



THE UNIVERSITY  
OF QUEENSLAND  
AUSTRALIA

CREATE CHANGE

The University of Queensland Surat Deep  
Aquifer Appraisal Project (UQ-SDAAP)  
Scoping study for material carbon abatement  
via carbon capture and storage

# Project Report

30 April 2019

## Authors

**Prof Andrew Garnett**, Director, Centre for Coal Seam Gas & UQ-SDAAP, The University of Queensland

**Prof Jim Underschultz**, Chair Petroleum Hydrodynamics, Centre for Coal Seam Gas, The University of Queensland

**Prof Peta Ashworth**, Chair of Sustainable Energy Futures, School of Chemical Engineering, The University of Queensland

## Project team

Mr Ahmed Harfoush

Ms Alexandra Wolhuter

Ms Alice Mahlbacher

Mr Alistair Innes-Walker

Ms Amy Hodson-Clarke

Dr Andrew La Croix

Mr Angus Veitch

Dr Ayrton Soares Ribeiro

Mr Carl Putzmann

Ms Carolyn Martin

Ms Christine Deeming

Mr Christopher Liens

Dr Claudia Nisa

Mr Degan Wye

Ms Dehlia MacDonald

Dr Des Owen

Ms Dianne Dimovski

Ms Elizabeth Delgado Alcantarino

Dr Harald Hoffman

Ms Helen Schultz

Mr Hossein Dashti

Mr Iain Rodger

Mr Ifti Altaf

Ms Jacqueline Robertson

Mr Jiahao Wang

Mr Jiang Kai

Mr Jianhua He

Mr Jochen Kassin

Dr Julie Pearce

Dr Katherine Witt

Dr Kwasi Ampofo

Ms Marian Sommer

Ms Michaela Farrow

Ms Michele Ferguson

Dr Mohammad Sedaghat

Ms Paulina Kaniewska

Dr Phil Hayes

Mr Rasheda Keen

Dr Sebastian Horning

Mr Sebastian Gonzalez

Ms Suzi Moore

Dr Vahab Honari

Ms Xiaoling Li

Mr Younas Yousafi

### **UQ professorial consultants**

Prof Brian Towler

Prof Joan Esterle

Prof Ray Johnson

Prof Sue Golding

Ass Prof Sue Vink

Prof Suzanne Hurter

Hon Prof Xinjing Wang

### **Consultancies/service providers**

Advisian Pty Ltd

ALS Environmental

Austar Gas Pty

Australian National University (ANU)

BizWordz

Bright Yellow

Curtin University

Gamma Energy Technology

Groundwater Logic

Hayes Geoscience

MGPalaeo

Pentagram Petrophysics

QCu Pty Ltd

Qualtrics

Terra Sana Consultants

## Acknowledgements

This report was prepared for The University of Queensland Surat Deep Aquifer Appraisal Project (UQ-SDAAP), a 3-year, \$5.5 million project funded by the Australian Government through the Carbon Capture and Storage Research Development and Demonstration (CCS RD&D) program, by Coal21, and The University of Queensland.

Software	Data Providers
CMG (CMOST)	Adelaide School of Petroleum (MICP analyses)
CMG (GEM)	ANU Centre for Advanced Microscopy (QEMSCAN)
Geoteric	Australia Pacific LNG (APLNG) (MAR data)
IHS Markit (WellTest)	Armour Energy (industry data)
Rock Flow Dynamics	Bridgeport Energy (Moonie field data & static model)
Schlumberger (Eclipse)	CS Energy (groundwater data)
Schlumberger (Petrel)	Carbon Transport & Storage Company (CTS Co) (subsurface data and technical review)
Schlumberger (PIPESIM)	GSQ Data Exploration Centre (access to drill core, and existing data sets). Dirk Kirste (mineral scripts)
Schlumberger (Techlog)	Geological Survey of Queensland (QDEX Database - Queensland Digital Exploration database)
	Office of Groundwater Impact Assessment (OGIA)
	Santos (industry data)
	Shell-QGC (Woleebee Creek GW4 and Kenya East GW7 data)
	Geological Survey of New South Wales (DIGS® - Digital 10Imaging Geological System database)
	Western Down Regional Council (regional data)

## Citation

Garnett AJ, Underschultz JR & Ashworth P (2019), Project Report: Scoping study for material carbon abatement via carbon capture and storage, The University of Queensland Surat Deep Aquifer Appraisal Project, The University of Queensland.

Referenced throughout the UQ-SDAAP reports as **Garnett et al. 2019d**.

## Publication details

Published by The University of Queensland © 2019 all rights reserved. This work is copyright. Apart from any use as permitted under the Copyright Act 1968, no part may be reproduced by any process without prior written permission from The University of Queensland.

ISBN: 978-1-74272-240-5

## Disclaimer

The information, opinions and views expressed in this document do not necessarily represent those of The University of Queensland, the Australian Government or Coal21. Researchers within or working with the UQ-SDAAP are bound by the same policies and procedures as other researchers within The University of Queensland, which are designed to ensure the integrity of research. The Australian Code for the Responsible Conduct of Research outlines expectations and responsibilities of researchers to further ensure independent and rigorous investigations.

# Contents

<b>1. Executive summary</b>	<b>21</b>
1.1 Summary statement	27
<b>2. Introduction</b>	<b>28</b>
<b>3. Societal and regional communities</b>	<b>30</b>
3.1 Introduction	31
3.2 How CCS is viewed in the context of other energy choices	32
3.2.1 National survey	32
3.2.2 Testing alternative messaging (framing) for increased understanding	42
3.3 The impact of alternative messaging approaches – on support for CCS	46
3.3.1 Workshops	46
3.3.2 International survey	49
3.4 Attitudes to groundwater and potential benefits the injection of CO <sub>2</sub> could have on improving water accessibility	54
3.4.1 Focus groups	54
3.5 The impact of how CCS is reported in the media	62
3.6 Important regulatory aspects of CCS in Queensland	65
3.7 Regional employment	66
3.8 Conclusion (socio-economic factors)	66
<b>4. Techno economic assessment of notional large-scale deployment</b>	<b>67</b>
4.1 Guide to this section	67
4.2 Introduction	68
4.3 Precipice Sandstone to Evergreen Formation: Geology of the Surat Basin	69
4.3.1 The storage play	72
4.3.2 Facies analysis	73
4.3.3 Sequence stratigraphic framework	82
4.3.4 Neural network wireline-facies	83
4.3.5 Seismic analysis	92
4.3.6 Mudstone palynology and age of sediments	102
4.3.7 Structural geology	103
4.3.8 Petrophysical analysis	121
4.3.9 MAR sector model	133
4.3.10 10 x 10 km sector-scale static reservoir models	135
4.3.11 Regional geological model	141
4.4 The container concept	146
4.4.1 The injection reservoir	148
4.4.2 The Transition Zone	149

4.4.3	The Ultimate Seal	150
4.4.4	The structure	153
<b>4.5</b>	<b>Evidence for containment potential</b>	<b>154</b>
4.5.1	Hydrocarbon systems analysis	155
4.5.2	Regional hydrogeological analysis	164
4.5.3	Fault zone analysis	174
4.5.4	Legacy wells	182
4.5.5	Sealing capacity of the Transition Zone and Ultimate Seal	185
4.5.6	Assessment of potential to fracture at the injection well	189
4.5.7	Water-CO <sub>2</sub> -rock reactive geochemistry	191
4.5.8	Summary of evidence for containment potential	197
<b>4.6</b>	<b>Evidence for injectivity</b>	<b>198</b>
4.6.1	Production tests and drill stem tests	198
4.6.2	Subsurface pressure constraints	199
4.6.3	Large-scale injectivity data (MAR)	200
4.6.4	Large-scale production data: Moonie oil field	210
4.6.5	Summary of evidence for injectivity	217
<b>4.7</b>	<b>Notional injection site identification and sweet spot analysis</b>	<b>218</b>
4.7.1	Risk minimising and avoidance philosophy	218
4.7.2	Application of “rules” to subsurface features constraints	220
4.7.3	Application of “rules” to surface constraints	224
4.7.4	Sweet spot identification, description and remaining uncertainties	224
<b>4.8</b>	<b>Notional injection site modelling and FDP – Reference case</b>	<b>226</b>
4.8.1	UQ-SDAAP field development philosophy	226
4.8.2	Translating the revised geology and static models	226
4.8.3	Boundary conditions	228
4.8.4	Fluid model	230
4.8.5	Transition Zone investigations	235
4.8.6	Injection well design	241
4.8.7	CO <sub>2</sub> injection scenarios and well lay-out	243
4.8.8	Injection sector test cases – upside and uncertainties	247
4.8.9	Field development simulations – testing rates and durations	252
4.8.10	Summary of site modelling test cases	256
<b>4.9</b>	<b>Pipeline network – a scoping investigation</b>	<b>257</b>
4.9.1	Methodology	257
4.9.2	Pipeline network final routing and sensitivities	259
<b>4.10</b>	<b>Surface facilities concepts</b>	<b>267</b>
4.10.1	General configuration	267
4.10.2	Well pad facilities basis of design – working assumptions	268
4.10.3	Well pad facilities high level operating philosophy	268
4.10.4	Description of surface and well site process facilities	268

4.10.5	Venting	270
4.10.6	Communications and control	270
4.10.7	Electrical power generation	271
4.10.8	Cost estimate summary	271
4.10.9	Summary of surface facilities	272
4.10.10	FDP Concept M&V for long term operations	272
4.10.11	Subsurface M&V for loss of containment	273
4.10.12	Summary of M&V	274
<b>4.11</b>	<b>Notional injection modelling and FDP reference cases – groundwater impact</b>	<b>275</b>
4.11.1	UQ-SDAAP groundwater modelling philosophy	275
4.11.2	Translating static and GEM model into a groundwater model	276
4.11.3	Model boundary conditions and time discretisation	277
4.11.4	CO <sub>2</sub> injection scenarios	278
4.11.5	Summary of groundwater modelling	282
<b>4.12</b>	<b>Notional injection modelling and FDP – sensitivity analysis</b>	<b>283</b>
4.12.1	Sensitivity analysis results	285
4.12.2	Summary of sensitivity analysis	300
<b>4.13</b>	<b>Notional injection modelling and FDP sensitivity analysis – groundwater impacts</b>	<b>302</b>
4.13.1	Sensitivity analysis results	302
4.13.2	Summary of sensitivity analysis and conclusions	304
<b>4.14</b>	<b>Retrofit deployment, hub scenarios, costs and cash-flow</b>	<b>305</b>
4.14.1	Introduction	305
4.14.2	What is a hub and how does development start?	305
4.14.3	Retrofit and post combustion capture	307
4.14.4	CO <sub>2</sub> hub scenarios	308
4.14.5	Activities and decisions on capital phasing	311
4.14.6	Implications for regional employment	317
4.14.7	Post-retrofit, power and emissions reductions and unit costs	318
4.14.8	LCOE and capital cost sensitivity analyses	319
<b>4.15</b>	<b>The calibrated <i>dynamic capacity</i> of the Surat Basin</b>	<b>321</b>
4.15.1	Typical capacity concepts	321
4.15.2	Dynamic capacity – concepts and communicating uncertainty	322
4.15.3	UQ-SDAAP calibrated, risked dynamic capacities and uncertainties	324
<b>4.16</b>	<b>Conclusion (technical feasibility)</b>	<b>327</b>
<b>5.</b>	<b>Next steps: actions required to progress CCS</b>	<b>328</b>
<b>5.1</b>	<b>Discussion</b>	<b>328</b>
<b>5.2</b>	<b>Overview – project forward risk assessment</b>	<b>330</b>
<b>5.3</b>	<b>Regulatory pathways (theme 1)</b>	<b>331</b>
<b>5.4</b>	<b>Community and stakeholder engagement (theme 2)</b>	<b>332</b>
5.4.1	Engaging with local communities	332
5.4.2	Awareness raising at the national level	332
5.4.3	Monitoring of attitudes	332

<b>5.5 Site-specific appraisal data gathering (theme 3)</b>	<b>333</b>
5.5.1 Technical storage project risks	333
5.5.2 Appraisal strategies	336
5.5.3 Appraisal well Blocky Sandstone Reservoir testing program	338
5.5.4 Vertical interference test	341
5.5.5 Costs and notional plans schedules	343
<b>5.6 Unit costs and discussion of the value of investment in appraisal</b>	<b>348</b>
5.6.1 Scoping level unit technical costs (scenario or project specific)	348
5.6.2 Accounting for appraisal costs.	349
5.6.3 Unit costs discussion leading to value of appraisal discussion	350
5.6.4 The impact of “at risk” appraisal costs on UTC (break-even) considerations	351
5.6.5 An alternative discussion on value of appraisal and appraisal decisions	353
5.6.6 Conclusions	354
<b>5.7 Venture set-up (theme 4)</b>	<b>355</b>
<b>5.8 Summary of critical success factors in moving beyond the next appraisal stage</b>	<b>356</b>
<b>6. References</b>	<b>357</b>
<b>7. UQ-SDAAP: project reports listing</b>	<b>372</b>
<b>8. Glossary of terms, acronyms and abbreviations</b>	<b>375</b>

# Tables

<b>Table 1</b>	Questionnaire structure.	36
<b>Table 2</b>	Perceived knowledge of the general public sample compared to COIs.	39
<b>Table 3</b>	Support for energy technologies across States.	40
<b>Table 4</b>	Support for energy technologies comparing general public and COIs.	42
<b>Table 5</b>	Regression model identifying support variables for CCS.	44
<b>Table 6</b>	Alternative versions of question order.	46
<b>Table 7</b>	Socio-demographic characteristics of participants across experimental conditions.	46
<b>Table 8</b>	Sequence of experiments in each workshop.	50
<b>Table 9</b>	Workshop survey questions.	50
<b>Table 10</b>	Combined pre and post-information support for energy technologies.	51
<b>Table 11</b>	Sequence of questions/materials in survey conditions.	52
<b>Table 12</b>	Socio-demographic characteristics of participants across countries.	53
<b>Table 13</b>	Combined pre- and post-information support for energy technologies, by survey condition.	54
<b>Table 14</b>	Do you believe global warming is happening or will happen in the next 30 years?	60
<b>Table 15</b>	When you think about carbon capture and storage (CCS), what first comes to mind?	61
<b>Table 16</b>	The number of articles in the dataset, broken down by region and source type.	65
<b>Table 17</b>	Reflector characteristics of the main seismic events.	95
<b>Table 18</b>	Characteristics of the major basement fault systems in the UQ-SDAAP study area interpreted from magnetic, Bouguer gravity and seismic data. Fault system azimuth orientation is taken from He et al. 2019 (paper in press).	112
<b>Table 19</b>	Core porosity statistics per facies.	128
<b>Table 20</b>	Core ambient air permeability statistics per facies.	128
<b>Table 21</b>	Core calculated water in-situ reservoir permeability statistics per facies.	128
<b>Table 22</b>	Core ambient vertical permeability statistics per facies.	129
<b>Table 23</b>	Core grain density statistics per facies.	129
<b>Table 24</b>	DSTs data inventory. BSR: Blocky Sandstone Reservoir, TZ: Transition Zone, BU: sub-Surat Unconformity, MLP_NORM: facies log, Y: Yes, N: No, Quality Scale: reliable data in green, data to be used with care in yellow and unreliable data in red. Thickness h is based on the DST interval.	130
<b>Table 25</b>	Permeability equations for the three regional permeability models.	134
<b>Table 26</b>	$K_v/K_h$ approximations used in the regional static reservoir models.	135
<b>Table 27</b>	C1-C4 concentrations of Moonie oil field production wells. Units = $\mu\text{g/L}$ . DL = 10 $\mu\text{g/L}$ .	184
<b>Table 28</b>	Fracture pressure cases for SDAAP models.	194
<b>Table 29</b>	Transient historical water balance in MG/day –whole model.	209
<b>Table 30</b>	UQ porosity-permeability transform for Moonie area categorised based on facies or groups of facies.	217
<b>Table 31</b>	Subsurface suitability criteria, risks represented and associated restriction function.	224
<b>Table 32</b>	Criteria weighting for subsurface analysis (initial weighting – a sensitivity analysis was undertaken and results in essentially the same high-graded sites).	225
<b>Table 33</b>	Factor values for top of Transition Zone depth.	226



<b>Table 34</b>	Factor values for Blocky Sandstone Reservoir thickness.	226
<b>Table 35</b>	Factor values for Blocky Sandstone Reservoir dip angle.	226
<b>Table 36</b>	Factor values for distance from Blocky Sandstone Reservoir zero edge.	226
<b>Table 37</b>	Factor values for bores/wells with a 15 km radius restriction function.	226
<b>Table 38</b>	Factor values bores/wells with 10 km radius restriction.	226
<b>Table 39</b>	Factor values for bores/wells with 5 km radius restriction.	226
<b>Table 40</b>	Factor values for bores/wells with 2 km radius restriction.	226
<b>Table 41</b>	Well performance after 10 years of injection for isothermal and non-isothermal simulations.	237
<b>Table 42</b>	Permeability fields used in the simulation scenarios.	247
<b>Table 43</b>	MKMK development scenarios. Wells reached the injectivity limit for low reservoir permeability cases (LowRes and HighTZ) – well redundancy not included (add at least one per site).	248
<b>Table 44</b>	MKTMKT development scenarios. Injectivity limits are similar to MKMK scenarios.	250
<b>Table 45</b>	MKTMKT extended development scenarios. Higher wellhead pressure is required to meet the injection target for MidRes.	250
<b>Table 46</b>	Notional injection sector model layers. The colour column refers to Figure 133.	253
<b>Table 47</b>	Mass rates for MKMK schedule.	256
<b>Table 48</b>	Mass rates for MKTMKT extended schedule.	256
<b>Table 49</b>	Weighting for each criteria in the base case and sensitivity analysis for the pipeline route selection.	262
<b>Table 50</b>	Pipeline route length (km).	268
<b>Table 51</b>	Pipeline route stream crossings.	268
<b>Table 52</b>	Pipeline route road, pipeline and rail crossings.	269
<b>Table 53</b>	Pipeline route powerline crossings.	269
<b>Table 54</b>	Basis of design (BoD) process conditions for pipeline CO <sub>2</sub> fluid.	270
<b>Table 55</b>	Summary P50 CAPEX estimate – 4 well configuration (\$2019, excludes owners' costs and escalation).	274
<b>Table 56</b>	Layering of the groundwater model compared to geological static and notional injection models.	279
<b>Table 57</b>	Parameters tested in the sensitivity studies. *indicates mean/typical values are shown in this table. Reference case in bold.	287
<b>Table 58</b>	Financial assumptions (Gamma Energy Technology 2019).	314
<b>Table 59</b>	Roll out scenario #1: cumulative installed capture rate and sequence.	314
<b>Table 60</b>	Summary of deployment sequence, retrofit jobs and cumulative capture rate installed.	317
<b>Table 61</b>	Comparison of scoping-level performance outcomes for three different retrofit scenarios.	321
<b>Table 62</b>	LCOE sensitivity to capacity factor assumptions (\$/MWh).	322
<b>Table 63</b>	Sensitivity of capital cost and parasitic loss to new technology (solvent).	323
<b>Table 64</b>	Impact on LCOE on funding source (WACC).	323
<b>Table 65</b>	Modelling parameters for well testing design for notional injection site in south-central Surat.	341
<b>Table 66</b>	Well testing sequences for the reference case in notional injection site.	342
<b>Table 67</b>	Parameters used during VIT scenarios in which water is injected into Hutton Sandstone and pressure changes observed in the Blocky Sandstone Reservoir.	345
<b>Table 68</b>	High level cost estimates (all costs are before market testing) for proposed appraisal program of both the north and south notional injection sites.	347
<b>Table 69</b>	Schematic of logging, coring and downhole testing program requirements.	349
<b>Table 70</b>	Summary of example deployment scenarios for unit cost discussions. 35271 Indicative unit appraisal costs for storage resources.	353
<b>Table 72</b>	Summary of high-level unit technical costs (UTCs) of 3 scenarios.	354

# Figures

<b>Figure 1</b>	Visualisation of a potential CCS initiative.	22
<b>Figure 2</b>	Power stations, pipeline routes and notional sites.	23
<b>Figure 3</b>	Illustration of minimum risk site selection.	25
<b>Figure 4</b>	Visualisation of a potential injection cross-section.	25
<b>Figure 5</b>	An indicative timescale over the life of the project to capitalise on the limited window of opportunity to draw maximum benefit from this initiative. This hinges on having a fully operational system in place as soon as possible in the useful life span of the three identified power stations to maximise the time for emissions capture. It is conceivable that capture can commence around 2030.	26
<b>Figure 6</b>	Geographical spread of respondents.	34
<b>Figure 7</b>	Perceived knowledge of each energy technology – general public sample (n=2383).	35
<b>Figure 8</b>	Support for each energy technology – general public sample (n=2383).	37
<b>Figure 9</b>	Energy technology frequency distributions (n=2383).	38
<b>Figure 10</b>	When you think about CCS, what first comes to mind?	40
<b>Figure 11</b>	When you think about renewable energy, what first comes to mind?	40
<b>Figure 12</b>	Support for each energy technology per condition, compared to ‘no information’ condition.	44
<b>Figure 13</b>	Perceptions of the advantages versus the risks of CCS.	52
<b>Figure 14</b>	Belief in global warming, by country.	53
<b>Figure 15</b>	General public’s word associations with the GAB.	56
<b>Figure 16</b>	The intensity of coverage of CCS in major geographic regions*.	63
<b>Figure 17</b>	(A) Geographic location of the Eromanga, Surat, and Clarence-Moreton basins in Australia. (B) The main structural features of the Surat Basin, and the location of wells used in cross sections, including the location of cored wells discussed in this report. (C) Structure-contour map (relative to sea level) of the base-Surat unconformity surface.	70
<b>Figure 18</b>	Comparison of various lithostratigraphic and sequence stratigraphic schemes for the Surat Basin, displayed next to the eustatic sea level curve developed by Haq et al. 1987. The Westgrove Ironstone Member has been dated using palynology to represent a regional transgression that correlates with the early Toaracian global sea level rise (Hallam & Wignall 1999). The Precipice Sandstone and Evergreen Formations were defined as supersequences by Hoffmann et al. 2009. More recently, three cycles (i.e. sequences) of deposition were interpreted by Wang et al. 2019.	71
<b>Figure 19</b>	The location of cored wells within the Surat Basin that were logged in detail as part of this study. A total of nine wells were examined, mostly occurring within the northern, north-eastern, and north-western parts of the basin.	74
<b>Figure 20</b>	Stratigraphic terminology used to describe the core, along with the modelling zones, and a litholog from Woleebee Creek GW4. The dashed line represents the location of the 2D seismic data.	76
<b>Figure 21</b>	Conceptual block model of Lowstand Systems Tract 1, the main reservoir interval investigated for CO <sub>2</sub> storage in the Surat Basin.	77
<b>Figure 22</b>	Conceptual block model for Transgressive Systems Tract 1, the unit overlying the main reservoir interval. The same depositional model is applicable to the transgressive systems tract within Sequence 2.	78
<b>Figure 23</b>	Conceptual block model for Highstand Systems Tract 1. The same model is applicable to the highstand systems tract from Sequence 2, as well as Highstand Systems Tract 3.	79
<b>Figure 24</b>	Conceptual block model for Lowstand System Tract 3, otherwise known as the Boxvale Sandstone. A similar model applies to the lowstand from Sequence 2.	80

<b>Figure 25</b>	Conceptual block model for Transgressive Systems Tract 3, the main interval containing ironstone.	81
<b>Figure 26</b>	Map showing the location of wells across the Surat Basin that were used for wireline log facies prediction. Their colour shows the number of distinct types of well logs that were available to improve their accuracy.	84
<b>Figure 27</b>	(A) The results of LDA showing how the 10 main WLF plot in multidimensional space and were grouped. (B and C) PCA for WLF displaying the wireline logs that were most important for determining WLF – gamma ray (GR), sonic, and neutron.	85
<b>Figure 28</b>	Schematic paleoenvironmental/facies map for the interval from J10-TS1. This is the main reservoir interval, consisting predominantly of the “Blocky Sandstone Reservoir” (i.e. Facies SA). Selected wells are marked to orient the reader.	87
<b>Figure 29</b>	Schematic paleoenvironmental/facies map for the interval from TS1-MFS1. This is the first part of the Transition Zone. Here begins the development of delta plain to subaqueous delta depositional environments that back-stepped towards the basin margins during a transgression in base level. Selected wells are marked to orient the reader.	88
<b>Figure 30</b>	Schematic paleoenvironmental/facies map for the interval from MFS1-SB. This is the middle section within the Transition Zone. At this point in time deltas prograded back towards the basin centre during a base level high stand. Selected wells are marked to orient the reader.	89
<b>Figure 31</b>	Schematic paleoenvironmental/facies map for the interval from SB2-TS3. This represents the top portion of the Transition Zone. A similar situation to the underlying interval occurs with deltaic and nearshore depositional settings back-stepped during sea level transgression and then prograded back to the basin centre during highstand. Selected wells are marked to orient the reader.	90
<b>Figure 32</b>	Schematic paleoenvironmental/facies map for the interval from TS3-J30. This is the Ultimate Seal interval for the basin. It is characterised by widespread ironstone and mudstone with very low porosity and permeability. Peculiar depositional conditions occurred in pulses allowing concentration of iron in the water column and nearshore realm. The top of the succession is overlain by the Hutton Sandstone. Selected wells are marked to orient the reader.	91
<b>Figure 33</b>	(A) Synthetic seismogram from Woleebee Creek GW4. (B) An east-west trending seismic section tied to Woleebee Creek GW4 that illustrates the sequence stratigraphic framework. The seismic data and synthetic seismogram are displayed in zero phase with SEG Y convention polarity. See Figure 17 for section location.	93
<b>Figure 34</b>	East-west trending seismic section showing the Lower Jurassic sequence stratigraphic framework across the northern part of the Surat Basin. The base of the Lower Jurassic (Seismic Event 5) is a regional unconformity typically manifest by truncation and onlap reflector terminations. Note that the reflectors between Seismic Event 4 and 5 onlap and thin toward both the western and eastern basin margins.	94
<b>Figure 35</b>	East-west trending seismic section showing the Lower Jurassic sequence framework across the central part of the Surat Basin.	94
<b>Figure 36</b>	(A) Regional 3D map illustrating 2D regional composite seismic lines for seismic interpretation correlation. Background map is the top of the J10 unconformity. (B) An example of regional seismic line Surat 78-4 from West to East depicting the base Surat. Stratigraphic panels in the seismic line depict the stratigraphic correlation and basal unit onlap. The location and orientation of the seismic line is marked with a red line in A. (C) A zoom in of the blue box of the central region of the figure B exhibiting the thinning and on-lapping of the Blocky Sandstone Reservoir towards the east. The yellow marker on the seismic lines represents the top of the Blocky Sandstone Reservoir TS1, magenta is the top of the Transition Zone, near J20 and white marker is the J10 Base Surat Unconformity.	95
<b>Figure 37</b>	Seismic Line AP10-21 illustrating paleo- topography control for the Blocky Sandstone Reservoir deposition. Note the double amplitude reflector near the Ferret 1 well, which is thicker with respect to a single amplitude reflector near the Dulacca 1 well (paleo-high). The cross section location is shown by the red line on the inset map.	96
<b>Figure 38</b>	Seismic Line BMR-84-14 (bottom inset), illustrating the seismic to well ties across the basin (the location of the seismic line is indicated by the red dotted line on the background map of depth to the Base Surat Unconformity). The seismic to well tie correlation indicates truncation of seismic event 4 (Top of the Blocky Sandstone Reservoir) in the east near the Daydream 1 well.	97
<b>Figure 39</b>	Structure contour map for base Surat J10 in depth. CI 200 m purple and dark blue denotes deep areas below 2000 m TVDSS. The red dotted line indicates the UQ-SDAAP model boundary. Inset square denotes location of Durham Ranch.	98

- Figure 40** Distribution of data used for the time depth conversion of seismic data. Red dots denote wells with velocity data. Lines in grey and blue are the 2D and 3D seismic data. Pink dots represent data obtained along the northern sub-crop of the Blocky Sandstone Reservoir. 99
- Figure 41** Isopach map of the Blocky Sandstone Reservoir where the red colour indicates near to zero thickness and purple represents >150 m thickness. The central east region shows a thinner area likely controlled by paleo-structures in a highly faulted region. 101
- Figure 42** Summary of the structural evolution of Bowen and Surat basins, where; (A) Stratigraphic nomenclature for the Surat and Bowen basins. Red arrows denote basin inversion events, Magenta parenthesis is Bowen Basin Strata and the Red parenthesis is Surat Basin Strata; (B) Are 1D burial history plots (Reza at- al 2009) for four wells in the basin with each well location displayed in figure C. Red arrows denote basin inversion events, Magenta parenthesis is Bowen Basin Strata and the Red parenthesis is Surat Basin Strata. (C) Regional map of the Surat-Bowen basins for the UQ-SDAAP area of study, exhibiting major tectonic elements (Korsch et al. 2009) and illustrating the structural evolution from west to east of the Bowen Basin. (D) Deformation synthesis for eastern Australia between the Carboniferous (left) and Permo-Triassic time (right) (Rosenbaum 2018). 104
- Figure 43** The isopach distribution for the Transition Zone and the Blocky Sandstone Reservoir combined, exhibiting areas of J20 truncation towards the south where the red dashed line is the near zero edge, depocenters are highlighted by green-blue colours and potential emerging land masses are indicated in orange polygons. The size of the “+” in the polygon indicates the interpreted degree of emergence related to the provenance contribution (increasing to the south). The red dotted line indicates the UQ-SDAAP model boundary. 105
- Figure 44** Schematic paleo-geographic reconstruction of the J10 Base Surat Unconformity for the Surat Basin where (A) is the Scotese paleo tectonic map at -170 ma. The red square shows the location of the Surat Basin. (B) A schematic convergent plate boundary (taken from PM-FIAS 2015 website “continent-ocean convergence formation of fold mountains”) exhibiting the volcanic setting and thrust belt postulated to be analogous of the mountain building along the east side of Surat during the Hunter-Bowen Orogeny prior and contemporaneous with deposition of the Blocky Sandstone Reservoir. (C) is a paleogeographic representation of the basin at -170 ma with the tectonic elements associated with the postulated convergent plate boundary. The green area represents an emerged land mass at that time. Grey represents the magmatic arc (New England Foldbelt), whereas the yellow and beige polygons represent the Surat and Clearance Moreton basin sedimentation respectively. Note a transfer zone and possible connection between the two basins. 106
- Figure 45** An OzSEEBASE map showing the regional tectonic elements of the Surat Basin (Top figure). Bottom figure: shows a composite E-W seismic line with the major faults and structures affecting the Bowen and Surat basins marked in red dashed lines. The yellow polygon denotes the Blocky Sandstone Reservoir. 108
- Figure 46** (A) Processed gravity data (from original data in D Geoscience Australia) using a 100 km high pass filter showing major lineaments in red, linked to major structural features. Magenta circles denote a high-density contrast linked to intrusions as seen in the total magnetic map C (red areas in map C). (B) A sequence of seismic lines oriented east-west (not scaled). The seismic profiles illustrate the different tectonic styles observed in the basin. (C) Total magnetic map (Geoscience Australia). (D) The regional gravity map. 110
- Figure 47** (A) A regional fault segmentation and classification analysis for the central and south east major fault trends. Colour code denotes the relative throw magnitude where red is high throw, magenta moderate and blue is low. (B) A stereonet plot of the fault segment orientations displayed by throw colour code. The maximum horizontal stress (Shmax) is also displayed in black arrows where the orientation is taking from Hills et al. (1988) map shown in C Faults with large throw in red are mainly oriented NW-SE almost perpendicular to the current Shmax in the basin. (C) Maximum Horizontal Stress Orientation after Hills et al. 1998 for Queensland Basins. The red dotted line indicates the UQ-SDAAP model boundary. 111
- Figure 48** The Moonie field location (white box) in relation to the regional OzSEEBASE Map. Blue and red dots are locations of interpreted faults crossing a seismic line. The red polygon is the approximate edge of the Blocky Sandstone Reservoir. B: A 3D schematic diagram of the Moonie fault highlighting dip trends (purple plane). C: Plan view of the Moonie fault showing the fault structural elements. Background map represents the structural contour map of the Top Blocky Sandstone Reservoir in depth, orange colours indicates shallow areas. Blue dots represent the Moonie well location. The red dotted line indicates the UQ-SDAAP model boundary. 112
- Figure 49** Left: Plan view and colour coded dip azimuth map along the fault plane. Contours denotes the top structure map of the Blocky Sandstone Reservoir. Dark colours along the fault plane (blue-green) represent higher dip values where each fault segment is indicated by a different colour. Right: Seismic cross sections (cross section location marked on the base map on the left) illustrating the various fault geometries for different Moonie fault segments (e.g. Section B runs along the centre of the field and highlights the steeply dipping fault plane in segment 5 (dark blue colour). 113
- Figure 50** BMR84 seismic cross section east of the Bennet Field. A high density of faults cutting through Jurassic section are highlighted in red dashed lines and by the blue box. 113

<b>Figure 51</b>	An example of seismic data showing how the folding of the Surat Basin strata changes with variable geometry of the reactivated basement fault (across the Moonie 3D seismic area). The histogram column shows the thickness ratio of the footwall to hanging wall.	114
<b>Figure 52</b>	(A) Fractured intervals observed in core (1032.24-1032.54 m) from the Upper Evergreen Formation of the Chinchilla 4 well, showing the fracture filled with calcite; (B) Core from the Reedy Creek MB3-H well, 1102.25 m, showing a low dip-angle slip fracture with smooth mirror, scratches and steps; (C) Core from the Reedy Creek MB3-H well, 1102.75 m, showing a vertical compression-shear fracture with scratches and steps. (D) Core image from the Southwood 1 well near the Moonie fault, 1988 m, showing sandstone calcite cemented fractures in sandstone; (E) An EDS calcium element map for part of the calcite filled fracture in figure E (image width 1 mm); (F) A Scanning Electron Microscopy (SEM) image of barite cement adjacent to a fracture mixed with K-feldspar altered to kaolinite. (H) An EDS spectrum of barite cement from the Chinchilla 4 well, 980 m; (I) an SEM image of pyrite cement. Ba: Barite; Ka: Kaolinite; KF: K-feldspar; Py: pyrite.	115
<b>Figure 53</b>	The seismic profile (SM95-01) across the Moonie fault and its interpretation of the sedimentary sequence geometry, showing the growth sequence.	116
<b>Figure 54</b>	A 3D view of the J10 structure map showing fault structural styles and schematic cartoons of seismic profiles across the major faults at various locations.	117
<b>Figure 55</b>	Structural elements for the central region of the Surat Basin. Left: An OzSEEBASE map highlighting structural anomalies oriented NE-SW in the yellow circle. Centre: a map of dip angle from a low pass filter of the gravity map where blue values indicate high dip angles. West directed dip angles are related to the Blocky Sandstone Reservoir truncation against the J10 unconformity. Right: A map of the J10 unconformity structural map dip angle that highlights the eastern faults.	118
<b>Figure 56</b>	(A) OzSEEBASE map illustrating the central part of the Surat Basin and the location of the seismic lines S78-2 and C1103. Red dotted lines refer to regional lineaments. (B) Seismic profile Surat 78-2 EW displaying a potential fault at the J10 unconformity surface near a gravity lineament A. (C) Seismic profile C11-03 displaying a normal fault propagating across the J10 unconformity. D: Throw in msec for both faults are -6 msc and the interval velocity is estimated to be around 4000 m/sec for this depth (Tasmania 1 well).	119
<b>Figure 57</b>	Fault juxtaposition scenarios for a 25 m throw fault in the Surat Basin central area.	120
<b>Figure 58</b>	UQ-SDAAP workflow for wireline log interpretation.	122
<b>Figure 59</b>	Map showing the distribution of wells with core analysis data from the Precipice Sandstone and Evergreen Formation utilised in the UQ-SDAAP petrophysical analysis.	123
<b>Figure 60</b>	Workflow for correcting core ambient air permeability to water in-situ reservoir permeability.	124
<b>Figure 61</b>	Methodology for estimating permeability from petrophysical data.	130
<b>Figure 62</b>	Workflow for estimating an upscaled $k_v/k_h$ ratio for a single lithology facies.	132
<b>Figure 63</b>	Map of the Surat Basin showing the location of the MAR sector model area.	134
<b>Figure 64</b>	Index map showing the location of the three-sector static model conceptualisation areas: Woleebeev Creek, Meandarra, and Moonie, respectively.	136
<b>Figure 65</b>	Facies modelling of the Meandarra sector model. (A) Object modelling of the lower Blocky Sandstone Reservoir. (B) object modelling of the upper Blocky Sandstone Reservoir. (C) Object modelling of the lower Transition Zone. (D) Object modelling of the middle Transition Zone. (E) Sequential Indicator Simulation of the upper Transition Zone. (F) Sequential Indicator Simulation of the Ultimate Seal.	138
<b>Figure 66</b>	Examples of the property modelling for the Meandarra sector model. (A) $V_{shale}$ . (B) Net to gross. (C) Total porosity. (D) Effective porosity. (E) Horizontal permeability. (F) Vertical permeability (water in-situ reservoir permeability). Note that $V_{shale}$ , total porosity and effective porosity were modelled parameters, whereas net to gross, horizontal permeability, and vertical permeability were calculated parameters.	139
<b>Figure 67</b>	(A) 3D perspective of the structural framework and model boundaries. Grey polygons denote faults, the white background represents structural contours for the J10 unconformity surface and the cross sections exhibit the sequence stratigraphic framework across the basin. (B) Modelled zones and layering for each stratigraphic unit. (C) An example of the layering discretisation.	143
<b>Figure 68</b>	Up-scaled facies classification from $V_{shale}$ compared to core facies data prediction. Vertical heterogeneity is captured in the up-scaled cells.	144
<b>Figure 69</b>	The isopach distribution (m) for the Transition Zone (TS1-TS3) where the blue dots are wells that penetrate the base of the Transition Zone and the blue outline represents the edge of the underlying Blocky Sandstone Reservoir.	151

<b>Figure 70</b>	The isopach distribution (m) for the Ultimate Seal (J30-TS3) where the red dots are wells that penetrate the base of the Ultimate Seal and the blue outline represents the edge of the underlying Blocky Sandstone Reservoir.	152
<b>Figure 71</b>	Burial history plot representative of the Bowen/Surat Basin. Timing and quantity of oil and gas generation for the 82-50 well using the geohistory model in part (A), and a 5% coal content within the Burunga Formation and the (B) measured compositional kinetics for oil and gas generation from German Creek coal #5334 and oil cracking kinetics of (Horsfield et al. 1991). (C) WinBury TM data in (Waples 1992) composite default kinetics for primary oil and gas generation, and secondary oil cracking (Boreham 1999).	156
<b>Figure 72</b>	The Hutton Sandstone (above the Evergreen Formation) structure top with the distribution of oil indicators. The total picks dataset is displayed by the grey crosses.	157
<b>Figure 73</b>	Cross section of the western edge of the Bowen and Surat basins showing Possible Migration pathways of hydrocarbons generated from Permian Source Rocks (Cadman 1998).	159
<b>Figure 74</b>	The distribution of hydrocarbon migration pathways west of the depositional limit of the Rewan Formation and Snake Creek Mudstone Member, across the Wunger Ridge and onto the Roma Shelf to various trapping and accumulation field locations (Cadman 1998).	160
<b>Figure 75</b>	Sandy Creek 2 well gamma ray petrophysical log with a matching pressure-elevation plot (Wu 2015). (Note that “Precipice SS” in this figure is in the UQ-SDAAP “Transition Zone”).	161
<b>Figure 76</b>	A pressure elevation plot (Augusta 2017) for the wells from the Borah Creek Field (note that “Precipice SS” in this figure is in the UQ-SDAAP “Transition Zone”).	162
<b>Figure 77</b>	A schematic representation of the lateral and vertical continuity of hydrocarbon accumulations in the stacked reservoir sands of the Kincora, Borah Creek and Sandy Creek fields on the Roma Shelf (Augusta 2017). Note that the ‘Wandoan Sandstone’ is below the sub-Surat unconformity.	163
<b>Figure 78</b>	The distribution of hydraulic head within the Blocky Sandstone Reservoir. Blue contours are hydraulic head with a 50 m interval. Well locations with hydraulic head data control points are posted in black and values highlighted by yellow shading are interpreted to be production affected.	166
<b>Figure 79</b>	Digital Elevation Model for the Surat Basin with red representing surface elevation greater than 250 m ASL and blue representing surface elevation less than 250 m ASL.	168
<b>Figure 80</b>	The alternative interpretation of the distribution of hydraulic head within the Blocky Sandstone Reservoir. Blue contours are hydraulic head with a 50 m interval. Well locations with hydraulic head data control points are posted in black and values highlighted by yellow shading are interpreted to be production affected.	170
<b>Figure 81</b>	The distribution of hydraulic head within the Hutton Sandstone Aquifer. Blue contours are hydraulic head with a 100 m interval.	171
<b>Figure 82</b>	Left: Seismic line BMR84-14 W-E showing the vertical seismic anomalies up to the near surface in the centre and the eastern flank. Right: Seismic line C11-03 N-S displaying the large number of features in the near surface along the mute seismic zone.	174
<b>Figure 83</b>	Location of seismic anomaly site	175
<b>Figure 84</b>	Conceptual representation of the effect of gas plume/cloud on raw laser methane meter data readings.	177
<b>Figure 85</b>	Laser methane survey results from vehicle and drone survey along Western Road and upstream and downstream of Two Mile Creek, and a control area in the east.	178
<b>Figure 86</b>	Major ion concentrations for Moonie produced water (from the Precipice Sandstone aquifer) from the 1960s when the wells were drilled (grey lines) and for recently acquired produced water samples from 2019 (black lines).	180
<b>Figure 87</b>	Potential leakage pathways along an existing well: between cement and casing (paths ‘A’ and ‘B’), through the cement (C), through the casing (D), through fractures (E), and between cement and formation (F). (Gasda et al. 2004).	183
<b>Figure 88</b>	The distribution of cement plug thickness for wells within 100 km radius of the Fantome 1 well (Yousafi 2018).	184
<b>Figure 89</b>	The distribution of legacy wells within 100 km radius of the Fantome 1 well, by decade (Yousafi 2018).	184
<b>Figure 90</b>	MICP data from Woleebee Creek GW4. Both plots show the same data, but the right-side plot uses a log scale for pressure. Dark blue lines are data from “Precipice Sandstone” (Blocky Sandstone Reservoir) while light blue lines are from “Evergreen Formation” (Transition Zone/Ultimate Seal).	186
<b>Figure 91</b>	Examples of natural mineral trapping alteration and natural fractures in core from the West Wandoan 1 well (WW1) Ultimate Seal, Moonie 31 and 38 wells Transition Zone, and Southwood 1 well Transition Zone. Ap = apatite, Sid = siderite, Py = pyrite, Zr = zircon, Ti = Ti-oxide cement, Cal = calcite, Si = silica cement.	187
<b>Figure 92</b>	Isothermal fracture pressure gradient in the Blocky Sandstone Reservoir as calculated from MEMs for two wells.	189

<b>Figure 93</b>	Mineral content with depth in the Moonie 38 well core for the Blocky Sandstone Reservoir (58 Sands, deeper two samples) and Transition Zone (56 Sands).	192
<b>Figure 94</b>	Photos and SEM examples of sampled core from the Moonie 38 and Southwood 1 wells. (A) and (B) Moonie 38 Transition Zone (56 Sands) at ~ 1726.7 m. (C) Moonie 38 Blocky Sandstone Reservoir (58 Sands) 1771.8 m. (D) and (E) Southwood 1 Transition Zone 1952.9 m. (F) Southwood 1 Transition Zone 1955.0 m. Sid = siderite, K-f = K-feldspar, Ka = kaolinite.	193
<b>Figure 95</b>	Predicted change in minerals and pH for the Moonie 38 well core samples over 1000 years simulation, with lower CO <sub>2</sub> fugacity (saturation) e.g. representing the edge of the plume. A)-B) Blocky Sandstone Reservoir (58 sands) 1771.8 m change in minerals and pH, C)-D) Transition Zone (56 Sands) 1727.7 m change in minerals and pH, and E)-F) Transition Zone (56 Sands) 1723.8 m change in minerals and pH.	194
<b>Figure 96</b>	MICP pore throat distributions measured for core samples from the Moonie 33, Moonie 38, Moonie 31, and Moonie 22 wells (labelled by M33 etc. and sample depth). Core samples are from the Transition Zone except those marked as the Blocky Sandstone Reservoir (BSR). Southwood 1 well samples (SW1) are from the Transition Zone, and two Ultimate Seal core samples from the West Wandoan 1 (WW1) and GSQ Chinchilla 4 (Chin 4) wells, labelled by depth in m (note-rounded to nearest m).	195
<b>Figure 97</b>	The groundwater model inversion area for MAR with observation bore locations showing the water level over the same time period as the MAR injection.	202
<b>Figure 98</b>	The groundwater model inversion area for MAR (heavy black border), with the APLNG hydraulic head distribution (top left), grid refinement near injection wells (bottom left) and head boundaries (top right).	203
<b>Figure 99</b>	The groundwater model inversion area for MAR with the discretisation highlighted near the Leichardt Burunga Fault System.	204
<b>Figure 100</b>	Modelled groundwater level calibration summary.	205
<b>Figure 101</b>	Selected inversion hydrographs of better quality.	206
<b>Figure 102</b>	Blocky Sandstone Reservoir MAR hydraulic conductivity (minimum error variance).	207
<b>Figure 103</b>	Blocky Sandstone Reservoir MAR inversion aquifer thickness.	207
<b>Figure 104</b>	Blocky Sandstone Reservoir MAR inversion transmissivity (minimum error variance).	208
<b>Figure 105</b>	Blocky Sandstone Reservoir MAR inversion intrinsic permeability (minimum error variance).	208
<b>Figure 106</b>	Blocky Sandstone Reservoir MAR inversion storativity and compressibility (minimum error variance).	209
<b>Figure 107</b>	Blocky Sandstone Reservoir MAR inversion hydraulic conductivity uncertainty.	209
<b>Figure 108</b>	Fluid type recovered during initial DST operations from wells testing the 56 Sand (UQ-SDAAP Transition Zone).	211
<b>Figure 109</b>	Fluid type recovery shown from DSTs that tested the 58 Sand in the Moonie field.	212
<b>Figure 110</b>	Evaluation of FWL in Blocky Sandstone Reservoir using hydraulic heads calculated from DSTs in Moonie wells.	213
<b>Figure 111</b>	Bridgeport Energy Moonie sector model area structure top of the 58 Sand depth map with inclusion of well locations and the Moonie fault.	214
<b>Figure 112</b>	Histograms of horizontal permeability for the 58 Sand of the Moonie model generated by the UQ-SDAAP porosity-permeability transform and the Bridgeport Energy original model (top) and their respective STOOIP values (bottom).	215
<b>Figure 113</b>	Moonie field oil production rate (top left), field water production rate (top left), field oil production cumulative (bottom). Red circles are historical data, light brown line and green line are for simulation runs with the Bridgeport Energy porosity-permeability model and UQ-SDAAP porosity-permeability transform, respectively.	216
<b>Figure 114</b>	Flow chart showing the UQ-SDAAP suitability analysis procedure.	220
<b>Figure 115</b>	Final suitability (low risk) map with notional injection locations and key power stations.	225
<b>Figure 116</b>	Location of the notional injection sector model (red box) relative to the top of the regional static model (left) and extent of Blocky Sandstone Reservoir (right). Colour indicates depth structure from sea level (blue/purple is deeper). notional injection sites shown as white squares.	227
<b>Figure 117</b>	The scale of the 'Pseudo- Boundary' area created by stretching three rows of cells in the notional injection sector model, shown overlain on the horizontal permeability distribution used in the groundwater model grid. The difference in permeability between the north and south parts of the groundwater model is due to two depo centres that are hypothesised by the UQ-SDAAP team. (Hayes et al. 2019a; Gonzalez et al. 2019b).	229

<b>Figure 118</b>	The structure and horizontal permeability of the Blocky Sandstone Reservoir in the notional injection sector reservoir model and ‘pseudo-boundary’. Note that the permeability in the ‘pseudo boundary’ has similar trend to the groundwater model grid shown in Figure 117.	230
<b>Figure 119</b>	CO <sub>2</sub> density from 20,000 to 40,000 kPa at 35, 50 and 70°C.	231
<b>Figure 120</b>	Pressure map after 10 years injecting CO <sub>2</sub> at 70°C (isothermal flow). The horizontal well trajectory is located at 775 m oriented north-south and the black rectangle sets the observation window for analysing profiles of pressure and densities.	232
<b>Figure 121</b>	Pressure and density of CO <sub>2</sub> and water for injecting CO <sub>2</sub> at 70°C (isothermal flow). This 2D cross section view of pressure and density within the injection reservoir, runs perpendicular to the horizontal well trajectory with the well located at 775 m on the horizontal axis.	233
<b>Figure 122</b>	Pressure and density of CO <sub>2</sub> and water for injecting CO <sub>2</sub> at 50°C (non-isothermal flow). This 2D cross section view of pressure and density within the injection reservoir, runs perpendicular to the horizontal well trajectory with the well located at 775 m on the horizontal axis.	233
<b>Figure 123</b>	Pressure and density of CO <sub>2</sub> and water for injecting CO <sub>2</sub> at 35°C (non-isothermal flow). This 2D cross section view of pressure and density within the injection reservoir, runs perpendicular to the horizontal well trajectory with the well located at 775 m on the horizontal axis.	234
<b>Figure 124</b>	Differences in the facies distribution between the three type areas for sector models. (A–C) show the facies evolution from the lower Blocky Sandstone Reservoir to the upper Blocky Sandstone Reservoir and then the lower Transition Zone in the Moonie sector. (D–F) shows the same progression for the Meandarra sector. Finally, (G–I) shows the facies progression for the Woleebee Creek sector.	236
<b>Figure 125</b>	Mass flow rates of CO <sub>2</sub> from the Blocky Sandstone Reservoir into the Transition Zone. Positive values indicate upwards flow, negative values are downwards flow. For comparison, well injection rate was >2,000 tonnes/d. Coloured background indicates periods discussed in text.	237
<b>Figure 126</b>	Ratio of cumulative flow of CO <sub>2</sub> into Transition Zone to cumulative injected CO <sub>2</sub> .	238
<b>Figure 127</b>	Saturation of supercritical CO <sub>2</sub> at the end of 30 years of injection for the Meandarra model. Horizontal well is in centre of model, running perpendicular to page. Red indicates higher CO <sub>2</sub> saturation. The boundary between the Transition Zone and Blocky Sandstone Reservoir is relatively clear across most of the model as the boundary between high CO <sub>2</sub> saturation below (orange) and low CO <sub>2</sub> saturation above (blue). In some more permeable areas near the centre of the model, capillary pressures are overcome and supercritical CO <sub>2</sub> is able to enter the Transition Zone (green patches higher in model).	238
<b>Figure 128</b>	Vertical profiles of supercritical CO <sub>2</sub> saturation in the column of cells where CO <sub>2</sub> migrated furthest vertically in the Meandarra model (approximately 300 m from the well completion). Shown at end of 30-year injection period (red) and 30 years after injection stops (green). Note that CO <sub>2</sub> saturation actually decreases in the Transition Zone after injection stops.	239
<b>Figure 129</b>	Flow rates of water (volumetric, reservoir conditions) from the Blocky Sandstone Reservoir to the Transition Zone. Positive values indicate flow upwards, negative values are flow downwards.	240
<b>Figure 130</b>	Illustrative vertical and horizontal well design. Horizontal well length could be several kilometres, and could kick off (i.e. become deviated) at shallower depth, depending on achievable build-up rates, extended reach requirements, and wellbore stability.	242
<b>Figure 131</b>	Six-well horizontal patterns for each injection site (North, South A and South B). Grid refinements were performed for each well grid blocks and its neighbour. From north to south, the injection centres (each with multi well pads) are called: 1) North, 2) South A and 3) South B.	244
<b>Figure 132</b>	North-South Cross-section of the reservoir layers around south A and B. Injection performance is modelled as “better” for South B because it is predicted to have a greater thickness. Note that the vertical axis scale is 100 times larger than the horizontal scale to clearly display the variations in thickness.	246
<b>Figure 133</b>	Map indicating extent of notional injections sector model (red) relative to Blocky Sandstone Reservoir structure (black) and the three notional injection sites (green).	249
<b>Figure 134</b>	West-east cross section indicating layering in notional injection sector model. Colours indicate parts of model as outlined in Table 46. Left side scale shows depth in metres (True Vertical Depth Subsea). The dark area at the top of the Blocky Sandstone Reservoir (yellow) in the deeper part of the model is the area where cells have been refined to more accurately model CO <sub>2</sub> plume migration. Also note the fault near the east of the figure.	250
<b>Figure 135</b>	Histograms of grid properties for Blocky Sandstone Reservoir cells in the base case notional injection sector model. Note x axis scales for horizontal (left) and vertical (centre) permeability are different. Vertical permeability is typically around 0.15 times horizontal permeability for cells in this model.	251



<b>Figure 136</b>	Histograms of grid properties for Transition Zone and Ultimate Seal cells in the base case notional injection sector model. Note x axis scales for horizontal (left) and vertical (centre) permeability are different, and also different from the equivalent histograms in Figure 135.	251
<b>Figure 137</b>	(A) Drainage relative permeability curves used for all cells in the base case notional injection sector model, (B) J-function curves for the Blocky Sandstone Reservoir (solid line) and Transition Zone/Ultimate Seal (dashed line), and (C) Capillary pressure curves calculated using the curves in 'b', and typical porosity/permeability values from the Blocky Sandstone Reservoir (solid line, $\Phi=0.12$ , $k=44\text{md}$ ) and Transition Zone/Ultimate Seal (dashed line, $\Phi=0.06$ , $k=0.05\text{md}$ ).	252
<b>Figure 138</b>	Well layouts for the MKMK schedule. Refined cells are visible around each well. The apparent “wobbling” of some of the north wells is due to these refined cells, but is not expected to affect the results of this particular study.	253
<b>Figure 139</b>	Well layout at South 1 notional injection site for all MKTMK simulations. The same layout was used at the other two notional injection sites. This figure shows one layer of cells only, which can be seen to “pinch-out” at the bottom left of the figure. Also note the refined cells around the wells. For reference large grid blocks are approximately 500 x 500 m, and well completions are approximately 3.75 km long.	254
<b>Figure 140</b>	An example of CMG GEMs AUTODRILL control for wells at the north notional injection site and MKTMK extended delivery schedule. Most of the time, all wells inject at the same rate. Arrows indicate points where wells become limited by wellhead pressure and either; (A) Injection is redistributed to other wells (blue arrows), or (B) All currently open wells are pressure limited, so the next well in the queue is opened and starts injection (red arrows).	255
<b>Figure 141</b>	Flow chart showing analysis methods.	258
<b>Figure 142</b>	Selected power stations in the study area and notional injection locations.	260
<b>Figure 143</b>	Pipeline routes: example from a “base case” analysis (note use of existing pipeline easements in the south near Moonie).	261
<b>Figure 144</b>	Pipeline routes; example from environment analysis.	262
<b>Figure 145</b>	Pipeline routes from social analysis.	263
<b>Figure 146</b>	Pipeline routes from ‘environmental’ analysis.	264
<b>Figure 147</b>	Surface facilities schematic.	269
<b>Figure 148</b>	Illustration of M&V options and concepts (Shell 2017).	274
<b>Figure 149</b>	Domain of the groundwater model (left) compared to the notional injection sector model (red box) and extent of Blocky Sandstone Reservoir (right). Colour indicates depth structure from sea level (blue/purple is deeper). Notional injection sites are shown as white squares.	277
<b>Figure 150</b>	Predicted groundwater head increase contours (A) in the top of Blocky Sandstone Reservoir and (B) Hutton Sandstone at the end of injection, after 39 years.	279
<b>Figure 151</b>	Predicted groundwater head increase contours (A) in the top of Blocky Sandstone Reservoir and (B) Hutton Sandstone 100 years after injection ceases.	279
<b>Figure 152</b>	Predicted groundwater head increase in the top of the Blocky Sandstone Reservoir during and after injection for: (A) Precipice wells closest to notional injection sites; (B) Selected wells located further north.	280
<b>Figure 153</b>	Predicted groundwater head increase in the Hutton Sandstone during and after injection for Hutton wells closest to notional injection sites.	281
<b>Figure 154</b>	(A) Drainage relative permeability curves used for all cells used in the high and low residual water saturation cases. (B) Drainage relative permeability (to $\text{CO}_2$ ) curves as used in the high and low relative permeability to $\text{CO}_2$ cases.	283
<b>Figure 155</b>	Mass of $\text{CO}_2$ injected per well for MKMK cases, presented as a percentage of reference case value (39.8 Mt/well).	285
<b>Figure 156</b>	Mass of $\text{CO}_2$ injected per well for MKTMK extended cases, presented as a percentage of reference case value (90.1 Mt/well).	286
<b>Figure 157</b>	Cumulative Mass of $\text{CO}_2$ injected for north notional injection site wells in the “MKMK – Low Reservoir $k_v$ case”. Note that the last well to start injecting (pink line) only injects for five years, and its cumulative injected $\text{CO}_2$ is just over 3 Mt, compared to 35 Mt for the previous well.	287
<b>Figure 158</b>	Mass of $\text{CO}_2$ injected per well for MKMK cases, excluding the well with the lowest injection, presented as a percentage of reference case value (44.5 Mt/well).	288

<b>Figure 159</b>	Mass of CO <sub>2</sub> injected per well for MKTMK extended cases, excluding the well with the lowest injection, presented as a percentage of reference case value (102.5 Mt/well).	288
<b>Figure 160</b>	Wells required per Mt of CO <sub>2</sub> injected for MKMK cases.	289
<b>Figure 161</b>	Wells required per Mt of CO <sub>2</sub> injected for MKTMK cases.	289
<b>Figure 162</b>	Wells required per Mt of CO <sub>2</sub> injected for MKMK cases, excluding the well with lowest injection.	290
<b>Figure 163</b>	Wells required per Mt of CO <sub>2</sub> injected for MKTMK cases, excluding the well with lowest injection.	290
<b>Figure 164</b>	Cumulative injection versus time for the 12 wells across the two southern notional injection sites in the MKTMK extended – low reservoir permeability case. Note that six of the 12 wells inject for less than 20 years (injection ends in 2088), and inject less than 30 Mt in total, or around 10% of the total injection for all 12 wells.	291
<b>Figure 165</b>	Supercritical CO <sub>2</sub> plumes at the northern notional injection site, 100 years after injection ends for MKMK – high porosity and MKMK – low porosity cases. Colour in first two plots indicates gas saturation, with grey indicating areas with saturations below the 0.1% cut off.	293
<b>Figure 166</b>	Supercritical CO <sub>2</sub> plumes at the northern notional injection site, 100 years after injection ends for MKTMK – high porosity and MKTMK – low porosity cases. Colour in first two plots indicates gas saturation, with grey indicating areas with saturations below the 0.1% cut off.	293
<b>Figure 167</b>	Comparison for the Supercritical CO <sub>2</sub> plumes at the northern notional injection site, 100 years after injection ends for MKMK – high porosity and MKTMK – low porosity cases. These were the smallest and largest plume sizes respectively. Colour in first two plots indicates gas saturation, with grey indicating areas with saturations below the 0.1% cut off.	293
<b>Figure 168</b>	MKMK – reference case, supercritical CO <sub>2</sub> plume 100 years after injection ends compared to Blocky Sandstone Reservoir in the UQ-SDAAP notional injection sector model to give indication of scale. The plume around the northern notional injection site in this figure is somewhere between the plume sizes shown in Figure 165.	294
<b>Figure 169</b>	Supercritical CO <sub>2</sub> plume areas versus time for the MKMK cases. Darker grey area indicates injection period. Black line is reference case. Dashed lines are those where desired injection rate could not be achieved due to poor injectivity and thus less CO <sub>2</sub> was injected in total (e.g. very low permeability case). Key parameters (those with most significant impact on plume area) are indicated, along with area of plume as a percentage of reference case. Swr is residual water saturation. Krgmax is the maximum relative permeability to CO <sub>2</sub> .	295
<b>Figure 170</b>	Supercritical CO <sub>2</sub> plume areas versus time for the MKTMK cases. Darker grey area indicates injection period. Black line is reference case. Dashed lines are those where desired injection rate could not be achieved due to poor injectivity and thus less CO <sub>2</sub> was injected in total. Key parameters (those with most significant impact on plume area) are indicated, along with area of plume as a percentage of reference case. Swr is residual water saturation. Krgmax is the maximum relative permeability to CO <sub>2</sub> .	295
<b>Figure 171</b>	Supercritical CO <sub>2</sub> plume areas at the northern notional injection site versus time for the MKTMK cases. Darker grey area indicates injection period. Black line is reference case. Dashed lines are those where desired injection rate could not be achieved due to poor injectivity and thus less CO <sub>2</sub> was injected in total. Key parameters (those with most significant impact on plume area) are indicated, along with area of plume as a percentage of reference case. Swr is residual water saturation. Krgmax is the maximum relative permeability to CO <sub>2</sub> .	296
<b>Figure 172</b>	Supercritical CO <sub>2</sub> plume areas at the southern notional injection site versus time for the MKTMK permeability cases. Darker grey area indicates injection period. Note that the low permeability case has the largest plume area at end of injection (due to higher well count), in but the high permeability case, the plume grows more quickly after injection stops.	297
<b>Figure 173</b>	Comparison of the supercritical CO <sub>2</sub> plume (red) with molality (green/blue colours) around the northern injection site in the MKTMK –high porosity case. The supercritical CO <sub>2</sub> plume is the same as that shown on the left in Figure 166. The minimum contour for the molality plume is at 0.002 mol/kg, and the darkest blue outside this indicates areas where CO <sub>2</sub> levels have not increased during injection.	298
<b>Figure 174</b>	Total area of increased molality in the top layer of the Blocky Sandstone Reservoir, plotted versus time for the MKTMK cases. The dark grey colour indicates the injection period. Key parameters (those with most significant impact on the area) are indicated, along with area of plume as a percentage of reference case.	298
<b>Figure 175</b>	Percent by volume at reservoir conditions of injected CO <sub>2</sub> that migrates into the Transition Zone for the MKTMK cases.	299
<b>Figure 176</b>	Sensitivity of predicted groundwater head increase to low, reference and high permeability cases in the upper Precipice Sandstone (upper Blocky Sandstone Reservoir) during and after injection for select wells.	303

<b>Figure 177</b>	Sensitivity of predicted groundwater head increase to low, reference and high permeability cases in the Hutton Sandstone (layer 1), during and after injection for selected wells.	303
<b>Figure 178</b>	A CO <sub>2</sub> hub system, showing a collection and storage hub (GCCSI 2016).	306
<b>Figure 179</b>	CCS hub concept (Bongers et al. 2017).	307
<b>Figure 180</b>	PCC simplified process (Bongers et al. 2018).	307
<b>Figure 181</b>	Typical black coal electricity power plant configuration with conventional SO <sub>x</sub> and NO <sub>x</sub> removal prior to CO <sub>2</sub> recovery (Bongers et al. 2018).	308
<b>Figure 182</b>	Notional injection sites and pipeline routes based on risk minimisation algorithms.	309
<b>Figure 183</b>	Generalised CCS decision framework (Garnett & Grieg 2014a pp 49).	312
<b>Figure 184</b>	Deployment scenario 1, impact on power generation and CO <sub>2</sub> captured/stored throughout sequential, partial retrofit.	315
<b>Figure 185</b>	Illustration of discrete investment (stop/go/review) decisions and cumulative capex and CO <sub>2</sub> captured/stored for roll-out scenario 1 (MKTMK).	316
<b>Figure 186</b>	High level estimate of employment and regional construction jobs generated by a large scale, CCS retrofit project.	317
<b>Figure 187</b>	Modified view of storage resource pyramid (Garnett 2017, modified after Kaldi & Gibson-Poole 2018).	321
<b>Figure 188</b>	Model for discussing confidence in dynamic capacity.	323
<b>Figure 189</b>	Model for discussing uncertainty in dynamic capacity.	323
<b>Figure 190</b>	Model for discussing late-life uncertainties in dynamic capacity.	324
<b>Figure 191</b>	Injection potential, uncertainty and capture profiles for northern site (scenario 1, nominal dates).	325
<b>Figure 192</b>	Injection potential, uncertainty and capture profiles for southern 2 sites (scenario 1, nominal dates).	326
<b>Figure 193</b>	Illustration: confidence in ~12.7 Mtpa now and (est.) after appraisal (20 to 40 years). It is expected that confidence in longer plateau periods would be influenced by early operations and M&V.	327
<b>Figure 194</b>	High level timeline to carbon abatement through retrofit.	329
<b>Figure 195</b>	UQ-SDAAP risk matrix (forward progress) appraisal and contingent deployment stages	330
<b>Figure 196</b>	Location map of the proposed notional injection sites in Surat Basin in Queensland, Australia.	334
<b>Figure 197</b>	Overview of suggested appraisal program.	337
<b>Figure 198</b>	Radius of investigation for the testing well located in notional injection site calculated at various build up periods in a low, mid and high case.	339
<b>Figure 199</b>	Log-log derivative response for the testing well in notional injection site at different pumping rates.	340
<b>Figure 200</b>	The log-log pressure derivative of an EWT generated by CMG reservoir simulation software and analysed by IHS WellTest software. The pumping rate of 1590 m <sup>3</sup> /day, 3 days DD and 200 days BU were used during this EWT design.	341
<b>Figure 201</b>	The pressure change in Blocky Sandstone Reservoir, Transition Zone and Ultimate Seal is generated by CMG reservoir simulation software when water is injected at 9660 m <sup>3</sup> /day for 200 days: (top) reference case and (bottom) one order of magnitude increase of permeability in the Transition Zone and Ultimate Seal.	342
<b>Figure 202</b>	Schematic of the completion diagram for the appraisal wells.	345
<b>Figure 203</b>	Schematic of the appraisal program (with the other required action themes).	346
<b>Figure 204</b>	Schematic of the completion diagram for the Hutton Sandstone pressure monitoring bore.	347
<b>Figure 205</b>	Illustrative scenario (MKTMK) time series for investment, CO <sub>2</sub> reduction and power generation	350
<b>Figure 206</b>	Sensitivity of carbon value or price required vs. overall perceived project risk (for MKTMK scenario).	352
<b>Figure 207</b>	Decision tree from appraisal to first FID and retrofit.	353
<b>Figure 208</b>	Impact of appraisal risk on required CCS retrofit success value.	354



# 1. Executive summary

The main aim of The University of Queensland Surat Deep Aquifer Appraisal Project (UQ-SDAAP) is to inform policy and decision makers as to whether or not material carbon abatement is feasible through implementing industrial-scale carbon capture and storage (CCS) in southern Queensland. ‘Material’ in this sense is taken as safely and securely injecting at least 5 million tonnes pa for at least 20 years. This is roughly equivalent to the emissions from one of the large, modern supercritical power plants in the area. In this study, a scheme with around 13 million tonnes pa has been matured for a 30 year duration under very conservative assumptions. This represents the UQ-SDAAP reference case CCS option.

This research shows that deep emission cuts could be achieved by the establishment of a large-scale CCS ‘Hub’ scheme conceptually built around retrofitting existing modern power plants (Millmerran, Kogan Creek and Tarong North). It does not discount the opportunity for new-build plants or additional capture from other emissions sources. The research demonstrates that a material abatement opportunity is likely to be a feasible option in the Surat Basin, though not yet quite ‘confirmed’.

There is a limited window for the main opportunity studied, which is tied to significantly reducing the emissions of the existing supercritical power stations. These power stations have a finite technical lifespan in the order of 35 years<sup>1</sup>. The sooner this abatement option is realised in the lifespan of these power stations, the greater the impact of the initiative. It is estimated that each year such a project is delayed would result in up to 13 million tonnes pa of carbon dioxide (CO<sub>2</sub>) less being captured. The establishment of secure, sustained high-rate CO<sub>2</sub> storage may also create opportunities for additional high emissions industries (such as hydrogen production or additional power generation). Recent work done in parallel with this study, indicates that pressure on power prices can be minimised by reducing total system cost and that to do this even more carbon abatement would be required via CCS as the NEM evolves into a low emissions network.

About 3-4 years are required to confirm this option, as much as 4-6 years to set up a commercial venture and permitting, and about 2-3 years to build the first of the required infrastructure. It is conceivable that commercial scale capture could commence around 2030. It is likely that there is adequate, secure, high rate CO<sub>2</sub> storage for the remaining life of the power stations, and probably a few decades more. The analysis so far indicates that material benefits are possible for a period in the order of at least three decades. The option should be seen as a critically important and material opportunity to make an orderly transition to a low-emission power generation mix. Carbon dioxide capture and injection schemes are inherently time-limited because CO<sub>2</sub> storage capacity is a limited resource, but estimates of those time limits from this research are sufficient to support large power plant and potentially other industrial investment decisions.

Surat Basin data-gathering activities, societal engagement and regulatory actions identified in this report need to start as soon as possible, ideally in 2019/20. Further, to quantify the full potential for east-coast carbon abatement for an orderly transition, a wider program of dynamic storage assessment in other basins is required.

The International Energy Agency emphasises that a full suite of technologies will be required to bring down emissions. They have positioned CCS as a key strategy to abate long-lived, high-intensity, stationary, industrial and power sector sources. Similarly, the recent 2018 Intergovernmental Panel on Climate Change “Special Report: Global Warming of 1.5°C” which explored the impacts of global warming at 1.5°C, identified CCS as a critical technology for managing the transition to a more sustainable energy future.

The study considered techno-economic, social and regulatory aspects of CCS. The main new contributions of this study are a more accurate understanding of the dynamic limits to safe, secure, high-rate storage and a promising new approach to public engagement on energy futures.

The research found that material abatement of southern Queensland emissions appears technically feasible with CCS as part of the future energy mix. However, in addition to the need for site-specific new data, the research highlighted a number of non-technical challenges that need to be addressed to establish CCS in southern Queensland. These include acceptance of the need for trade-offs between carbon abatement aims, regional jobs, aquifer recharge and groundwater use.

This UQ-SDAAP study investigated scenarios for carbon mitigation for the power sector in Queensland using CCS. The area of focus was the Surat Basin, which had been identified for its strong potential for CCS development in earlier studies. Note that the project also included significant engagement with Chinese collaborators in CCS in that country. This is the subject of a separate report.

CCS deployment could comprise the sequential retrofitting of up to three modern, supercritical, coal-fired power plants<sup>2</sup> in southern Queensland with storage in the Precipice Sandstone in the deepest part of the Surat Basin (shown schematically in Figure 1, with the notional geographic locations shown in Figure 2). These plants currently support a significant number of regional jobs, provide critical baseload power, and are currently expected to maintain (unabated) operations well into the mid-2050s.

<sup>1</sup> Note that power station life is notoriously difficult to estimate. Commercial factors can lead to early shut-down, and late-life extensions also commonly allow plants to run beyond their notional, technical end dates.

<sup>2</sup> Millmerran, Kogan Creek, and possibly Tarong North

Figure 1 Visualisation of a potential CCS initiative.

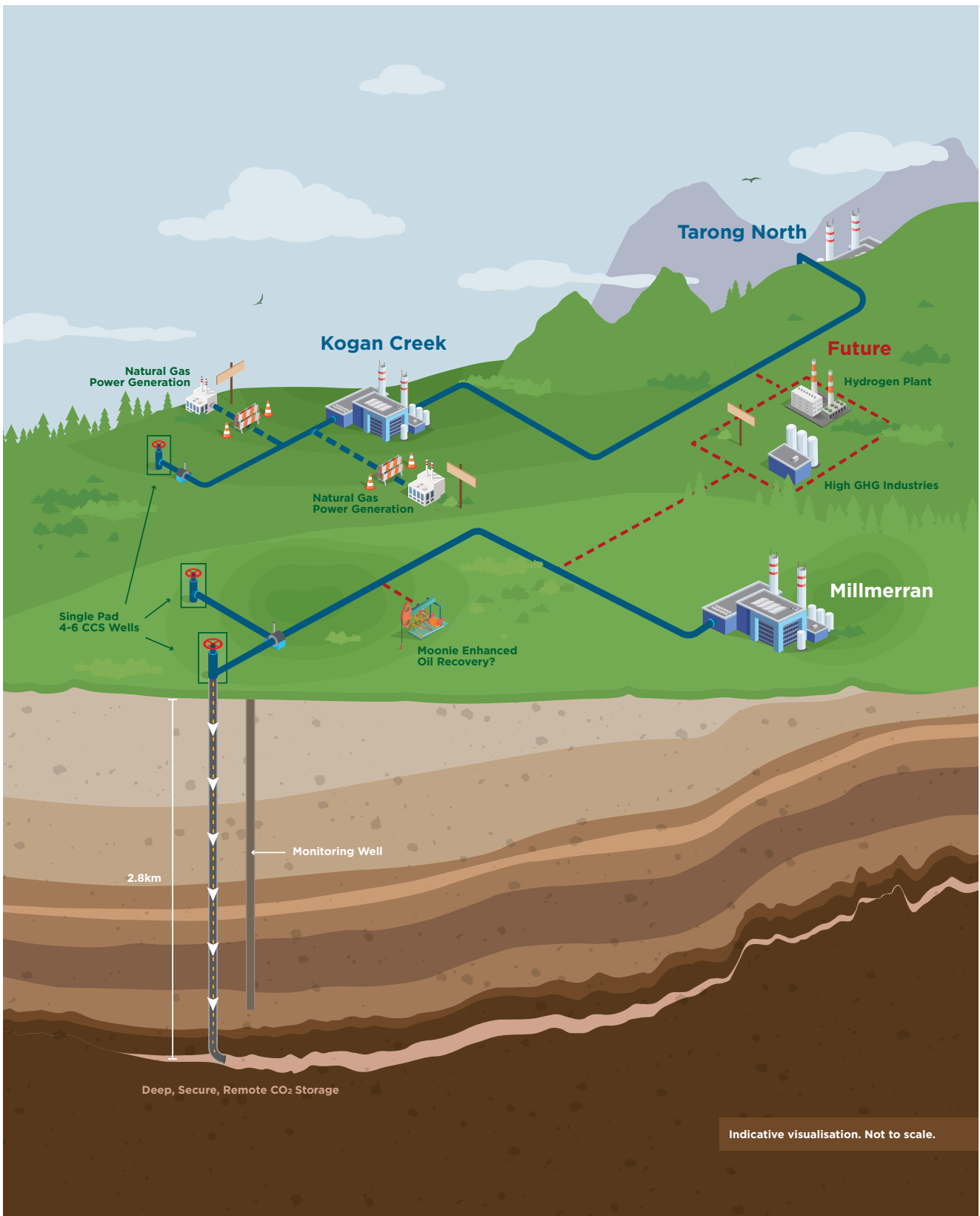
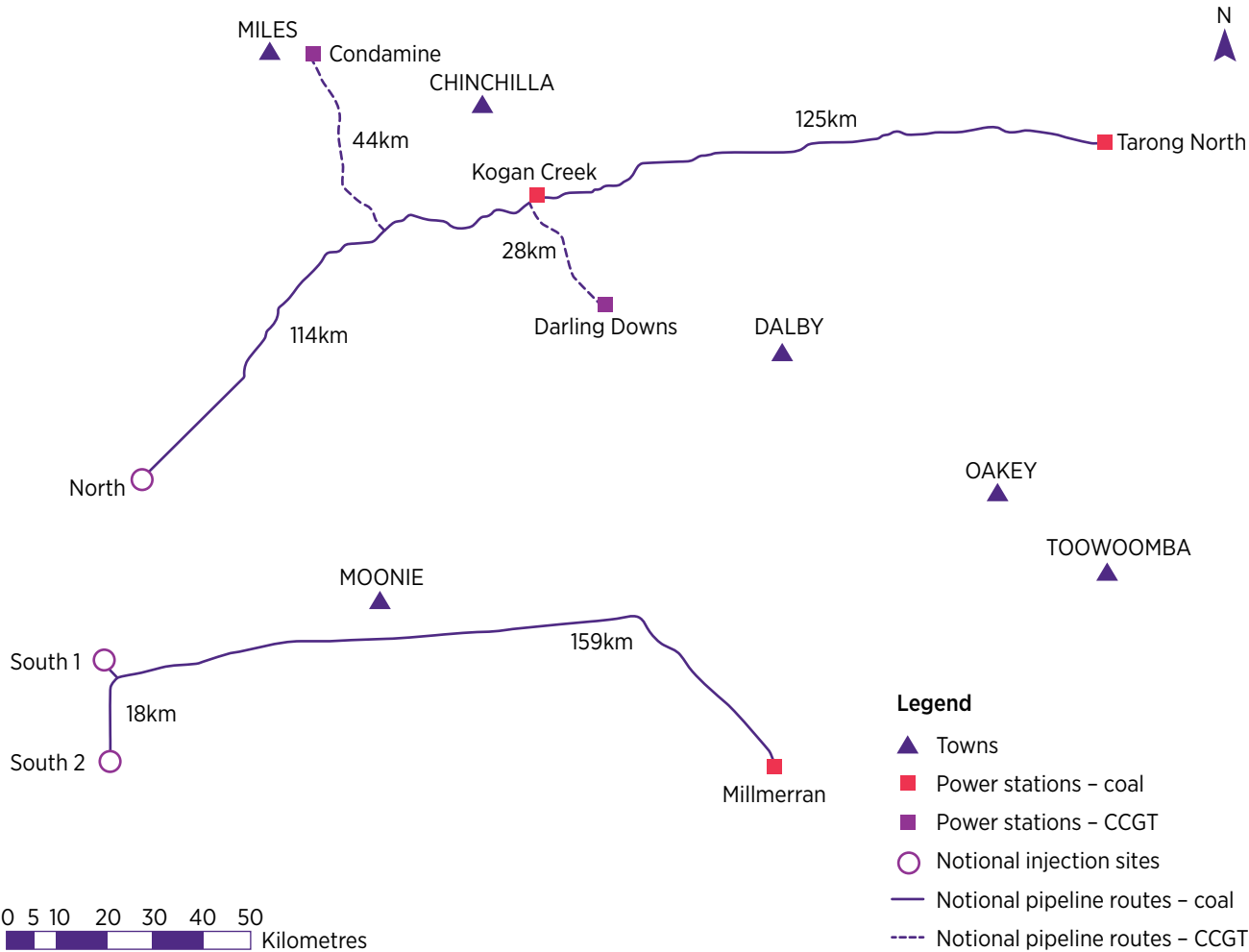


**Figure 2** Power stations, pipeline routes and notional sites.



CO<sub>2</sub> captured at the three identified plants could be transported via pipeline to two or three remote well pads. At each pad, there would be injection via 4-6 wells where UQ-SDAAP has determined the lowest risk zones (Figure 3). The notional injection sites would be more than 80 km from current water abstraction sites and would be much deeper. The injection sites are at a depth of over 2.3 km in the deepest part of the Surat Basin (Figure 4). The maximum lateral movement of the CO<sub>2</sub> away from the wells is expected to be typically within a 10 km radius.

Development of a CCS Hub could result in the following benefits:

1. **Low-emissions baseload power:** A CCS Hub would gradually convert and abate existing plants resulting, in up to 1.62 GW of installed, low-carbon, net *baseload* power in the national electricity market (NEM) for 30 years or more (the reference case for UQ-SDAAP was 13 Mt/yr for 30 years). It could deliver annually up to 12,800 GWh of baseload<sup>3</sup> power. For fully retrofitted plants<sup>4</sup>, emissions intensity would be an average of 135 kg CO<sub>2</sub>e/MWh<sup>5</sup>, and the base case levelised cost of electricity (LCOE) would be less than \$70/MWh<sup>6</sup>
2. **Material emissions reductions:** On current data, it seems likely that a hub could safely capture and inject about 13 million tonnes pa of CO<sub>2</sub> for around 30 years, with indefinite secure retention. UQ-SDAAP scenarios have been modelled conservatively. There is considerable upside with some scenarios extending the plateau for three or more decades culminating in around 650 million tonnes. If new data supports this, it would require that future CO<sub>2</sub> sources would be “plumbed in”. Notwithstanding this, even the “limited” retrofit scheme can contribute significantly beyond Australia’s current Conference of Parties 21, nationally determined contributions (COP21 NDC commitments)
3. **Regional employment:** CCS could create about 250 new regional jobs in the retrofit and construction phase, as well as either safeguarding, or even extending the need for, approximately 500 existing regional jobs in the power plants and adjacent mines. Indirect employment multipliers in the local economy have not been assessed in this study, however previous work has suggested this would be statistically significant
4. **Enabled low-carbon economy:** The creation of a CO<sub>2</sub> transport and storage hub infrastructure could potentially enable additional, traditionally high CO<sub>2</sub> intensity industries. This includes, but is not limited to, the production of hydrogen from coal or natural gas or a hybrid approach with renewables

**The main trade-off for these benefits** would be that an area of around a 10 km radius of the Precipice Sandstone at a depth of over 2.3 km, immediately around the injection sites, would *not be available for future groundwater abstraction*.

The remote location and aquifers identified as lowest risk in this study are currently considered to be too deep for economically viable groundwater abstraction, and the water quality has yet to be confirmed.

An additional *consequential upside of deep injection* would be:

5. **Groundwater levels raised:** Groundwater would be displaced laterally from the injection site. This would raise water levels (pressures) in existing, sometimes depleted, groundwater abstraction bores in the target formation, in the ‘far-field’ and to a lesser extent in the overlying Hutton Sandstone aquifer. The increased water levels could persist for over 100 years. There would be no CO<sub>2</sub> contamination in these areas of regional pressure rise, making the water easier to access for alternatives uses, such as agriculture and town water supplies (potentially up to hundreds of kilometres away from the 10 km radius CO<sub>2</sub> plume).

While techno-economic studies suggest that such a scheme could be a real option, social science studies highlight the importance of public engagement about the context of future energy choices in a carbon-constrained world.

Currently, there are also ambiguities in the Queensland regulations that need to be addressed to facilitate the establishment of CCS technology and to build stakeholder confidence in CCS.

The opportunity mapped in this report would be a unique, long-term project in Australia. A suitable project creation and delivery vehicle is needed to effect the full scope of work required.

<sup>3</sup> Queensland generated approximately 7200 GWh of intermittent solar in 2016-17.

<sup>4</sup> There are options for partial refit that would still result in material emissions abatement, though LCOE and emissions intensity would be higher

<sup>5</sup> Typical emissions intensity for baseload modern supercritical power is 960 kgCO<sub>2</sub>e/MWh.

<sup>6</sup> Note that unless otherwise stated in this report all cost estimates should be considered scoping level estimates only and are cited in real terms 2018 dollars



Figure 3 Illustration of minimum risk site selection

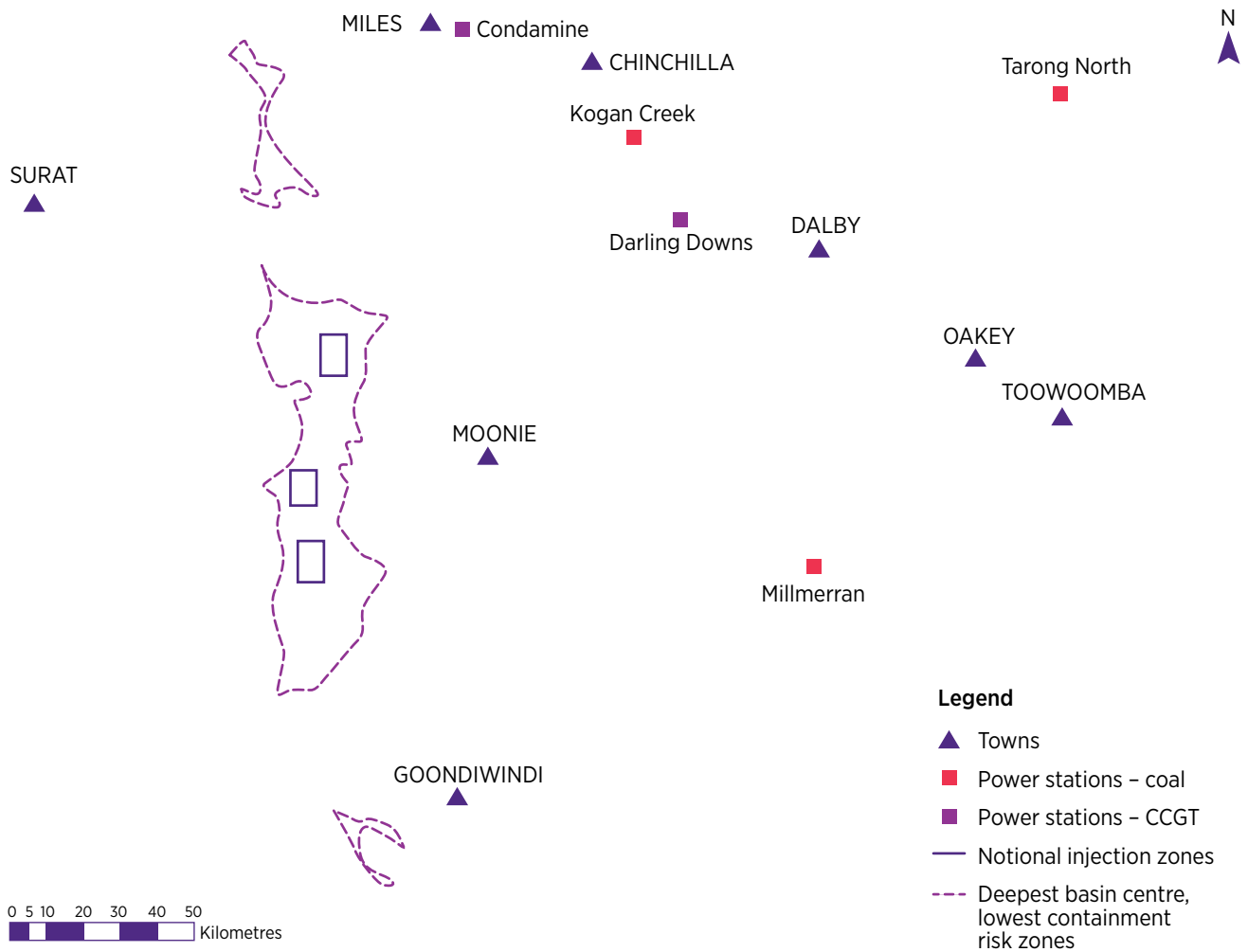
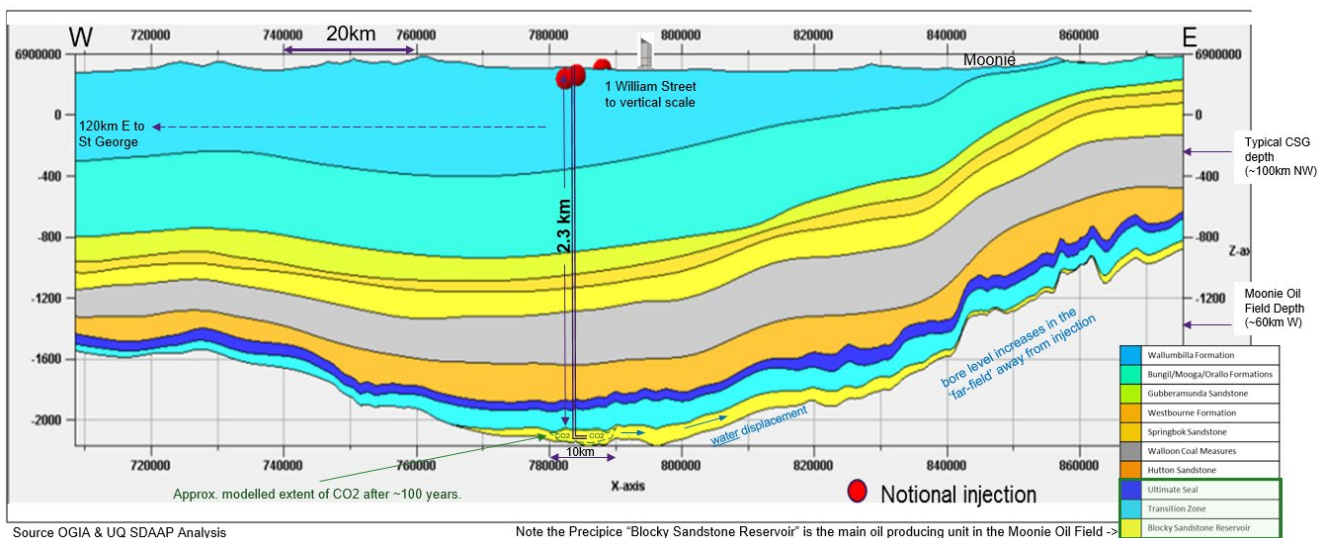


Figure 4 Visualisation of a potential injection cross-section.

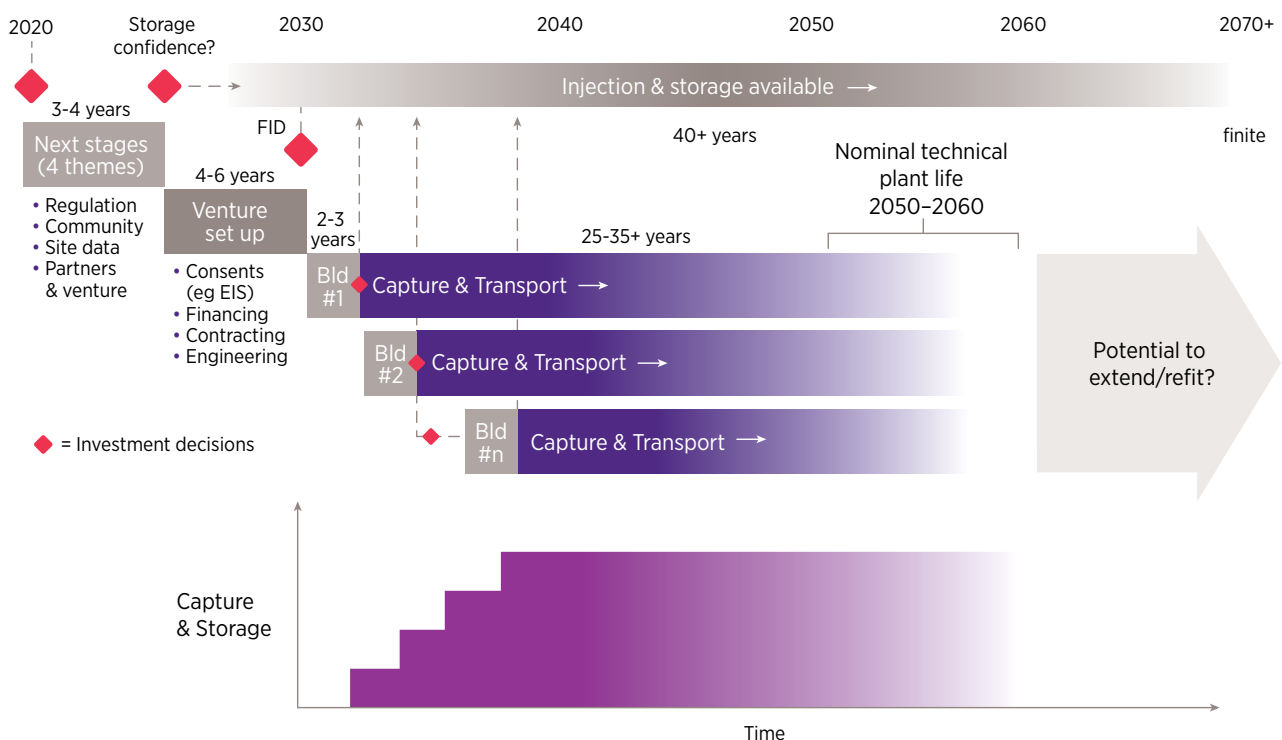


## How a material CSS option could be (incrementally) rolled out

If all data continues to support secure storage and other non-technical matters are resolved in the next 3-4 years, the *first* retrofit for industrial-scale capture could be operational in circa 10 years' time. The way forward can be thought of in three main stages (Figure 5):

1. The first investment required is around \$100 million<sup>7</sup>. This would include a 3-4 year work program, including site appraisal and various engagement activities. Some capture and transport engineering studies could be undertaken in parallel
2. In year three or four, a decision would be required to invest around \$110 million. This would cover a further period of an estimated 4-6 years<sup>8</sup>, working up to a Final Investment Decision (FID) on the first retrofit. The period is required to prepare for regulatory approvals, financing and funding agreements, engineering definition from prefeasibility to detailed engineering design, commercial and venture set-up, contracting and procurement. It will also include the installation of a deep aquifer monitoring network. A significant amount of time is expected to be required for first-of-a-kind environmental approvals
3. A sequential retrofit is suggested with plants partially retrofitted and a controlled incremental commitment of capital investment. The FID for the first plant would be needed in about years 8 to 10 (depending on approvals). This would be around \$1.06 billion and would include the building of one of the pipelines. Construction would start shortly after. Subsequent FIDs in the range \$650 million to \$1.1 billion could follow approximately every 2-3 years, depending on individual decisions on the scale of retrofit (investment could be halted at each step). The total period from first FID would be about 10-13 years of construction and commissioning

**Figure 5** An indicative timescale over the life of the project to capitalise on the limited window of opportunity to draw maximum benefit from this initiative. This hinges on having a fully operational system in place as soon as possible in the useful life span of the three identified power stations to maximise the time for emissions capture. It is conceivable that capture can commence around 2030.



**There is considerable opportunity to reduce these time frames,** given sufficient state and federal government support and prioritisation.

<sup>7</sup> It could be as low as \$30 million and 2 years to determine unsuitability.

<sup>8</sup> The largest elements of schedule uncertainty are related to environmental approvals, project financing and, related to this, final market positioning.

## 1.1 Summary statement

The transition of Australia's energy system to a low-carbon economy will require the deployment of several technologies that provide both intermittent and baseload power (or non-synchronous and synchronous power).

Secure, high rate CO<sub>2</sub> storage looks feasible for a period of several decades, but for a large-scale CCS hub project, there are important social dimensions that need to be managed. A deeper discussion and education on trade-offs and choices is required. There would be local impacts and benefits in terms of jobs, investment and groundwater impacts, and national benefits in terms of power grid stability and lower national emissions.

To keep this option open and increase the confidence that it could be implemented when required, it is essential to progress in four key areas:

1. Ongoing key stakeholder and community engagement
2. Mapping out a regulatory pathway
3. Gathering critically important site-specific data
4. Establishing a suitable vehicle or entity to manage this process

Within the first four years, a clear *line-of-sight* needs to be generated which supports both large-scale, partial public financing for the ultimate retrofit sequence, as well a commercial model that creates a special place (e.g. government Power Purchase Agreement (PPA) or dispatch rules) in the NEM for low-carbon baseload achieved via this mechanism.

With respect to the retrofit scenario developed in this research, time is of the essence because there are long-lived emissions sources in southern Queensland that provide a critical baseload generation service within the NEM. These are estimated to retire in the years 2050-2060 time frame. Retrofit requires a certain remaining active life for it to be justifiable. Construction should ideally commence within the next 10 years in order to provide a significant period of material emissions reductions for these assets and to potentially attract other abatement opportunities (e.g. hydrogen). There is significant work to be done in the interim – all of which needs support and funding.

Notwithstanding this, UQ-SDAAP research indicates that there is potential in the Surat Basin for sustained, high-rate injection even beyond the life of the existing power plants. Importantly, other work suggests that the availability of more storage potential than is articulated in this study, could greatly assist in reducing total system costs and keeping power prices down. There is a need to explore, including drilling and testing, other Basins to quantify their dynamic potential.

Retrofit requires a certain remaining active life for it to be justifiable. Construction should ideally commence within the next 10 years in order to provide a significant period of material emissions reductions for these assets.

## 2. Introduction

**The UQ-SDAAP is a project related to future large scale carbon abatement. Previous studies identified aquifers deep within the basin to be of possible interest in safely and securely storing CO<sub>2</sub> (Bradshaw et al. 2011 and Hodgkinson and Grigorescu 2013).**

The project aims to better inform public debate and policy makers on whether or not large-scale CCS could be a feasible, real and material option in Queensland, more specifically in the Surat Basin. “Material” in this sense was taken to mean at least 5 million tonnes pa of emissions reductions for at least 20 years (roughly equivalent to a large power station). “Feasible” was taken to mean (i) demonstrably lowest risk storage locations; (ii) high levels of technical confidence; (iii) a robust, conservative capture scenario minimising disruption to power supplies; (iv) no obvious showstoppers for pipeline routes; and, (v) reasonable cost estimates, in line with published estimates. In the event, a scale of around 12.7 Mtpa for over 20 years seems technically feasible with technical uncertainties that can be addressed through new data gathering. The main risks and uncertainties are non-technical.

Based on the results of this circa 3 year research project, a robust case is shown for progressing with the next stage of community and regulatory engagement and with extensive technical, site-specific data gathering needed to mature such an option for Queensland

External analysis (International Energy Agency (2019)), indicates that transition to a low carbon global economy involves the continued use of fossil fuels for several decades. Fossil fuels have been and will likely continue to be critical to economic and social development across the globe, particularly in the fast-developing Asia-Pacific region. Australia is a leading exporter of fossil fuels with primary markets in Asia that are increasingly moving to reduce emissions from their use. An immediate transition challenge is to continue to supply energy while abating carbon.

On this basis, the Australian Government has set up the Carbon Capture and Storage Research Development and Demonstration (CCS RD&D) Fund, providing up to \$25 million for research, development and demonstration activities in supporting Australian industry to innovate and adapt new technologies and processes, in particular for transport and storage of CO<sub>2</sub>. The University of Queensland Surat Deep Aquifer Appraisal Project (UQ-SDAAP) is one of the projects funded under this scheme.

While globally, saline aquifer storage is considered to represent the majority of available storage capacity (PICC 2005 suggests ~90%), most of Australia’s onshore deep aquifers tend to have ‘better’ water quality between fresh and ~10,000 mg/L (see, for example Hambermehl 1980 in the case of the Great Artesian Basin (GAB)). This adds an extra community and social science component to evaluating choices and trade-offs in balancing the need for greenhouse gas emissions reductions against technically feasible carbon storage options.

### The project has two main parts:

1. A social science program that exploring attitudes to CCS and trade-offs in terms of making future energy choices
2. A techno-economic assessment on notional large-scale deployment of CCS in the Surat Basin. Through the acquisition and analysis of critical static and dynamic geological and engineering data, the project increases our understanding of storage reservoir and regional aquifer properties and characteristics

The aim of the UQ-SDAAP research is not to advocate or oppose carbon storage in the Surat Basin, but to collect data and conduct new analysis regarding various CCS scenarios and their potential impact. The research did not require injection of any CO<sub>2</sub> underground to perform the assessment. Likewise, the project has not required the any construction of new wells for testing. Existing wells and data were used for the research. Complimentary to the project is an international collaboration and partnerships with key Chinese research entities and companies. Both the technical and social science research have been shared with Chinese collaborators, and a number of PhD students have been supported in each country.

This final report of the UQ-SDAAP project details the findings of the \$5.5 million, 3 year project. Chapters 3 and 4 bring together the scientific technical body of knowledge assembled during the project. Chapter 5 builds on the findings with an outline of the recommended actions, timelines and estimates of the costs and investments needed to mature the possible development of CCS in Queensland's Surat Basin.

# 3. Societal and regional communities

**The project's consideration of technical and non-technical risks to carbon abatement via large-scale carbon capture and storage (CCS) indicates that the central matters to overcome are in the social and regulatory domain.**

Public perception and evaluation of the CCS technology is critical for its commercial deployment. Early discussions about CCS have not been without controversy and perceptions of risk in relation to CCS have tended to be high for those who do not know much about the process. Given the slow progress of CCS projects and the importance of understanding and gaining public support for CCS in developing the technology, socio-economic studies formed an essential component of this project.

An intensive program of surveys, workshops and focus groups have been undertaken. This has delivered an important suite of information that will be critical to progressing a CCS initiative in Queensland and beyond and included:

1. An up-to-date assessment of current knowledge of and support for CCS across Australia
2. A set of factors and message frames that may enhance support for CCS
3. An understanding of how CCS is portrayed in the media and the impact of that on knowledge levels of the public
4. The development of a key international collaboration and knowledge sharing relationship with China

The insights delivered by this social research component has resulted in the UQ-SDAAP recommending the development of a social program as a critical success factor in progressing a longer term CCS initiative for Queensland. This would entail an ongoing and active process of community engagement, with an increased understanding of the trade-offs and benefits of CCS in the context of other energy options.

## 3.1 Introduction

As carbon intensive fossil fuels continue to dominate much of the world's energy generation and industrial activities, CCS (or CCUS as it is now often referred to globally, to incorporate carbon *utilisation* as well as storage) is one technology that has been proposed to play a major role in mitigating greenhouse gas emissions (e.g. IEA 2013). In addition to developed countries reliant on fossil fuels, CCS is also relevant to a number of fast-developing and developing countries whose future CO<sub>2</sub> emissions are expected to continue to rise (Dütschke et al. 2016). In light of the recent Intergovernmental Panel on Climate Change (IPCC) report 2018 examining the impacts of global warming at 1.5°C, CCS and other carbon dioxide removal (CDR) technologies have been identified as critical technologies for managing the transition to a more sustainable energy future (Boot-Handford et al. 2014).

However, early discussions about CCS have not been without controversy. Opponents argue that it promotes 'dirty energy' and if deployed, its impact may lead to a technology lock-in that hinders the development of more renewable energy options (Marshall 2016). Similarly, as some CCS projects have been put on hold or cancelled due to public opposition and failing to gain or sustain support from political leaders (Wallquist et al. 2012; Hammond & Shackley 2010), it has been recognised that the public's perception and evaluation of CCS technology is critical for its commercial deployment (L'Orange Seigo et al. 2014).

Reviews examining the psychological, social and cultural factors that underlie the support (or lack of it) for CCS projects (e.g. Ashworth et al. 2013; de Coninck & Benson 2014; L'Orange Seigo et al. 2014) show that public understanding and awareness of the technology have been the most frequently analysed topic. The research consistently shows a lack of knowledge and familiarity with CO<sub>2</sub> and the process of CCS (e.g. Wallquist et al. 2012; Jeanneret, Muriuki & Ashworth 2014; Hobman & Ashworth 2013). However, this poor knowledge does not hinder individuals from forming an opinion about CCS and often fosters misconceptions about the technology (e.g. Itaoka et al. 2013).

Risk perceptions and attitudes towards CCS are the next most investigated factors. The early research identified that perceptions of risk about CCS tend to be high — with a variety of stakeholders expressing concerns about the possible negative human and environmental impacts of the technology (e.g. Howell et al. 2012). The research also showed that risk perceptions can be modulated by local contexts and personal experiences with how different companies have operated in certain countries (e.g. Bradbury et al. 2011). Perceptions of risk have also been shown to be closely related to trust in information sources which has also been examined in social CCS research (e.g. Ashworth 2010, Terwel et al. 2009).

### Why an assessment of public knowledge and attitudes relating to CCS was needed

The scope of the UQ-SDAAP project was broad. It included the following objectives:

#### *Whole-of-chain integration and cross-cutting issues*

- Examining the complex issues of basin resource management and CO<sub>2</sub> enhanced water recovery in a basin with significant CSG development and groundwater use
- Looking at the fundamentals of engagement in contentious science, undertaking social baseline assessments and undertaking regulator capability build

#### *Development of international collaboration and partnerships*

- Engaging with key Chinese research entities and a major Chinese oil company in both technical and social streams, with complementary research streams in each country and a number of workshop and conference engagements in the design phases

Given the slow progress of CCS projects and the relative importance of understanding and gaining public support for CCS, socio-economic studies were deemed an essential component of this project.

The core objectives for this component included:

1. Undertaking an up-to-date assessment of current knowledge of, and support for CCS across Australia
2. Identifying the factors and message frames that may enhance support for CCS
3. Understanding how CCS is being portrayed in the media
4. Undertaking knowledge sharing and comparative research with China

It was envisaged that as the project progressed, the socio-economic research would converge with the technical program of research. This has already begun. A recent project investigated the public's response to enhanced water recovery for the GAB using managed aquifer recharge (MAR) processes with CCS. This is a separate area of research to the reinjection of water currently being trialled by the coal seam gas (CSG) industry.

The following sections detail an overview of the total package of social science research. While the essential components have been summarised here, more detailed results can be found in *Ferguson et al. 2019a*.

## 3.2 How CCS is viewed in the context of other energy choices

### UQ-SDAAP commenced their socio-economic research program with a large-scale assessment of the Australian public's current views towards CCS in the context of key energy technology choices.

A nationally representative survey was run between June and August 2017. This was followed by a second survey examining how different messaging can increase the salience and mental accessibility of particular topics or information around energy technologies. Social science research has shown that how information is presented may lead to shifts in individuals' preferences.

The findings of these surveys have significantly advanced understanding of the public's current views across four key areas:

1. Which factors are associated with support for different energy sources and technologies
2. Which factors are specifically associated with support for CCS
3. Which socio-economic and demographic groups are more or less likely to support CCS
4. Whether exposure to energy technologies influences the level of support for various technologies

The research showed that those who believe they have a good understanding of CCS are more likely to support it. Given the low levels of understanding about the technology which currently prevail, it points to a high likelihood that a concerted communications and engagement program using trusted sources would greatly increase public support of a CCS initiative such as this in Queensland.

The 'message framing' survey allowed the research team to drill down into the effectiveness of a range of alternative messaging approaches to promote increased understanding and informed decision-making about CCS.

### 3.2.1 National survey

#### 3.2.1.1 Introduction

To undertake an up-to-date assessment of the Australian public's current views towards CCS in the context of other energy technology choices, a nationally representative survey of individuals aged 18 years of age and older (95% confidence level and +/-1.76% confidence interval) was run between June and August 2017.

#### 3.2.1.2 Questionnaire design

To monitor changes in the public's views towards CCS over time, a level of replicability was maintained with previous surveys (for example: Ashworth et al. 2009a; 2009b; 2011; 2013) as shown in Table 1.



**Table 1** Questionnaire structure.

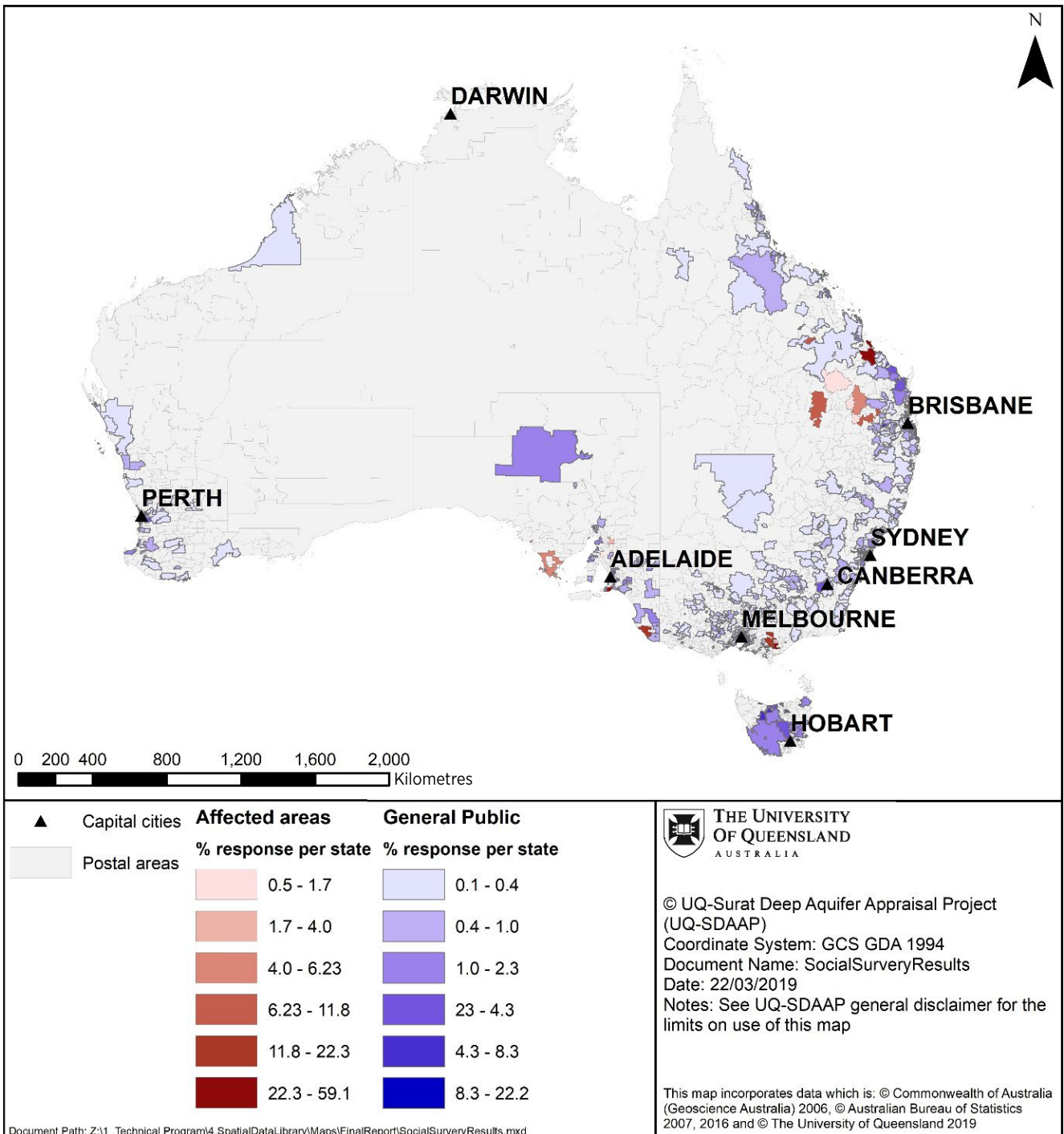
Section	Topic	Example Questions	Source
1	Screening questions	Age Gender Postcode	NA
2	Knowledge	<b>Objective knowledge</b> e.g. “How is most electricity in Australia generated?” and <b>perceived knowledge</b> e.g. “Please indicate your current level of knowledge about the following energy sources and technologies” (scale from 1 = no knowledge to 7 = expert knowledge)	Adapted from Jeanneret et al. 2014
3	Support for energy technologies and public funding preferences	Stated support e.g. “Please indicate how strongly you agree or disagree with the following options as potential ways of generating Australia’s future energy needs” (scale from 1 = strongly disagree to 7 = strongly agree)	Adapted from Jeanneret et al. 2014
4	Economic trade-offs and reliability concerns	Willingness to pay e.g. “I would give part of my income if I were certain that the money would be used to prevent environmental pollution” (scale from 1 = strongly disagree to 7 = strongly agree); Please indicate below how concerned you are that in the next 10-20 years electricity will become unaffordable for you? (scale from 1 = not at all concerned to 7 = extremely concerned)	Adapted from OECD EPIC survey; WVS
5	Climate change	Perceptions about global warming e.g. “Do you believe global warming is happening now or will happen in the next 30 years? How serious do you think are the environmental problems facing the world? (1 = not at all serious to 7 = extremely serious)	Adapted from OECD EPIC survey; WVS
6	CCS versus renewable energy perceptions	E.g. How likely do you think the following consequences are as a result of using CCS technology? e.g. An increase in the risk of a major accident involving the public occurring (1 = very unlikely to 7 = very likely); With regard to renewable energy projects to what extent do you trust renewable energy industries to e.g. act in the best interest of society? (1 = not at all to 5 = trust a lot)	Adapted from Huijts et al. 2012; 2014
7	Socio-demographic Information	E.g. Educational level, income level, household composition, political preferences	Adapted from Jeanneret et al. 2014

### 3.2.1.3 Sample demographics

After data cleaning, the final sample included 2383 individuals from across Australia as well as individuals randomly selected from specific regions (n=550). These regions, or communities of interest (COIs), were strategically chosen because of their exposure to energy projects. The aim was to further test whether geographic proximity and context influenced opinions, and to provide greater insights into any differences in attitudes that emerge across the various regions and demographic subgroups. The regions chosen included those living close to CSG and proposed CCS projects in Queensland (n=186), wind farms in South Australia (n=176) and brown coal mines and coal-fired power station closures in Victoria (n=188) (refer Figure 6).

Of those who responded to the questionnaire, 51% were female with an average age of 48 years. The majority (69%) resided in urban areas and approximately one-third of respondents had attained a level of education up to and including Year 12, while another third had completed a Bachelor degree or above. Median income was between AU\$60-\$90K pa. Around one-third of participants voted for the Australian Labor Party, and another third voted for the Coalition (Liberal Party and National Party combined), while 10% voted for the Australian Greens. A comprehensive summary of demographics can be found at Ferguson et al. 2019a.

**Figure 6** Geographical spread of respondents.

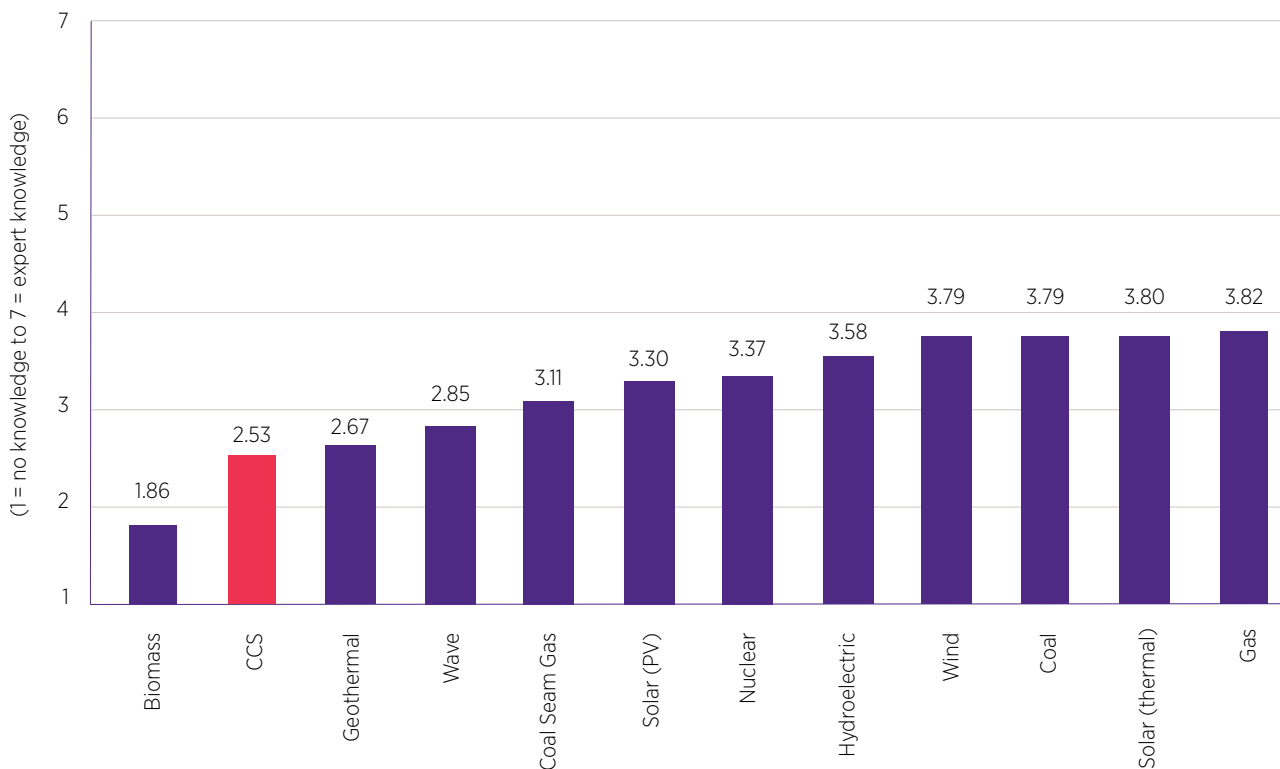


### 3.2.1.4 Results

#### 3.2.1.4.1 Knowledge of CCS and other energy technologies

On average participants self-reported having limited knowledge (that is, a mean below 4 on a 7-point Likert scale) about energy sources and technologies (Figure 7). Overall, there has been almost no increase in the public's knowledge and awareness of CCS, with it receiving lowest self-rated knowledge besides biomass and similar to geothermal and wave energy. Comparing the general public's self-rated knowledge with data from Australian nationally representative samples in 2011 and 2013 (Jeanneret et al. 2014), the data suggests that, on average, there was a decrease in self-rated knowledge about all energy sources and technologies. For CCS, the mean self-rated knowledge was 2.86 in 2011, 2.99 in 2013 and 2.53 in 2017.

**Figure 7** Perceived knowledge of each energy technology – general public sample (n=2383).



When viewed on a state-by-state basis, there were some variations between state average levels of perceived knowledge. Respondents from New South Wales (NSW) reported higher levels of knowledge about coal ( $\bar{x}$  = 3.88) and CSG ( $\bar{x}$  = 3.33) than other states and higher levels of knowledge about CCS ( $\bar{x}$  = 2.64), although these levels were still generally low. Conversely, Western Australian (WA) respondents reported knowing less about CSG ( $\bar{x}$  = 2.71) and CCS ( $\bar{x}$  = 2.42) than the remaining states.

However, comparing the views of the general public to the COIs (refer Table 2), the results demonstrate that individuals from the COIs perceived themselves to be more knowledgeable about coal (general public  $\bar{x}$  = 3.79 versus above 4 for COIs with  $p < 0.05$ ). The Queensland COI reported higher levels of perceived knowledge for CSG compared to all other groups ( $\bar{x}$  = 3.84 vs ratings around 3 with  $p < 0.05$ ) and the Victorian COI reported knowing significantly less about geothermal ( $\bar{x}$  = 2.39) than the other groups. In contrast, the South Australian COI reported significantly higher levels of perceived knowledge for renewable energies including solar (thermal and photovoltaic), wave and wind. There were no differences between the four groups for biomass, gas, CCS, hydroelectricity and nuclear. Contrary to our initial hypothesis, the Queensland COI reported knowing marginally less about CCS than the general public and the other COIs, but the difference was not large enough to be statistically significant.

**Table 2** Perceived knowledge of the general public sample compared to COIs.

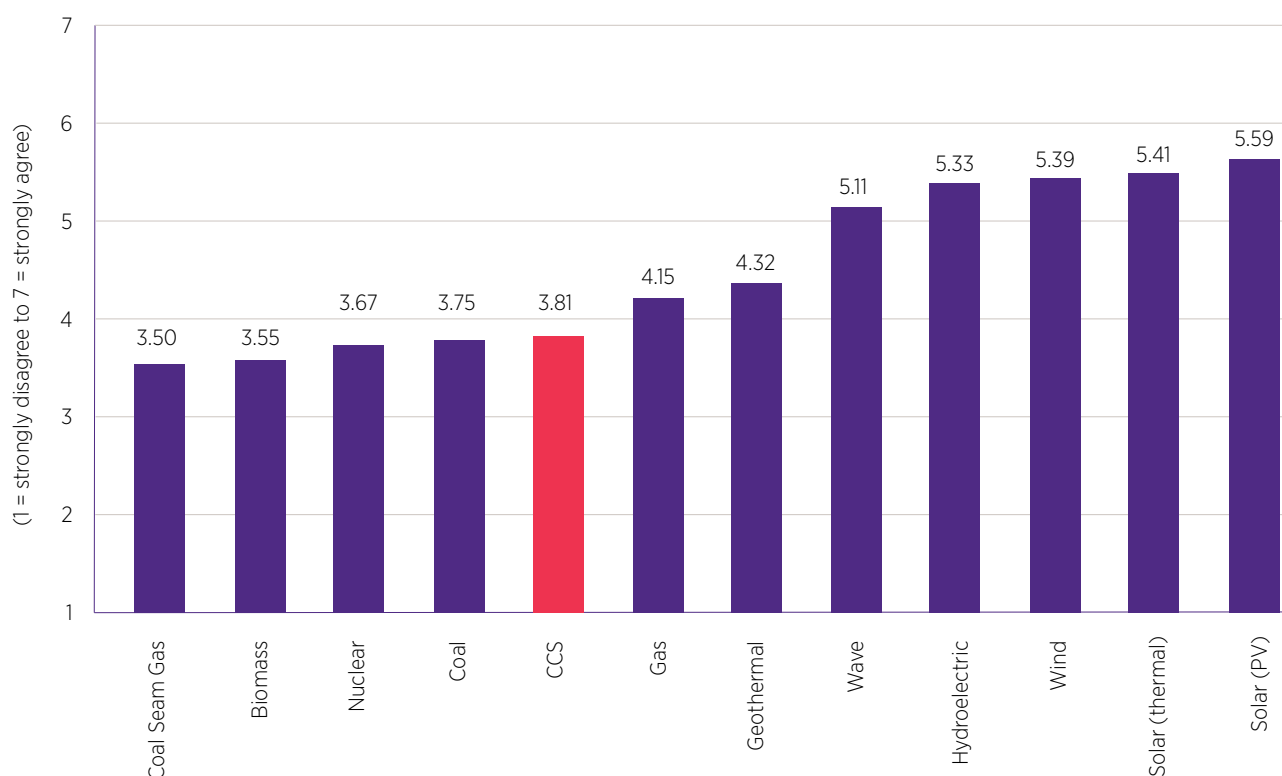
	General Public	Communities of Interest		
	(n=2383)	QLD (n=186)	VIC (n=188)	SA (n=176)
Biomass	1.86	1.91	1.75	2.03
Coal**	3.79	4.24	4.38	4.01
Coal Seam Gas**	3.11	3.84	2.91	3.24
Gas	3.82	3.87	3.98	4.01
<b>CCS</b>	<b>2.53</b>	<b>2.48</b>	<b>2.60</b>	<b>2.65</b>
Geothermal**	2.67	2.57	2.39	2.90
Hydroelectric	3.58	3.55	3.40	3.80
Nuclear	3.37	3.14	3.10	3.40
Solar (thermal)**	3.80	3.74	3.64	4.18
Solar (PV)**	3.30	3.62	3.12	3.89
Wave**	2.85	2.66	2.45	3.12
Wind**	3.79	3.75	3.72	4.29
<b>Total</b>	<b>3.21</b>	<b>3.28</b>	<b>3.12</b>	<b>3.46</b>

Mean scores where 1 = no knowledge, 4 = moderate knowledge and 7 = expert knowledge. (\* p<0.1; \*\*p<0.05)

### 3.2.1.4.2 Support for CCS compared with other energy technologies

It appears that in many ways CCS remains an enigma to most. Subsequently support for CCS as part of the energy mix is relatively low as shown in Figure 8. Between the states and territories (Table 3), support for the various technologies differed with only gas and geothermal showing no significant differences. The significant differences identified included:

- NSW and QLD reported significantly higher support for coal and CSG than the average support expressed in WA
- NSW reported significantly higher support for CCS than WA
- Nuclear energy received higher support in NSW compared to QLD and WA
- SA and WA reported higher support for solar (thermal) than all other states
- WA had the highest support for wind, wave and solar (photovoltaic) compared to all other states

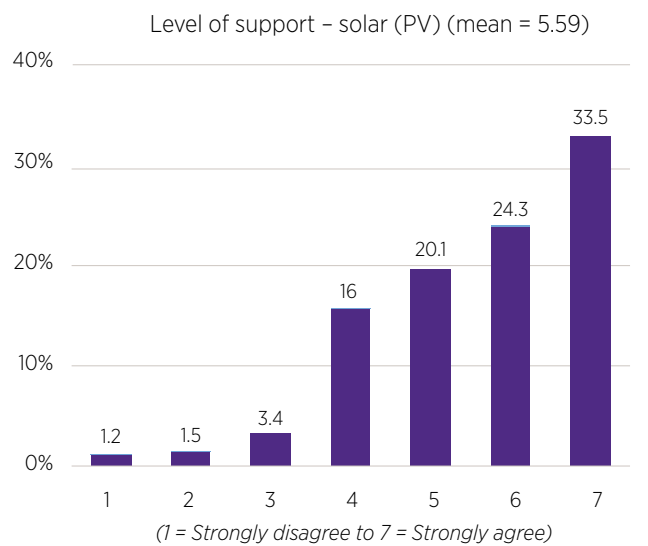
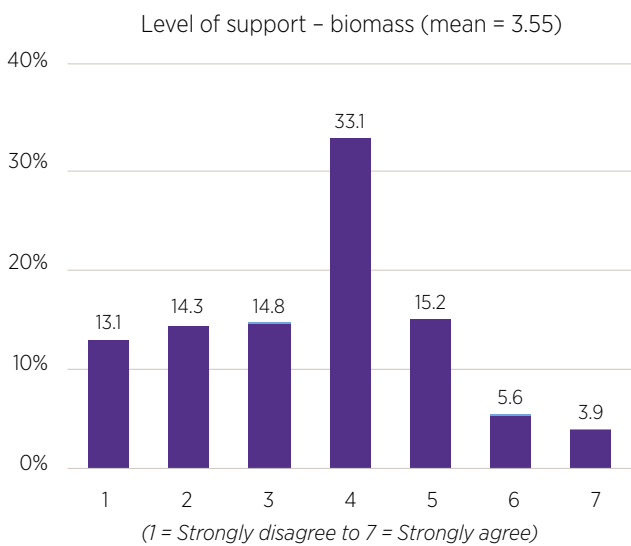
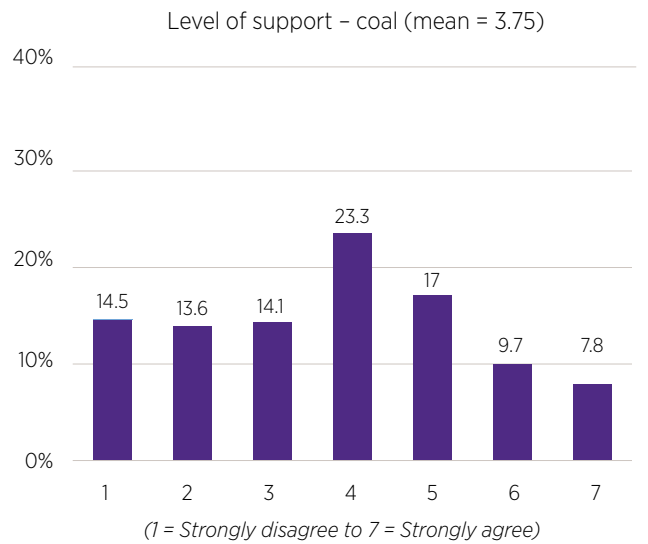
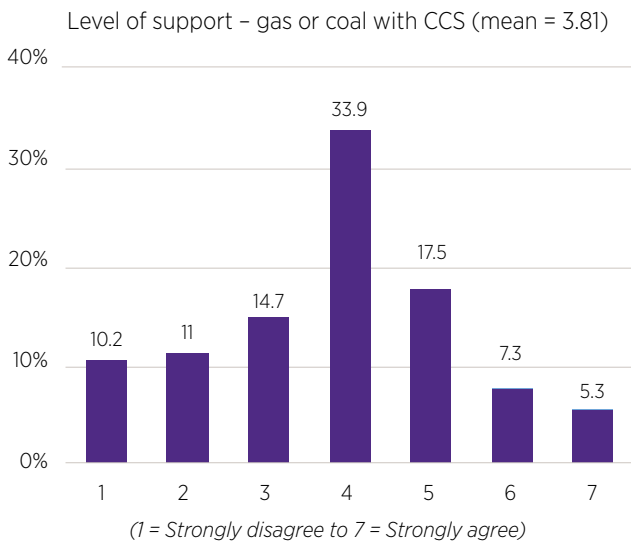
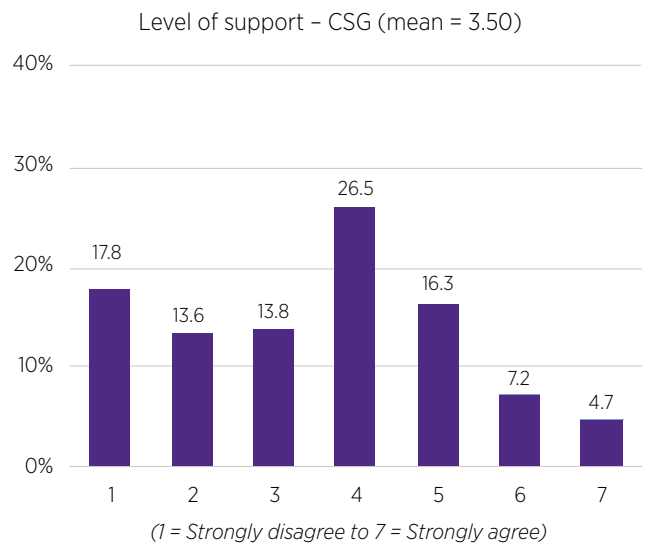
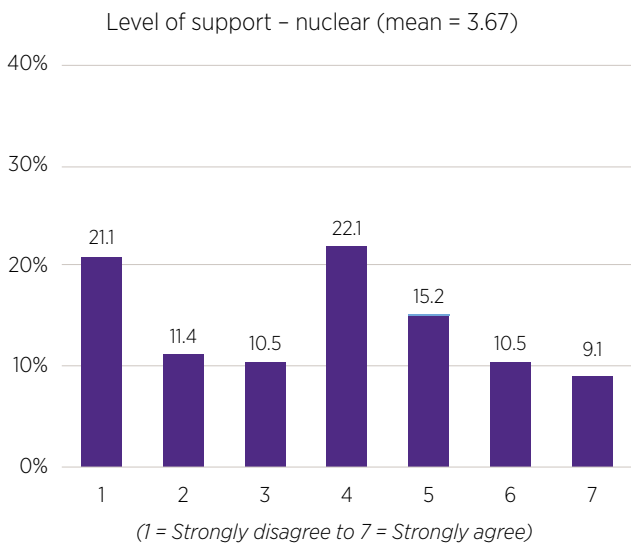
**Figure 8** Support for each energy technology – general public sample (n=2383).**Table 3** Support for energy technologies across states.

	NSW (n=780)	VIC (n=600)	QLD (n=463)	SA (n=177)	WA (n=257)
Biomass**	3.61	3.48	3.62	3.71	3.27
Coal**	3.97	3.66	3.87	3.67	3.22
Coal Seam Gas**	3.59	3.46	3.60	3.58	3.14
Gas	4.23	4.08	4.13	4.27	4.04
CCS*	3.92	3.77	3.79	3.88	3.59
Geothermal	4.37	4.32	4.29	4.35	4.27
Hydroelectric	5.34	5.28	5.44	5.20	5.23
Nuclear**	3.88	3.61	3.50	3.78	3.38
Solar (thermal)	5.34	5.42	5.43	5.47	5.51
Solar (PV)**	5.46	5.66	5.66	5.50	5.80
Wave**	5.01	5.11	5.16	5.06	5.43
Wind**	5.22	5.49	5.41	5.28	5.63

Mean scores where 1 = strongly disagree, 4 = neither agree nor disagree and 7 = strongly agree (\* p<0.1; \*\*p<0.05)

Investigating the frequency distributions of each technology revealed further variations between levels of support for the various energy technologies (Figure 9). Nuclear (21%) and CSG (18%) were the technologies with the highest proportions of 'strongly disagree' responses. The histograms reflect a group displaying staunch opposition to these technologies, which is consistent with their controversial nature. Although biomass has a similar mean score to both nuclear and CSG (Figure 8), this is due to the large proportion of respondents (33%) who 'neither agreed nor disagreed', rather than being strongly opposed to the technology. This was also the case for CCS (33%) and geothermal (29%) where a large percentage sat on the fence in relation to these technologies. Similarly, gas (29%), CSG (26%) and coal (23%), had almost one-quarter of those in the population who 'neither agreed nor disagreed', which suggests there remains some tolerance for these technologies across Australia.

**Figure 9** Energy technology frequency distributions (n=2383).



Substantial differences were found between the general public and the COIs around support for different technologies, particularly between South Australia and Victoria (Table 4). As hypothesised, the Victorian COI was more supportive of coal, gas and CCS with mean ratings of above 4, while the South Australia COI supported coal and CCS significantly less than the other groups. However, the South Australian COI reported the highest support, significantly higher than all other groups, for geothermal energy and for the renewable energies solar (both thermal and photovoltaic) and wind; and also had a significantly higher proportion of individuals who strongly disagreed with support for coal (27%) and CSG (30%). These results highlight the regional differences between the COIs and the sources of energy technologies they most rely on. Contrary to our initial hypothesis, support for CSG was higher in the Queensland COI than the general public and the other COIs, which suggests a growing acceptance of this technology in that region.

**Table 4** Support for energy technologies comparing general public and COIs.

	General Public	Communities of Interest		
	(n=2383)	QLD (n=186)	VIC (n=188)	SA (n=176)
Biomass**	3.55	3.63	3.71	3.20
Coal**	3.75	4.01	4.49	3.27
Coal Seam Gas**	3.50	3.77	3.58	2.96
Gas**	4.15	4.05	4.51	4.14
<b>CCS*</b>	<b>3.81</b>	<b>3.81</b>	<b>4.02</b>	<b>3.61</b>
Geothermal**	4.32	4.14	4.13	4.60
Hydroelectric	5.33	5.42	5.15	5.42
Nuclear*	3.67	3.45	3.35	3.86
Solar (thermal)**	5.41	5.45	5.30	5.78
Solar (PV)**	5.59	5.75	5.47	5.93
Wave	5.11	5.11	4.86	5.22
Wind*	5.39	5.39	5.26	5.66

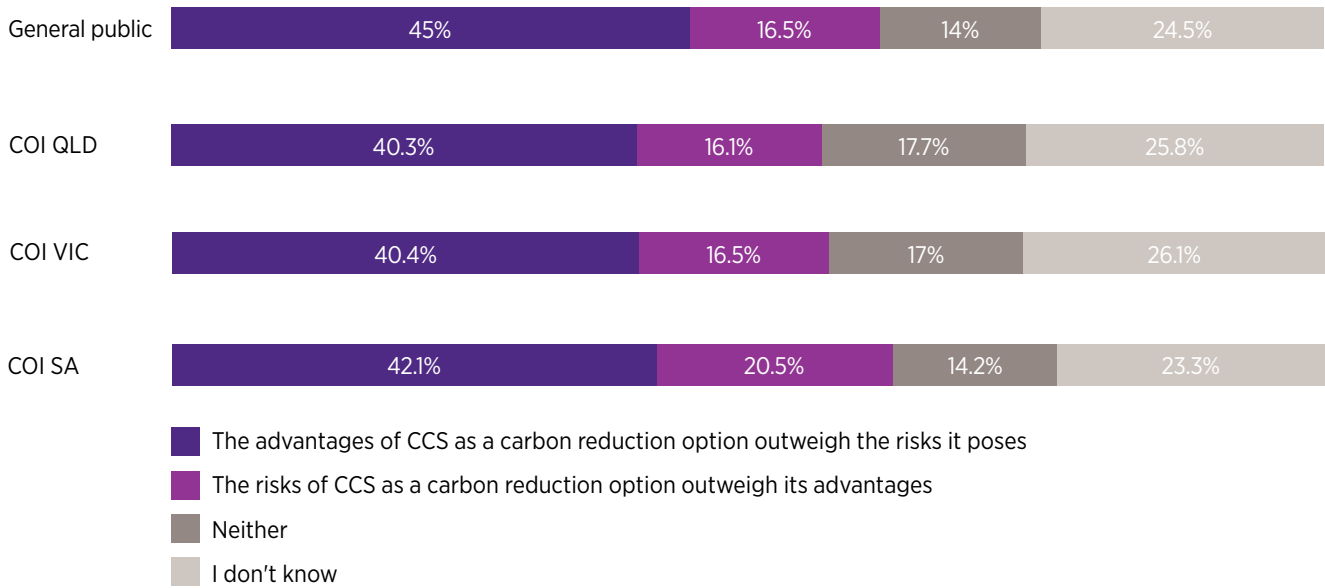
Mean scores where 1 = strongly disagree, 4 = neither agree nor disagree and 7 = strongly agree (\* p<0.1; \*\*p<0.05)

### 3.2.1.4.3 Perceived risks and benefits of CCS compared with renewable energy

It has been suggested that given the lack of knowledge, both objective and self-reported, of CCS and other technologies, stated levels of support should be treated with caution as they can only be classified as pseudo-opinions (de Best-Waldhober et al. 2009). Therefore, to provide participants with more information a short video was shown which discussed the roles of CCS, renewable energy and energy efficiency as options for mitigating carbon emissions. A set of questions about the potential risks and benefits of CCS and renewable technologies were then asked in order to understand how individuals perceived the two technologies following the information provided in a video. The two sets of questions were presented in a randomised order to prevent any order bias. Consistent with previous research, support for CCS was lower than renewables, while almost one-quarter responded that they did not know if the advantages of CCS outweighed the risks or vice versa.

Figure 10 below demonstrates that results were consistent across the four groups. Less than half of the individuals in all sample groups considered that the advantages of CCS as a carbon reduction option outweigh the risks it may pose. The South Australian COI had a slightly higher proportion of individuals (20.5%) who considered that the risks of CCS outweigh its advantages, but this difference was not statistically significant. The proportion of participants who saw neither net risks nor net benefits was around 15% of participants across all groups, suggesting a neutral rather than negative attitude towards CCS technology.

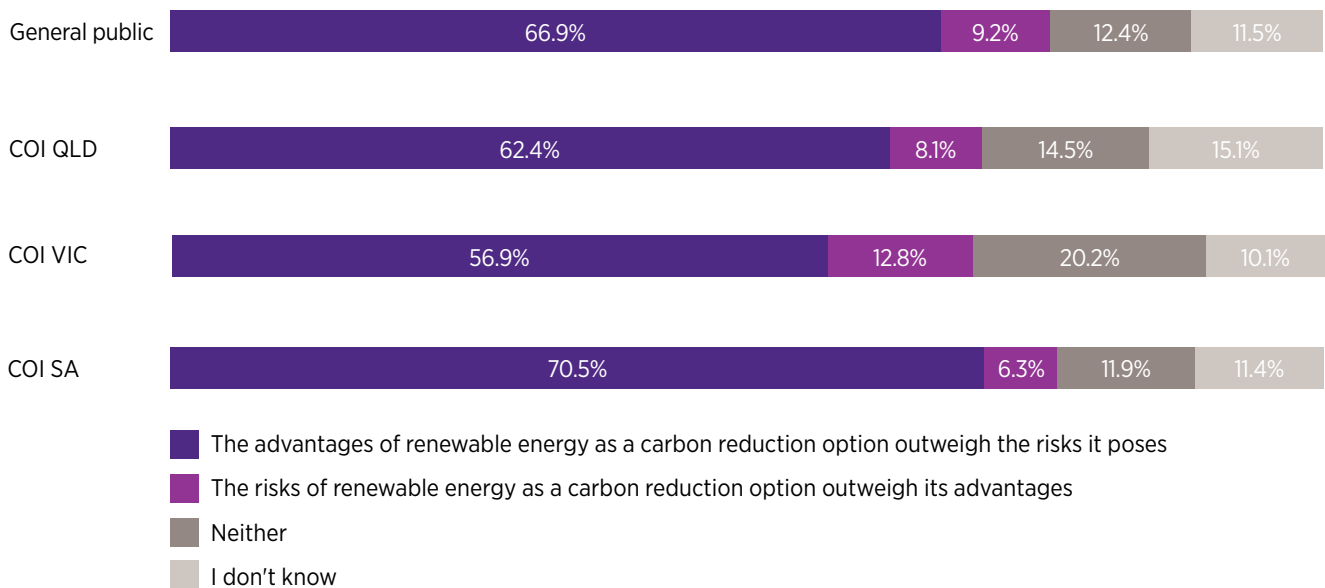
**Figure 10** When you think about CCS, what first comes to mind?



*Pearson chi2 (9) = 6.42, Pr = 0.697*

Perceptions about renewable energy followed a different pattern where all groups were largely favourable towards renewable energy (Figure 11). The majority of participants considered that the advantages of renewable energy outweighed its possible risks, ranging from 70.5% in the South Australian COI, to 57% in the Victorian COI. A smaller proportion of individuals in each group (6-13%) considered that the risks of renewables outweigh their advantages, compared to the same response for CCS. The average proportion of participants who saw neither net risks nor net benefits was about the same for renewables as it was for CCS. However, the proportion of participants who did not know about the risks and benefits of renewable energy options was considerably lower than the proportion of those who did not know about CCS.

**Figure 11** When you think about renewable energy, what first comes to mind?



*Pearson chi2 (9) = 18.97, Pr = 0.025*

When asked to identify the risks and benefits of CCS, the key benefit was perceived to be reducing CO<sub>2</sub> emissions. This was followed by increased employment which suggests participants saw opportunities for new employment in such an industry. Risk perceptions were higher in the COIs in Queensland and South Australia, mainly related to risks in the transport and storage of carbon dioxide. On investigation, the perceived benefits of CCS was weakly correlated to support for CCS.



### 3.2.1.4.4 Correlates of support for CCS

Regression analyses were used to show the influence of a range of independent variables on public support for CCS (Table 5). Respondents who believe they have a good understanding of CCS are more likely to support it ( $p < 0.001$ ). In keeping with perceived knowledge, the coefficients suggest that those who are males and more highly educated are also more likely to support CCS. Not surprising, those who perceive the social, economic and environmental benefits of CCS to outweigh any risks are more likely to be supportive of it.

The model suggests that in Australia, those who prioritise longer term outcomes over the shorter term, economic growth over the environment, who more highly rate the transparency and fairness of the decision-making processes to determine whether to implement CCS, and who trust government and the CCS industry to act in the best interests of society, are more likely to support CCS.

Surprisingly, Australians who agree that global warming is happening (or will happen in the near future) ( $p < 0.001$ ) and that human activities have contributed to global warming ( $p < 0.01$ ) are less likely to support CCS. As well, those Australians who feel some personal or moral responsibility for contributing to energy problems and their solutions do not tend to support CCS.

**Table 5** Regression model identifying support variables for CCS.

Variables	B	SE B	$\beta$
Self-rated knowledge: gas or coal with Carbon Capture and Storage	0.153***	(0.021)	0.153***
Gender	-0.112	(0.062)	-0.036
Age	0.004'	(0.002)	0.049'
Education level			
Up to Year 11 or equivalent	0.000	(.)	0.000
Year 12 or equivalent	-0.007	(0.106)	-0.002
TAFE/Technical Certificate/Diploma	-0.030	(0.090)	-0.009
Bachelor degree	0.113	(0.100)	0.030
Postgraduate qualification	0.099	(0.113)	0.021
Global warming is happening (yes)	-0.397***	(0.075)	-0.119***
Humans cause global warming (yes)	-0.180**	(0.068)	-0.056**
Ascription of responsibility (AR)	-0.075**	(0.027)	-0.078**
Personal norms (PN)	-0.010	(0.028)	-0.009
Long-term orientation (individual)	0.102**	(0.034)	0.064**
Collectivism (individual)	-0.049	(0.028)	-0.039
Top priority – economic growth	0.480***	(0.072)	0.143***
CCS – Perceived Risks (PR)	-0.014	(0.024)	-0.012
CCS – Perceived Benefits (PB)	0.128***	(0.035)	0.095***
CCS – Trust in government	0.174***	(0.038)	0.124***
CCS – Trust in industry	0.093'	(0.044)	0.062'
CCS – Fairness & transparency of decision-making process	0.091*	(0.040)	0.057'
Constant	1.615***	(0.293)	.
<b>Observations</b>	<b>2370</b>		
<b>R<sup>2</sup></b>	<b>0.181</b>		

## 3.2.2 Testing alternative messaging (framing) for increased understanding

### 3.2.2.1 Introduction

While our research reported above identified current knowledge and support for CCS, conducting this survey provided an opportunity to examine the relative effectiveness of *alternative* message frames in promoting increased understanding and informed decision-making about CCS.

A growing body of research has explored framing effects and prompts/cues on perceptions of climate change and support for climate policy and is well-established in the social sciences (Bernauer & McGrath 2016; Bolsen & Druckman 2018). There are fewer published studies in the area of energy sources and technologies (see Bolsen, Druckman & Cook 2014; Bruine de Bruin & Wong-Parodi 2014).

To promote increased understanding and informed decision-making about CCS, the impact of increasing the salience of related topics on participants' reported levels of support for energy technologies and CCS was examined. The increase in salience was tested by varying the first group of questions participants were presented within the survey. The motivation behind testing variations in the first topic presented is based on *question order effects*. Survey questionnaire design research has demonstrated that the order in which questions are asked can alter the context, or *frame*, in which subsequent questions are interpreted, and can influence how participants respond to subsequent questions, thus producing different results (Bruine de Bruin 2011; Oldendick 2008). Much of the literature on order effects in questionnaire design is aimed at reducing unintentional bias and statistical noise. However, in social science experimental questions can also be purposefully ordered to increase the salience and mental accessibility of particular topics or information, and thus act as prompts/cues, 'in line with literature showing that people base survey responses on whatever information most easily comes to mind' (Druckman 2015; Kahneman & Frederick 2002).

It was hypothesised that this experimental design would lead to a better understanding of how the salience of different information topics may lead to shifts in individuals' preferences. This project aimed to examine the salience of the following topics on levels of support for CCS and other energy technology options:

- Objective and perceived knowledge about energy technologies
- Economic trade-offs – cost and reliability of energy technologies
- Beliefs about climate change – occurrence and causes
- Energy efficiency behaviours and pro-environmental actions

### 3.2.2.2 Survey design – to test the impact of message framing

In addition to the main survey (Version A, Table 1), four different versions of the survey were presented to a random sample of around 125 individuals. All versions began with screening questions (age, gender, and postcode). The initial questions preceding the support questions for each version are outlined below and in Table 6.

#### Version A – Knowledge – salience: objective and perceived knowledge (KN)

The first questions presented focused on objective knowledge of energy topics and perceived knowledge about different energy sources and technologies. This was the format used in the formerly reported nationally representative data. Therefore, the group of participants was randomly selected from the larger sample (subsample n=125, randomly selected from n=2383). This version allowed identification of the effect of participants' knowledge on the individuals' preferences and support for different energy technologies.

#### Version B – No information – no questions presented before stated preferences (control group) (NI)

No questions were presented before asking participants to rate their support for the various energy sources and technologies under analysis. This version allowed us to identify individuals' baseline preferences and support for different energies without having considered any preceding information.

#### Version C – Cost and reliability – salience: economic trade-offs and reliability concerns (CR)

Initial questions related to the financial implications of using just renewable energy, attitudes about energy reliability standards and perceptions of energy security. This version allowed us to identify individuals' preferences and support for different energies after having considered the multiple economic and financial implications of them, as well as individuals' concerns for future energy reliability.

### Version D – Climate change – salience: beliefs about occurrence and causes of global warming (CC)

The first questions presented were about beliefs about whether global warming is occurring, the causes of global warming, the perceived severity of a variety of environmental problems, and environmental attitudes. This version allowed us to identify individuals' preferences and support for different energies after having considered their beliefs about climate change and global warming, as well as their concerns for the various environmental problems we face as a society.

### Version E – Energy behaviours – salience: energy efficiency behaviours (EB)

The first questions presented were about the frequency respondents perform a variety of pro-environmental behaviours, e.g. saving water, recycling, reducing air conditioning usage, and washing clothes with full loads only; as well as subscription to Green Power. This version allowed us to identify individuals' preferences and support for different energies after having considered their own individual and household contribution and their daily behaviours in terms of energy consumption and energy resources use.

**Table 6** Alternative versions of question order.

Section order	1	2	3	4	5	6	7
Version A	KN	Support	CR	CC	EB	CCS versus renewable energy perceptions	Socio-demographic information
Version B (control)	Support (NI)	KN	CR	CC	EB		
Version C	CR	Support	CC	EB	KN		
Version D	CC	Support	CR	EB	KN		
Version E	EB	Support	KN	CC	CR		

### 3.2.2.3 Sample demographics

The first group of participants was randomly selected from the larger project described above (subsample n=125, randomly selected from n=2383). An additional 500 surveys were completed for the four experimental groups, with a total of 469 of these surveys being retained after data cleaning. Although these participants were shown a questionnaire with a variation in the order of questions, the participants were equally included in the national randomisation process. This means that these participants were not selected from a particular area, but randomly collected across Australia, however the sample of participants between the conditions was balanced in terms of age (mean age 46-49), gender and state location (Table 7).

**Table 7** Socio-demographic characteristics of participants across experimental conditions.

Sample		No Information	Knowledge	Cost & Reliability	Climate Change	Energy Behaviours	Total
Gender	Male	50.8%	51.2%	51.3%	45.9%	42.9%	288
	Female	49.2%	48.8%	48.7%	54.1%	57.1%	306
Age	Mean	48.7	47.8	49.9	47.5	50.6	48.9
	(SD)	(17.4)	(16.7)	(16.0)	(17.4)	(17.4)	(17.0)
<b>Total</b>		<b>122</b>	<b>125</b>	<b>119</b>	<b>109</b>	<b>119</b>	<b>594</b>

### 3.2.2.4 Results

Examining the differences between levels of support for individual energy technologies according to the experimental condition, an interesting difference between the technologies arose (Figure 12). Compared to the NI group, the KN group recorded significantly lower support for renewable energy technologies, including wind, solar (PV), and hydroelectric. In contrast, participants in the EB group had higher support for all energy technologies except for hydroelectricity and wind, and significantly higher support for gas, nuclear, CCS and biomass – a group of technologies that typically receive the lowest support in other surveys.

Participants in the KN group reported a strong bias towards alternatives that perpetuate the status quo, demonstrating higher levels of support for conventional energy technologies that have been around for longer and with which the general population are most familiar, and that are seen as reliable and more affordable. The results suggest that there is a frame effect related to the knowledge questions that generated a *status quo bias* (Bolsen, Druckman & Cook 2014; Samuelson & Zeckhauser 1988). Although the objective knowledge questions were themselves framed neutrally, they nonetheless increased the emphasis on and salience of the topics covered, i.e. electricity generation, household energy use and costs, and national energy needs.

**Figure 12** Support for each energy technology per condition, compared to 'no information' condition.



Mean scores: 1 = strongly disagree, 4 = neither agree nor disagree and 7 = strongly agree (\* p<0.05)

However, when it came to the trade-offs between the economic and environmental costs and reliability of energy technologies, hypothetically, prompting participants with these questions should increase support for technologies that are considered cheaper and more reliable. Yet, of all the experimental conditions, this demonstrated the least effect. There were no significant differences in comparison to the NI group and not even a statistical trend in some direction (p-values do not remotely approach significance). In an attempt to uncover the motives that influenced individual preferences, participants were asked to indicate the extent to which they considered various factors when deciding whether to support energy technologies. Economic issues, and installation/maintenance costs, were significant factors in the CR group when compared to the NI group. As there were no similar differences between the other conditions (KN, CC and EB) compared to the NI group, it would appear that prompting participants with questions that increase the salience of economic and environmental cost and reliability trade-offs, as in the CR condition, may have some effect on the factors underlying support. However, this did not seem to translate in different energy support ratings.

When using the CC frame, compared to the NI group, there was a tendency towards an increase in support for coal, CSG, CCS and nuclear, and lower support for renewables, particularly wind energy. These results were unexpected as prompting with climate change questions should, in theory, increase the salience of the need for supporting energy technologies that are perceived as producing lower emissions – typically identified as renewable energy technologies. Whether this pattern of results differed according to beliefs about global warming was examined. For participants who indicated they were uncertain, did not know or did not believe that climate change was happening, there were no significant differences in levels of support for energy technologies between those in the CC group compared to the NI group (note that these groups were  $n < 40$ , thus analyses lacked statistical power). The responses showed higher levels of support for fossil fuel-related energies and nuclear, and lower support for renewable energies. It was more surprising that this pattern was also seen for participants who do believe that global warming is happening. There were significant increases for support in the CC group compared to the NI group for coal ( $\bar{x} = 3.57$  vs  $\bar{x} = 3.01$ ,  $p < 0.05$ ), and for nuclear ( $\bar{x} = 3.74$  vs  $\bar{x} = 3.07$ ,  $p < 0.05$ ).

A closely corresponding pattern of results was found when examining beliefs about the causes of global warming. Participants in the CC group who believe global warming is caused mostly by natural changes in the environment, or by both natural changes and human activities, were significantly less supportive of wind energy compared to the NI group ( $\bar{x} = 5.01$  vs  $\bar{x} = 5.69$ ,  $p < 0.05$ ) and hydroelectricity ( $\bar{x} = 5.43$  vs  $\bar{x} = 5.90$ ,  $p < 0.05$ ). However, CC group participants who believe that global warming is caused mostly by human activities were more supportive of all energy technologies compared to the NI group, and support for CCS was significantly higher ( $\bar{x} = 4.23$  vs  $\bar{x} = 3.48$ ,  $p < 0.05$ ).

These results suggest that a psychological mechanism is triggered when participants are prompted with climate change questions – even for those who believe that global warming is happening and is caused mostly by human activity. These findings did not appear to be mediated by prompting with the questions regarding values, norms and beliefs included in the climate change section, as there were no significant differences in levels of support when these variables were added to regression analyses. One possible explanation is that of ‘techno-optimism’, which Gardezi and Arbuckle 2018 define as ‘a belief that human ingenuity, through improved science and technology, will ultimately provide remedies to most current and future threats to human well-being’, such as climate change. In their study of farmers’ attitudes towards climate change adaptation, they found that techno-optimism can reduce farmers’ support for climate change adaptation and to express a preference to delay adaptation-related actions. In this instance it is possible that respondents thought that all possible technologies, including fossil fuels, will be required as we adapt to climate change, particularly for developing the new technologies that require large amounts of conventional energy to power the transition.

## 3.3 The impact of alternative messaging approaches – on support for CCS

**The significantly different results that arose around support for CCS depending on the way the messages were framed in previous surveying warranted further investigation in this area.**

UQ-SDAAP took a two pronged approach; conducting pilot-scale face-to-face experimental workshops, which then led to a broader pilot-scale international survey.

The aim was to further test the impact on expressed support for CCS and other energy technologies when leading with the frame of energy efficiency behaviours. Some additional information was provided to participants during the survey, which yielded important insights into the forming of opinions and views when given information on the topic from respected and trusted sources.

The initial analyses of the message testing workshops and international survey suggest that providing objective, balanced and understandable information about CCS is associated with higher levels of support for CCS, and with more balanced perspectives on the potential risks and benefits of CCS technologies and projects.

However, in contrast to the results of the message framing survey, priming participants with the Energy Behaviour frame in the international survey was not associated with higher levels of support for CCS.

One limitation of these studies is that they are cross-sectional and can therefore only give a snapshot of participants' knowledge, perceptions of and acceptance of CCS and other energy technologies at a time. It would be insightful to design a future study that can re-test a set of participants some months later to explore whether levels of support remain at higher levels after provision of information.

### 3.3.1 Workshops

#### 3.3.1.1 Introduction

Face-to-face experiments were run at UQ computer labs with three different groups of participants in December 2018. The aim was to further test the impact on expressed support for CCS and other energy technologies when leading with the frame of energy efficiency behaviours as well as including some information provision. A key consideration for this activity was to locate respected and trusted information sources (i.e. NGOs, experts, research) that were freely available in different formats (i.e. videos, internet fact sheets and numerical tables and graphs).

Table 8 summarises the individual workshop processes. In all three workshops, participants were first asked to complete a short survey online. They were then shown a video of a researcher discussing the merits of CCS. In the first workshop, participants were then asked to respond to a follow up survey. Their responses to two other videos on CCS were subsequently tested. Their responses to these were explored through some online questions and group discussion. In the second workshop the process was the same except that following the video, participants viewed a web page on frequently asked questions (FAQ) on the Bellona website. Bellona is a Norwegian NGO that works across a range of issues, including energy. Participants were given the opportunity to explore more pages about CCS on the Bellona website if they wished to, before testing their responses and group discussion as per the first workshop. In the third workshop, after viewing the Bellona information, participants were given a paper handout of a comparison of different types of power plants' CO<sub>2</sub> emissions versus the average amount of energy each type produced, followed by testing responses and group discussion.

**Table 8** Sequence of experiments in each workshop.

Activity	Rationale	Frame 1	Frame 2	Frame 3
Pre-survey	Salience of EB frame and baseline support	x	x	x
CCS expert video – Dr Julio Freedman <sup>9</sup> in plenary on large screen	Video and trust in experts	x	x	x
Bellona fact sheet <sup>10</sup> & internet browsing – individual activity on computer	Internet, risks and benefits, trust in NGO		x	x
CEDM Technology Fact sheets <sup>11</sup> – Comparison of power plants' CO <sub>2</sub> emissions vs energy produced – individual activity with paper handout	Academic information, numbers and graphs			x
Post-survey	Support for CCS	x	x	x

### 3.3.1.2 Survey design

Questions included in the survey replicated the specific sequence order of the Energy Behaviours frame questions along with various support questions (Table 9). By introducing different sources sequentially across the groups, the influence of each of the sources on participants' attitudes by using pre and post surveys replicating the key questions from the original survey (refer Table 1) could be monitored.

**Table 9** Workshop survey questions.

Section	Topic	Example Questions	Source
1	Energy Behaviours	Frequency with which people perform a variety of energy efficiency and pro-environmental behaviours, e.g. reducing air conditioning usage, washing clothes with full loads only, saving water, recycling, as well as subscription to Green Power	Adapted from OECD EPIC survey; WVS
2	Support for energy technologies and public funding preferences	Stated support e.g. <i>"Please indicate how strongly you agree or disagree with the following options as potential ways of generating Australia's future energy needs"</i> (scale from 1 = strongly disagree to 7 = strongly agree)	Adapted from Jeanneret et al. 2014
3	Knowledge of energy technologies	E.g. <i>"Before today, which of the following carbon dioxide mitigation methods have you heard about?"</i> (scale: 1 "Never heard about it", 2 "Heard about it", 3 "Know it very well").	Adapted from Yang et al. 2016
4	<b>Socio-demographic Information</b>	E.g. Educational level, income level, household composition, political preferences	Adapted from Jeanneret et al. 2014
5	Advantages vs risks of CCS	E.g. <i>"When you think about carbon capture and storage (CCS), what first comes to mind?"</i> a. The advantages of CCS as a carbon reduction option outweigh the risks it poses b. The risks of CCS as a carbon reduction option outweigh its advantages c. Neither d. Don't know	Adapted from Steg et al. 2005
6	Risks and benefits of CCS	E.g. <i>"CCS can reduce CO<sub>2</sub> emissions"</i> (scale from 1 = strongly disagree to 7 = strongly agree)	Adapted from Yang et al. 2016; L'Orange Seigo et al. 2014
7	Trust	Trust in sources of information about CCS; trust in monitoring of CCS sites, e.g. <i>"To what extent do you trust information about CCS if it were to come from the following sources?"</i> (scale 1 = not at all to 5 = trust a lot)	L'Orange Seigo et al. 2014
8	Materials presented	Legitimacy of, effectiveness of and trust in the information presented in the video/fact sheet	Druckman et al. 2018
9	Climate change	Perceptions about global warming e.g., "Do you believe global warming is happening now or will happen in the next 30 years?"	Adapted from OECD EPIC survey; WVS

<sup>9</sup> [www.thirdway.org/video/julio-explains-it-all-why-we-need-carbon-capture-for-climate](http://www.thirdway.org/video/julio-explains-it-all-why-we-need-carbon-capture-for-climate)

<sup>10</sup> [www.bellona.org/about-ccs/faq-about-ccs](http://www.bellona.org/about-ccs/faq-about-ccs)

<sup>11</sup> [www.cedmcenter.org/tools-for-cedm/informing-the-public-about-low-carbon-technologies](http://www.cedmcenter.org/tools-for-cedm/informing-the-public-about-low-carbon-technologies)

### 3.3.1.3 Sample demographics

Recruitment of participants for the experimental workshops was done through an online call for volunteers via the UQ News website, and through forwarding the call for participants through social networks of the researchers including a number of student groups. Initially it had been anticipated that up to six workshops would be conducted, however, because of the time of the year (close to Christmas) there were only enough participants for three. In total 26 individuals attended the workshops. Across the groups there were more females (73%) than males, with the average age of participants being 30 years of age. Participants included students, UQ staff, and members of the community.

### 3.3.1.4 Results

Analysis of the mean responses across all experiments showed an increase in support for CCS and nuclear power while support for coal, solar PV and wind reduced slightly. It is highly unusual to see such high support ( $\bar{x} = 5$ ) for CCS, and these results tentatively suggest that priming with different formats and types of information about CCS may lead to increased levels of support. Despite priming the pre-information survey with the Energy Behaviour questions, the pre-information mean for CCS was slightly lower than that of the no Information (control) condition in our message framing survey ( $\bar{x} = 3.65$  vs  $\bar{x} = 3.85$ ), which does not lend support to our previous message framing survey results. However, in the absence of control groups this needed to be further tested.

**Table 10** Combined pre and post-information support for energy technologies.

Technology	n	Pre-information		Post-information		
		Mean	(SD)	Mean	(SD)	Difference
Coal	23	2.39	(1.50)	2.35	(1.64)	- 0.04
CCS	23	3.65	(1.43)	5.04	(1.33)	+ 1.39***
Nuclear	23	3.56	(1.80)	4.04	(2.078)	+ 0.48
Solar PV	23	6.65	(0.71)	6.61	(0.83)	- 0.04
Wind	23	6.61	(0.78)	6.48	(0.99)	- 0.13

Mean scores: 1 = strongly disagree, 4 = neither agree nor disagree and 7 = strongly agree (paired t-test \*  $p < 0.05$ ; \*\*  $p < 0.01$ ; \*\*\*  $p < 0.001$ )

To test the effectiveness of the different information that was shared with the groups, the individual group results were examined. While the group sizes are too small to make any generalisations, the results from each of the experimental groups demonstrate that support for CCS increased in all groups. The largest increase arose in Group 2 which had a combination of the video and then the Bellona FAQ webpage with time to click on other components of the Bellona website. While the support for CCS was positive across all groups for the other technologies this was not always the case. In the third group, where individuals were also provided with information comparing CO<sub>2</sub> emissions versus energy produced there was a decrease in support for solar PV and wind and an increase in support for coal and nuclear. It appears that the volume of energy produced by the different technologies, despite their CO<sub>2</sub> emissions, influenced this support (although with such small numbers of participants, these preliminary results should be interpreted with caution).



## 3.3.2 International survey

### 3.3.2.1 Introduction

The findings from the workshops informed the design of an international experimental survey across five countries.

UQ-SDAAP's aim was to explore if the results from both the message frame survey and experimental workshops could be replicated across differing national contexts.

### 3.3.2.2 Survey questionnaire design and sample demographics

Between 10-20 March 2019 an online survey was run (n=1015) with approximately 200 randomly sampled participants in five countries: Australia, China, India, the United Kingdom (UK) and the United States (US).

The survey questionnaire largely replicated the workshop survey and design. UQ-SDAAP again used the CCS expert video featuring Dr Julio Freedman. We created a factsheet which aimed to present objective information, including risks and benefits, of CCS, similar to the Bellona website information accessed in the workshops. The design was based on feedback from our workshop participants and previous research (e.g. de Best-Waldhober et al. 2009; Brunsting et al. 2011) that demonstrates a public preference for accurate, balanced and understandable information. A modified and updated power plant comparison was designed, based on the CEDM fact sheet, using US Department of Energy statistics to calculate CO<sub>2</sub> emissions and energy generation across a range of energy technologies (Appendix F). For respondents in the China sample, the questionnaire and materials were translated into Chinese, and the video was sub-titled in Chinese. In all other countries, the materials were presented in English.

Participants were randomised to one of four experimental conditions. Condition 1 was used as a control group, as per the 'No Information' condition in our message framing national survey, in order to further test the effect of the Energy Behaviour frame on the pre-information levels of support for energy technologies. Conditions 2-4 replicated the three workshop frames. Table 2.11 summarises the survey flow and conditions.

**Table 11** Sequence of questions/materials in survey conditions.

(Refer to Table 9 for topic/sources)		Condition			
		1 (control) (n= 255)	2 (n=253)	3 (n=255)	4 (n=252)
1	Energy Behaviours		x	x	x
2	Support for energy technologies and public funding preferences	x	x	x	x
3	Knowledge of energy technologies	x	x	x	x
4	CCS expert video – Dr Julio Freedman	x	x	x	x
5	CCS factsheet			x	x
6	Power plant comparison factsheet				x
		All conditions			
7	Repeat measure: Support for energy technologies and public funding preferences			x	
8	Advantages vs risks of CCS			x	
9	Risks and benefits of CCS			x	
10	Trust			x	
11	Materials presented			x	
12	Climate change			x	
13	Socio-demographic Information			x	

Table 12 presents the sample demographics across the five countries. Participants were aged 18 years and over, and the sampling aimed to be nationally representative for age, gender and region. There were slightly higher proportions of female participants in Australia, the UK and the US, and notably higher proportions of male participants in China. The overall mean age of participants was 39.3 years, with lower mean ages in India (30.7) and China (34.8).

**Table 12** Socio-demographic characteristics of participants across countries.

Sample		Australia	China	India	United Kingdom	United States	Total	(%)
Gender	Male	45%	58%	52%	48%	45%	503	49.6%
	Female	55%	42%	48%	52%	55%	512	50.4%
Age	Mean	42.5	34.8	30.7	43.9	44.7	39.3	
	(SD)	(12.1)	(10.2)	(9.3)	(12.0)	(14.8)	(13.1)	
<b>Total</b>		<b>202</b>	<b>203</b>	<b>201</b>	<b>204</b>	<b>205</b>	<b>1015</b>	<b>100%</b>

### 3.3.2.3 Initial results

#### 3.3.2.3.1 Comparative support for energy technologies across conditions

Analysis of the pre-information and post-information mean responses showed a significant increase in support for both CCS and nuclear energy technologies across all conditions (Table 13). Support for coal also increased in conditions 1, 2 and 3, although it received the lowest level of support of the five energy technologies. Support for solar PV and wind was highest across all conditions, although post-information support for solar PV decreased slightly in condition 1. Support for solar PV also decreased in condition 4, where individuals were provided with information comparing CO<sub>2</sub> emissions versus energy produced for several energy technologies, as it had in the corresponding workshop group (group 3). The post-information mean for CCS ( $\bar{x} = 5.11$ ) lends weight to our workshop findings, which suggests that priming with information about CCS may lead to higher levels of support. Compared to the results from the experimental workshops, coal, CCS and nuclear all had higher pre-information mean levels of support, while solar PV and wind had lower pre-information means. However, contrary to the findings of our national message framing survey, priming with energy efficiency behaviours in conditions 2-4 did not lead to significantly higher baseline levels of support for CCS compared to our control group (condition 1). There were no significant differences between the conditions for post-information mean levels of support for any of the energy technologies.

**Table 13** Combined pre- and post-information support for energy technologies, by survey condition.

Technology	Condition	n	Pre-information		Post-information		
			Mean	(SD)	Mean	(SD)	Difference
COAL	1	255	3.85	(1.73)	3.99	(1.75)	+ 0.13
	2	253	3.73	(1.81)	3.94	(1.86)	+ 0.21**
	3	252	3.82	(1.81)	4.24	(1.84)	+ 0.42***
	4	255	3.95	(1.70)	3.95	(1.88)	0.0
	<b>Total</b>	<b>1015</b>	<b>3.84</b>	<b>(1.76)</b>	<b>4.03</b>	<b>(1.83)</b>	<b>+ 0.19</b>
CCS	1	255	4.34	(1.59)	5.00	(1.56)	+ 0.66***
	2	253	4.17	(1.57)	5.20	(1.46)	+ 1.02***
	3	252	4.37	(1.58)	5.14	(1.59)	+ 0.77***
	4	255	4.65	(1.41)	5.09	(1.47)	+ 0.44***
	<b>Total</b>	<b>1015</b>	<b>4.38</b>	<b>(1.54)</b>	<b>5.11</b>	<b>(1.52)</b>	<b>+ 0.73</b>
NUCLEAR	1	255	4.18	(1.79)	4.55	(1.68)	+ 0.37***
	2	253	4.21	(1.69)	4.68	(1.59)	+ 0.47***
	3	252	4.22	(1.80)	4.71	(1.65)	+ 0.49***
	4	255	4.25	(1.66)	4.79	(1.62)	+ 0.54***
	<b>Total</b>	<b>1015</b>	<b>4.21</b>	<b>(1.73)</b>	<b>4.68</b>	<b>(1.63)</b>	<b>+ 0.47</b>
SOLAR PV	1	255	5.65	(1.30)	5.60	(1.40)	- 0.05
	2	253	5.53	(1.43)	5.71	(1.35)	+ 0.18***
	3	252	5.71	(1.36)	5.80	(1.17)	+ 0.09
	4	255	5.67	(1.35)	5.55	(1.36)	- 0.12
	<b>Total</b>	<b>1015</b>	<b>5.64</b>	<b>(1.36)</b>	<b>5.67</b>	<b>(1.32)</b>	<b>+ 0.03</b>
WIND	1	255	5.40	(1.53)	5.44	(1.49)	+ 0.05
	2	253	5.49	(1.43)	5.74	(1.28)	+ 0.25***
	3	252	5.46	(1.42)	5.63	(1.32)	+ 0.17**
	4	255	5.45	(1.37)	5.53	(1.38)	+ 0.07
	<b>Total</b>	<b>1015</b>	<b>5.45</b>	<b>(1.44)</b>	<b>5.58</b>	<b>(1.37)</b>	<b>+ 0.13</b>

Mean scores: 1 = strongly disagree, 4 = neither agree nor disagree and 7 = strongly agree (paired t-test \*p<0.05; \*\*p<0.01; \*\*\*p<0.001)

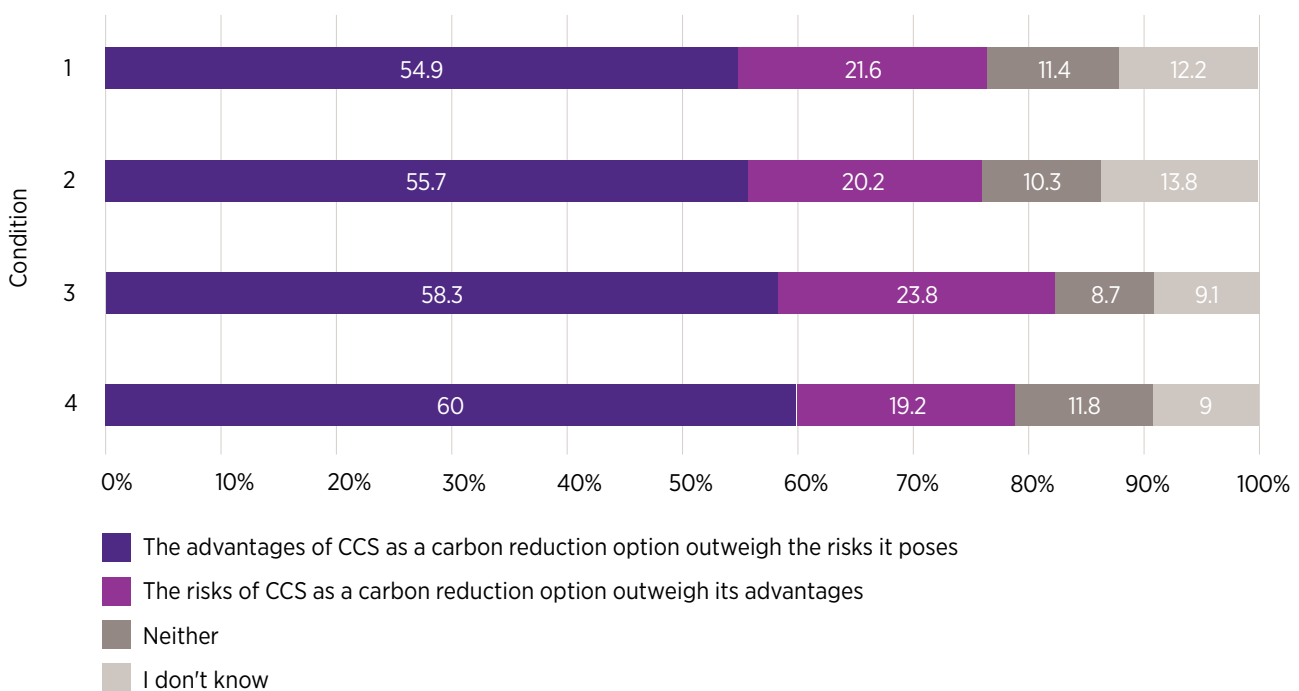
Self-reported levels of knowledge about types of CO<sub>2</sub> mitigation methods, which included several energy technologies, appeared to be associated with support for different energy technologies, in line with similar findings from our national survey. Across all countries, participants indicated that they had the highest self-reported levels of knowledge (on a scale of 1 = Never heard about it to 3 = Know it very well) of solar energy ( $\bar{x}$  = 2.50) and wind energy ( $\bar{x}$  = 2.40), and lower levels of knowledge of CCS ( $\bar{x}$  = 1.65). Participants who indicated that they had higher levels of knowledge about CCS also indicated that they had higher mean pre-information levels of support for CCS, notably in China ( $\bar{x}$  = 5.27) and India ( $\bar{x}$  = 5.23). Our findings further confirm that support of an energy technology is influenced by exposure and familiarity.

### 3.3.2.3.2 Perceived risks and benefits of CCS

Across all four conditions, more than 50% of participants indicated that they thought the advantages of CCS outweigh the risks, and this increased slightly (but not significantly) by condition (Figure 13). The results for participants in condition 1 and 2, who viewed the video only, were almost identical. In comparison, the proportion of participants in condition 3 (video and CCS factsheet) who thought that the advantages of CCS outweigh the risks increased slightly, as did the proportion of those who thought that the risks outweigh the advantages. Sixty percent of participants in condition 4 (video, CCS factsheet, and power plant comparison factsheet) thought that the advantages outweighed the risks. In both conditions 3 and 4, it appears that information provision had the effect of increasing the proportion of participants who thought that the advantages outweigh the risks, and reducing the proportion of participants who indicated that they don't know whether the advantages outweigh the risks, or vice versa. However, providing objective information about CCS in condition 3 appeared to slightly increase the perception of risks, while adding a comparison of CCS and other energy technologies in condition 4 appeared to reduce concerns about risks. Across all conditions, participants who said they had higher levels of knowledge of CCS were more likely to have firmer views and see either advantages or risks, and were less likely to indicate 'neither' or 'don't know' ( $\chi^2$ ,  $p < 0.01$ ).

**Figure 13** Perceptions of the advantages versus the risks of CCS.

**When you think about carbon capture and storage (CCS), what first comes to mind?**



Pearson  $\chi^2(9) = 7.3534$  Pr = 0.600

Perceptions of specific potential risks and benefits of CCS followed a similar pattern. Across all conditions, participants indicated that the key risks were that CO<sub>2</sub> capture leakage would cause ecological damage (scale of 1 = strongly disagree to 7 = strongly agree:  $\bar{x} = 4.80$ ) and that the technology was still in the developmental stage and relatively immature ( $\bar{x} = 4.83$ ). Participants in conditions 1 and 2 indicated that the main benefit of CCS projects was jobs creation ( $\bar{x} = 5.19$  and  $\bar{x} = 5.28$ ), while participants in conditions 3 and 4 agreed the main benefit of CCS technologies was environmental protection ( $\bar{x} = 5.41$  and  $\bar{x} = 5.37$ ). Generally, participants in conditions 3 and 4 reported slightly higher mean scores for all benefits and slightly lower mean scores for risks than those in conditions 1 and 2, so it would seem that providing more information helps to slightly reduce perceptions of risks and increase perceptions of benefits. Participants also indicated that they thought CCS is more beneficial for future generations (scale of 1 = not at all beneficial to 3 = very beneficial:  $\bar{x} = 2.55$ ), than for participants personally ( $\bar{x} = 2.14$ ), or for their country's society ( $\bar{x} = 2.41$ ). Mean scores were almost identical between conditions, and similar across countries. In addition, participants agreed that their government should formulate CCS-related laws, regulations and standards (scale of 1 = strongly disagree to 7 = strongly agree:  $\bar{x} = 5.32$ ).

### 3.3.2.3.3 Trust in sources of information about CCS and trust in institutions to monitor CCS sites

Participants were asked to indicate their level of trust in sources of information about the risks and benefits, and pros and cons of CCS (on a scale of 1 = not at all to 5 = trust a lot). While the results did not vary between conditions, they did vary by country, as might be expected. Levels of trust were very similar in Australia, the UK and the US, and were highest in India. Across all countries, there were generally higher levels of trust in university researchers ( $\bar{x}$  = 3.85) and in publicly funded research organisations (e.g. CSIRO in Australia) ( $\bar{x}$  = 3.68), followed by non-government organisations (NGOs,  $\bar{x}$  = 3.52). Trust in energy companies that operate CCS sites was highest in India and China ( $\bar{x}$  = 4.08 and  $\bar{x}$  = 3.62), compared to an average mean of 3.15 in Australia/the UK/the US. Average levels of trust in government at local, state and national level were closer to neutral, but were notably higher in India than in other countries (no questions about the government were included in the Chinese version of the survey). It is worth noting that India scores highly on the Power Distance dimension of Hofstede's Six Dimensions of Culture, indicating an appreciation for hierarchy and respect for authority (Hofstede Insights), and that this may account for some of the difference in levels of trust. In all countries, a neutral and technically qualified third-party monitor was more highly trusted to monitor the safe operation of CCS sites ( $\bar{x}$  = 3.83) than for energy companies that operate CCS sites or the government.

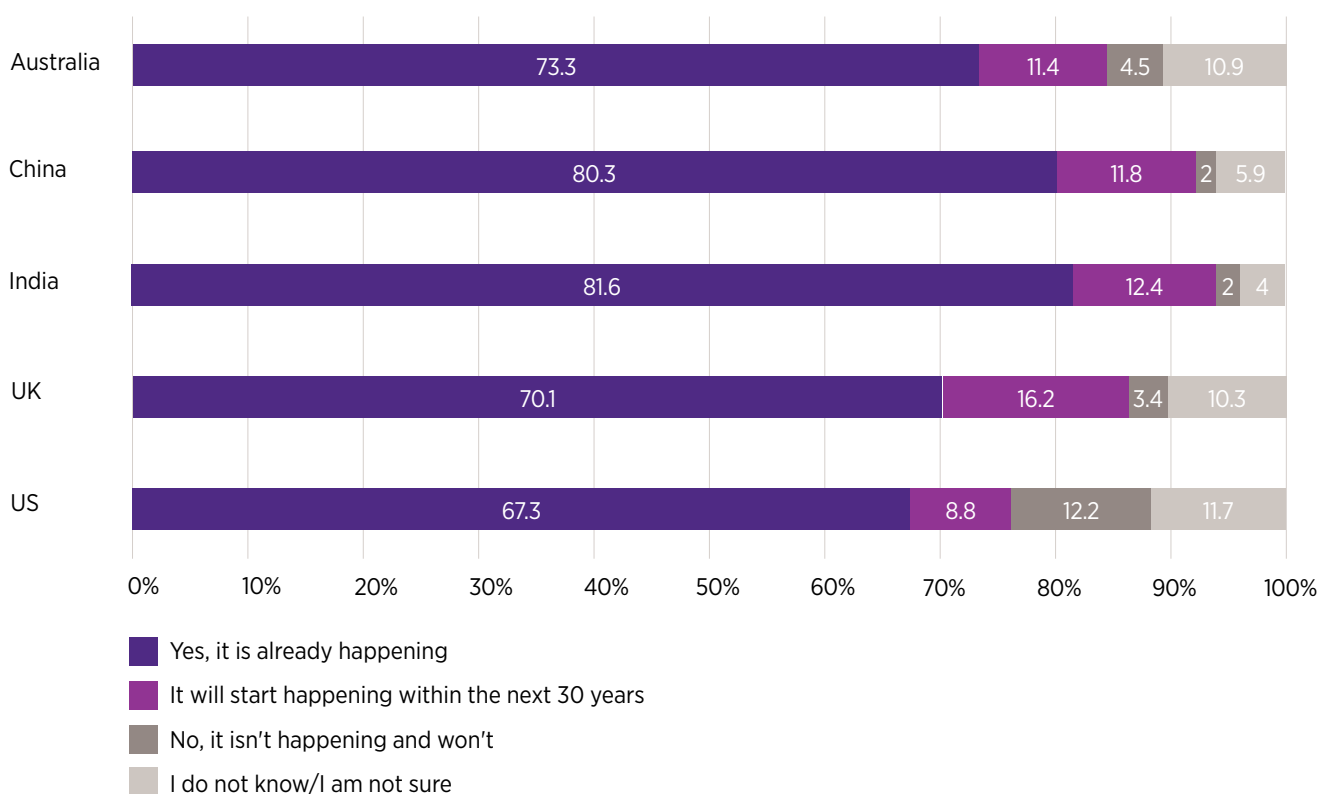
Participants were also asked to rate the information presented in the video and the two factsheets on three dimensions: legitimacy (1 = not at all legitimate to 5 = definitely legitimate); effectiveness (1 = definitely not effective to 7 = definitely effective) and trustworthiness (1 = not at all to 5 = trust a lot). Across the dimensions, all mean scores were above neutral, indicating that participants thought the information presented was somewhat legitimate and effective, and that they somewhat trusted the information. Participants suggested a variety of preferred formats for information about CCS, including educational information. Videos, media articles, and research articles were the most frequently listed.

### 3.3.2.3.4 Belief in climate change

At the international level, climate change mitigation has been a key motivating factor for CCS and its ongoing development. UQ-SDAAP was interested in exploring differences between countries regarding belief in climate change. As shown in Figure 14 below, a significantly higher proportion of participants in India (94%) and China (92%) believe that global warming is happening now or will start happening in the next 30 years, compared to the US in particular, where almost a quarter of participants reported either that global warming is not happening (12%), or that they don't know/are not sure (12%). In the Australian sample, 73% of participants agreed that global warming is already happening, which is slightly higher than the national average in the 2017 survey where 69% agreed it was already happening (Nisa et al. 2018).

**Figure 14** Belief in global warming, by country.

**Do you believe global warming is happening now or will happen in the next 30 years?**



## 3.4 Attitudes to groundwater and potential benefits the injection of CO<sub>2</sub> could have on improving water accessibility

**A potential benefit of injecting CO<sub>2</sub> is that the plume may help enhance water recovery in the nearby areas. It does this by putting additional pressure on the aquifer at the injection site, resulting in the water being pushed further along, in this case, to potentially more accessible locations for many stakeholders in the area.**

Early indications are that the process may help increase water levels up to 100 km away from the re-injection site.

While the prospects of this process are encouraging, the project team believed that there may be concerns which would need to be addressed concerning implementation of this new technology. This is an essential step in gaining public confidence and ensuring the process is endorsed by local stakeholders.

A number of focus groups were set up to test the concept on a range of stakeholders, including those with a direct interest, a sample of the general public less impacted by the process, and a sample of policy makers.

### 3.4.1 Focus groups

#### 3.4.1.1 Introduction

A core component of this research has been assessing the potential of the Surat Basin for storing CO<sub>2</sub> especially because of its proximity to some coal and gas fired power plants with an expected lifetime use out to the 2040s and '50s. However, the Surat Basin is also well recognised for its strong agricultural base with much of its water being supplied by the Great Artesian Basin (GAB).

It was timely to test the concept of using the injection of CO<sub>2</sub> for enhanced water recovery (EWR) on a range of stakeholders, including those with a direct interest in the GAB, a sample of the general public less impacted by the process and policy makers.

While farmers in the area have enjoyed unlimited access to free-flowing water from the GAB, with the noticeable drop in water levels of the GAB, more recently there has been a concerted effort by the Queensland Government and other stakeholders to ensure all bores are metered and overall water use is more closely monitored. Since 2015, in an effort to stem the decline in water levels of the basin, the CSG industry has been trialling the use of managed aquifer recharge (MAR) processes. Its trials have used fresh water obtained from their reverse osmosis plants. Early results have indicated that this process has been successful with increases in water levels being observed up to 100 km away from the re-injection site.

To further test the concept of re-pressurising water in the GAB, the technical team have also undertaken modelling to see if injecting CO<sub>2</sub> into the aquifer would bring about a similar result for EWR. The early modelling results have been promising. It was important to test the concept of using the injection of CO<sub>2</sub> for EWR on a range of stakeholders. The identified stakeholders included farmers, landholders and towns-people with an interest in the GAB being located in the Surat Basin area, the general public living in Brisbane and therefore less impacted by the process, and Queensland policy makers.

The main objectives of the focus groups was to:

- Identify participants' current knowledge and understanding of water use and perceptions of the GAB
- Identify participants' current knowledge and understanding of MAR
- Identify participants' current perceptions and attitudes towards climate change
- Identify participants' current knowledge and understanding of carbon capture and storage (CCS)
- Document participants' perceptions of the risks and benefits of CCS
- Record the technical questions participants already have about MAR and CCS
- Document participants' responses when presented with information about new understandings of the GAB, and the possible role of CCS in EWR as a component of MAR

- Identify barriers and enablers to the proposed uses of CCS in EWR
- Ascertain the key challenges for acceptance, perceived concerns and opportunities, and the trade-offs participants would be willing to consider
- Determine other questions/further information they would like/need to help them in their decision making and to feel more comfortable
- Ascertain the types of topics they believe might need more research

### 3.4.1.2 Focus group methods

A series of focus groups of approximately 2.5 hours in length in Toowoomba (1), Chinchilla (2), St George (1), Goondiwindi (1) and Brisbane (1) were run in October and November, 2018. Note that one of the Chinchilla groups had members of the Great Artesian Basin Sustainability Alliance which meant many of those were very knowledgeable about the concept. Of the two Brisbane groups, one of these focused on policy makers who worked in the water space and also had a solid understanding of the GAB. Because of their position in policy, their responses are reported below separately in this section. Recruitment for the focus groups used a variety of methods including emails to key bodies working across the GAB as well as personal emails and use of a marketing recruitment company.

On arrival, participants were asked to complete a short survey at the beginning of the focus group to better understand their views before any information was presented. After some initial discussions about the GAB and individual responses to it, they were provided with short videos on climate change<sup>12</sup> and CCS<sup>13</sup>. Following some discussion on their reactions to the video, our hydrogeology and CCS expert, Professor Jim Underschultz, provided an overview of the concept of MAR and EWR using water reinjection and CO<sub>2</sub> injection (Ferguson et al. 2019b). Following the presentation, participants were led through a series of questions to understand their responses to the concept of using CO<sub>2</sub> injection for EWR.

In total, seven focus groups were run. Six of the focus groups were conducted with the general public and group size ranged from four to 12 participants resulting in 47 members of the general public participating in the research. Another 10 individuals attended a focus group in Brisbane which was run specifically for policy makers.

### 3.4.1.3 Sample demographics

The general public focus groups were made up of 55% male participants, and average age of the group (n=46) was 52.5 years of age. The participants shared a range of education levels with 18 achieving Year 12 (n=5) or below (n=13) and seven reporting having attained a certificate education. Of the rest, seven had an Advanced Diploma/Diploma; another seven a Bachelor or Honours degree and eight had attained a Postgraduate degree. Twenty of the participants identified as either farmers, graziers and landholders or some combination of these. Another 18 identified themselves as town/city residents. Three were business owners, one a community member and four identified themselves as students living in the city.

Ten policy practitioners from relevant Queensland and Australian Government departments participated in a focus group in Brisbane in late October. Unlike the other focus groups, participants were selectively invited to participate, based on their roles and experience relating to water and/or CCS and connected areas such as mining, risk assessment, resource policy for agricultural land use, and water health. Several participants had extensive experience with community engagement. Eight participants were male and two female, and the majority were at the senior or principal policy officer level.

### 3.4.1.4 Results

#### 3.4.1.4.1 General public results

##### Understanding of the GAB and sustainable water use

As shown in Figure 15 below, water was the key word that arose in response to the written survey question: *What is the first thing that comes to mind when you hear the words Great Artesian Basin?* Further analysis of the written comments revealed 75 different responses. Coding these into themes revealed 16 referred to the GAB as water, while another 12 were more specific referring to it as an underground water resource and two of those specifically mentioning the word aquifer. Similarly, there were 11 who recognised its large or huge size. Another 10 noted the precious nature of the GAB as a water resource with another eight specifically noting the need to preserve, protect and manage it with these six also noting current *unsustainable* use of the Basin. There were another six who mentioned the value it provides to Australia as an economic resource and five also noted the links between the GAB and the agriculture and farming sector. One mentioned links to school.

<sup>12</sup> BoM & CSIRO: State of the Climate 201

<sup>13</sup> Zero emissions platform: The hard facts behind CO<sub>2</sub> capture and storage





When asked about the meaning of sustainable water use, the main response was about re-use, not wasting water and having water available for generations to come. It was observed that many people do not seem to understand this term. Again, there were suggestions that those living in the country were more likely to conserve water than city folk who are less immediately impacted by droughts and water levels. That said, most of those who were in the Brisbane focus group were aware of the need for water recycling and reuse. However, they also noted that it can be difficult and although the intent to conserve and reuse water exists, it does not always happen in real life.

“ So, sustainable water, at our home, is all about re-using that water as many times as possible before it goes out onto the fruit trees and all of that. FG002

To me sustainable means for the long, long term. Not just for a lifetime or a generation or my farming career or whatever. To me it means water supply that we understand and can look after well enough to know that it's sustainable for generations. FG005

I think a lot of people are aware that we should make sustainable use of water, but in reality it's like – we are suggesting to use our washing water to irrigate the grass – but in the reality it's like people don't and it wastes to the drain. FG007

### Thoughts on climate change

As noted previously, climate change mitigation has been a key motivating factor for CCS and its ongoing development. To understand the participants' views in relation to climate change, on the pre-survey they were asked the question “Do you believe global warming is happening now or will happen in the next 30 years?” Of the 42 usable responses there were 31 (74%) who agreed that yes, it is already happening; three (7%) who disagreed and felt no, it was not happening and won't; while eight (19%) responded that they did not know or were not sure. Note that the number of those who agreed was slightly higher in the focus groups than the national average in the earlier survey where 69% agreed it was already happening (Nisa et al. 2018). However, in the national survey another 9% felt climate change would start happening in the next 30 years.

**Table 14** Do you believe global warming is happening or will happen in the next 30 years?

	18 - 34		35 - 54		55+		Total	
	No.	%	No.	%	No.	%	No.	%
Yes, it is already happening	7	87.5	6	50	17	81	30	73
No, it is not happening	0	0	2	17	1	5	3	7
I do not know/I am not sure	1	12.5	4	33	3	14	8	20
<b>Total</b>	<b>8</b>	<b>100</b>	<b>12</b>	<b>100</b>	<b>21</b>	<b>100</b>	<b>41</b>	<b>100</b>

Pearson chi2 (4) = 5.1555 Pr = 0.272

The quotes below represent some of the themes that emerged when discussing climate change across the focus groups. In the regional groups, some participants were less comfortable discussing the issue of climate change as it seems they attributed a level of blame from the city folk for their use of water and the land. This was also reflected in a feeling of unappreciation of the role of agriculture in both providing food for Australia as well as exports.

“ I listened to what science has got to say, and I'm only alive now because of what scientists have done for cancer treatment which I've had, so I believe in what the scientists say and the numbers, and 97% agree that climate change is happening. FG001

Science and agriculture are continually going up against each other. And usually agriculture is getting a knock on the head which I think's quite wrong. FG005

Regardless of all these things we've talked about, how do we deal with that amount of CO<sub>2</sub> in the next 30 years? FG005

## Responses to CCS

The brief survey included a question about the potential advantages and risks of CCS. Table 15 (below) demonstrates that participant's perceptions of CCS, prior to the focus group discussion and technical presentation, were mixed. Of the 38 useable responses, nearly half of participants (45%) did not know if the advantages of CCS outweighed the risks or vice versa (45%). Around one-third of participants (34%) felt that the risks outweighed the benefits, and of these participants, 75% were aged 55 years and above.

**Table 15** When you think about carbon capture and storage (CCS), what first comes to mind?

	18 - 34		35 - 54		55+		Total	
	No.	%	No.	%	No.	%	No.	%
The advantages of CCS as a carbon reduction option outweigh the risks it poses	3	37.5	0	0	1	5.3	4	10.5
The risks of CCS as a carbon reduction option outweighs its advantages	0	0	3	27.3	10	52.6	13	34
Neither	1	12.5	1	9.1	2	10.5	4	10.5
I do not know	4	50	7	63.6	6	31.6	17	45
<b>Total</b>	<b>8</b>	<b>100</b>	<b>12</b>	<b>100</b>	<b>21</b>	<b>100</b>	<b>38</b>	<b>100</b>

Pearson chi2 (6) = 13.68, Pr = 0.033

Participants were first exposed to the concept of CCS through the zero emission platform video and then subsequently as part of the expert presentation which focused on MAR using either the reinjection of water or CO<sub>2</sub> to raise water levels in the basin. Across the groups there were varying levels of knowledge and familiarity with the concept of CCS. Despite this the questions that arose in relation to CCS were quite similar to previous research in this area.

The major themes that arose centred around safety. Would it stay underground and what might be the risks if there was a leak? Does seismicity affect storage, or conversely can CO<sub>2</sub> injection cause a seismic reaction? What will it cost? How efficient is CCS, and what is the power required? Who pays? Who is responsible for monitoring? Is it just a band-aid solution? Can we trust the science? How much space is there for storage and how long will that last? How is it converted to liquid? How is it transported?

The quotes below reflect some of the themes that arose in the discussions:

“ Just safety and storage again coming – leaking back up to the surface. Sustainability of keeping it there. FG001

And I guess one way is just to, you know, bury it – put it aside and bury it. That will bring our targets down. So I wonder about the politics behind all of this. FG003

Who is doing it – where is the funding possibly coming from? And would it be open season for private companies? Who is leading it or running it would influence whether I'd approve of it. Who is benefitting? Who is profiting? FG007

I probably want more research into the health and environmental impacts, and how it's going to affect the water. But it is still only a band-aid solution and there's only so much space. FG007

## Responses to MAR

When asked how many had heard of the term MAR approximately 18 of the participants across the groups indicated they had. However, there were varying depths of knowledge about the concept, with some very knowledgeable and others only having just heard of it. Once presented with an explanation of the concept, many of the participants were quite receptive to the idea. Most participants saw great benefits with raising the water levels to enable easier access and obviating the need to build deeper wells. However, this was with the caveat that it would not mess with the existing water and that ongoing management principles were in place to ensure more sustainable use. This is reflected in the quotes below:

“ I was quite shocked about the increase in CSG water for the last 2 years, and it's a good example for me because I hadn't heard anything about it. And the people there don't seem to be suffering any ill health... FG007

You've got to give them a bit of credibility that they weren't bugging everything. Some are pumping – the QGC mob are pumping their water to the Glebe Weir and I'm one of the recipients along – the pipeline goes through my place. I'm using that water for stock and domestic. Nothing wrong with it. FG003

I've got no problem with reasonable quality water being put back in to recharge it. Because we took it out, so we should just put it back where it came from. FG003

This is putting water back in? Yeah, I think it's a great idea. FG001

Reactions to the use of CO<sub>2</sub> for enhanced water recovery were generally more cautious. Some questioned whether it would have a negative impact on the overall sustainable use of water from the GAB. Other participants suggested that it should not be considered as an option at all. However, there were others who were more positive and thought that it was worth exploring for the benefits of reducing CO<sub>2</sub> and enhancing access to water. That said, it was recognised in several of the groups that the concept of making water easier to access with CO<sub>2</sub> was not sustainable, particularly in light of the earlier discussions about the meaning of sustainable water use.

“ So I'm hoping that if we do recharge – which I think is a wonderful idea – that we're very, very careful about what we're recharging with. FG005

My question at the moment is if you're pumping this gas down into the Great Artesian Basin, are you just not making it easier to extract the water one way or the other so that it is going to run out sooner one day down the track? FG001

Unsurprisingly the biggest concern was the potential for the CO<sub>2</sub> to leak or mix with the fresh water causing fresh water in the GAB to become more acidic, rendering it useless for agricultural use. It is safe to say that being able to guarantee water quality would not be affected was the number one concern for all participants. The quotes below reflect the sentiment of the discussions surrounding this point:

“ Those sorts of things lead me to absolute conviction, if there's such a thing, that we shouldn't be mucking around with it. Leave the CO<sub>2</sub> out of it. FG003

So this contaminating the water, which A1 touched on then, you don't want to be putting anything down there that's going to damage what is there. That's number one concern. FG004

What if things move as the earth moves and there is a fault, what happens with that CO<sub>2</sub> when it hits Great Artesian water? FG005

Who would be managing the risks and who would claim it if anything did happen? FG007

“ It needs to be put on the table. It needs funding. They’ve got to do something with it. I’m not really excited about it in the basin but if that’s the best spot for it. FG002

But the concept, I think it’s great. It’s a great concept. You’re sort of killing two birds with one stone. You’re getting rid of the emissions out of the atmosphere and storing them down in the – somewhere down there. FG004

### Broader issues in relation to CCS

As the discussions ensued in the groups, there were a number of broader considerations that arose in relation to CCS. The points below reflect what participants felt would be important if CCS was to have any chance of success over the longer term. That is not to say that all were supportive of the concept. However, they recognised that like any new technology which has perceived risks and concerns, there were important conditions that are essential to take into account. In no order of priority, these included:

- Developments in science and technology learning – *people’s perceptions change and people understand, as generations go on, people understand processes better*
- A need for bi-partisan support, the power of politics and vested interests – *I often think that science is like, the Science Minister is working against the Agriculture Minister, you know what I mean? They just do not seem to come together*
- The need for education – *And it’s that awareness raising that needs to be done throughout the community, not just with the kids*
- Not In My Backyard (NIMBY) – *Public perceptions in our western society is that I think we all talk about these things, but underneath that is the, but I don’t want it to affect my lifestyle. Or like, put your dump out there but not here*
- First mover disadvantage – *We can do something here in Australia that helps the environment but adds to the cost of our production, and if another country is using poor practices and human rights poor practices to produce something, we’re the ones over here that will still go and buy that cheap t-shirt*
- Track record and lack of trust – *But the implementation of quick emotive short-term solutions by governments and vested interests makes me fearful*
- The potential for unintended consequences – *It seems feasible if we can monitor water, but I keep thinking about cane toads and rats*
- The need to explore trade-offs – *In my opinion, before you ever sink that sort of money, you’re talking big dollars, which someone said before, but that big dollars could be spent on batteries and solar panels*

#### 3.4.1.4.2 Policy maker results

##### Observations of lay public attitudes to the GAB and sustainability

Policy makers noted they had seen a big change in both general public and landholder attitudes towards water since the Millennium drought. However, their perceptions were that people still do not understand the concept of sustainability; that they are more focused on local concerns and less interested if their area is not directly impacted; and that they do not think long-term enough, e.g. 500 years. They also observed that people do not understand the complexity of the GAB system, and that an accurate lay understanding of the GAB is very important in terms of management of the GAB. Participants even suggested the need for another surrogate term for sustainability in the GAB (for the lay person) as the traditional concept of water sustainability (i.e. recharge and discharge), does not work in the GAB where sustainability is about maintaining pressure rather than recharge = discharge. They also noted that there is a problem with the way the media describes and reports the GAB, and that education is needed for both media and lay public. However, they were adamant that this is not due to a lack of available materials about the GAB, or about water and sustainability.

##### Knowledge and support for MAR with water

Around half of the group were familiar with the concept of MAR. Overall, perceptions of MAR were positive. Policy narratives have more recently shifted to water storage, or ‘banking’ after excess surface water events. In light of climate change predictions of longer droughts and more severe rainfall events, it was acknowledged that there will be more demand for storage, and with no significant new dams planned in the future, MAR can also help to offset evaporation from existing dams. Participants observed there is a lack of a policy framework or incentives for MAR in Queensland at present, despite having some of the largest MAR projects in Australia. The discussion included potential impacts on water quality and risk management obligations. It was felt that social licence to operate considerations were also an issue, best evidenced through the discussions around recycled water.

### Knowledge of and support for CCS in EWR

All participants had heard of CCS, however their knowledge about the technology and the process for storing CO<sub>2</sub> was generally limited. There was mixed support for CCS, and major concerns centred on both short and long-term risks, trade-offs, costs and regulation. This included the difficulties for policy practitioners to guide risk assessments for what is seen as a relatively new, innovative, unproven and unknown technology in Queensland. It was suggested that, technical feasibility and general pushback to new technologies aside, the real struggle is dealing with public perceptions and difficulties with communicating or selling the concept of CCS.

Participants felt that using climate change mitigation as the driver for CCS could be problematic. As one participant explained:

“...When you explain this driver to them [to landholders], they’ll say, “What are you talking about and why are you coming in my backyard to solve the world’s problems?” and that’s the kind of modern-day view. So how we communicate, and I think that’s where there’s already some debate and conversation about climate change, is it’s not real to them”.

Responses to the technical presentation echoed those of the community focus groups. EWR using CCS was seen as potentially feasible, with more research needed on risks and costs, as well as the need for drivers such as a carbon tax or financial incentives. Key technical issues identified were the risks to water quality and pressure changes, and the potential for an increased rate of water use and depletion. Some participants highlighted the importance of acknowledging competing uses in light of recent experiences with CSG.

“ (The GAB is) more than just a storage site for CO<sub>2</sub>, it’s an aquifer. The proponents of CCS haven’t tried to deal with that issue or address the fact that there’s competing uses.

Other participants expressed strong concerns that a freshwater aquifer could be polluted, with potentially negligible benefits for climate change mitigation.

Participants suggested that MAR using water was “a no brainer” and probably easy to sell to the community. However, some felt that the way CCS had been presented as part of EWR, without enough discussion of the risks and how to address them, “looked like one problem leading into another problem down the track”, particularly given the close analogies with CSG. There was concern that while MAR was much needed as a water storage solution, “it doesn’t help to link it to suggesting that it’s going to solve long-term drawdown problems in the GAB because it never will”, and that by linking MAR to CCS, it could potentially impair perceptions of and support for both. Given that the Queensland Government has put considerable investment into educating the public about environmental contaminants, it was thought likely that people would immediately see CO<sub>2</sub> as a contaminant. As one participant explained, people were already concerned “about stuff being injected into the Precipice [Aquifer] that wasn’t there before...it’s a real perception as well as a lack of knowledge”.

Participants highlighted the need to learn lessons from underground coal gasification, and understand the legacy issues: to recognise that people have a lack of trust in government and industry, and off the back of Linc [Energy], there is a lack of trust in the regulator. Some participants related experiences with landholders not believing data and emphasised that presenting information is not enough. Sometimes the community just won’t accept it and don’t respect where it has come from. One participant commented:

“ It doesn’t matter how good your science is, how good your data is...our country is paralysed on climate change... people don’t have the knowledge and they don’t know how to bring that into their everyday life.

There was a general consensus that there is a real need to increase the conversations in the public about these issues. Communication is crucial, and even if it’s good science, it will take a lot of education and time to get people to understand.

#### 3.4.1.4.3 Focus group conclusions

The results of the focus groups demonstrate that there is a mixed response to using CCS as part of an EWR process in the Surat Basin. While some participants were encouraged by the prospects of the process, it was clear across all groups, that there were a number of concerns that would need to be addressed if public confidence was to be gained and the process endorsed. It seems that policy makers and the lay public were in agreement on most of these. What will be critical is that communication about any of these topics will be paramount and opportunities to raise awareness of such processes should be implemented both at the community level, in schools and across larger society.

### 3.5 The impact of how CCS is reported in the media

The media, in all of its forms, has been shown to be a critical influencer on stakeholder attitudes. The information portrayed in the media can have a huge impact, both positive and negative, on attitudes towards technologies. Therefore, examining how CCS is being portrayed in the media, the issues that are being discussed and by whom, are important factors when considering further communication and engagement activities.

As part of the social research component, an analysis of global and Australian media coverage of CCS technologies was undertaken from January 2003 to 30 September 2018 using Factiva as our database for articles. The main aim of the analysis was to examine how the volume and content of global and Australian media coverage of CCS have changed over time and in response to events such as project and policy announcements.

The data analysed was a collection of 4668 media articles from 621 different sources. As can be seen in Table 14, the majority of the articles analysed came from Australia, the United States, Canada, and the United Kingdom with only limited coverage of media from Asian and non-English speaking countries. It is worth noting that the dataset does not necessarily offer a complete representation of media coverage in each country. Rather, it reflects the sources that Factiva happens to catalogue. Furthermore, the completeness of coverage is likely to vary from country to country. Compounding this effect is that only articles in English were retrieved, leading to the omission of many sources in countries where English is not the primary language. Finally, in our analysis no attempt was made to normalise the volume of coverage from each country against variables such as the population size or number of media outlets in the country.

**Table 16** The number of articles in the dataset, broken down by region and source type.

Source Type	Australia	United States	Other	Global	Canada	Western Europe	Total
Newspapers*	715	366	351	-	502	471	<b>2,405</b>
Wires: Newswires	221	40	261	630	162	62	<b>1,376</b>
Magazines & journals*	-	239	19	-	1	10	<b>269</b>
Websites: News	15	157	94	-	-	1	<b>267</b>
Unknown	2	74	94	72	-	-	<b>242</b>
Other	69	27	5	-	4	4	<b>109</b>
<b>Total</b>	<b>1,022</b>	<b>903</b>	<b>824</b>	<b>702</b>	<b>669</b>	<b>548</b>	

\*Includes both print edition and online titles

The dataset assembled contains media articles from many different countries in addition to outlets with a global distribution. Figure 16 summarises the geographic composition of the dataset, showing the intensity of coverage over time in each continental region. The figure also indicates the overall number of articles in the dataset from each region. Not included in Figure 16 are sources with a global distribution (these are primarily newswires), which account for a total of 702 articles. The data also excludes sources that are not available in Factiva for the full period shown. The data has been filtered in this manner to ensure comparability over time. However, filtering in this manner excludes much of the available data for some countries, especially those in Asia and Africa. Figure 16 therefore shows an incomplete picture of coverage from these regions, particularly in the years after 2008.

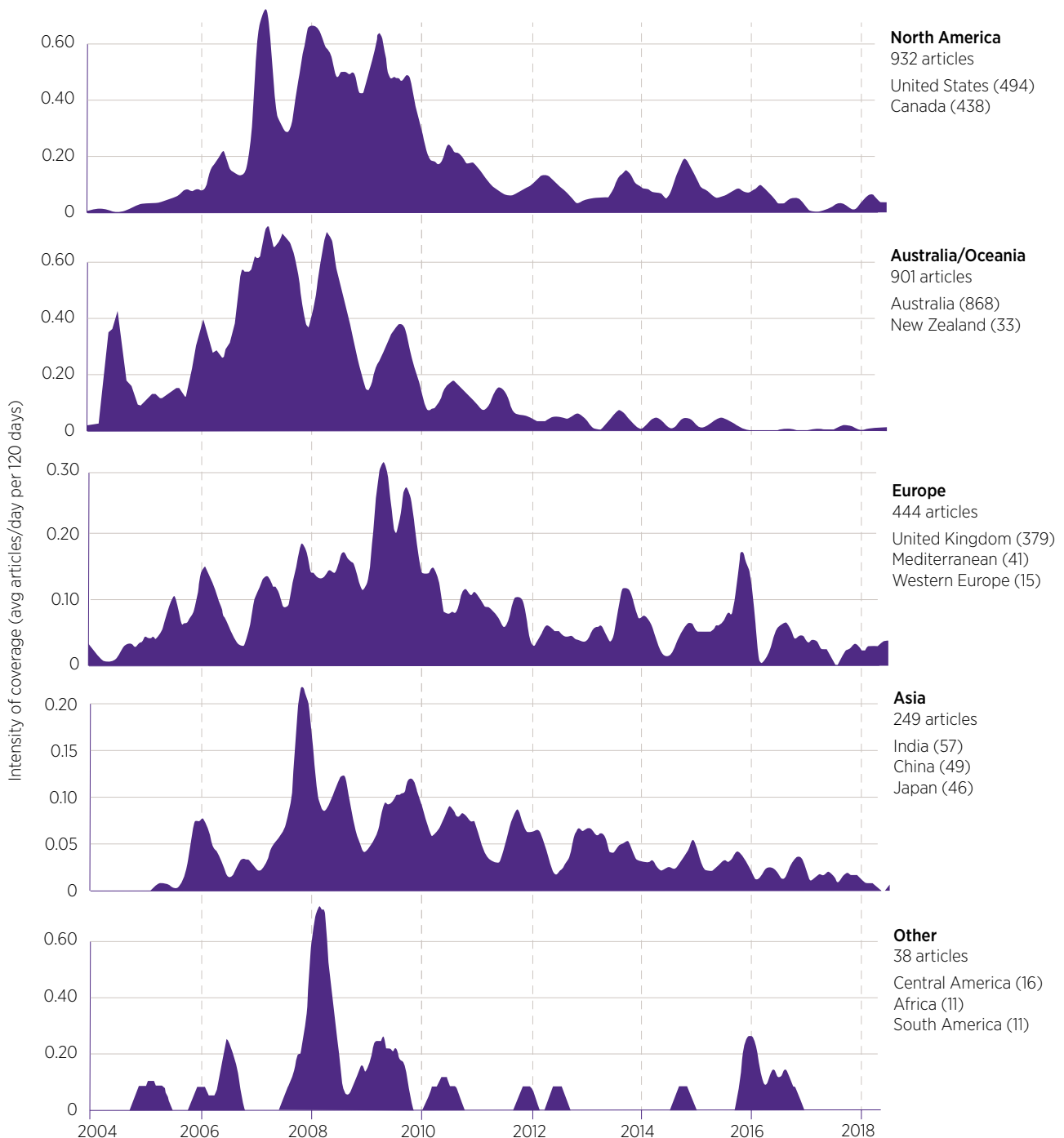
Globally, the volume of coverage of CCS started to grow in 2004 and reached its highest levels in 2007 and 2008. The volume of coverage dropped sharply in 2010 and has remained at relatively low levels ever since. Although relative to peak levels, the volume of coverage in Europe has not fallen as dramatically as it has in Australia and North America. Spikes in coverage have in most cases been driven by announcements about policies and funding arrangements relating to CCS projects. The data also shows that global relevant events, such as climate conferences, have generally not had much of an impact on the level of coverage of CCS.

When CCS is portrayed in the media, the most frequently mentioned persons are overwhelmingly political figures (presidents, prime ministers, premiers, governors) or government officials (chief scientists, secretaries for energy or environment). Researchers, climate scientists and resource company executives also feature in the coverage. Much less prominent are representatives of environmental and social advocacy groups.

The proportion of content relating specifically to geosequestration has declined since 2014. Meanwhile, the amount of content dedicated to other aspects of CCS, including carbon capture technologies and their integration with other industrial processes such as cement and biofuels production, has been steadily increasing since at least 2004. Also becoming more prominent in the coverage is content about alternative carbon sequestration methods such as direct air capture and soil sequestration.

The most frequently discussed topics in the global media coverage can be classified under two broad themes: *energy governance* (including the regulation of emissions and fossil fuels, and the funding and subsidisation of CCS and other power generation projects) and *CCS projects*. Together, these two themes account for about half of the content in the dataset. The proportion of coverage devoted to energy governance has declined gradually over time, perhaps reflecting a lessening of involvement from governments in supporting, financing and regulating CCS projects. Another prominent theme in the coverage (accounting for 16% of all content) is *climate and energy politics*. The prominence of this theme declined between 2006 and 2013, but since then has been rising, and accounted for more than 20% of all content in 2018.

**Figure 16** The intensity of coverage of CCS in major geographic regions\*.



\* Note that this data does not include sources with a global distribution or whose regional affiliation is unknown.

The trends in volume and content of coverage over time within the Australian media were broadly similar. However, relative to the peak level, the volume of Australian coverage dropped to even lower levels than occurred elsewhere. There are just 47 Australian articles in the dataset from February 2014 onwards. From January 2016, there are just 14 articles. The highest spike in coverage occurred in June 2008, when the then federal Resources Minister, Martin Ferguson, unveiled a world-first legislative framework for CO<sub>2</sub> geosequestration – a move that came on the heels of BP and Rio Tinto abandoning a geosequestration trial project in deep-sea formations near Perth. The last significant spike in Australian media coverage of CCS occurred in September 2009, after the then federal Environment Minister, Peter Garrett, granted approval to the Gorgon LNG project.

Many of the top terms in the Australian coverage were also prominent in the global coverage. One set of terms that is more prominent in the Australian coverage relates to carbon sequestration via land, soil, or trees. Also, more prominent in the Australian coverage between 2010 and 2014 is the word *community*. As with the global coverage, the Australian coverage of CCS up until 2010 was dominated by references to government actors. From 2010 onwards, however, individuals and organisations involved in scientific research and pilot projects appear to have received at least as much attention as political figures.

The amount of content discussing CCS projects is smaller in the Australian media coverage than in the international coverage, accounting for just 13% of content as opposed to 20%. This is unsurprising, given that no CCS projects in Australia to date have advanced beyond pilot and demonstration phases. More prominent in Australia, however, has been coverage about *geosequestration* and *climate and energy politics*, which account for 16% and 20% of all content respectively. Of the 14 Australian articles in the dataset published since January 2016, only eight relate to CCS in the sense being considered in this report. The remaining six relate to other carbon capture methods, including tree planting, soil sequestration, and direct air capture. Of the eight relevant articles, only one adopts an openly critical stance towards CCS, while three express a positive sentiment.

In the context of recent publications from organisations such as the IPCC and International Energy Agency, the findings suggest that there is something of a disparity between public and expert views towards CCS. At the same time as prominent experts in climate and energy policy are calling for renewed investment in CCS in order to avert dangerous climate change, most media outlets appear to have largely lost interest in the technology, or view it with increasing scepticism. The extent to which the media coverage examined here is reflective of public sentiment towards CCS cannot be determined from this analysis alone. However, these findings highlight the possibility that any moves in the short term by governments to invest heavily in CCS could be met with opposition from a sceptical and uninformed public.

The lack of coverage of CCS also highlights an opportunity for communication. If there was interest to raise awareness of the technology it would be possible to proactively engage journalists and associated media outlets to encourage more sharing of information and discussion. While this can be a double-edged sword if a journalist is extremely opposed to the technology, given the low levels of knowledge about CCS that have been identified in the survey work, providing some editorial pieces or project updates could provide a nice platform for raising the profile of CCS. This could be coupled with the identifying need and opportunity to attach CCS to existing coal and gas fired power plants which have a long lifetime ahead of them because of their more recent construction. Coupled with the knowledge from the message testing it appears there are some clear ways this communication could take place.



## 3.6 Important regulatory aspects of CCS in Queensland

The large-scale implementation of CCS would require the development, adaptation or modification of a number of regulations. This includes Queensland's existing green house gas (GHG) and environmental and water regulations. A regulatory roadmap needs to be constructed with the Queensland Government. Furthermore, interaction (if any) with the federal *Environment Protection and Biodiversity Conservation Act 1999* needs to be defined.

**The interplay of various state (and federal) legislation needs to be clarified by reference to a realistic, working case example. While this may be done in parallel with the next phase of site-specific data gathering, it must be done before any large investment decisions can be made on ultimate deployment.**

UQ-SDAAP's research focused specifically on the *Queensland* regulatory environment. The study has not addressed the matter of tenement award or the processes thereof. It is important for the state government to note, however, that the best, lowest risk areas identified by UQ-SDAAP appear to be within a single GHG storage exploration tenement EPQ-10. Careful governance of any award, assurance of suitable work plans and then of operator performance will be required to ensure this acreage is matured in a robust and timely manner and is available to large scale emitters.

Queensland policies, Acts and associated regulations allow for injection and storage of greenhouse gases (*Greenhouse Gas Storage Act 2009*). However, this legislation interacts significantly with a raft of other legislation. This includes sections governing the protection of the environment (*Environmental Protection Act 1994*), interference with groundwater resources (*Water Act 2000*) and the fate of any industrial wastes (*Waste Reduction and Recycling Act 2011*). Activities may also interact with federal legislation, most notably where it relates to conservation of biodiversity and sites, or possible water resources of national environmental significance (*Environment Protection and Biodiversity Conservation Act 1999*) if application of the existing 'water trigger' were to be extended.

The regulatory pathway in Queensland for industrial-scale GHG injection and storage in aquifers that have historically been defined as being part of the Great Artesian Basin, is not clear.

The target areas for injection are, however, in remote and very deep locations and are far removed from abstraction or economic use. The impact of injection operations on groundwater quality (lower pH) would be localised. However, the consequential upside is that water levels (pressure) would be raised over a very wide area, well beyond the tenements. With respect to water quality, changes to quality that renders it incapable of being used for agriculture or stock and domestic may be considered 'environmental harm', even if that water is too deep for economically viable abstraction. So, impacts to water quality within the GHG storage reservoirs and tenements will necessarily have to be authorised by the environmental authority under the *Environmental Protection Act 1994*. It is important to note that the relevant Acts do not authorise indirect impacts or impacts outside of the storage space. Certainly, they cannot authorise impacts off-tenement – beneficial or otherwise.

The key statute that governs hydraulic pressure changes and water quality is through the water-related legal and regulatory framework. However, there are multiple mechanisms in the overarching governance framework relating to GHG injection in Queensland that also plays a part in governing the incidental impacts of the activity, such as the emanating increase in formation. The UQ-SDAAP study suggests that the current framework may not successfully manage these, but that lessons from recent development experience in coal seam gas and other jurisdictions might be applied to improve it.

Technically, injection of GHG into groundwater aquifers (as promoted via Queensland's *Greenhouse Gas Storage Act 2009*) will be 'interfering' with those aquifers (as governed, for example, by the *Water Act 2000*) with implications for licensing and conditions thereof. 'Interfering' has a broad meaning and could include potentially beneficial as well as detrimental aspects. More clarity is also needed on whether CO<sub>2</sub> captured from flue gas would be categorised as a 'waste stream' of an industrial process (i.e. power generation).

The UQ-SDAAP study found that it would be important to conduct early engagement with the regulator in five key areas:

1. Whether a waste stream of CO<sub>2</sub> would be classified as an 'end of waste' product
2. Whether deep aquifer storage of CO<sub>2</sub> could be considered a public amenity. It is important to note that Managed Aquifer Recharge (MAR), as practiced by coal seam gas operator APLNG, is considered beneficial use
3. Whether remote pressure inflation or water level increases off-tenement would be recognised as a benefit and can be allowed through some appropriate instrument
4. Whether this benefit and/or GHG emissions mitigation could be argued to trade off against what might be classed as environmental 'harm' or changes to localised groundwater quality
5. It may be that water licences currently held by some extractors (mining, petroleum and gas resource extractors and, to a lesser extent, stock and domestic users and Aboriginal and Torres Strait Islander people) may need to be curtailed in the local injection area to prevent interference with an emplaced CO<sub>2</sub> plume

Pragmatically, it will be important to select injection sites with the lowest inherent environmental risk. The target aquifer would be as far removed from active abstraction bores as possible, and where they are so deep as to be beyond practical economic reach for other users.

The regulatory issues that require addressing in order to address large-scale CCS are clearly laid out, but are interlocked and complex to address. Focussed efforts around realistic deployment of projects should assist in defining a pathway, or at least in identifying where legislation might need to be amended.

## 3.7 Regional employment

Part B of this report, describes the potential for large-scale carbon abatement via CCS in Queensland through several scenarios (Section 4.14). High level analysis (Gamma Energy Technology, 2019) indicates that such a deployment might create around about 250 new regional jobs in the retro-fit and construction phase. In addition, a large-scale deployment could safeguard, or even extend the need for, approximately 500 existing regional jobs in the power plants and adjacent mines.

Indirect employment multipliers in the local economy have not been assessed in this study, however previous work has suggested this would be statistically significant (Fleming & Measham 2014), and in the range of 1 to 4 or 6 (Knights & Hoods 2009; and Rolfe, Lawrence & Rynne 2011).

## 3.8 Conclusion (socio-economic factors)

There are a number of clear activities that will be required to overcome the low levels of knowledge about CCS that exist in society. This will be particularly important in regional areas across the Surat Basin, if the CCS hub project was to be progressed.

Required actions, in no order of priority, include:

- **A clear regulatory roadmap.** To consent for large scale injection of CO<sub>2</sub> captured from industrial processes (e.g. flue gas) into the precipice aquifer. Clear support and cooperation from the state government. Clarity on federal government requirements
- **Further engagement** with local communities including influential stakeholders, local employees in mines and plants and associated jobs and schools
- **Raising awareness** at a national level. Research shows a clear link between knowledge of CCS and support for it. More active “blogs” are suggested focussing on baseload power needs, jobs and other CCS differentiators. Influential stakeholders need to be engaged across the regions. In particular, policy makers, both state and federal, will need to be included on the discussions about latest requirements and changes around regulatory requirements
- **Monitoring of attitudes.** Surveys started as part of this project should be repeated in 2019 and again beyond
- **Alternative message framing.** The early results of the experimental workshops and international survey provide some positive insights into how best to inform the public about CCS. These results need further investigation both at the local, national and international level

Further details about additional work are included in section 5.4.

Research shows a clear link between knowledge of CCS and support for it. Awareness raising is needed nationally.

# 4. Techno economic assessment of notional large-scale deployment

## 4.1 Guide to this section

This techno-economic assessment section of the report (section 4) starts by presenting a fundamental revision of the geology of the deepest and oldest parts of the Surat Basin (section 4.3). This section is key to understanding the data availability and the basic science that drives estimates of storage security and injection performance. Based on these observations and a revised geology, the concept of a subsurface ‘container’ is then developed to describe an area where CO<sub>2</sub> may notionally be injected at high rate for a limited period of time to be securely and indefinitely stored (section 4.4). The definition of a container is central to understanding the rate limitations of the basin and is needed to develop a “lowest risk” methodology for site screening. The likely dynamic response of the basin to large-scale injection is “calibrated” with substantial new evidence from many different and independent sources, this supports the case for *secure* long-term storage in the selected play and high-graded areas (section 4.5). Investigation of evidence for containment and identification of potential leakage modes or routes, together with a clear development philosophy (section 4.7.1) has been developed and risk-minimisation rules (rather than cost optimisation rules) applied. Finally, for CCS to be a valid climate change mitigation approach, there not only needs to be high confidence in containment; it must be feasible and involve *material* rates of CO<sub>2</sub> injection (section 2). Substantial, new and diverse evidence that relatively high rates can be achieved and sustained (section 4.6) has been used to calibrate the assessment.

All this evidence and analysis is brought together to lowest containment-risk potential injection sites (section 4.7). Then a feasible robust, notional field development plan is investigated with sound well engineering solutions which can reduce containment risk and surface footprint (sections 4.8, 4.10 and 4.12). There are no technical show stoppers. There are however localised (<10 km) groundwater impacts and more widespread, potentially beneficial, far-field pressure rises in the Precipice Sandstone which have been deeply investigated (sections 4.11 and 4.13). Given the regulatory uncertainties mentioned in section 3.6, significant engagement is needed on these impacts.

As a further sense check, sensitivities and notional pipeline routes have been investigated from the three main power plants (Millmerran, Kogan Creek and Tarong North – section 4.9). Scoping level capture scenarios have been evaluated (section 4.14) within an overall philosophy which results in a rolling, partial retrofit enabling both minimal disruption to power generation. The philosophy and roll-out concept result in a stage-gated investment pathway, avoiding the need to take “one very large” decision for full deployment. Impacts on LCOE, capital investment, and regional jobs are briefly highlighted).

To summarise the evaluation, the concept of dynamic capacity is elucidating and estimates from this research given along with a discussion on confidence levels (section 4.15).

The conclusions from these sections are that large-scale injection of around 12.7 million tonnes pa for 30+ years (and probably beyond the life of the existing, most modern plants) can likely be securely stored by injecting into the deepest, lowermost aquifer of the Surat Basin by transporting captured CO<sub>2</sub> by pipeline to two or three remote well pads. However, more site-specific data is required from these notional injection sites to increase technical confidence before development decisions can be made.

## 4.2 Introduction

Geological carbon storage concepts have historically been categorised into three main options: depleted hydrocarbon reservoirs; un-minable coal seams; and deep aquifers (Holloway 2001). Studies such as Nordbotten et al. 2005 have consistently demonstrated that deep aquifer storage by far represents the largest potential storage capacity globally. The experience from CO<sub>2</sub> injection at pilot projects (e.g. Frio in Texas, Otway in Australia and Nagaoka in Japan) and commercial operations (e.g. Sleipner, Snøhvit, In Salah and various acid-gas injection) show that CO<sub>2</sub> geological storage in saline aquifers is technically feasible (Michael et al. 2010). However, these projects are not necessarily representative of geological conditions elsewhere. Importantly, they have not been conducted at the very large, industrial scale (> 5 million tonnes pa) required to make material emission cuts at climate abatement scale. Therefore, site-specific characterisation and appraisal is required and the nature of this assessment or appraisal must consider data and studies required to increase confidence in industrial scale operations i.e. material rates and decadal durations of injection. This is not to say that appraisal must employ these rates over long durations, rather that the data gathered must allow for assessment of the dynamic response of the aquifer/seal complex for such a scenario.

Assessment of any geological formation for CCS potential has the fundamental objective of understanding injectivity, capacity and containment of CO<sub>2</sub> (Bachu et al. 2007). The development of a broadly applicable method for determining CO<sub>2</sub> storage capacity at an early stage of site selection and characterisation is a critical component for stakeholders to make informed decisions regarding the potential implementation of large-scale CO<sub>2</sub> storage. Historically, carbon storage capacity estimates have been based on static geological models with the capacity being a function of the available pore space with a discount defined by a storage efficiency factor (Bachu et al. 2007, Bradshaw et al. 2007 and Bachu 2008) and often couched in terms of the petroleum resources management system (e.g. SPE 2016) that also include economic and technical operational considerations. However, it has been noted that static-based capacity calculations have limited benefit in estimating dynamic 'practical capacity' (Garnett, Greig and Oettinger 2012: p. 353 & 441). The historic, static approach represents largely a fallacy of construction. For any proposed sequestration site or sites, the challenge at hand is not to sequester a given volume CO<sub>2</sub> but to sequester a given rate for a sustained, defined period. Static methods either fail to recognise that mitigation is a rate-governed challenge and/or make implicit assumptions that large static capacities can support a large sustained injection rate and that, somehow, sustainable injection rate is mainly a function of capacity.

UQ-SDAAP is therefore a departure from historic, *static* capacity related estimates and is an attempt to produce a dynamically calibrated storage assessment. It seeks to answer the questions: what injection rates are safely achievable, and where and how long can these be sustained? The project investigates fundamental geological properties that impact fluid and pressure propagation in the sub-surface, and incorporates new and extensive data sets from large-scale and long-term injection and production operations to provide a dynamic storage capacity estimate consistent with the geological environment, a notional field development plan and key risk minimising development principles.

This UQ-SDAAP techno-economic assessment of notional large-scale deployment of CCS in the Surat Basin relies on previous work that identified geological strata of interest for commercial-scale carbon storage in Australia and Queensland. The GEODISC program of the Australian Petroleum Cooperative Research Centre (APCRC) assessed and ranked sedimentary basins across Australia for their carbon storage potential relative to major point source emissions (Bradshaw et al. 2002 and Allinson et al. 2003) and identified that the Surat Basin has significant notional storage capacity. Further, Bradshaw et al. 2011 and Hodgkinson and Grigorescu 2013 high-graded the Precipice Sandstone to Evergreen Formation stratigraphic succession as the most prospective reservoir and seal pair in the Surat Basin due to good fluid flow properties, as well as pressure, depth, and temperature characteristics making the strata favourable for carbon storage.

This UQ-SDAAP study, builds heavily on previous investments made by Australian Government, ACALET and the Queensland Government. Between 2009 and 2010, the ZeroGen project evaluated the potential for large-scale CCS in the Surat Basin (Garnett et al. 2012: pp 363-469). That study concluded that the Precipice Sandstone to Evergreen Formation strata offered the most material, dynamic potential and that "...uncertainty rather than risk ..." (ibid, p.364) dominated the evaluation. The study also recommended a significant appraisal program (not since undertaken) with a specific focus on evaluating the possible interference of increasing injection pressure and groundwater systems (ibid, p.386). From a technical perspective, the study concluded that the "... greatest predictive uncertainties are (i) reservoir connectivity and hence the build-up of pressure over time and (ii) the facies intersected by the wells..." (ibid, p.428). These uncertainties have been significantly reduced by this research. An additional key, technical uncertainty (presence of faults) has been highlighted. UQ-SDAAP had initially intended to acquire extended well water production test data from legacy oil and gas exploration wells. However, this proved not to be possible. Technical issues and progress on clarifying regulations is described in Garnett 2019c.

Based on this previous work, the UQ-SDAAP project also focuses its techno-economic assessment on the Precipice Sandstone to Evergreen Formation strata of the Surat Basin of Australia with particular emphasis on a revision of geological fundamentals, calibration with extensive flow test data and on area-wide, groundwater impact assessment. It should be noted that within the Surat Basin, the Precipice Sandstone is often considered to be the lowermost aquifer of the Great Artesian Basin (Habermehl 1980).

The safe development of any natural resource is a combination of the given geological parameters and of engineering choices made such as well location, well trajectory, well count, site facilities operations and flow assurance. Storage fields will need to be operated within carefully studied pressure constraints and these together with a development plan which dictates the final estimates of sustainable injection rates, duration of operations and the basis of design for capture plants. Notional injection development scenarios are devised, which assume a ramp-up period as power plants are sequentially retrofit followed by continued injection for a sustained period of 30-40 years.

### 4.3 Precipice Sandstone to Evergreen Formation: Geology of the Surat Basin

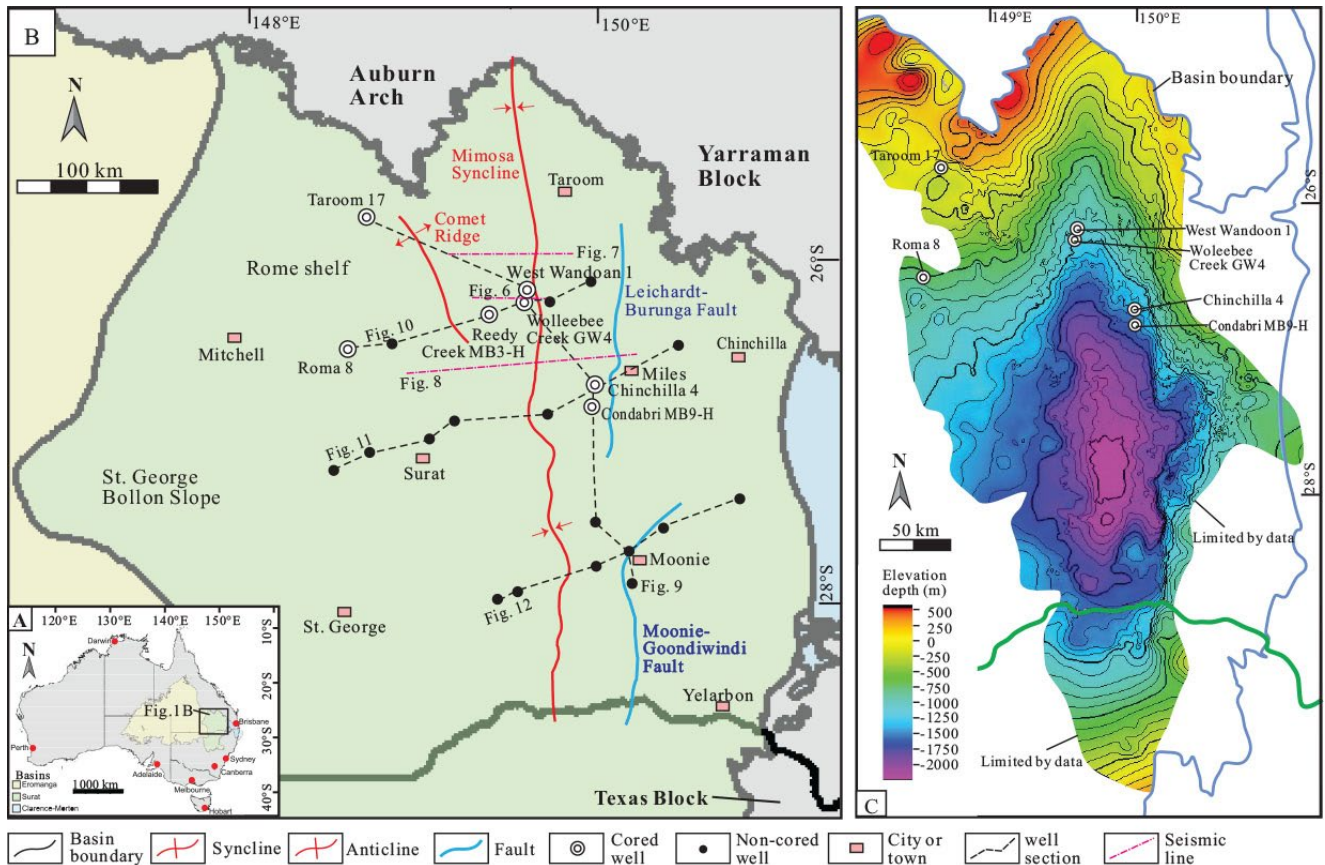
**Predictions of reservoir/aquifer and seal quality need to be made in areas in-between where well data exists. Making confident predictions requires that geological models to be built that are internally consistent with all the available geotechnical data as well as with fundamental geological concepts of how the geological environments were laid down, because this drives key correlative principles. UQ-SDAAP has used all data with both traditional and machine learning techniques to build a significantly revised geological understanding, resulting in much higher confidence in the containment and limited movement of any injected CO<sub>2</sub>. An overview of the main technical interpretations is given in this section.**

The concept of a “play” has been developed across a very wide region to define the aerial distribution of key geological strata. This geological revision has significantly improved confidence that notionally injected CO<sub>2</sub> would be securely contained. The play in question includes the Precipice Sandstone and Evergreen Formation that define the notional CO<sub>2</sub> storage container, and which represent the lowermost geological units of the Surat Basin. This new work (together with new modelling) has substantially underpinned an increase in confidence that a plume can be retained in a local area of the storage complex and that pressures can be managed within safe limits.

The Surat Basin has an area of ~327, 000 km<sup>2</sup> and stretches from 25° to 33° S, and from 147° to 152° E in eastern Australia (Figure 17). A series of structural highs separate surrounding time-equivalent basins – the Eromanga and Clarence-Morton basins (Power & Devine 1970; Exon 1976; Green et al. 1997). The Surat Basin developed as a shallow platform depression following uplift, exposure and non-deposition atop the Bowen and Gunnedah basins (Exon 1976; Green et al. 1997), and therefore partly rests upon Palaeozoic rocks.

UQ-SDAAP has used all data with both traditional and machine learning techniques to build a significantly revised geological understanding, resulting in much higher confidence in the containment and limited movement of any injected CO<sub>2</sub>.

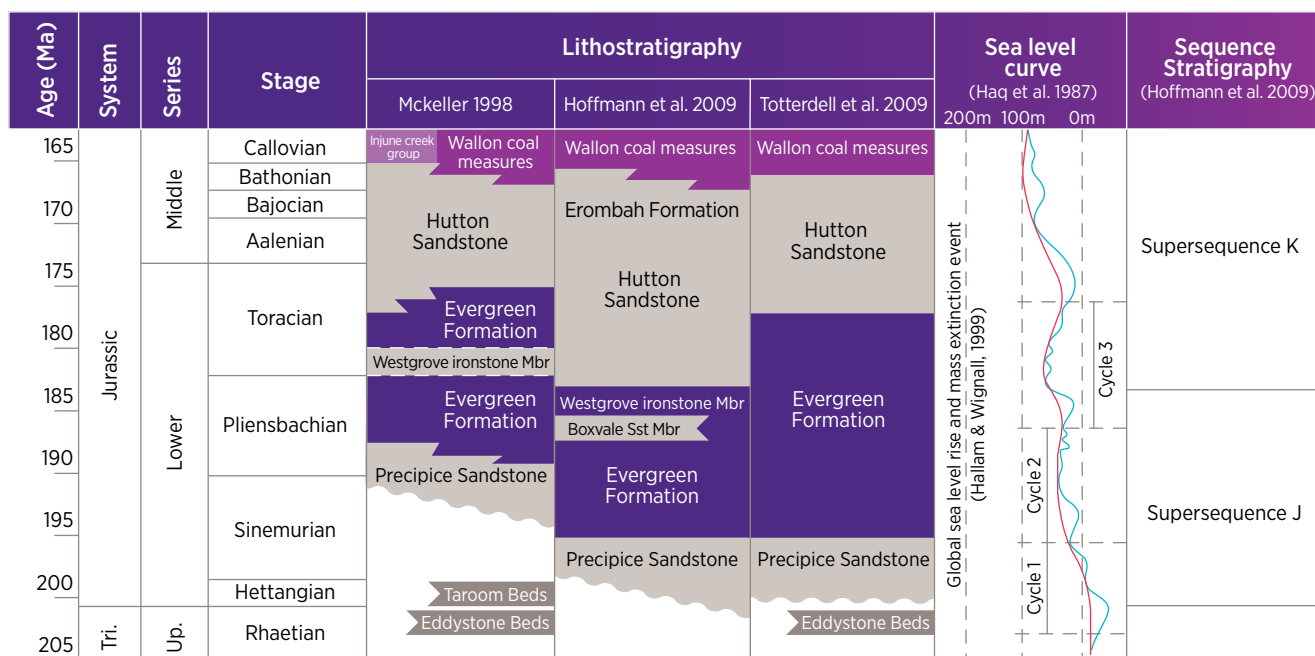
**Figure 17** (A) Geographic location of the Eromanga, Surat, and Clarence-Moreton basins in Australia. (B) The main structural features of the Surat Basin, and the location of wells used in cross sections, including the location of cored wells discussed in this report. (C) Structure-contour map (relative to sea level) of the base-Surat unconformity surface.



The axis of the basin is arranged north to south along the Mimosa Syncline (Exon 1976; Hoffmann et al. 2009). The Leichardt-Burunga and Moonie-Goondiwindi fault systems are two major structural features interpreted as reactivated incipient basement faults of the underlying Bowen Basin (Raza et al. 2009). Wide acceptance of the mechanisms of basin formation has not yet been achieved. Varying datasets suggest possible mechanisms including thermal subsidence (Korsch et al. 1989), dynamic platform tilting (Gallagher et al. 1994; Korsch and Totterdell 2009; Waschbusch et al. 2009), and intraplate rifting (Fielding 1996). Nonetheless, some combination of a thermally relaxing tectonic regime and regional subsidence were responsible for the widespread deposition of the Precipice Sandstone and Evergreen Formation (Green et al. 1997).

The sedimentary fill in the Surat Basin exceeds 2500 m of siliciclastics and coal. Several lithostratigraphic frameworks exist for the basin varying in name and depositional age of units, although none are universally accepted (e.g. Power & Devine 1970; Exon 1976; Exon and Burger 1981; McKellar 1998; Hoffmann et al. 2009; Totterdell et al. 2009; Ziolkowski et al. 2014; Wainman et al. 2015; Figure 18).

**Figure 18** Comparison of various lithostratigraphic and sequence stratigraphic schemes for the Surat Basin, displayed next to the eustatic sea level curve developed by Haq et al. 1987. The Westgrove Ironstone Member has been dated using palynology to represent a regional transgression that correlates with the early Toarcian global sea level rise (Hallam & Wignall 1999). The Precipice Sandstone and Evergreen Formations were defined as supersequences by Hoffmann et al. 2009. More recently, three cycles (i.e. sequences) of deposition were interpreted by Wang et al. 2019.



Sequence stratigraphy has also been applied in the Surat Basin (e.g. Hoffmann et al. 2009, Totterdell et al. 2009, Ziolkowski et al. 2014). Early workers recognised six major cycles in the Jurassic-Cretaceous, each of which lasted for approximately 10 to 20 million years and broadly correspond to second-order global tectonic and sedimentation cycles (Exon & Burger 1981, Burke 2011). The earliest cycle was thought to characterise the Precipice Sandstone to Evergreen Formation strata (Exon & Burger 1981). Subsequently, a higher resolution sequence stratigraphic interpretation was proposed by Ziolkowski et al. 2014. However, the resulting framework used a limited dataset consisting of two cores, only a few seismic lines, and a wireline log. This is not believed to be sufficient to determine basin-wide sequence stratigraphy.

The Precipice Sandstone and Evergreen Formation have been previously interpreted as non-marine deposits in an intracratonic setting (Exon 1976; Exon & Senior 1976; Gallagher et al. 1994; Green et al. 1997). The Precipice Sandstone is commonly interpreted to represent high-energy, braided river deposits because of its consistently thick coarse-grained cross-stratified sandstone intervals with only thin, interspersed mudstone intervals. The Evergreen Formation, on the other hand, has been considered to represent meandering river and freshwater lacustrine deposits (Exon 1976, Exon & Burger 1981). Although the Westgrove Ironstone Member appears to show subtle marine influence (Exon 1976), it has been interpreted that full marine conditions did not become established in the basin (Green et al. 1997; Cook et al. 2013). Recent studies have indicated that there was more significant marine influence in the Surat during the early Jurassic (Martin et al. 2018; Bianchi et al. 2018).

### 4.3.1 The storage play

**A “play” in the carbon storage context is a combination of stratigraphy forming both an injection reservoir and an overlying seal or “seal complex”. The main geological properties and types of containment or injectivity risks of a play can be considered to be common across the play segment, making it a suitable unit of geological analysis for ultimate performance assessment.**

The lack of a basin-wide stratigraphic scheme that is linked to paleodepositional interpretations has hindered predictive confidence in reservoir performance modelling for CO<sub>2</sub> sequestration in the Surat Basin. The poorly constrained stratigraphy makes predicting reservoir-seal effectiveness difficult. Particularly, the Precipice Sandstone was previously considered to be overlain by a muddy Evergreen Formation, which was the basis for subdividing the two formations (Exon 1976; Green et al. 1997; Martin et al. 2017). However, a poorer quality sandy and silty transitional interval that is sometimes called the “Upper Precipice” (e.g. Ziolkowski et al. 2014; Martin et al. 2018) has caused confusion about where to place the contact between the two formations. Due to an inconsistently applied nomenclature, the architecture of reservoirs and seals described in this section are not well communicated in the broader literature. This is especially evident on the western margin of the basin (e.g. on the Roma Shelf) where sandstones that have been thought to be correlative to the Precipice Sandstone, occur stratigraphically higher.

In order to better describe the stratigraphy and understand the lateral continuity of various reservoir and sealing geobodies of the Precipice Sandstone to Evergreen Formation stratigraphic succession making up the storage play, the following sections present the results of an integrative study using core, wireline logs, and seismic data, to construct a detailed sequence stratigraphic framework for explaining the distribution of facies across the basin. This enables a better understanding of the architecture of reservoirs and seals and provides a better context to describe the lower Jurassic System in the Surat Basin. The outcome of this work is fundamental to building a range of geologically robust static models at various scales and locations that are parameterised to both capture the geological uncertainty and provide the base case scenario for dynamic simulation of carbon storage that informs notional injection site analysis and sweet spot identification.

The UQ-SDAAP project developed the following workflow for characterising the Surat Basin Precipice Sandstone to Evergreen Formation stratigraphy and for building various static geological sector models:

1. Facies analysis: Examine available cores to conduct facies analysis and establish key sequence stratigraphic surfaces and depositional cycles
2. Sequence stratigraphic framework: For the wells with core descriptions (point 1), match the key sequence stratigraphic surfaces and depositional cycles with petrophysical log signatures to define a set of control wells with sequence stratigraphic picks. Use the control wells to extend the sequence stratigraphic picks to other wells with petrophysical logs but no core
3. Neural network wireline-facies: Using the control wells (point 2) and facies analysis (point 1), use machine learning (i.e. neural networks) to determine wireline-facies from petrophysical logs that match the core facies (point 1). Use the subsidiary wells with sequence stratigraphic picks but no core and allow the trained neural network to determine wireline-facies in these wells
4. Seismic analysis: Using the control wells (point 2) and subsidiary wells with sequence stratigraphic picks but no core (point 3) to create synthetic seismic profiles from petrophysical logs. Tie the synthetic seismic profile at each well to actual seismic data (available in 3D and 2D). Identify the sequence stratigraphic picks that are correlatable on the 3D and 2D seismic data and trace these surfaces through the available seismic volumes away from wells but with iterative crosschecking between well and seismic data
5. Mudstone palynology and biostratigraphy: The advantage of sequence stratigraphic correlation is that the lateral tracing of depositional units of similar geological age and that have a genetic relationship to each other. Seismic reflection horizons commonly approximate time-boundaries allowing for the integration of core, well log, and seismic data to be used to construct a sequence stratigraphic framework. Palynology can provide age-calibration of stratigraphic correlation and serve as independent validation of correlations. The palynology can also provide information regarding depositional environment to support facies interpretations from core
6. Structural geology: Using data from points 1-5, faults and other structural features are identified across the UQ-SDAAP study area. Fault zone architecture is identified including juxtaposition analysis and geomechanical fault stability analysis
7. Petrophysical analysis: Using the data from points 1-3 and defined petrophysical workflows, calculate the volume of shale, total porosity, effective porosity and permeability for control and subsidiary wells. The calculated petrophysical permeability is calibrated with available core plug analysis (laboratory determined permeability) and drill stem test (DST) interpreted permeability. The calculated petrophysical porosity and permeability data is analysed for trends with geographic location, depth, facies and sequence stratigraphic unit



8. Geological sector models: Well and seismic control in the sweet spot location of notional injection is lacking, therefore more than one conceptual geological model is needed to capture the full range of uncertainty in facies distribution and stratigraphy to predict fluid flow properties of the strata. Using data from points 1-4, three 10 x 10 km sector models were built representing three geological conceptualisations for the notional injection locations. Information from point 5 was used to parameterise each of the three sector models using a base case, high case, and low case for fluid flow properties (porosity and permeability). These models were used to test the range of expected fluid flow behaviour of the play in the notional injection areas
9. Regional geological model: Using data from points 1-4, a regional geological model was constructed. Information from point 5 was used to parameterise the model using a base case, high case, and low case for fluid flow properties (porosity and permeability). The regional geological model was used to build a large-scale dynamic simulation of notional CO<sub>2</sub> injection at commercially material scale and to test the range of possible impacts on groundwater resources

### 4.3.2 Facies analysis

**As noted previously by Garnett et al. 2012, improved facies prediction is critical for reducing uncertainty of CO<sub>2</sub> storage performance in the Precipice Sandstone and Evergreen Formation. Initial stages of facies analysis requires either drill core or outcrop or both. Our understanding of the depositional facies gained from examination of core and outcrop across the Basin is substantially increased.**

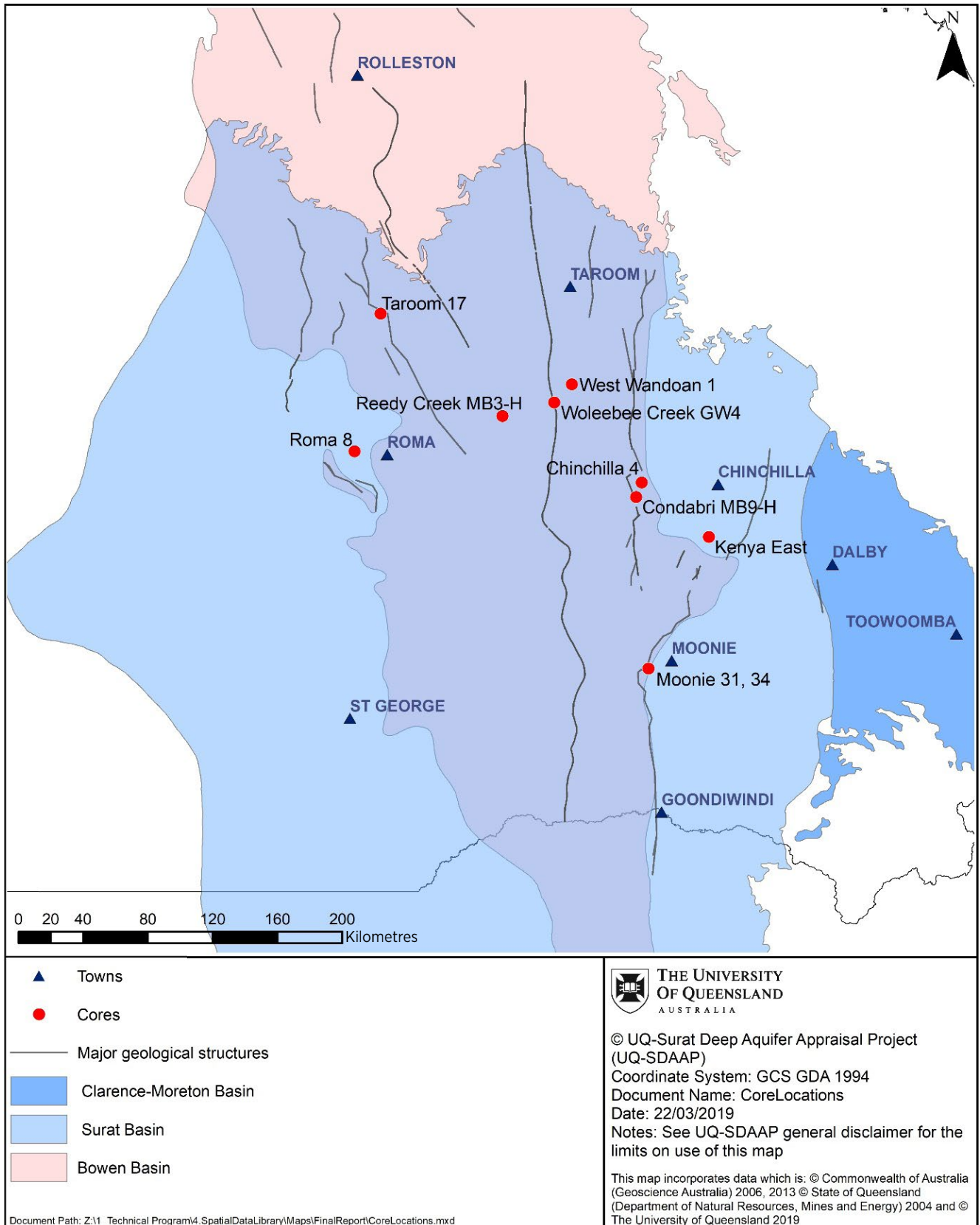
Nine wells with significant sections of core from the Precipice Sandstone and Evergreen Formation were examined for their sedimentological and ichnological characteristics. These were, in alphabetic order: Chinchilla 4, Condabri MB9-H, Kenya East GW7, Moonie 34, Reedy Creek MB3-H, Roma 8, Taroom 17, West Wandoan 1, Woleebee Creek GW4 (Figure 19). From analysis of over 2000 m of cumulative section, 19 distinct depositional facies were identified that range from 0.11 to 11.56 m thick. The facies were grouped into five main facies associations corresponding to: (1) braided channel complex, (2) lower delta plain, (3) subaqueous delta, (4) tidal flats, and (5) shoreface. The methodology employed was to make paleoenvironmental interpretations of the strata that aid sequence stratigraphic correlations across the basin. The facies and facies associations were used to construct the sequence stratigraphic framework by identifying depositional hiatuses. These were used to map the distribution of geobodies in the subsurface and populate them with fluid flow properties (e.g. porosity and permeability).

For the core descriptions, textural observations included lithology, grain size, grain sorting, and roundness. Sedimentological data such as bedding style, physical sedimentary structures, cementation, and accessory aspects were also recorded. Finally, information about the ichnological aspects of the strata were recorded such as ichnogenera identification, trace fossil size, diversity, bioturbation intensity using the BI-scale (Taylor and Goldring 1993), and the distribution characteristics of burrowing between beds. In concert, these data were used to make paleoenvironmental interpretations of the strata using process-response inferences following the methods and philosophy outlined in Middleton 1978 and Dalrymple 2010.

Following a classification of facies approach, the units were organised into groups of facies that occur together and are considered to be genetically or environmentally related (c.f. Dalrymple 2010). Facies associations are larger scale sedimentary packages that are interpreted to represent entire depositional environments (i.e. delta plain, channel complex, etc.). This is in contrast to facies-scale packages that are the result of distinct depositional processes occurring at the sub-environment scale (i.e. mouth bar, interdistributary bay, etc.).

The report by La Croix et al. 2019a provides a detailed description of the facies analysis workflow and how it was applied to the UQ-SDAAP project. In this report, each sedimentary facies was described in detail and an interpretation is provided in terms of the formative depositional processes and environments that represent that facies. Facies association descriptions and interpretations then follow, and all the results are summarised in a set of tables. Finally, individual cored intervals for the Precipice Sandstone and Evergreen Formation are documented from the base (bottom) up, showing how facies and facies associations are stacked vertically through the section.

**Figure 19** The location of cored wells within the Surat Basin that were logged in detail as part of this study. A total of nine wells were examined, mostly occurring within the northern, north-eastern, and north-western parts of the basin.



### 4.3.2.1 Results

From all the available core data examined, the following 19 facies were recognised:

1. Facies G1: Interbedded Conglomerate and Sandstone (>30% Granules and Coarser)
2. Facies G2: Mud-Clast Breccia (>30% Granules and Coarser)
3. Facies S1: Coarse Grained Planar-Tabular to Trough Cross Stratified Sandstone (>90% Sand)
4. Facies S2: Planar-Tabular Cross Stratified Grading into Current Ripple Laminated Sandstone (>90% Sand)
5. Facies S3: Wave to Combined-Flow Ripple Laminated Sandstone (>90% Sand)
6. Facies S4: Structureless to Planar-Parallel Laminated Sandstone (>90% Sand)
7. Facies S5: Bioturbated Sandstone and Muddy Sandstone (>90% sand)
8. Facies S6: Bioturbated Muddy Sandstone with Wave-Ripple Lamination and Hummocky Cross-Stratified Interbeds (>90% Sand)
9. Facies M1: Planar-Parallel Laminated Mudstone with Thin Sandstone Laminae (>90% Mud; Silt and Clay)
10. Facies M2: Structureless Mudstone (>90% Mud; Silt and Clay)
11. Facies M3: Bioturbated Sandy Mudstone (>90% Mud; Silt and Clay)
12. Facies M4: Bioturbated Sandy Mudstone with Wave-Ripple Laminated to Hummocky Cross Stratified Interbeds (>90% Mud; Silt and Clay)
13. Facies SM1: Mixed-Influence Sand Dominated Heterolithics (90%>Sand>70%)
14. Facies SM2: Mixed-Influence Heterolithics with Sub-equal Proportions of Sandstone and Mudstone (70%>Sand>30%)
15. Facies SM3: Mixed-Influence Mud Dominated Heterolithics (30%>Sand>10%)
16. Facies SM4: Tide-Dominated Heterolithics (90%>Sand>10%)
17. Facies O1: Coal
18. Facies O2: Carbonaceous Sandstone and Siltstone
19. Facies O3: Ironstone (Oolitic and Cemented Types)

These were grouped into the following 5 facies associations:

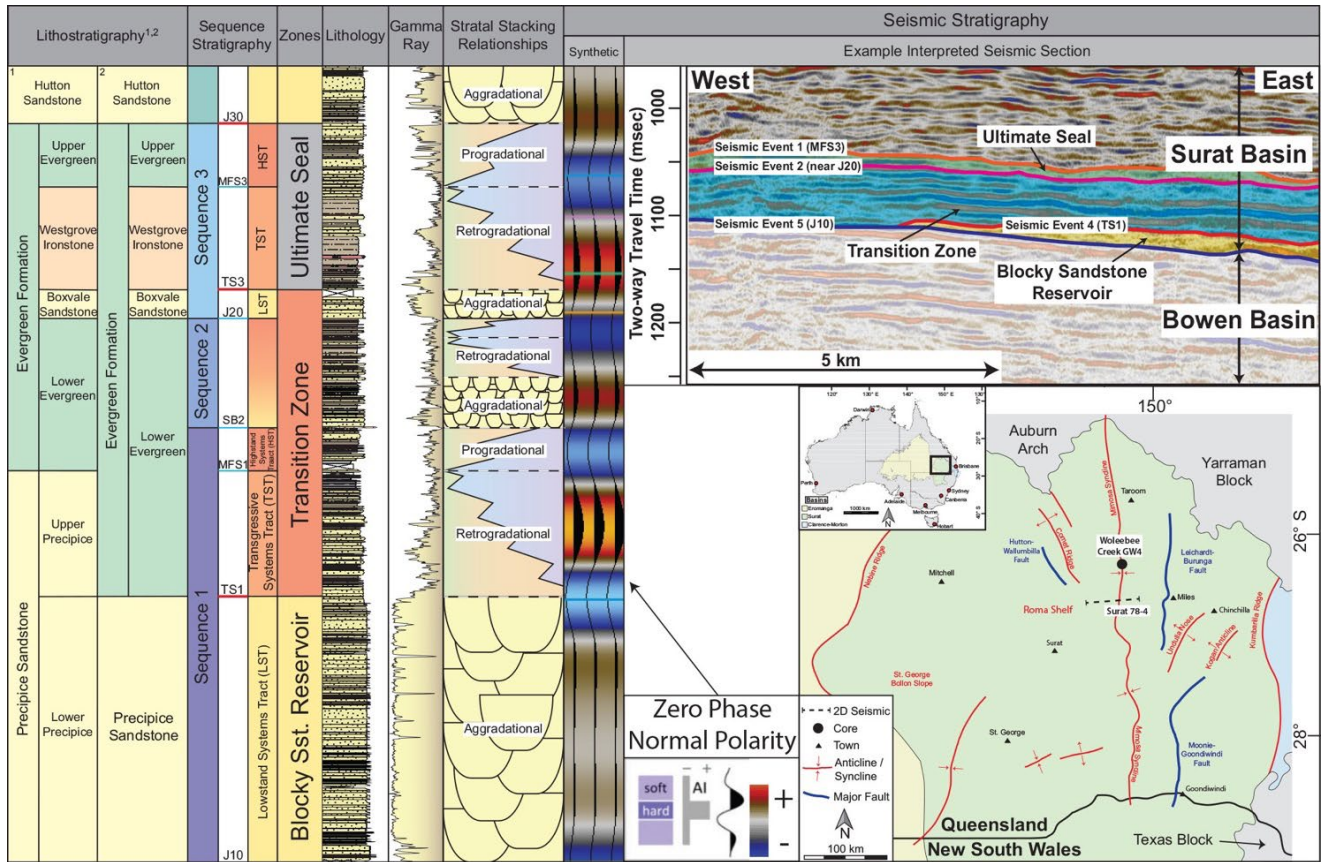
1. Facies Association 1 (FA1): Alluvial to Subaerial Delta Braid-Plain
2. Facies Association 2 (FA2): Subaerial Delta
3. Facies Association 3 (FA3): Subaqueous Delta
4. Facies Association 4 (FA4): Tidal Flats
5. Facies Association 5 (FA5): Shoreface

The core descriptions are also used to define sequence stratigraphic surfaces and depositional cycles. The Precipice Sandstone and Evergreen Formation consists of three sequences from base to top. In theory each sequence consists of a basal unconformity, a transgressive surface, a maximum flooding surface, and are marked by an unconformity at the top (which is also the base of the overlying sequence). These segment the sequences into a lowstand systems tract, transgressive systems tract, and highstand systems tract, respectively. However, only the basal and top sequences have their transgressive surface and maximum flooding surface picked at the scale of the UQ-SDAAP; the second sequence of the three was relatively thin and these surfaces were difficult to trace across most of the basin (See Figure 20).

For reference in subsequent sections, the deepest parts of the Blocky Sand Reservoir are the most attractive for high-rate, secure injection of CO<sub>2</sub> and have been considered as such. The more complex, laterally and vertically heterogeneous Transition Zone acts as a baffle to pressure transmission and any vertical flow of CO<sub>2</sub> from the Blocky Sandstone Reservoir into the Ultimate Seal. The Ultimate Seal acts as the final cap-rock which retains the CO<sub>2</sub> (in fact in modelling, no CO<sub>2</sub> reaches the base of the Ultimate Seal in any scenario and very little if, any enters, the Transition Zone).

The defined UQ-SDAAP stratigraphy is composed of the surfaces: J10 (base-Surat unconformity), TS1, MFS1, SB2, J20, TS3, MFS3, and J30 (top Evergreen) from base to top. In terms of the notional storage complex, the Blocky Sandstone Reservoir is between the surfaces J10 and TS1, the Transition Zone is between the surfaces TS1 and TS3 and the Ultimate Seal is between the surfaces TS3 and J30. **Figure 20 is a key index for terminology used in the remainder of the report.**

**Figure 20** Stratigraphic terminology used to describe the core, along with the modelling zones, and a litholog from Woleebee Creek GW4. The dashed line represents the location of the 2D seismic data.



<sup>1</sup>after Exon et al. 1967, Gray 1968, Rigby and Kanstler 1987, Martin et al. 2018  
<sup>2</sup>after Mollan et al. 1972, Green et al. 1997, Wang et al. in press

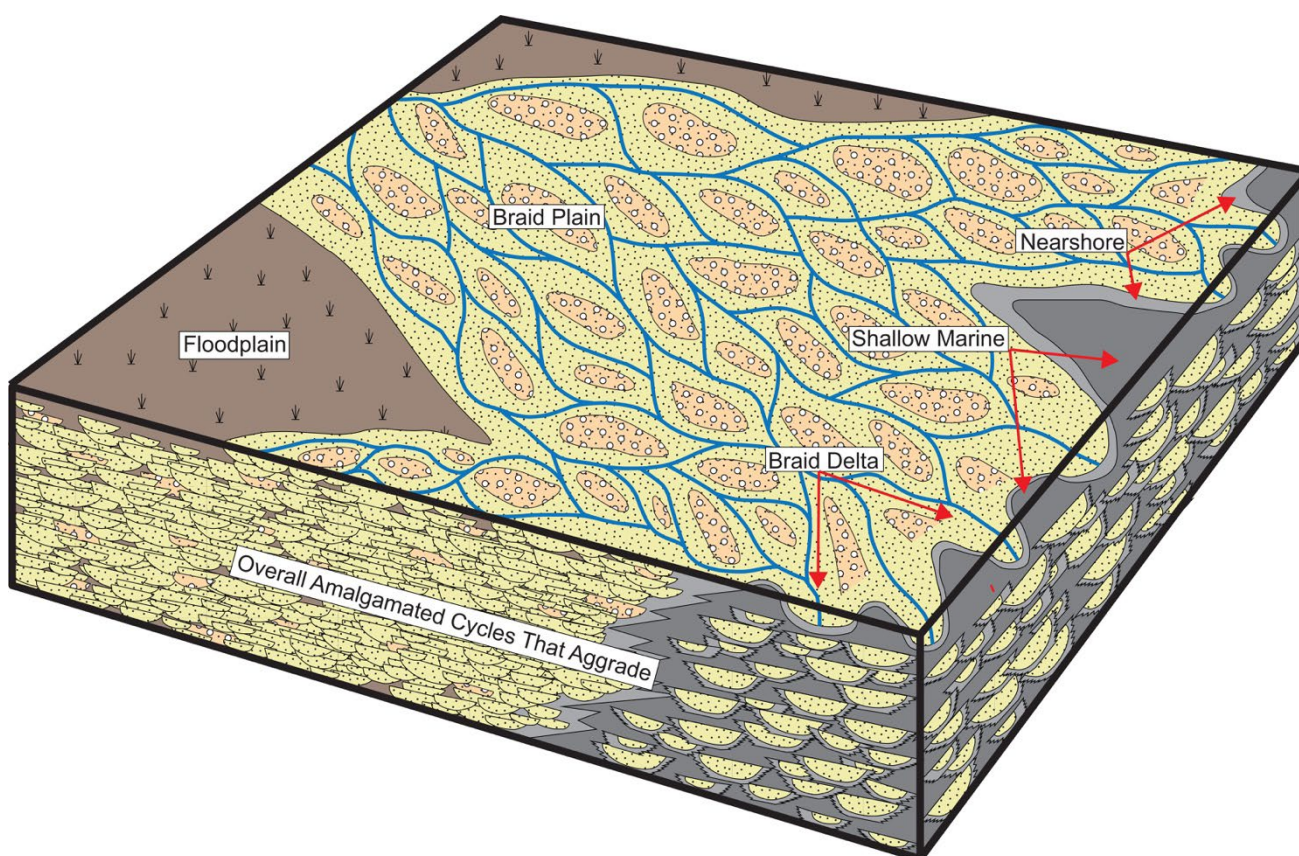
### 4.3.2.2 Analysis and discussion

Conceptual block models were constructed for the main components of the Precipice–Evergreen succession. These models show the major depositional environments, and their stratal stacking relationships to help better envision the distribution of facies and flow units within the basin. However, they do not hold any significance with respect to the orientation of depositional systems or the relative proportion of environments, a topic that is addressed in the technical report dealing with neural network facies predictions and paleogeographic distribution of facies (Section 4.1.4).

#### 4.3.2.2.1 Lowstand Systems Tract 1 (J10–TS1) – Blocky Sandstone Reservoir

Figure 21 shows the conceptual depositional model for the Blocky Sandstone Reservoir (Precipice Sandstone) between J10 and TS1, representing the lowstand systems tract. The model indicates that the bulk of accommodation space was filled with sediments representing braided channel complexes (FA1), with subordinate shallow marine environments such as the subaqueous delta (FA3). These were stacked in an aggradational pattern, neither prograding nor retrograding.

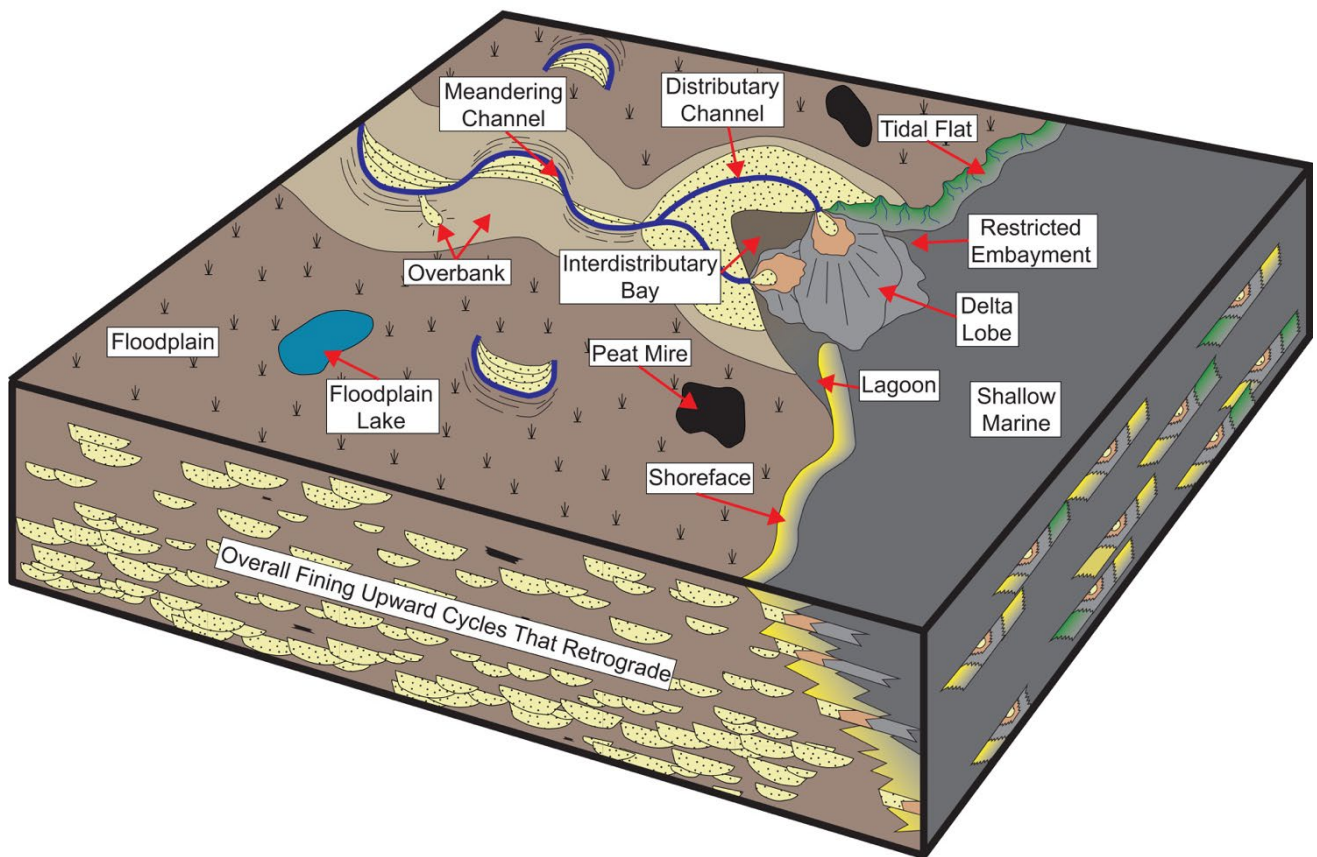
**Figure 21** Conceptual block model of Lowstand Systems Tract 1, the main reservoir interval investigated for CO<sub>2</sub> storage in the Surat Basin.



#### 4.3.2.2.2 Transgressive Systems Tract 1 (TS1-MFS1) – lower part of the Transition Zone

A conceptual depositional model for Transgressive Systems Tract 1 is indicated in Figure 22, the part of the succession lying between TS1 and MFS. The model indicates that deposition occurred within a complex palaeogeography consisting of a large-scale deltaic system, which itself comprises a delta plain (FA2), subaqueous delta (FA3), and with subordinate elements of tidal (FA4) and shoreface (FA5) systems. Strata shows overall backstepping relationships with deepening of sedimentary environments with time. A similar depositional model is suggested for the minor transgressive systems tract contained within Sequence 2.

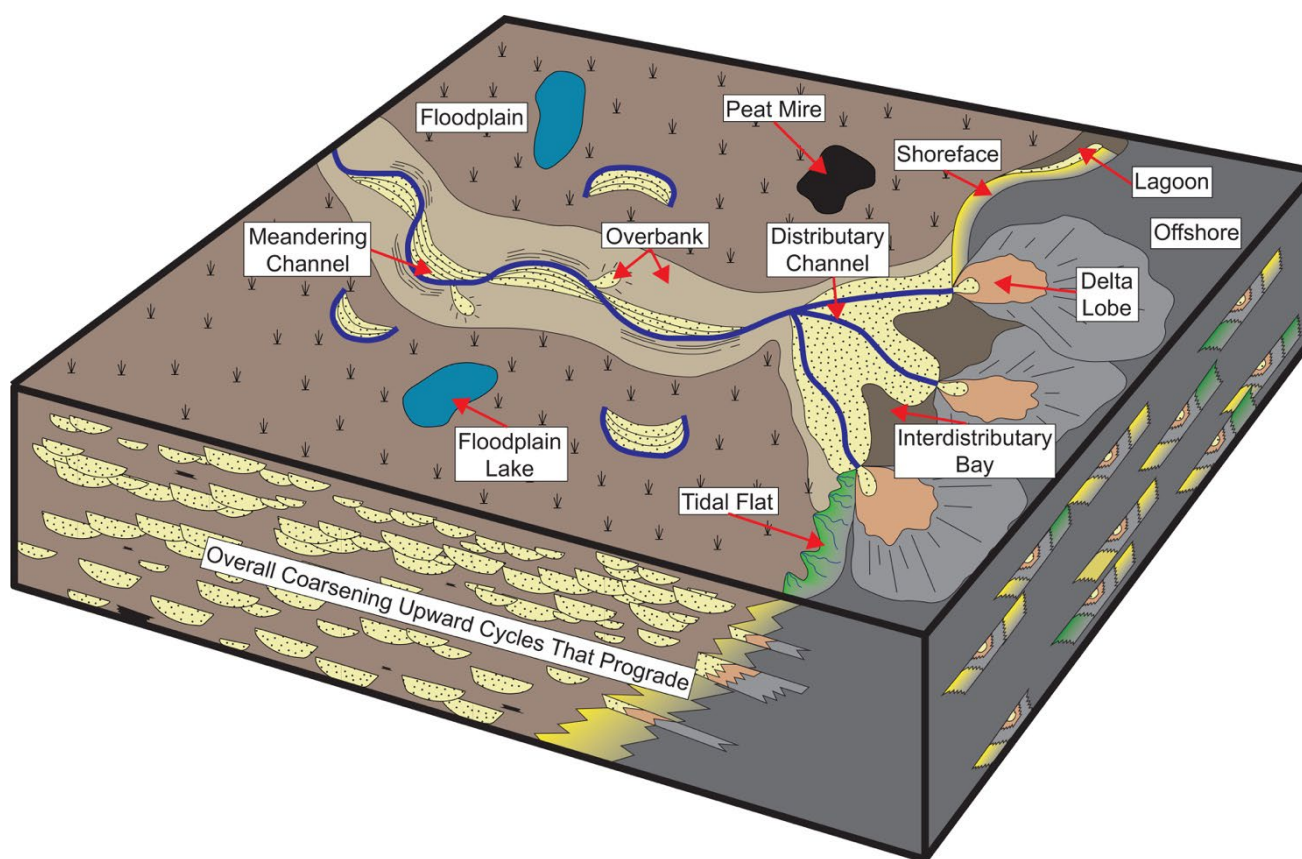
**Figure 22** Conceptual block model for Transgressive Systems Tract 1, the unit overlying the main reservoir interval. The same depositional model is applicable to the transgressive systems tract within Sequence 2.



#### 4.3.2.2.3 Highstand Systems Tract 1 (MFS1-SB2) – middle part of the Transition Zone

The depositional model for Highstand Systems Tract 1, between MFS1 and SB2, is displayed in Figure 23. Deposition of the highstand was within the same palaeogeography that the transgressive systems tract was deposited, though depositional environments were progradational overall. Thus, cross-cutting and complex facies relationships were common – possibly the result of low depositional gradients where small changes in relative base level resulted in large shifts in environments of deposition. Nonetheless, the highstand consisted of delta plain (FA2), subaqueous delta (FA3), and with subordinate elements of tidal (FA4) and shoreface (FA5) systems. Within Sequence 2, the thin highstand probably had a similar arrangement of facies and environments; so too did Highstand Systems Tract 3, although it probably had increasing marine influence on deposition.

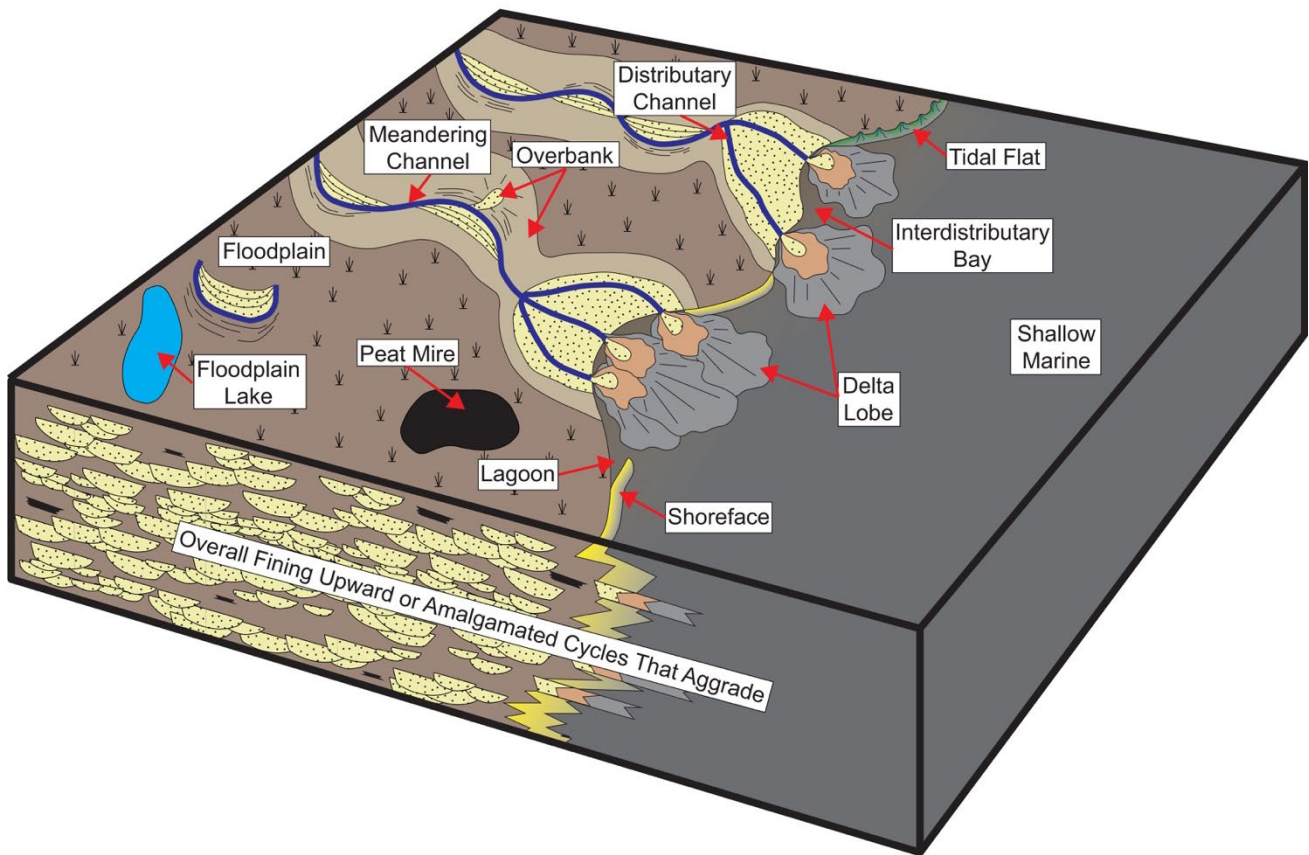
**Figure 23** Conceptual block model for Highstand Systems Tract 1. The same model is applicable to the highstand systems tract from Sequence 2, as well as Highstand Systems Tract 3.



#### 4.3.2.2.4 Lowstand Systems Tract 3 (J20-TS3) – upper part of the Transition Zone

The model for Lowstand Systems Tract is shown in Figure 24. The same large-scale fluvio-deltaic system that was occupying the Surat Basin was present up until this time (broadly equivalent to the Boxvale Sandstone Member). Complex facies relationships prevailed, but overall depositional environments comprised delta plain (FA2), subaqueous delta (FA3), and with subordinate elements of tidal (FA4) and shoreface (FA5) systems. These did not show progradation or retrogradation at the sequence scale, thus, are inferred to be stacked in an aggradational fashion. The lowstand systems tract from Sequence 2 probably looked similar.

**Figure 24** Conceptual block model for Lowstand System Tract 3, otherwise known as the Boxvale Sandstone. A similar model applies to the lowstand from Sequence 2.

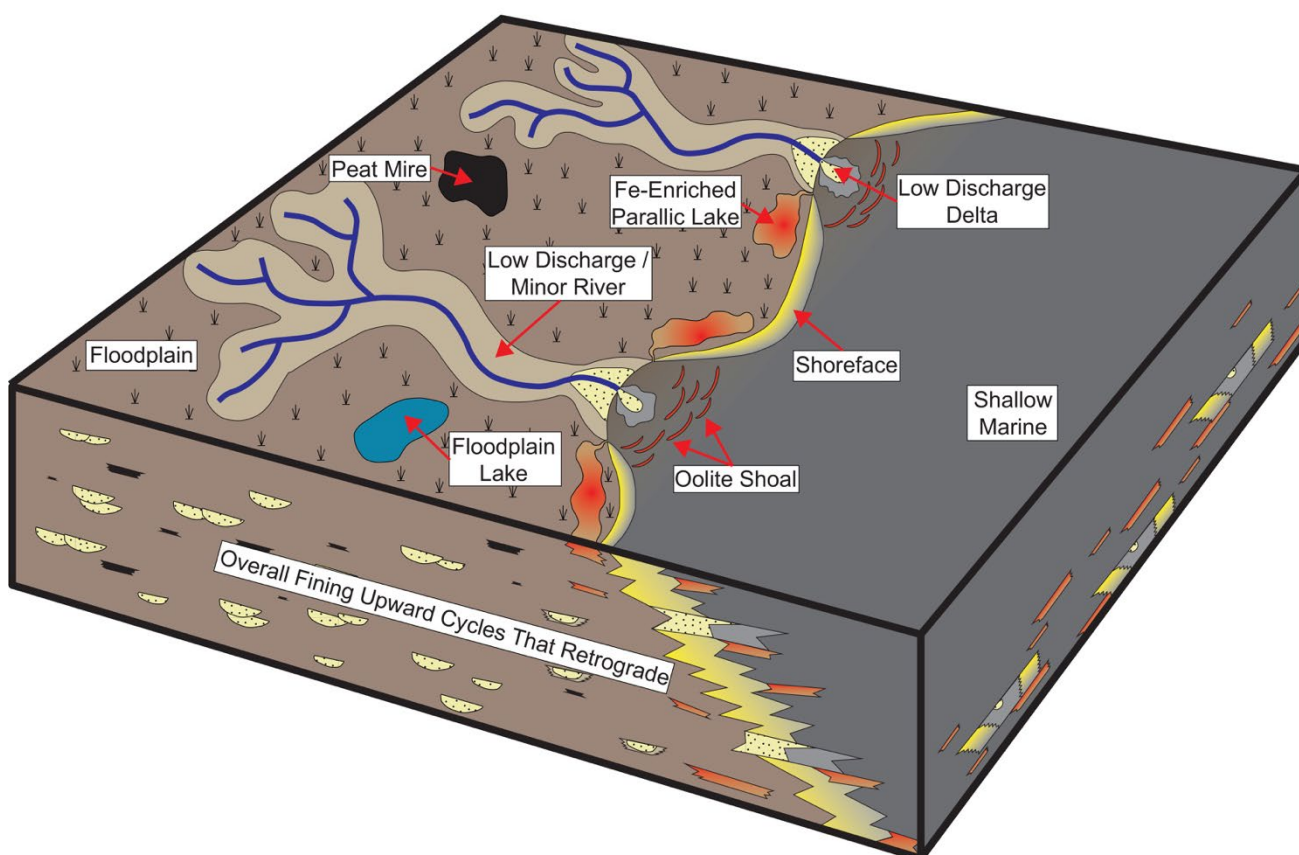




#### 4.3.2.2.5 Transgressive Systems Tract 3 (TS3-MFS3) – Ultimate Seal

The conceptual model for Transgressive System Tract 2, the interval containing ironstone horizons, is depicted in Figure 25. The overall depositional setting is envisioned as a low gradient system, with minor rivers and streams flowing into a marine basin. During deposition of Transgressive Systems Tract 3, the delta plain and shallow marine realm were still of low gradient, such that small changes in base level would have resulted in large shifts of facies belts. Portions of the delta plain (FA2), subaqueous delta (FA3), and minor tidal (FA4) and shoreface (FA5) elements would have been present and overall deposition would have been under deepening conditions with time as environments were transgressed by rising relative sea level. The dominant environment consisted of a restricted delta front or estuary where iron-enrichment was able to take place under slight wave agitation resulting in deposition of the oolitic ironstone bands. Minor paralic lakes and bays probably also would have accumulated ironstone, being in connection to the basin and sharing similar chemistry.

**Figure 25** Conceptual block model for Transgressive Systems Tract 3, the main interval containing ironstone.



### 4.3.3 Sequence stratigraphic framework

**Critical to confidence in injection and containment prediction is the lateral prediction of properties away from well control. Rather than rely on historic correlations, UQ-SDAAP has undertaken a fundamental revision of the lowermost Jurassic stratigraphy that comprise the storage play into a sequence stratigraphic framework. This has led to increased confidence in both injection and sealing prediction and performance.**

Integration of core, wireline logs, and seismic data were used to construct a sequence stratigraphic framework in which to interpret the facies and flow units of the Precipice Sandstone and Evergreen Formation. Three third-order sequences were identified: SQ1-SQ3, from base to top. Each sequence consists of three main parts: (1) a lowstand systems tract (LST) comprising aggradational-stacked facies successions, (2) a transgressive systems tract (TST) in which facies retrograde towards the basin margins, and (3) a highstand systems tract (HST) where facies prograde into the basin-centre. The main reservoir interval, the Blocky Sand Reservoir (Precipice Sandstone), represents the LST of SQ1. The Transition Zone through which pressure and potentially small amounts of CO<sub>2</sub> migration is anticipated to occur, corresponds to the TST and HST of SQ1. All of SQ2 and the LST of SQ3 – corresponding to the Boxvale Member (Evergreen Formation) – are also part of the Transition Zone. Finally, the Ultimate Seal is composed of the TST and HST of SQ3. These equate to the Westgrove Ironstone Member and the Upper Evergreen Formation.

The report by La Croix et al. 2019b provides a detailed description of the sequence stratigraphic correlation workflow and how it was applied to the UQ-SDAAP project. The three mapped sequences approximately coincide with global sea-level cycles documented for the early Jurassic (Haq et al. 1987). Two episodes of accelerated tectonic subsidence were responsible for the thinning and onlap of SQ1 and SQ3 on the basin margins. In contrast, weak tectonic subsidence was responsible for the overall finer grained sediment, the uniformity of thickness, and widespread distribution of SQ2. The new stratigraphic framework serves as a means to subdivide and segregate the Blocky Sandstone Reservoir, Transition Zone, and Ultimate Seal within the various static geological models for carbon storage.

#### 4.3.3.1 Analysis and discussion

**The main geological conclusions are: (1) the distribution of the Blocky Sandstone Reservoir for prospective CO<sub>2</sub> storage in the Surat Basin has a more restricted vertical and lateral distribution than has been previously recognised (2) The Transition Zone increases in sandstone content and thickness towards the basin margins where the sandstones are poorly-connected and generally low permeability due to their depositional affinity with distributary channels. The Transition Zone becomes more mudstone rich towards the basin centre where mudstone intervals act as localised seals or baffles; and, (3) the Ultimate Seal has good sealing potential because geobodies are widespread and overall fine-grained with very low bulk permeability.**

The construction of a sequence stratigraphic framework gives important insights into the architecture of lower Jurassic reservoirs and seals for CO<sub>2</sub> storage. The Storage Container is not accurately described as a simple reservoir-seal pair. Rather, the Blocky Sandstone Reservoir forms the main notional injection reservoir and the Ultimate Seal (upper part of the Evergreen Formation) forms the main seal with these two units being separated by a Transition Zone. The main geological conclusions regarding these three units can be described in more detailed sequence stratigraphic terminology as:

1. The distribution of the major sandstone unit for prospective CO<sub>2</sub> storage in the Surat Basin (the Precipice Sandstone) has a more restricted vertical and lateral distribution than has been recognised by previous workers. The UQ-SDAAP project calls the main reservoir the “Blocky Sandstone Reservoir”

The Storage Container is not accurately described as a simple reservoir-seal pair. Rather, the Blocky Sandstone Reservoir forms the main notional injection reservoir and the Ultimate Seal (upper part of the Evergreen Formation) forms the main seal with these two units being separated by a Transition Zone.

2. The sandy transitional interval occurring in the TST of SQ1, was deposited during the early stages of relative base level rise, retreated towards and overlapped the eastern and the western basin margins. It increases in sandstone content and thickness towards the basin margins, as geobodies backstepped and retrograded. Importantly, these sandstone layers should not be misidentified as the Precipice Sandstone, with a case example being the Roma 8 core
3. Sand bodies in the transitional interval are poorly-connected due to their depositional affinity with distributary channels, and are generally of lower permeability than the Blocky Sandstone Reservoir. Overall, they have far less desirable reservoir characteristics compared with the Precipice Sandstone
4. There are thin mudstone intervals in the upper portion of the TST and the HST of SQ1 that act as localised seals or baffles
5. SQ2 is a good regional seal because of its low proportion of sandstone, thickness (40-50 m) and widespread distribution
6. The Boxvale Sandstone, which is discontinuously distributed across the central portion of the basin. In the UQ-SDAAP project this unit falls within the Transition Zone
7. The TST and HST of SQ3 have good sealing potential because they are widespread and overall fine-grained. The UQ-SDAAP project calls this interval the Ultimate Seal

#### 4.3.4 Neural network wireline-facies

**UQ-SDAAP has applied modern correlative and pattern recognition (machine learning) techniques for the first time in this basin. This compensates to some extent for sparse, old and incomplete data, and maximises the use of historical data in constraining the new geological interpretation. This data is used to define the paleo-depositional environments for the main geological components of the storage complex.**

The need for wireline log facies derives from the fact that core data is sparse across the basin, and is entirely absent from the region of interest for basin centred reservoir modelling. Thus, with the ability to recognise geological units using wireline logs alone, the available data set to characterise the Surat Basin's palaeogeography is enhanced and can be used to predict the distribution of geobodies and flow units.

Based on data from nine cored wells with a total thickness of ~2000 m, 20 core facies were defined by their texture, as well as their sedimentological and ichnological characteristics (described in La Croix et al. 2019a). Statistical analysis was undertaken on six wireline log parameters – gamma ray, density, sonic, neutron, photoelectric factor, and deep resistivity – to simplify the core facies into 10 representative wireline log facies with unique ranges of petrophysical parameters (some of the 20 facies recognisable in core are not uniquely distinguishable in wireline logs alone). Markov Chain analysis was then applied to the wireline log facies to determine the significance of vertical facies transitions, which ultimately supported the interpretation that facies group into five distinct associations: channel-levee complex, subaerial delta, subaqueous delta, tidal flats, and shoreface.

From the facies analysis and statistical classification, a neural network was applied to predict the wireline log facies where suitable logs occur but no core exists. Results show that the accuracy of prediction ranges from 66% to 99% (ca. 83%) depending on the facies. Accordingly, cross-validation accuracy ranges from 48-97% (ca. 71%) depending on the facies. As expected, the accuracy of facies recognition decreases step wise with decreasing log input data, such that when only gamma ray, density, and sonic are used to train neural networks the accuracy drops to between 40- 90%, depending upon the facies. This was considered the lowermost threshold for acceptable facies determination for this project (and was accompanied by expert discussion and visual validation). Figure 26 is a map showing the distribution of wells and the corresponding number of logs present in each well. The highest concentration of wells are on the Roma Shelf and in the north-western part of the basin. From the facies analysis of core (La Croix et al. 2019a) nineteen facies were identified (core facies; CF) based on their sedimentological characteristics. The CF types included conglomerates and breccias (Facies G1 and G2), sandstones (Facies S1, S2, S3, S4, S5, and S6), mudstones (Facies M1, M2, M3, and M4), heterolithics (Facies SM1, SM2, SM3 and SM4), as well as organic and miscellaneous facies (Facies O1, O2 and O3). The CF were simplified into 10 representative wireline log facies (WLF) using the LDA method (Figure 27). Some CFs were not recognised in log because they did not have discrete petrophysical properties that allowed their differentiation, such as G1, G2, SM5 and O2 (see La Croix et al. 2019a). Other CFs were grouped together into a single WLF (Figure 27) because of their similar log response characteristics.

Finally, the predicted wireline log facies were used to map the distribution of facies and depositional environments across the basin. These maps were the backbone of static reservoir modelling efforts, and proved to be a useful tool for helping define carbon storage play segments, and were a means to understand the distribution and nature of flow units in the basin-centre where data is otherwise sparse. The report by La Croix et al. 2019c provides a detailed description of the neural network wireline-facies workflow and how it was applied to the UQ-SDAAP project.

**Figure 26** Map showing the location of wells across the Surat Basin that were used for wireline log facies prediction. Their colour shows the number of distinct types of well logs that were available to improve their accuracy.

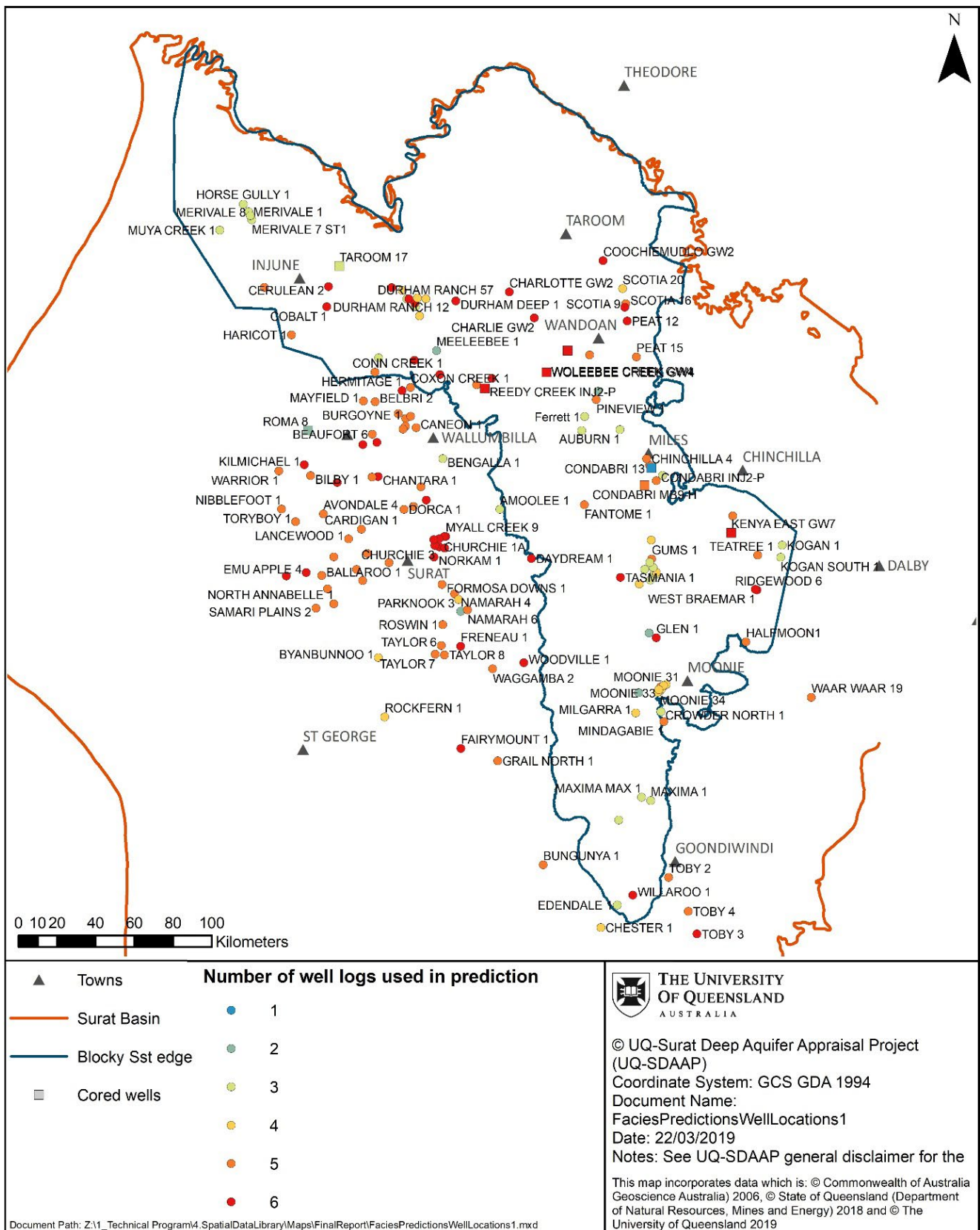
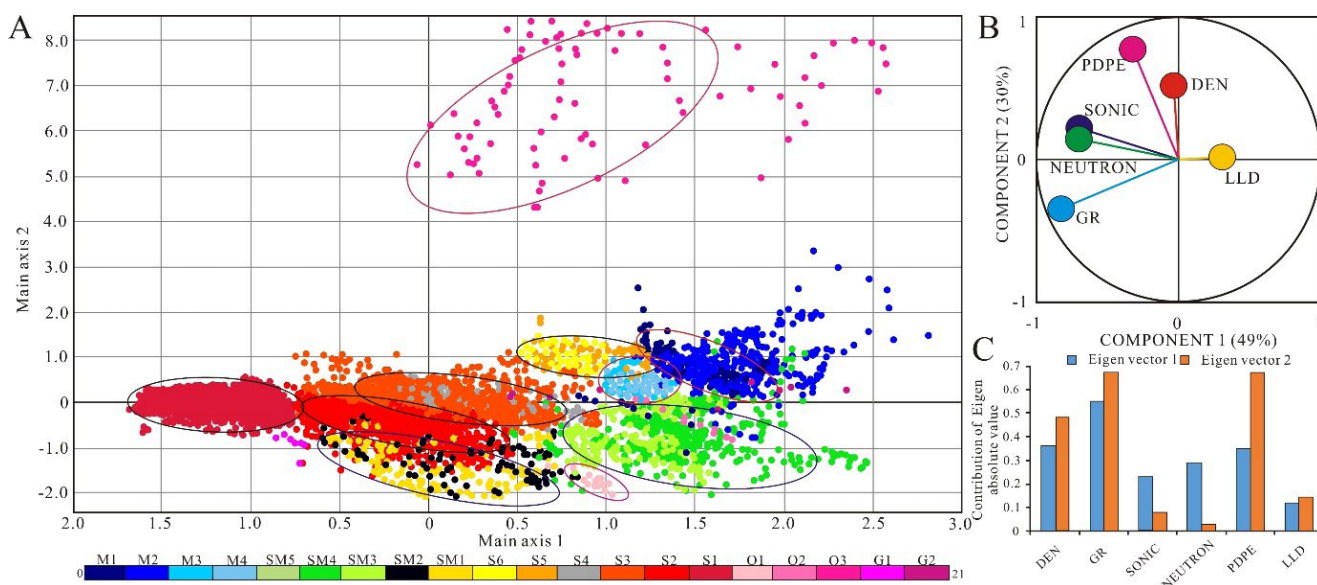


**Figure 27** (A) The results of LDA showing how the 10 main WLF plot in multidimensional space and were grouped. (B and C) PCA for WLF displaying the wireline logs that were most important for determining WLF – gamma ray (GR), sonic, and neutron.



#### 4.3.4.1 Mapping wireline-facies across the basin

The results from the robust MLPC model was applied to the uncored intervals in the wells with at least four wireline logs to develop a better understanding of the facies distribution and depositional setting across the Surat Basin for five major stratigraphic intervals: J10-TS1, TS1-MFS1, MFS1-SB2, SB2-TS3, TS3-J30 (see sequence stratigraphy and facies analysis chapters). Facies interpretations were combined with maps of  $V_{shale}$  to better understand the orientation of major facies belts. These in turn were compared against pie-chart maps showing the facies proportions at each location. The “most of” facies (i.e. facies comprising the greatest thickness within each interval of interest) were used in combination with the gamma ray log motif to map the palaeogeography for each major interval.

The Early Jurassic land surface consisted of elevated basement blocks in the southwest (Auburn Arch), northeast (Yarraman Block), and southeast (Texas High; Green et al. 1997). These exposed basement blocks provided the main sedimentary input into the Surat Basin. The main source areas were: the southwestern block, composed of siliceous sedimentary rocks, metasediments, schists, gneisses, and granites; the Auburn Arch and Yarraman Block, consisting largely of granite and gneiss; and the New England Fold Belt, composed mainly of indurated fine-grained sediments (Green et al. 1997). At this time, The Precipice Sandstone covered most of the Basin and was dominated by sediments deposited within a braided plain system (+/- braided delta influence; Figure 28). However, the southwestern part of the basin lacked thick sandstone deposits due to the high elevation of the land surface on the Wunger Ridge (Exon 1976).

During the deposition of the Lower Evergreen Formation (TS1-MFS1), base level rise occurred rapidly, and facies zonation became more prominent (Figure 29). The TST of SQ1 was composed of meandering river, delta plain, and subaqueous delta (delta front and prodelta) sediments. More basinal facies were limited to a narrow belt in the central basin. Many large-scale deltas were building out towards the central basin (e.g. near the West Wandoan 1 and Trelinga 1 wells) from the northwest margin extending into the basin for a distance of at least 53 km (Figure 29). Younger deposits cut through older strata with complex cross-cutting relationships derived from allogenic shifts in environments. However, on the eastern margin of the basin, delta lobes did not extend very far from their provenance areas (i.e. from the Auburn Arch and Yarraman Block). This appears to have been partially controlled by palaeogeomorphology. From the south, delta systems had much greater axial extents than on the east and west sides of the basin. Minor shoreface environments were distributed in the north-eastern part of basin and tidal settings were distributed in the south. During the HST of SQ1 (TS1-SB2), major sedimentary environments consisted subaqueous delta and basinal settings, with much less extensive delta plains (Figure 30). Only the north-western and south-eastern part of basin contained isolated delta systems, whereas in the rest of the basin these were connected by long coastlines fed by many rivers. This was coupled with enhanced marine influence and an overall increase in water depths. The West Wandoan 1, Woleebee Creek GW4, and Trelinga 1 wells are interpreted to be located near the locus of deposition – representing the “basin centre”.

The sedimentary facies from SB2 to TS3 mainly consist of meandering river and delta plain deposits with associated subaqueous deltas (Figure 31). Large deltaic systems from the northwest and southeast prograde back towards the central basin. Sediment input with a southeast provenance is interpreted to have increased greatly. However, delta systems with east provenance were less important and their corresponding delta plains were much smaller in aerial extent. Near the top of the Evergreen Formation between TS3 and SB4, the entire basin became heavily influenced by marine processes and marine water flooded the central and the north-eastern parts of basin (Figure 32). Sediment input was mainly derived from a western and south-eastern provenance. Through time the eastern provenance was flooded and became the epicentre of oolitic shoals. Shorefaces mainly develop in the northeast, facing the open sea, whereas the tidal environments were mainly restricted mainly to a narrow strip in the south.

Overall, the stratal stacking patterns are indicative of progressive backstepping of depositional environments up-section and towards the basin margins in the Precipice-Evergreen succession. Marine influence became increasingly more prominent up section, though occurred in discrete pulses probably derived from a combination of autogenic (i.e. lobe switching, channel avulsion) and allogenic (base level fluctuation due to tectonics or global forcing) control. In the early stages (below J20), the main sediment provenance was the Wunger Ridge in the southwest. The southeast near the Moonie-Goondiwindi Fault system and northeast were secondary sediment sources. During later stages, sediment input from the southeast increased at the same time as the north-eastern basin margin was being transgressed. This resulted in overall decreasing importance of the northeast as a source of sediment input. It is likely that a connection to the sea, although still speculative, would have occurred in this part of the basin (cf. Bianchi et al. 2018).

**Figure 28** Schematic paleoenvironmental/facies map for the interval from J10-TS1. This is the main reservoir interval, consisting predominantly of the “Blocky Sandstone Reservoir” (i.e. Facies SA). Selected wells are marked to orient the reader.

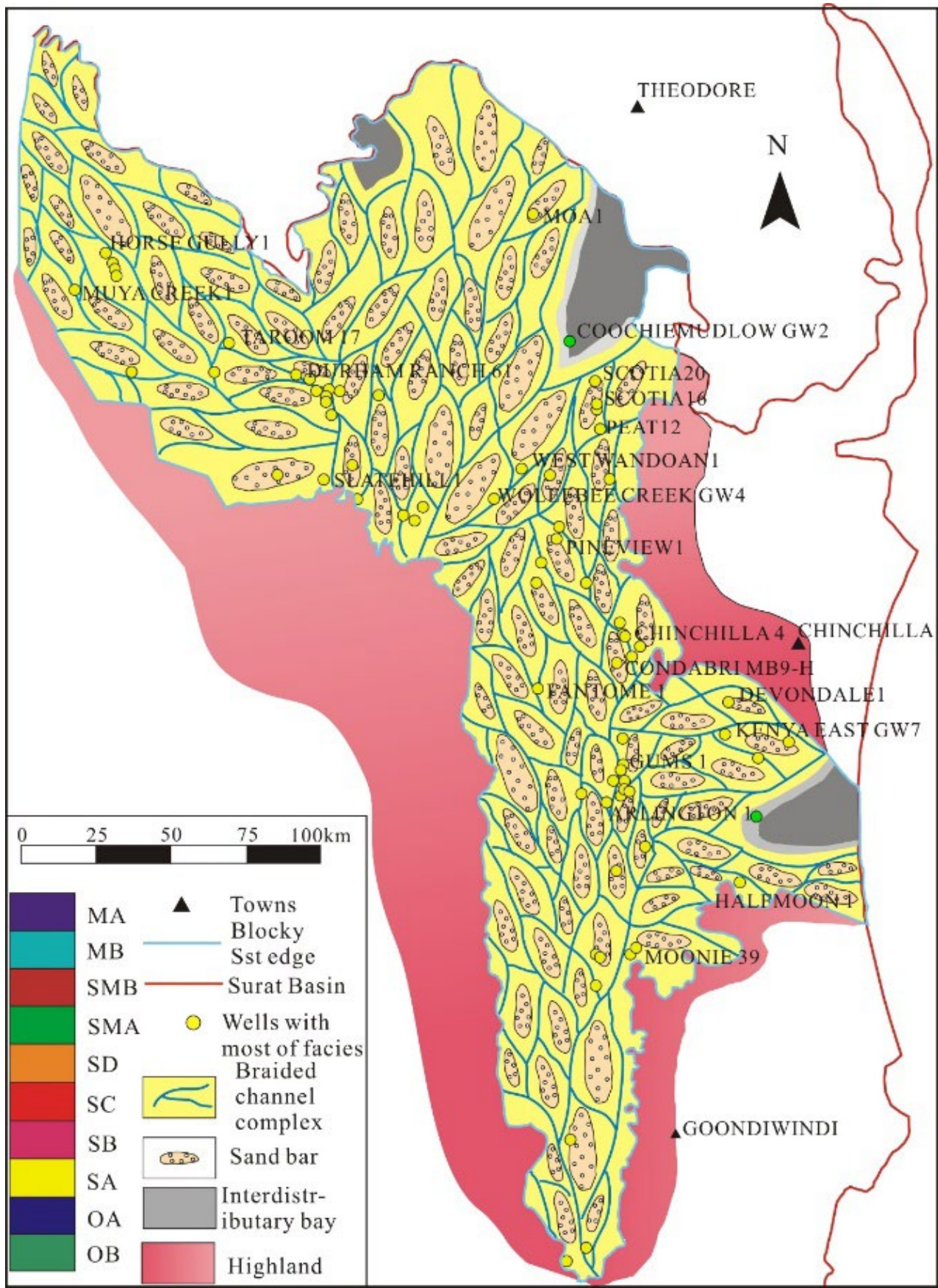


**Figure 29** Schematic paleoenvironmental/facies map for the interval from TS1-MFS1. This is the first part of the Transition Zone. Here begins the development of delta plain to subaqueous delta depositional environments that back-stepped towards the basin margins during a transgression in base level. Selected wells are marked to orient the reader.

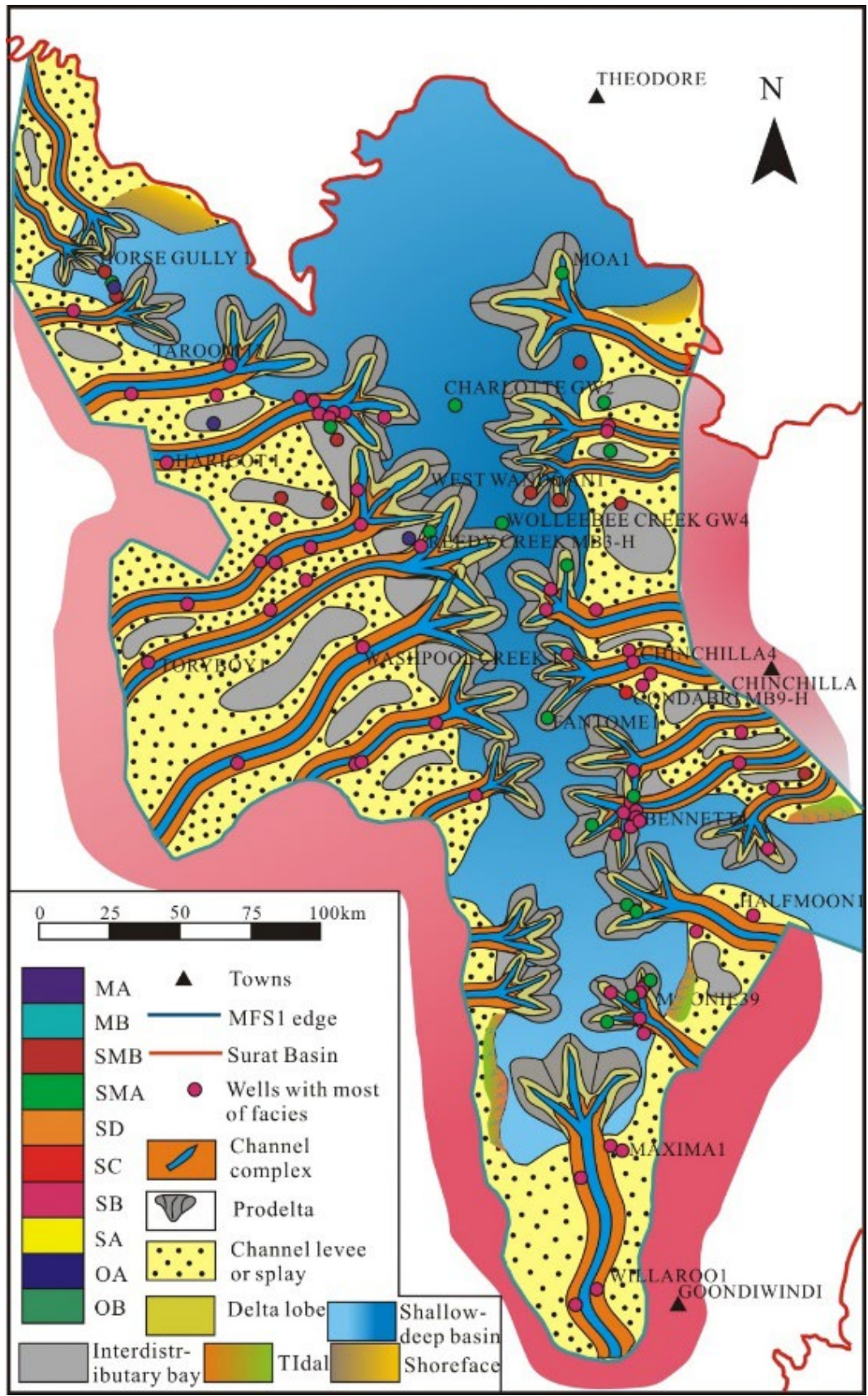




**Figure 30** Schematic paleoenvironmental/facies map for the interval from MFS1-SB. This is the middle section within the Transition Zone. At this point in time deltas prograded back towards the basin centre during a base level high stand. Selected wells are marked to orient the reader.

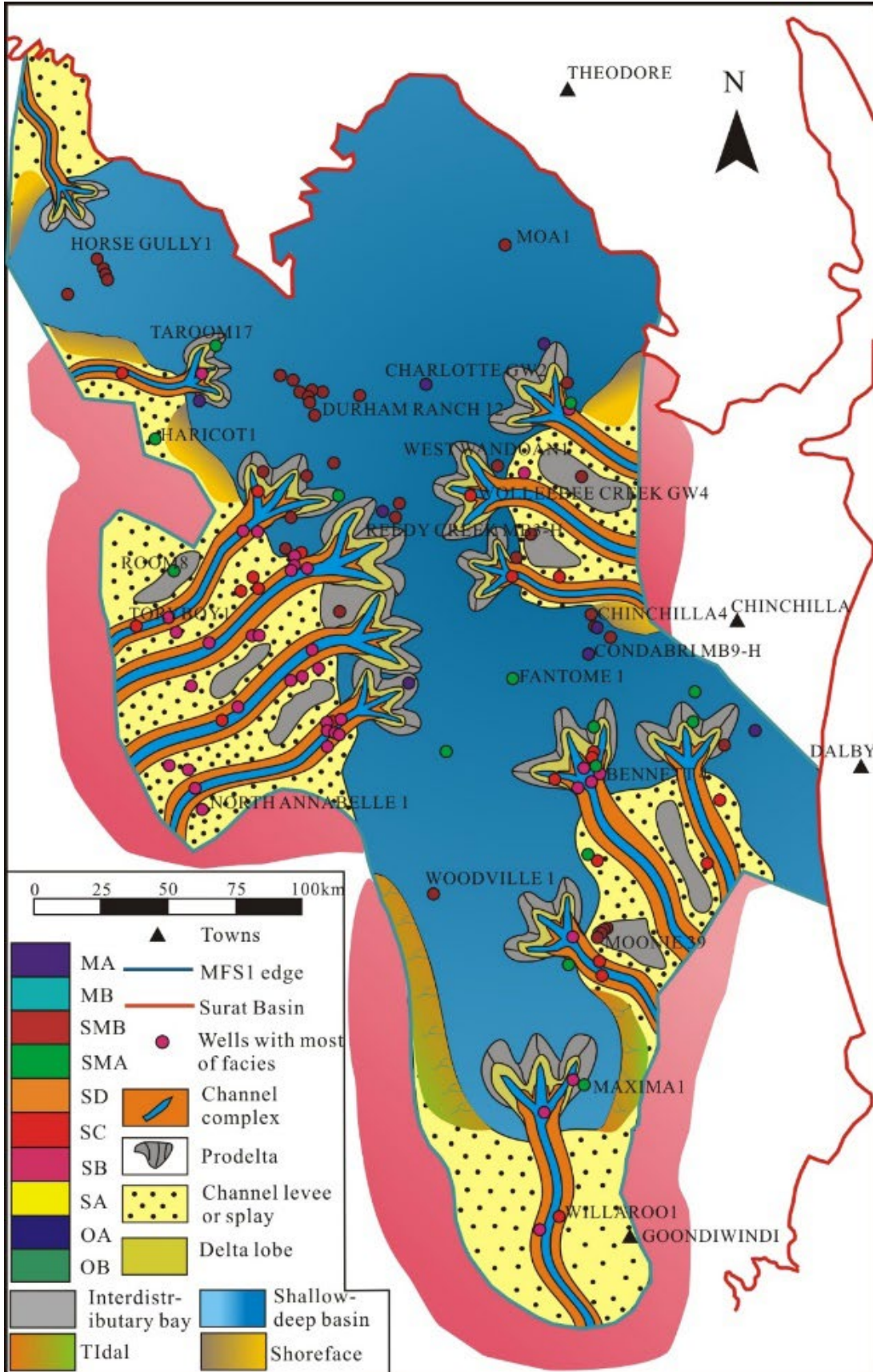


**Figure 31** Schematic paleoenvironmental/facies map for the interval from SB2-TS3. This represents the top portion of the Transition Zone. A similar situation to the underlying interval occurs with deltaic and nearshore depositional settings back-stepped during sea level transgression and then prograded back to the basin centre during highstand. Selected wells are marked to orient the reader.

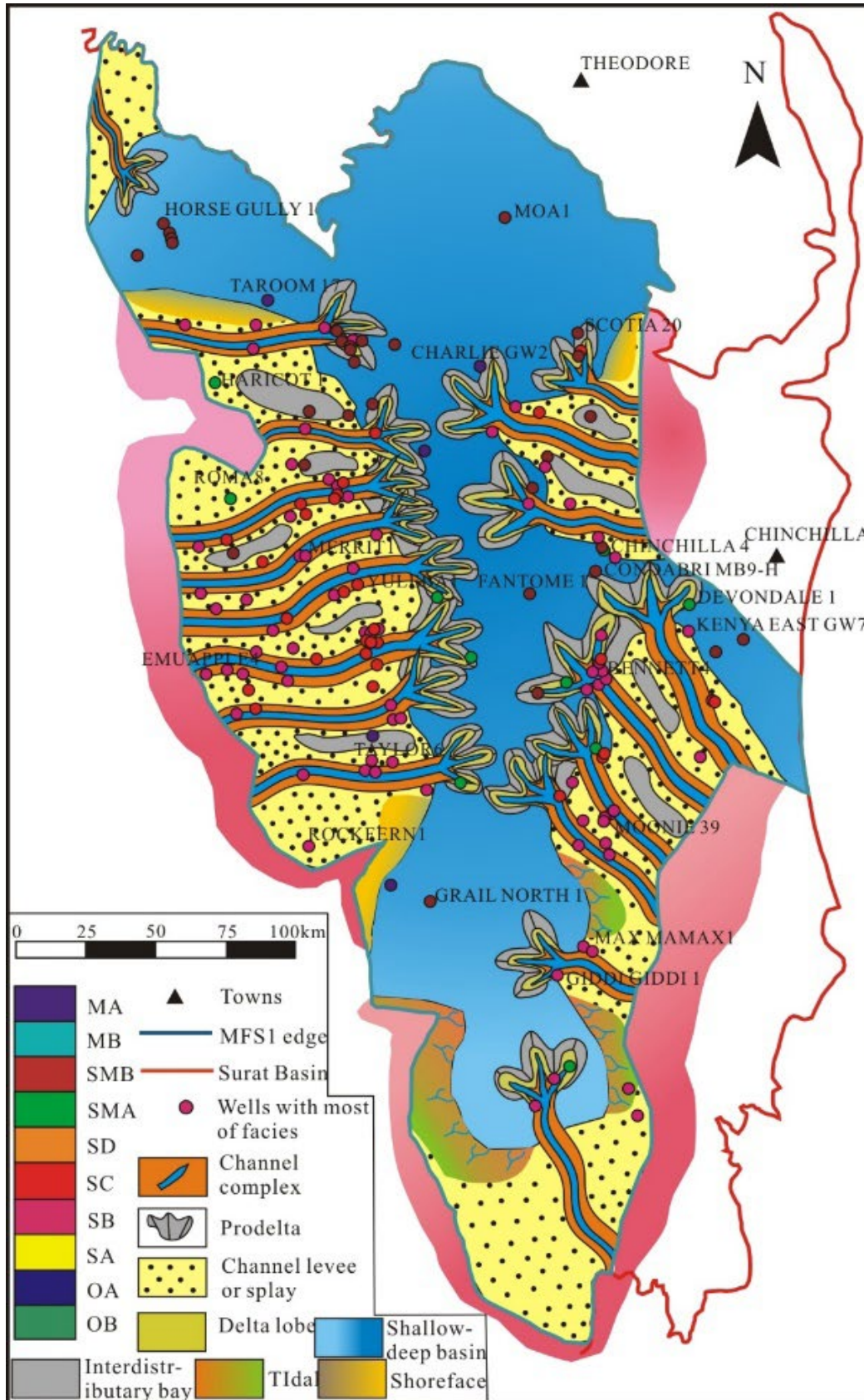
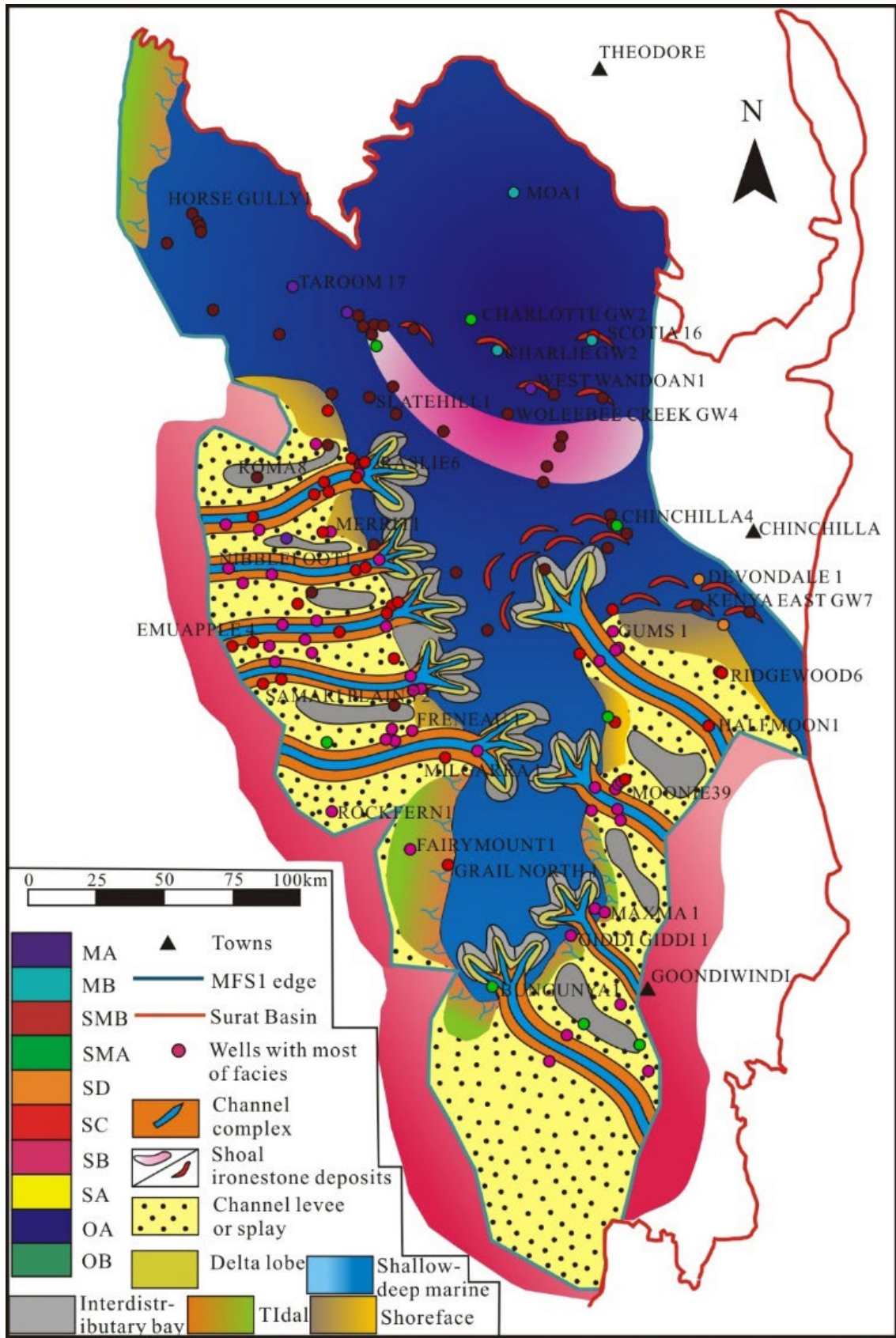


**Figure 32** Schematic paleoenvironmental/facies map for the interval from TS3-J30. This is the Ultimate Seal interval for the basin. It is characterised by widespread ironstone and mudstone with very low porosity and permeability. Peculiar depositional conditions occurred in pulses allowing concentration of iron in the water column and nearshore realm. The top of the succession is overlain by the Hutton Sandstone. Selected wells are marked to orient the reader.



The paleo-environmental interpretations for the various sequence stratigraphic intervals are a fundamentally important interpretive outcome for the UQ-SDAAP project because:

1. They provide an interpretive framework that is constrained by and consistent with all of the core, wireline logs and seismic data
2. In regions of little or no data control, the paleo-environmental interpretations provide constraints on the range of geologically plausible scenarios that could exist
3. This range of geologically plausible scenarios determines the range of porosity and permeability that could exist, which are used to populate the dynamic model rock properties for uncertainty analysis

### 4.3.5 Seismic analysis

**The fundamental revisions of stratigraphy (described in previous sections), have been integrated with (mostly) 2D seismic data of several vintages to further constrain and improve lateral prediction of the nature and extent of the Storage Play. This has significantly improved the understanding of aerial limits of the extent of the Blocky Sandstone Reservoir as well as the continuity of the Transition Zone and Ultimate Seal.**

Within the UQ-SDAAP geographic and stratigraphic area of interest (the Precipice Sandstone to Evergreen Formation), the main stratigraphic zones defined in the project (Figure 20) are correlated to the five seismic events (Table 17). Seismic Event 5 corresponds to the base of the Surat Basin (“J10” or Sub-Surat Unconformity). Seismic Event 4 (stratigraphic horizon “TS1”) represents the top of the Blocky Sandstone Reservoir. Seismic Event 3 occurs near the maximum flooding surface (“MFS1”) part way through the Transition Zone. The surface separating the Boxvale Sandstone Member below from the overlying Westgrove Ironstone Member is called Seismic Event 2 (“TS3” and “near J20”). Finally, Seismic Event 1 approximates the stratigraphic surface MFS3 in the middle of the Ultimate Seal (middle of the Upper Evergreen Formation). Note that the base of the Hutton Sandstone (top of Evergreen Formation) termed the “J30” does not exhibit a good seismic reflection or acoustic impedance contrast. Thus, it is not clearly constrained using seismic data and therefore was not able to be traced in the regional seismic framework. Seismic events 3 and 1 were localised features, and were not deemed to be basin-wide stratigraphic surface and are schematically shown in an east-west oriented seismic section tied to the Woleebee Creek GW4 well (Figure 33).

**Table 17** Reflector characteristics of the main seismic events.

Horizon	Seismic Event	Stratigraphic Top	Age	Horizon Colour	Lithology	Reflector Characteristics
Near MFS3	1	Ultimate Seal	Jurassic	Yellow	Shale, Silt	Low amplitude value (blue trough). No good lateral continuity
TS3 (Top Boxvale-Base Iron Stone Member)	2	Transition Zone	Jurassic	Red	Sand, Silt	Strong and continuous high amplitude (red peak) with a good vertical contrast between the Ultimate Seal and Transition Zone
Near MFS1	3		Jurassic	Green	Shale, Silt	Distinct positive amplitude (red peak) with generally strong vertical contrast on the margins of the basin.
Top Blocky Sandstone Reservoir TS1	4	Blocky Sandstone Reservoir	Jurassic	Blue	Sand	Strong low amplitude value (blue trough) marked by strong vertical density and velocity contrast across the basin indicating the top of the Blocky Sandstone reservoir
Unconformity SB1 or “J10”	5	Triassic Bowen Basin Strata	Jurassic/ Triassic	Orange	Silt, Shale, Clay & Sand	No significant change in seismic attributes, angular unconformity on underlying Bowen Basin sediments in some areas.

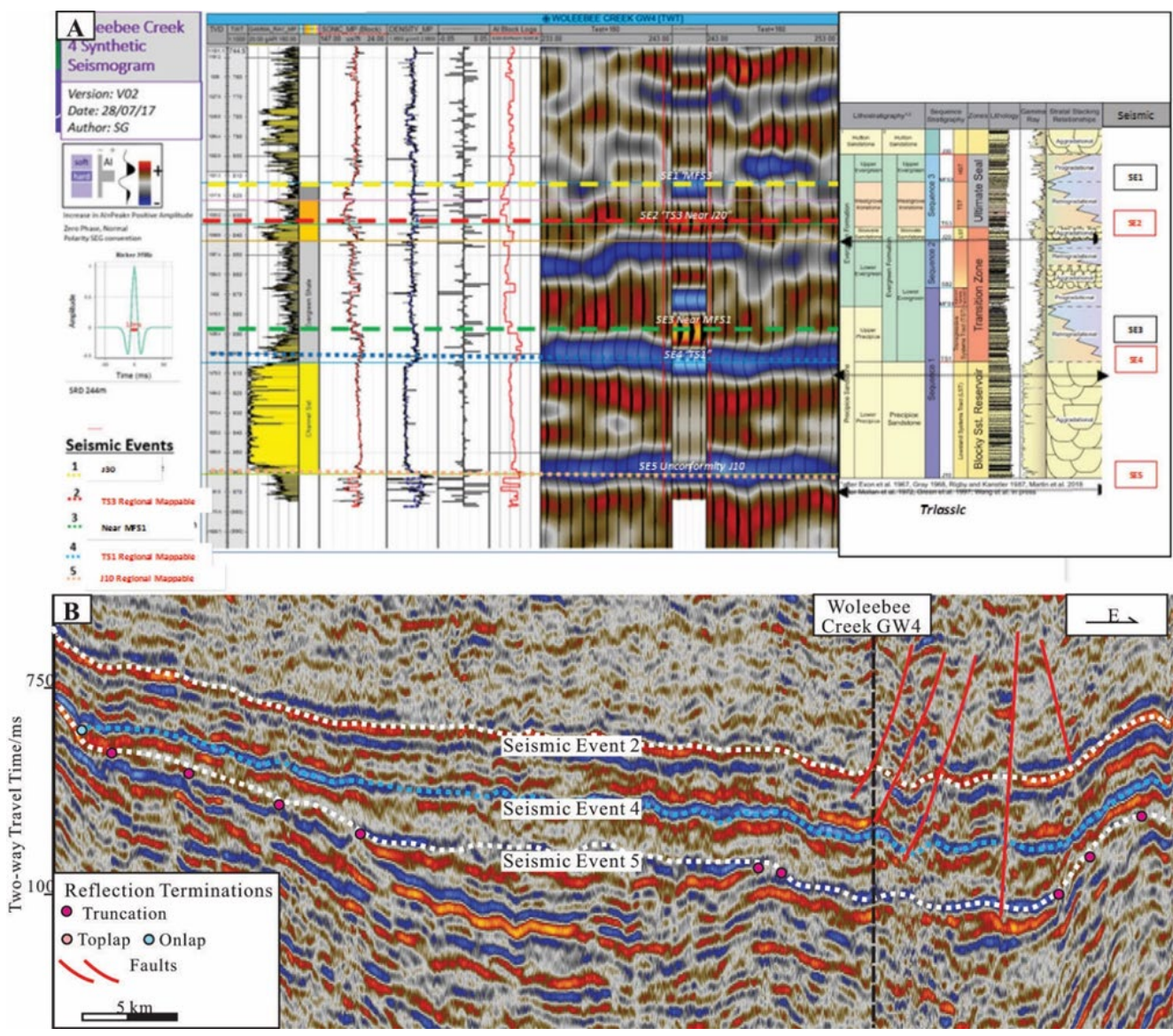
In SQ3 between Seismic Events 1 and 2, discontinuous and weak-amplitude reflections occur, which are caused by velocity and density anomalies related to the ironstone and cemented sandstone. However, with reference to Figure 33, Seismic Event 2 is a basin-wide, continuous reflection at the interface between the base of the “Ultimate Seal” and top of the “Transition Zone”. Given the extensive and consistent ironstone lithologies close to the top of the Transition Zone, the reflector continuity and consistency of Seismic Event 2 is supportive of an interpretation of a continuous and consistent Ultimate Seal (at bulk scale).

As a whole, the seismic reflection properties such as continuity and amplitude are closely related to sedimentary facies types and extent. The LST of SQ1 is composed of the coarsest sediments, is dominantly distributary channel facies, and is represented by the poorest-continuity and weakest-amplitude reflections between Seismic Events 4 and 5 on seismic sections. This is the Blocky Sandstone Reservoir Interval which is the proposed target for large-scale injection. Importantly, it thins toward both the western and eastern margins of the basin with an overall lenticular shape.

By contrast, the interval between Seismic Events 2 and 4, are represented by continuous near horizontal reflections with overall even thicknesses, corresponding to upward increasing mudstone and siltstone that have much greater lateral continuity. This Transition Zone interval is a buffer or baffle zone and lies above any injected CO<sub>2</sub>.

The sequence stratigraphic framework in the north Surat Basin is displayed in an east-west oriented seismic section (Figure 34). The reflector Seismic Event 5 is demarcated by underlying, angular truncation terminations, indicating increasing denudation (uplift & erosion) towards the western and eastern margins of the current basin centre. Erosion into an underlying anticline of the Bowen Basin strata on the eastern side of the basin implies that Pre-Jurassic compressional tectonics were responsible for the development of the base-Surat Unconformity (i.e. J10). Discontinuous, low amplitude reflectors within the Blocky Sandstone Reservoir, between Seismic Events 4 and 5, corresponding to the LST of SQ1, onlapping and thinning toward both the western and eastern basin margins. Within the Transition Zone, there are continuous high-amplitude reflections both in the TST-HST of SQ1 and SQ2, between Seismic Event 2 and 4. In SQ3 reflections weaken and decrease in continuity upward between Seismic Events 1 and 2, the latter being approximately the base of the Ultimate Seal.

**Figure 33** (A) Synthetic seismogram from Woleebee Creek GW4. (B) An east-west trending seismic section tied to Woleebee Creek GW4 that illustrates the sequence stratigraphic framework. The seismic data and synthetic seismogram are displayed in zero phase with SEGY convention polarity. See Figure 17 for section location.



As shown in Figure 35, the sequence boundary marks and internal reflection features cross the middle of the Surat Basin. Noticeably, the interval between Seismic Events 4 and 5, relating to the LST of SQ1 have multistep internal onlap terminations and it pinches out both at the western and eastern margins of this basin.

**Figure 34** East-west trending seismic section showing the Lower Jurassic sequence stratigraphic framework across the northern part of the Surat Basin. The base of the Lower Jurassic (Seismic Event 5) is a regional unconformity typically manifest by truncation and onlap reflector terminations. Note that the reflectors between Seismic Event 4 and 5 onlap and thin toward both the western and eastern basin margins.

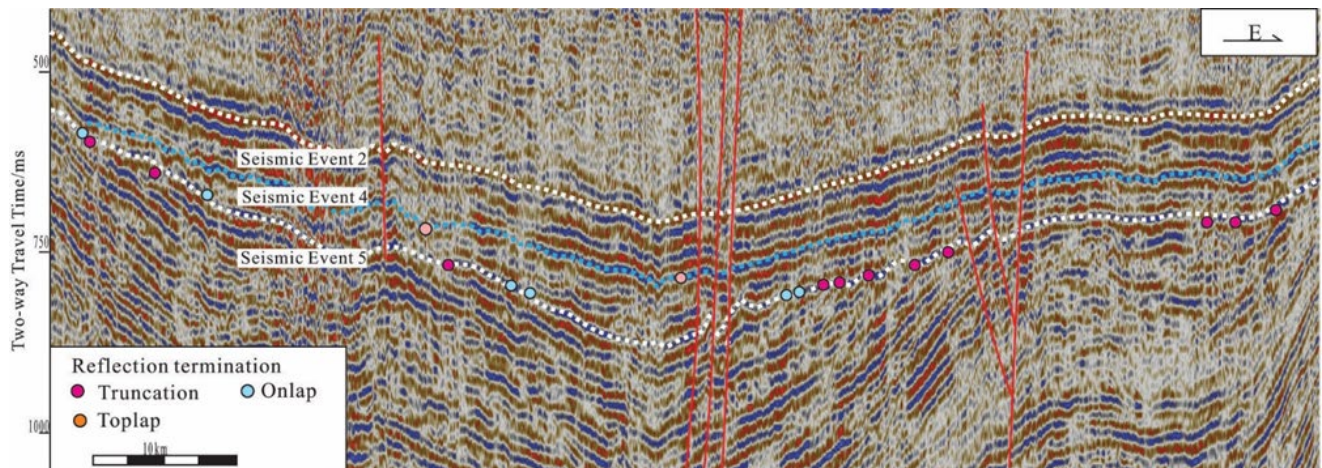
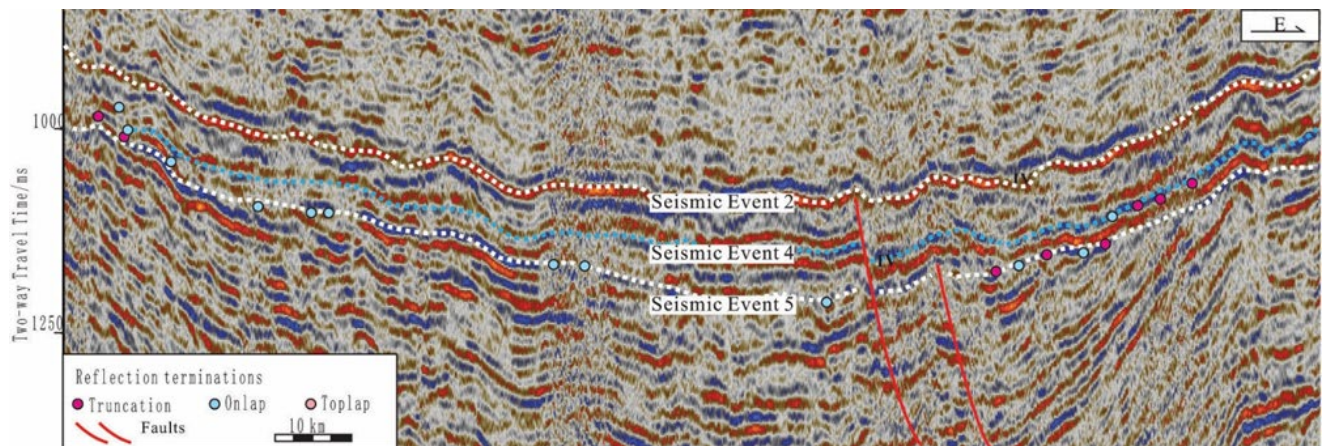


**Figure 35** East-west trending seismic section showing the Lower Jurassic sequence framework across the central part of the Surat Basin.



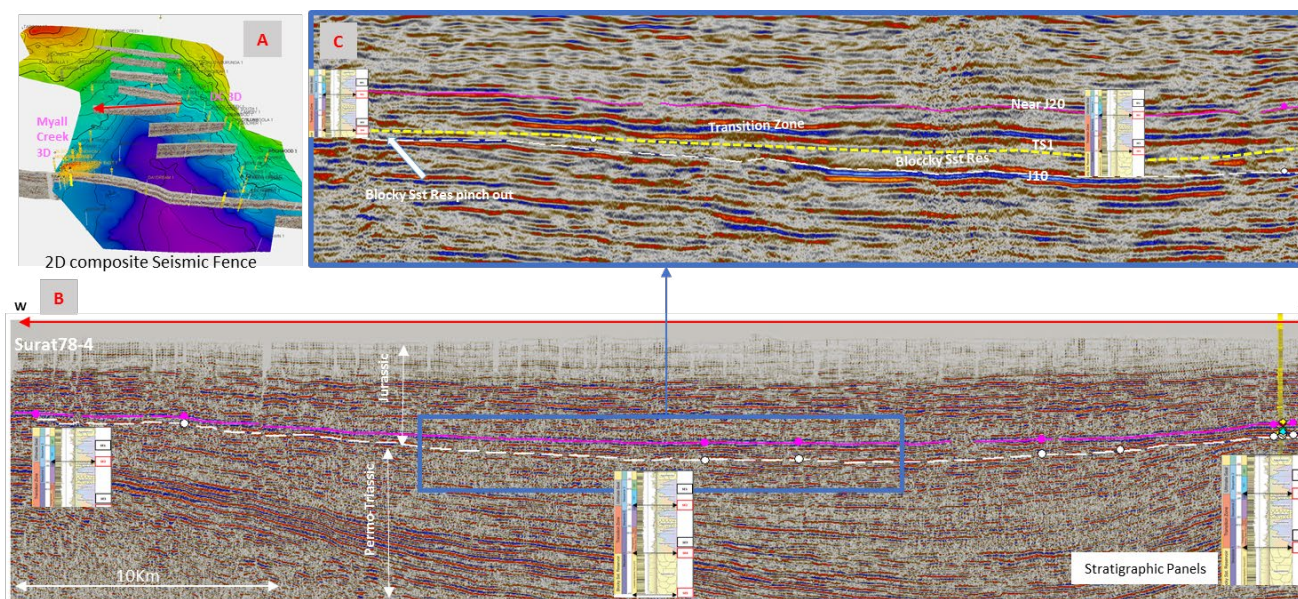
The report by Gonzalez et al. 2019a provides a detailed description of the seismic analysis workflow and how it was applied for the UQ-SDAAP project.

### 4.3.5.1 Seismic interpretation

The seismic interpretation for the regional seismic events, was mainly calibrated using 3D seismic data tied to wells with check-shot data and synthetic seismograms. These correlations were then extended to 2D seismic lines. Seismic correlation loops were conducted following the SEG-Y convention. The interpretation was initialised on localised seismic loops (field scale) offsetting the seismic reflections from the 3D areas into nearby wells along 2D composite seismic lines. This iteration was performed on several possible loops connecting well data to ensure the seismic traces are consistent from well to well, minimising the mis-ties and keeping the reflector trend between the lines.

The absence of 2D seismic data connecting the basin margins through the centre and the lack of wells providing seismic ties connecting the sparse east-west seismic lines in the centre of the basin, creates uncertainty in mapping the lateral continuity of the seismic reflectors. To overcome this, 2D fence seismic panels connecting 3D seismic data together were generated to estimate the regional trend of seismic features across the basin (Figure 36A). The integration of a regional overview of the seismic data from basin margins help to depict the stratigraphic thinning and potential areas for truncation (onlaps) affecting the basal units (Figure 36B-C).

**Figure 36** (A) Regional 3D map illustrating 2D regional composite seismic lines for seismic interpretation correlation. Background map is the top of the J10 unconformity. (B) An example of regional seismic line Surat 78-4 from West to East depicting the base Surat. Stratigraphic panels in the seismic line depict the stratigraphic correlation and basal unit onlap. The location and orientation of the seismic line is marked with a red line in A. (C) A zoom in of the blue box of the central region of the figure B exhibiting the thinning and on-lapping of the Blocky Sandstone Reservoir towards the east. The yellow marker on the seismic lines represents the top of the Blocky Sandstone Reservoir TS1, magenta is the top of the Transition Zone, near J20 and white marker is the J10 Base Surat Unconformity.



Seismic and well data integration from the flanks of the basin depict that the Blocky Sandstone Reservoir (Seismic event 4- TS1) is not a continuous single lithostratigraphic unit as has previously been interpreted. Rather, the Blocky Sandstone Reservoir is confined to the east and basin-centre regions within pre-existing topographic lows of the Base Surat Unconformity. The Blocky Sandstone Reservoir pinches out and onlaps onto topographic highs toward the flanks of the basin. Figure 36 and Figure 38 illustrates a well to seismic tie correlation along the best quality regional 2D seismic line BMR-84-14, from Myall Creek in the West to the Leichardt field in the East. Seismic Event 2 (Near J20) is the most consistent and continuous seismic reflector identified for the UQ-SDAAP project in most of the seismic lines. This seismic event is therefore used as the reference horizon for flattening cross sections in Petrel with the aim of highlighting subtle Transition Zone and Blocky Sandstone sedimentation and structural patterns. Even though Seismic Event 3 (MFS1) is correlated in synthetic seismograms for wells in the central part of the basin (Figure 38), the seismic reflector is not continuous regionally and is associated with a series of discontinuous sandy bodies consistent with the facies analysis from core and wireline logs (La Croix et al. 2019a).

Summarising: seismic interpretation provides critical data control away from wells that serves to constrain the uncertainty of the static geological model. It has also identified some geometric features of the various sequence stratigraphic intervals that have important implications to the anticipated flow behaviour of the defined Container. These include:

- The Blocky Sandstone Reservoir has limited geographic extent and pinches out against the sub-Surat Unconformity to the western edge of the Surat Basin and to the south into New South Wales. The eastern edge becomes thin, filling in the topography of the sub-Surat Unconformity surface but also extends to the east (south of the town of Roma) apparently into the Clarence Morton Basin. This geometry restricts the reservoir volume, thus impacting the anticipated pressure response to commercially material CO<sub>2</sub> injection
- The seismic reflectors within the Transition Zone interval are discontinuous. This corroborates the facies interpretation that suggests the geobodies of these depositional environments are of limited lateral extent. The anticipated fluid response would be for limited vertical migration of CO<sub>2</sub> and transmission of pressure through a geological system of discontinuous baffles
- The Ultimate Seal strata marks a return to regionally correlatable seismic reflectors that are more geographically wide-spread than the underlying extent of the Blocky Sandstone Reservoir. This suggests that the Ultimate Seal is likely to have regionally continuous strata unlike the Transition Zone below. In addition, its sealing characteristics are more widespread than the distribution of either the Transition Zone or Blocky Sandstone Reservoir

**Figure 37** Seismic Line AP10-21 illustrating paleo- topography control for the Blocky Sandstone Reservoir deposition. Note the double amplitude reflector near the Ferret 1 well, which is thicker with respect to a single amplitude reflector near the Dulacca 1 well (paleo-high). The cross section location is shown by the red line on the inset map.

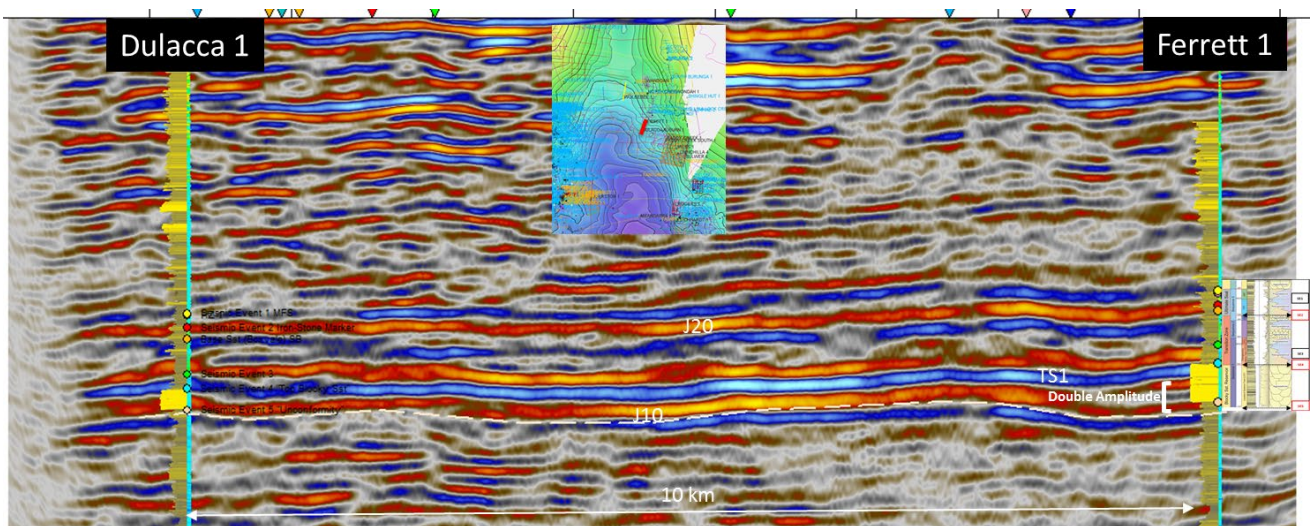
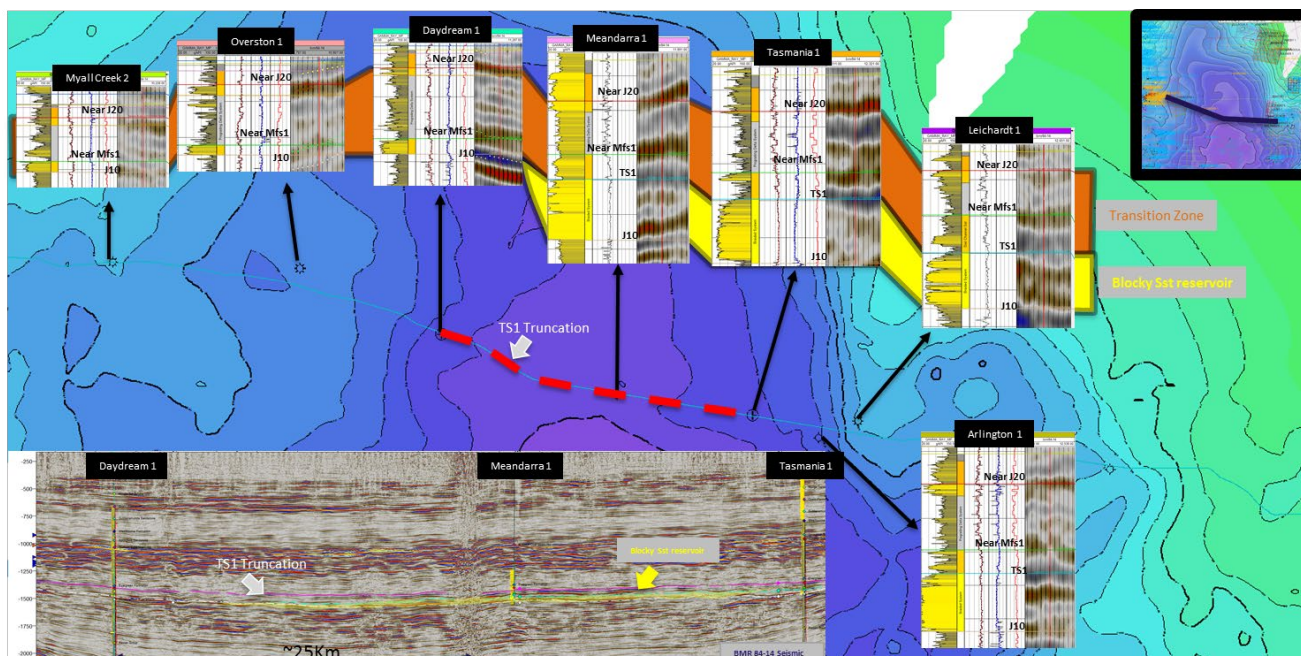




**Figure 38** Seismic Line BMR-84-14 (bottom inset), illustrating the seismic to well ties across the basin (the location of the seismic line is indicated by the red dotted line on the background map of depth to the Base Surat Unconformity). The seismic to well tie correlation indicates truncation of seismic event 4 (Top of the Blocky Sandstone Reservoir) in the east near the Daydream 1 well.



#### 4.3.5.2 Time-depth conversion and mapping

Seismic interpretations described thus far were made in two-way time (TWT). Time horizon structures were generated for the regional mappable seismic horizons J10, TS1 and Near J20 with their respective isochores (i.e. J10-TS1 = Blocky Sandstone Reservoir) which depicts the extent of the various stratigraphic zones in the basin. The most important aspect of the time depth conversion was to build a coherent 3D velocity model. Due to lack of representative seismic and well velocity data and the differences in structural and stratigraphic conditions between the east and west margins of the Surat Basin (where most of the data is available) a suitable regional 3D velocity model was not constructed. Therefore, to link the time-domain of seismic data and the depth-domain of well data, a velocity model was built based using check-shot data. The well velocity data was obtained from the time depth relationship (TDR) from wells with check-shot information. The time depth relationships were extrapolated to areas lacking well data. Sparse data commonly generates a pitfall of crossing grids while gridding thin layers near to truncation areas and paleo-highs. To overcome this issue, a stacking method for time depth conversion using a base reference grid and isochore maps with its respective interval velocities was selected to prevent crossing grids when data is sparse. For this method, the base Surat (J10 unconformity) was selected as the reference surface for the stacking process because this is the surface that creates the paleo-topography condition for the Blocky Sandstone Reservoir sedimentation (Figure 39).

Data used for the generation of the depth conversion is illustrated in Figure 40. A total of 32 offset wells (red dots on Figure 40) were found to have good quality check-shot data and these were used to tie with the respective seismic survey values. In addition, a time depth relationship was also developed and calibrated for wells with good sonic and density logs using check-shots from the nearby wells with velocity data available. The seismic data selected for time depth conversion covers the stratigraphic extent of the Blocky Sandstone Reservoir, Transition Zone and Ultimate Seal. The seismic data in the northern part of the basin has poorer resolution and lies generally at shallower depth (often too shallow for effective CO<sub>2</sub> storage). However well data and outcrop data from this region was integrated with the seismic data to help constrain the extrapolation of the seismic horizon grids. The time-depth conversion process provided the fundamental mechanism of getting seismic data into the same depth frame of reference as the well based geology data and it is the frame of reference that is relevant to buoyancy driven fluid migration process in multiphase systems such as CO<sub>2</sub> and formation water.

The notional injection sites were selected in location where the regional dip of the container strata is close to zero. This will limit the expected lateral extent of CO<sub>2</sub> migration post injection. Current uncertainties in the dip of strata are low, although more data coverage is still needed in the deepest part of the basin mainly to confirm absence of major faults.

**Figure 39** Structure contour map for base Surat J10 in depth. CI 200 m purple and dark blue denotes deep areas below 2000 m TVDSS. The red dotted line indicates the UQ-SDAAP model boundary. Inset square denotes location of Durham Ranch.

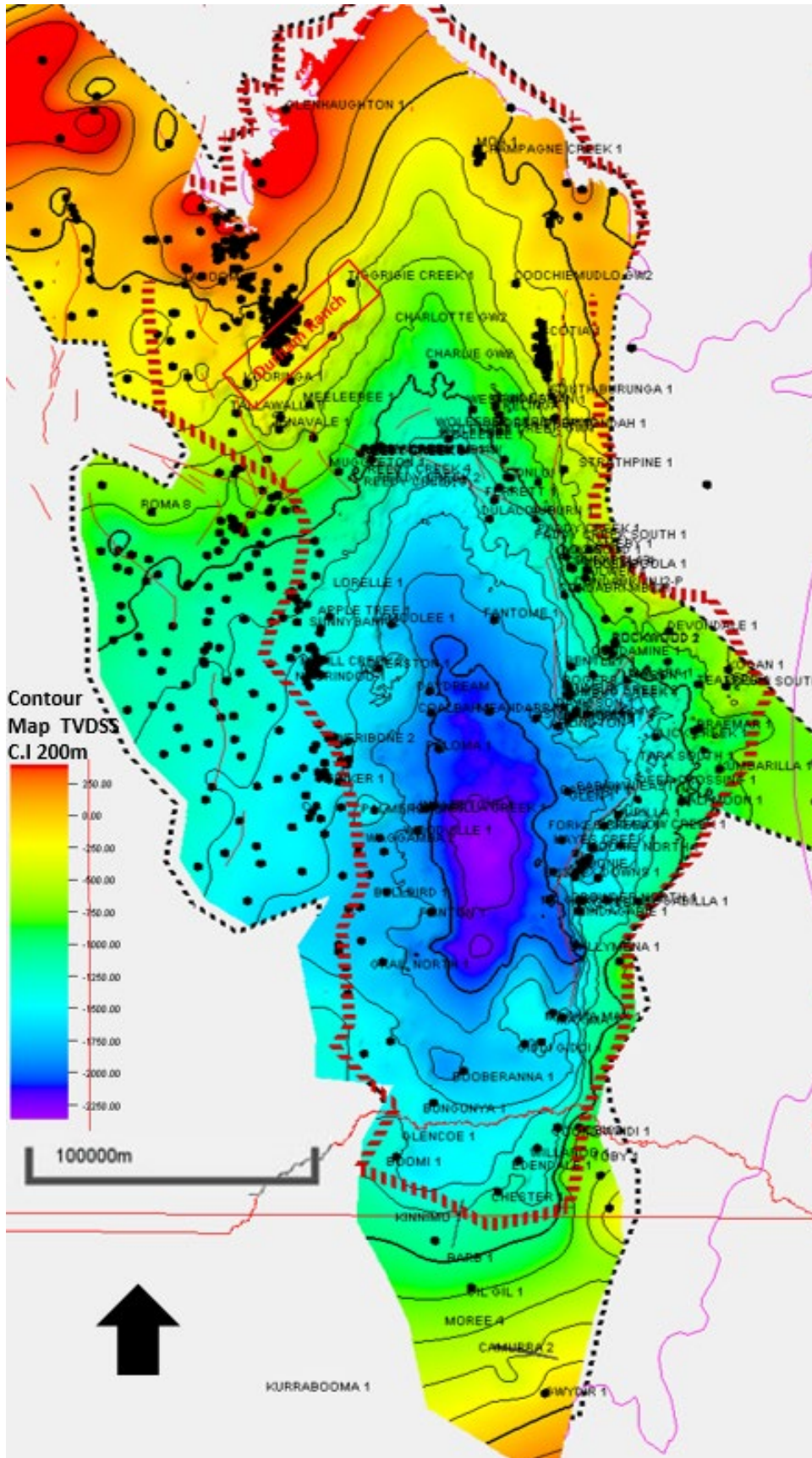
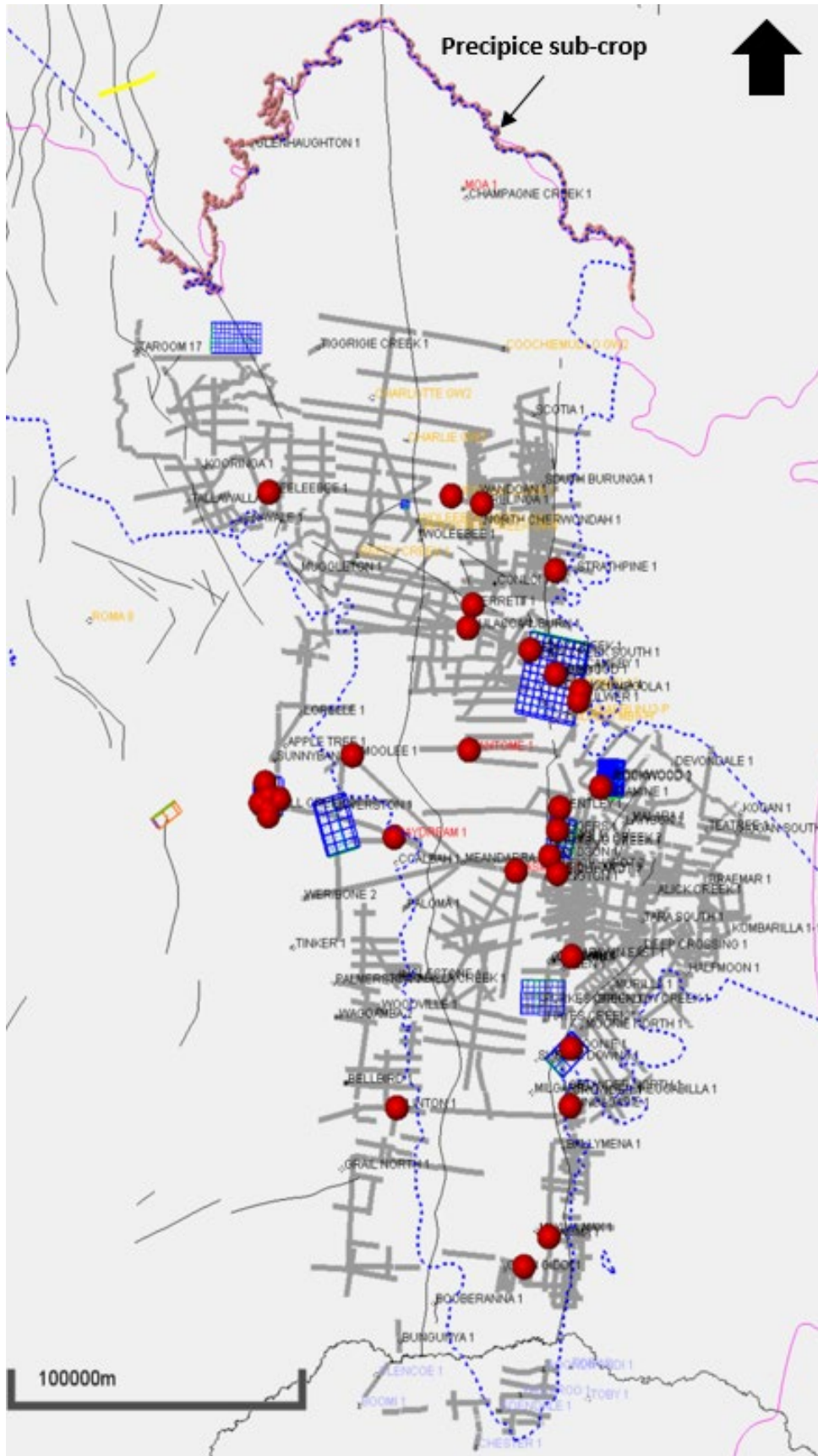


**Figure 40** Distribution of data used for the time depth conversion of seismic data. Red dots denote wells with velocity data. Lines in grey and blue are the 2D and 3D seismic data. Pink dots represent data obtained along the northern sub-crop of the Blocky Sandstone Reservoir.



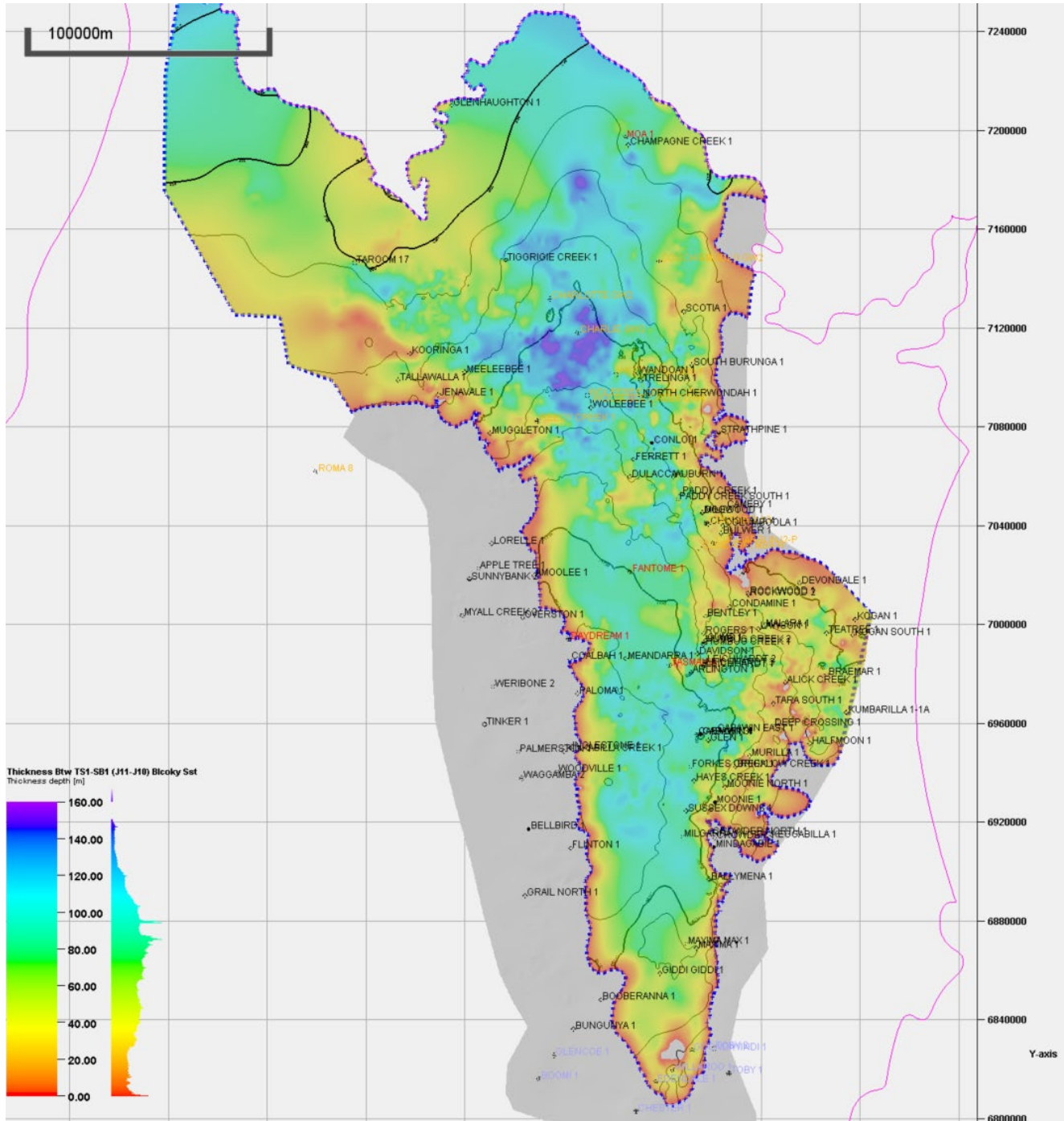
### 4.3.5.3 Discussion and results

A model of the distribution, thickness and depth of the Blocky Sandstone Reservoir, Transition Zone and Ultimate Seal is a key outcome from the seismic analysis linked with the sequence stratigraphic analysis (La Croix et al. 2019b). Based on the sequence stratigraphic concepts, the extent of the Blocky Sandstone Reservoir is limited towards the West onto the Wunger Ridge and Roma Shelf. In the south the unit becomes narrower from east to west and becomes shallower with respect to ground level, eventually pinching out against Permo-Triassic sediments approximately 20 km south of the Queensland and New South Wales border. Depositional trends on the eastern side of the basin appear to be controlled by uplift of the Late Triassic Hunter Orogeny, which exhumed the New England fold belt (Rosenbaun et al. 2018) leaving a narrow passage from the central part of the basin potentially connecting it with the Clarence Moreton Basin to the east (Figure 41). The paleogeographic depositional extent towards the north is still under debate as the units' shallow towards ground level and a substantial thickness of section is missing due to erosion.

The top of the Transition Zone, or Seismic Event 2 (Near J20), loses strong contrast in acoustic impedance towards the New South Wales border. This could be attributed to changes in lithological contrast where the wells exhibit fewer ironstone bands of the Westgrove Ironstone Member and where the Ultimate Seal becomes siltier. Alternatively, sandier lithologies underneath the Seismic Event 2 in the Transition Zone could account for the reduced impedance contrast. These two scenarios are not mutually exclusive. The importance of this observation is the fact that a sandier overall lithology and a thinner ironstone interval could result in a degradation of seal of the Ultimate Seal south of the Queensland boarder with NSW. The extent of the reflector and the nature of the underlying unit (the Transition Zone) structurally follows the Seismic Event 4 (Top of Blocky Sandstone Reservoir) in a "basin filling style" but with its extent covering further over the Wunger Ridge and Roma Shelf. However, the Seismic Event 2 also ultimately pinches out further south into New South Wales and towards the East, onlapping the underlying New England Foldbelt rocks.

**The integration of core, well log and seismic data within a sequence stratigraphic framework guided by a paleo-depositional environment interpretation has resulted in a new set of stratigraphic correlations that define the three main geological units of the Storage Complex. The thickness map of the Block Sandstone Reservoir presented in Figure 41 is a key outcome that will feed through further dynamic reservoir modelling. Note that the thickest areas (blue and purple) define a northern and southern depositional centre with a thin area (yellow) trending E-W separating them. This is an important and fundamental aspect of the depositional system. It will guide the next stages of petrophysical analysis and ultimately the assignment of rock properties to the dynamic model simulations.**

**Figure 41** Isopach map of the Blocky Sandstone Reservoir where the red colour indicates near to zero thickness and purple represents >150 m thickness. The central east region shows a thinner area likely controlled by paleo-structures in a highly faulted region.



### 4.3.6 Mudstone palynology and age of sediments

As discussed above, the revision of basin sequence stratigraphy and detailed, partly automated, facies analysis has been integrated with extensive seismic interpretation with the premise that the correlations are time equivalent in geological age of strata. An additional independent dataset (palynology) was also integrated to further increase confidence in predictions and verify their validity.

Biostratigraphic correlation is one of the most widely utilised methods for determining age-relationships of sediments in geological successions. However, interpreting the age of strata using fossil taxa or groups of fossil taxa contains an inherent degree of error and uncertainty. The uncertainties relate to sample quality, sample size and sampling interval, the resolution of the biostratigraphic zonation, and the fact that the stratigraphic record is incomplete (Cope 1995). Good, clean samples are important for quality biostratigraphic assessment to avoid the convoluting ages due to caving, reworking, or post-depositional mixing. Sample size and sampling interval have an important control on the resolution of age-determinations. There are stochastic effects related to the size of samples analysed and the amount of effort used to examine them (Cooper et al. 2000). Similarly, the vertical spacing between samples can impart uncertainty related to the lowest and highest occurrence of particular taxa; these never represent their true first and last occurrence. Therefore, good taxonomic understanding of the particular group of fossils being used for biostratigraphy is essential (Cope 1995; Pol & Norell 2006). However, not all time-intervals and groups are understood to the same resolution (e.g. Loydell 1993, Shackleton et al. 2000, Berggren et al. 1995; Kaufmann 2006). Since biostratigraphy is in essence an indirect dating method, this requires ties to geochronometric datasets at other locations. Finally, the stratigraphic record is incomplete in nature (Miall 2010), and this probably presents the largest uncertainty in achieving the highest possible resolution in depositional ages.

Another aspect of biostratigraphic analysis is the interpretation of depositional environment. Based on the suite of palynomorphs and their relative proportions, inferences can be made about the types of vegetation that were present in the environment (Farley 1990b; Batten 1974; Frederiksen 1985). These can then lend insights about faunal production, climate and latitude, and be used to help differentiate between subaerial, freshwater, and marine-influenced depositional settings (Czarnecki et al. 2014; Farley 1990a). The main types of palynomorphs recorded include spores, pollen, and algae – these are the most common non-marine forms. On the other hand, marine-indicators generally consist of dinoflagellate cysts, acritarchs, copepod eggs, and types of marine algae (de Vernal 2009). Of course, the relationship between palynomorph and environment is much more complicated with numerous other factors affecting the distribution of forms including windblown transport (Andersen 1974; Birks 1981), redeposition and sediment mixing (Davis 1968; Davis 1973), reworking of older palynomorphs, and unstable depositional settings in terms of water table fluctuations, and autogenic shifts in environment. These ultimately mean that interpretations based on palynology need to be couched in the context of other lines of evidence including stratigraphy, sedimentology, and ichnology.

A palynological analysis of core from the Precipice Sandstone and Evergreen Formations in the Surat Basin was undertaken to better refine our stratigraphy and interpretations of depositional environments. The research sought to address uncertainties in the age-relationships between sequence stratigraphic units to ensure our correlations were sound and to better predict lateral continuity of strata. Moreover, the paleoenvironmental information gleaned from the analysis was important for assessing the validity of facies interpretations and the size and distribution of geobodies. Ultimately, by reducing our uncertainty, better static reservoir models could be built. A total of 71 core samples from the Chinchilla 4, Condabri MB9-H, Kenya East GW7, Reedy Creek MB3-H, Roma 8, Taroom 17, West Wandoan 1, and Woleebee Creek GW4 wells were processed by MGPalaeo at their Malaga Laboratory in Western Australia. The report by La Croix et al. 2019d provides a detailed description of the Palynological Analysis workflow, detailed results by well and how it was applied for the UQ-SDAAP project.

#### 4.3.6.1 Results and discussion

Results of the palynological analysis showed that by and large the Precipice Sandstone fits into the APJ2 spore-pollen zone of Price 1997 or C. torosa zone of Helby et al. 2004 suggesting that it ranges from Hettangian to Pleinsbachian in age (Early Jurassic). The Evergreen Formation shows palynozonation within the APJ3 spore-pollen zone (Price 1997) or the A. fissus zone (Helby et al. 2004) with an age varying between Toriacian to Bajocian (Early to Middle Jurassic). The few samples collected from higher stratigraphic intervals (i.e. the Hutton Sandstone) generally fit into the APJ3 zone (Price 1997) placing it within the Middle Jurassic, but younger than the Evergreen Formation.

Paleoenvironmental interpretations of the samples showed an overall dominance of freshwater-continental origin for the mudstones. However, a proportion of the samples suggested subtle marine influence on deposition due to the presence of acritarchs and dinoflagellate cysts. These are scattered between wells and stratigraphic levels, though show an overall concentration above the J20 unconformity and upwards into the Westgrove Ironstone Member and Upper Evergreen Formation. The results don't necessarily contravene interpretations based upon sedimentology and ichnology, as there are many possible explanations for the distribution of palynomorphs. In fact, it is thought that these results support the idea that depositional environments shifted substantially due to small changes in base level and a very shallow dipping depositional gradient. These palynological results are not dissimilar to what is observed in modern large-scale delta systems such as the Mississippi River Delta, USA (Chmura 1994; Darrell 1973) and the Fraser River Delta, Canada (Czarnecki et al. 2014).

The palynology data provides confidence in the sequence stratigraphic correlations. It confirms that the combination of matching sequence boundaries in core and on log analysis, linked with regionally correlatable seismic reflectors, produced time correlative sequence stratigraphic interpretations consistent with depositional processes. These then have higher predictability away from well control. The data is also consistent with the depositional environment interpretations presented earlier (section 4.1.4).

### 4.3.7 Structural geology

Deposition in settings such as the lowermost Jurassic of the Surat Basin responds to both local and global factors that influence base-level. The degree to which local structures may have influence stratigraphy (tectono-stratigraphy) has been investigated, in part, to ensure consistency across the data sets. In addition, because faults might be potential leakage routes or pressure barriers, mapping the location of local structures (faults) and interpreting their likely geometry, juxtaposition and timing of activation or re-activation, is critical for containment risk analysis. The main risk reduction strategy taken has been to avoid or maximise distance to known faults and also to minimise pressure build up. Importantly, this new UQ-SDAAP study has interpreted a small number of high angle, low offset vertical faults in the areas of most interest as possible storage sites. The faults appear to project up to (near) surface, within the seismic data mute zone. They appear to have been formed or reactivated at least in the later Cretaceous and possibly much more recently. Existing data poorly constrains the lateral extent of fault density, so the acquisition of new data will be critical to further site maturation.

A basin-wide structural interpretation of the Precipice Sandstone and Evergreen Formation has limitations due to the general absence of 3D seismic data, poor quality 2D seismic data, and a general lack of published surface observations pertaining to the basin structure. However, there are locations where excellent data exists and this provides insights to the regional structure. Hillis et al. (1999) have reported that the majority of the faults (80%) in the uppermost kilometre of the crust are reverse, while in the northern and southern Bowen Basin, 17% of the faults are strike-slip, and only 3% are normal faults. It is important to note that there are several geological periods of deformation and strain, and that more recent strike slip and reverse faults are mainly reactivated older structures.

The UQ-SDAAP fault interpretation for the basin integrates seismic data and other geophysical datasets such as Bouger gravity and magnetics to depict regional structural grain or patterns. Processed gravity data were used to validate the relationship between paleotopographic elevation at the Sub Surat Unconformity surface and pre-existing tectonic features. Seismic data confirm that pre-existing basement fault geometries had a fundamental influence on the location of deposition and subsequent folding of the overlying sedimentary succession. For this reason, the UQ-SDAAP project investigated the characteristics of Permo-Triassic structural settings that underlie the Precipice Sandstone to Evergreen Formation strata. In this study, the fault interpretation is focused on the central and southern parts of the basin near to the notional injection site locations. Structural data and interpretations from the north were consolidated from the fault and fractures project performed by the UQ Centre for Coal Seam Gas Fault and Fractures project (Copley et al. 2017). Major faults were mapped along 2D seismic lines but they could not necessarily be correlated and mapped as continuous fault planes due to the wide separation between seismic lines. In these cases, the location of a fault crossing a 2D line and information on dip angle, dip orientation and throw (within the 2D line) were recorded with regional structural trends inferred from gravity maps (OzSEEBASE Map).

The report by Gonzalez et al. 2019a provides a detailed description of the Structural and Tectonic Analysis workflow and how it was applied for the UQ-SDAAP project.

The main risk reduction strategy taken has been to avoid or maximise distance to known faults and also to minimise pressure build up.

### 4.3.7.1 Regional tectonic setting

The structural framework for the J10 Sub-Surat Unconformity surface forms a gentle dipping to flat paleo-topographic surface that developed after several millions of years of Bowen Basin inversion and erosion. The main tectonic events that led to the J10 unconformity development are summarised in the Figure 42 where part A shows the stratigraphic column and B shows examples of 1D burial history plots (Reza et al. 2009). Initial Bowen Basin deposition and subsidence is bracketed by the magenta parenthesis that is terminated by basin inversion and erosion (red arrow at the top of the magenta bracket). This corresponds to first period of uplift on the burial history plots. This is followed by Surat Basin subsidence and sedimentation (red parenthesis) and a final period of basin inversion, uplift and erosion (the second red arrow and the second period of uplift on the burial history plots).

The three main tectonic stages of basin development are also identified in Figure 42C and D (Rosenbaun et al. 2018), where the Kanibiam Orogeny in the Carboniferous creates the western flank of the Bowen Basin (e.g. Roma Shelf and Wunger Ridge). Subsequently, in the Early Permian a rifting event took place that generating the Taroom Trough, which is the Bowen Basin major depocenter with up to 7 km of burial. Subsequently the Hunter Bowen orogeny in the late Permian and early Triassic resulted in deformation and basin inversion with uplift of nearly 4 km (Rosenbaun et al. 2018). This lateral shortening, uplift and mountain building was followed by extensive erosion that generated the J10 unconformity and defined both the topographic surface and the source regions of sediment that was to fill the Mimosa Syncline and form the Surat Basin.

Figure 43 depicts the isopach between the near J20 surface and the J10 Base Surat Unconformity. The near J20 surface underlays the Westgrove Ironstone Member. The isopach is like a “mould” of the paleotopography on the Base Surat Unconformity that contributed to both sediment supply (positive areas of the topography) and fill (negative areas of the topography). Note that the Surat deposition in the Mimosa Syncline is slightly shifted westward of the underlying Taroom Trough of the Bowen Basin, possibly due to tilting linked to the Hunter Bowen deformation.

**Figure 42** Summary of the structural evolution of Bowen and Surat basins, where; (A) Stratigraphic nomenclature for the Surat and Bowen basins. Red arrows denote basin inversion events, Magenta parenthesis is Bowen Basin Strata and the Red parenthesis is Surat Basin Strata; (B) Are 1D burial history plots (Reza at- al 2009) for four wells in the basin with each well location displayed in figure C. Red arrows denote basin inversion events, Magenta parenthesis is Bowen Basin Strata and the Red parenthesis is Surat Basin Strata. (C) Regional map of the Surat-Bowen basins for the UQ-SDAAP area of study, exhibiting major tectonic elements (Korsch et al. 2009) and illustrating the structural evolution from west to east of the Bowen Basin. (D) Deformation synthesis for eastern Australia between the Carboniferous (left) and Permo-Triassic time (right) (Rosenbaum 2018).

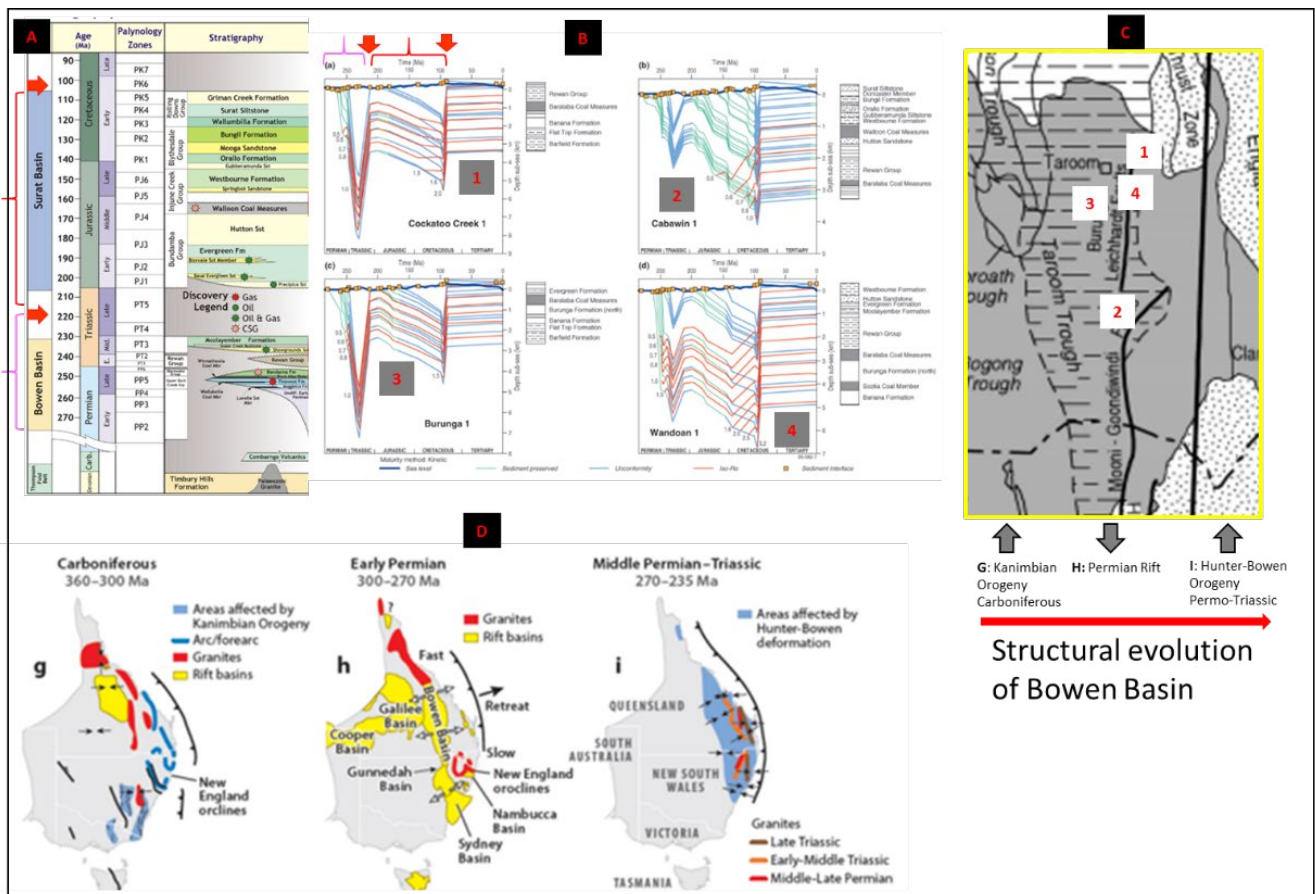
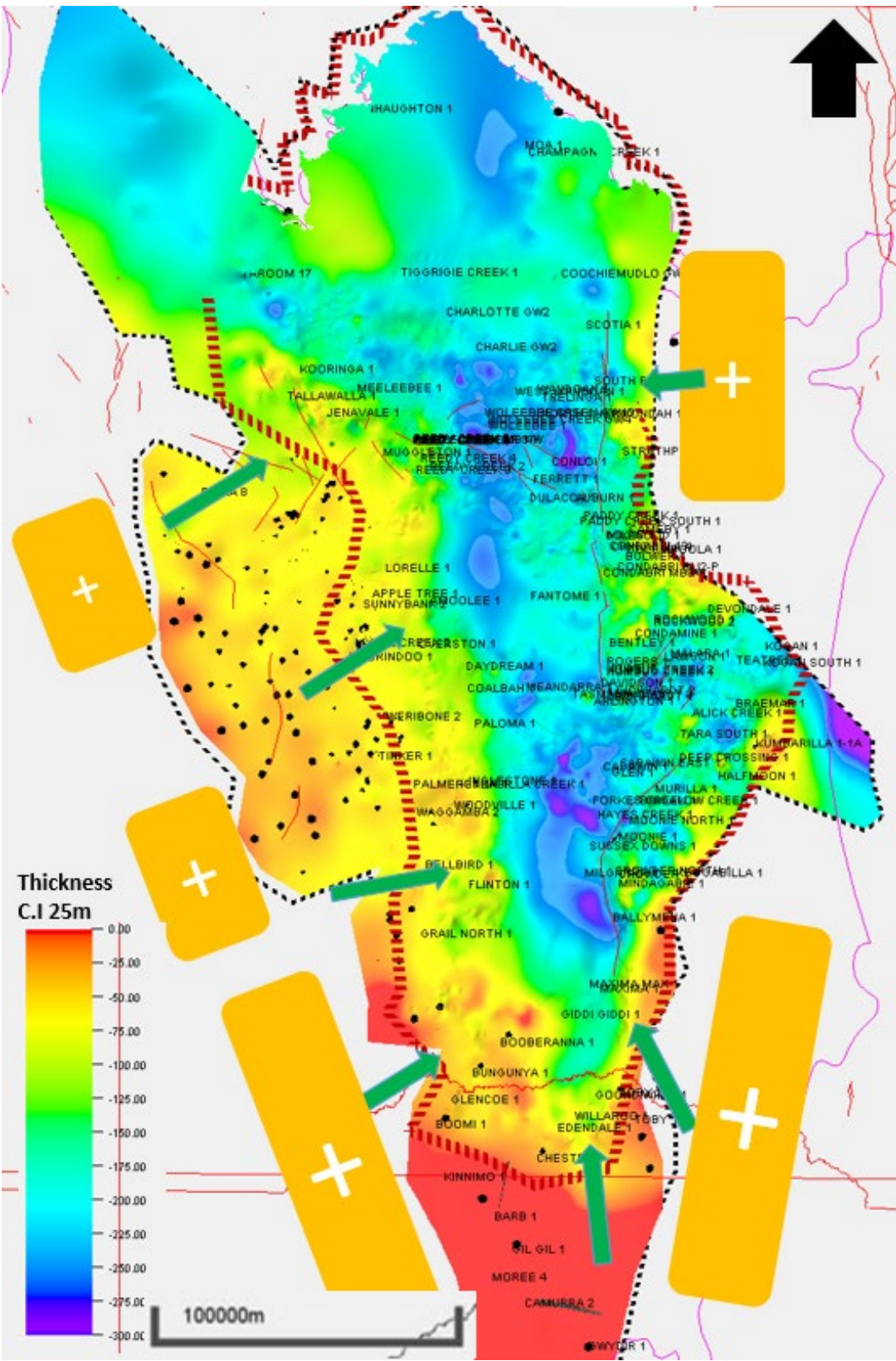




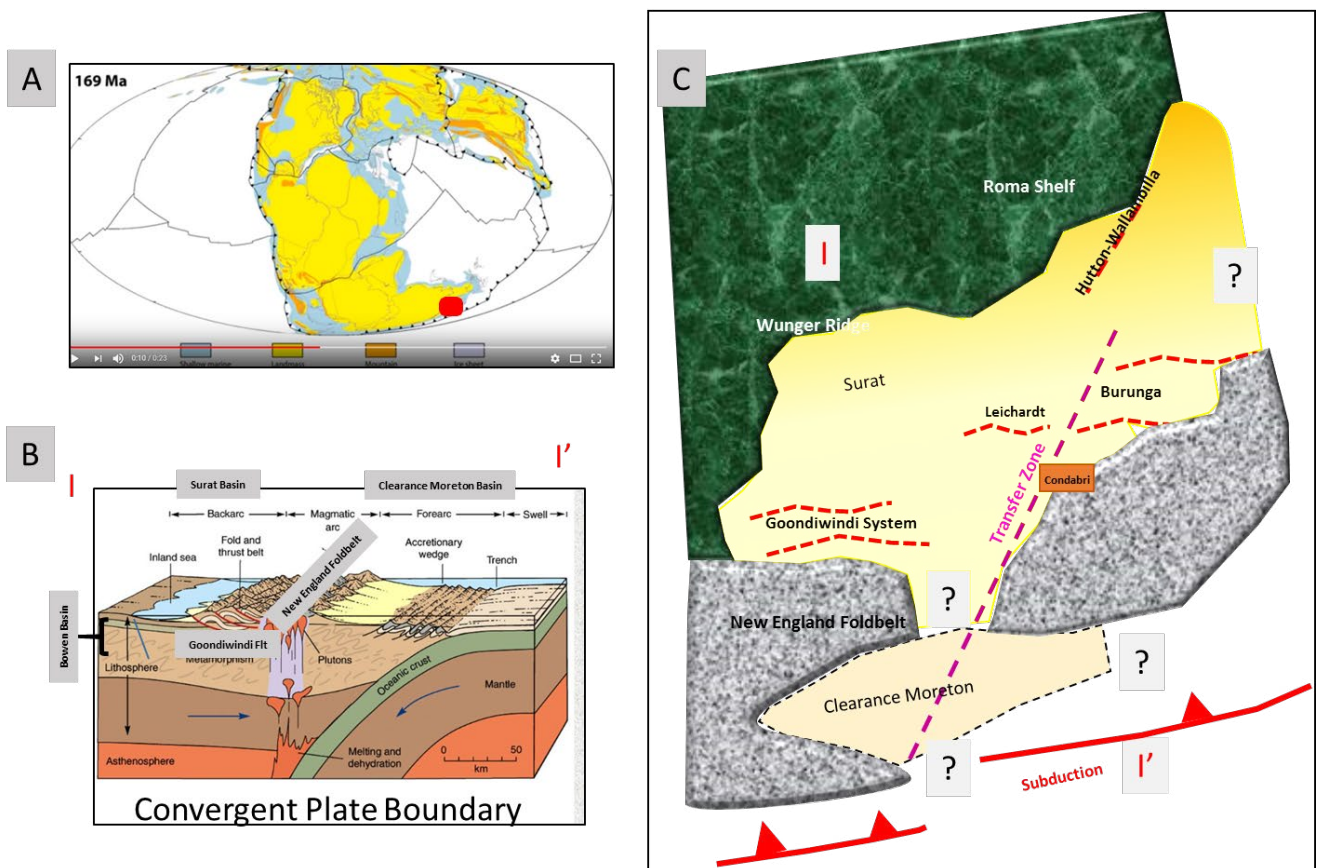
**Figure 43** The isopach distribution for the Transition Zone and the Blocky Sandstone Reservoir combined, exhibiting areas of J20 truncation towards the south where the red dashed line is the near zero edge, depocenters are highlighted by green-blue colours and potential emerging land masses are indicated in orange polygons. The size of the “+” in the polygon indicates the interpreted degree of emergence related to the provenance contribution (increasing to the south). The red dotted line indicates the UQ-SDAAP model boundary.



A schematic paleogeographic reconstruction of the Base-Mid Jurassic around 170 Ma is shown in Figure 44. The regional tectonic reconstruction model only includes the results of the seismic interpretation data in this study and is subject to a broader regional data integration from the eastern Australian and Papua New Guinean margins.

The closest plate tectonic boundary postulated to explain the Jurassic evolution of the Surat Basin is a convergent plate boundary. The schematic paleogeography in Figure 44 C is rotated to express the Australian location at Jurassic time. The yellow polygon denotes the extent of the Blocky Sandstone Reservoir. There is uncertainty on the extent of the basin on the east side of the map or if a connection to the Clearance-Moreton Basin exists. The major thick red line with triangles denotes the subduction zone and dotted red lines denote the major structural elements in the Surat Basin.

**Figure 44** Schematic paleo-geographic reconstruction of the J10 Base Surat Unconformity for the Surat Basin where (A) is the Scotese paleo tectonic- map at -170 Ma. The red square shows the location of the Surat Basin. (B) A schematic convergent plate boundary (taken from PM-FIAS 2015 website “continent-ocean convergence formation of fold mountains”) exhibiting the volcanic setting and thrust belt postulated to be analogous of the mountain building along the east side of Surat Basin during the Hunter-Bowen Orogeny prior and contemporaneous with deposition of the Blocky Sandstone Reservoir. (C) is a paleogeographic representation of the basin at -170 Ma with the tectonic elements associated with the postulated convergent plate boundary. The green area represents an emerged land mass at that time. Grey represents the magmatic arc (New England Foldbelt), whereas the yellow and beige polygons represent the Surat and Clearance Moreton basin sedimentation respectively. Note a transfer zone and possible connection between the two basins.



The Magmatic Arc (grey polygon) in Figure 44 C is postulated to be the eastern Hunter-Bowen Orogeny mountain building site with a fold and thrust belt component in the back-arc location (Figure 44 B). This event causes the NW-SE shortening and deformation of the Bowen Basin strata and erosion of this topography ultimately formed at least one source for Blocky Sandstone Reservoir sedimentation. The green polygon represents the emerged mass land on the north-western side of the incipient Surat Basin (Wunger Ridge, Roma Shelf and Gunnedah Basin in NSW) that was shedding sediment and contributing to Basal Sandstone Reservoir deposition as well. Figure 44 B is a schematic of a generic convergent plate boundary illustrating geographically the tectonic settings in relation to Surat and Clearance Moreton basins. The orientation I-I' in Figure 44 B is also located on Figure 44 C where the subduction zone is near I' and the Clearance Moreton Basin lie in a forearc setting. It is postulated that the simple geometry depicted in Figure 44 B, is complicated by a Transfer Zone (marked by a pink dashed line in Figure 44 C) that could explain a connection between the Clearance Moreton and Surat basins. The trend of this transfer zone is similar to the Hutton-Wallumbilla fault system on the eastern side of the Surat Basin and runs parallel to the current N-NW striking fault directions in the Condabri area.

A significant outcome of the geological characterisation, which combined facies analysis in a sequence stratigraphic framework linked with regionally trackable seismic reflectors, is that the Blocky Sandstone Reservoir thickness distribution defines two depositional centres with a thin area joining them. In the context of the paleodepositional environment this suggests two separate major braided fluvial systems, one in the north and one in the south, each with its own provenance source areas. The southern system may be draining to the east into the Clarence Morton Basin with the northern one draining to the northeast.

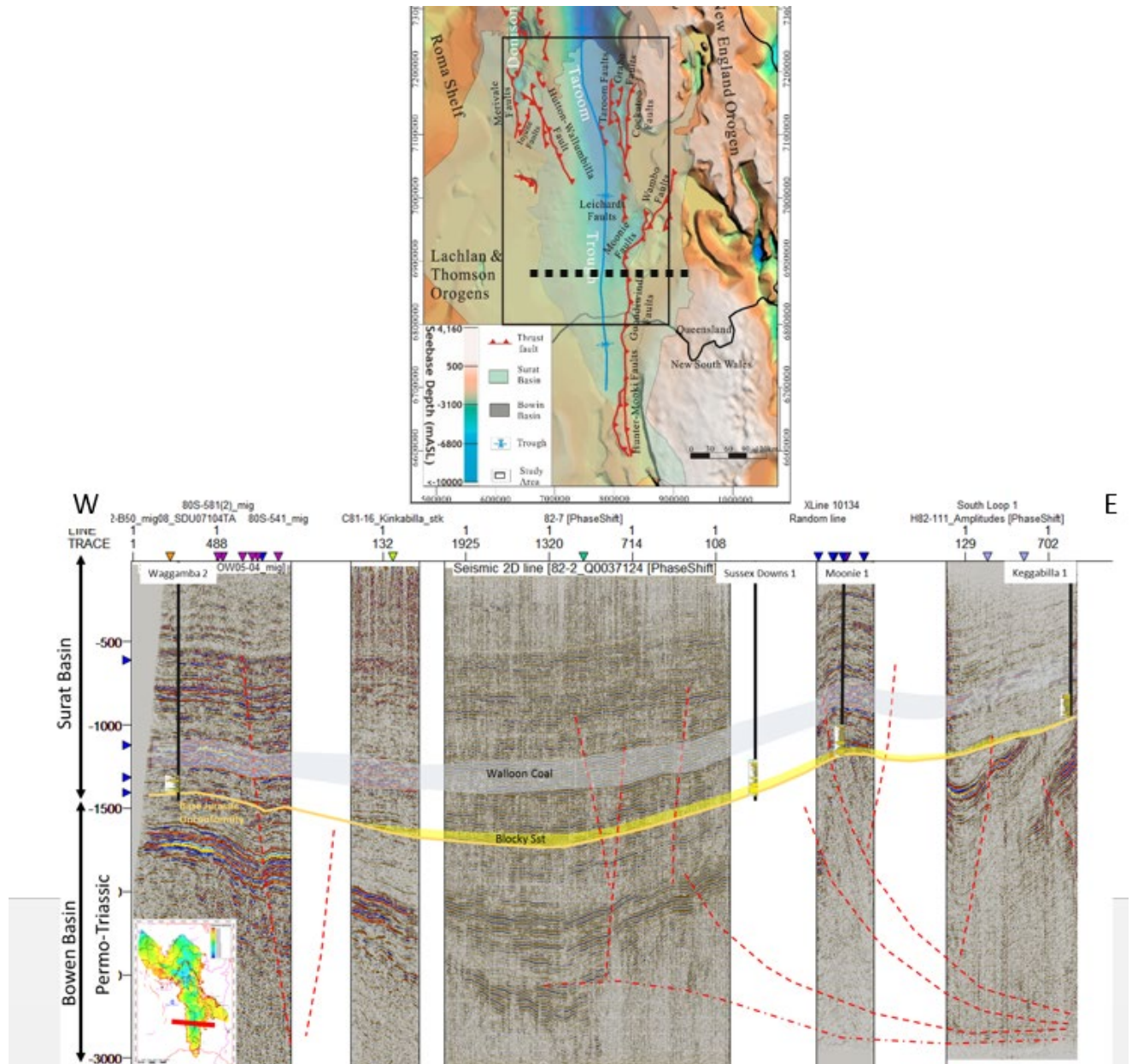
#### 4.3.7.2 Major fault trends

The UQ-SDAAP project has a focus on the Precipice Sandstone to Evergreen Formation stratigraphy that form the first sediments deposited in the Surat Basin. This analysis considered both the major faults that occur in the immediately underlying Bowen Basin strata that influence Surat Basin deposition, but also the major faults with in the Surat Basin strata. Figure 45 displays the main tectonic features of the Bowen and Surat basins, including the major faults obtained from previous regional interpretations in various public domain literature (e.g. Korsch et al. 2009 and Reza et al. 2009).

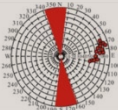
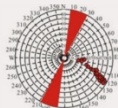
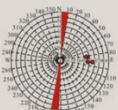
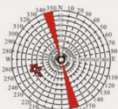
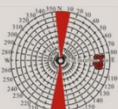
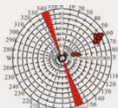
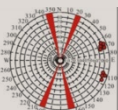
The major fault zones of the eastern Surat/Bowen basins can be divided into five key regions from south to north: Goondiwindi, Moonie, Leichhardt, Burunga and Cockatoo (Figure 45). This series of fault zones forms the eastern boundary of the Bowen Basin. Major deformation and shortening occurred at the end of Bowen Basin sedimentation in response to the late Permian to early Triassic Hunter-Bowen Orogeny (Fielding et al. 1990; Korsch et al. 2009 and Reza et al. 2009). In the western part of the basin, the Merivale and the Hutton-Wallumbilla Fault Systems formed the western margin of an extensive uplift on the Roma shelf extending ~100 km or more in a north-south trend. Korsch et al. 2009 and Reza et al. 2009 suggest that further deformation in the late Triassic consistent with transpression and reactivation of pre-existing structures resulted in complex fault architecture. The major faults have their key characteristics itemised in Table 18.

A significant outcome of the geological characterisation, is that the Blocky Sandstone Reservoir thickness distribution defines two depositional centres with a thin area joining them.

**Figure 45** An OzSEEBASE map showing the regional tectonic elements of the Surat Basin (Top figure). Bottom figure: shows a composite E-W seismic line with the major faults and structures affecting the Bowen and Surat basins marked in red dashed lines. The yellow polygon denotes the Blocky Sandstone Reservoir.



**Table 18** Characteristics of the major basement fault systems in the UQ-SDAAP study area interpreted from magnetic, Bouguer gravity and seismic data. Fault system azimuth orientation is taken from He et al. 2019 (paper in press).

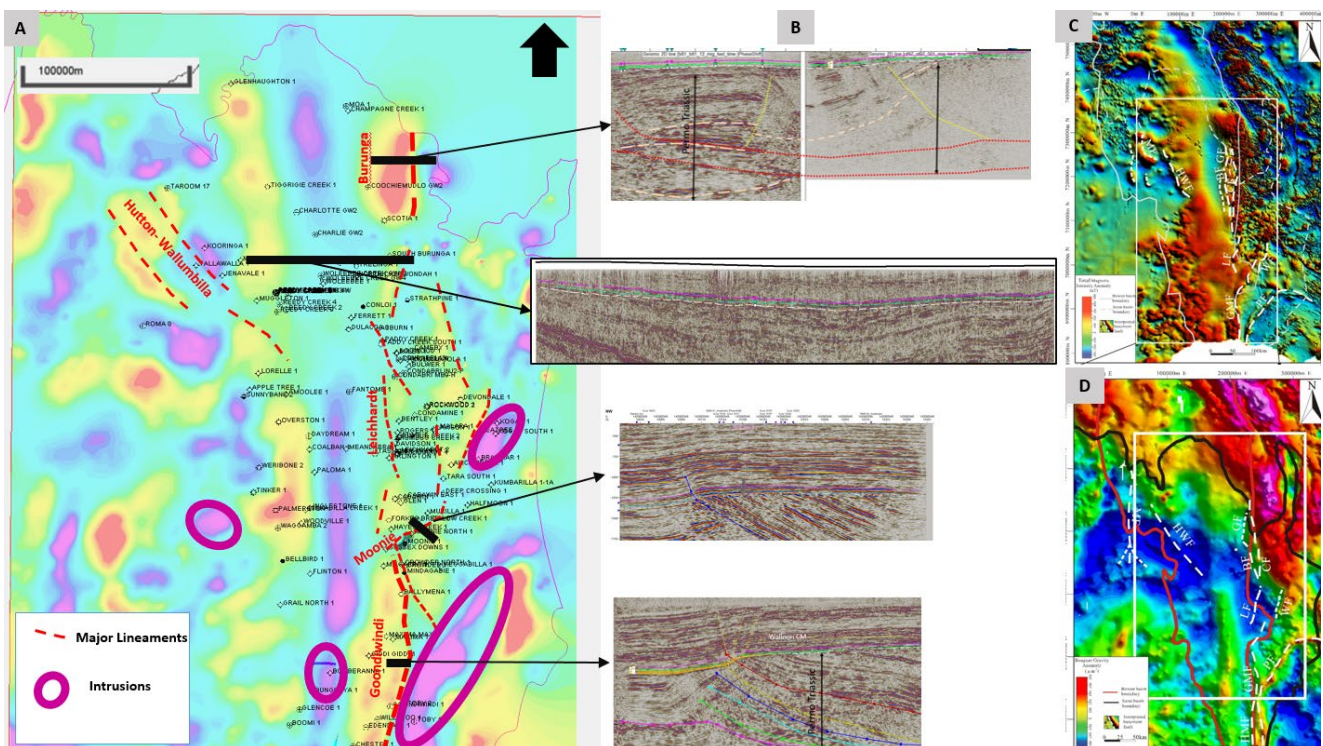
Fault System	Structural Style	Fault System Azimuth	Fault System Length (km)	Main Characteristic	Timing and Evolution
Goondiwindi	Reverse Fault Basement involved		80	Duplex style fault system with variations from high angle to low angle fault planes	Form in the Early to Middle Permian with evidence of reactivation at base Jurassic
Moonie	Reverse Fault Basement involved northern section and cover-decollement in the southern section		90	Continuation of the Goondiwindi System in the north with abrupt change in azimuth orientation (NE). Fault segmented in the Moonie Field section	Form in the Early to Middle Permian with evidence of reactivation at base Jurassic
Leichardt	High angle vertical reverse fault Cover decollements		30	High angle fault with generating a gentle Permian fold with throw >550 m. Form the Leichardt and Bennet field structures.	Form in the Early to Late Triassic. Possible reactivation in strike slip movement during Jurassic
Burunga	Reverse Fault Cover decollements		70	Listric and low angle reverse structure. Large throws ranging from 100 m to 600 m. This fault system generates the Burunga Permian anticline structure.	Form in the early to Late Triassic. No major evidences on fault reactivation Post-Triassic
Cockatoo	Reverse Fault Basement involved		100	Middle to high angle reverse fault with fault throws increasing from south to north.	Form in the Middle to Late Permian. No major evidences on fault reactivation Post-Triassic
Hutton-Wallumbilla	Reverse Fault Basement involved southern section and cover-decollement in the northern section		90	Low angle fault bend fault style in the north section and high angle trust fault in the south	Form in the Middle to Late Permian. Strong reactivation after deposition of Surat Basin (Cretaceous?)
Merivale	Reverse Fault Basement involved		80	High angle reverse fault system generating a Permian horst block	Form in the Early Permian. No clear evidence of fault reactivation at the base Jurassic

The major fault systems on the eastern flank of the basin are basement-involved with generally a north or northeast strike direction (Goondiwindi, Moonie, Burunga, Leichardt, and Cockatoo faults). These fault systems are often associated with pre-existing normal faults that formed during Early Permian rifting in the Bowen Basin with a reverse reactivation component that occurred in the late Permian to early Triassic (Hunter Bowen Orogeny) (Korsch et al. 2009 and Reza et al. 2009). These faults were variously reactivated during Jurassic-Cretaceous time with a possible strike-slip orientation as result of the Coral Sea rifting event (Gaina et al. 1998). However, they generally have not noticeably (based on available seismic resolution) propagated upwards (or may have only slightly propagated) into the lower strata of the Surat Basin. However, at some locations a high fault density in the Surat Basin is observed such near the Moonie oil field where fault reactivation reaches shallower depths.

Figure 46 summarises the different tectonic styles observed in the Bowen/Surat basins from an integration of data such as: processed gravity data Figure 46 A, regional seismic profiles Figure 46 B, total magnetic map Figure 46 C and Bouguer gravity map Figure 46 D. The seismic profiles in the south-eastern part of the basin show that the Goondiwindi Fault System is a series of the Surat Basin. The northern region shows flatter decollement of an imbricated system with antithetic faults creating large Permo-Triassic anticline features (Burunga Anticline) that are not reflected in the Surat Basin. The Leichardt fault system that is not illustrated in the seismic profiles is a vertical fault reactivated after Surat deposition with a possible reactivation also during Jurassic time. This fault system seems to have strike slip movement and has a deep decollement on a regional Permian imbricate fault.

There is a general lack of observable faults in the centre and southwest part of the Surat Basin and it is less affected tectonically than the northern and eastern margins. High density contrast in Figure 46 A represented by magenta colours are associated with thick Permo-Triassic strata along the Mimosa syncline axis. However, some magenta coloured areas indicate volcanic anomalies that can be correlated with the magnetic map (red areas in Figure 46 C). As an example, areas east of the Goondiwindi Fault show high-density contrast (Figure 46 A) that are related to volcanic intrusions (Figure 46 C) reported in well data. The volcanic areas in the processed gravity map (Figure 46 A) are marked in magenta ellipses.

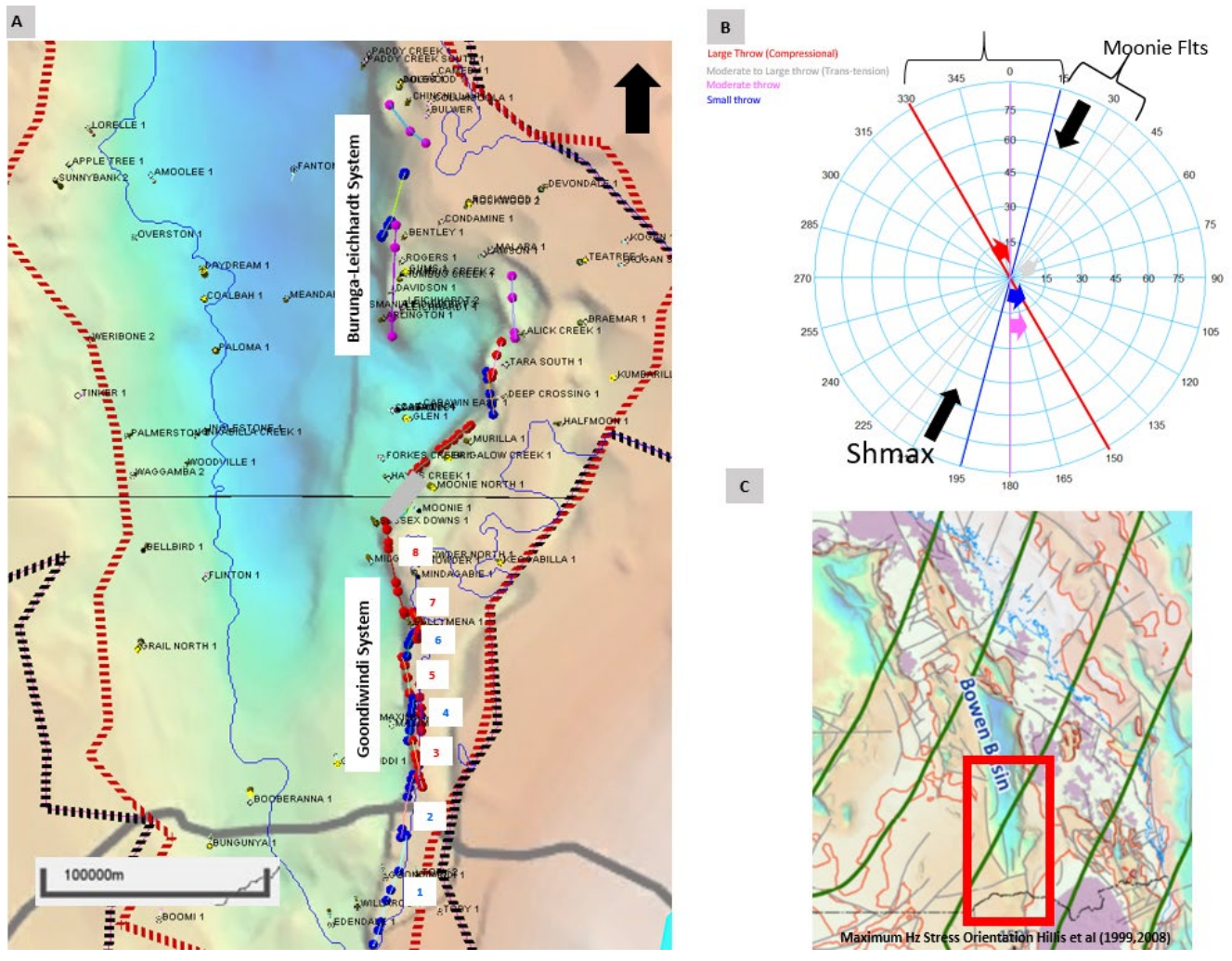
**Figure 46** (A) Processed gravity data (from original data in D Geoscience Australia) using a 100 km high pass filter showing major lineaments in red, linked to major structural features. Magenta circles denote a high-density contrast linked to intrusions as seen in the total magnetic map C (red areas in map C). (B) A sequence of seismic lines oriented east-west (not scaled). The seismic profiles illustrate the different tectonic styles observed in the basin. (C) Total magnetic map (Geoscience Australia). (D) The regional gravity map.



Other regional structural elements were mapped on the Roma Shelf area such as the Wallumbilla-Hutton Fault System with a strike direction N-NW (Figure 45). Figure 47 exhibits the fault segmentation interpretation and fault orientation relative to the current maximum horizontal stress (Hillis et al. 1998) for the Goondiwindi, Moonie, Burunga, and Leichardt Fault Systems. Fault segment lengths have been identified by changes in fault parameters (azimuth and dip). Colour codes denote relatively high medium and low throws by red, purple and blue respectively. The segmentation of the regional faults reveals a series of en-échelon faults oriented roughly parallel to the N-S regional structural grain. For instance, the Goondiwindi fault system is interpreted and mapped with a series of eight different offset fault segments along the regional trend. The segments vary in azimuth and throw and demonstrate variable degrees of propagation into the Surat Basin strata depending on the local architecture of the structures in the underlying Bowen Basin strata (Figure 46B and Figure 47A).

The azimuth variation of individual faults ranges from NE-NW with dip angles from 15 to 60 degrees (Figure 47B). Fault segments with higher throws are predominantly N to NW orientation, which is nearly perpendicular to the direction of maximum horizontal stress (SW-NE) (Hillis et al. 1998, Figure 47C). Fault azimuths parallel to maximum horizontal stress tend to have low throw.

**Figure 47** (A) A regional fault segmentation and classification analysis for the central and south east major fault trends. Colour code denotes the relative throw magnitude where red is high throw, magenta moderate and blue is low. (B) A stereonet plot of the fault segment orientations displayed by throw colour code. The maximum horizontal stress ( $S_{hmax}$ ) is also displayed in black arrows where the orientation is taking from Hills et al. (1988) map shown in C Faults with large throw in red are mainly oriented NW-SE almost perpendicular to the current  $S_{hmax}$  in the basin. (C) Maximum Horizontal Stress Orientation after Hills et al. 1998 for Queensland Basins. The red dotted line indicates the UQ-SDAAP model boundary.



### 4.3.7.3 Case study areas with 3D seismic

Areas with high data density and modern data sets have been investigated to inform interpretations in low data density areas in the basin centre.

In some areas with higher resolution 3D seismic data, fault geometries such as throw and dip angle can be resolved sufficiently to observe rapid changes along strike. This indicates complex discontinuous or segmented en-échelon fault segments perhaps linked by relays rather than continuous fault planes. The Moonie oil field potentially has its original free water level controlled by certain segments of the Moonie fault, which forms part of the larger Goondiwindi–Moonie fault system trend (Figure 48). Note that there is a bend in the strike of the regionally mapped Goondiwindi Moonie fault system, close to the location of the Moonie oil field. For this reason, the Moonie fault system is treated separately from the Goondiwindi trend in this study.

Previously, the Moonie fault has been mapped as a single segment reverse fault dipping south-east (Copley et al. 2017). A dip azimuth fault analysis by UQ-SDAAP of the Moonie 3D seismic volume reveals that the geometry of the Moonie fault (~15 km long) is comprised by six discrete segments. Each has a distinctive fault dip and azimuth (Figure 49). The total length of each segment ranges from 2 to 5 km and the dip angle at the Base Surat Unconformity ranges from 15 to 35 degrees with the higher angle observed in the centre where the throw is greatest. This was used as an analogy for interpreting the 2D seismic areas to help define fault segmentation patterns for other regional fault zones.

The Moonie fault system is unlikely to present a continuous flow barrier at regional scale and so is not likely to cause rapid pressure build up if large scale injection takes place in the deep basin centre to the west.

### 4.3.7.4 Timing for fault reactivation and further propagation to the Surat Basin

The seismic interpretation confirms a relative continuity of the Jurassic sediments without major faulting except for the areas on the eastern and north-western basin margins. These areas shown fault reactivation of deeper structures through the overlying Surat Basin strata. The most complexly faulted area of the Surat sedimentary succession is located northeast of the Moonie Field where the Blocky Sandstone Reservoir thins and on-laps paleo-highs of the J10 sub Surat Unconformity. Here, more recent reactivation (with a strike-slip component and small throw) of Permo-Triassic faults is observed to extend into the Surat Basin strata (see Figure 50), occasionally to the base of alluvial sediments.

**Figure 48** (A) The Moonie field location (white box) in relation to the regional OzSEEBASE Map. Blue and red dots are locations of interpreted faults crossing a seismic line. The red polygon is the approximate edge of the Blocky Sandstone Reservoir. (B) A 3D schematic diagram of the Moonie fault highlighting dip trends (purple plane). (C) Plan view of the Moonie fault showing the fault structural elements. Background map represents the structural contour map of the Top Blocky Sandstone Reservoir in depth, orange colours indicates shallow areas. Blue dots represent the Moonie well location. The red dotted line indicates the UQ-SDAAP model boundary.

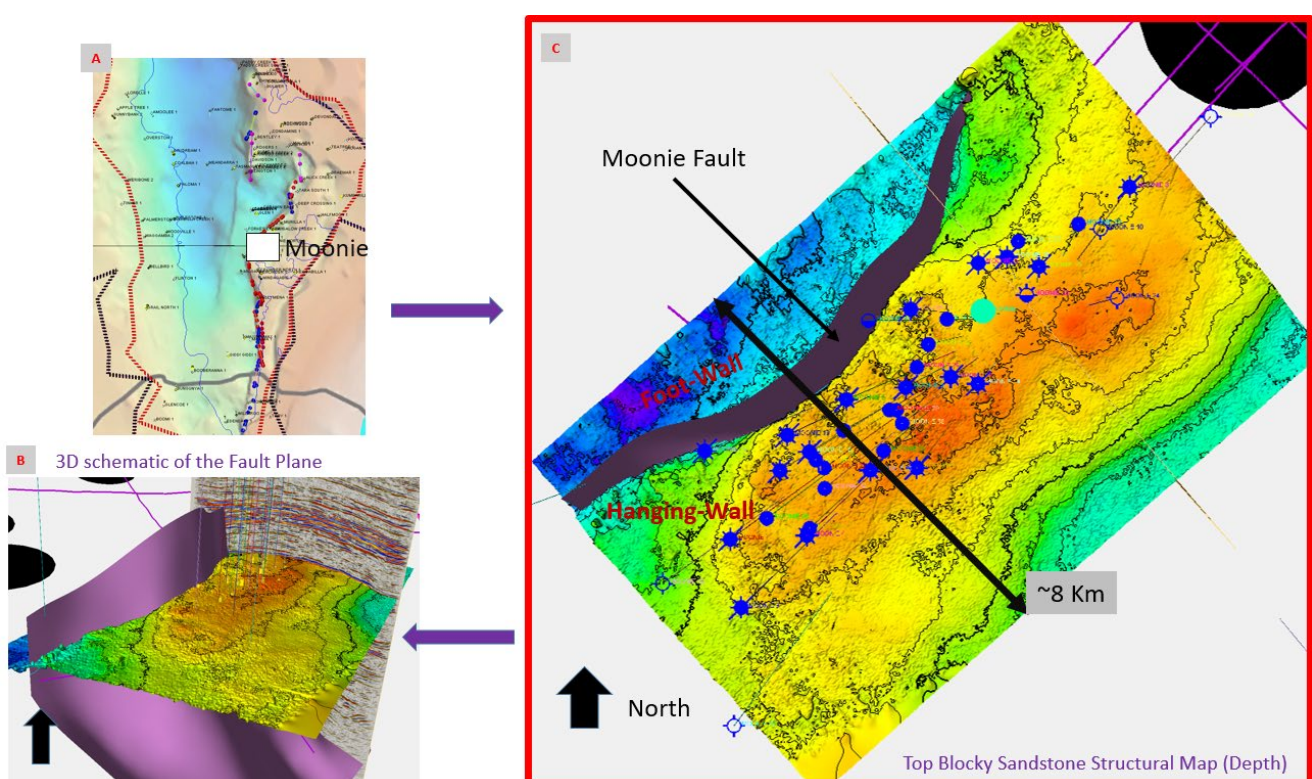




**Figure 49** Left: Plan view and colour coded dip azimuth map along the fault plane. Contours denotes the top structure map of the Blocky Sandstone Reservoir. Dark colours along the fault plane (blue-green) represent higher dip values where each fault segment is indicated by a different colour. Right: Seismic cross sections (cross section location marked on the base map on the left) illustrating the various fault geometries for different Moonie fault segments (e.g. Section B runs along the centre of the field and highlights the steeply dipping fault plane in segment 5 (dark blue colour)).

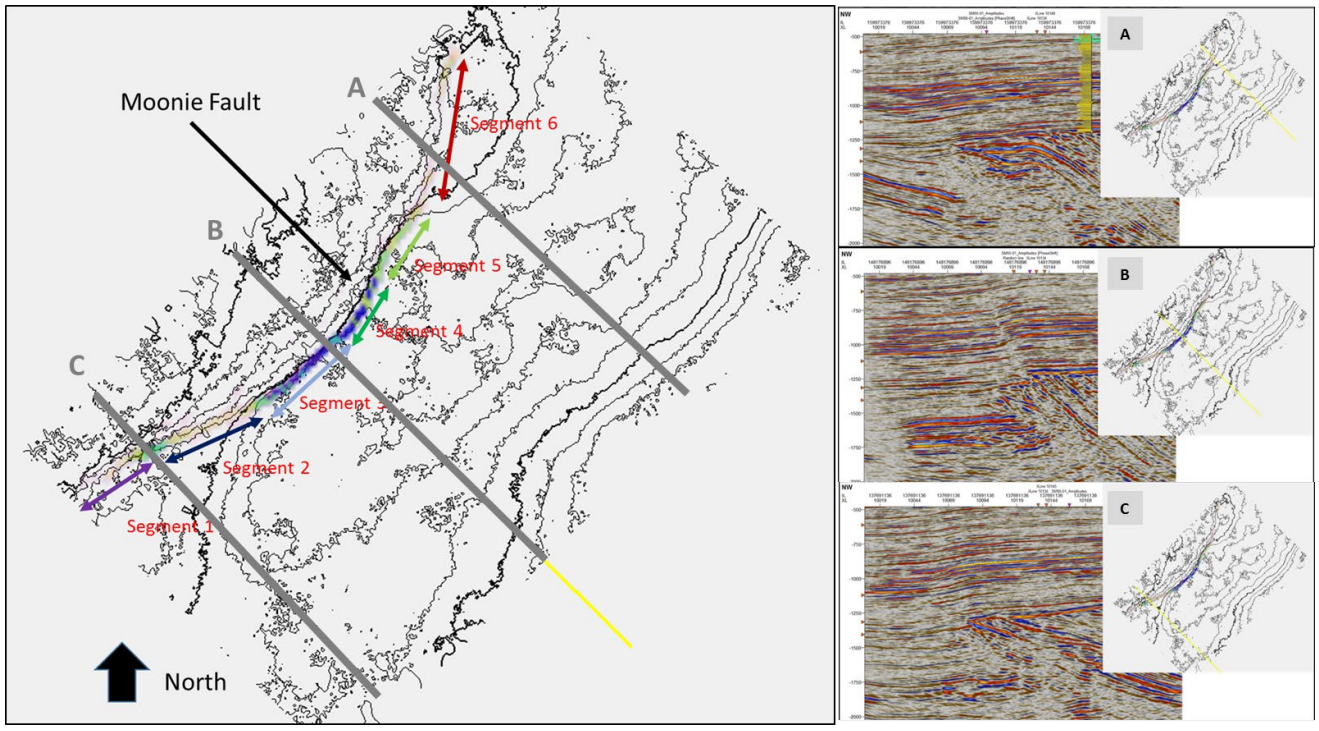
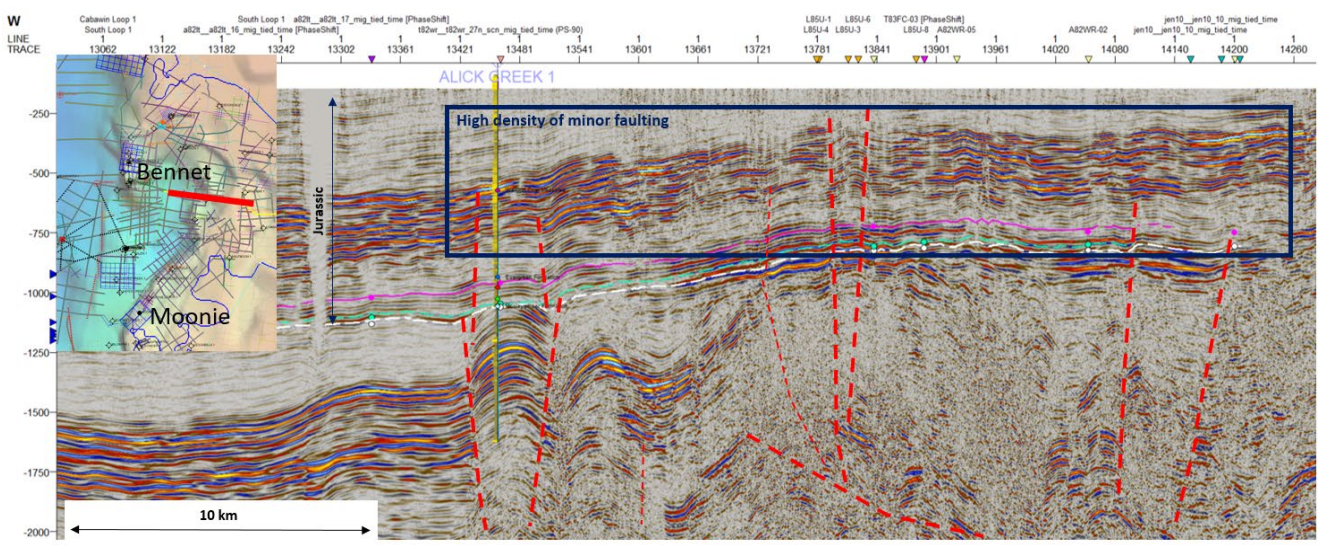
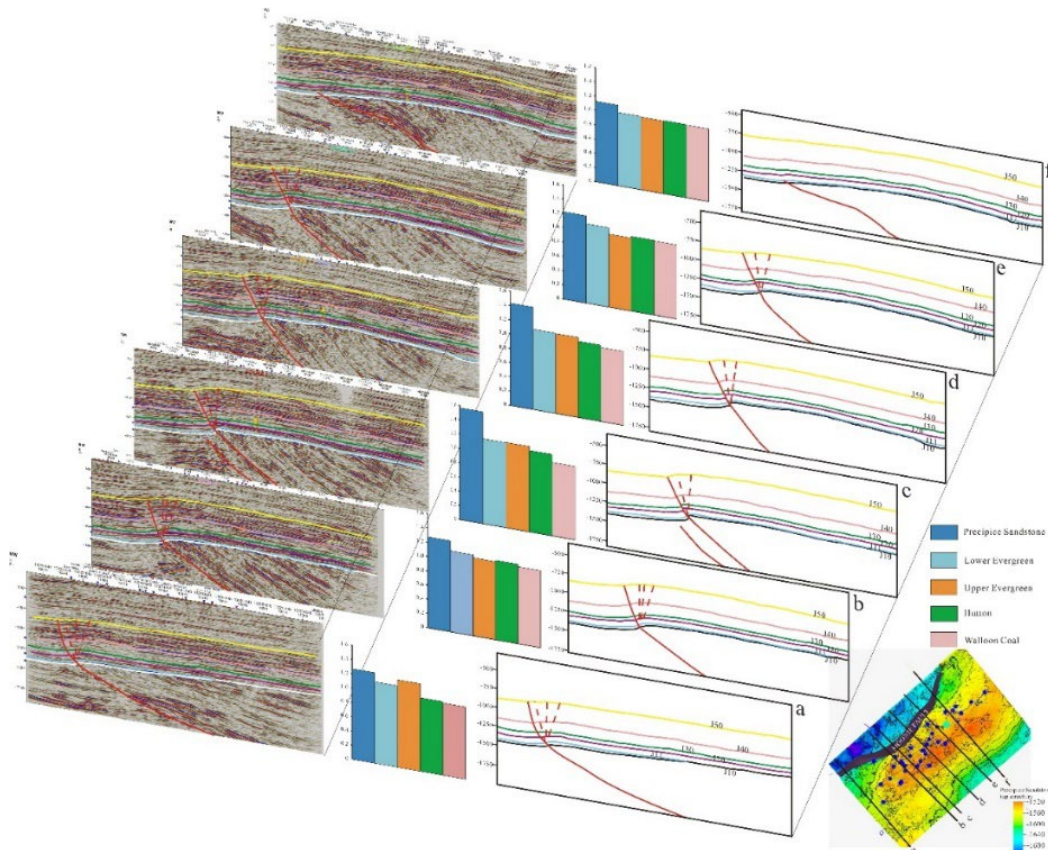


**Figure 50** BMR84 seismic cross section east of the Bennet Field. A high density of faults cutting through Jurassic section are highlighted in red dashed lines and by the blue box.



It is very common for pre-existing basement faults to have a systematic influence on folding deformation of strata above (Allmendinger et al. 2004). In this study, the Moonie 3D seismic was considered as a case study area to examine the influence of the pre-existing Bowen Basin faults on overlying Surat Basin strata because of the high quality of seismic imaging. As shown in the Figure 50, the variable geometry of the pre-existing basement in the Bowen Basin succession resulted in the different folding deformation styles in overlying Surat Basin strata.

**Figure 51** An example of seismic data showing how the folding of the Surat Basin strata changes with variable geometry of the reactivated basement fault (across the Moonie 3D seismic area). The histogram column shows the thickness ratio of the footwall to hanging wall.



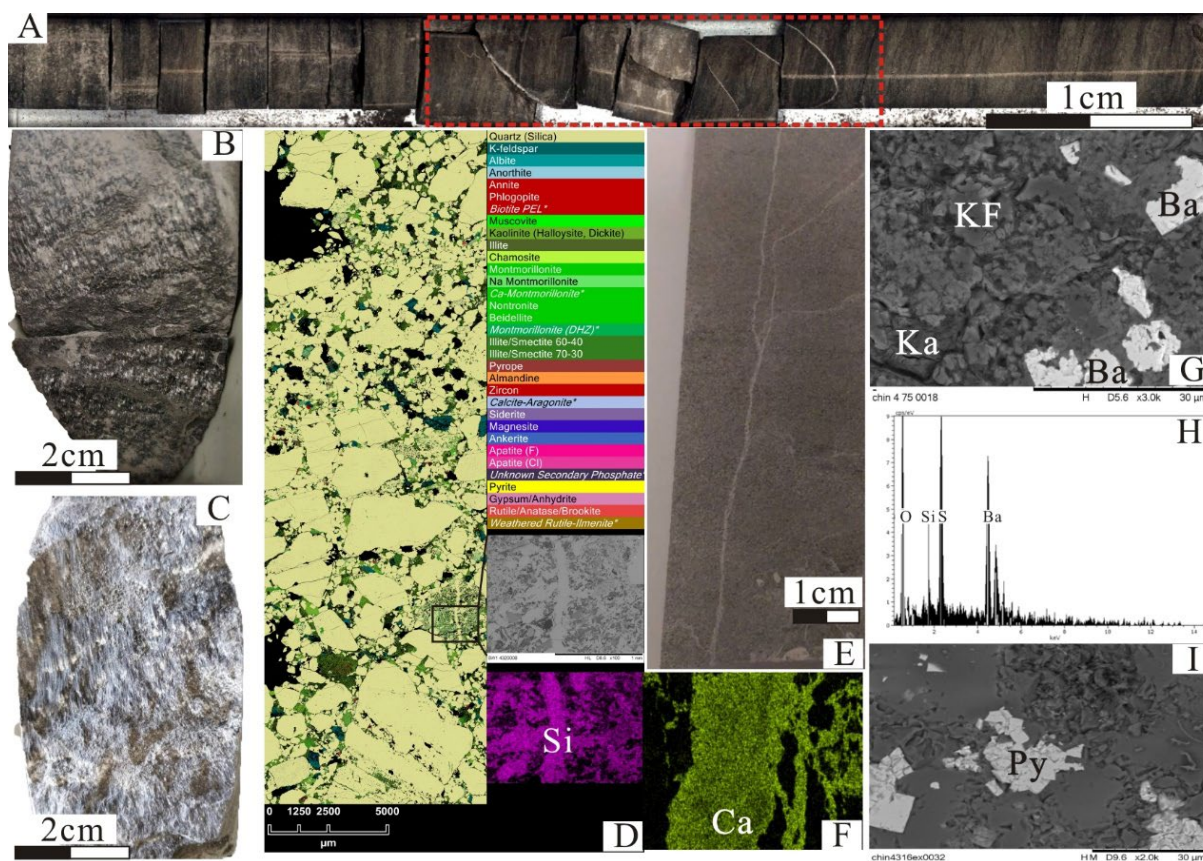
According to the modelling results and seismic profile observations, three types of pre-existing basement reactivation were found in the study area:

- Normal faulting in the Early Permian was reversed, then strongly reactivated at high angle and developing a narrow monocline. It demonstrates a high magnitude of hanging wall thinning and footwall thickening
- Listric trishear faulting with the dip increasing during the compression deformation, then reactivated with medium-high fault dip and developing a wide monocline. It demonstrates a low magnitude of hanging wall thinning and footwall thickening
- Low angle faulting related to fault-bend folding followed by little reactivation, thus developing a flat monocline. It demonstrates little influence on the Surat Basin stratigraphic succession

The timing of pre-existing basement fault reactivation is not well constrained in the Surat Basin, but the fact that these structures are associated with fracturing and syn or post-depositional fold deformation can provide some indirect constraints. Recent studies provide information on Late Cretaceous-Cenozoic deformation in southeast Queensland (Babaahmadi and Rosenbaum 2014, 2015). However, the exact tectonic events that led to this deformation remain poorly constrained.

Results from Precipice Sandstone to Evergreen Formation core and thin-section observations indicate fractures present near the J20 boundary. These are characterised by low angle slip fractures or high angle structural fractures showing smooth mirror surfaces, scratches and steps (Figure 52 A-C). They include two sets of fractures in the core and thin-section (Figure 52 D and E), indicating two tectonic events. One set of fractures were developed in the early stage of deformation and were filled with calcite or silica (Figure 52 D and F). Moreover, along or near this early fracture set, different hydrothermal minerals (e.g. barite and pyrite) occur in the mineral assemblage (Figure 52 G-I). This suggests hydrothermal fluids from a deep-seated source migrated up through the faults and/or fracture channels. Further data on fracture fills is given in Pearce et al. 2019a. The geochemistry data from several mineral fills (mainly calcite) in fractures of various cores in the Surat Basin analysed in a separate project further support the notion of hydrothermal fluid migration (Golding et al. 2016).

**Figure 52** (A) Fractured intervals observed in core (1032.24-1032.54 m) from the Upper Evergreen Formation of the Chinchilla 4 well, showing the fracture filled with calcite; (B) Core from the Reedy Creek MB3-H well, 1102.25 m, showing a low dip-angle slip fracture with smooth mirror, scratches and steps; (C) Core from the Reedy Creek MB3-H well, 1102.75 m, showing a vertical compression-shear fracture with scratches and steps. (D) Core image from the Southwood 1 well near the Moonie fault, 1988 m, showing sandstone lomite cemented fractures in sandstone; (E) An EDS calcium element map for part of the calcite filled fracture in figure E (image width 1 mm); (F) A Scanning Electron Microscopy (SEM) image of barite cement adjacent to a fracture mixed with K-feldspar altered to kaolinite. (H) An EDS spectrum of barite cement from the Chinchilla 4 well, 980 m; (I) an SEM image of pyrite cement. Ba: Barite; Ka: Kaolinite; KF: K-feldspar; Py: pyrite.

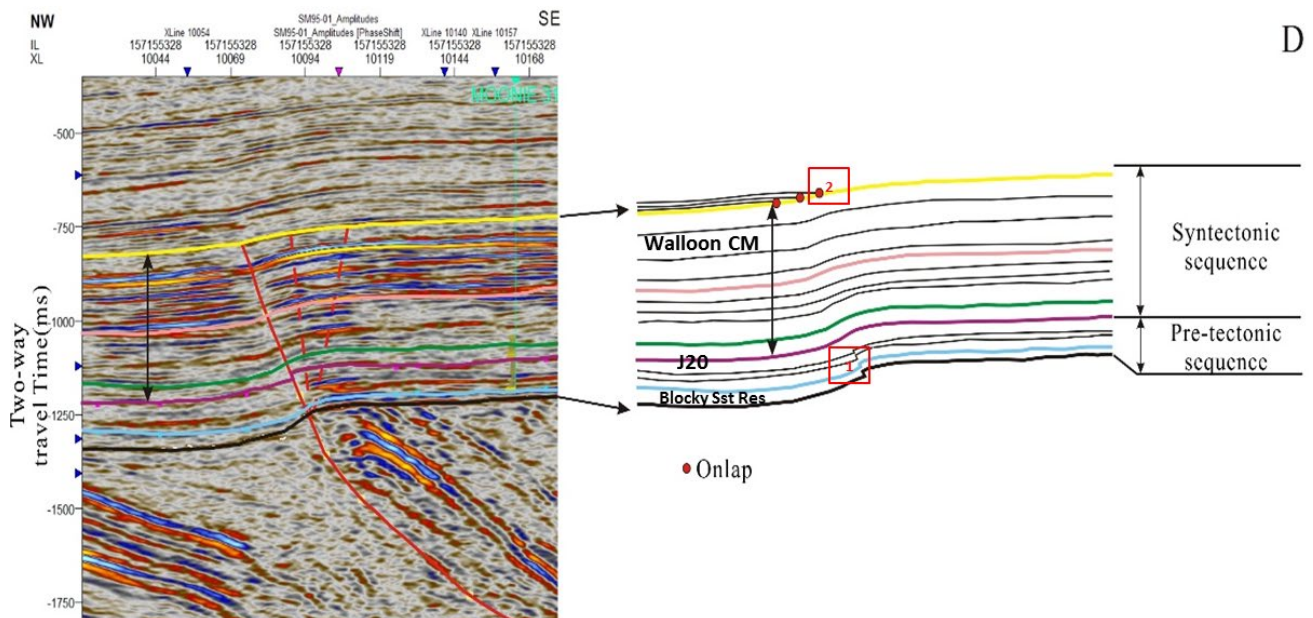


Evidence of cretaceous and/or younger reactivation of pre-existing fault trends, increases potential fault seal risk in the basin centre where high angle faults are seen to extend close to surface. Faults will need to be mapped and distances from faults to injection wells maximised.

The compaction trend observed from sonic transit time data can reflect subsidence rate and quantitatively evaluate the exhumation or erosion thickness (Corcoran and Dore 2005). The difference of sonic transit time above the Blocky Sandstone Reservoir between the Sussex Downs 1 and Moonie 1 wells across the Moonie fault does not show any strong variation suggesting a small compaction difference. This compaction trend difference below the Walloon Coal Measures is more likely to be related to a syn-depositional fault propagation. From the 3D seismic, the Moonie fault cuts the J10-TS1 boundary and then the fold propagates up to the top of the Walloon Coal Measures where the overlying sediments gently onlap. As a result, the Moonie fault could have had two episodes of reactivation: i) at the base Jurassic; syn-depositional at J10-J20 and ii) folded after Walloon Coal Measures deposition (Figure 53).

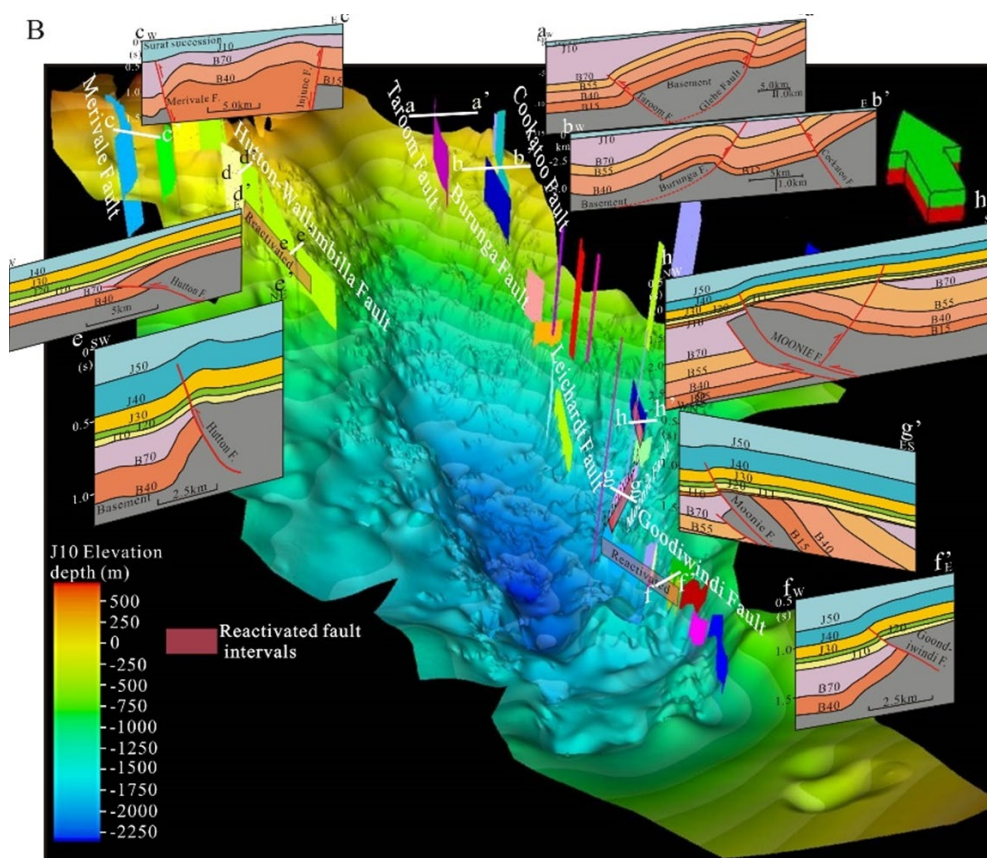
In a regional context, most of major fault deformation was controlled by the decollements in the basement rocks and was bounded by tight folds often composed of lower Permian strata. The structure styles are dominated by both thin-skinned structure (e.g. fault-propagation fold and fault-bend fold) and thick-skinned structure (e.g. reverse fault).

**Figure 53** The seismic profile (SM95-01) across the Moonie fault and its interpretation of the sedimentary sequence geometry, showing the growth sequence.



The movements of many faults ceased in the Late Triassic. However, a few faults were reactivated and this reactivation is variable along the trend. For example, the Burunga anticline is one of the larger Bowen Basin structures tightly folded with over 1 km of net uplift, whereas, the overlying Surat Basin section only develops a subtle fold indicating little reactivation. In comparison, the Hutton-Wallumbilla fault system has Surat Basin strata uplift nearly equal to that in Bowen Basin but only reactivated along the southern portion (Figure 54). The same observation was made along some portions of Goondiwindi and Moonie faults, with offset continuing across the Surat Basin succession. Very few of the faults that formed in the Bowen Basin are reactivated along similar fault planes into the Surat Basin succession, but rather the Surat Basin strain is only loosely linked to the underlying Bowen Basin structures.

**Figure 54** A 3D view of the J10 structure map showing fault structural styles and schematic cartoons of seismic profiles across the major faults at various locations.



#### 4.3.7.5 Tectonic elements in the Mimosa synclinal axis

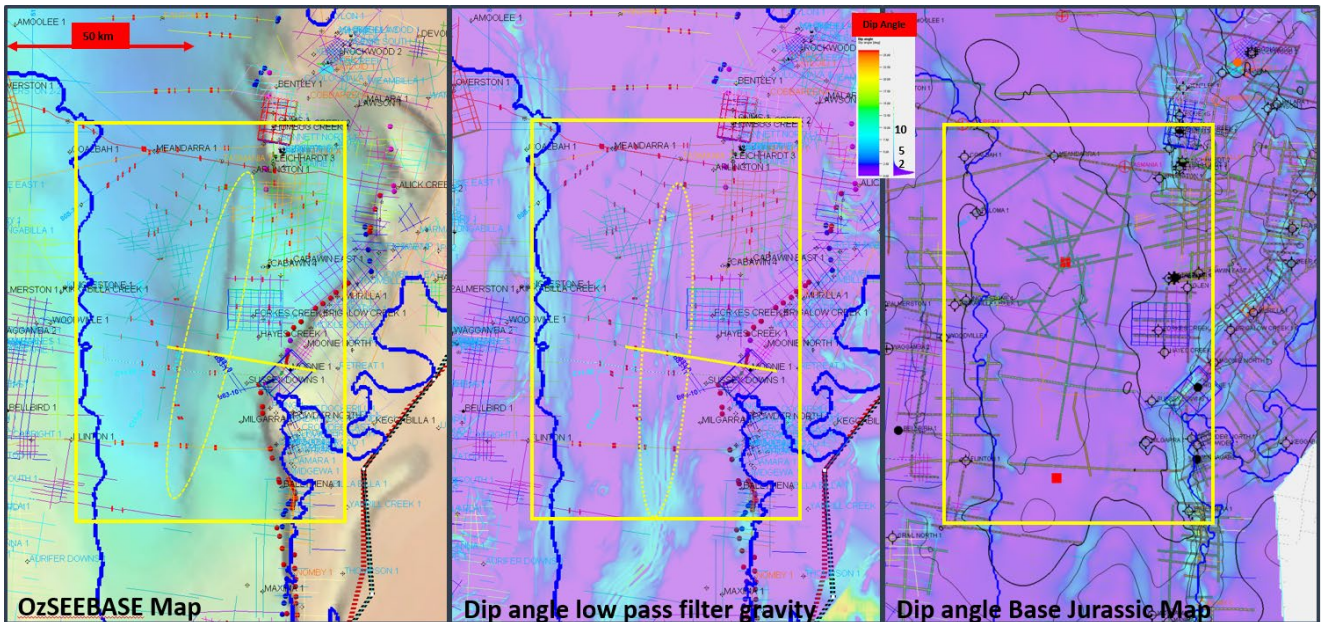
The notional injection sector in the southern depositional centre for the Blocky Sandstone Reservoir is near the Mimosa synclinal axis. It is important to understand the likelihood of faulting in this region as it could impact the viability of commercial-scale carbon storage. Unfortunately, the structural configuration of this area is poorly constrained due to low seismic data coverage. Thus, regional gravity, OzSEEBASE maps integrated with seismic fault interpretation and results from the Moonie field as an analogue, are combined to assess the structural elements for the basin-centre.

Figure 55 depicts the data consolidation from the OzSEEBASE and dip angle data obtained from gravity and structural maps. The OzSEEBASE map shows lineaments trending NE-SW as an en-échelon pattern possibly related to an extension of the Leichardt and Bennet fault to the south. The dip angle maps from the low pass filter map and the J10 sub Surat Unconformity structural map show a relatively flat area with angles less than 2 degrees in purple. Nevertheless, the gravity horizontal derivative map shows some lineations that could either be correlated with a deep structural feature or a strong Permo-Triassic sub-crop contrast. Lineations to the east represent the steep dip increase in the Permian strata where the J10 unconformity is truncated.

While there are a few anomalies in the centre of the basin that could be associated with deep faults, grid extrapolation in these areas with low density data does not reveal any detail. The faults are inferred from OzSEEBASE and gravity maps and their lengths are *arbitrarily* mapped based on fault segmentation similar to the Moonie fault.

More seismic data coverage is required in the basin-centre to help identify new and improve the correlation of those identified in this study.

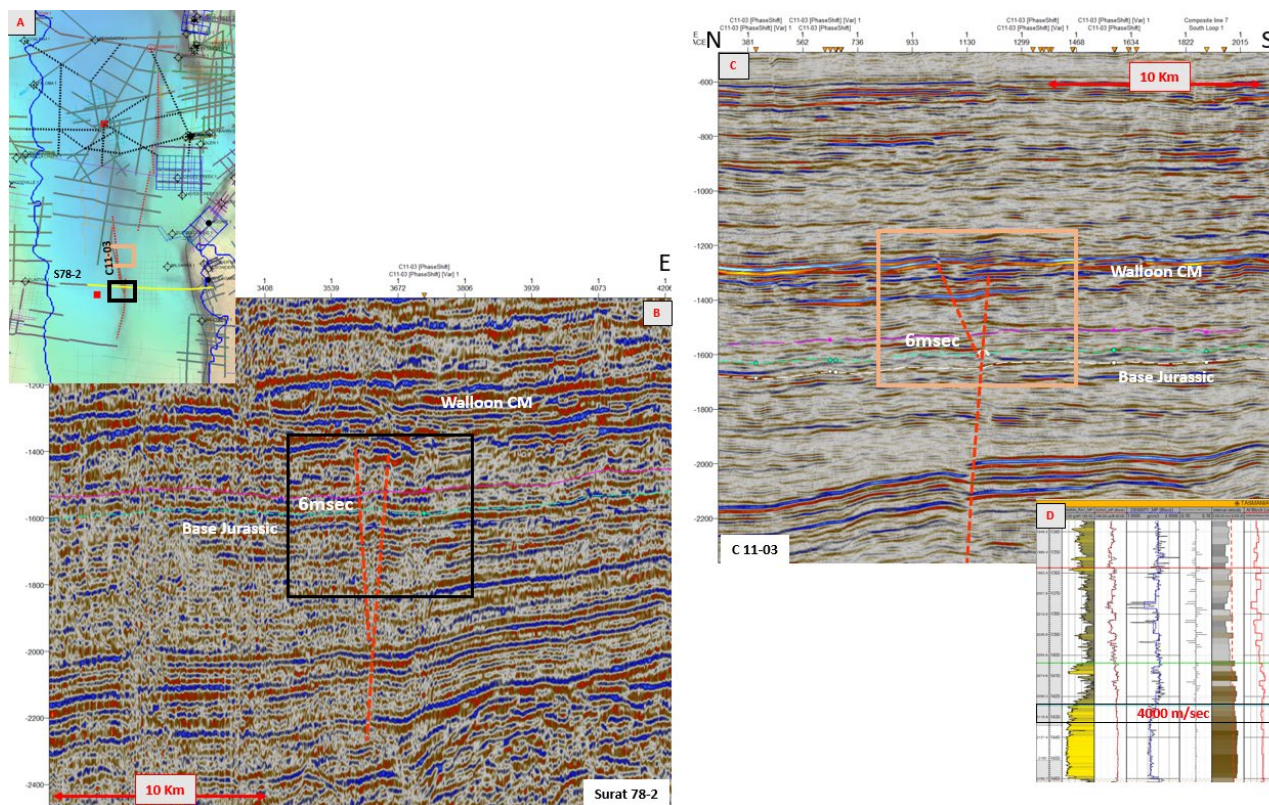
**Figure 55** Structural elements for the central region of the Surat Basin. Left: An OzSEEBASE map highlighting structural anomalies oriented NE-SW in the yellow circle. Centre: a map of dip angle from a low pass filter of the gravity map where blue values indicate high dip angles. West directed dip angles are related to the Blocky Sandstone Reservoir truncation against the J10 unconformity. Right: A map of the J10 unconformity structural map dip angle that highlights the eastern faults.



The few available 2D seismic lines reveal small throw faults from pre-existing Permo-Triassic structures cutting through the J10 unconformity, that coincide geographically with the lineaments observed in the OzSEEBASE map (Figure 55). The nature of the faults such as length and geometry are unknown and the orientation is assumed to follow the trends observed in the OZSEEBASE map. Two seismic lines in the central south part of the area of interest include:

1. C11-03 in the north-south direction shows an extended Permo-Triassic normal fault extending across the J10 unconformity with an offset of around 6 msec (Figure 56)
2. Surat 78-2 in an east-west orientation indicates a transpressional fault architecture at the level of the J10 unconformity. The quality of this seismic line is poor and reprocessing could validate and or refute this interpretation

**Figure 56** (A) OzSEEBASE map illustrating the central part of the Surat Basin and the location of the seismic lines S78-2 and C1103. Red dotted lines refer to regional lineaments. (B) Seismic profile Surat 78-2 EW displaying a potential fault at the J10 unconformity surface near a gravity lineament A. (C) Seismic profile C11-03 displaying a normal fault propagating across the J10 unconformity. (D) Throw in msec for both faults are ~6 msec and the interval velocity is estimated to be around 4000 m/sec for this depth (Tasmania 1 well).



Considering the low fault offset of 6 msec and a seismic velocity of 4000 m/sec at the Blocky Sandstone Reservoir depth, the fault throw is estimated to be around 25 m, which is at the limit of seismic resolution.

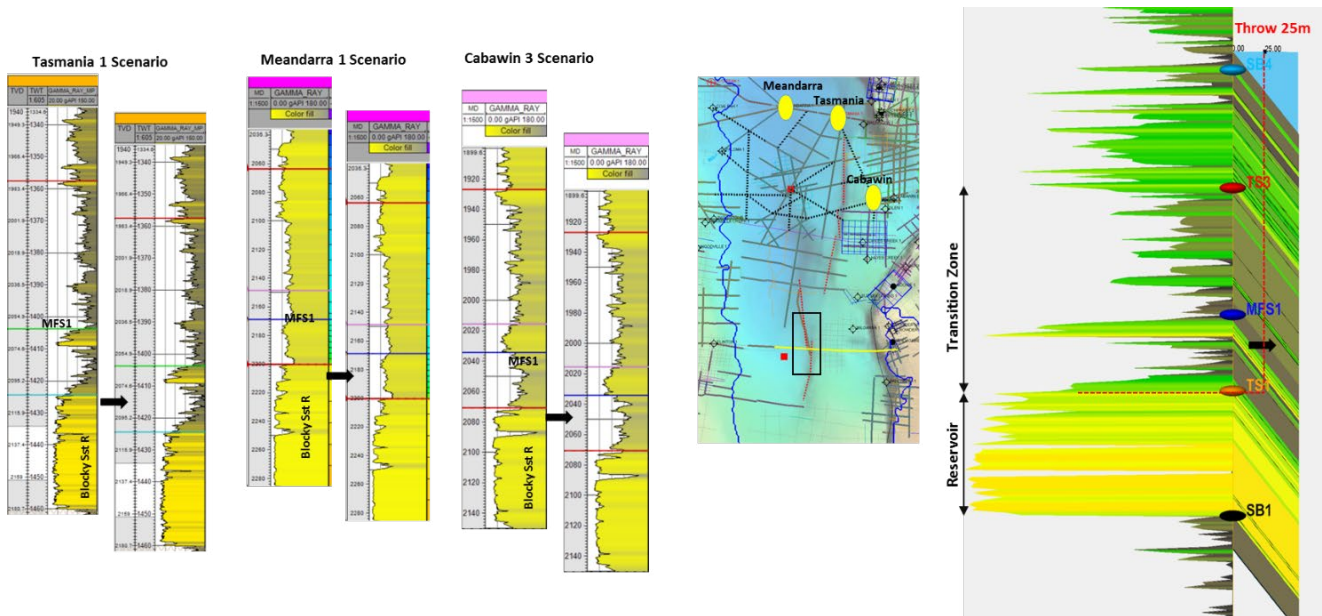
A juxtaposition analysis has been performed considering a 25 m throw and using the three deep well scenarios in the vicinity (Meandarra 1, Tasmania 1 and Cabawin 3) on the assumption that these wells reflect the stratigraphy distribution for the deepest part of the Surat Basin. As the fault regime is not clear from seismic data, a worst-case scenario of fault connectivity is analysed. This locates the downthrown of the fault towards the east flank where the Blocky Sandstone Reservoir is in contact with shallower reservoir units towards the east. At 25 m throw all three wells show Juxtapositions of the Blocky Sandstone Reservoir with high gamma ray values (mudstone) at the base of the Transition Zone. (Figure 57). With throw increases up to 40 m the Blocky Sandstone Reservoir would be juxtaposed with the upper sandy section of the MFS1- TS1 unit of the Transition Zone observed in the Tasmania 1 well.

Summarising structural geology interpretation: the occurrence of faults near a commercial-scale carbon storage project are important as they present both a risk of up-fault or across fault leakage of CO<sub>2</sub> or if the fault is of low permeability the fault could present a pressure transmission barrier that limits the reservoir volume and allows the injection reservoir pressure to increase sooner than anticipated. Both could negatively impact on the CO<sub>2</sub> storage project. The structural analysis in the UQ-SDAAP project includes both juxtaposition and fault reactivation analysis.

The main findings include:

- The region around the notional injection sites are relatively un-structured, however the potential for relatively young, small throw, strike slip, high angle faults has been identified
- Small throw basin centred faults generally may not pose a juxtaposition across fault leakage risk but need to be identified so that wells can avoid them
- Previously mapped large-scale fault trends in the Bowen Basin were reactivated to various degrees in Surat Basin deposition often with only a loose mechanical linkage
- The Moonie field provides a good case study due to the availability of 3D seismic coupled with the hydrocarbon migration history
- It is unlikely that the Moonie fault system will create a regional flow barrier (due to segmentation) that would cause increased pressure rises in response to deep basin injection.

Figure 57 Fault juxtaposition scenarios for a 25 m throw fault in the Surat Basin central area.





### 4.3.8 Petrophysical analysis

Extensive data conditioning, cross-correlation and calibration has been undertaken that significantly better defines the flow and seal properties compared to previous studies (Garnett et al 2012). Following the work in this research, uncertainty ranges are better understood and this has allowed for three main poro-perm reservoir scenarios (low, medium, high) to be constructed. These are used in static models and dynamic simulation in subsequent sections. To the maximum extent possible, all available dynamic injection and production data have been incorporated to calibrate the petrophysical parameters with real, measured, in-situ flow measurements. Important residual uncertainties remain, mainly due to the distance from the nearest control points to the key areas of interest and because these areas are 300-400 m deeper than any hard data point. The only way to further reduce these uncertainties is via site-specific drilling, coring, logging and testing and the associated routine core analysis and special core analysis.

The petrophysical analysis provides a critical link between the geological characterisation and the dynamic reservoir or groundwater simulation as it provides a methodology of parameterising the key rock properties into the cells of the various static geological models, required by the single phase or multiphase flow simulators. The petrophysical analysis integrates data from core, DST and well logs to establish a predictive framework for estimating porosity and permeability away from data control. The reports by Harfoush et al. 2019a, 2019b, 2019c and Honari et al. 2019a, provide a detailed description of the petrophysical analysis workflow and how it was applied for the UQ-SDAAP project.

#### 4.3.8.1 Data and methodology

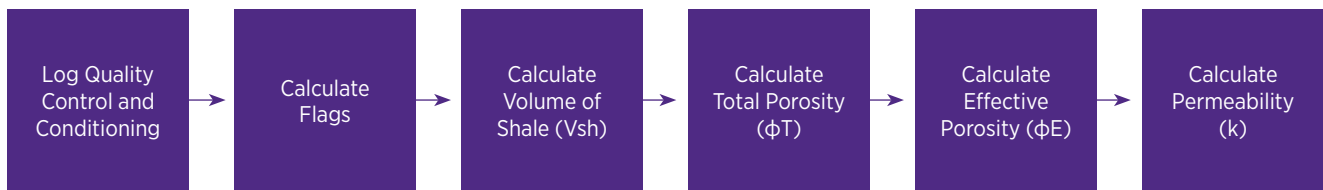
The UQ-SDAAP project evaluated the wireline logs from 285 wells to assess the petrophysical properties needed to parameterise the various static geological models. The key petrophysical properties required include:

- Volume of Shale ( $V_{\text{shale}}$ )
- Total Porosity ( $\phi_T$ )
- Effective Porosity ( $\phi_E$ )
- Permeability ( $k$ )
- Flags for occurrences of Coal and Ironstone lithologies

Figure 58 shows the workflow used to evaluate and interpret the wireline logs. First, a quality check was conducted to standardise the dataset. For example, different vintages of logs and different logging contractors use different units and logging techniques and some data may only exist as scanned image files (requires digitisation). The log quality control (LQC) process harmonised the data to solve these problems in advance of analysis.

After creating the flags to highlight coal and ironstone lithologies (dealt with differently than petrophysics for clastic sedimentary rock), the petrophysical properties were calculated sequentially according to the defined workflow, starting with volume of shale and ending with permeability. With the exception of the Moonie oil field wells, all of the wells in the UQ-SDAAP study have pore space saturated with formation water. This simplifies the petrophysical workflow somewhat. For the Moonie oil field wells, the pore space has a combination of water and hydrocarbon saturation and thus the relative saturation needed to be accounted for. Thus, the Moonie oil field wells were treated with an extra step in the processing.

**Figure 58** UQ-SDAAP workflow for wireline log interpretation.



Since not all wells have the same suite of wireline logs, some of the calculated parameters ( $V_{\text{shale}}$ ,  $\phi_T$ ,  $\phi_E$ , and  $k$ ) were not possible to determine. Of the 285 wells available,  $V_{\text{shale}}$  was determined for all 285 wells, calculated total and effective porosities for 208 wells, and calculated permeability for 73 wells. Of the 285 wells, all had gamma ray logs, 132 wells had neutron logs, 179 had density logs, 91 had photoelectric factor logs, 230 had compressional slowness logs, and 204 had resistivity logs.

The report of Harfoush et al. 2019a describes this process in detail. The UQ-SDAAP research used Schlumberger's Techlog™ for petrophysical analysis and the Python programming language to run codes that helped in conditioning and processing the data. The NeuraLog™ software was used to digitise a significant number of legacy wireline logs.

Petrophysical analysis (as described above) was performed on four groups of wells. The well grouping was based on geographic area with priority given to areas around the various geological sector models (La Croix et al. 2019d). These different groups of wells were inserted into four different databases to increase software efficiency. A different approach in conditioning and assigning shale parameters to the different groups/databases was used. This depended on geographic location, depth range, and the availability of data in each database. The four different well groups were:

- The managed aquifer recharge (MAR) area including the northern part of the Blocky Sandstone Reservoir – this data group is hereafter referred to as the “MAR Petrophysics Database” (MARPD)
- Myall creek area – this data group is hereafter referred to as the “Myall Creek Petrophysics Database” (MCPD)
- Moonie field area – this data group is hereafter referred to as the “Moonie Petrophysics Database” (MPD)
- The remaining wells in the centre, south and western parts of the Blocky Sandstone Reservoir distribution – this data group is hereafter referred to as the “Southern Depocentre Petrophysical Database (SDPD)”

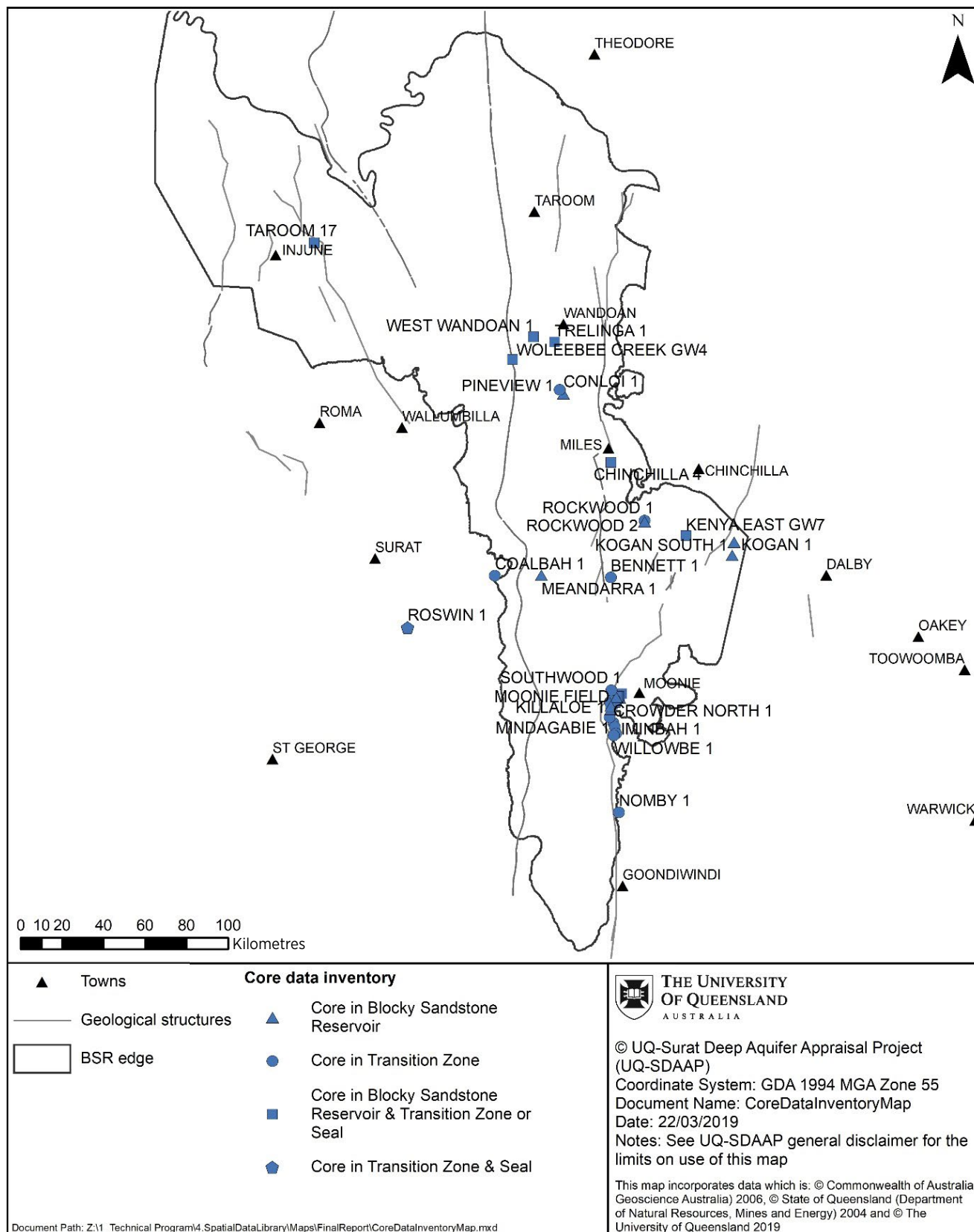
With the petrophysical properties ( $V_{\text{shale}}$ ,  $\phi_T$ ,  $\phi_E$ , and  $k$ ) calculated, statistical analysis and distribution maps were used to understand how they varied by grouping them in various ways. This included analysis for geographical trends or vertical trends with depth, grouped by stratigraphic zone (Block Sandstone Reservoir, Transition Zone or Ultimate Seal), grouped by facies, grouped by geographic sub-area (MARPD, MCPD, MPD and SDPD). For each of these groupings a statistical characterisation of the various petrophysical properties was provided, together with uncertainty parameters. The report of Harfoush et al. 2019a describes these outcomes in detail.

**Summarising petrophysics: the petrophysical assessment corroborated that there are important differences in the typical rock properties of the Blocky Sandstone Reservoir between the northern and southern depositional centres with the north having generally higher permeability and very little clay content. The south has more clay and generally lower permeability even when considering the depth trends and environmental factors such as pressure and temperature etc. These differences are likely related to the different source regions for the northern and southern depositional areas.**

#### 4.3.8.2 Core plug analysis

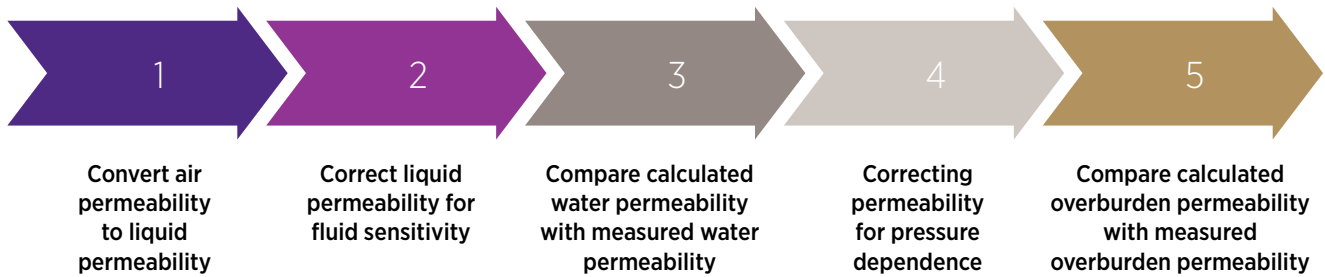
Historically, when some oil and gas wells were drilled, samples of rock core were extracted and sent to the laboratory to have various measurements such as porosity and permeability conducted. This data for the UD-SDAAP strata of interest provided actual measurements of certain petrophysical properties calculated from logs as previously described. As such they proved an excellent calibration data set for the petrophysical workflow. Core data was obtained from the publicly accessible Queensland state QPED database and core analysis reports from the QDEX database. The distribution of wells having core data in the UQ-SDAAP study region for the strata of interest (Precipice Sandstone to Evergreen Formation) are shown in Figure 59 showing the distribution of wells with core analysis data from the Precipice Sandstone and Evergreen Formation utilised in the UQ-SDAAP petrophysical analysis.

**Figure 59** Map showing the distribution of wells with core analysis data from the Precipice Sandstone and Evergreen Formation utilised in the UQ-SDAAP petrophysical analysis.



Before the core data can be used in the calibration of the petrophysics workflows, it first needs to be quality checked and corrected to *in-situ* conditions. For example, core plug permeability measurements are normally conducted at laboratory temperature and pressure conditions and permeability is measured relative to either air or helium. The measured values need to be corrected to the pressure at the depth from which the core was originally taken from the well and the permeability needs to be converted relative to formation water. This was done according to the methodology illustrated in Figure 60 (see Harfoush et al. 2019b for details).

**Figure 60** Workflow for correcting core ambient air permeability to water in-situ reservoir permeability.



The core data tends to be biased by nature to higher permeability zones, since the plugs are usually selected in specific places in the recovered core that are of interest to the core owner (usually a resource company), thus such statistics might not be representative of the entire formation. It should be noted that is not always the case. For example, Woleebec Creek GW4 was drilled for data/research purposes and the core plugs were generally sampled at regular intervals. Despite the general bias, the data when combined with other tools (e.g. logs, DST, etc.) are a good indication of the trends and the range of values to be expected.

According to core data analysis, the Blocky Sandstone Reservoir exhibits good reservoir qualities (i.e. relatively high porosity and permeability). Average core porosities range from 20.4% in the north, around the MARPD area, where the reservoir is relatively shallow, to an average of 16.4% in the MPD area where the reservoir is deeper. The core porosity data exhibits some variation, evident in the MPD area, where core porosity ranges from 13% to 18%. Analysis of the core water in-situ reservoir permeability demonstrates relatively high permeability values as well, ranging from an average of 2500 mD in the MARPD region to 360 mD at the MPD area. Again, heterogeneity is evident from the variation of average core water in-situ reservoir permeability within the MPD area (from 14 mD to 1057 mD).

The core analysis for plugs taken from the Transition Zone shows variation across the basin. Average core porosities range from 7% to 21%. Average core water in-situ reservoir permeability ranges from 0.01 mD to 829 mD. This heterogeneity relates to the different facies and stratigraphic zones that plugs have been taken from. There were only five cored wells with core plugs taken within the Ultimate Seal, and they all demonstrate an average core porosity between 9 % and 10%, and core water in-situ reservoir permeability of *less than* 0.1 mD (probably an effective measurement limit).

The UQ-SDAAP project used neural network algorithms trained on wells with core observations for predicting facies from logs with no core (*La Croix et al. 2019c*). The core data was studied with respect to the facies assigned to them in order to understand how different these facies are to each other from a rock property perspective. The results are displayed in Table 19 to Table 23. The largest number of samples were for facies SA, the predominant facies of the Blocky Sandstone Reservoir, having a total of 551 samples, while facies MB, OA and OB did not have any available core data.

**Table 19** Core porosity statistics per facies

Facies	No. Samples	Minimum (v/v)	Arithmetic Mean (v/v)	Maximum (v/v)	Standard Deviation (v/v)
<b>SA</b>	<b>551</b>	<b>0.061</b>	<b>0.194</b>	<b>0.261</b>	<b>0.031</b>
SB	212	0.041	0.116	0.228	0.048
SC	72	0.028	0.082	0.191	0.029
SD	3	0.077	0.087	0.103	0.014
SMA	191	0.004	0.115	0.308	0.061
SMB	109	0.019	0.083	0.162	0.027
MA	73	0.025	0.087	0.166	0.025
MB	-	-	-	-	-
OA	-	-	-	-	-
OB	-	-	-	-	-

**Table 20** Core ambient air permeability statistics per facies

Facies	No. Samples	Minimum (mD)	Arithmetic Mean (mD)	Maximum (mD)	Standard Deviation (mD)
<b>SA</b>	<b>441</b>	<b>0.016</b>	<b>2097.83</b>	<b>15789</b>	<b>2355.91</b>
SB	163	0.002	44.62	1575	200.74
SC	46	0.001	1.79	78	11.49
SD	2	0.01	0.028	0.045	-
SMA	130	0.001	43.16	1304	160.73
SMB	54	0.001	0.09	0.75	0.16
MA	44	0.001	0.592	13	2.03
MB	-	-	-	-	-
OA	-	-	-	-	-
OB	-	-	-	-	-

**Table 21** Core calculated water in-situ reservoir permeability statistics per facies

Facies	No. Samples	Minimum (mD)	Arithmetic Mean (mD)	Maximum (mD)	Standard Deviation (mD)
<b>SA</b>	<b>446</b>	<b>0.003</b>	<b>1641.56</b>	<b>12393</b>	<b>1846</b>
SB	158	0.0001	17.13	834.47	97.13
SC	45	4.70E-05	0.74	32.26	4.81
SD	2	0.0011	0.0044	0.0077	-
SMA	120	2.46E-05	11.55	523.19	54.19
SMB	54	2.37E-05	0.015	0.15	2.56
MA	41	1.58E-05	0.073	1.574	0.255
MB	-	-	-	-	-
OA	-	-	-	-	-
OB	-	-	-	-	-

**Table 22** Core ambient vertical permeability statistics per facies

Facies	No. Samples	Minimum (mD)	Arithmetic Mean (mD)	Maximum (mD)	Standard Deviation (mD)
<b>SA</b>	<b>140</b>	<b>0.5</b>	<b>1391.88</b>	<b>8030</b>	<b>1795.08</b>
SB	48	0.001	42.83	1161	184.55
SC	11	0.001	1.55	17	5.12
SD	-	-	-	-	-
SMA	33	0.001	8.98	128	24.24
SMB	19	0.001	0.005	0.037	0.008
MA	15	0.001	0.084	0.9	0.23
MB	-	-	-	-	-
OA	-	-	-	-	-
OB	-	-	-	-	-

**Table 23** Core grain density statistics per facies

Facies	No. Samples	Minimum (g/cc)	Arithmetic Mean (g/cc)	Maximum (g/cc)	Standard Deviation (g/cc)
<b>SA</b>	<b>361</b>	<b>2.63</b>	<b>2.648</b>	<b>2.72</b>	<b>0.01</b>
SB	132	2.54	2.659	3.01	0.05
SC	56	2.58	2.643	3.01	0.05
SD	2	2.58	2.600	2.62	-
SMA	111	-	2.639	3.20	0.14
SMB	94	2.45	2.636	3.16	0.08
MA	65	2.59	2.666	3.14	0.11
MB	-	-	-	-	-
OA	-	-	-	-	-
OB	-	-	-	-	-

### 4.3.8.3 Drill stem test interpretations

Historically, when some oil and gas wells have been drilled, they test the wells production potential with a temporary completion called a drill stem test (DST). This allows the operator to sequentially flow and shut in the completed interval and record the downhole pressure, among other things. The pressure time increments recorded during the flow phase of a DST can be interpreted to estimate the formation permeability. This data for the UQ-SDAAP strata of interest, provides alternative and independent measurements of permeability. As such, it proved an excellent calibration data set for the petrophysical workflow. DST data was obtained from the publicly accessible Queensland state QDEX database. The UQ-SDAAP project analysed 79 DSTs from 60 different wells across the UQ-SDAAP project region and stratigraphy of interest. Out of these 79 wells:

- 23 DSTs were conducted within the Blocky Sandstone Reservoir
- 40 DSTs were conducted in the Transition Zone
- 10 DSTs were conducted where the interval covered both the bottom of the Transition Zone and the top of the Blocky Sandstone Reservoir
- Four DSTs were conducted where the interval crossed the sub-Surat Unconformity (Blyth Creek 1, Marmadua 2, Paloma 1 and Wingnut 2 wells)
- One DST that was completed totally below the sub-Surat Unconformity (the Cherwondah 2 well)

Table 24 lists the DST data inventory, showing relevant information about the DST's interval, quality (green for reliable, yellow for data to be used with care and red for unreliable as determined by the DST analysis – see Honari et al. 2019a), and the availability of wireline interpretation and facies predictions for the well.

**Table 24** DSTs data inventory. BSR: Blocky Sandstone Reservoir, TZ: Transition Zone, BU: sub-Surat Unconformity, MLP\_NORM: facies log, Y: Yes, N: No, Quality Scale: reliable data in green, data to be used with care in yellow and unreliable data in red. Thickness h is based on the DST interval.

Well	DST interval (m MD)	Zone	k.h (mD.ft)	h (ft)	k (mD)	Quality	Logs Evaluated?	MLP_NORM Present?
Arlington 1	2115.5 - 2122.5	BSR	502.28	23.00	22.00	Yellow	Y	Y
Bennett 1	1625.0 - 1632.0	TZ	498.70	23.00	22.00	Red	Y	Y
Bennett 1	1651.0 - 1659.0	TZ/BSR	12389.00	26.00	480.00	Red	Y	Y
Bennett 2	1616.3 - 1629.8	TZ	335.22	44.30	7.60	Yellow	Y	Y
Bennett 2	1620.6 - 1625.8	TZ	772.00	17.00	45.00	Red	Y	Y
Bennett 2	1649.0 - 1653.8	BSR	923.50	10.00	92.00	Green	Y	Y
Bennett 4	1616.0 - 1620.5	TZ	611.30	15.00	41.00	Red	Y	Y
Bennett 4	1643.0 - 1646.5	TZ/BSR	2.44	3.00	0.81	Red	Y	Y
Bennett 4	1650.0 - 1659.3	BSR	491.02	24.00	20.00	Yellow	Y	Y
Bennett North 1	1628.9 - 1638.0	BSR	991.40	17.00	58.00	Green	Y	Y
Bentley 1	1481.7 - 1521.3	TZ/BSR	1896.90	10.80	180.00	Yellow	Y	Y
Blyth Creek 1	1154.0 - 1164.0	TZ	1421.25	18.00	79.00	Red	N	N
Blyth Creek 1	1165.0 - 1169.0	TZ/BU	210.77	7.00	30.00	Yellow	N	N
Brigalow Creek 1	1676.4 - 1685.5	TZ	4782.60	18.00	270.00	Red	Y	N
Bulwer 1	1136.3 - 1141.2	BSR	7030.70	16.00	440.00	Red	Y	Y
Cherwondah 2	1200.0 - 1204.0	BU	27.10	8.00	3.40	Green	N	N
Cabawin 2	2039.0 - 2045.4	TZ	111.90	21.00	5.30	Red	N	N
Coalbah 1	2209.6 - 2236.9	TZ	0.43	36.00	0.01	Green	Y	N
Colgoon 1	1432.3 - 1437.1	Unknown	0.46	3.00	0.15	Red	N	N

Well	DST interval (m MD)	Zone	k.h (mD.ft)	h (ft)	k (mD)	Quality	Logs Evaluated?	MLP_NORM Present?
Dulacca 1	1584.0 - 1589.0	BSR	1265.86	16.00	79.00		Y	Y
Ferrett 1	1579.0 - 1582.5	TZ/BSR	7846.50	12.00	650.00		Y	Y
Giligulgul 1	1300.0 - 1305.5	BSR	110.75	10.00	11.00		N	Y
Humbug Creek 1	1646.8 - 1650.8	BSR	488.40	13.00	38.00		Y	Y
Humbug Creek 1	1646.5 - 1656.6	BSR	1397.80	33.00	42.00		Y	Y
Inglestone 1	2185.4 - 2196.0	TZ	1171.95	35.00	33.00		N	N
Leichhardt 1	1676.4 - 1681.0	TZ	3.44	15.00	0.23		Y	Y
Leichhardt 1	1677.9 - 1685.5	TZ	981.90	25.00	39.00		Y	Y
Leichhardt 1	1706.9 - 1719.0	TZ/BSR	1123.05	34.00	33.00		Y	Y
Mackie 1	1144.5 - 1149.0	TZ	159.30	15.00	11.00		N	N
Marmadua 2	1348.7 - 1362.5	BSR/BU	32.35	35.00	0.92		N	N
Mascotte 1	1187.0 - 1197.0	TZ	775.75	30.00	26.00		N	N
Meribah 1	1985.2 - 1991.6	TZ	722.25	19.00	38.00		N	N
Merrit 1	1269.0 - 1289.0	TZ	747.10	15.00	50.00		Y	Y
Moonie 1	1719.0 - 1722.7 1724.0 - 1725.5	TZ	617.00	17.00	36.00		N	N
Moonie 13	1769.7 - 1774.0	TZ	2540.00	14.00	180.00		N	N
Moonie 13	1731.8 - 1735.0	TZ	25.30	10.00	2.50		N	N
Moonie 15	1718.8 - 1726.4	TZ	73.00	25.00	2.90		N	N
Moonie 16	1785.2 - 1794.7	TZ/BSR	158.00	31.00	5.10		Y	N
Moonie 19	1727.6 - 1738.0	TZ	14.40	34.00	0.42		N	N
Moonie 2	1719.6 - 1729.0	TZ	2875.30	31.00	93.00		N	N
Moonie 20	1721.2 - 1733.7	TZ	7805.00	41.00	190.00		N	N
Moonie 21	1716.0 - 1734.3	TZ	4.50	60.00	0.08		Y	N
Moonie 23	1774.8 - 1780.7	BSR	1790.00	19.00	94.00		Y	N
Moonie 24	1800.0 - 1806.0	BSR	27135.00	20.00	1400.00		Y	N
Moonie 25	1797.5 - 1803.5	BSR	1011.40	20.00	51.00		Y	N
Moonie 26	1767.5 - 1770.3	BSR	562.80	9.00	63.00		N	N
Moonie 27	1717.8 - 1727.0	TZ	92.40	30.00	3.10		Y	N
Moonie 28	1723.0 - 1730.3	TZ	23.10	24.00	0.96		Y	N
Moonie 28	1766.2 - 1769.3	BSR	2589.00	10.00	260.00		Y	N
Moonie 29	1718.2 - 1723.6	TZ	68.00	18.00	3.80		N	N
Moonie 29	1723.6 - 1728.2	TZ	1607.50	15.00	110.00		N	N
Moonie 3	1778.5 - 1787.7	TZ/BSR	2711.80	30.00	90.00		N	N
Moonie 31	1728.8 - 1733.4	TZ	28.00	15.00	1.90		Y	Y
Moonie 32	1728.2 - 1733.7	TZ	985.00	18.00	55.00		N	N



Well	DST interval (m MD)	Zone	k.h (mD.ft)	h (ft)	k (mD)	Quality	Logs Evaluated?	MLP_NORM Present?
Moonie 32	1723.6 - 1728.2	TZ	534.00	15.00	36.00		N	N
Moonie 33	1764.1 - 1767.1	BSR	1800.00	10.00	180.00		Y	Y
Moonie 33	1770.2 - 1773.2	BSR	520.00	10.00	52.00		Y	Y
Moonie 33	1773.2 - 1776.3	BSR	448.00	10.00	45.00		Y	Y
Moonie 34	1773.9 - 1776.9	BSR	341.00	10.00	34.00		Y	Y
Moonie 34	1776.9 - 1780.0	BSR	189.10	10.00	19.00		Y	Y
Moonie 34	1771.7 - 1774.5	BSR	3747.00	9.00	420.00		Y	Y
Moonie 38	1720.6 - 1727.0	TZ	1739.20	21.00	83.00		Y	N
Moonie 39	1719.0 - 1735.2	TZ	4110.00	53.00	78.00		Y	Y
Moonie 8	1774.0 - 1780.0	TZ/BSR	397.50	20.00	20.00		N	N
Paloma 1	2277.2 - 2338.1	TZ/BU	20.72	20.00	1.00		Y	Y
Pickanjinnie 10	1244.0 - 1262.0	TZ	337.20	22.00	15.00		N	N
Pineview 1	1340.2 - 1342.0	TZ	5.03	6.00	0.84		Y	Y
Range 1	1147.9 - 1165.2	TZ/BSR	3390.40	57.00	59.00		N	N
Rockwood 1	1143.0 - 1159.0	TZ	54.80	40.00	1.40		N	N
Rockwood 1	1185.0 - 1197.0	TZ/BSR	56.98	20.00	2.90		N	N
Stakeyard 2	1229.0 - 1248.0	TZ	12.44	23.00	0.54		N	N
Surlick Creek 1	1316.0 - 1335.0	TZ	2.98	52.30	0.06		N	N
Tey 1	1566.7 - 1569.7	TZ	896.60	10.00	90.00		N	N
Tinhut 1	834.0 - 858.0	TZ	358.10	79.00	4.50		N	N
Trelinga 1	982.0 - 1002.0	TZ	0.71	65.00	0.01		Y	Y
Undulla 1	1693.0 - 1721.2	BSR	15398.75	93.00	170.00		N	N
Wingnut 2	1136.9 - 1147.6	TZ/BU	11.32	20.00	0.57		Y	Y
Woleebee Creek GW4	1468.0 - 1478.7	BSR			2500.00		Y	Y
Woleebee Creek GW4	1468.6 - 1573.6	BSR			2800.00		Y	Y

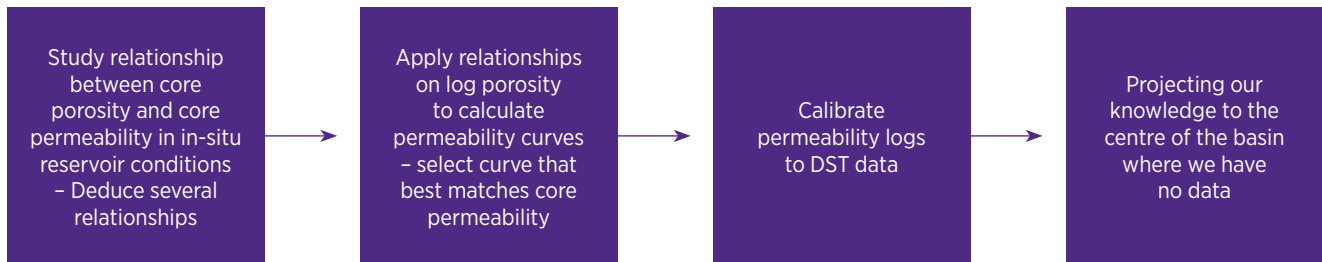
Details of the DST interpretations and details of the DST to Petrophysical log calibrations can be found in Honari et al. 2019a.

#### 4.3.8.4 Applying the petrophysics to static geological model parameterisation

The existing permeability data that was available for the Blocky Sandstone Reservoir, Transition Zone, and Ultimate Seal were either measured in the laboratory on core samples or interpreted from drill stem test (DST) analysis. The core measurements provide permeability data at a centimetre to microscopic scale. The DST measurements provide an estimate of permeability at the metre or larger scale depending on its design.

The UQ-SDAAP project used the petrophysical methodology described in Figure 61 to estimate permeability from logs.

**Figure 61** Methodology for estimating permeability from petrophysical data.



The methodology can be described in more detail as follows:

1. Convert the measured core porosity and permeability data to *in-situ* reservoir conditions and then deduce porosity-permeability transforms
2. Calculate permeability logs for each well using porosity logs from wireline data interpretation and the transforms created from step 1
3. Calibrate the permeability logs to DST permeability data. This is performed by averaging the permeability curves within the DST intervals (for wells with DST data) and comparing the results with DST derived permeability. Corrections are then applied to the transform equations, such that the calculated permeability logs match with DST data
4. From the learnings of this analyses, high-base and low-case scenarios were produced for estimating permeability in parts of the basin where there is no well data
5. Finally, the log derived permeability that was calibrated with DST's to the results of the groundwater inverse modelling of the MAR Sector area (Hayes et al. 2019a) was compared

In order to incorporate the petrophysics results into the static geological models (parameterisation), the selected transforms (high base and low), corrected to DSTs, were applied to the porosity values in each cell in the various 10 km<sup>2</sup> sector models (see La Croix et al. 2019d for a description of the sector models) to generate three permeability scenarios for each model cell.

#### 4.3.8.5 Porosity-permeability transforms for 10 x 10 km sector models

The first step in modelling permeability was to derive a relationship between core porosity and core permeability under reservoir conditions. There are many alternative methodologies to achieve this such as those described by Kozeny-Carman relationship (Carman 1956), the work of Timur A 1960 and the work of Ahmed, Crary & Coates 1991. However, the equations developed in these studies are dependent on rock properties such as irreducible water saturation, grain size, pore surface area, and others. In the UQ-SDAAP study, the lack of information regarding these properties presents a challenge. As a result, empirical transform equations, unique to our stratigraphic interval of interest were created. This workflow revealed that the corrections were dependent on the facies type (see La Croix et al. 2019a for a description of the various core facies). As a result, the neural network (see La Croix et al. 2019b) wireline facies output was able to be used as an input to *in-situ* reservoir condition corrections for wells with core data and wireline facies logs. An exception to this was for core data from the Moonie field within the Blocky Sandstone Reservoir and permeability values higher than 1 mD. In this case, it was assumed that they all belonged to core facies SA, and these were corrected to *in-situ* reservoir conditions accordingly.

After continuous permeability logs for wells with wireline facies was calculated, the research checked whether the log derived values (upscaled) match the permeability estimated from DST interpretations. This is because the permeability derived from DSTs represents a larger reservoir volume than permeability derived from well logs. This was checked by averaging the permeability logs (in case of the Moonie field the curve KHLOG10\_LIN) over the DST interval, using arithmetic and geometric means, and compared the product of permeability and thickness, k.h for both methods. In case of a discrepancy, an explanation for the discrepancy was identified such as a mechanical problem with the DST, or a correction to the log permeability was found.

Table 25 lists the permeability equations derived from core porosity permeability cross-plots and the result of comparing the Blocky Sandstone Reservoir log derived permeability with permeability from DST interpretations for the four regional clusters named MAR, Woleebee Creek, Moonie and Central permeability scenarios (not to be confused with the static and dynamic models and areas).

**Table 25** Permeability equations for the three regional permeability models.

Permeability Model	Facies	Permeability Equation
Northern Depositional Centre of Blocky Sandstone Reservoir. To be called the MAR Permeability Scenario	SA	$KH_{MAR} = 10^{(20.02 * PHIT - 1.24)}$
	DST comparison for SA	No correction was needed. Log data matched DST data.
	SB, SC, SD and SMA	$KH_{MAR} = 10^{(-0.67 * V_{SH} + 25.64 * PHIT - 4.11)}$
	Remaining facies	$KH_{MAR} = 0.01 \text{ mD}$
Woleebee Creek GW4 well. To be called the Woleebee Creek Permeability Scenario	SA	$KH_{WCK} = 10^{(11.77 * PHIT + 0.88)}$
	DST comparison for SA	No correction was needed. Log data matched DST data.
	SB, SC, SD and SMA	$KH_{WCK} = 10^{(-0.98 * V_{SH} + 21.12 * PHIT - 3.83)}$
	Remaining facies	$KH_{WCK} = 0.01 \text{ mD}$
Southern Depositional Centre of Blocky Sandstone Reservoir. (Moonie Field). To be called the Moonie Permeability Scenario	SA	$KH_{LOG10\_LIN} = 10^{(-2.30 * V_{SH} + 14.05 * PHIT - 0.20)}$
	DST comparison for SA	$KH_{MOONIE} = 1.0354 * KH_{LOG10\_LIN}$
	SB, SC, SD and SMA	$KH_{MOONIE} = 10^{(-2.35 * V_{SH} + 14.95 * PHIT - 1.04)}$
	Remaining facies	$KH_{MOONIE} = 0.01 \text{ mD}$
Wells with DST around Leichhardt Fault in the centre of the basin. To be called Central Permeability Scenario	SA	$KH_{LOG11\_SW} = 10^{(13.13 * PHIT + 0.18)}$
	DST comparison for SA	$KH_{CENTRAL} = 0.0004 * (KH_{LOG11\_SW})^{1.9026}$
	SB, SC, SD and SMA	$KH_{CENTRAL} = KH_{LOG11\_SW} = 10^{(-0.99 * V_{SH} + 30.67 * PHIT - 3.91)}$
	Remaining facies	$KH_{CENTRAL} = 0.01 \text{ mD}$

In the 10 x 10 km sector models, the equations of the different permeability scenarios in Table 25 was applied to the total porosity and  $V_{shale}$  values in each cell to parameterise permeability in these models.

#### 4.3.8.6 Permeability for the regional geological and notional injection sector models

In the regional static geological model, the permeability was populated from permeability curves PERM, that were based on the four permeability scenarios MAR, Woleebee Creek, Moonie and Central as in Table 25. However, for the notional injection sector model the Moonie permeability scenario was determined to be the appropriate base case scenario for the Blocky Sandstone Reservoir.

The Moonie permeability model was calculated from core total porosity and shale volume. The notional injection sector model was developed based on effective porosity. Thus, the permeability equation has been edited substituting PHIT with PHIE (effective porosity) to be used in the notional injection sector model. This forms the base case permeability for the notional injection sector model. The average  $V_{shale}$  in the wells around the area selected for the notional injection sector model is nearly 0.1 v/v. There is a possibility that the centre of the basin has cleaner sand (La Croix 2019a) and thus an average  $V_{shale}$  of less than 0.1 v/v. For this reason, a core porosity – permeability regression using only core plugs with  $V_{shale}$  less than 0.1 v/v was created. This forms the high permeability case for the notional injection sector model. Since there was no petrophysical basis for developing a low case scenario, a statistical low case scenario was created arbitrarily by dividing the values of permeability in the base case scenario in half.

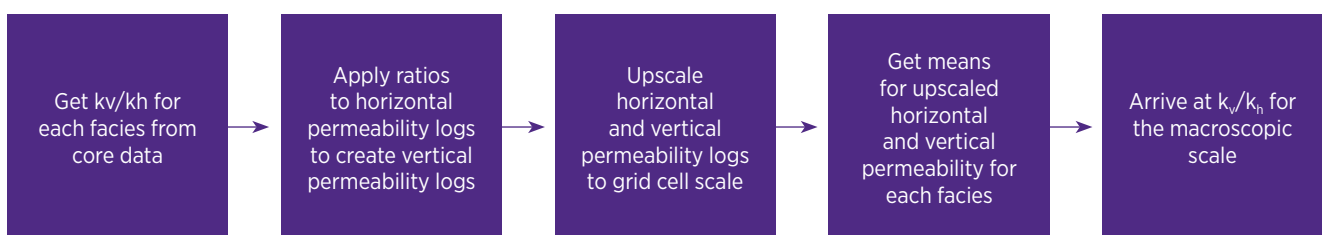
### 4.3.8.7 Estimating vertical permeability ( $k_v$ )

Vertical permeability at the reservoir scale has a critical role to play with regards to accurately determining the migration characteristics of CO<sub>2</sub> and transmission of pressure in dynamic reservoir models. Vertical permeability is normally roughly perpendicular to bedding and thus even thin beds of low permeability material can greatly affect the vertical permeability. Availability of vertical permeability data was limited to core data from five wells, and different approaches were taken to derive upscaled vertical to horizontal permeability ( $k_v/k_h$ ) ratios (reservoir scale) from these core data (plug scale).

Different approaches were taken to calculate  $k_v/k_h$  according to the assigned facies, and to whether plugs had both horizontal and vertical permeability measurements or not. From a facies perspective, heterolithic facies such as SMA and SMB were treated differently than homogeneous facies. Figure 62 shows the method for estimating upscaled  $k_v/k_h$  used in parameterising the various static geological sector models.

Two different methods were used to calculate core  $k_v/k_h$  for the homogenous facies: using cross plots and histograms.

**Figure 62** Workflow for estimating an upscaled  $k_v/k_h$  ratio for a single lithology facies.



Due to the regional static reservoir model being constructed using a different approach than that for the 10 x 10 km sector models it was not appropriate to utilise the tables of  $k_v/k_h$  described above for parameterising the regional model. The regional model used a  $V_{shale}$ -based classification of grid blocks for the purpose of populating porosity and permeability (see Gonzalez et al. 2019b). The 10 x 10 km sector models used core and neural-network based facies classification to determine porosity and permeability (see La Croix et al. 2019d). To have internally consistent  $k_v/k_h$  between models some approximations were made to convert the facies-based to  $V_{shale}$ -based values. These are displayed in Table 26.

**Table 26**  $K_v/K_h$  approximations used in the regional static reservoir models.

$V_{shale}$ Classifier	$K_v/K_h$
Sandstone	0.2
Silty Sandstone	0.02
Siltstone	0.003
Shale	0.02

### 4.3.8.8 Porosity depth trends

One of the important uncertainties for the UQ-SDAAP project is in characterising the static and dynamic properties for the notional injection sector that occurs in the deepest part of the basin where there is a lack of data. Porosity depth trends were used to extrapolate porosity values from more shallow areas constrained by data to the centre of the basin.

There are two categories of static geological models that require different depth trends. The model categories are:

- The 10 x 10 km sector models (La Croix et al. 2019d)
- The regional basin model and notional injection sector model (Gonzalez et al. 2019b)

Total porosity and effective porosity was estimated in the 10 x 10 km sector models (La Croix et al. 2019d). The purpose of modelling effective porosity was to represent volume, whereas the total porosity was populated to calculate permeability using the MAR, Moonie and central permeability scenarios. Since the 10 x 10 km sector models were located in the southern depositional centre for the Blocky Sandstone Reservoir, there was no need to create depth trends for the northern part of the reservoir. Modelling was conditioned to facies using probability distribution functions. Thus, 10 x 10 km sector modelling required:

- Depth trends of total porosity per facies
- Depth trends of effective porosity per facies

For regional basin and notional injection sector models, only effective porosity and log-derived  $V_{\text{shale}}$ -based facies rather than core-derived litho-facies (see Gonzalez et al. 2019b) were used. The depth trend for the Northern depositional centre was required to guide the porosity distribution for that region. Thus, the regional modelling required:

- Depth trends for effective porosity per stratigraphic zone in the southern depositional centre part of the regional model
- Depth trends for effective porosity per stratigraphic zone in the northern depositional centre part of the regional model

All the models used the true vertical depth sub-sea (TVSS) as the depth reference, and thus, the depth trends were created for porosity *versus* TVSS.

**Summarising the application of petrophysics: the petrophysical analysis forms an important constrained and calibrated methodology for populating the static geological model cells with geologically realistic porosity and permeability values that are linked to well control and facies analysis and have been calibrated with core plug analysis and well test data such as DSTs. Importantly, the petrophysical analysis also provides an uncertainty quantification that allows for a low medium and high scenario to be applied that feeds uncertainty analysis of the dynamic simulation.**

The report of Harfoush et al. 2019c describes the workflow and implementation for the UQ-SDAAP project in detail.

### 4.3.9 MAR sector model

**Groundwater impact assessment is central to this project. This section describes how groundwater dynamic studies are used to inform pressure transmission in response to large-scale injection. In the northern part of the Surat Basin, Asia Pacific LNG (APLNG) and Shell/QGC have been operating or have trialled MAR. This involves the large-scale injection of treated water in the Precipice Sandstone. The companies, as well as Santos, gave extensive access to this data to UQ-SDAAP as well as helped with technical advice and discussions. This proved invaluable in calibrating the small-scale flow-properties of the aquifer as well as long range continuity and heterogeneity (critical to evaluation of possible pressure build-up over time). Critically, the model shows that pressure transmission is very long range in the Blocky Sand Reservoir and the Transition Zone/Ultimate Seal complex does not transmit this pressure vertically (the overall play, sealing concept is support by MAR evidence).**

For clarity, the MAR area (in the northern depositional centre) is not a location that the UQ-SDAAP identified for notional CO<sub>2</sub> injection (section 47), however the existing MAR activities together with the associated monitoring bore network provide an excellent data set for the Blocky Sandstone Reservoir dynamic pressure response. The calibration of this data set to UQ-SDAAP dynamic models can be corrected to deeper conditions and used to validate parameters of the Storage Play in the southern depositional centre where notional CO<sub>2</sub> injection sites have been identified. Generally speaking, the investigation showed the Blocky Sand Reservoir to be extensive and relatively homogenous with little internal structure over tens of kilometres, which could give rise to pressure increases. It also showed the potential for more sophisticated groundwater modelling to be undertaken to investigate inter-play between continued MAR and later (very remote) CO<sub>2</sub> injection operations (discussed in later sections).

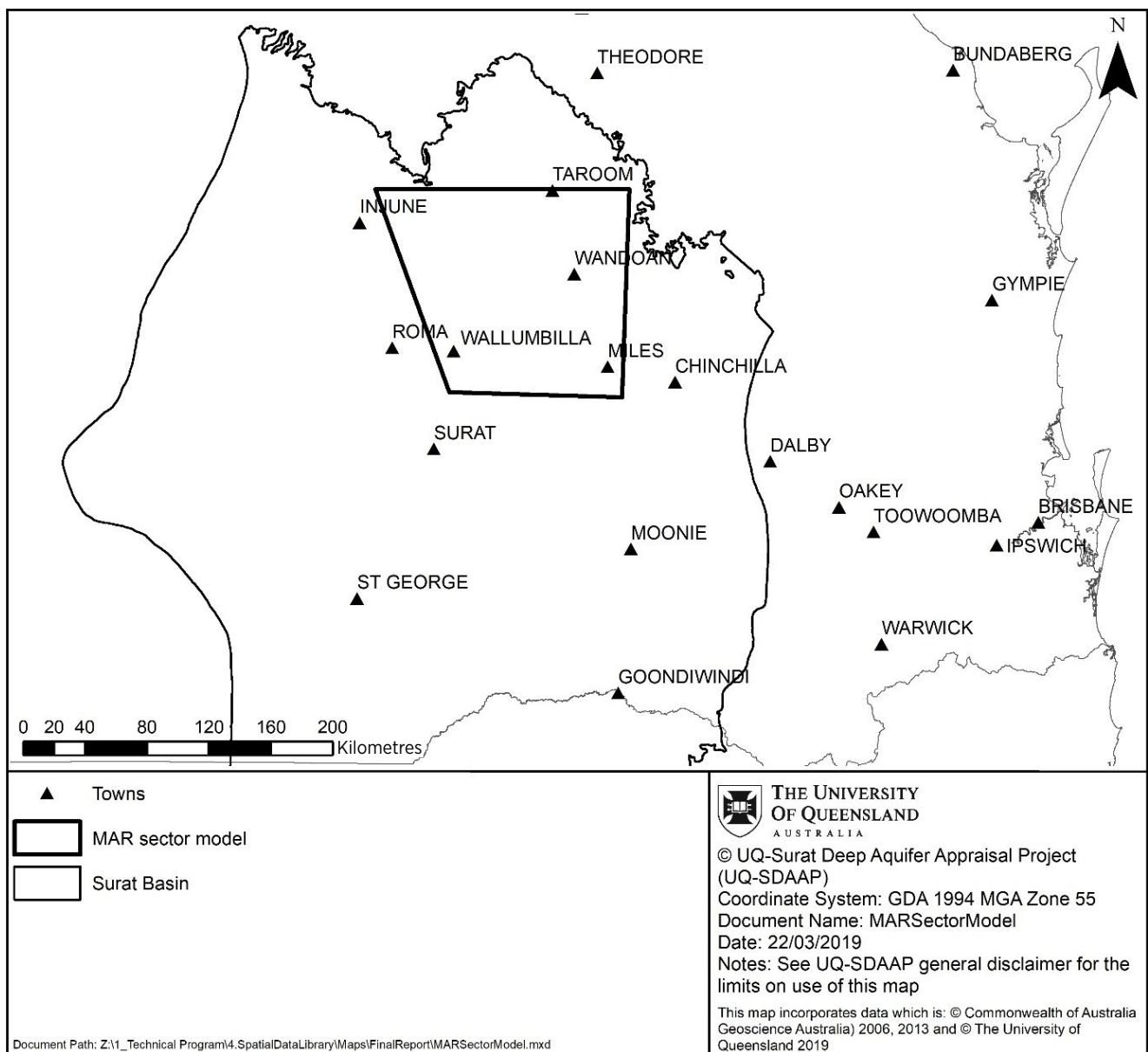
A key calibration area for the project was the northern depositional centre of the Blocky Sandstone Reservoir (see La Croix et al. 2019a, 2019b and 2019c). This area was the best constrained by core, well logs and seismic data.

The MAR activity provided the UQ-SDAAP a significant dynamic data set (i.e. many monitoring wells across the region recording the pressure change with time since the start of injecting some 20 ML per day into the Precipice Aquifer at Reedy Creek and Spring Gully) that could be used to historically match dynamic model simulations. As a result, the MAR sector model (Figure 63) was the first dynamic simulations to be performed in the UQ-SDAAP overall workflow. These early simulations were used as learnings of the expected behaviour of the system and how this related to the early understanding of the stratigraphic architecture. The learnings then informed the ongoing geological characterisation and subsequent dynamic modelling of other sectors more directly related to the notional CO<sub>2</sub> injection sites. A detailed explanation of the MAR sector model can be found in Sedaghat et al. 2019a.

### 4.3.9.1 MAR sector static model

The results of the UQ-SDAAP static and dynamic modelling of the MAR sector revealed that the Blocky Sandstone Reservoir is likely characterised by a dual permeability system at some locations and that permeability is strongly scale-dependent, where the matrix permeability is characterised by the petrophysical analysis. However, only larger scale pump testing (DST's or larger pumping tests including commercial production or injection) may reveal added fracture permeability. The dynamic data set from the MAR operations in the northern depositional centre together with the Precipice Sandstone monitoring bore network allowed for a history match of dynamic simulation scenarios to gain an understanding of bulk rock properties of the Blocky Sandstone Reservoir at various scales and their implications to modelled fluid flow. The learnings from this early modelling were subsequently incorporated into the ongoing geological characterisation and dynamic simulation workflows of the UQ-SDAAP project. A detailed explanation of the MAR sector model can be found in Sedaghat et al. 2019a.

**Figure 63** Map of the Surat Basin showing the location of the MAR sector model area.



### 4.3.10 10 x 10 km sector-scale static reservoir models

Since the notional injection sweet spots are located in the centre of the Surat Basin in a region with very little data control, there is uncertainty in many of the geological parameters and properties that may impact the dynamic simulation of CO<sub>2</sub> injection. To overcome this uncertainty, *initial* 10 x 10 km dynamic models were run on three separate geologically plausible realisations for the basin-centre each with a high, medium and low case for permeability. This initial investigation informed later work on static and dynamic modelling in support of field development planning.

The lowest risk, large-scale carbon storage option in the Surat Basin is the Blocky Sandstone Reservoir, at over 2.3 km in the deepest part of the Mimosa Syncline (sections 4.5 and 4.7). This is also the location of least historic interest to the oil and gas industry as it is unstructured and therefore has the least seismic and well control. Extensive data gathering is recommended later in this report (section 5.3). Uncertainty at this time has been evaluated through discrete sub-surface scenario analysis in which different property and heterogeneity characteristics for the Basal Sandstone Reservoir and the Transition Zone have been combined, each scenario grounded in data from type-wells or play segments.

To test the likely, large-scale injection performance at the basin-centre, three 10 x 10 km sector-scale static reservoir models were built. These captured the range of geological uncertainty in facies distribution and reservoir properties by considering sectors of the Surat Basin with different paleogeographic implications: the Moonie Sector, the Meandarra Sector, and the Woleebee Creek Sector (Figure 64). The main purpose of the models was to capture necessary detail particularly at the interface between the Blocky Sandstone Reservoir and the Transition Zone for each of the three geological scenarios.

Deterministic (object) modelling was used for the Blocky Sandstone Reservoir and lower Transition Zone. The dimensions, orientations, and sizes of geobodies were based on literature and modern deposition environments but designed to be characteristic of the basin-centre. Stochastic modelling was implemented for the upper portion of the Transition Zone and the Ultimate Seal. This was due to early dynamic simulation demonstrating that these zones were less sensitive to the distribution of facies. Reservoir properties including  $V_{\text{shale}}$ , net to gross, porosity, and permeability were modelled using stochastic means, or were calculated based on petrophysical equations.

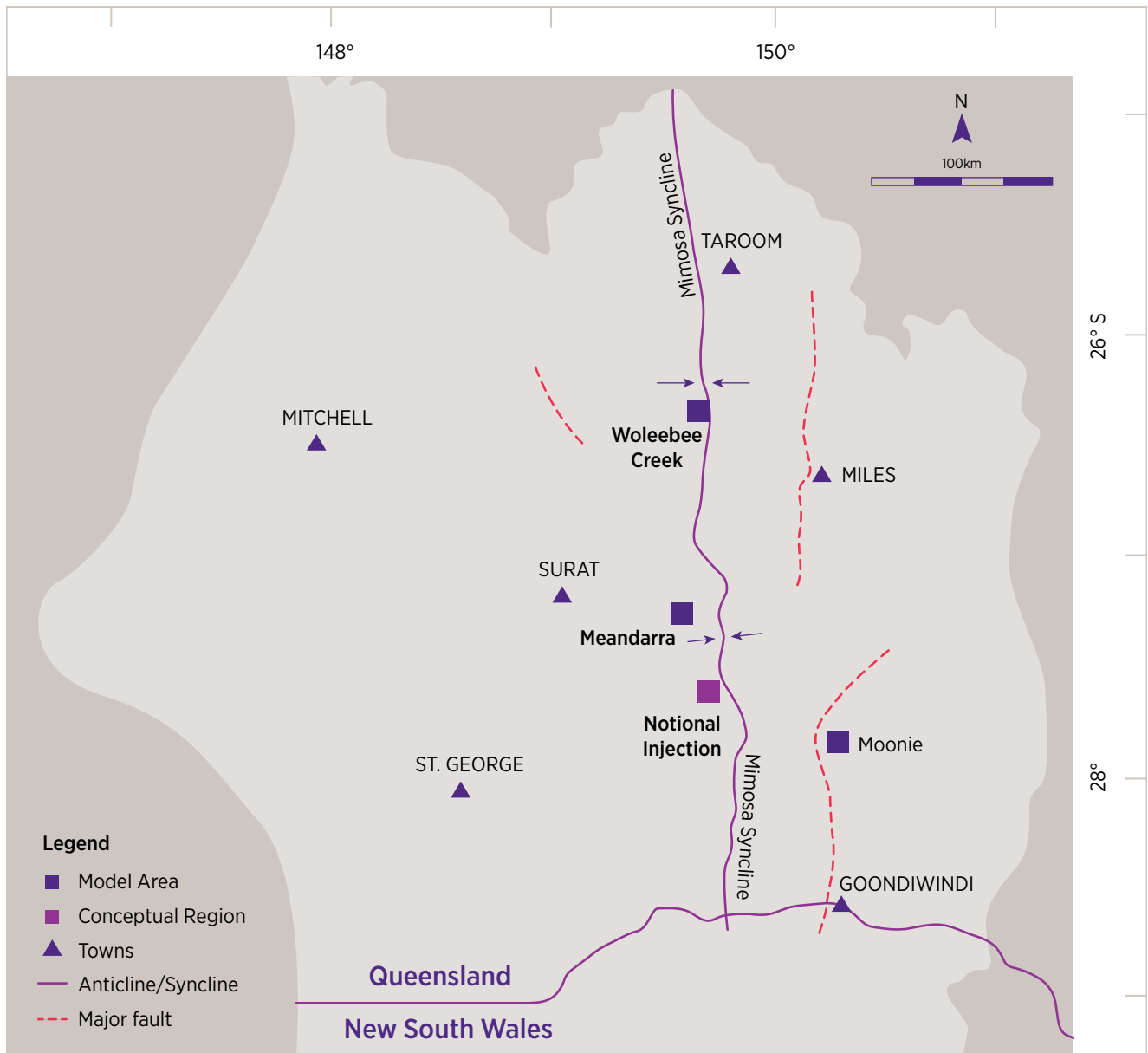
Results of the static reservoir modelling showed that the Woleebee Creek Sector had a clean, porous, and permeable Blocky Sandstone Reservoir interval, a heterogeneous silty and muddy Transition Zone with the lowest porosity and permeability of the three sector models, and an Ultimate Seal that was very low porosity and permeability. The Meandarra Sector displayed the lowest quality. The Blocky Sandstone Reservoir displayed comparatively low porosity and permeability, a mid-case Transition Zone with moderate porosity and permeability, and an Ultimate Seal very similar to Woleebee Creek Sector model. Finally, the Moonie sector model had an overall clean, porous, and permeable Blocky Sandstone Reservoir, the sandiest and most porous and permeable Transition Zone of the three sector models, and an Ultimate Seal almost identical to Woleebee Creek and Meandarra sector models. The distribution of facies and reservoir properties in the static models supports the notion that the Transition Zone has the potential to provide seal qualities overlying the Blocky Sandstone Reservoir. In all cases, the Ultimate Seal showed excellent sealing properties.

The report by La Croix et al. 2019e provides a detailed description of the structural and tectonic analysis workflow and how it was applied for the UQ-SDAAP project.

#### 4.3.10.1 Data and methodology

Representing geological complexity in reservoir models is important to adequately assess the feasibility of CO<sub>2</sub> storage in the subsurface. Rock properties, such as porosity and permeability, are strongly impacted by the heterogeneity of sedimentary facies, as is the mineralogy of the rock. These in turn influence the carbon storage performance of the notional injection site. Thus, it is important to characterise facies and their architecture at multiple scales because facies play a first-order control on these properties. This ensures that the fluid flow behaviour modelled by the reservoir simulation represents geologically realistic scenarios across the range of uncertainty (Bianchi et al. 2015; Ringrose & Bentley 2015).

**Figure 64** Index map showing the location of the three-sector static model conceptualisation areas: Woleebee Creek, Meandarra, and Moonie, respectively.



A variety of methods have been developed to model the distribution of geological strata, each with various strengths and weaknesses. These are generally characterised as either stochastic or deterministic methods (de Marsily et al. 2005; Koltermann & Gorelick 1996). Stochastic approaches generate a series of equally probable realisations of subsurface heterogeneity. The advantage of stochastic modelling is the ability to capture uncertainty in the geology and provide the parameterisation of grid cells. A drawback of stochastic models is the difficulty in reproducing complex and interconnected geologically realistic structures, which are common to most siliciclastic depositional systems (He et al. 2014; Refsgaard et al. 2012). Deterministic approaches use direct or indirect geological information to build unique models of heterogeneity. These types of models obey stratigraphic and facies relationships (i.e. Walther's Law), but tend to be more interpretive, relying on the model builder's conceptualisation of geological systems. The major pitfall of deterministic models is the perceived difficulty in applying reservoir rock properties to the geology, as these are not necessarily linked one for one (Xu & Dowd 2003; Perrin et al. 2005; Mallet 2002; Turner 2006). Other alternate means exist that attempt to impart geological information within a statistical framework, such as multi-point statistics (Hu & Chugunova 2008) and transition probability approaches (Carle & Fogg 1997; Carle & Fogg 1996), but these can be challenging to apply in three-dimensional analysis.



A deterministic approach was used to capture the reservoir characteristics and sealing potential of the Blocky Sandstone Reservoir and Transition Zone, respectively, surrounding a notional CO<sub>2</sub> injection well at the basin-centre. Due to the large degree of uncertainty in the geology, a series of three sector-scale 10 x 10 km reservoir models were constructed based on our regional understanding of the palaeogeography. This helped produce several geologically-reasonable play segment situations each with their own geobody distributions that captured the range of geological uncertainty that exists for the basin centre location. As the basin-centre is largely lacking in seismic, core, and wireline log data the various geometries and orientations of geobodies were conceptualised using facies analysis of core (La Croix et al. 2019a), wireline log facies from neural networks (see La Croix et al. 2019c), and from sequence stratigraphy using wireline logs and seismic (see La Croix et al. 2019b). The models were then populated with reservoir properties using a facies-driven approach, and ultimately used for dynamic flow simulation.

The dataset used for sector modelling consisted of paleogeographic maps of the Precipice Sandstone–Evergreen Formation interval (Gonzalez et al. 2019a), as well as petrophysical properties derived from core and wireline log analysis (see Harfoush et al. 2019a, 2019b, 2019c and Honari et al. 2019a).

Paleogeographic maps were used as a predictive tool for understanding the distribution of sedimentary facies and depositional environments for the major stratigraphic subdivisions. The stratal packages were defined as the intervals between J10–TS1, TS1–MFS1, MFS1–SB2, SB2–TS3, and TS3–J30, respectively (Figure 20). This was the most convenient and meaningful way to split the Precipice Sandstone–Evergreen Formation succession, as the surfaces were straightforward to correlate and map across the basin. The subdivision captured the detail of the Blocky Sandstone Reservoir interval (J10–TS1; see Sequence Stratigraphy Report), the component stratal architecture of the Transition Zone (TS1–MFS1, MFS1–SB2, and SB2–TS3), as well as the Ultimate Seal (TS3–J30). However, grouping units together for mapping and modelling was necessary in situations where the strata between two surfaces were thin or discontinuous across the basin. The best example of this is the Boxvale Sandstone Member, which was grouped to be included in the uppermost portion of the Transition Zone (SB2–TS3), though technically is defined as occurring between J20 and TS3.

The paleogeographic maps were the main outcome of the core analysis and facies from neural networks workflow (see La Croix et al. 2019c). In summary, a facies classification scheme was defined from core observations (see La Croix et al. 2019c). Next, the wireline log signature of the core facies was simplified into a smaller set of wireline log facies (WLF) with similar ranges of petrophysical parameters using statistical methods. Then, an artificial neural network was trained to recognise the WLF using the cored wells to cross validate. Finally, WLF were determined from 189 wells within the basin that had a suitable suite of logs. From these, the proportion of WLF in each of the stratigraphic intervals mentioned above were calculated. The facies distributions were generated by mapping the dominant WLF for each well in each interval. The paleogeographic maps were then used to understand and predict the variation in geological heterogeneity and depositional environments at the basin-centre where data was lacking.

#### 4.3.10.2 Model philosophy for the basin-centre

To capture the uncertainty of facies distributions at the basin-centre, 10 x 10 km static reservoir sector models were built of three contrasting paleogeographic regions: 1) the Moonie region – thought to be the most proximal in terms of the position of sedimentary environments relative to a paleo-shoreline; 2) the Meandarra region – which was interpreted to represent the most likely depositional position; and, 3) the Woleebee Creek region – representing the most distal of the three situations with respect to a paleo-shoreline. Sedimentary facies, their proportions, geometry, and distribution were transposed into the sector model to the correct depth and orientation for the position within the basin-centre. The three regions were only used as a conceptual basis for the distribution of sedimentary facies, which then drove the model parameterisation with porosity and permeability distributions corrected to *in-situ* conditions of the basin centre location. However, the data derived from petrophysics applies to the *regions as a whole* rather than any individual wells within the region. Static reservoir modelling consisted of three components: 1) building the model structure, 2) modelling facies, and 3) property modelling. Each modelling phase drew upon a different dataset that is described in other sections of this and subsidiary technical reports.

##### 4.3.10.2.1 Model structure

The sector-scale models were built using the regional stratigraphic horizons that were mapped across the basin: J10, TS1, MFS1, SB2, TS3, and J30 (see La Croix et al. 2019b and Gonzalez et al. 2019a). However, the interval from J10–TS1 was split into two using a horizon (J10a) running parallel to and sitting 15 m below TS1. This resulted in a model consisting of six major zones, or layers. The top of each model occurs at a depth of approximately 1910 m subsea. The base of each model sits at approximately 2120 m subsea, thus each model had a cumulative thickness of 190 m.

Layering of the models varied by zone in an effort to capture detail at specific stratigraphic intervals. This was especially the case near the top of the Blocky Sandstone Reservoir and within the Transition Zone where it was important to understand the detailed geological characteristics occurring at the interface.

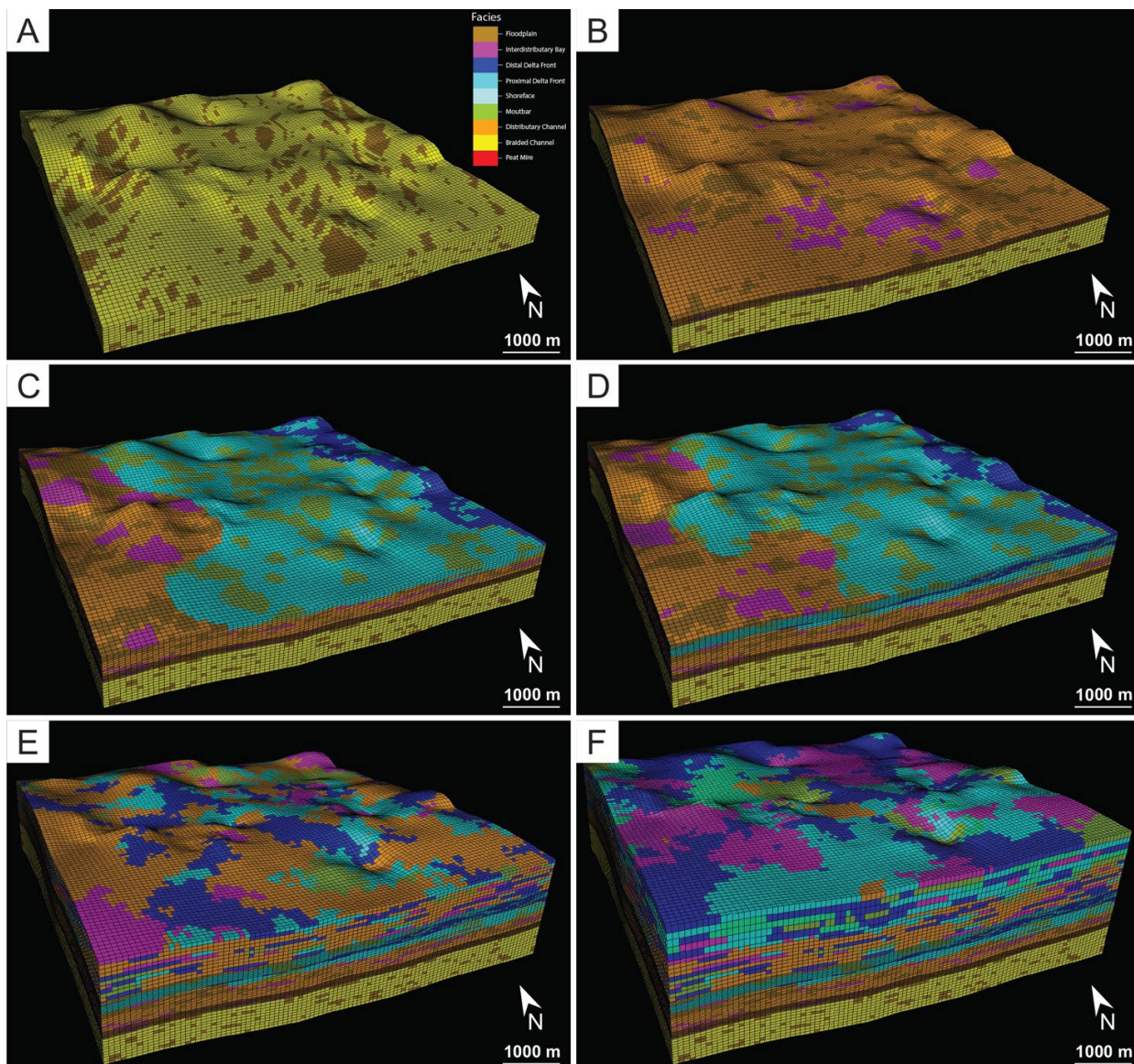
Grid cells in the ‘j’ and ‘k’ directions (i.e. both horizontal directions) were 100 x 100 m. This resulted in the 10 x 10 km model consisting of 100 cells x 100 cells x 55 cells; The total number of cells within the model was 550,000.

#### 4.3.10.2.2 Facies modelling

Facies were modelled as geobody objects in the lowermost four zones, representing the Blocky Sandstone Reservoir and lower Transition Zone. On the other hand, the upper two zones (representing the upper Transition Zone and Ultimate Seal) were modelled using stochastic means. In order to “object model” geobodies, first the overall proportion of facies per zone was estimated by considering the regional paleogeographic maps (see La Croix et al. 2019c). Next, a background frame of core facies was used to embed the geobody objects. This background consisted of core facies MA to represent the delta plain, SMA to represent the proximal subaqueous delta, and SMB to represent the distal subaqueous delta. Within this background, various geobodies were populated with a range of size distributions and orientations relative to their position in the basin (Figure 65). Orientations were based upon our best understanding of the paleogeography. Size distributions were based upon observations from core and with reference to literature values (see La Croix et al. 2019 c and 2019e for details).

Stochastic facies modelling of the Ultimate Seal was undertaken using Sequential Indicator Simulation (SIS; Journel 1983; Journel & Issaks 1984; Journel & Alabert 1988; Deutsch 2006). The relative proportion of facies were estimated based on paleogeographic maps for their respective intervals. Then, a range of anisotropy in the major, minor, and vertical directions were applied (i.e. variograms). A spherical variogram with no azimuth or dip direction was chosen, due to the lack of directional trend information available from the basin.

**Figure 65** Facies modelling of the Meandarra sector model. (A) Object modelling of the lower Blocky Sandstone Reservoir. (B) object modelling of the upper Blocky Sandstone Reservoir. (C) Object modelling of the lower Transition Zone. (D) Object modelling of the middle Transition Zone. (E) Sequential Indicator Simulation of the upper Transition Zone. (F) Sequential Indicator Simulation of the Ultimate Seal.

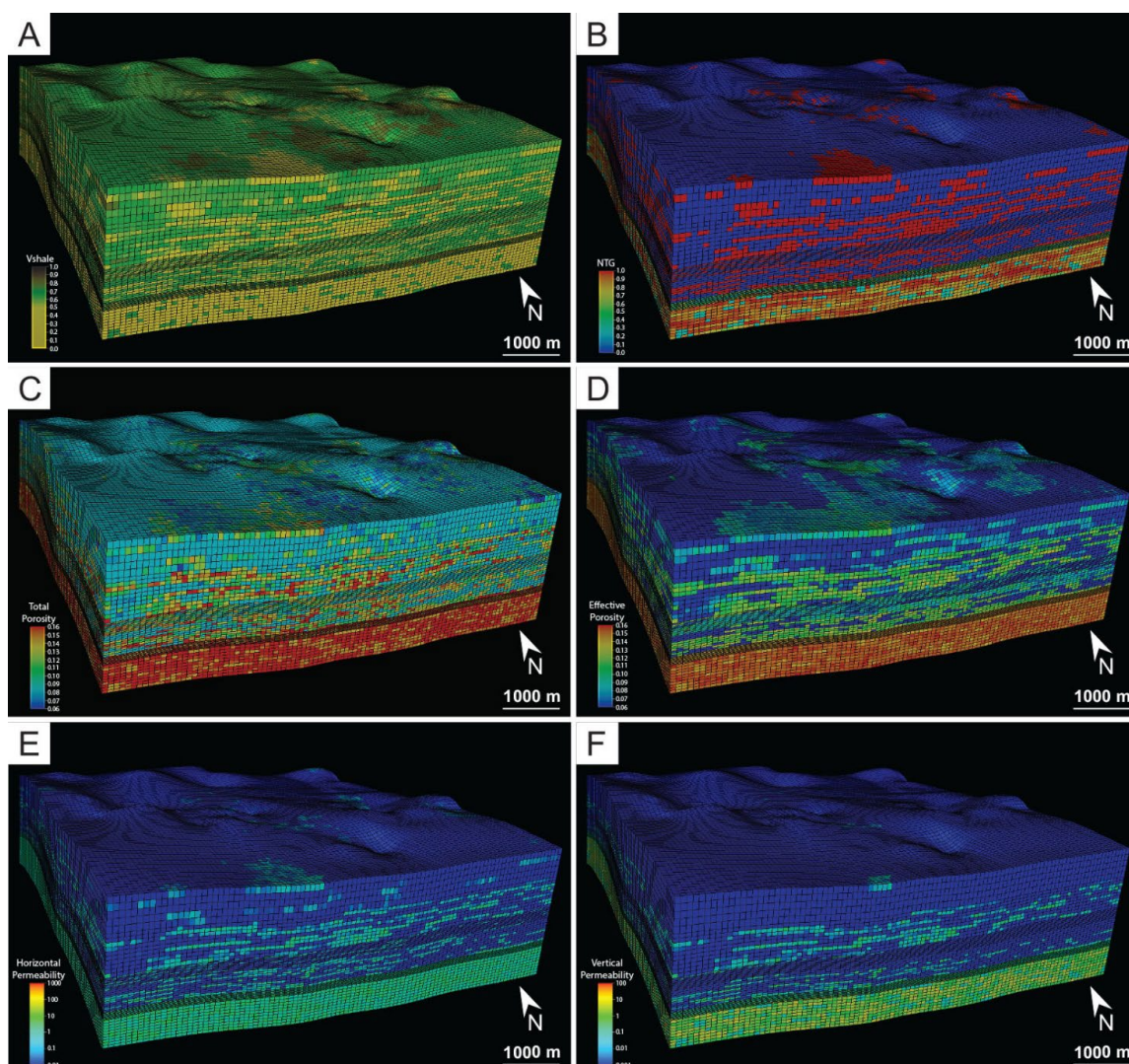


#### 4.3.10.2.3 Property modelling

Petrophysical data was used to populate model cells with appropriate rock properties. Properties that were modelled include: ‘shaliness’ ( $V_{\text{shale}}$ ), net to gross (NTG), total ( $\Phi_T$ ) and effective porosity ( $\Phi_E$ ), and horizontal ( $k_h$ ) and vertical permeability ( $k_v$ ). They were calculated on a per-facies basis using WLF. Generally, properties fell into two broad categories: modelled parameters and calculated parameters. Modelled parameters were derived from detailed petrophysical analysis (see Harfoush et al. 2019a, 2019b, 2019c and Honari et al. 2019a) and distributed through the sector-scale static models (see below) with a correction for *in-situ* conditions of the basin centre location. Calculated parameters were calculated based on the modelled parameters but were not distributed using deterministic or stochastic means. The parameters that were modelled consisted of  $V_{\text{shale}}$ ,  $\Phi_T$ , and  $\Phi_E$ . The calculated parameters were NTG,  $k_h$ , and  $k_v$ . See La Croix et al. 2019e for details on the petrophysical characterisation of the 10 x 10 km sector models.

Petrophysical modelling used Sequential Gaussian Simulation (SGS; Deutsch & Journel 1992; Verly 1993; Lee et al. 2007) for sand-dominated facies (Figure 66). Mud-dominated facies, on the other hand, were modelled using assigned constant values: the mean log-derived value for the central basin region. Sandy facies were distributed using the minimum, maximum, and standard deviation for most properties. Distribution functions were used for SGS of all sandy facies for  $V_{\text{shale}}$ . Distribution functions were also used for SGS modelling of  $\Phi_T$  and  $\Phi_E$  for facies SMA. Each distribution function was based upon the upscaled log-derived values from the central basin. Finally, a range of anisotropy in the major, minor, and vertical directions were applied (i.e. variograms). A spherical variogram with no azimuth or dip orientation was chosen, due to the lack of directional trend information available from the basin. See La Croix et al. 2019e for details.

**Figure 66** Examples of the property modelling for the Meandarra sector model. (A)  $V_{\text{shale}}$ . (B) Net to gross. (C) Total porosity. (D) Effective porosity. (E) Horizontal permeability. (F) Vertical permeability (water in-situ reservoir permeability). Note that  $V_{\text{shale}}$ , total porosity and effective porosity were modelled parameters, whereas net to gross, horizontal permeability, and vertical permeability were calculated parameters.



### 4.3.10.3 Discussion of results

All three sector models consisted of six zones; two to represent the Blocky Sandstone Reservoir, three representing the Transition Zone, and one for the Ultimate Seal. The stratigraphically lowest four zones were object-modelled using paleogeographic conceptualisation to determine the relative proportion of facies. Geobody objects were modelled with a range of sizes and orientations based on dimensions documented in the literature or known from modern depositional systems:

- The Moonie sector captures the facies from a proximal position relative to a paleo-shoreline
- The Meandarra sector model showed a more distal facies relationship, and one that is thought to be most representative of the basin-centre area where notional injection sites have been selected
- The Woleebee Creek sector demonstrated how facies would be distributed in the most distal position relative to a paleo-shoreline

The uppermost two layers within all the models used sequential indicator simulation to stochastically model the distribution of facies based upon their relative proportions. The three models capture the range of geologically-reasonable uncertainty in the Precipice Sandstone-Evergreen Formation succession within the Surat Basin.

Facies distributions were the basis for modelling reservoir properties in the static models. Six main properties were modelled:  $V_{\text{shale}}$ , NTG,  $\Phi_E$ ,  $\Phi_T$ ,  $K_h$ , and  $K_v$ . Of these,  $V_{\text{shale}}$ ,  $\Phi_E$ , and  $\Phi_T$  were modelled using sequential gaussian simulation and were based on a detailed petrophysics workflow. In contrast, NTG,  $K_h$ , and  $K_v$  were calculated parameters and ultimately tied to the distribution of shale and porosity. Permeability modelling used porosity-permeability transforms characteristic of the specific sector areas. The results of the property modelling generally showed a cleaner and more porous and permeable Blocky Sandstone Reservoir in the Moonie and Woleebee Creek sectors compared with the Meandarra sector model. The Transition Zone, on the other hand, was dirtiest, with the lowest porosity and permeability in the Woleebee Creek sector. The Moonie sector had the cleanest and most porous and permeable Transition Zone with the Meandarra sector lying somewhere midway between the two. Finally, the Ultimate Seal interval was overall similar between all three sector models. In all cases, the Ultimate Seal showed low proportions of sandstone, low porosity, and low permeability. These results attest to the potential for pressure and flow dampening in the Transition Zone and showed good sealing potential of the Ultimate Seal in all three model situations.

**Summarising the sector models: the 10 x 10 sector models provided UQ-SDAAP a range of three geological conceptualisations. These are consistent with available data, defining the range of uncertainty in the facies models and paleo depositional environments. For each of the three realisations there was also a low, medium and high rock property scenario based on the uncertainty defined in the petrophysical analysis. Together this created nine combinations of different but supportable, geological scenarios and rock property parameterisations with which to run dynamic simulations of notional CO<sub>2</sub> injection.**

### 4.3.11 Regional geological model

Site-specific models need to be integrated in and consistent with wider, regional models. Large-scale CO<sub>2</sub> injection storage may have only small physical sub-surface footprint (<10 km) where the CO<sub>2</sub> can move. However, pressure in the sub-surface is transmitted much further. The direction and magnitude of pressure inflation needs to be assessed across areas far greater than those typically modelled in reservoir simulators. For this, regional structural and stratigraphic variability needs to be defined over hundreds of kilometres. The pressure “source term” needs detailed two phase modelling. The far-field “response” to this requires a different, single phase, groundwater modelling approach. The two approaches need to be consistent where the models meet.

The UQ-SDAAP research created a regional geological model of the Precipice Sandstone to Evergreen Formation strata in the Surat Basin. It integrates existing seismic data, well data, and their associated geological interpretations using Petrel 2016 software. The aim was to produce a 3D geological model that combines all the subsurface geological understanding to depict the spatial distribution of reservoirs and seals that is consistent with all available data. Subsurface data integration supported a conceptual geological model creation. In addition, using the play concept developed for the Precipice Sandstone and Evergreen Formation, subsurface fluid flow and its implications for CO<sub>2</sub> storage can then be assessed. Constructing large-scale models for the Surat Basin has limitations relating to areas of sparse data and this carries with it a relatively high degree of uncertainty. However, the uncertainty was mitigated by using our conceptual understanding of the geology to infill data gaps in a geologically consistent manner.

The regional geological model is used as the base case reference for the regional groundwater and notional injection sector dynamic simulations. The report by Gonzalez et al. 2019b provides a detailed description of the regional basin model development workflow and how it was applied for the UQ-SDAAP project.

#### 4.3.11.1 Methodology and input data

The 3D regional geological model integrated deterministic data such as petrophysical logs, drill stem tests, well tops, structural surfaces from seismic and wells, and paleo-geographic maps of depositional systems into a probabilistic distribution of facies and rock properties. The construction of the regional geological model is comprised of three phases: 1) structural modelling, 2) facies modelling, and 3) property modelling, which was co-dependent of the facies modelling.

1. The structural modelling inputs the stratigraphic surfaces and major fault structures mapped from seismic interpretation (Gonzalez et al. 2019a). This provides a stratigraphic framework which is based on the “play concept” that defines three main stratigraphic zones: 1) Blocky Sandstone Reservoir, 2) Transition Zone, and 3) the Ultimate Seal (La Croix et al. 2019b)
2. The 3D facies model was created from a simplified facies criteria obtained from a  $V_{\text{shale}}$  “cut off” for all wells with  $V_{\text{shale}}$  logs. Considering the regional scale of the model and the need for computational efficiency, the detailed facies information was required to be simplified in comparison to the approach taken for the 10 x 10km sector models (La Croix et al. 2019e). The learnings from the 10 x 10kmm sector modelling were used to define four facies classifiers for the regional geological model ( $V_{\text{shale}}$  Facies Sand, Silty Sand, Silt and Mud). The 3D model facies were laterally trended using paleogeographic maps and in the vertical direction the  $V_{\text{shale}}$  facies were up-scaled using the proportions that were “most of” and cell volume to represent the most dominant facies present at each stratigraphic interval or layer
3. The property model represents the 3D effective porosity (PHIE) and the 3D horizontal permeability (kh). Continuous wireline logs were calculated for ‘shaliness’ ( $V_{\text{shale}}$ ), effective porosity (FE), and horizontal permeability (kh) (see Harfoush et al. 2019a, 2019b, 2019c and Honari et al. 2019a). These were used to determine reservoir properties at locations away from data control for each stratigraphic zone in the model. The property model inputs are defined by well data distribution functions and histograms, porosity depth trends for the sandier facies guided by geographically distributed property maps. Statistical well function distributions were adjusted using the 2D maps to fill spatial data gaps. The regional geological model was not characterised for vertical permeability. This was dealt with in the dynamic modelling for the regional groundwater or notional injection sector models (Rodger et al. 2019c and Hayes et al. 2019b)

The regional static model was populated using Gaussian Random Function Simulation (GRFS) that referenced variograms, correlation coefficients, and depth trends to constrain the vertical and lateral distribution of properties. These required substantial professional judgement based on our best understanding of the variable geology of each zone. Co-kriging was used to trend well data into a lateral spatial distribution.

The input data used for building the regional geological model included maps, seismic and well data.

#### 4.3.11.1.1 Maps

- Total of five paleogeographic maps; one for each of the main stratigraphic zones
- A digital elevation (topographic map)
- A regional geological map depicting the main tectonic events of the basin

#### 4.3.11.1.2 Seismic data

Seismic data coverage was concentrated in the northern part, as well as the eastern and western margins of the basin. Full details of seismic data used in the model can be found in Gonzalez et al. 2019a. In summary, seismic interpretation primarily focused on tracing three horizons (i.e. seismic events) across the basin:

- Top Transition Zone Near J20 (Seismic Event 2)
- Top Blocky Sandstone Reservoir TS1 (Seismic Event 4)
- Base Jurassic J10 (Seismic Event 5)

Note that three additional surfaces were 'phantomed' from the above horizons, two of them were used to subdivide the Transition zone into three zones (TS1-MFS1; MFS1-SB2 and SB2-TS3) and the third one represented the Top of the ultimate seal J30.

#### 4.3.11.1.3 Well data

The well data input for defining the spatial distribution of property data was extracted from wells containing a full suite of logs, whereas well tops were derived from all the possible wells correlated in the basin. Available wireline logs have been interpreted, and the results used as the major input for the property model. The property model was based on ~70 wells with  $k_r$  and 207 with PHIE and 285 with  $V_{shale}$  data (see Honari et al. 2019a).

### 4.3.11.2 Discussion and results

The regional geological model was defined by three main zones from bottom to top:

1. Blocky Sandstone Reservoir, roughly equivalent to the Precipice Sandstone
2. Transition Zone: roughly equivalent to the lower Evergreen Formation and comprising silty shale and sandy interbedded units
3. Ultimate Seal: roughly equivalent to the Westgrove Ironstone Member as well as silty and shale layers of the Upper Evergreen Formation

In order to characterise the impact to fluid flow of the various sandy strata and capture a higher level of detail within the Transition Zone, subzones were used (Figure 67). The subdivision in the Transition Zone is given by: the Lower Subzone (TS1-MFS1); the Mid Subzone (MFS1-SB2); and the Upper Subzone (SB2-TS3) (Figure 67). This sub-zonation followed conformable surfaces in the UQ-SDAAP sequence stratigraphic characterisation for TS1-MFS1 and MFS1-SB2 and a percentage distribution for the upper subzone SB2-TS3 (see Gonzalez et al. 2019a and 2019b for details).

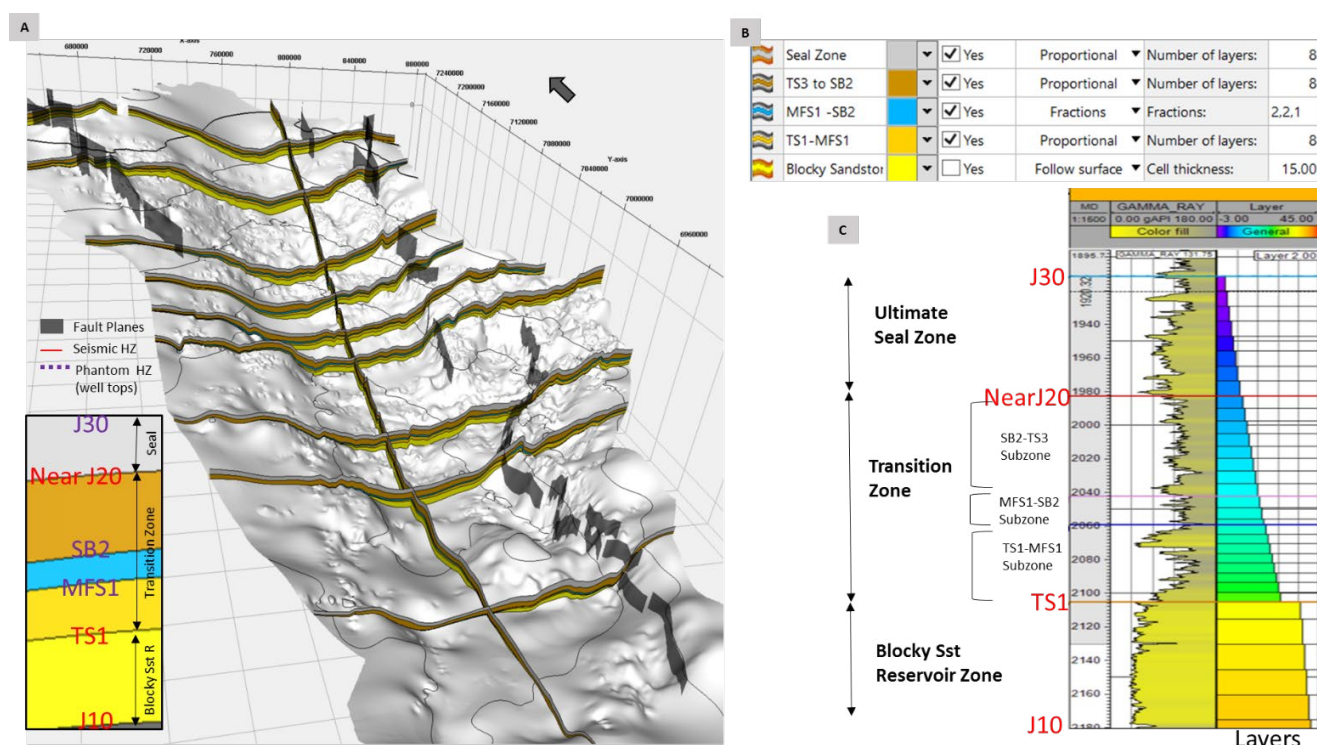
#### 4.3.11.2.1 Structure

The static model was discretised in the lateral direction using a 250 x 250 m grid. In the vertical direction, the geological zones defined by the seismic and phantomed horizons were divided into layers. Resolution of layering was defined based on depositional cyclicity. For instance, a homogeneous lateral shale unit such as, MFS1-SB2 would have less resolution in layering, whereas more detailed layering is applied near the boundary between the Blocky Sandstone Reservoir and the Transition Zone. This is because  $CO_2$  migration due to buoyancy is more likely near this boundary (based on results of the 10 x 10 km sector model simulation results) and this is also where the Transition Zone tends to be sandier and siltier. Due to the regional scale and homogeneity in the lithological characteristics of the Blocky Sandstone Reservoir, the layering for this zone was devised with the aim to capture the bulk sandy properties, which was around 15 m thick (Figure 67). Thin muddy layers within the Blocky Sandstone Reservoir range from 1 to 2 metres thickness and were not able to be explicitly captured in a regional model. However, the low permeability values for this muddy lithology was taken into account in the Blocky Sandstone Reservoir parameterisation.

In order to represent the Blocky Sandstone Reservoir truncation against the Base Surat Unconformity, the layering option in Petrel was selected that followed the top of the Blocky Sandstone Reservoir surface TS1. Proportional layering was then applied to all the subzones in the Transition Zone and the Ultimate Seal Zone, except for the MFS1-SB2 Subzone, which is determined by fractions of the total zone thickness. The layering process is summarised below:

- Ultimate Seal Zone: 8 proportional layers
- SB2-TS3 Sub-zone of the Transition Zone: 8 proportional layers
- MFS1-SB2 Sub-zone of the Transition Zone: Fraction layers with the relative portions of 2, 2, and 1 (e.g. the first layer is 2 times thicker than the bottom layer)
- TS1-MFS1 Sub-zone of the Transition Zone: 8 proportional layers
- Blocky Sandstone Reservoir Zone: Layers every 15 m following the top surface, allowing truncation (onlapping) for the bottom layers

**Figure 67** (A) 3D perspective of the structural framework and model boundaries. Grey polygons denote faults, the white background represents structural contours for the J10 unconformity surface and the cross sections exhibit the sequence stratigraphic framework across the basin. (B) Modelled zones and layering for each stratigraphic unit. (C) An example of the layering discretisation.



All the major faults were interpreted or combined with those mapped as part of the Faults and Fractures Project (Copley et al. 2017) and are incorporated into the regional static model Figure 67. A total of 30 faults located at the base of the Surat Basin were gridded, cut and their fault planes extrapolated through the relevant stratigraphy. Further, pillar gridding refinement may be required for local models. This has a direct impact on estimated connectivity across these faults, therefore re-evaluation of throws and fault geometries is necessary.

#### 4.3.11.2.2 Facies

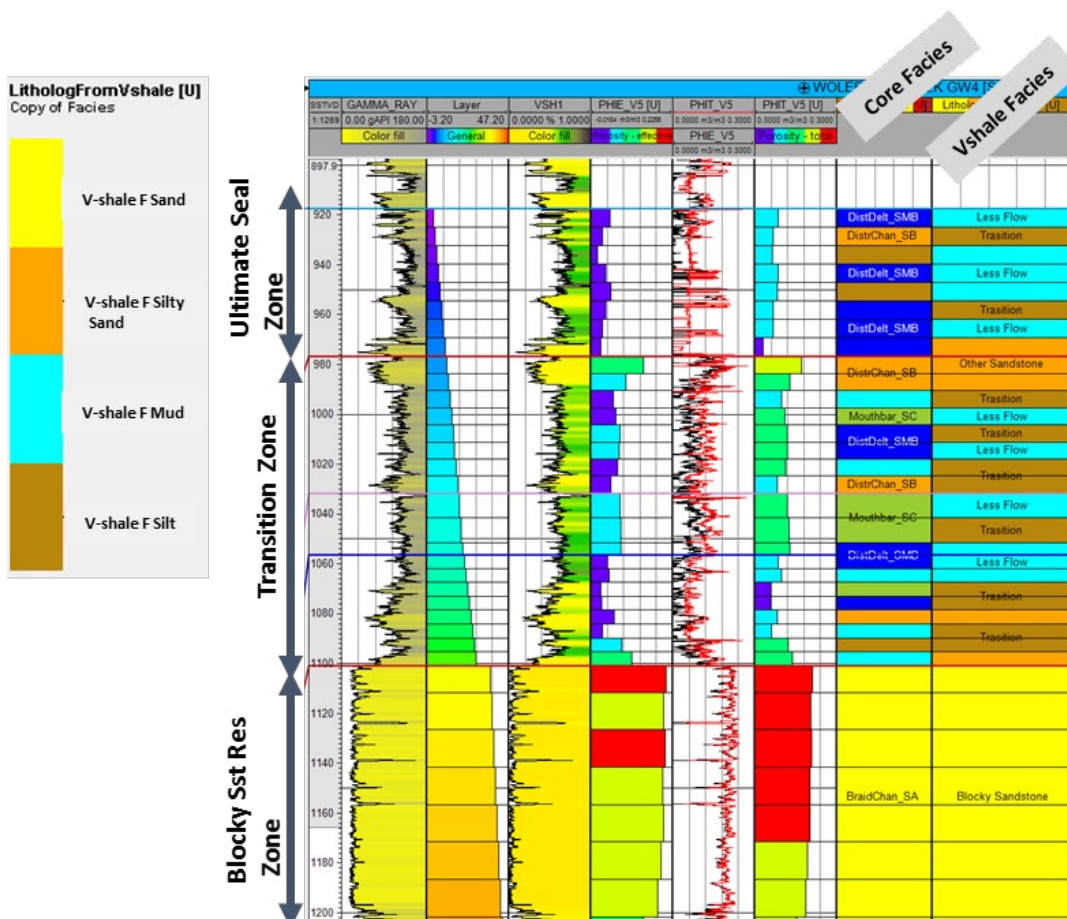
A facies model was constructed with the aim of integrating various geological data with the regional depositional trends conceptualised from the paleogeographic maps (La Croix et al. 2019c). Facies were also used to guide the population of rock properties across areas of the basin where data was otherwise sparse. Considering the regional scale of the model, the facies model was simplified into four gamma ray derived  $V_{shale}$  facies (Gonzalez et al. 2019b) instead of the 19 core facies (La Croix et al. 2019a). The  $V_{shale}$  facies classification was derived from  $V_{shale}$  cut offs obtained from wells with gamma ray logs as follow:

- $V_{shale}$  Facies Sand (Braided system and localised fluvial channels)  $V_{shale} < 15\%$
- $V_{shale}$  Facies Silty Sand (Fluvial to distributary channels)  $V_{shale} 15\% - 35\%$
- $V_{shale}$  Facies Silt (Muddy Sandstone layers)  $V_{shale} > 35\% - 60\%$
- $V_{shale}$  Facies Mud (Shales and muddy layers)  $V_{shale} > 60\%$

The  $V_{shale}$  cut offs and the  $V_{shale}$  up-scaled facies obtained from the “most of” method was fine-tuned using core facies prediction from machine learning and neural network models (La Croix et al. 2019c) to get geologically-realistic  $V_{shale}$  cut off values for each facies. For instance, Figure 68 compares core facies classification and  $V_{shale}$  derived facies. The  $V_{shale}$  facies tend to group differently than the core facies. Facies dissimilarity are more obvious in the mid  $V_{shale}$  range, whereas the lower  $V_{shale}$  intervals are better correlated. There is no direct facies correlation for the mid  $V_{shale}$  range as the facies association from core data includes results from a full suite well logs. As an example, the  $V_{shale}$  Facies Silt can be contrasted to a wider core facies association such as: SB (distributary channels sands), SMB (interbedded sandstone and muds) and SC (splays sandstone) as observed in Figure 68. This variation is associated with changes in rock properties. As a result, the  $V_{shale}$  Facies Silt cut off was intended to capture the uncertainty in the vertical and lateral distribution of the rock properties. Conversely, this intermediate classification is considered to be re-defined as a  $V_{shale}$  Facies Silty Sand or  $V_{shale}$  Facies Mud with their respective statistical distribution for further sensitive analysis and dynamic simulation case scenarios. (Rodger et al. 2019e).

In general, the stratigraphic  $V_{shale}$  facies variation in the vertical section can be summarised by sandy lithologies at the Blocky Sandstone Reservoir to interbedded silt and shale strata in the Transition Zone and predominantly shale units at the top of the Ultimate Seal Zone.

**Figure 68** Up-scaled facies classification from  $V_{shale}$  compared to core facies data prediction. Vertical heterogeneity is captured in the up-scaled cells.





#### 4.3.11.2.3 Rock properties

The reservoir property model is developed to represent a single value of effective porosity (PHIE) and horizontal permeability ( $k_h$ ) in each cell, and this forms a major input for dynamic reservoir simulation. Effective porosity and horizontal permeability data were derived from well logs, core, and DST analysis where well log data is calibrated against and converted to a continuous vertical representation of calculates PHIE and  $k_h$ . This forms the main input to the regional property modelling (see Harfoush et al. 2019a, 2019b, 2019c and Honari et al. 2019a).

The PHIE and  $k_h$  was determined from continuous petrophysical logs. PHIE and  $k_h$  were up-scaled using the arithmetic mean and populated throughout the model in 3D considering vertical and horizontal trends. In areas where wells do not occur, porosity-depth trends were applied for sandier facies (i.e.  $V_{shale}$  Facies Sands and Facies Silty Sand) focused on the Blocky Sandstone Reservoir taking into account porosity reduction with depth. Following the (vertical) up-scaling at the well locations, the grid was populated in the lateral direction to fill the 3D modelling domain and the GRFS method was used in Petrel. The rock properties were distributed and conditioned to the facies distribution for each stratigraphic zone. The vertical and lateral variation within the data was obtained from: i) variograms, ii) histogram of statistical analyses and iii) co-kriging secondary variables such as: a vertical function (porosity depth trends for  $V_{shale}$  Facies Sands and Facies Silty Sand) and a horizontal variable provided by the input of 2D property maps for each  $V_{shale}$  facies.

The variograms are subject to well data density. The range, which is the maximum distance where sample values are dependent on each other, was selected after running several iterations to get the closest regional trends associated to paleogeographic input and the geological concept model (i.e. porosity data from the north part of the basin is not representative to the central and south region, therefore the ranges were truncated and restricted to areas of influence).

The statistical distribution (PHIE and  $k_h$  histograms) uses the standard method in Petrel and a general distribution function. The general distribution function was selected for a combination of a best fit histogram obtained from the well data input range and for the expected values and trends from the 2D property maps. This data combination is more common for  $k_h$  distributions due to a paucity of permeability logs. The 2D property maps were intended to fill the data gap geographically, following the conceptual geological model. The 2D property maps for PHIE and  $k_h$  were constructed for each  $V_{shale}$  facies using GRFS and co-kriging it to their respective 2D  $V_{shale}$  fraction map.

The co-kriging variables for the vertical functions use the depth trends for the sandier facies obtained from petrophysical log and core calibration. For the horizontal functions, the generated 2D property maps are used as input. This surface is converted with a 3D trend having identical values for all cell with similar x, y coordinates.

**Summarising the regional geological model: the final regional geological model provides the basis of generating the regional groundwater static model and the notional injection sector static model. These were then used for dynamic simulation (sections 4.6, 4.8, 4.11, 4.12 and 4.13). The report by Gonzalez et al. 2019b provides a detailed description of the regional basin model development workflow and how it was applied for the UQ-SDAAP project.**

## 4.4 The container concept

For climate change mitigation to be accomplished through CCS, the large majority of CO<sub>2</sub> injected into the sub-surface must be securely contained indefinitely. To demonstrate containment requires the definition of a “container”. The leakage risk must be analysed within the context of this defined container. A container comprises the intended injection and storage reservoir and an overlying seal or seal complex that defines a vertical extent. The container also has to have defined, lateral boundaries. If CO<sub>2</sub> migrates outside the defined container (i.e. above the seal complex and/or beyond the lateral boundaries), it can be considered to have leaked. For clarity, this is not the same as causing “damage” either in terms of the local environment or in terms of increased emissions to atmosphere, because, even in these cases, there are many mechanisms that could cause the CO<sub>2</sub> to become trapped or fixed (e.g. residual or mineral trapping). Furthermore, to define “damage” requires an assessment of the amount leaked and the sensitivity of the receiving environment. In any case, a container should be selected and defined as having very low risk of any leakage (and thus significantly lower risk of ‘damage’).

The containers (up to three sites) proposed in this chapter comprise the Precipice Sandstone of the lowermost Jurassic as the injection/storage reservoir. These are geographically located in the deepest part of the basin where the strata are relatively flat lying. The reservoir is overlain by a seal complex, which is comprised of a thick Transition Zone that acts as a baffle or a buffer to vertical CO<sub>2</sub> migration, and an overlying Ultimate Seal. The lateral extent of the container will be defined as the furthest modelled extent of an emplaced plume plus a margin. This is expected to be a distance of around 10 km radius from a notional injection well site.

The basic geological requirements for commercial-scale geological carbon storage have been documented previously (Bachu et al. 2007; NETL 2008; Michael et al. 2010; Neele et al. 2011). UQ-SDAAP has built further on these:

1. Depth, where the *in-situ* pressure and temperature conditions result in supercritical CO<sub>2</sub> (normally deeper than -800-1000 m below ground surface), noting that increasing depth increases the CO<sub>2</sub> density and thus also results in decreasing buoyancy forces on emplaced CO<sub>2</sub>
2. Injectivity, where the storage reservoir has sufficient permeability and thickness to accept the injected CO<sub>2</sub> at an economic rate for an economic duration and preferably with minimum surface footprint (not too many injection wells) without exceeding critical pressure constraints where pressures in the formation are to be managed lower than (i) the temperature adjusted fracture pressure of the sealing formations at the injection well site; (ii) fault reactivation or fault valving pressures for any naturally occurring faults in the Play; and (iii) the CO<sub>2</sub> capillary entry pressure at the seal
3. Storage capacity, where there is sufficient accessible pore space within the injection reservoir to accommodate the volume to be stored
4. Containment, where geological features limit the migration of injected CO<sub>2</sub> (laterally or vertically) beyond its intended location

The UQ-SDAAP project considers that a certain combination of injectivity and storage capacity, termed “dynamic storage capacity”, to be a critical concept in successfully evaluating economically viable carbon storage sites. This concept incorporates the time dependent injectivity of wells, where the rate of injection declines as the formation pressure increases. This can be dependent on the storage aquifer rock properties and the location of near and far field lateral barriers or changes in reservoir transmissivity.

For the UQ-SDAAP project, the Blocky Sandstone Reservoir is considered to be the injection reservoir; the transition zone to form a combination of seals; intra-formational baffles and possibly secondary storage reservoirs; and the Ultimate Seal to be the seal.

In order to conceptualise the complicated heterogeneous nature of geological systems, the proposed 3D volume of geological strata that meet the four geological criteria described above, are often referred to as the “geological storage complex”. For examples of this from other major carbon storage projects see Mathieson et al. 2011 (In Salah), Whittaker et al. 2011 (Weyburn), Liebscher et al. 2013 (Ketzin), and Chadwick et al. 2014 (Sleipner). The definition of a storage complex is based on the occurrence of the injected supercritical CO<sub>2</sub> phase over time in the sub-surface. The geological storage complex normally has elements of four main components, including:

1. An injection reservoir, where the strata have sufficient porosity and permeability to allow injection at the intended rate (injectivity), and sufficient reservoir volume (porosity x thickness x map area) to accommodate the intended CO<sub>2</sub> volume (capacity)
2. Intraformational baffles, which are relatively low permeability strata that impede but may not completely prevent upwards migration of buoyant CO<sub>2</sub> out of the injection reservoir
3. Possible secondary storage reservoirs, which are relatively high porosity and permeability units separated from the injection reservoir by intra-formational seals and baffles. Secondary storage reservoirs could receive migrated CO<sub>2</sub>, but this added storage capacity is anticipated to be minor compared to that of the injection reservoir; and
4. A seal, that forms the upper part of the storage complex and impedes CO<sub>2</sub> migration

For the UQ-SDAAP project, the Blocky Sandstone Reservoir is considered to be the injection reservoir; the Transition Zone to form a combination of seals; intra-formational Baffles and possibly secondary storage reservoirs; and the Ultimate Seal to be the seal.

The report by La Croix et al. 2019b provides a detailed description of the sequence stratigraphic correlation workflow and how it was applied to the UQ-SDAAP project. It provides the geological definition of the Blocky Sandstone Reservoir, the Transition Zone, and the Ultimate Seal.

In addition to the geological storage complex, within which the injected CO<sub>2</sub> will be contained, a CO<sub>2</sub> injection project must also consider the impacts of CO<sub>2</sub> injection and storage beyond the boundaries of the geological storage complex (i.e. beyond the CO<sub>2</sub> plume itself). The Canadian Standards on geological storage of carbon dioxide (CSA Z741, 2012) states that the project operator shall define the surface and subsurface physical boundaries of the storage project. Where:

“ The subsurface physical boundary includes the subsurface volume and its overlying surface area wherein CO<sub>2</sub> injection could impose important physical effects. Examples of important physical effects can include pore fluid displacement and impacts upon known subsurface resources or the exploitation thereof (e.g. impacts from fluid-pressure increase). The project operator shall estimate the nature and boundaries of subsurface effects and update and improve such estimates throughout the project’s life cycle as new data become available.

This sub-surface physical boundary is referred to as the “Area of Review” in the Canadian Standards on geological storage of carbon dioxide (CSA Z741 2012) and also often in the literature (e.g. Buscheck et al. 2012). For reference and comparison, the *Queensland Greenhouse Gas Storage Act 2009* can be found at: [www.legislation.qld.gov.au/view/html/inforce/2018-10-25/act-2009-003](http://www.legislation.qld.gov.au/view/html/inforce/2018-10-25/act-2009-003).

## 4.4.1 The injection reservoir

**Work done by UQ-SDAAP confirms the presence of an injection reservoir with long term, high-rate potential, wherein pressure build-up can likely be monitored and managed well within secure containment specifications. UQ-SDAAP's new work, shows that the Blocky Sandstone Reservoir is aurally limited to the south, west and east and importantly it is relatively flat lying such that injected CO<sub>2</sub> would not migrate more than a few kilometres beyond any injection sites. Site-specific dynamic data are still required.**

In the UQ-SDAAP the injection reservoir is the Blocky Sandstone Reservoir (La Croix et al. 2019a, b), located between the sequence stratigraphic horizons J10 and TS1 (Figure 20). The Early Jurassic land surface on which the Blocky Sandstone Reservoir was deposited, consisted of elevated basement blocks in the southwest (Auburn Arch), northeast (Yarraman Block), and southeast (Texas High; Green et al. 1997). These exposed basement blocks provided the main sedimentary input into the Surat Basin. The Auburn Arch shed sediment from siliceous sedimentary rocks, metasediments, schists, gneisses, and granites. The Auburn Arch and Yarraman Block, provided a sediment source consisting largely of granite and gneiss. Finally, the New England Fold Belt was a source of indurated fine-grained sediment that was cannibalised and deposited in the adjacent Surat Basin (Green et al. 1997). The base-Surat Unconformity (J10) is mapped as a structure surface and shown in Figure 39 showing the shape of the basin. At this time, the Blocky Sandstone Reservoir dominantly occurred along the basin axis and was structurally restricted from east to west. The unit was dominated by sediments deposited within a braid plain system (+/- braided delta influence; Figure 28). However, the south-western part of the basin lacked thick sandstone deposits due to the high structural elevation of the land surface on the Wunger Ridge and Roma Shelf (UQ-SDAAP in agreement with Exon 1976).

Based on sequence stratigraphic mapping, the extent of the Blocky Sandstone Reservoir is limited towards the west onto the Wunger Ridge and Roma Shelf. In the south the unit is narrower from east to west and shallower with respect to ground level, eventually pinching out against Permo-Triassic sediments approximately 20 km south of the Queensland and New South Wales border. Deposition on the eastern side of the basin was controlled by uplift associated with the Permian to Late Triassic Hunter-Bowen Orogeny, which exhumed the New England fold belt (Rosenbaun et al. 2018) leaving a narrow passage connecting the central portion of the Surat Basin with the Clarence-Moreton Basin to the east. This is clearly shown in the isopach distribution of the Blocky Sandstone Reservoir (Figure 41). The paleogeography and depositional extent towards the north is still under debate as the units' shallow towards ground level and a substantial thickness of section is missing due to erosion.

The injection reservoir has relatively high permeability (Harfoush et al. 2019a, 2019b, 2019c and Honari et al. 2019a):

- Core plug measurements of horizontal maximum corrected water permeability ranging from 14 to 2500 mD (arithmetic average of 540 mD)
- DST interpreted permeability ranging from 11 to 2800 mD (arithmetic average of 390 mD)
- Petrophysical log derived corrected water permeability ranging from 4.7 to 3900 mD (arithmetic average of 890 mD)
- Groundwater model inversion of the MAR area permeability ranging from 470 to 190,000 mD (arithmetic average of 37,000 mD). From a reservoir engineering perspective these permeability values are extremely high and may be related to fracturing of the Precipice Sandstone (see Section 4.6.3.3).

**It is important to note that regional stratigraphic reviews conclude that there may be a different provenance or provenance-mix for the northern depositional centre (MAR sector) and southern depositional centre (notional injection sector) parts of the play as well as a different burial histories. Each of these depositional centres should be considered a different play segment (or even play) and while the depositional architecture is probably informative of heterogeneity in the South, the absolute values and ranges of permeability are not.**

## 4.4.2 The Transition Zone

The Transition Zone occurs between the sequence stratigraphic horizons TS1 and TS3 (Figure 20) and its deposition spans three cycles (La Croix et al. 2019b):

1. Between TS1 and MFS1 base level rise occurred rapidly, and facies zonation became increasingly prominent (Figure 29). The TST of SQ1 was composed of meandering river, delta plain, delta front, and prodelta sediments. Basinal facies were limited to a narrow belt near the basin-centre. Many large-scale deltas built out towards the central basin (e.g. near the West Wandoan 1 and Trelinga 1 wells) from the northwest margin extending into the basin for a distance of at least 53 km (Figure 29). Younger deposits cut through older strata with complex cross-cutting relationships derived from allogenic shifts in environments. However, on the eastern margin of the basin, delta lobes did not extend very far from their provenance areas (i.e. from the Auburn Arch and Yarraman Block). This appears to have been partially controlled by the presence of large faults such as the Moonie and Goondiwindi fault systems. From the south, delta systems had much greater axial extents than on the east and west sides of the basin. Minor shoreface and tidal environments were distributed between deltaic systems, on the parts of the shoreline distal to fluvial sediment input
2. During the HST of SQ1 (TS1-SB2), major sedimentary environments consisted of delta front and prodelta settings, with subordinate delta plains (Figure 30). Only the north-western and south-eastern part of basin contained isolated delta systems, whereas in the rest of the basin these were connected by long coastlines fed by many rivers. This was coupled with enhanced marine influence and an overall increase in water depths. The West Wandoan 1, Woleebee Creek GW4, and Trelinga 1 wells are interpreted to be located near the locus of deposition – representing the “basin centre”
3. The sedimentary facies from SB2 to TS3 mainly consist of meandering river and delta plain deposits with associated delta front and prodelta sediments (Figure 31). Large deltaic systems from the northwest and southeast prograde back towards the central basin. Sediment input with a southeast provenance is interpreted to have increased greatly. However, delta systems with east provenance were less important and their corresponding delta plains were much smaller in aerial extent

The Transition Zone isopach map (Figure 69) shows that above the Blocky Sandstone Reservoir the Transition Zone is more than ~40 m thick and generally over 100 m thick. The thinnest regions are south near the NSW border where the unit thins dramatically and west of the Block Sandstone Reservoir depositional edge.

It's important to note, that the likely thinning of the Transition Zone puts a southerly limit when seeking “lowest containment risk” site options and focusses the search to the north in the current basin-centre.

The Transition Zone is both laterally and vertically heterogeneous indicating low chance of finding strata with high permeability which are connected over large distances or conversely low permeability strata connected over large distances. Data shows relatively low bulk permeability (Harfoush et al. 2019a, 2019b, 2019c and Honari et al. 2019a) with:

- Core plug measurements of horizontal maximum corrected water permeability ranging from 0.01 to 820 mD (arithmetic average of 130 mD)
- DST interpreted permeability ranging from 0.01 to 270 mD (arithmetic average of 41 mD)
- Petrophysical log derived corrected water permeability ranging from 0.002 to 680 mD (arithmetic average of 46 mD)

It should be noted that the flow behaviour of such highly heterogeneous formations cannot be represented in dynamic simulation by arithmetic mean values of core permeabilities (not only, but not least because these result from biased sampling by oil and gas operator's intent on investigating sandstones).

**The sequence stratigraphic analysis of the Transition Zone suggests that the finer grained, lowest permeability ‘maximum flooding surfaces’ are regionally extensive and correlatable, whereas the intermediate sandstones are localised (and also likely not connected – see, section 4.5). The lower permeability layers are likely more laterally continuous than the sandstone layers.**

### 4.4.3 The Ultimate Seal

**UQ-SDAAP (and other) research supports the existence of a wide-spread, relatively consistent, very low permeability sealing formation. It is proven to have contained gas and oil over millions of years and also to create a regional barrier separating different hydrochemical (aquifer quality) and water pressure gradients. In the northern part of the study area, it is also shown (as combined with the Transition Zone) not to transmit injection over-pressures caused by MAR operations (section 4.3.9) over the period of observation thus far.**

The Ultimate Seal is defined as the stratigraphic interval sandwiched between the sequence stratigraphic surfaces TS3 and J30 (Figure 20). This corresponds to the base of the Westgrove Ironstone Member to the top of the Evergreen Formation (La Croix et al. 2019b). Between TS3 and J30, the entire basin was heavily influenced by marine processes, and marine water flooded the central and north-eastern parts of basin (Figure 32). Sediment input was mainly derived from a western and south-eastern provenance. Through time though, the eastern sediment source became flooded and the basin developed abundant oolitic shoals. Shorefaces mainly developed in the northeast, facing the open sea, whereas the tidal environments were mainly restricted to a narrow strip in the south, sheltered from the largest wave-fetch.

The distribution of the Ultimate Seal isopach (Figure 70) shows that above the Blocky Sandstone Reservoir the Ultimate Seal is generally more than 40 m thick (with a few exceptions) and some areas as much as 100 m thick. It tends to thin towards the southern edge of the study area near the NSW border.

The Ultimate Seal has extremely low permeability (Harfoush et al. 2019a, 2019b, 2019c and Honari et al. 2019a) with core plug measurements of horizontal maximum corrected water permeability ranging from 0.003 to 0.086 mD (arithmetic average of 0.037 mD), and petrophysical log derived corrected water permeability is unreliable for this low permeability formation. There is no interpretable DST data from which to derive permeability in the Ultimate Seal. New, site specific data is required. Ideally this would be core permeability tests and vertical interference tests (section 5.3).

**Figure 69** The isopach distribution (m) for the Transition Zone (TS1-TS3) where the blue dots are wells that penetrate the base of the Transition Zone and the blue outline represents the edge of the underlying Blocky Sandstone Reservoir.

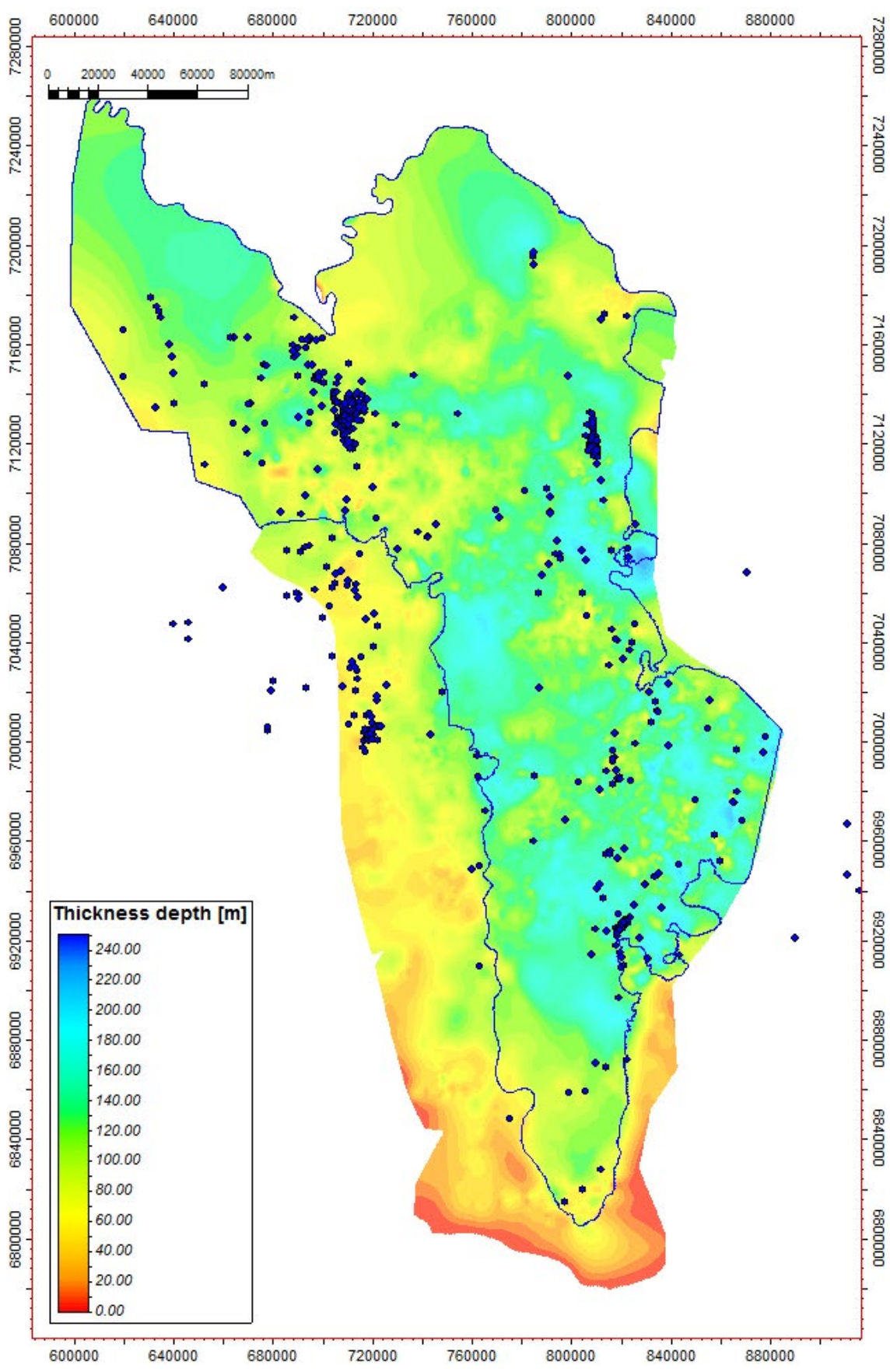
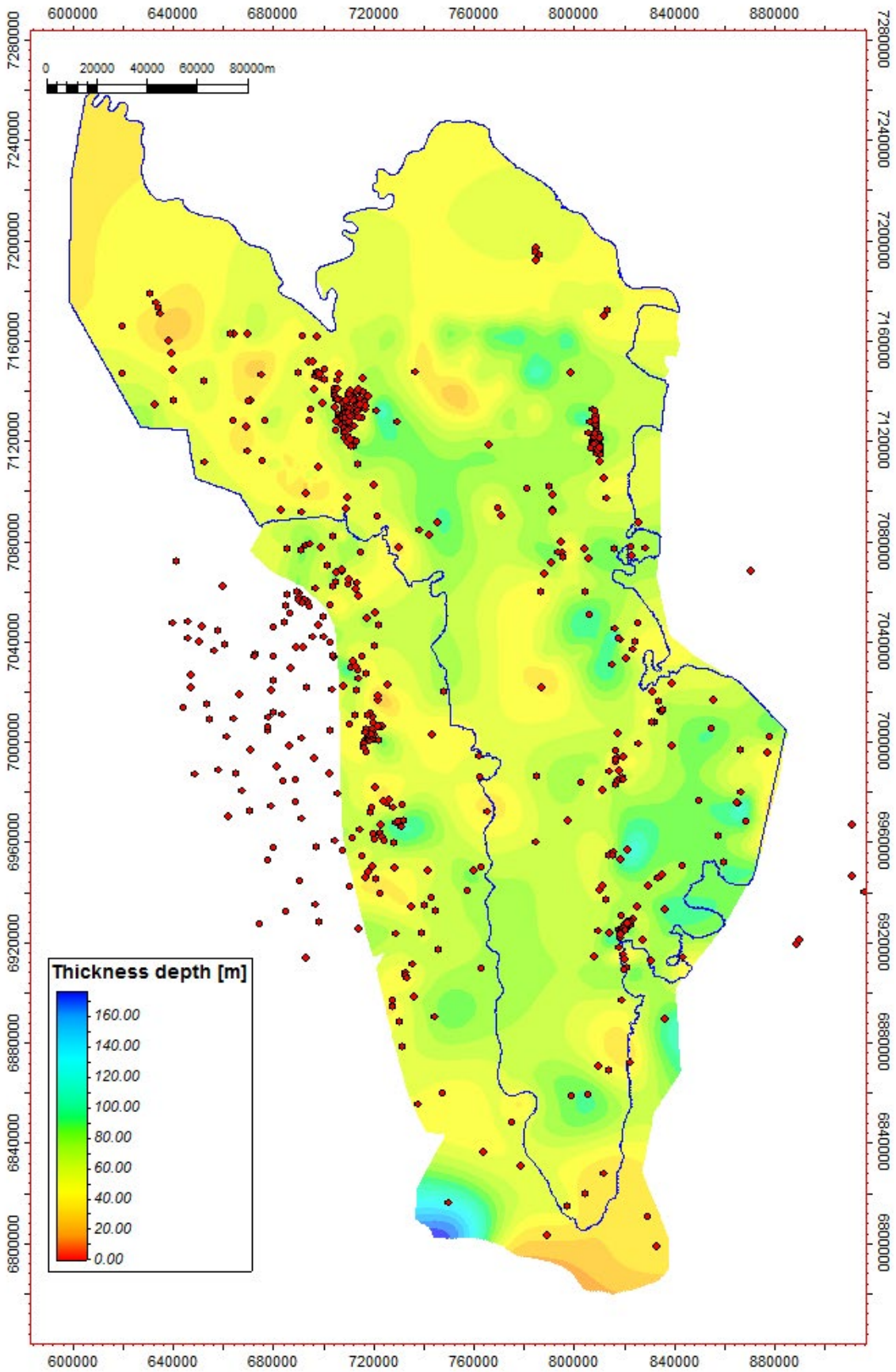


**Figure 70** The isopach distribution (m) for the Ultimate Seal (J30-TS3) where the red dots are wells that penetrate the base of the Ultimate Seal and the blue outline represents the edge of the underlying Blocky Sandstone Reservoir.





#### 4.4.4 The structure

Faults can provide lateral barriers to the migration of formation fluids (or propagation of fluid pressure) or fluid conduits either vertically between aquifers or to the ground surface. Some faults can be a barrier and conduit simultaneously at different locations along the fault plane (Mallants et al. 2018). As a result, faults form a key geological risk to carbon storage projects and require meticulous assessment to understand thoroughly. While the Moonie fault complex likely does not provide a lateral barrier to flow or pressure, seismic evidence of reactivation in the Cretaceous or younger, indicates the need to better map and avoid, where possible, faults in the basin centre to reduce the albeit small risk of vertical communication.

The UQ-SDAAP project focussed on the Precipice Sandstone to Evergreen Formation stratigraphy, which formed the first sediments deposited in the Surat Basin. Therefore, the project was interested in both the major faults that occur in the immediately underlying Bowen Basin strata that influence Surat Basin deposition, but also the major faults within the Surat Basin strata itself. Figure 45 displays the main tectonic features of the Bowen and Surat basins, including the major faults obtained from previous regional interpretations in various public domain literature (e.g. Korsch et al. 2009 and Reza et al. 2009). In addition to the major faults there is some evidence that minor late stage structures, perhaps with significant strike-slip displacement, occur in the central parts of the basin. The structural geology is described in detail in section 4.3.7 of this report as well as by Gonzalez et al. 2019a. Supporting the structural geology work, the various UQ-SDAAP workflows that included core examination often recorded fractures. These are often notably identified in close proximity to major faults (see section 4.5.5 and Pearce et al. 2019a). Finally, the groundwater inversion of the MAR area identified extremely high bulk permeability for the blocky sandstone reservoir that was in excess of that identified for the same rocks from the petrophysics analysis. This suggests that there may be a dual permeability system in that area, one associated with the matrix permeability identifiable in the petrophysical analysis and the other associated with a fracture network. In turn, that fracture network may have a spatial association with faults.

## 4.5 Evidence for containment potential

In line with the approaches taken throughout this project, confidence levels in CO<sub>2</sub> containment have been increased through the interpretation and integration of several data-sets and data-types. All data interpreted so far are supportive of long-term secure storage of rates of CO<sub>2</sub> of the order of around 13 Mtpa for at least 20-30 years and probably longer. Evidence also supports how the flow properties of the Transition Zone, as a series of barriers and baffles has been modelled and that the Ultimate Seal is likely to be regionally viable except where intersected by large faults. In order to *assure* containment, dynamic capacity has to be constrained and may only be used within clear pressure limits. While there is opportunity for resource optimisation (not included in this study) that can either increase the maximum rate or duration of injection, the container can only be used once.

As defined in the earlier discussion of the container concept (section 4.4), a key aspect of carbon storage site evaluation is to assess the potential for loss of containment and migration of CO<sub>2</sub> out of the storage complex. Loss of containment could be through one of four mechanisms:

1. Leakage through unidentified permeable zones within the seal
2. Leakage through faults as a result of insufficient capillary sealing capacity or mechanical fault reactivation caused by the increase in pore pressure as CO<sub>2</sub> is injected
3. Leakage from well bores, especially legacy well bores, where there may be failure of well bore integrity (i.e. due to cement, casing, or bonding with the formation from poor well construction or reactive geochemical changes due to prolonged exposure of the casing and cement to CO<sub>2</sub>)
4. Leakage via lateral migration out of the geographically defined storage complex boundaries

There are various lines of evidence that can identify regions of the area of review as either having high or low risk of lateral and vertical containment of injected CO<sub>2</sub>. The lines of evidence include:

- Hydrocarbon systems analysis: the Bowen and Surat basins have produced large volumes of hydrocarbons over geological time that has been expelled from source rocks and migrated through the strata as well as (possibly) faults and fractures. Some of the migrating hydrocarbons were trapped in known accumulations such as the Moonie oil field or several commercial accumulations on the Roma Shelf, while much of the remainder migrated to the surface and escaped over geological time. Hydrocarbon migration indicators and the location of trapped hydrocarbon can shed light on the leak points and migration pathways. In certain circumstances, virgin hydrocarbon column heights can be used to indicate minimum seal retention pressures. This can inform the assessment of seal potential for carbon storage applications
- Regional hydrogeology: comparing the difference in hydraulic head between aquifers with intervening aquitards (seals) can identify regions where strata have either high or low hydraulic resistance. This can be related to the seal capacity for carbon storage. Similarly, the gradient in hydraulic head across faults is indicative of fault seal capacity. The formation water chemistry distribution can be used as supporting evidence of hydraulic continuity of discontinuity
- Fault zone architecture and *in-situ* stress can be linked to assess fault seal capacity and vertical leakage risk. The geotechnical analysis of fault zones can identify fault orientations more or less at risk of reactivation given an anticipated increase in formation pressure with CO<sub>2</sub> injection
- The location, age, design and abandonment method of legacy wells can be assessed in relation to their location relative to the notional injection site for their leakage risk

## 4.5.1 Hydrocarbon systems analysis

**There are existing accumulations of oil and gas in the basin i.e. areas where very long term containment of fluids and pressures is proven. Analysis of the hydrocarbon habitat of these accumulations and understanding of hydrocarbon migration is essential to assessing containment risk. Evidence discussed hereunder is supportive of the play and container concept.**

The University of Queensland Centre for Coal Seam Gas conducted a Bowen/Surat Hydrocarbon Systems Analysis study (Underschultz et al. 2015) that also resulted in a publication (Underschultz et al. 2016). This work provided a review of previous work and included new analysis of hydrocarbon migration indicators from mud logs, core, well tests, and cuttings. This work was later updated and reported by Schintee et al. 2018 with additional mud log data.

Constructing a burial and uplift history of the Bowen and Surat basins, together with some assumptions about the geothermal gradient and paleo heat flow, provides information about the time period over which various organic-rich source rocks passed through the oil and gas generation windows. A representative burial history curve for the Bowen and Surat basins is shown in Figure 71. In the case of the Bowen Basin there are six major source rock horizons: the Triassic Moolayember Formation, the Permian Baralaba Coal Measures, the Burunga Formation, the Banana Formation, the Flat Top to Buffel formations and the Reids Dome Beds (Boreham et al. 1996, and Carmichael and Boreham 1997). In the Surat Basin the Jurassic Evergreen Formation and Walloon Coal Measures are the main source rock intervals. Bowen Basin formation occurred in three stages (Fielding et al. 2001):

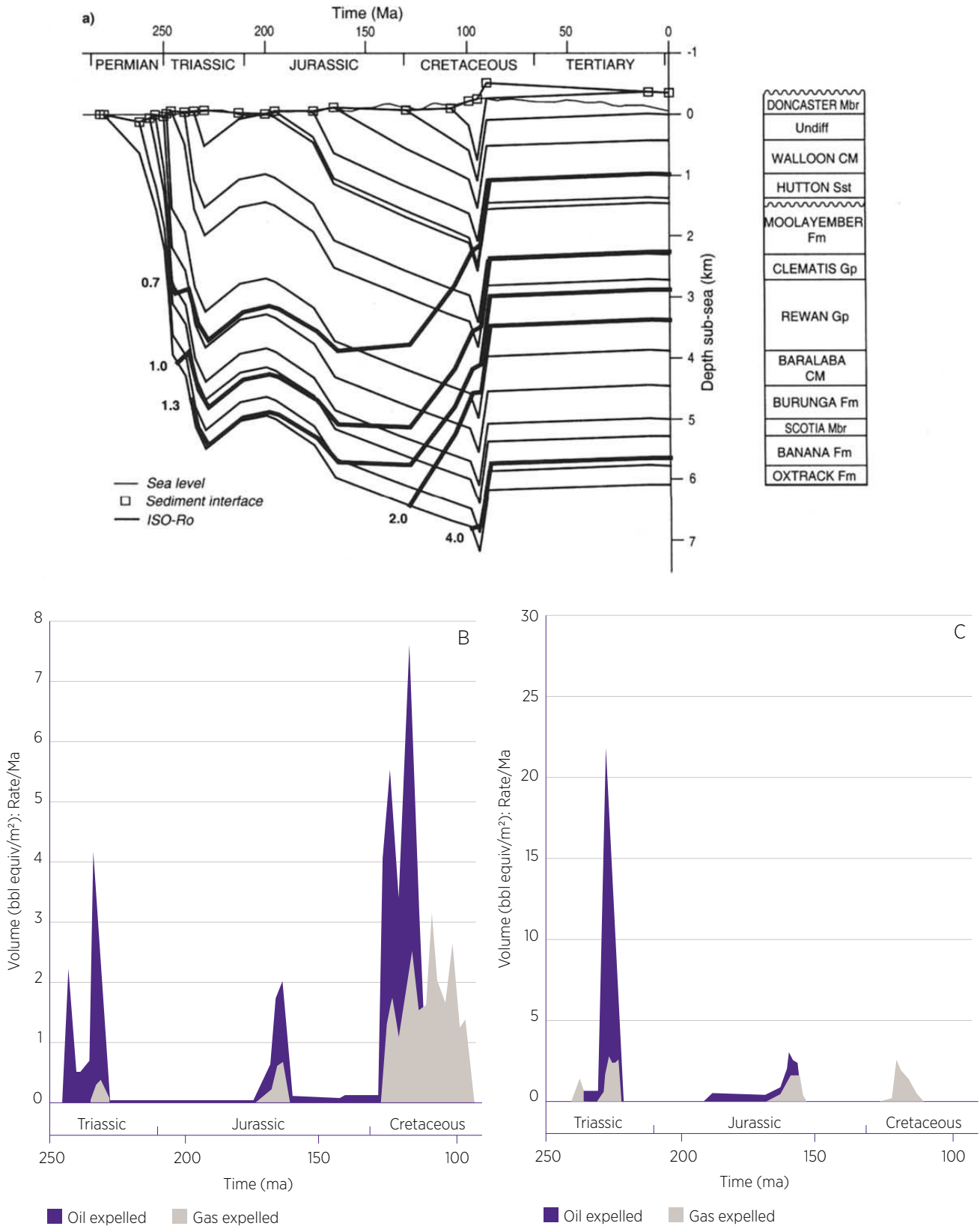
1. An early permian period of extensional subsidence with associated volcanic activity
2. An early late permian passive thermal subsidence phase
3. A late permian to middle triassic phase of foreland thrust load-induced subsidence

The Bowen Basin subsidence culminated at about 230 Ma and was most significant in the northern end of the Taroom Trough decreasing to the south (Underschultz et al. 2016). Preserved permian source rocks only in the northern and central parts of the Taroom Trough reached a high enough temperature and pressure to generate oil, with perhaps the start of gas generation at peak burial in this subsidence event. The subsequent Surat subsidence culminated at about 100 Ma and was relatively greater in the southern and eastern regions of the Mimosa Syncline (very roughly coincident with the underlying Taroom Trough). Here a much broader area of preserved source rock (both Permian and Jurassic) generated hydrocarbon with mainly gas in the northern and central Taroom trough from Permian sources and mainly oil in other areas. Jurassic source rocks only barely reached the start of oil generation in some locations (Underschultz et al. 2016).

In addition to the commonly considered thermogenic source of hydrocarbons, there are also organic rich sedimentary rocks that form sources of gas due to biogenic processes. This is commonly thought to occur in the shallower parts of the sedimentary basin at temperatures less than about 70°C where bacteria are viable. Thermal maturation indicators (vitrinite reflectance) suggest the Walloon Coal Measures probably never reached thermogenic gas generation (Golding et al. 2013; Hamilton et al. 2014). This would suggest that any thermogenic hydrocarbon observed in strata younger than the Evergreen Formation more than likely migrated there from a source rock somewhere deeper in the basin.

Regional mapping of total organic content (TOC) and hydrogen index (HI) values for each of the identified source rocks, combined with the burial and thermal history model, can be used to estimate oil and gas yields for each source rock (Boreham 1994 and 1995). This work suggested that >90% of the oil and ~65% of the gas that migrated within the Bowen and Surat basins was generated from the Permian Baralaba Coal Measures and Burunga Formation (Shaw et al. 2000). The Buffel-Bandana source rocks contribute another 30% of the gas in the Bowen and Surat basins. Modelled hydrocarbon volumes generated are >20,000,000 PJ (>3400 billion barrels of oil) and >16,000,000 (>2700 billion oil equivalent barrels) of gas but with uncertainty on the order of 50% (Shaw et al 2000). Estimates of oil resources in the Bowen and Surat basins (produced and remaining) are about 352 PJ (>57 million barrels of oil) and 34,415 PJ gas (conventional and CSG) or >5.6 billion barrels of oil equivalent (Bureau of Resources and Energy Economics (BREE) 2014). Even considering the large uncertainty in the volumes generated, there is still a three-orders of magnitude difference between generated hydrocarbons and those trapped. The difference can be considered in four categories: 1) a large percentage of the generated hydrocarbon remains in the source rock; 2) there are remaining undiscovered hydrocarbons trapped within the basins; 3) the Great Artesian Basin aquifers contain large volumes of dissolved hydrocarbon in situ; and 4) large volumes of hydrocarbons have been lost to surface over geological time via formation water migration and/or separate gas phase migration (Shaw et al. 2000).

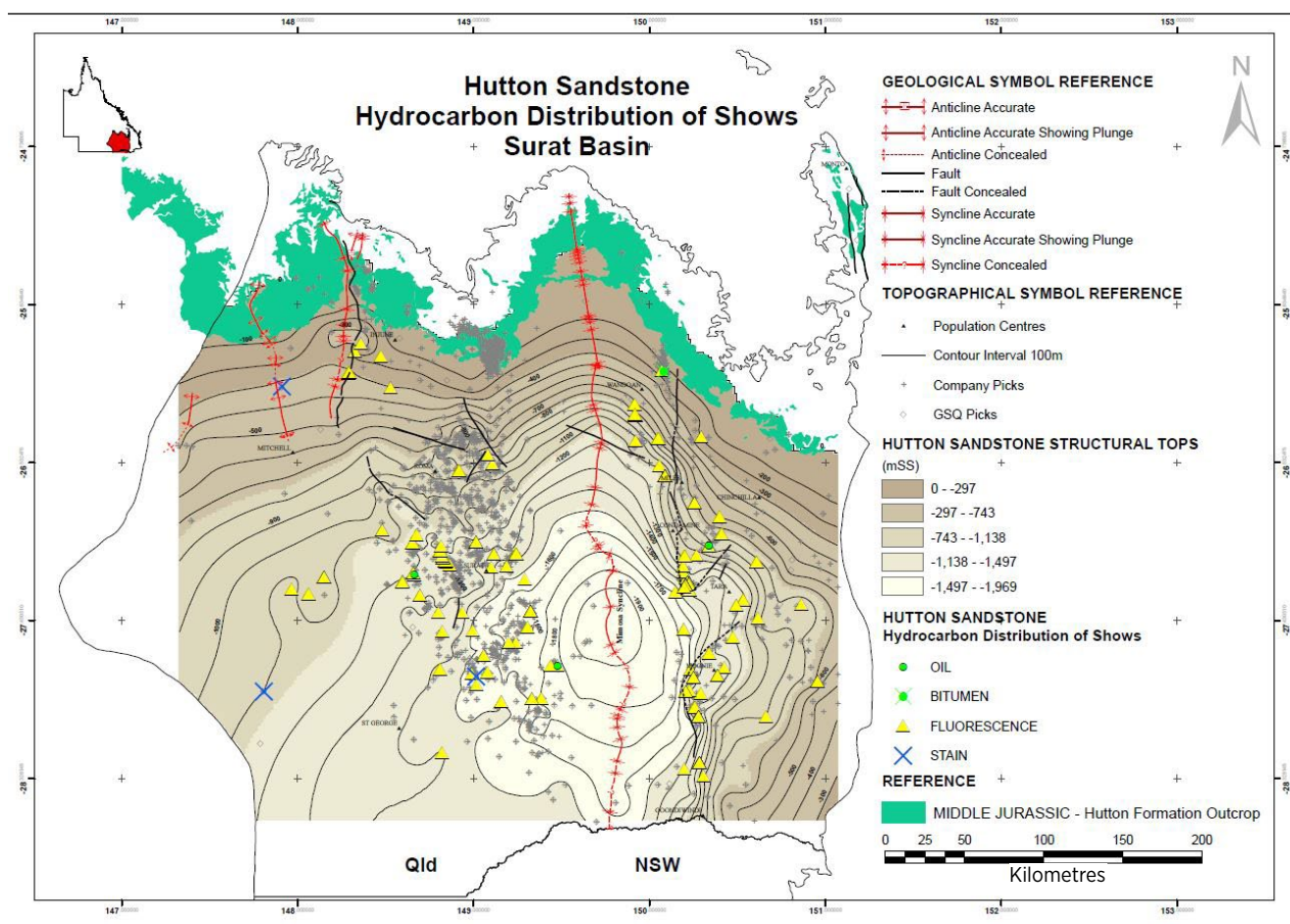
**Figure 71** Burial history plot representative of the Bowen/Surat Basin. Timing and quantity of oil and gas generation for the 82-50 well using the geohistory model in part (A), and a 5% coal content within the Burunga Formation and the (B) measured compositional kinetics for oil and gas generation from German Creek coal #5334 and oil cracking kinetics of (Horsfield et al. 1991). (C) WinBury TM data in (Waples 1992) composite default kinetics for primary oil and gas generation, and secondary oil cracking (Boreham 1999).



Evidence of the fate of missing hydrocarbons can be found in hydrocarbon indicators. These include staining, fluorescence, and shows in core and cuttings, hydrocarbon samples from drill stem test and wireline testing, and gas detected in the mud returns during drilling. The stratigraphic and geographic distribution of hydrocarbon indicators can be compared with the location of discovered conventional and unconventional reserves. While the full details of this analysis can be found in reports generated by the UQ Centre for Coal Seam Gas (Underschultz et al. 2015, 2016), it is particularly instructive for considering containment of CO<sub>2</sub> storage in the Blocky Sandstone Reservoir to examine the distribution of hydrocarbon migration indicators in the Hutton Sandstone. This is because any thermogenic hydrocarbons located in the Hutton Sandstone can be surmised to have most likely originated (been generated) from the Bowen Basin. Finding them in the Hutton Sandstone would suggest that they managed to migrate across the intervening Evergreen Formation that makes up the UQ-SDAAP Transition Zone and Ultimate Seal. Whilst this could have taken geological time periods of up to or greater than 100 million years, it still is an indication of where the seals in the basin may be compromised and warrant closer scrutiny.

Figure 72 presents the distribution of oil indicators in the Hutton Sandstone. Gas is not shown because there was not sufficient detail to determine if the gas is thermogenic or biogenic (biogenic gas can be generated at shallow depths and thus is not necessarily indicative of a migration path across the Evergreen Formation). Oil indicator data includes fluorescence of core or cuttings, oil staining on core or cuttings, observation of bitumen in core and cuttings or oil samples from well testing. Here there is a broad distribution of wells that penetrate the Hutton Sandstone (grey crosses), but a relatively restricted distribution of oil indicators on the east side of the Mimosa Syncline associated with the main fault trends. On the western side of the Mimosa Syncline there remains a less focused wide distribution of oil indicator data. The distribution would suggest that over geological time oil has migrated up the Moonie-Goondiwindi fault systems at certain locations. This is consistent with the accumulation of oil in the Moonie oil field in the underlying Precipice Sandstone that must have originated from Permian source rocks deeper in the underlying Bowen Basin.

**Figure 72** The Hutton Sandstone (above the Evergreen Formation) structure top with the distribution of oil indicators. The total picks dataset is displayed by the grey crosses.



Many of the oil shows on the western side of the Mimosa Syncline occur west of the Blocky Sandstone Reservoir pinch-out edge over the Roma Shelf. This is also the location of a number of commercial oil and gas fields occur in the strata on either side of the sub-Surat Unconformity surface. The UQ Masters of Petroleum Engineering program has been running a series of student post mortem field analysis on the various fields in this area and these often show insightful analysis on the vertical hydraulic connectivity between reservoir sands in this region that have implications for understanding the general hydraulic connectivity (or lack of) between the Blocky Sandstone Reservoir and the Hutton Formation. The UQ-SDAAP project can use these field studies to assess the performance of the Transition Zone and to what degree it acts as a barrier to flow. This information can then be used to assess the likely seal performance of the Transition Zone and Ultimate seal for future notional CO<sub>2</sub> storage. The next section looks at individual commercial hydrocarbon accumulations and evidence for Transition Zone and Ultimate Seal performance at various locations around the Surat Basin.

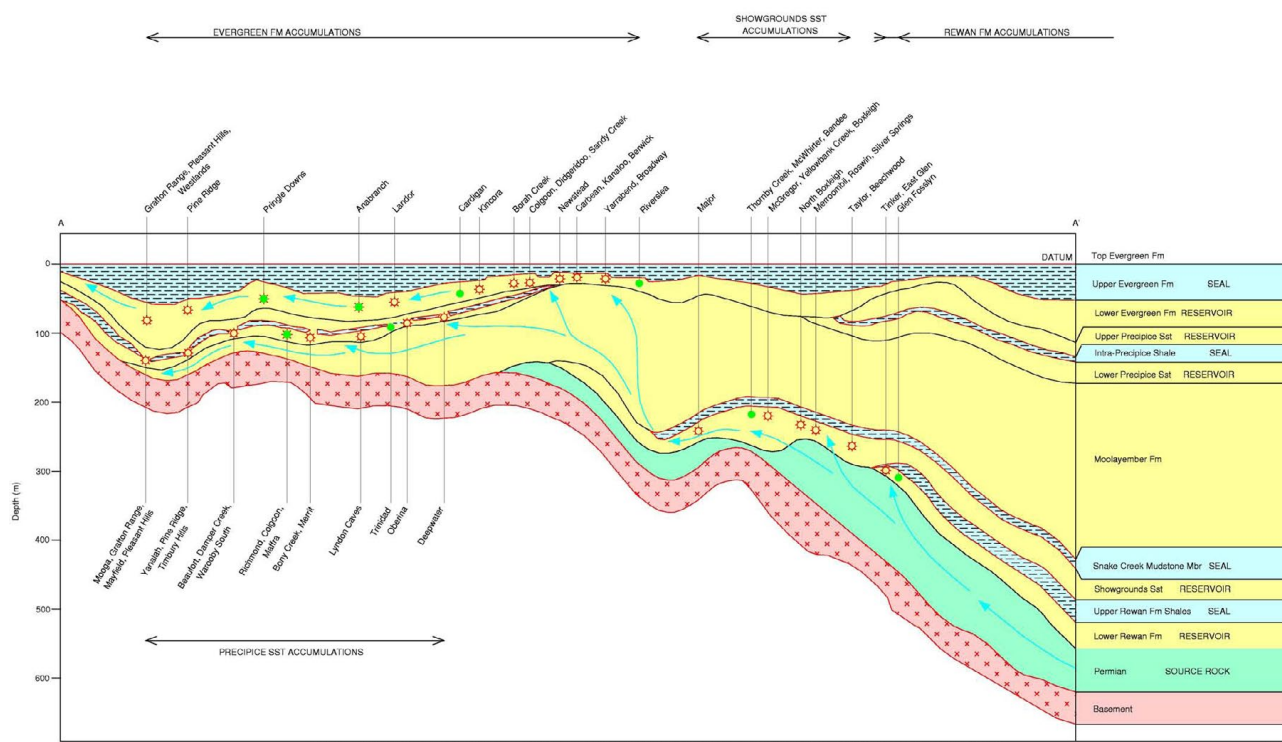
#### 4.5.1.1 Moonie oil field

On the eastern side of the Mimosa Syncline there are a number of hydrocarbon accumulations beneath the Evergreen Formation (Transition Zone) with the Moonie oil field being the most significant. These are mainly associated with the Moonie-Goondiwindi Fault System that is postulated to have provided the migration pathway from deeper Permian source rocks. The Moonie field has two oil bearing formations, the Evergreen Formation “56 Sand” that is equivalent to a sandstone within the UQ-SDAAP Transition Zone, has limited production history. The Precipice Sandstone “58 Sand” that is roughly equivalent to the UQ-SDAAP Blocky Sandstone Reservoir is the main producing reservoir. The hydrocarbon saturation in the 56 Sand (Transition Zone) is patchy, representing only a small portion of the total production and can be thought of as a “thief zone” with the main reservoir being the 58 Sand (Blocky Sandstone Reservoir). The field size is determined by the 4-way structural closure of folding associated with faulting on the local segment of the Moonie-Goondiwindi Fault System. Three core samples were analysed using mercury injection capillary pressure (MICP) analysis (conducted by Bridgeport Energy), which indicated air/mercury threshold pressures of 15,396 kPa, 42,147 kPa and 48,332 kPa, equivalent to seal capacities of 319 m, 953 m and 1100 m of oil. The column height at Moonie is far less than theoretically possible based on this top seal, capillary seal capacity and it’s thought to have its free water level controlled by either a structural spill point or a fault seal spill point. Other minor accumulations in similar geological and structural settings include the Alton and Bennett trends. The location of these thermogenic hydrocarbons in the Blocky Sandstone Reservoir with minor patchy saturation within the overlying Transition Zone suggest that the Transitions Zone provides effective seal capacity for trapped hydrocarbons, generally consistent with the interpretation of the paleogeography (La Croix et al. 2019c) and facies interpretation (La Croix et al. 2019a) presented in the UQ-SDAAP study.

#### 4.5.1.2 Roma Shelf hydrocarbon field analysis

Several UQ Masters of Petroleum Engineering students conducted research projects involving a post mortem field analysis on historical field data on the Roma Shelf to the west of the Blocky Sand Reservoir pinch-out. To date there are research reports on Borah Creek Field (Agusta 2017), Colgoon, Digeridoo and Digger fields (Kelson 2017), Kincora Field (Jacome 2016), Sandy Creek Field (Wu 2015), Carbean Field (Liao 2015), Newstead (Kashoob 2018), Yarrabend (Subhi 2017), and Yellowbank Field (Tehseenullah 2015). In the area of the Roma Shelf, the strata that the sub-Surat Unconformity erodes into is the Moolayember Formation (or equivalent Wandoan Formation), in some locations, it has properties of a low permeability sandstone/siltstone or tight sandstone/siltstone. Overlying the sub-Surat Unconformity in this area, the strata are within the UQ-SDAAP defined Transition Zone. Historically, the equivalent basal Evergreen Formation sandstone (sometimes called the upper Precipice Sandstone, see La Croix et al. 2019a, 2019 b and 209c) and Boxvale Sandstone Member (sometimes called the Mid-Evergreen Sand) makes up recognised reservoir units that host gas, condensate and liquid components. Cadman 1998 proposed a hydrocarbon migration pathway form the deeper part of the Bowen Basin westwards and north-westwards up dip through the lower Rewan Formation and Showgrounds Sandstone carrier beds past the western edge of the overlying upper Rewan Formation shales and Snake Creek Mudstone member respectively. West of the top seals zero edge the hydrocarbons could migrate upwards to stratigraphically younger strata straddling the sub-Surat Unconformity where they could become trapped (see Figure 73). The same concept, but in plan view, is demonstrated by Cadman 1998 in Figure 74.

**Figure 73** Cross section of the western edge of the Bowen and Surat basins showing Possible Migration pathways of hydrocarbons generated from Permian Source Rocks (Cadman 1998).



This is a summary of the various post mortem field investigations in the view of understanding vertical and lateral hydraulic connectivity of the various reservoir sandstone units within the UQ-SDAAP defined Transition Zone. Kelson 2017, Augusta 2017, Jacome 2016, Wu 2015, Liao 2015 and Tehseenullah 2015 all report stacked hydrocarbon accumulations in the Wandoan Formation, Precipice Sandstone or Basal Evergreen Sand and Boxvale Sandstone Member or what is termed a “Mid Evergreen Sand”.

“ All of this historical stratigraphic nomenclature is equivalent to the UQ-SDAAP Transition Zone below the Ultimate Seal and not the Basal Sandstone Reservoir. The data confirms that there are effective intra-Transition Zone seals and there is some evidence that there is limited continuity to intra-Transition Zone sand.

(See La Croix et al. 2019a).

Data generally shows that the hydrocarbon pressure gradients on pressure elevation plots are separate for each of the stacked reservoir sands, however occasionally there is some evidence for more than one sandstone falling on a common gradient at certain well locations (see for example Figure 75 for the Sandy Creek 2 well where the Wandoan Formation and Precipice Sandstone can be interpreted to fall on a common gas gradient). Similarly, Augusta 2017 shows that what they term the Wandoan Formation and Basal Evergreen Sand can be interpreted to represent a single hydrocarbon column at the Borah Creek field (Figure 76). Here the Borah Creek 5 well is interpreted as being separate laterally from the rest of the Borah Creek field potentially due to production induced pressure decline.

The sandstones in the Transition Zone in the areas where hydrocarbon accumulations are found, are poorly or not interconnected. These areas are more sand-prone than the deep basin areas studied for potential injection (section 4.3).

For all of the post mortem field evaluations, hydrocarbon reservoirs in what they term as the mid Evergreen Formation or Boxvale Sandstone Member are interpreted to be separate from those in deeper reservoir units.

**Figure 74** The distribution of hydrocarbon migration pathways west of the depositional limit of the Rewan Formation and Snake Creek Mudstone Member, across the Wunger Ridge and onto the Roma Shelf to various trapping and accumulation field locations (Cadman 1998).

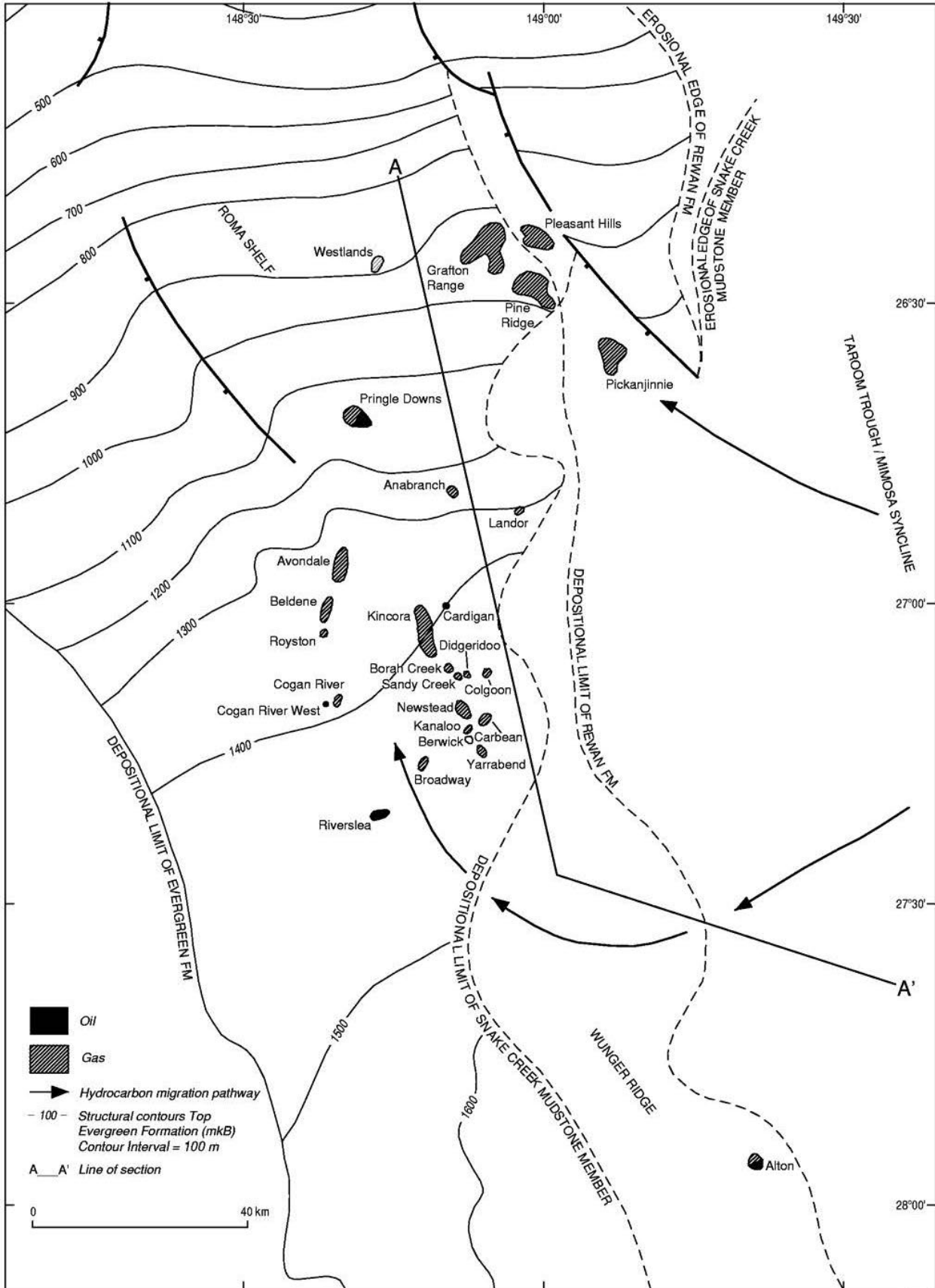




**Figure 75** Sandy Creek 2 well gamma ray petrophysical log with a matching pressure-elevation plot (Wu 2015). (Note that “Precipice SS” in this figure is in the UQ-SDAAP “Transition Zone”).

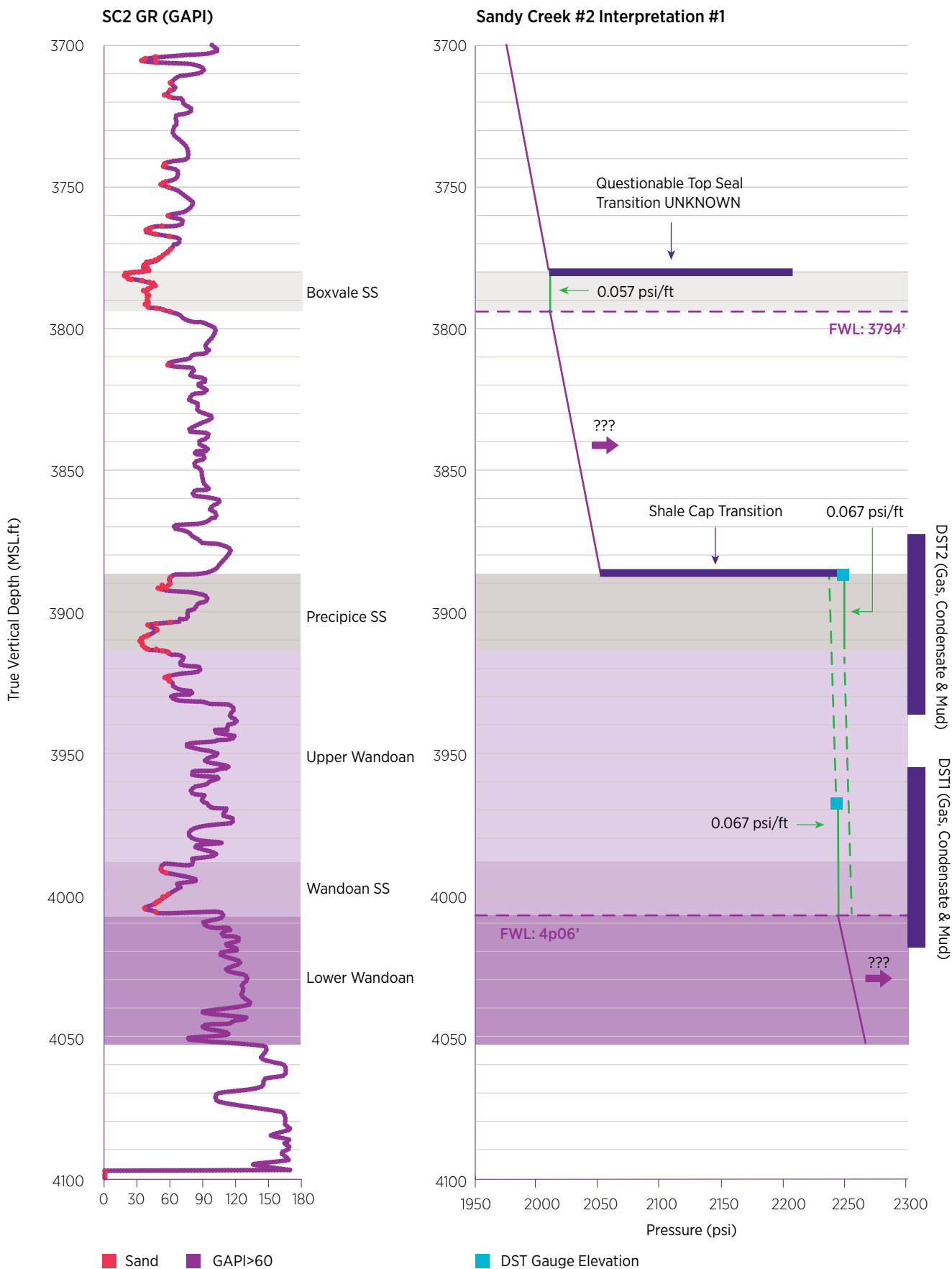
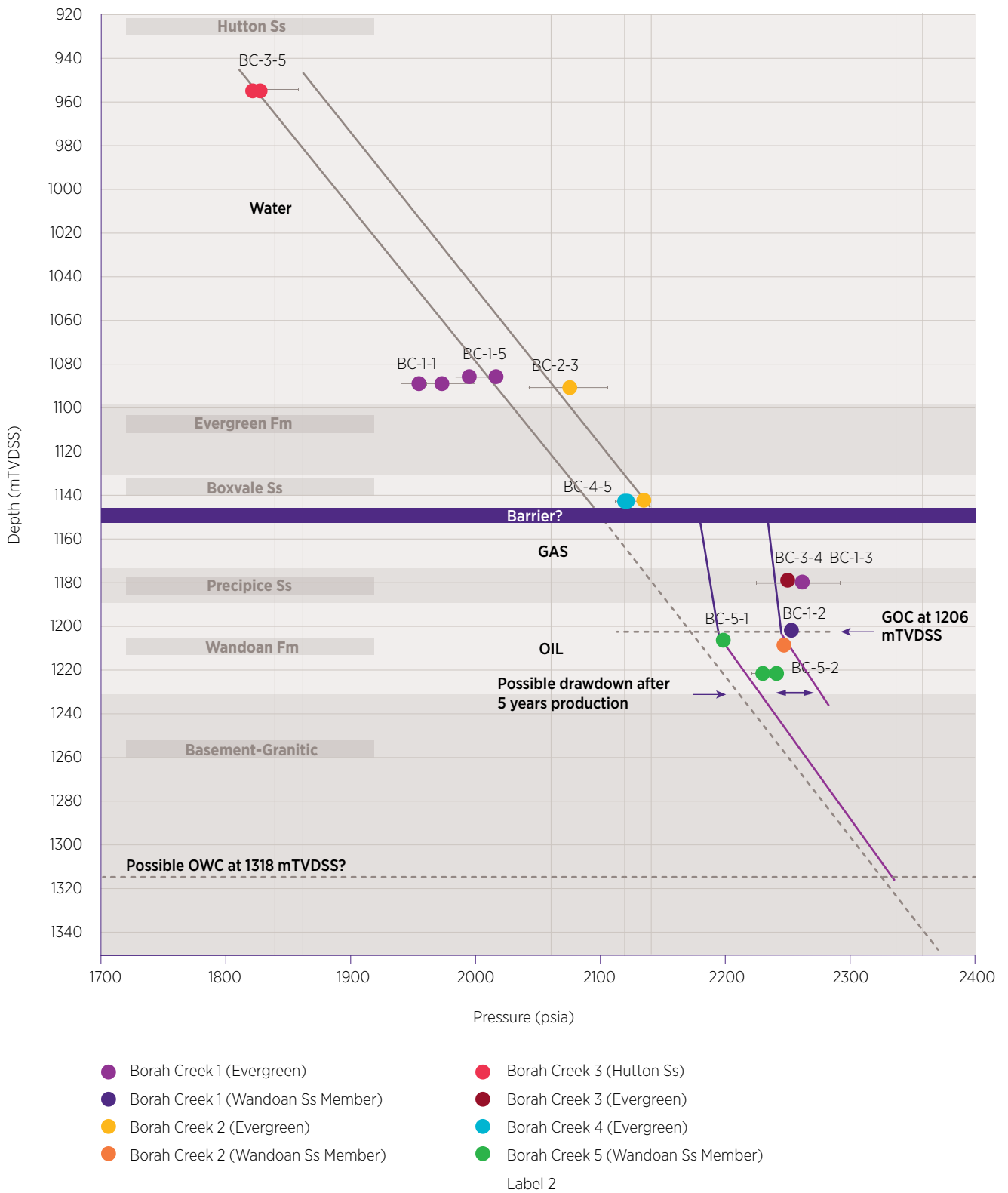


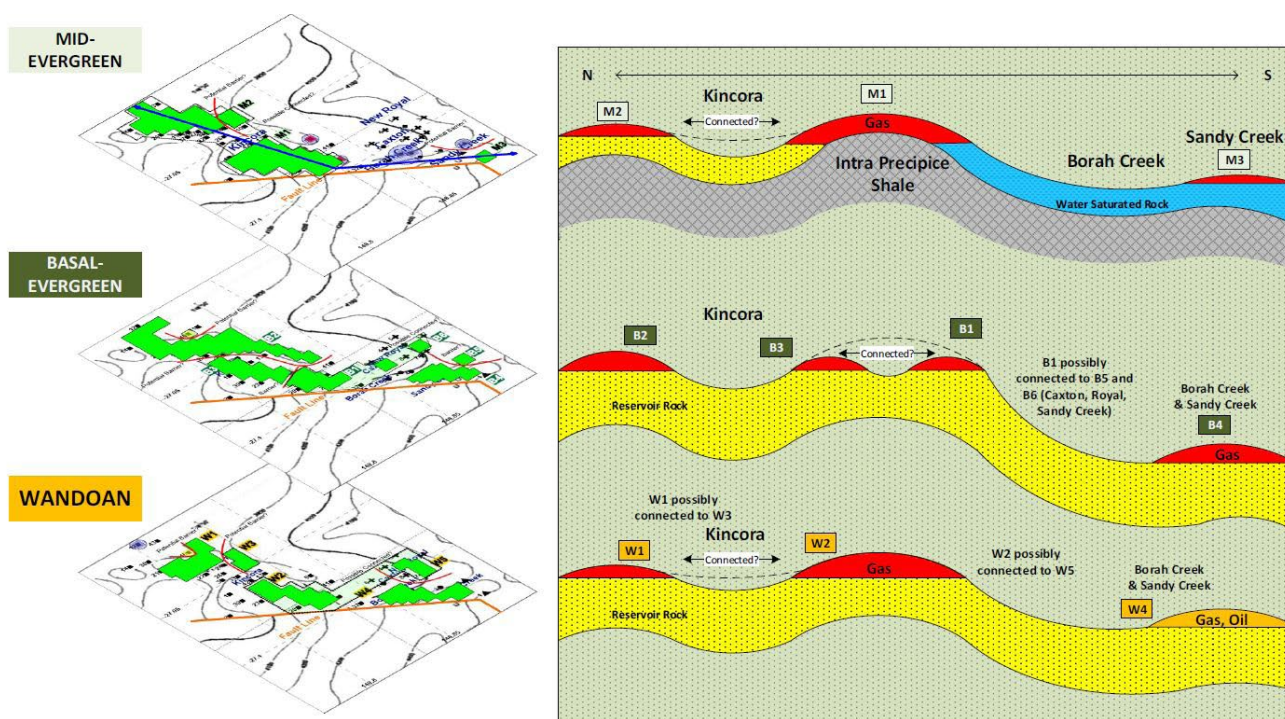
**Figure 76** A pressure elevation plot (Augusta 2017) for the wells from the Borah Creek Field (note that “Precipice SS” in this figure is in the UQ-SDAAP “Transition Zone”).



Augusta 2017 has also attempted to assess the likelihood of lateral connection of hydrocarbon phases between adjacent fields (Kincora, Borah Creek, and Sandy Creek). Figure 77 provides a schematic cross-section summarising the analysis. This shows the potential for Borah Creek and Sandy Creek to represent a laterally continuous hydrocarbon reservoir within what they term as the Wandoan Formation and also within the Basal Evergreen Sandstone reservoir. However, the Kincora Field is clearly laterally disconnected.

Recognising that the stratigraphic nomenclature of the post mortem field analysis (Augusta 2017, Jacome 2016; Wu 2015; Liao 2015; Tehseenullah 2015) is internally inconsistent and equivalent to the UQ-SDAAP defined Transition Zone, the work can be used to assess the likely vertical and lateral hydraulic connectivity of the sandy units of this stratigraphic section. Thermogenic hydrocarbons (gas accumulations with a liquids component) generated from deeper Permian source rocks have migrated and accumulated in the sands occurring below and immediately above the sub-Surat Unconformity surface on the Roma Shelf. The hydrocarbons form relatively patchy saturation with accumulation being mainly related to folded structural closures associated with local faults with some element of stratigraphic pinch-out likely in these channelised systems. With a few exceptions, the individual stacked reservoir sandstones represent separate hydrocarbon accumulations suggesting that the intervening low permeability baffles effectively provide effective seals at geological time scales albeit individually of limited lateral extent. This generally is consistent with the depositional environment interpretation (La Croix et al. 2019c) and facies interpretation (La Croix et al. 2019a) presented in the UQ-SDAAP project.

**Figure 77** A schematic representation of the lateral and vertical continuity of hydrocarbon accumulations in the stacked reservoir sands of the Kincora, Borah Creek and Sandy Creek fields on the Roma Shelf (Augusta 2017). Note that the 'Wandoan Sandstone' is below the sub-Surat unconformity.



## 4.5.2 Regional hydrogeological analysis

The regional hydrogeology of the Surat Basin, particularly the Hutton Sandstone Aquifer immediately above the Ultimate Seal and the Precipice Sandstone aquifer (equivalent to the Block Sandstone Reservoir) provides insights into the locations where there may or may not be hydraulic communication either between the aquifers or between an aquifer and the surface (recharge and discharge features). This can be gleaned from examination of the distribution of hydraulic head (see Bachu 1995 for an explanation of hydraulic head) within each of the aquifers and the difference in hydraulic head between them. Similarly, the distribution of hydrochemistry of groundwater within each of the aquifers is insightful. Locations of recharge and discharge can also be further examined at surface by sampling springs and surface water drainage. Analysis of these water samples may reveal evidence of mixing older water of deep aquifer provenance with younger surface or shallow groundwater. Data examined hereunder are supportive of the seal and seal complex hypothesis in the deep basin centre.

Substantial work has been conducted on regional hydrogeological and hydrochemical analysis. Hitchon and Hays 1971 provided an early analysis of the hydrogeology and how this related to the hydrocarbon occurrences in the Surat Basin. These studies provide both a hydraulic head map and a salinity map where they interpreted recharge in the northwest and on the eastern side of the basin along the Great Dividing Range with discharge to the Balonne River and in the southwest from a sub-surface pinch-out of the Precipice Sandstone upwards through the overlying cover. Hitchon and Hays (1971) describe the Precipice Sandstone aquifer as a “low fluid potential drain” resulting from its high permeability and lateral continuity but they don’t speculate on where the “drain” discharges other than upwards through the overlying sedimentary succession. The salinity ranges from fresh to as high as 4000 mg/L. One of the areas of relatively high salinity is in the area near Roma where there are also hydrocarbon accumulations and what Hitchon and Hays 1971 interpret to be discharge to the Balonne River. Interestingly the UQ-SDAAP project interpret this water chemistry data to be within the Transition Zone. What remains unanswered in the Hitchon and Hays conceptual hydrogeological model is how there can be a high permeability connection from the Precipice Sandstone aquifer at depth and discharge to the surface. Habermehl and co-authors have published extensively on various aspects of Australia’s Great Artesian Basin (e.g. Habermehl 1980, Calf and Habermehl 1984, Torgersen et al. 1991, and Herczeg et al. 1991) including the Surat Basin, where they have characterised regional flow systems with recharge to aquifers on the basin’s eastern margins and flow systems generally towards the southwest. The development of coal seam gas in the Surat Basin over the last 15 years has led to an extraordinary increase in data (wells, core, petrophysical logs, well testing, seismic, fluid sample, monitoring bores etc.). With this new data, researchers began to map out more complex flow systems within Surat Basin aquifers. Hodgkinson et al. 2010 and OGIA 2016a and 2016b recognised, for example, that there are local flow directions towards the northeast on the northeast side of the Great Dividing Range in the Surat Basin.

Underschultz & Vink 2015 observed that the low values of hydraulic head in the Hutton Sandstone aquifer driving this north-easterly direct flow on the northeast edge of the Surat Basin matched the Dawson River valley surface elevation – suggesting subcrop and outcrop surface topographic control imposing a low hydraulic head boundary condition and discharge at that location.

The UQ-SDAAP project has reviewed all the previous hydrogeological conceptualisations for the Surat Basin Precipice Sandstone and Hutton Sandstone aquifers, re-analysed the available DST data from the Blocky Sandstone Reservoir (Honari et al. 2019a) and reviewed the available water level data from bores. This analysis includes, where possible, a Horner extrapolation to determine formation pressure. An updated view of the hydrogeological conceptualisation based on all currently available data is developed as part of the UQ-SDAAP outputs that can be used to help establish boundary and initial conditions for the groundwater modelling and for testing concepts of regional seal performance.

#### 4.5.2.1 Hydraulic head of the Blocky Sandstone Reservoir and Hutton Sandstone Aquifer

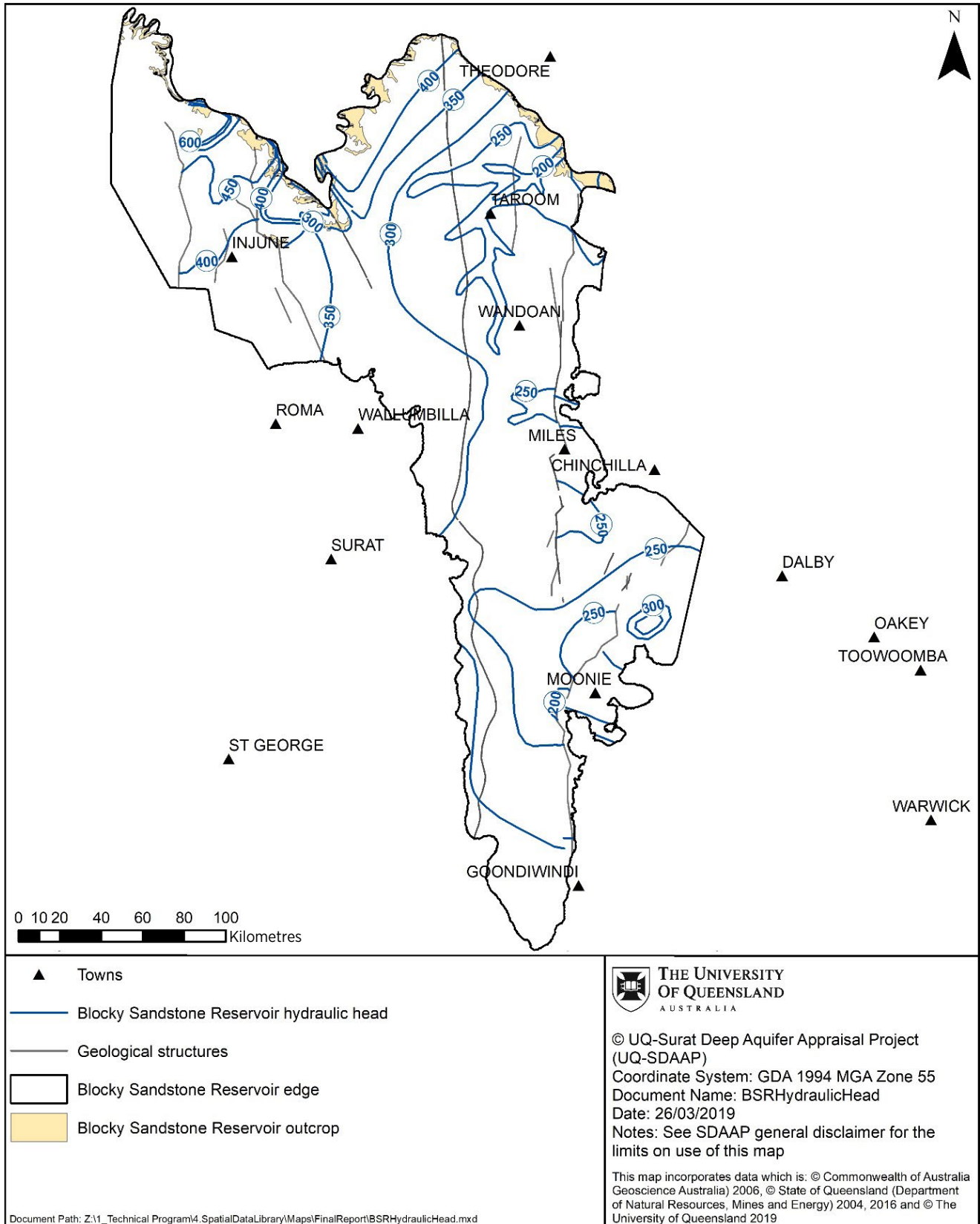
It is important to consider the purpose of the hydraulic head analysis in advance of mapping data. Over time, there may be many human induced stressors of the aquifer in question and these can transiently induce changes in hydraulic head measurements near the stressor. Stressors could be oil, gas or water extraction such as from commercial oil and gas field production as well as significant water users such as feedlot and piggery bores, town water supply bores or power station bores. In addition, there has been a commercial-scale managed aquifer recharge scheme in recent years injecting water into the Blocky Sandstone Reservoir. If considering the use of any water supply bore as a water level data source, no matter how large the extractor, one must determine if the water level reading is affected by recent pumping. For this reason, dedicated monitoring bores can often generate better quality data.

In the case of the UQ-SDAAP project and its desire to understand the hydraulic performance of the Blocky Sandstone Reservoir, Transition Zone and Ultimate Seal, it's important to first consider the hydraulic state of the Blocky Sandstone Reservoir and the Hutton Sandstone Aquifer (above the Ultimate Seal) prior to any impacts of human activity. How the Blocky Sandstone Reservoir and Hutton Sandstone Aquifer respond hydraulically over time to the mentioned stressors can then be considered.

Of the available data, the DST data from oil and gas wells is normally collected at the time of drilling the well and thus represents the formation pressure prior to significant disturbance of the aquifer. This may not be true if, for example, the well is a development well in the Moonie field - if it was drilled after field production has already begun. In the case of Moonie, wells drilled up to Moonie 18 were prior to commercial oil production and those drilled subsequently are variously impacted by production induced pressure decline. Similarly, water level data utilised from bores needs to be filtered to only utilise observations unaffected by pumping. An additional difficulty with water level data from bores is that these wells often do not contain any other supporting information (such as modern petrophysical logs) that can be used to confirm the stratigraphic unit within which the bore is completed. If this information is lacking, the screened interval depths can be compared to the regional geological model to estimate the stratigraphic interval that the well is completed in. The data set available for the Blocky Sandstone Reservoir and Hutton Sandstone, deemed to be unaffected by pumping or production, is displayed with well data control locations and contoured for hydraulic head. Rather than using an automatic gridding and contouring algorithm, the hydraulic head values are manually contoured using a digitisation option in graphics software. This allows for the hydraulic head contours to be influenced by water table boundary conditions in outcrops and for the tendency of the system to have preferentially connected regions of low hydraulic head connecting hydraulic drains to discharge locations and high hydraulic head connected to recharge locations. This is not possible with most automated contouring algorithms.

The hydraulic head distribution of the Block Sandstone Reservoir is shown in Figure 78. The hydraulic head distribution defined a relatively flat surface between 250 and 350 m across a broad region. This is consistent with a hydraulically well connected relatively high transmissivity (related to permeability and thickness) aquifer that does not support steep hydraulic gradients. Areas of high hydraulic head such as in the extreme northwest of the map (more than 600 m of hydraulic head), along the outcrop northwest of Taroom (more than 400 m of hydraulic head) and in the extreme east-central area (excess of 400 m of hydraulic head) are associated where relatively high topography areas (i.e. higher than that the hydraulic head value) that may be influencing recharge to the aquifer. Conversely, areas of relatively low hydraulic head (less than 250 m) can conceptually be linked to possible discharge. For this to occur, the low values of hydraulic head must physically be hydraulically linked to a water table or surface water elevation of at least that low of an elevation above sea level (i.e. less than 250 m ASL). If this is not the case, some other physical reason for a groundwater sink needs to be considered. For example, the area of less than 250 m hydraulic head in the north central part of the area coincides with the Dawson River (north east of Taroom), the elevation of which becomes less than 180 m ASL in the same region (Underschultz & Vink 2015). There are also several areas of less than 250 m hydraulic head distributed along the various fault liniments including at Moonie. Finally, there is an east-west trending region of less than 250 m hydraulic head to the east of Moonie extending to the eastern edge of the mapped area.

**Figure 78** The distribution of hydraulic head within the Blocky Sandstone Reservoir. Blue contours are hydraulic head with a 50 m interval. Well locations with hydraulic head data control points are posted in black and values highlighted by yellow shading are interpreted to be production affected.



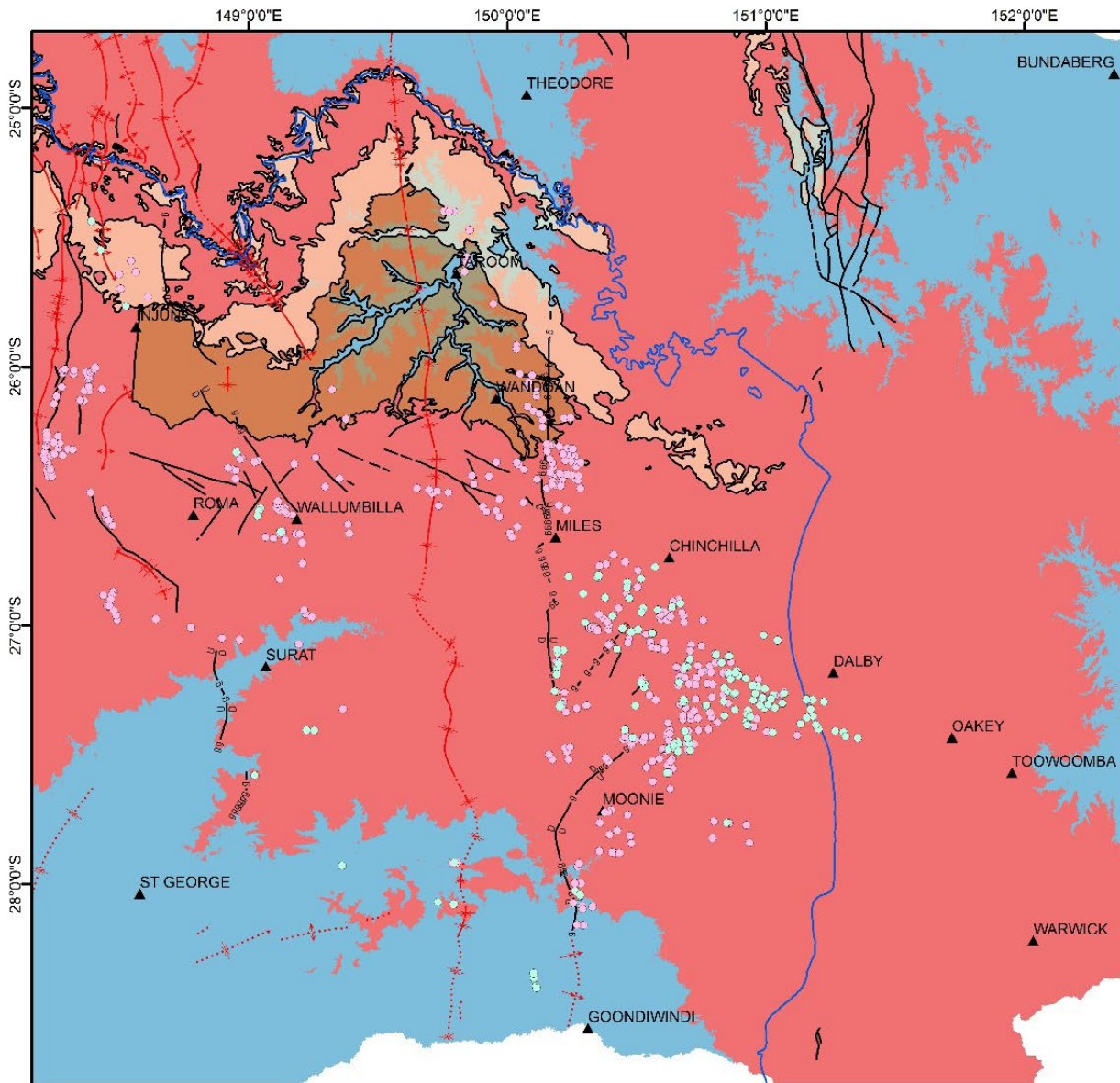
If the digital elevation model for the study area is examined for regions with a surface elevation of less than 250 m (Figure 79) that coincide with Blocky Sandstone Reservoir hydraulic head values less than 250 m hydraulic head, one can hypothesise about the potential for discharge at that location. This assumes that the water table is reasonably close to the land surface as an approximation. Figure 79 shows the DEM model, colour-coded with red being greater and blue being less than 250 m ASL. There are four regions where the surface elevation is less than 250 m ASL:

1. In the extreme northeast: however, this region occurs east of the Blocky Sandstone Reservoir outcrop edge and thus is not relevant
2. In the north-central area coincident with the Dawson River drainage system: this coincides with the low hydraulic head in the Blocky Sandstone Reservoir in exactly the same area and the Dawson River Valley itself is the site of many observed Springs (OGIA 2016b and 2016d). The hypothesis is that this forms a major boundary condition control on the hydraulic head distribution for the Blocky Sandstone Reservoir
3. In the east-central edge of the study area near Toowoomba: this location coincides with the eastern edge of the east-west trending low hydraulic head extending east from Moonie. The low topography east of Toowoomba is part of the Brisbane River drainage, but is located within the Clarence Morten Basin. The hypothesis is that the Blocky Sandstone Reservoir strata extend from the Surat Basin eastward into the Clarence Morton basin where they subcrop or outcrop along the Brisbane River drainage, and that this forms a major boundary condition control on the hydraulic head distribution for the Blocky Sandstone Reservoir. This is in agreement with OGIA 2016b where they suggest that the “the Precipice Sandstone, interconnects around the northern end of the Kumbarilla Ridge (Ransley & Smerdon 2012). The upper unit of the Woogaroo Subgroup—the Ripley Road Sandstone (previously termed the Helidon Sandstone)—is the equivalent of the Precipice Sandstone”
4. In the south-west corner of the mapped area: this region has a complex geometry related to a number of surface drainage systems including the Weir River (north of Moonie), Condamine River (near the town of Surat), Wyaga Creek (east of St George). The area north of Moonie coincides with the location of the Moonie-Goondiwindi fault system and near the location of a low hydraulic head region (<250 m) of the Blocky Sandstone Reservoir. With this information, it is hypothesised that hydraulic communication up a segment of the Moonie fault may provide hydraulic communication between the Blocky Sandstone Reservoir low topography surface discharge (or subsurface discharge to the water table). This forms a major boundary condition control on the hydraulic head distribution for the Blocky Sandstone Reservoir

The analysis of surface topography with hydraulic head lows in the Blocky Sandstone Reservoir is satisfying in that there are a number of locations where the coincidence makes physical sense with the possibility of discharge. However, there are other areas of low hydraulic head (<250 m) located along the north south fault trends (see Figure 78) where there is no related surface low. In this case, if the hydraulic head contours are correct, it means either there is a sink (pumping) within the Blocky Sandstone Reservoir at these locations or the formation water is leaving the Blocky Sandstone Reservoir and migrating up or down to an adjacent aquifer with similar or lower hydraulic head (if surface discharge is not an option).

The three hypothesised discharge points for the Blocky Sandstone Reservoir where the hydraulic head distribution and surface topography match, can be tested by field sampling these locations for soil gas or surface water chemistry that may indicate Blocky Sandstone Reservoir discharge. UQ-SDAAP investigated each of these regions and the details of the fieldwork with interpretive results are described below and will also be part of student Masters Thesis documents.

**Figure 79** Digital Elevation Model for the Surat Basin with red representing surface elevation greater than 250 m ASL and blue representing surface elevation less than 250 m ASL.



**Legend**

- |                            |                                     |  |
|----------------------------|-------------------------------------|--|
| ▲ Towns                    | <b>SURAT_BASIN_STRUCTURE</b>        | ⋯⋯⋯ Anticline Concealed                      |
| ● BaseSuratWCMKeystone     | — Fault Accurate                    | ⋯⋯⋯ Anticline Concealed Double Plunge Away   |
| ● BaseSuratFaultPoints     | — Fault Accurate Rel. Disp. U/D     | ⋯⋯⋯ Anticline Concealed Showing Plunge       |
| □ Surat Basin              | - - - - - Fault Concealed           | ⋯⋯⋯ Monocline Concealed                      |
| <b>Surface rock units</b>  | ▭ Fault From Seismic                | — Syncline Accurate                          |
| ■ Injune Creek Group       | ▭ Fault From Seismic With Down/Up   | — Syncline Accurate Showing Multiple Plunges |
| ■ Hutton Sandstone         | ▭ Fault From Seismic With Up/Down   | — Syncline Accurate Showing Plunge           |
| ■ Precipice Sandstone      | ⋈ Anticline Accurate                | ⋯⋯⋯ Syncline Concealed                       |
| <b>DEM</b>                 | ⋈ Anticline Accurate Showing Plunge | ⋯⋯⋯ Syncline Concealed Showing Plunge        |
| <b>&lt;VALUE&gt;</b>       |                                     |  |
| ■ -18.17508888 - 250       |                                     |  |
| ■ 250.0000001 - 1,602.4823 |                                     |  |



An alternative hydraulic head contouring of the Blocky Sandstone Reservoir is presented in Figure 80 that still honours the data control but where the various regions of less than 250 m of hydraulic head are linked either to a drain at the Dawson Valley or east of Toowoomba. This avoids the need for up-fault discharge near Moonie and it also ties in the other small areas of low hydraulic head along the north-south fault trend. It presents a possible but perhaps less realistic hydrogeological conceptualisation as it requires relatively narrow regions to be hydraulically connected over long distances. Nonetheless, this represents a plausible alternative conceptualisation.

The hydraulic head distribution for the Hutton Sandstone aquifer is shown in Figure 81. It has a larger lateral hydraulic gradient than the Blocky Sandstone Reservoir with values ranging from more than 500 m to less than 200 m of hydraulic head. This suggests that the hydraulic transmissivity is lower than that for the Precipice Sandstone aquifer. There is a similar pattern however to the locations of possible recharge (high hydraulic head in areas of high topography) and discharge (low values of hydraulic head in topographically low regions) with possible recharge in the far northwest and far-east part of the study area. In addition, there is a small area of higher hydraulic head (>300 m) in the outcrop area of high topography northwest of Taroom. In the case of the Hutton Sandstone Aquifer, it appears that the discharge is almost entirely focused on the Dawson River with few other localised lows (sinks). This could partially be the result of a general lack of data control in the southern parts of the study area. This hydrogeological conceptualisation is consistent with Suckow et al. 2018 who examined environmental isotopes and noble gases and discovered mixing trends that suggested the Hutton Sandstone Aquifer is a dual permeability system with groundwater age determinations consistent with discharge to the northeast at the Dawson River with a mixing of relatively old and recently recharged formation water.

**Figure 80** The alternative interpretation of the distribution of hydraulic head within the Blocky Sandstone Reservoir. Blue contours are hydraulic head with a 50 m interval. Well locations with hydraulic head data control points are posted in black and values highlighted by yellow shading are interpreted to be production affected.

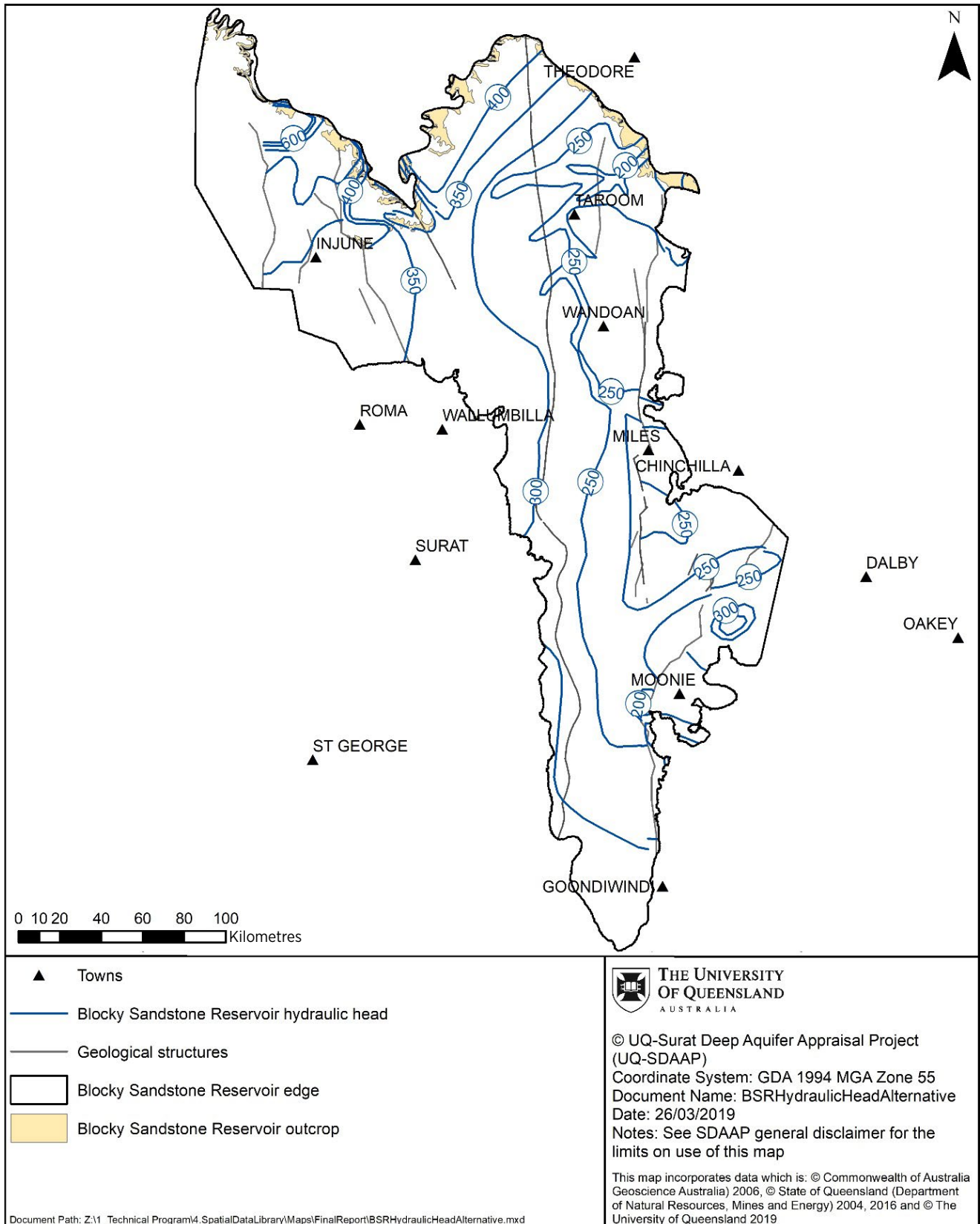
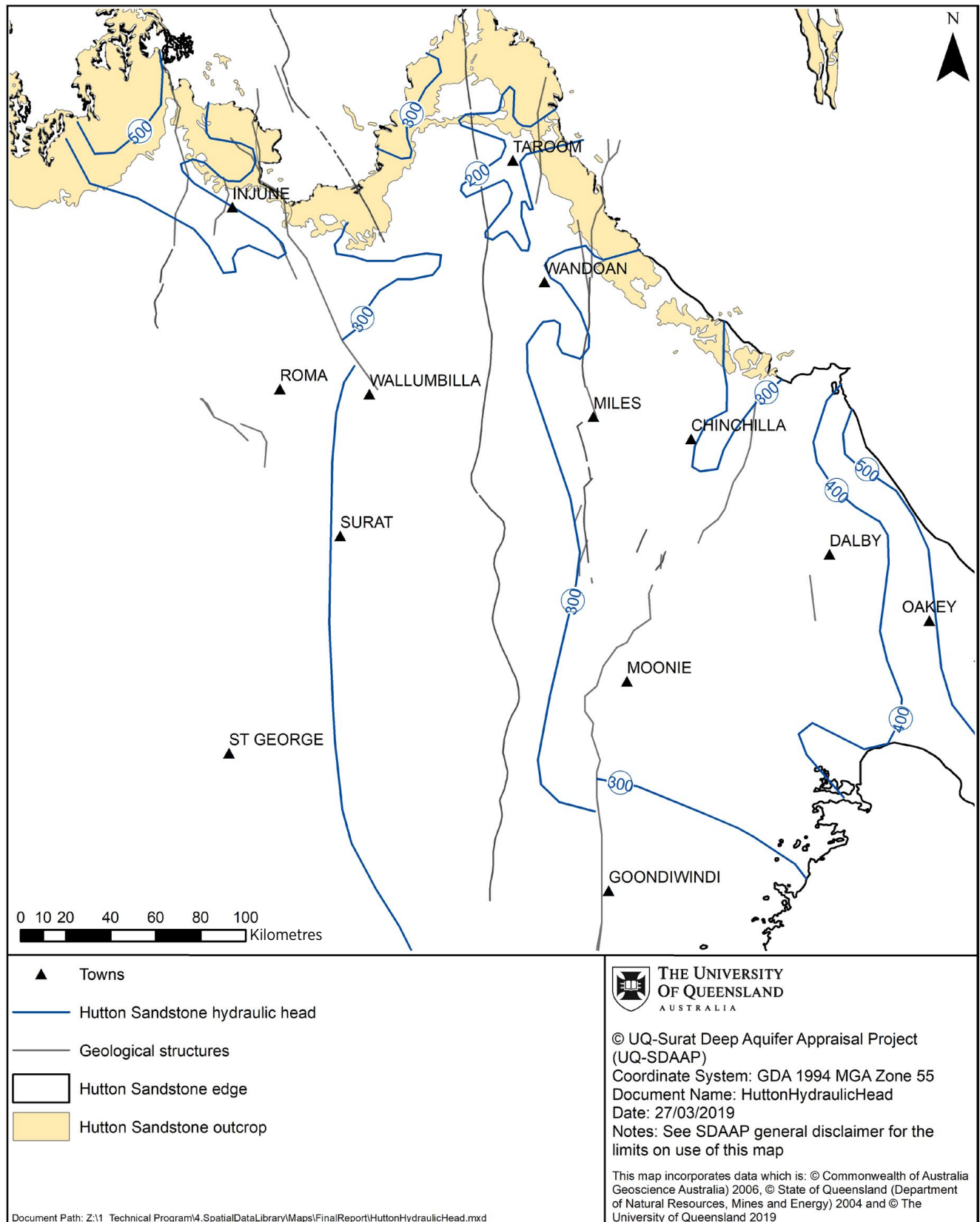


**Figure 81** The distribution of hydraulic head within the Hutton Sandstone Aquifer. Blue contours are hydraulic head with a 100 m interval.



The regional hydraulic head maps for the Blocky Sandstone Reservoir (below the Transition Zone and Ultimate Seal) and the Hutton Sandstone aquifer (above the Ultimate Seal) can be compared to see the vertical hydraulic gradient between the two. A large difference in hydraulic head indicates that the intervening strata (the Transition Zone and Ultimate Seal) have sufficiently low bulk permeability to sustain such a high hydraulic gradient over geological time. A small difference (say less than -5 m) is indeterminate since it could be due to better vertical hydraulic transmissivity or it could be coincidental. OGIA 2016a created a distribution of calculated head difference between the Precipice Sandstone and Hutton Sandstone aquifers in their Hydrogeological Conceptualisation Report for the Surat Cumulative Management Area showing differences of >5 m. The hydraulic head difference observed between the Blocky Sandstone Reservoir (Figure 79) and the Hutton Sandstone (Figure 81) would support that the intervening Transition Zone and Ultimate Seal are regionally of low bulk vertical permeability.

#### 4.5.2.2 Field work on the Dawson River and Lockyer Valley discharge

The regional hydrogeology conceptual models have identified that both the Hutton Sandstone and the Precipice Sandstone aquifers likely discharge to the Dawson River drainage system on the northeast edge of the basin, and that the Precipice Sandstone aquifer may also have a hydraulic connection to discharge in the Lockyer Valley in the Clarence Morten Basin near Toowoomba. The Office of Groundwater Impact Assessment has conducted several investigations on discharge features of the Surat and Bowen basins including the “Identification of gaining streams in the Surat Cumulative Management Area” (OGIA 2017) and, “Springs in the Surat Cumulative Management Area” (OGIA 2016). UQ-SDAAP funded complementary master’s student research projects to investigate surface water systems in these two regions and determine if there are any hydrochemical signatures that can be linked to the aquifer hydrochemistry. Findings from these projects are summarised below.

##### 4.5.2.2.1 Discharge features examined by OGIA

Data available from gauging the flow in surface water drainage features (rivers and creeks) can show either “gaining” or “losing” sections where the surface drainage is increasing or decreasing in volume. In certain circumstances, this can be linked to either discharging or recharging conditions to unconfined aquifers. These conditions can also inform aquifer connectivity to alluvial systems in certain instances where the bedrock aquifer is subcropping at the base of the alluvium. OGIA has examined a number of recharge and discharge features in the Cumulative Management Area (CMA) including the location of gaining water courses associated with unconfined aquifer discharge. In the entire CMA, OGIA found that “the majority of the identified potentially gaining streams are in the Dawson River catchment. In particular, on the northern slopes of the Great Dividing Range between Wandoan and Roma...” (OGIA 2017 page 13). This is consistent with the UQ-SDAAP observations from the regional hydraulic head distributions for the Hutton Sandstone and Precipice Sandstone aquifers. In terms of spring discharge, OGIA 2016 (pp 9) note that “The occurrence and distribution of springs in the Surat CMA are primarily driven by regional and local geology, topography and groundwater flow regimes. Most springs are located along and near the northern and central outcrop areas of the Surat and Bowen basins and are associated with the Gubberamunda, Hutton, Clematis and Precipice sandstones. In addition to topography, structures such as faults influence the occurrence and distribution of springs. Regional faulting features such as the Hutton Wallumbilla Fault and the Leichhardt-Burunga Fault are associated with springs in the central area of the Surat CMA, including the Lucky Last and Boggomoss spring complexes”. Out of 40 identified watercourse springs, OGIA 2016 links 14 to the Hutton Sandstone aquifer and eight to the Precipice Sandstone aquifer (more than half).

##### 4.5.2.2.2 Dawson River run of river radon sampling

The UQ-SDAAP project conducted a run of river sampling program for the Dawson River in areas where the surface elevation is less than 180 m and coincident with the Hutton Sandstone and Precipice Sandstone outcrops. Radon ( $^{222}\text{Rn}$ ) is a radiogenic isotope that has a natural emission source in mafic minerals that make up rocks in the subsurface. With time groundwater in deep aquifers pick up this random signature that represents a higher activity than typical in surface water or more recently recharged shallow aquifer water. As such, an anomalously high  $^{222}\text{Rn}$  value in sample from a run of river water sampling campaign can indicate groundwater discharge locations. The run of river samples along the Dawson River did not show anomalously high values. This could be due to there being little groundwater discharge to surface water or due to the Precipice and Hutton sandstone aquifers having a high quartz component of the mineralogy and thus not having a significant source of  $^{222}\text{Rn}$ .

#### 4.5.2.2.3 Lockyer Valley surface water sampling

The UQ-SDAAP project regional hydrogeology conceptualisation work indicates the possibility of the Blocky Sandstone aquifer of the Surat Basin potentially extending eastward into the Clarence Morton Basin where it may discharge at surface elevations of less than 250 m in the Lockyer Valley. This is consistent with the geological interpretation of the Blocky Sandstone Reservoir (Gonzalez et al. 2019b). Wye 2019 conducted a Master of Science research titled “The Lockyer Valley; Great Artesian Basin groundwater discharge to the east of the Great Dividing Range” supported by the UQ-SDAAP project. Four field trips were undertaken to collect surface water samples from a range of creeks across the study area. Physical parameters, major ions, trace metals, stable isotopes and radon were assessed. Field sample data and groundwater bore data from the Queensland Government Groundwater Database were analysed and used in combination with geological and hydrogeological knowledge of the region as the basis for the study, with the goal of generating a better understanding of the local and regional groundwater systems. An area of mixing between the Clarence-Moreton Basin aquifers of the GAB and the overlying alluvial aquifers was inferred in the locality of Soda Spring and Lockyer Creeks. Soda Spring Creek samples were shown to be Na-Cl dominant and align closely with the water chemistry of Clarence-Moreton Basin formations. Soda Spring Creek samples also had the highest TDS values of 6000 and 5300 ppm and were shown to be unevaporated, indicating non-alluvial origin. It was concluded that Soda Spring Creek waters are of mixed origin and likely partially comprised of water from the GAB. This helps increase the overall understanding of flow directions and mixing in this region and the connectivity between the Surat and Clarence-Moreton Basins (Wye 2019). The full details of this work can be found the report of Wye 2019.

#### 4.5.2.3 Summary of hydrogeological analysis

**A combination of literature reviews of historical published work, new analyses of recently available gas industry data and fit for purpose field data acquisition programs have be integrated to develop a new understanding of the Precipice Sandstone and Hutton Sandstone aquifers. This was combined with the geological findings of the UQ-SDAAP work that updates the stratigraphic correlation into a seismo-sequence stratigraphic framework and observations of monitoring bore response to the gas industry managed aquifer injection. New conceptual models of the hydrogeology have been developed that are consistent with all observations. With this in mind, the following observations have been made:**

1. The Blocky Sandstone Reservoir forms the basal aquifer system of the Surat Basin and it has limited geographic extent making it more suitable for storage than previously considered. The Blocky Sandstone Reservoir pinches out in the deep subsurface in the southern depositional centre. It comes to outcrop boundary conditions in the northern depositional centre and is hypothesised to be connected in laterally equivalent stata of the Woogaroo Subgroup (Rabier et al 2019) to outcrop in the Lockyer valley of the Clarence Morton Basin to the east
2. West of the Blocky Sandstone Reservoir pinch-out, there are disconnected Transition Zone sandstone geobodies that previously were referred to as “Precipice Sandstone”. **The observation well network recording pressure response to managed aquifer injection proves that these sands are hydraulically disconnected from the Blocky Sandstone Reservoir.** The Transition Zone is a poor vertical conductor of fluids and pressures
3. Considering points 1) and 2), the conceptual hydrogeological model for the Blocky Sandstone Reservoir suggests that it is highly permeable and hydraulically connected across the northern and southern depositional centres with relatively low hydraulic head connected to discharge at the Dawson River in the northeast and to the Lockyer Valley in the east. This is supported by hydrochemistry and isotope analysis
4. The Hutton Sandstone forms a generally lower permeability aquifer where the hydraulic head across at least the northern half of the Surat Basin is affected by discharge to the Dawson River in the northeast. This is supported by hydrochemistry and isotope analysis
5. The difference in hydraulic head observed between the Blocky Sandstone Reservoir and the Hutton Sandstone together with the seismo-sequence stratigraphic correlation, facies analysis and the managed aquifer recharge monitoring bore network would suggest that the seal complex i.e. **Transition Zone combined with the Ultimate Seal is an effective regional vertical hydraulic barrier**

### 4.5.3 Fault zone analysis

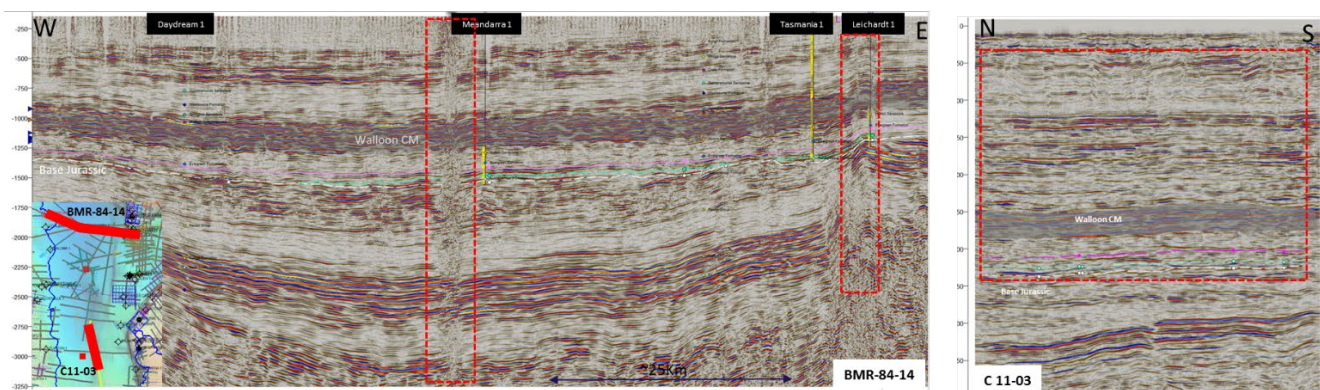
Faults are a containment risk factor. This research has mapped and characterised fault geometries and pressures to the degree possible on existing data. New data was acquired in several areas to investigate possible evidence of fault-related vertical transmission of methane. The data did not support this hypothesis. More, site-specific, 2D seismic data is required. The current assessment is that fault density in the basin centre is likely to be low and so, it seems likely that locations can be found for injection wells which minimise interaction of plume dynamics and faults.

Earlier in this report (sections 4.3.5 and 4.3.7) describe the major fault trends and section 4.5.1 described the hydrocarbon systems with certain migration pathways that may relate to faults, with the Moonie oil field being a prime example. Since the Moonie oil field is not filled to the structural spill point of the top seal and since there are hydrocarbon migration indicators trending along the Moonie fault segments in the overlying Hutton Sandstone, it would suggest that some aspect of fault seal may be controlling the original Moonie oil field free water level. This could simply be up-fault leakage (at least at the geological time scale) due to the fault zone architecture within the prevailing stress field. Gonzalez et al. 2019b describes the characterisation of major faults in the UQ-SDAAP project area and assess the up-fault leakage potential.

Other seismic anomalies and features that have been noted in the seismic analysis across the Surat Basin and require further investigation include geometries and indicators indicating that certain fault segments could be connecting Permian strata to the surface. Examples are highlighted in seismic lines C-11-03 and BMR84-14 (Figure 82). The seismic line BMR84-14 exhibits a strong and abrupt vertical seismic interference at the centre of the basin near the Meandarra 1 well. A first impression of this anomaly is that it could be associated with a gas chimney. However, reprocessing or acquisition parameters could also be an explanation, while the anomaly towards the east of the same line could be associated with reactivation of the Leichardt fault that propagates near to the surface. Further south in the seismic line C11-03, a chaotic seismic pattern near the surface could be interpreted as strain, however, it does not show roots through to the underlying units. This suggests the potential for some faults to have a decollement into Permian or shallower strata.

The UQ-SDAAP project selected one of these features to investigate further in an effort to confirm or refute the possibility of hydraulic communication to surface. The most detectible feature would be if a fault were to be generating a “gas chimney”. This is essentially a region of potentially enhanced permeability perhaps associated with the faults damage zone that allows vertical methane migration and results in a characteristic anomalous seismic signature as described above for seismic line BMR84-14 displayed in Figure 82. In this case, an anomalously high methane signature in the atmosphere, soil gas or in surface water could corroborate if there is vertical leakage occurring or not. This would particularly be true if any detected gas were of thermogenic origin (i.e. likely generated in the Bowen Basin source rocks).

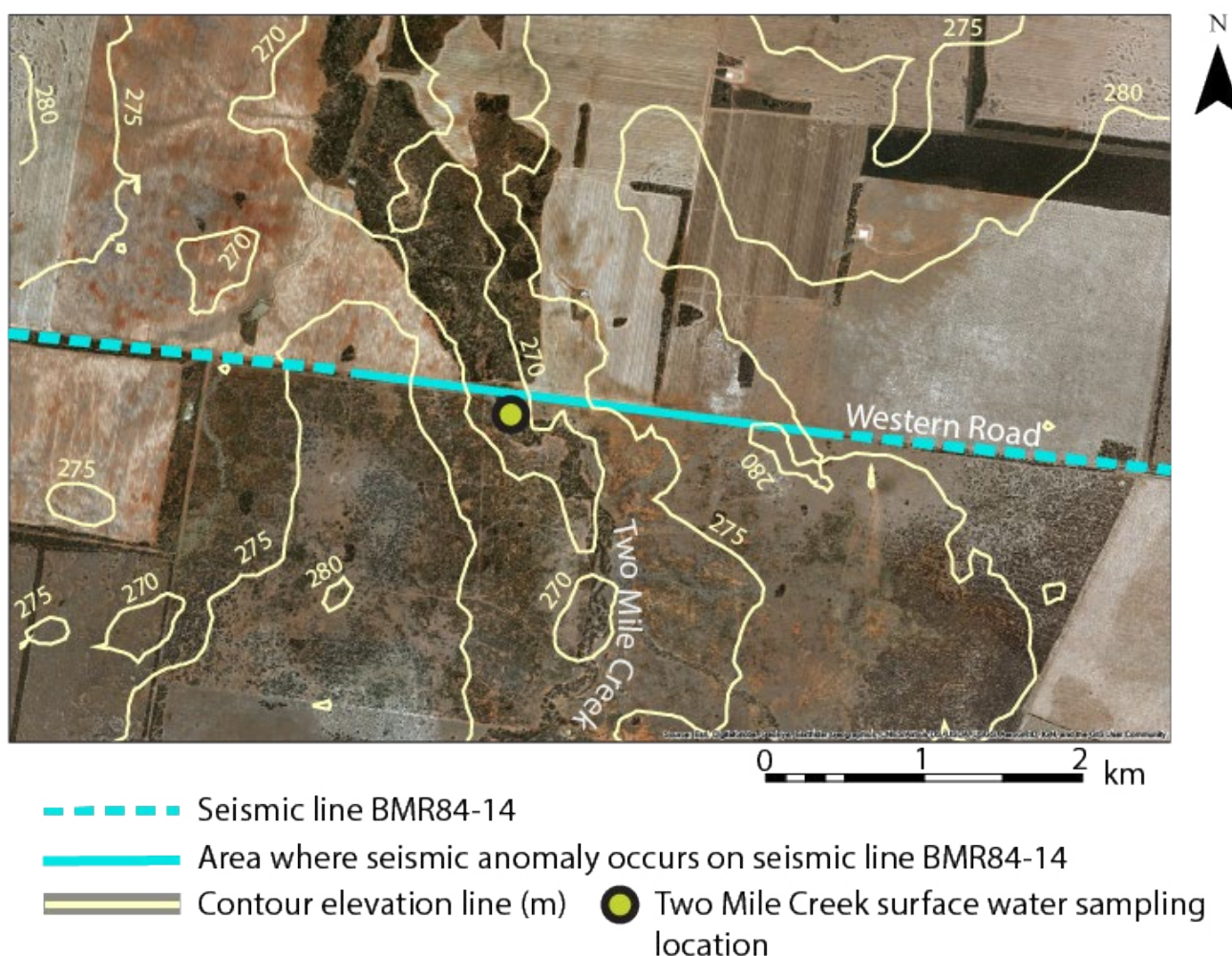
**Figure 82** Left: Seismic line BMR84-14 W-E showing the vertical seismic anomalies up to the near surface in the centre and the eastern flank. Right: Seismic line C11-03 N-S displaying the large number of features in the near surface along the mute seismic zone.



#### 4.5.3.1 Field work investigating seismic anomalies resembling gas chimneys

One of the seismic anomalies that resembles a gas chimney in Figure 82 occurs along approximately 2.7 km of Western Road. The topography of this area is relatively flat, and the seismic anomaly intersects the upper reaches of a first order tributary of the Condamine River, Two-Mile Creek. This creek is ephemeral, and only flows intermittently during storm events. Adjacent land use is agriculture, comprising cattle and cropping, with some sparse native vegetation present. Figure 83 provides an aerial image, including contour elevation, of the study area to highlight topographical constraints.

**Figure 83** Location of seismic anomaly site



In order to assess possible gas migration from the deep Surat or Bowen basins, a number of atmospheric gas survey techniques were performed in combination with dissolved hydrocarbon gas samples from a local, gassy bore and surface water sites. The target gas for these surveys was methane, although dissolved C2-C6 were also sampled at the bore site. Methane was determined as an appropriate target gas due to its ubiquity in Surat Basin aquifers (Underschultz et al. 2016). Considering this, the following hypothesis was developed:

“ The detection of methane plumes (laser meter surveys) in combination with measured fluxes of methane along the seismic anomaly, but absent in the control area, is evidence of subsurface methane fluxes due to site-specific geological phenomena identified by the seismic data.

In order to test that the fluxes of any detected methane were directly associated with the identified seismic anomaly, a control site was also required. A control site with similar terrain but in an area not overlying the seismic anomaly was selected.

The gas surveys consisted of two sequential methane gas survey techniques at both the seismic anomaly site and the control site. Gas plume detection was conducted via methane gas scanning surveys using a prototype laser detector via:

- Traversing a specific section of Western Road (seismic anomaly site) or track (control site) in a vehicle travelling -10-15 km/h
- At specific locations where methane gas plumes were identified in 1) flux hoods coupled to gas flux meters to determine the flux of methane over time and 2) the concentration of different gases, respectively

In addition to the above, a gassy bore (located at the control site, -880 m deep and open -800-880 m) and two surface water sites, located at the intersection of the seismic anomaly and Two Mile Creek, were also sampled for dissolved C1-C4 hydrocarbon gases. This approach was used because methane derived from the Precipice Sandstone aquifer is likely to be associated with the presence of higher chain (C2-C4) hydrocarbons, with the gassy bore samples used as a broad indicator of deep aquifer gases (Underschultz et al. 2016). It is anticipated that any vertical flux of C1-C4 gases along the seismic anomaly from the deep subsurface would result in dissolved hydrocarbons in surface water at this site.

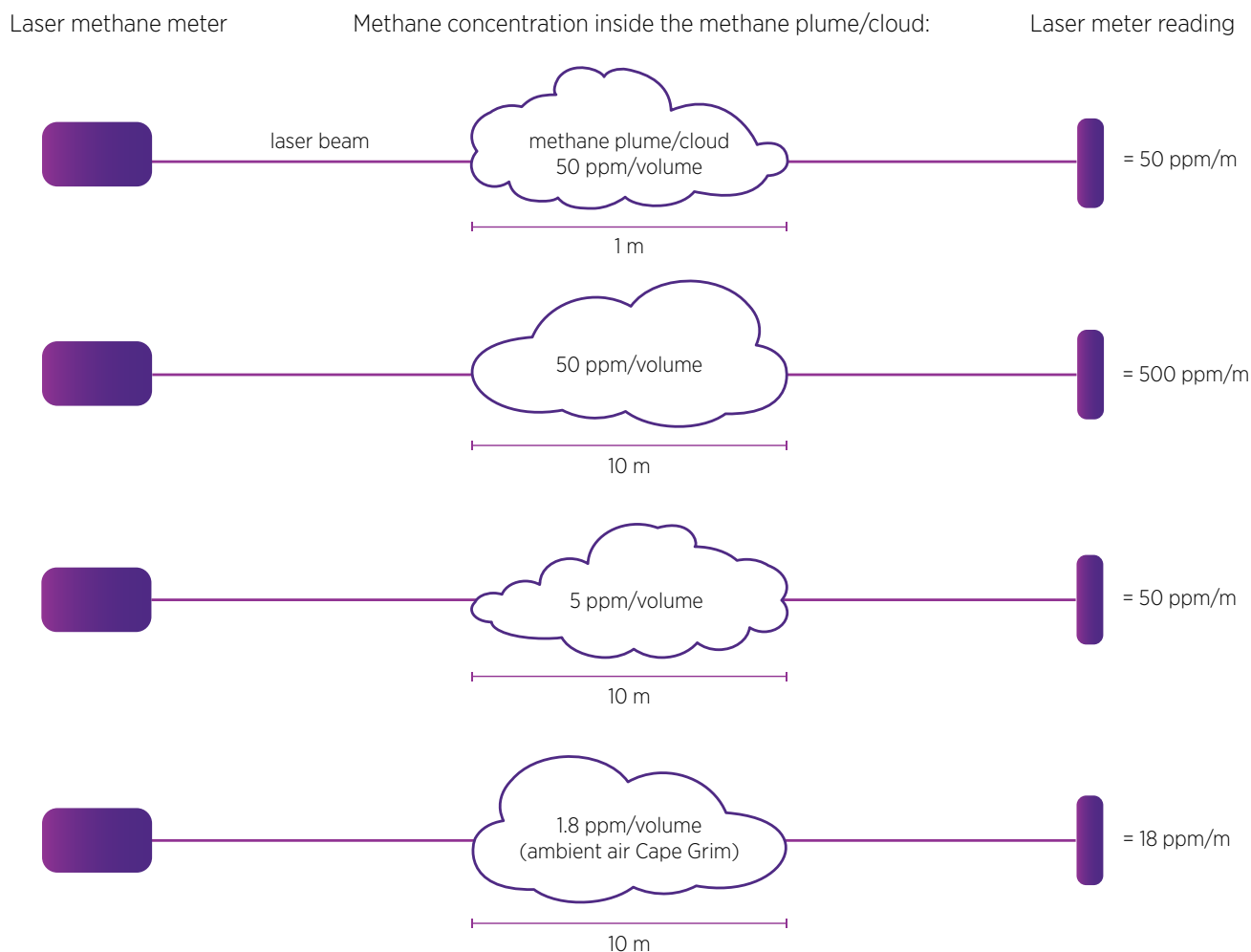
The methane gas surveys were conducted by Terra Sana Consultants Pty Ltd on 11 December 2018, and details of these surveys included in this report are derived from a report provided by Terra Sana to The University of Queensland on 12 February 2019 (Terra Sana Consultants 2019). Laser methane detector data was collected using a prototype open-path absorption spectroscopy detector (detection limit 1 ppm/m, detection speed 0.1 s, detection distance 0.5-100 metres) coupled with a real-time data acquisition system. Surface and groundwater sampling was conducted by The University of Queensland on 11 December 2018. Samples for dissolved hydrocarbons (C1-C4 gases) were collected by filling 40 ml glass vials with rubber butyl stoppers using a syringe, and ensuring no headspace. The C1-C4 hydrocarbon gases were analysed at the Australian Laboratory Services laboratory in Melbourne, Victoria (procedure ALS EP033-LL, detection limit = 1 µg/L).

#### 4.5.3.1.1 Laser methane detection

Laser methane sensors work by emitting a laser beam with a specific wavelength, and then measuring the reflection of a laser beam pointed at a surface. Methane adsorbs part of the beam, and this adsorption changes the reflected beam, which allows a methane measurement in the air to be made. The laser reading is dependent upon the distance that the laser beam travels through a gas cloud containing methane. Therefore, the units of data collected from laser methane detectors are always per unit of distance, e.g. metre, for example ppm/m, %Volume/m or %LEL/m. Data readings are most often presented in ppm/m, which changes due to length of the plume (Figure 84). For example, a ppm/m reading of 50 ppm can be indicative of a 1 m long methane plume (or “cloud”) with an internal methane concentration of 50 ppm/volume, or, alternatively it can be indicative of a 10 m long methane plume, with an internal methane concentration of 5 ppm/volume. As a result, the laser meter ppm/m readings also change depending on the angle that the beam enters a plume; for example, measurement parallel to the plume’s longest dimension results in a higher value than measurement in a perpendicular direction. Given this, laser methane data needs to be interpreted in context, and generally are only effective at detecting possible methane plumes from point-sources following repeated stationary measurements at individual sites.



**Figure 84** Conceptual representation of the effect of gas plume/cloud on raw laser methane meter data readings.



During a methane survey, a laser methane detector is used by pointing the laser beam at the ground surface and traversing a transect with the laser data continually logging. Readings below 25 ppm/m are generally considered within background limits, although higher readings (up to 500 ppm/m) may occur due to a number of factors not related to a point source methane leak, including: measurement error; dust or other interference; and the presence of multiple or diffuse sources of methane nearby. For this survey, when readings along the seismic anomaly transect were detected greater than 100 ppm/m, the vehicle was stopped and repeated measurements were made around the area from different angles where a high reading was detected. Under a scenario where a point-source of methane discharge was occurring, a plume of methane would be detected by the laser methane detector: this would be confirmed by repeated, stationary high ppm/m readings at the site. If repeated, stationary measurements could not be confirmed it would be concluded that a point-source plume of methane does not exist at that site.

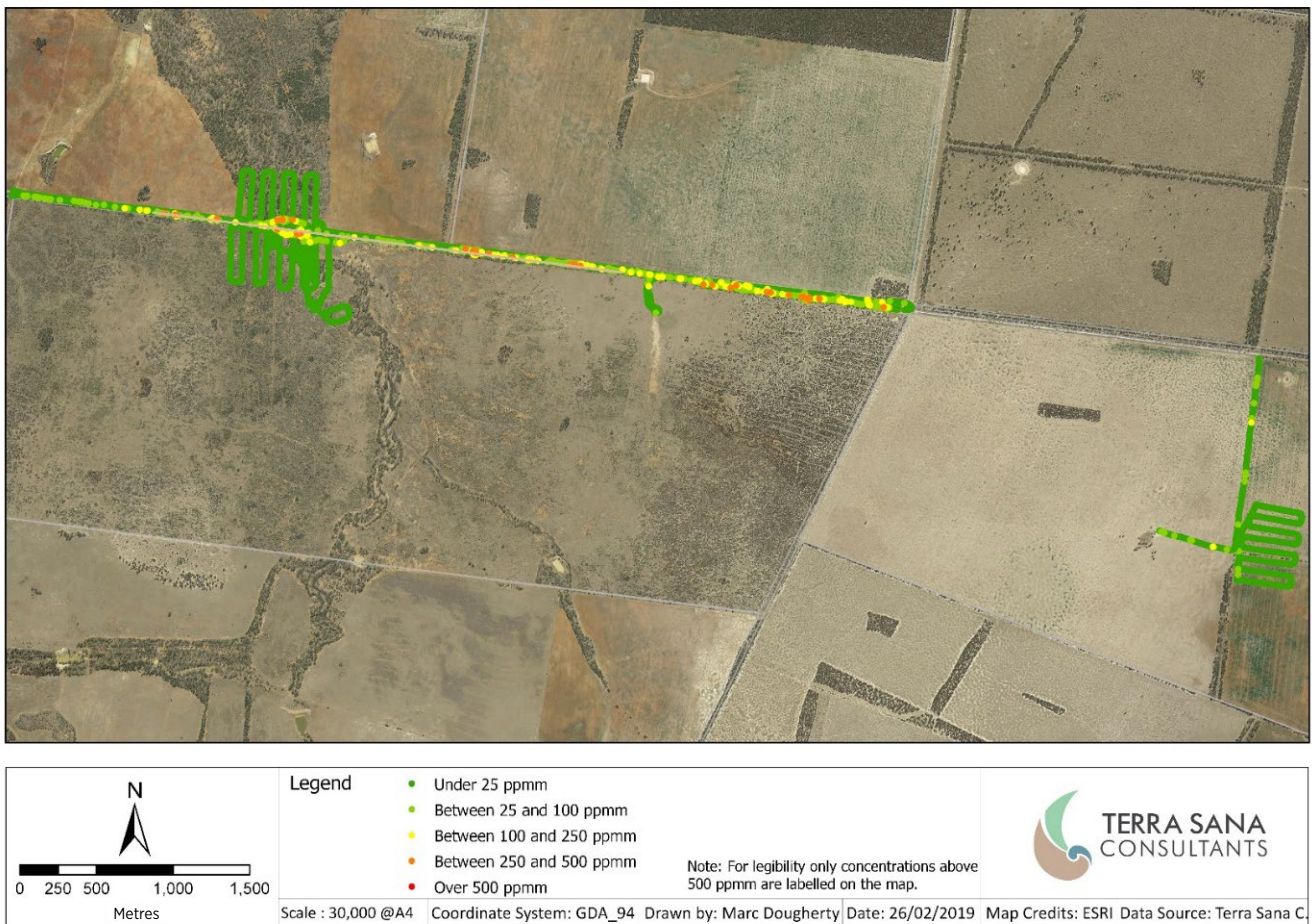
#### 4.5.3.1.2 Results

Gas plume detection surveys using the handheld laser meter and the drone surveys did not detect methane ppm/m readings above expected background methane ppm/m readings in the area, either in the area above the seismic anomaly or at the control site (Figure 85). As a result, flux chamber measurements were not conducted. A single high reading of 5005 ppm/m was observed at a gassy bore (RN 14906): this bore was continually pumping via a solar pump and geographically separated from the seismic anomaly location.

Dissolved hydrocarbon analysis of groundwater samples taken at the gassy bore RN 14906 showed methane and ethane concentrations of 12,400 µg/L and 3 µg/L, respectively. This high methane and low ethane concentration is typical of the predominantly biogenic methane gas sources throughout the Surat Basin aquifers (Hamilton et al. 2014; Baublys et al. 2015; Owen et al. 2016). Analysis of dissolved hydrocarbons from two surface water samples taken from standing pools at the intersection of Two Mile Creek and Western Road showed methane concentrations of 8 µg/L and 3 µg/L respectively, with no other hydrocarbons present. These low methane concentrations are most likely generated in-situ in the stagnant pools; considering the no-flow condition and the presence of cattle manure in and around the pool, these dissolved methane concentrations are unexpectedly low for these conditions.

Summarising: overall, the field survey for atmospheric methane and surface water hydrochemistry and isotope analysis investigation found **no evidence of gas leakage from the subsurface** at the location of a possible high angle low offset structure with gas chimney signature on seismic analysis. It seems that the anomaly in the seismic imaging could be due to a processing artefact.

**Figure 85** Laser methane survey results from vehicle and drone survey along Western Road and upstream and downstream of Two Mile Creek, and a control area in the east.



#### 4.5.3.2 Field work investigating up fault leakage potential on the Moonie fault

There are several lines of evidence that would suggest that certain segments of the Moonie-Goondiwindi fault system may be providing hydraulic communication between the Blocky Sandstone Reservoir and surficial aquifers or the ground surface. This includes the hydrocarbon systems analysis (section 3.3.1), the regional hydraulic head analysis (section 3.3.2) and the Moonie oil field assessment (section 3.4.4). Based on this, the UQ-SDAAP project sponsored a masters student project to collect and examine hydrochemical evidence from surface and subsurface water samples to confirm or refute hydraulic communication along various Moonie fault segments (Mahlbacher 2019).

The Moonie fault system runs north from the NSW border near Goondiwindi to Moonie, and then north east from Moonie. The fault system intersects the overlying drainage features (streams) of the Weir River and tributaries and the Moonie River. North of Moonie, where the fault system heads north east, the fault system directly underlies the Moonie River for approximately 45 linear kilometres (Figure 48). At a number of points along these river systems, the fault system intersects: drainage features where the hydraulic head in the Blocky Sandstone aquifer is ~250 m and the surface elevation is 250 m or less (see section 4.3.2.1). The combination of these hydrogeological and geomorphological features suggests there is potential for the Blocky Sandstone Reservoir to discharge to shallow overlying drainage features. Two conceptual hypotheses were considered to investigate this potential connectivity in the Moonie area.

Both conceptual hypotheses would assume that the fault system is acting as a conduit for either groundwater or gas to the surface, along certain segments of fault system where it also intersects a surface drainage feature.

The water in the Precipice Sandstone aquifer is relatively fresh compared to many other Great Artesian Basin aquifers and has a Na-HCO<sub>3</sub> character (Grigorescu 2011b). The aquifer is generally thought to be isolated from the overlying Hutton Sandstone by the shale-rich Evergreen Formation aquitard (Hodgkinson et al. 2010). The majority of the hydrochemistry data of the Precipice Sandstone aquifer belong to wells in the northern depositional centre Surat Basin, close to the recharge areas. Ransley et al. 2015 and OGIA 2016 reported some regional variability in water quality in the Precipice Sandstone aquifer from fresh (northern Surat Basin) to brackish (in southern and eastern parts of the Surat Basin) with TDS ranging from 100 to 6000 mg/L with chloride content generally increasing with increasing TDS (Grigorescu 2011b).

Hydrochemical data from the Blocky Sandstone Reservoir are available from the Moonie oil field. Some of the well completion reports for Moonie wells (drilled between 1962 and 1965) contain water analysis data (major ions, pH and resistivity). A data quality review of this data found the following issues:

- No potassium measurements for 8 wells
- No fluoride measurements for all wells
- The absence of magnesium measurements for 6 wells (either not measured or below detection limit)
- Reported “measured total solids” being inconsistent (usually lower) than a total dissolved solids (TDS) calculated from the measured ion concentrations

As a result, this early Moonie oil field hydrochemistry data had a limited application; however, pH, calculated TDS and measured ion concentrations for 11 of 14 of the analyses were considered within an acceptable accuracy for this study. These 11 come from 8 different wells (M2, M4, M13, M18, M23, M24, M25a/M25b). The charge balance error of the 8 usable analyses is less than 5%.

Within the targeted area there are three different rivers/creeks that are tributaries to the Barwon River, which flows into the Murray-Darling drainage system. The Moonie River is a mainly an ephemeral river (DNRM 2015) flowing generally to the south-west and is joined by 13 minor tributaries before reaching its confluence with the Barwon River. The Moonie River is coincident with the Moonie fault over a short distance until crossing the highway north of the town of Moonie. Streamflow data from the water monitoring portal (*ibid*) for a gauging station at Flinton, approximately 90 km west-south-west of Moonie, indicate a mean annual flow volume of 10673 ML with the stream flowing 51-80% of the time. Between the towns of Moonie and Goondiwindi, the Weir River flows south-westwards towards the Barwon River catchment. Its headwaters are in western slopes of the Great Dividing Range in the state forests west of Moonie and is a main tributary to the Moonie River. A Weir River gauging station is located 55 km south-south-west of Moonie that shows an annual mean flow volume of 6521 ML with the stream flowing 20-50% of the time (*ibid*). Finally, Wyaga Creek is a small ephemeral tributary of the Weir River with a confluence north of Goondiwindi.

#### 4.5.3.2.1 New hydrochemical data

The above hypotheses were tested using a combination of hydrochemical (electrical conductivity (EC), pH and major ions), isotope (<sup>222</sup>Rn, δ<sup>2</sup>H-H<sub>2</sub>O, δ<sup>18</sup>O-H<sub>2</sub>O) and dissolved hydrocarbon gas composition data (C1-C4 hydrocarbons) collected along the surface drainage expressions. Sampling sites along the surface drainage system were focussed around the area overlying/near the underlying Moonie fault system. Samples for these parameters were taken in three locations:

1. Precipice groundwater samples from Moonie oilfield production wells (n=7). These samples were used to characterise the hydrochemical, isotope and hydrocarbon gas composition of deep Precipice groundwater/gases near the fault
2. Selected sites along the Weir River and its tributaries, upstream and downstream of the intersection with (n=9): i) the underlying Moonie fault system; ii) the 250 m pressure head estimation contour; and iii) the 250 m surface elevation contour
3. Selected sites along the Moonie River, upstream and downstream of the intersection with: i) the underlying Moonie fault system (n=11); ii) the 250 m pressure head estimation contour; and iii) the 250 m surface elevation contour, as well as along the upstream section of the Moonie River that directly overlies the Moonie Fault system

At all sites, EC (µS/cm), temperature and pH were measured. Water samples were taken at all sites by filling HDPE bottles and analysed for major and minor ions, including fluoride and including sulfate. Samples for dissolved hydrocarbons (C1-C4 gases) were collected and analysed.

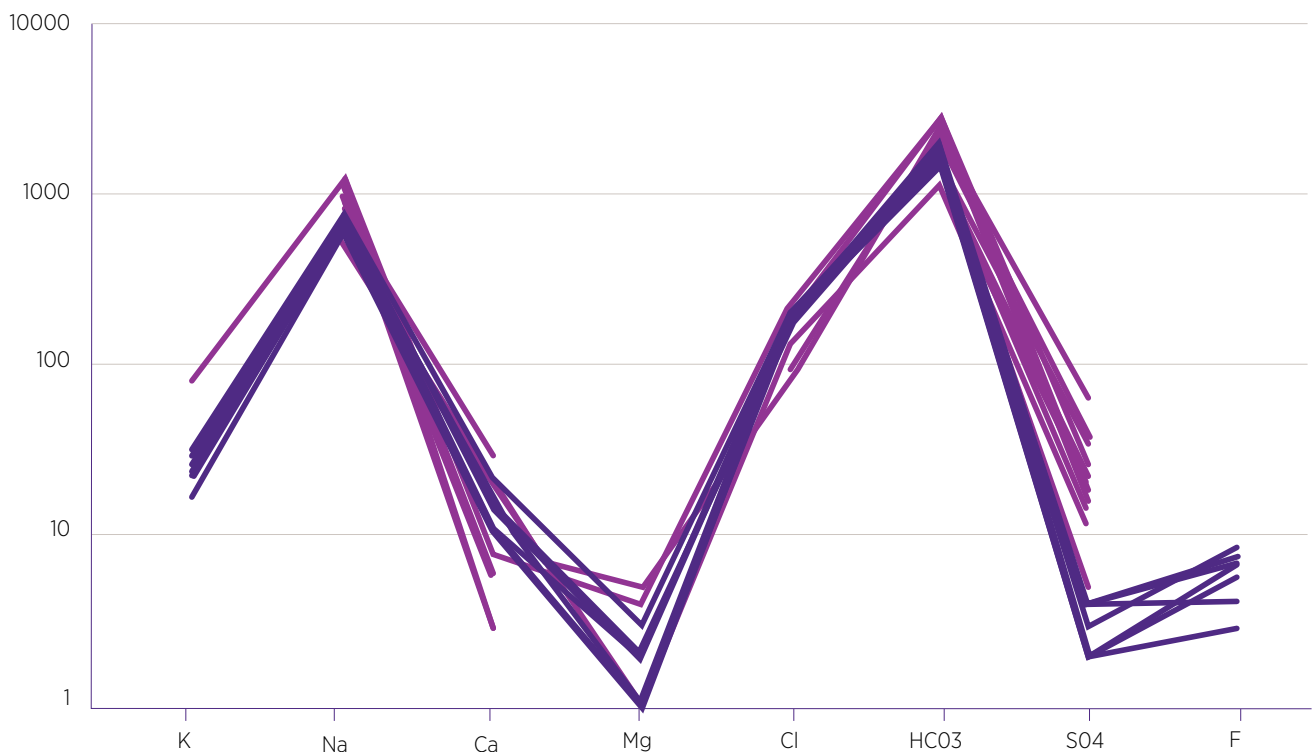
Stable isotopes of water (δ<sup>2</sup>H-H<sub>2</sub>O, δ<sup>18</sup>O-H<sub>2</sub>O) were analysed at UC Davis' Stable Isotope facility using a Laser Water Isotope Analyser V2 (Los Gatos Research, Inc. Mountain View, CA, USA). For isotopes, each sample was injected at least six times. The average of the last four injections is used for isotope ratio calculations. Isotope ratios for each sample were standardised against reference waters that have been calibrated using VSMOW. Precision for water samples is typically ±0.3 per mil for 18O and ±2.0 per mil for D/H. Final isotope values are reported relative to VSMOW.

A RAD-7 (DurrIDGE Co.) instrument was used to measure <sup>222</sup>Rn activities (Bequerels per m<sup>3</sup> of water (Bq m<sup>-3</sup>)) in surface water. Methods for analysis followed those described in Burnett and Dulaiova 2006. Sampling involved filling 1L HDPE bottles with no headspace at the stream site. Approximately 0.5 L of the sample was then transferred to a bottom-filling a glass flask and <sup>222</sup>Rn was subsequently degassed for 5 minutes into a closed air loop of known volume. Counting times were 2 hours for surface water and 20 minutes for groundwater.

#### 4.5.3.2.2 Discussion and interpretation of up fault leakage

Groundwater salinity from the original Moonie oil field wells that were tested when drilled (1960's) was slightly brackish, with TDS ranging from 1800 mg/L to 4000 mg/L. Samples collected in 2018 after decades of production had a smaller TDS range, 2500-3000 mg/L (Figure 86). Samples from the 1960s also had relatively higher sulfate than those collected in 2018, with an average concentration of 28.5 mg/L and 6 mg/L, respectively. It is not clear if these small temporal differences in hydrochemistry are due to changes in hydrochemistry that are associated with spatial variability of aquifer hydrochemistry and long-term groundwater pumping due to oil production, or are associated with some contamination (e.g. residual drilling fluids) in the earlier samples. In any case, the data is sufficient to characterise Moonie oil-production well hydrochemistry as slightly brackish Na-HCO<sub>3</sub> water types. This water type is common in sedimentary and alluvial aquifers of the Surat (Baublys et al. 2015; Owen and Cox 2015; Ransley et al. 2015; Owen et al. 2016a), and as such, major ion hydrochemistry does not provide a robust stand-alone indicator for possible Moonie fault migration. However, given the water is brackish, any discharge along the fault to surface drainage systems could produce a detectable change in EC, and this parameter was used to assess potential discharge in combination with other data.

**Figure 86** Major ion concentrations for Moonie produced water (from the Precipice Sandstone aquifer) from the 1960 when the wells were drilled (grey lines) and for recently acquired produced water samples form 2019 (black lines).



#### Hydrocarbon gas composition

Hydrocarbon composition of thermogenic methane, such as that associated with oil reserves, can be distinguished by the ratio of C1 to the sum of C2-C6 gases, where C1 is methane, and C2-C6 are higher chain hydrocarbons such as ethane, propane, butane etc. C1/C2-C3 ratios < 100 are typical of thermogenic gases, i.e. they are hydrocarbon gases not produced via microbial processes (Bernard et al. 1977; Golding et al. 2013). All the Moonie oil field samples had C1/C2-C6 ratios of dissolved hydrocarbons < 100 (min = 4, max = 19), which is indicative of thermogenic hydrocarbon (Table 27). This result is expected, given the oil reserve at this location is near the fault in the Precipice Sandstone aquifer (see section 3.3.1).

**Table 27** C1-C4 concentrations of Moonie oil field production wells. Units = µg/L. DL = 10 µg/L

Well	Methane	Ethene	Ethane	Propene	Propane	Butene	Butane	Bernard Parameter
M2	5190	<10	109	<10	314	<10	894	4
M21	2480	<10	117	<10	296	<10	384	3
M30	6040	<10	79	<10	74	<10	162	19
M31	3800	<10	72	<10	118	<10	333	7
M32	3470	<10	66	<10	111	<10	203	9
M34	2080	<10	50	<10	175	<10	295	4
M37	5200	<10	123	<10	182	<10	629	6

Since hydrocarbon composition in other overlying commercial reservoirs (e.g. Walloon Coal Measures coal seam gas production) in the Surat Basin are predominantly biogenic gases comprised mostly of methane, the C1/(C2-C4) ratios are typically > 100 (Hamilton et al. 2014; Baublys et al. 2015; Owen et al. 2016b). As a result, the thermogenic, low C1/(C2-C4) ratios of the Moonie oil field hydrocarbon provide a distinct hydrocarbon indicator of deep Precipice Sandstone Moonie oil field gases near the fault zone. This was used as a potential indicator of gas migration along the Moonie fault to surface drainage systems.

#### Fault-to-surface connectivity indicators

The conceptual hypotheses assumes that the likely points of connectivity from the fault to the surface could occur along one or more of the Moonie fault segments. Where these intersect overlying streams of elevation at or below 250 m elevation, they could represent hydraulically realistic discharge locations given that the hydraulic head in the Blocky Sandstone Reservoir at this location is about 250 m. Based on the existing information on Precipice Sandstone aquifer hydrochemistry, and using a combination of hydrochemical, isotope and gas composition data, the following theoretical indicators of potential evidence of connectivity between the fault (Precipice Sandstone aquifer) and surficial drainage features were developed:

For hydraulic connection, a combination of:

- An increase in stream EC
- A change in pH
- High Radon ( $^{222}\text{Rn}$ ) activities (> 1000 Bq / m<sup>3</sup>) that indicate deep (non-hyporheic) groundwater contributions to the stream
- Dissolved hydrocarbon gases, including the presence of higher chain hydrocarbons such as ethane, propane and butane. Dissolved gas C1/(C2-C3) ratios < 100 would be strong indicators of gas migration from the deeper precipice along the fault to the surface

Or, for gas migration only:

- Dissolved hydrocarbon gases, including the presence of higher chain hydrocarbons such as ethane, propane and butane. Dissolved gas C1/(C2-C3) ratios < 100 would be strong indicators of gas migration from the deeper precipice along the fault to the surface

Even though hydrocarbon gases may migrate independently of groundwater, due to buoyancy, it is logical to expect that any free gas would equilibrate with overlying surface water, resulting in a dissolved gas component in surface waters. As a general rule, if connectivity was occurring due to the fault acting as a discharge point-source of groundwater and/or gases, sharp changes in the above-listed parameters could be expected at/near the points of discharge and subsequent downstream dilution. In order to address this, both upstream and downstream of the potential fault-to-surface connectivity areas for relevant streams was sampled.

#### Surface water sites

**No evidence of point source-discharge of groundwater or gases to surface waters** drainage systems along or across the underlying Moonie fault system was found. This result could be due to there being no migration pathways, or due to the original pathways being shut down today by 30+ years of Moonie production aquifer pressure depletion. It would suggest that perhaps the second hydraulic head interpretation for the Blocky Sandstone Reservoir (see section 3.3.2) is the preferred option where the entire of the aquifer system is dominated by northward and north eastward flow toward discharge either at the Dawson River in the north or the Lockyer Valley in the Clarence Morton basin to the east. Details of the Moonie hydrochemical analysis and fieldwork can be found in Mahlbacher 2019.

### 4.5.3.3 Fault reactivation potential

It is important to examine the implications of fault reactivation in the presence of changing formation pressure during CO<sub>2</sub> injection. As the pore pressure rises due to fluid injection the stress field in the reservoir changes, which could lead to unwanted seismicity along pre-existing faults, as has been observed in some geothermal projects (Deichmann et al. 2007; Moeck et al. 2009). The pressure at which a pre-existing fault slips can be estimated based on a characterisation of the in-situ stresses in the reservoir, the fault zone architecture and the subsequent stress changes caused by pore pressure increase. Due to the uncertainties regarding the stresses in the deeper part of the Surat Basin, and in the location and geometries of potential faults, a Monte Carlo approach to estimate fault reactivation pressures was used. This was similar in principal to the method described by Walsh III and Zoback 2016. A detailed description of the analysis for UQ-SDAAP is presented in Rodger et al. 2019a.

The slip tendency was first calculated at initial pore-pressure (assumed to be hydrostatic), and then recalculated as pore-pressure was increased. This step-wise method was employed due to the potential for changes in the stress regime as pore-pressure changes, which alters the angle used in the calculation of slip tendency. When slip tendency reached a value of one (indicating a fault slip event) the associated pressure increase was recorded, and the 'experiment' was repeated using new input parameters. After ten-thousand 'experiments' the results were combined. The analysis was performed considering two cases. The first was the theoretical worst-case scenario where the fault had zero cohesion. For the second, the cohesion was considered as a uniform distribution between zero and the cohesive strength of the intact rock from the formation.

For the cohesionless case at a depth of 2350 m, the resulting P90<sup>14</sup> value for the pressure increase at which fault slip would be expected is approximately 30,100 kPa, with a mean value from all 'experiments' of 34,200 kPa. These values suggest that the pressure at which fault slip would occur are P90 = 53,150 kPa; mean = 57,250 kPa. This is likely to be higher than the FBHP set to avoid inducing fractures in the Blocky Sandstone Reservoir) of any injection well, even in this theoretical worst case. Any cohesion that existed would increase the pressure required to cause fault slip. Since pressure during injection decreases away from the well, any potential injection sites should be located away from significantly faulted areas (to reduce the risk of CO<sub>2</sub> leakage through faults). **It is very unlikely that fault slip would occur due to injection operations if these BHP limits were adhered to.**

### 4.5.3.4 Summary of fault analysis and up-fault leakage potential

**There is conflicting evidence regarding the hydraulic transmissivity of the Moonie Goondiwindi fault system. The hydrocarbon system analysis and Moonie oil field analysis would suggest that over geological time hydrocarbons have migrated between deeper source rocks and shallow aquifers up segments of the fault system. This would imply some similar hydraulic connection of the formation water system, although there is no present day hydrochemical or hydraulic evidence to suggest that the Blocky Sandstone Reservoir has a hydraulic connection either to a shallow aquifer or the water table. This may be due to pressure draw-down effects of decades of Moonie oil field production. Therefore, the degree of hydraulic connection or isolation provided by the Moonie Goondiwindi fault system to the Blocky Sandstone Reservoir remains unclear.**

Based on geomechanical analysis and a statistical approach to likely fault orientation, the risk of fault reactivation is small even for large-scale injection. The largest risk that has been identified is that very small offset strike slip faults may exist but are unresolved with the current seismic data coverage. Were these faults to occur near a notional injection well, it is likely to induce a barrier to the lateral propagation of injection pressure. This could result in more rapid than anticipated injection pressure increase that could limit effective injectivity.

## 4.5.4 Legacy wells

**In carbon storage "containers" (section 4.4), contain legacy wells represent a leakage risk if the injected CO<sub>2</sub> were to come into contact with the well at some stage in the project lifecycle. The main response to this is to maximise the offset between injection sites and the location of these wells as has been assumed in this research (section 4.7). In addition, further characterisation is required (section 5.3) and special measures would be taken in any field development to baseline and monitor such potential leak features (section 4.10). UQ-SDAAP research suggests that the risk can largely be avoided and residual risk can be monitored.**

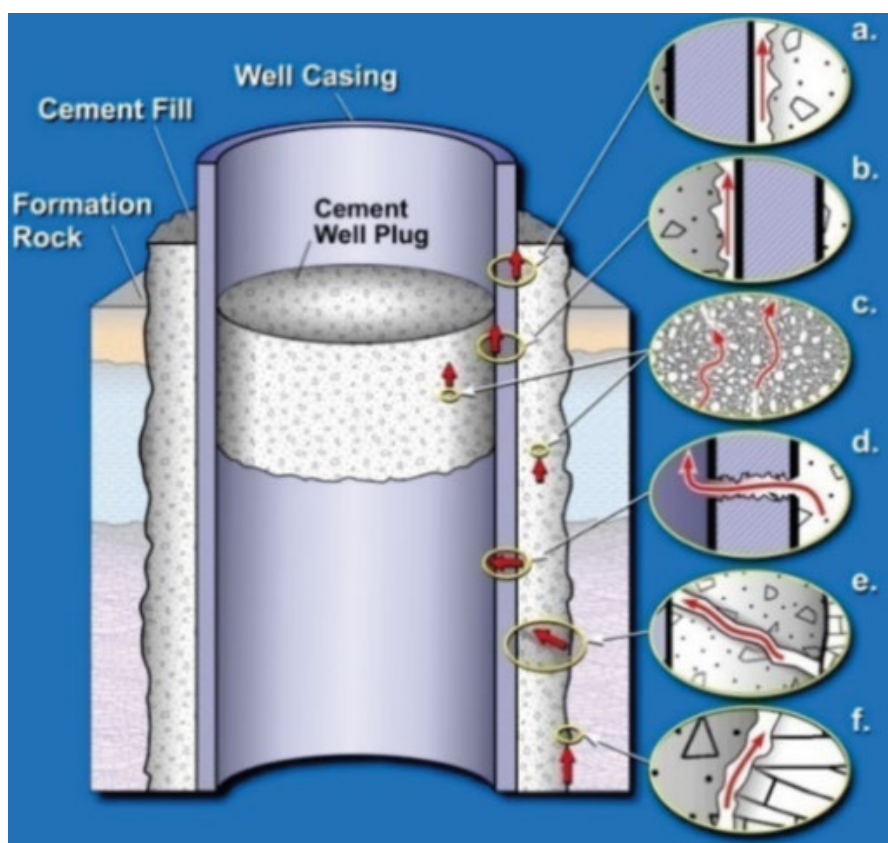
The main leakage pathways for CO<sub>2</sub> along the wellbore is the leakage through the cement plug inside the casing and leakage along the cement/casing or cement/formation interfaces (Carey et al. 2007). During well construction, open-hole sections are covered by running a steel casing and cementing the casing to the formation by circulating a cement slurry down the casing and up the annular space. The cement protects the steel casing from formation fluids or injected fluids and prevents these fluids from migrating upwards through the annular space. Defects that might occur during the well construction and well operation

<sup>14</sup> P90 refers to the value which is exceeded by 90% of the estimates (i.e. a low case)

can affect the well integrity (Manceau et al. 2015). Some key locations subject to failure of well integrity are depicted in Figure 87. While newly developed wells (including the CO<sub>2</sub> injection and monitoring wells for the CCS project) are governed by current regulations and designed to sustain integrity according to current base practice, wells drilled and abandoned in the past may have been subject to less strict governance, and therefore are considered to be the greater risk to long-term storage integrity.

Bachu and Watson 2009 analysed more than 300,000 wells in Alberta, Canada, where they found the majority of leakage incidents are due to time-independent mechanical factors as a result of issues during well construction or abandonment (mainly cementing) and not to time-dependent factors such as geochemical cement degradation. Therefore, in theory wells can be evaluated for cement/casing and cement/formation bonding to establish integrity risk to upward migration of CO<sub>2</sub> and/or CO<sub>2</sub>-saturated brine. In practice, there is a general lack of knowledge about legacy wells completion condition, and formerly abandoned wells may no longer be accessible. Consequently, they cannot be easily assessed for well integrity and remediated if required (van der Kuip et al. 2011). If these wells cannot be assessed as to their individual risk level, then the site selection process can choose to avoid or, where possible, re-complete them (Bachu and Celia 2009).

**Figure 87** Potential leakage pathways along an existing well: between cement and casing (paths 'A' and 'B'), through the cement (C), through the casing (D), through fractures (E), and between cement and formation (F). (Gasda et al. 2004).



The UQ-SDAAP evaluation considered a large area of the south-central Surat Basin (a 100 km radius from the Fantome 1 well [a well of interest for dynamic testing near the deepest part of Surat Basin in the early stages of the UQ-SDAAP project]). In this region are 242 wells that penetrate the top of the Blocky Sandstone Reservoir (Yosafi 2018). Of these, 45 are producing or are suspended oil or gas wells with production casing to total depth (i.e. these are accessible for casing integrity evaluation and remediation if required), 103 have been converted to water bores with a cement plug arrangement with some open-hole sections, and 94 are permanently plugged and abandoned (P&A) with some combination of cement plugs and open-hole sections. Of the 197 water bore conversions of P&A's there are 147 that have sufficient information in well completion reports to determine the location of cement plugs relative to casing and open-hole sections. Of the 197 wells, 79 have cement plugs within the Blocky Sandstone Reservoir, 34 have cement plugs within the Transition Zone and 37 have plugs within the Ultimate Seal (Yosafi 2018). The average cement plug length is 51 m with ~75% of the plugs having a length between 40-50 m (Figure 88). The majority of the wells were drilled either during the 1960s or the 1980s (Figure 89). The UQ-SDAAP project took the approach of conducting this initial cursory evaluation of the legacy well risk, however in the notional site selection process an "avoidance" strategy was adopted to obtain the lowest possible risk (see Wolhuter et al. 2019 a). Any future actual site selection process would likely re-consider legacy wells in the vicinity of any proposed sites to be considered for carbon storage.

**Figure 88** The distribution of cement plug thickness for wells within 100 km radius of the Fantome 1 well (Yousafi 2018).

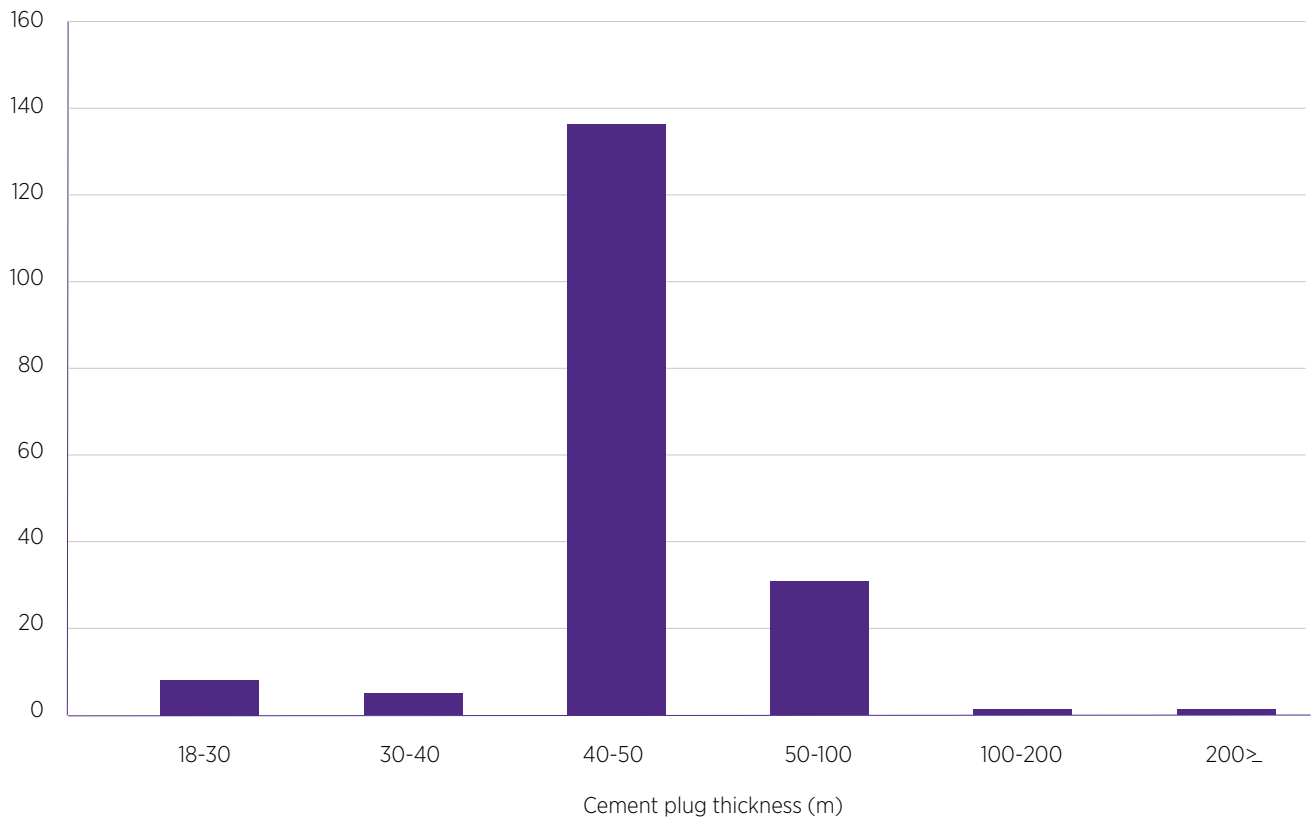
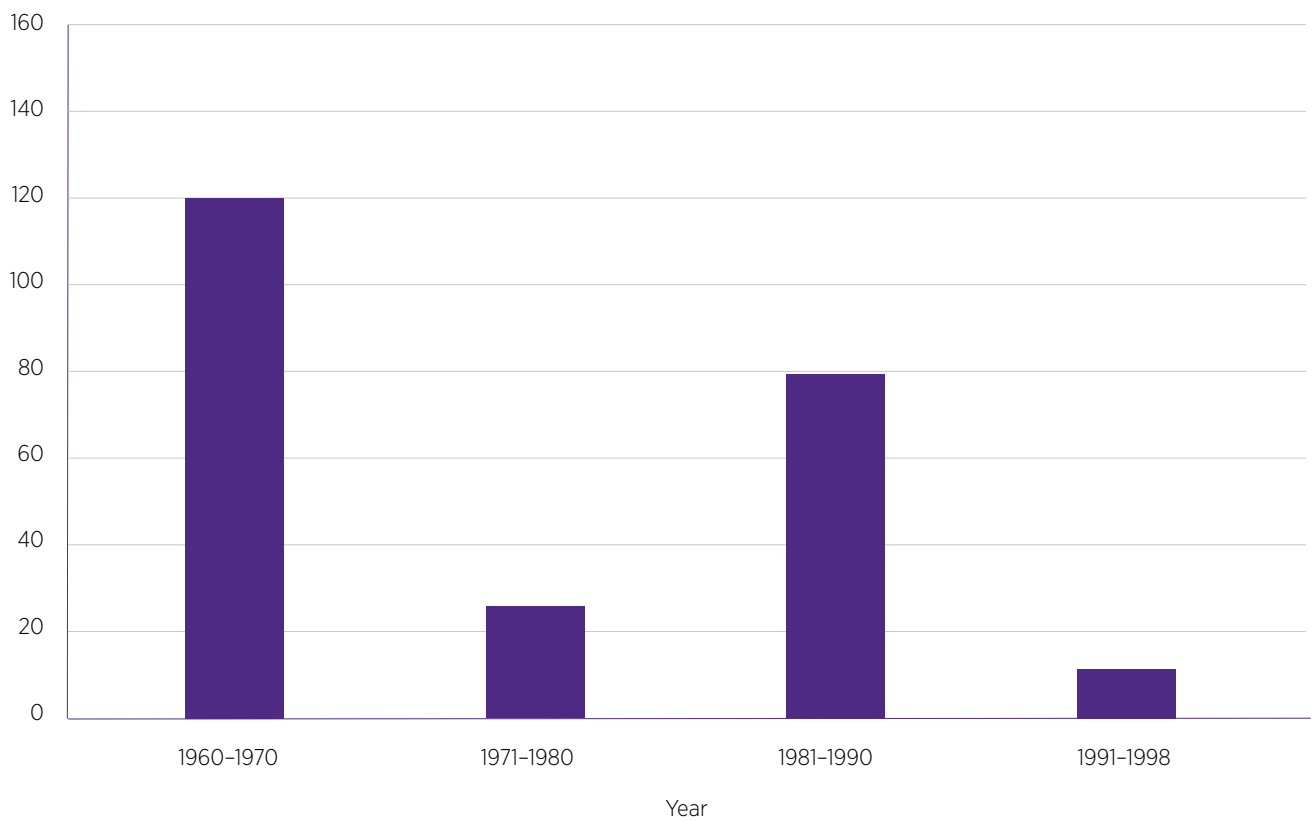


**Figure 89** The distribution of legacy wells within 100 km radius of the Fantome 1 well, by decade (Yousafi 2018).





## 4.5.5 Sealing capacity of the Transition Zone and Ultimate Seal

**Geological evidence and reasoning, as well as significant managed aquifer recharge, hydrogeological and hydrocarbon data and analysis are consistent with a valid seal hypothesis. Scenario modelling described hereunder, further supports a prediction that little or no injected CO<sub>2</sub> would invade the Transition Zone and none would reach the base of the Ultimate Seal within the 100-year modelling timeframe. Site specific data is now needed to quantify key pressure limits.**

The Transition Zone is the lithologically heterogeneous interval between the top of the Blocky Sandstone Reservoir and bottom of the Ultimate Seal. In general, the majority of the Transition Zone appears to be low permeability (<1 mD). Some extremely low permeability (or tight) parts of the Transition Zone could act as seals, the lateral extent is not fully resolved. Sequence stratigraphic analysis suggests that mid Transition Zone “Maximum Flooding Surfaces” (MFS-1, Figure 20) is regionally correlatable, though does not form a continuous seismic reflection event. This could be because it is either discontinuous or too thin to resolve.

Other sandier parts have sufficient porosity and permeability to be considered reservoirs, such as the “56 Sands” in the Moonie oil field or the Lower Evergreen Formation Sandstone intervals on the Roma Shelf (e.g. Borah Creek, Colgoon, Digeridoo, Digger, Kincora, Sandy Creek, Carbean, Newstead, Yarrabend and Yellowbank fields). The overall lateral flow behaviour of the Transition Zone, in any area, is largely dependent on the presence and connectedness of high permeability sandy streaks. The vertical flow and pressure transmission is dependent on the continuity of the main flooding event (MFS-1).

The Ultimate Seal marked by the laterally continuous ironstones (La Croix et al. 2019a) represents the lowest bulk permeability of the UQ-SDAAP study area stratigraphy (Harfoush et al. 2019a, 2019b and Honari et al. 2019a). It is lithologically consistent, correlatable over a wide area and is represented by a continuous seismic reflector throughout the study area (Figure 20).

The assessment of sealing capacity for carbon storage the Transition Zone and Ultimate Seal must be considered in the framework of multi-phase flow (CO<sub>2</sub> and formation water) where wettability and the relative saturation by each phase significantly impact the relative permeability of each phase. Capillary pressure is the difference in pressure across the interface between two immiscible fluids caused by capillary forces. Considering an oil/water system in a single capillary tube, the capillary pressure can be calculated using the Young-Laplace equation:

$$p_{oil} - p_{water} = P_c = \frac{2\sigma \cos \theta}{r}$$

Where,  $p$  is the phase pressure,  $P_c$  is capillary pressure,  $\sigma$  (in some literature  $\gamma$ ) is the interfacial tension,  $\theta$  is the wetting angle of the liquid on the solid surface (which indicates the wettability of the system), and  $r$  is the radius of the capillary tube. It is important to note that increasing  $r$  (the radius of the capillary tube) decreases the capillary pressure.

Capillary pressures are particularly important when considering the behaviour of the CO<sub>2</sub>-water system in the Transition Zone and Ultimate Seal if CO<sub>2</sub> is the non-wetting phase. Seals in hydrocarbon bearing formations where the hydrocarbon is the non-wetting phase are often “membrane seals”, where migration of hydrocarbons is prevented by capillary effects rather than simply by low leakage rates, as is the case for hydraulic seals. Membrane seals can fail, allowing hydrocarbons to migrate through them, if the capillary threshold pressure is exceeded. This is the pressure at which “a continuous thread of non-wetting fluid extends across the sample” (Underschultz 2007). The threshold pressure is slightly higher than the capillary entry pressure. While the non-wetting phase could *enter* a seal at the capillary entry pressure, it could not pass *through* until the threshold pressure is reached. Often seal capacity is estimated by calculating the height of a column of fluid (e.g. oil or gas) which would cause the pressure due to the buoyancy of the hydrocarbon to equal the threshold pressure of the seal. In essence, this would be the point where any further increase of the column height would raise the pressure beyond the threshold pressure and cause the membrane seal to fail.

### 4.5.5.1 Capillary pressure data

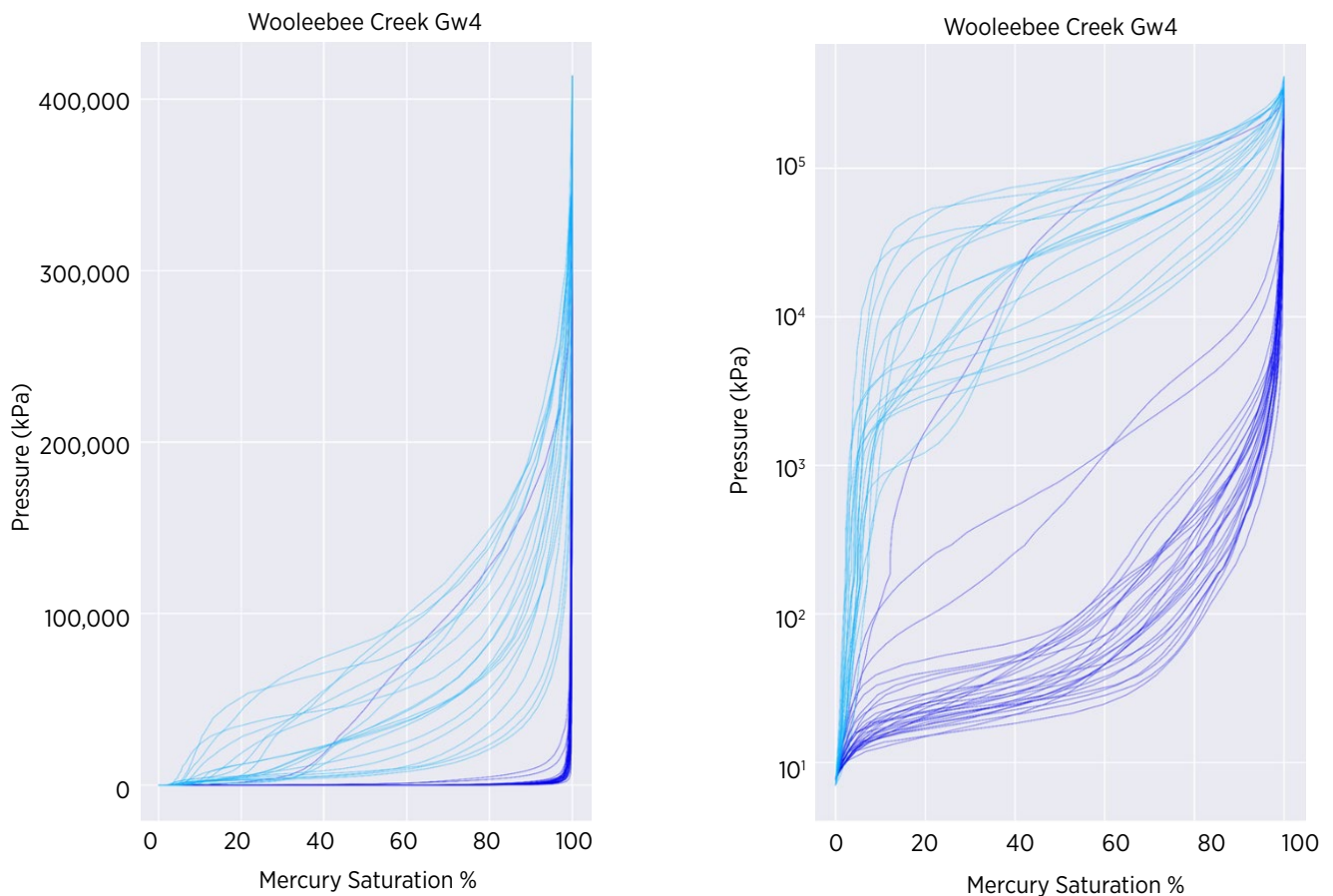
Relevant capillary pressure data was available from 3 wells:

- MICP data, including raw data, from Moonie 12 (Transition Zone only)
- MICP data, including raw data, from Woleebee Creek GW 4 (all three zones).
- CO<sub>2</sub>/Brine plots and analysis from West Wandoan 1 SCAL (Blocky Sandstone Reservoir Only)

The data from Moonie 12 was a seal capacity report to Bridgeport Energy, which had been used to determine whether or not the “Seal” in the Moonie field (which is considered part of the Transition Zone in the UQ-SDAAP scheme) had sufficiently high threshold pressure that hydrocarbons would “spill” out of the Moonie anticline before a membrane seal failure occurred. Three core samples were analysed using mercury injection capillary pressure (MICP) analysis, which indicated air/mercury threshold pressures of 15,396 kPa, 42,147 kPa and 48,332 kPa, equivalent to seal capacities of 319 m, 953 m and 1100 m of oil. The capillary pressure curves from Moonie 12 were not used directly in creating the curves used in the UQ-SDAAP numerical simulations, but are reported here to allow comparison.

Extensive MICP data from all three zones was available from Woleebee Creek GW4 and was used as the basis for estimating capillary pressure curves which would be used in the UQ-SDAAP Models. The MICP curves from this well are shown in Figure 90. Air-mercury threshold pressures for the Blocky Sandstone Reservoir were typically between 12.5 kPa and 25 kPa, while the Transition Zone and Ultimate Seal threshold pressures were *much* higher, ranging from 1100 kPa to 63,000 kPa. These higher pressures were consistent with the results from Moonie 12. The Woleebee Creek GW4 data, and a description of how it was used to create input curves for UQ-SDAAP models, is discussed in more detail in Section 4.8.

**Figure 90** MICP data from Woleebee Creek GW4. Both plots show the same data, but the right-side plot uses a log scale for pressure. Dark blue lines are data from “Precipice Sandstone” (Blocky Sandstone Reservoir) while light blue lines are from “Evergreen Formation” (Transition Zone/Ultimate Seal).



Some CO<sub>2</sub>-brine capillary pressure data for the Blocky Sandstone Reservoir was available from the SCAL reports for West Wandoan 1 (the same analysis which provided relative permeability data). Capillary pressure curves were fit to the experimental data based on the Van Genuchten model:

$$P_c = P_e \left( \left( \frac{S_w - S_{wr}}{1 - S_{wr}} \right)^{1/\lambda} - 1 \right)^{(1-\lambda)}$$

Where  $S_{wr}$  is the residual water saturation,  $P_e$  represents the entry pressure, and  $\lambda$  alters the curvature. The report on this analysis indicates the best fit for most plugs was achieved using  $P_e = 1.72\text{kPa}$ ,  $S_{wr} = 0.26$  and  $\lambda = 0.4$ . The experimental data was scattered. Higher permeability plugs (greater than 2000mD) needed higher values of  $\lambda$  for the Van Genuchten model to fit the data, but all models used  $P_e$  less than 17.5kPa (ANLEC 2016).

Limited relative permeability data is available for the Blocky Sandstone Reservoir, Transition Zone and Ultimate Seal in the UQ-SDAAP study area. The data that is available suggests that the Blocky Sandstone Reservoir is likely to have lower relative permeability to CO<sub>2</sub> compared with other analogous sandstones described in the literature, which may limit injectivity.

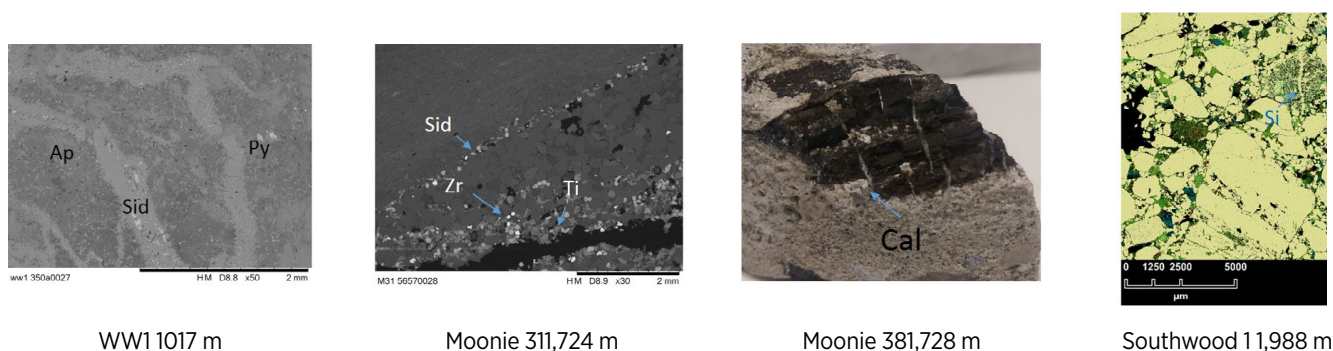
Capillary pressure data is particularly important in the Transition Zone as it determines whether or not CO<sub>2</sub> is likely to migrate vertically during and after injection. The data that is available suggests that some parts of the Transition Zone act as a good membrane intraformational seal (assuming that it is water wetting), as seen in the Woleebee Creek GW4 and Moonie 12 wells. However, it is unclear how representative these samples are of the Transition Zone across the Surat Basin, and particularly in the areas identified as notional injection sweet-spots. The Transition Zone in the Woleebee Creek GW4 well has generally very low permeability (typically <0.1 md, and in some cases reported as 0.00 md or “N/A”), and thus may indicate higher capillary pressures than would be seen elsewhere in the basin. Note that core sampling of the Moonie 12 well was targeting a seal, and thus samples were likely bias towards high capillary pressures. Details of the capillary pressure data and analysis for UQ-SDAAP can be found in Rodger et al. 2019b.

#### 4.5.5.2 Impact of fractures

Various drill cores sampled, showed evidence of natural fractures, fracture fills of carbonate minerals and presence of hydrothermal minerals that could be related to previous natural CO<sub>2</sub> alteration (natural analogues). Examples include in the Transition Zone (Evergreen Formation) and Ultimate Seal (Westgrove Ironstone Member) in the GSQ Chinchilla 4 and West Wandoan 1 wells, parts of the Moonie 38 well Transition Zone, the mudstones in the Transition Zone (between the 58 and 56 sands) of the Moonie 31 well, calcite cemented zones in the Moonie 22 well, and the Southwood 1 Transition Zone core (Figure 91).

Natural fracture fill minerals include siderite, calcite, Ti-oxides, apatite, pyrite, silica, and barite cements. Fractured quartz grains in the Southwood 1 (e.g. Figure 91) and various Moonie wells could indicate potential for fracture flow, given the relatively high permeabilities in the Moonie reservoir sands (58 and 56 Sands). Natural analogue data is useful to understand processes over geological timescales and is essential to validate geochemical model outputs. For example, alteration processes predicted in this chapter include plagioclase and chlorite conversion to siderite and ankerite. This is consistent with observations in natural systems with high CO<sub>2</sub> content (Higgs et al. 2015; Watson et al. 2004).

**Figure 91** Examples of natural mineral trapping alteration and natural fractures in core from the West Wandoan 1 well (WW1) Ultimate Seal, Moonie 31 and 38 wells Transition Zone, and Southwood 1 well Transition Zone. Ap = apatite, Sid = siderite, Py = pyrite, Zr = zircon, Ti = Ti-oxide cement, Cal = calcite, Si = silica cement.



For more details on the analysis of fractures observed in core for the UQ-SDAAP area of interest, see Pearce et al. 2019.

Evidence of natural fractures, fractured quartz grains, or previous hydrothermal fluid movement were present in several Moonie and Southwood 1 wells core samples (along with the Ultimate Seal in several managed aquifer recharge (MAR) sector northern wells). Given the high reported bulk permeabilities in the Moonie reservoir sands (58 and 56 Sands) for example it is possible that these are influenced by fracture permeability. The Southwood 1 well Transition Zone core samples also appeared different to those in the MAR sector northern wells, being more quartz rich and containing small amounts of disseminated siderite cements, and fractured quartz grains.

#### 4.5.5.3 Vertical migration in the Transition Zone from dynamic simulation

Sector scale static models of three various possible Transition Zone stratigraphic conceptualisations were constructed to capture the range of uncertainty in Transition Zone flow characteristics (see La Croix et al 2019e). Numerical simulations were used to ‘test’ these different Transition Zone conceptualisations in order to assess how much water and CO<sub>2</sub> are likely to flow into (or through) the Transition Zone in each case. These models also assess the likely temperature reduction in the Transition Zone caused by CO<sub>2</sub> injection, which is important due to the thermal effects on fracture pressures (see Rodger et al. 2019a).

Static models of the three Transition Zone conceptualisations were named after wells which were considered to best represent each: Moonie (most sandy and permeable), Meandarra (base case), and Woleebee Creek (least sandy and permeable). These models covered a 10 x 10 km area, extending from the top of the Ultimate Seal to the base-Surat Unconformity at the base of the Blocky Sandstone Reservoir (approx.190 m total thickness). Two additional cases were run using the Moonie-type static model (the model that resulted in the most flow into the Transition Zone). Both had zero capillary pressure throughout, representing CO<sub>2</sub> wet relative permeability cases and thus no membrane seal effects. In these cases, the flow rate of CO<sub>2</sub> through the Transition Zone is limited only by permeability, not by capillary effects. In the second of these cases, the well was controlled to inject while limited by wellhead pressure at 15 MPa. This final case represented a worst-case scenario for vertical CO<sub>2</sub> migration, where the pressure around the well would be high during injection (and thus increase viscous flow), but capillary effects would not limit the vertical migration of CO<sub>2</sub>. In all cases, simulations included 30 years of injection and continued for another 30 years post-injection. The details of the Transition Zone modelling workflow for the three sector models are described in Rodger et al. 2019c.

Dynamic simulations indicate that, in any of these cases, the Transition Zone acts as an effective barrier, limiting vertical migration of CO<sub>2</sub>. It seems that, even for the sandiest and most permeable Transition Zone types, the Transition Zone is likely to have such low permeability that any flow (of CO<sub>2</sub> or water) through it will be limited.

Even in a worst-case scenario, which combined the most permeable and most sandy Transition Zone type, zero capillary pressure and high injection rates, only 3.6% of the injected CO<sub>2</sub> entered the Transition Zone in the 30-year injection period and 30 years post injection. **Even in this worst case, the CO<sub>2</sub> did not migrate beyond the lowest 10 m of the Transition Zone during the simulation period.**

In all cases, the lowest part of the Transition Zone was cooled by up to 15°C during the simulation, which caused an apparent reduction in pressure in parts of the Transition Zone where the permeability was low and fluid flow was near zero. An example of this occurring in a field trial is described by Ennis-King et al. 2011.

These models indicate that the Transition Zone is an effective barrier to vertical CO<sub>2</sub> migration. However, future efforts should focus on reducing uncertainty in model parameters through an appraisal plan that can provide additional information on the depositional setting and petrophysical properties (including wettability and capillary pressure) of the Transition Zone (especially near the notional injection site where current data control is poor). This would most reasonably be achieved by drilling a well to the base-Surat unconformity, and collecting core.

## 4.5.6 Assessment of potential to fracture at the injection well

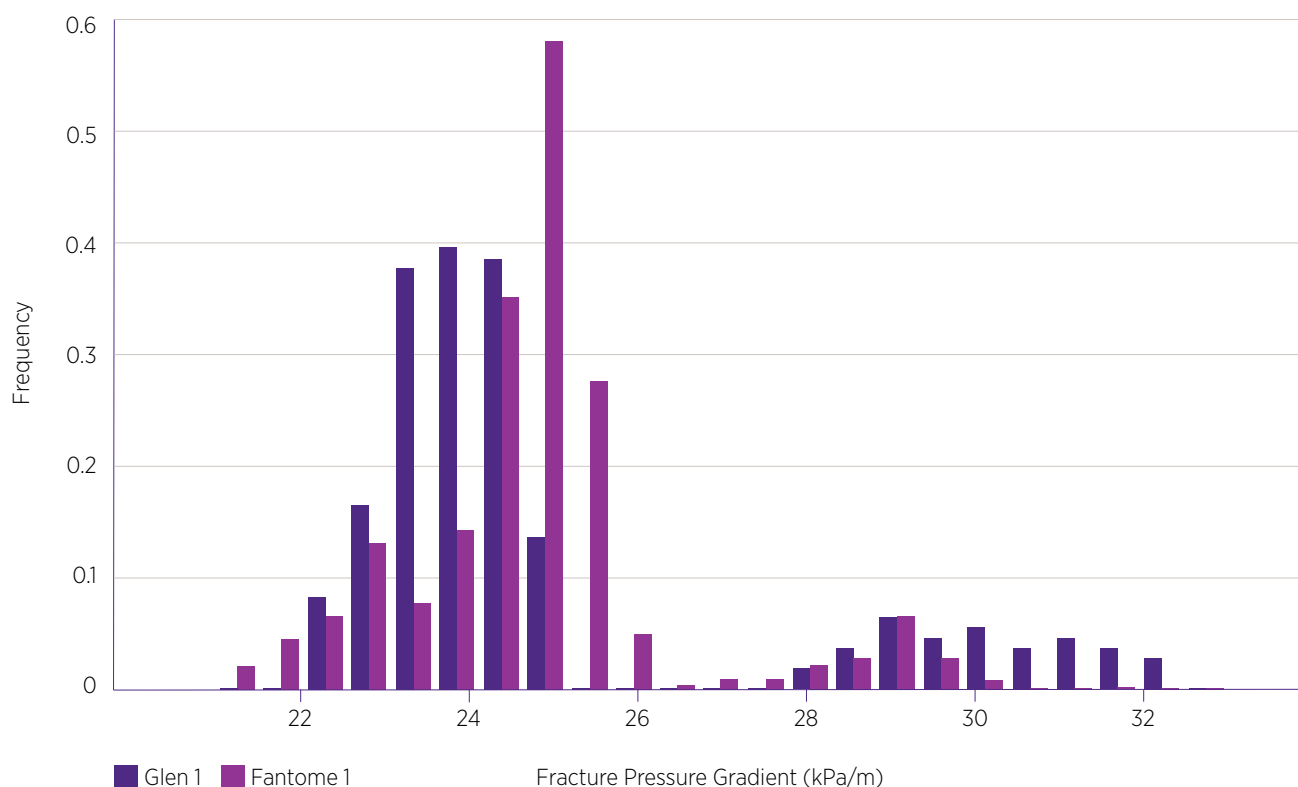
Consideration of containment potential must assess the risk of fractures induced by the injection operations themselves. In essence this risk is manageable by maintaining injection pressures below some critical limit. However, reducing these pressures will lead to reduced injection rates and could impact materiality. Analysis discussed hereunder, shows that a feasible and easily manageable injection scheme can be operated well below fracture pressure estimates for the Transition Zone or Ultimate Seal, even accounting for reductions in temperature.

If the pressure around the injection well is increased sufficiently, it is possible to mechanically break the rock, inducing fractures. The pressure at which this occurs is the fracture pressure<sup>15</sup> of the formation. In many cases fracturing the formation around the well while injecting, is acceptable, and is often beneficial as it improves permeability and increases injection rates. In other situations, it may be necessary to avoid fracturing, e.g. if there are concerns around fractures propagating into or through an overlying sealing formation. If this is the case, the bottomhole pressure (BHP) of the injection well should not be allowed to increase above the fracture pressure. In fact, a safety margin should be employed to ensure this does not occur, with BHP limited to some fraction of the estimated fracture pressure. In this case 90% of the fracture pressure will be used as the BHP limit of injection wells, as had been used in Canadian CO<sub>2</sub> injection operations (Bachu and Gunter 2005).

In order to estimate the fracture pressure for the Blocky Sandstone Reservoir identified as the notional target for CO<sub>2</sub> storage by the UQ-SDAAP, mechanical earth models (MEMs) were created for wells which had the required datasets (See Appendix A of Rodger et al. 2019a for details). MEMs are numerical models representing the geomechanical state of the subsurface, and include the *in-situ* stresses and rock mechanical properties of the formations. These models are calibrated by ensuring the minimum stress calculated in the MEM for a well matches the minimum stress determined by injection tests carried out in the well and validated using wellbore stability analysis.

MEM wellbore stability analysis for two representative Surat Basin wells with the required input datasets (i.e. Fantome 1 and Glen 1), indicated that isothermal formation fracture gradients are expected to be ~22.20 kPa/m (0.98 psi/ft) (Figure 92). This value will be used as the base case isothermal fracture gradient, with 21.20 kPa/m and 23.20 kPa/m being the low and high case values to allow some sensitivity analysis. Uncertainty in the fracture gradient, should be reduced by suitable testing (e.g. DFITs or XLOTs) during an appraisal program.

**Figure 92** Isothermal fracture pressure gradient in the Blocky Sandstone Reservoir as calculated from MEMs for two wells.



<sup>15</sup> Fracture pressure (or gradient) can be used to describe a number of different pressures. In this case it refers to the formation breakdown pressure, i.e. the pressure at which intact rock around the well breaks, creating new fractures.

An additional consideration when assessing the actual fracture pressure as a limit for the injection well BHP, is the further reduction in fracture pressure due to thermal effects of injecting relatively cool CO<sub>2</sub> in a relatively warm reservoir.

#### 4.5.6.1 Thermal effects on stresses and fracture pressure

When a relatively cool fluid is injected into a relatively warm reservoir, the rock is cooled around the injection well. The cooled region grows in volume with time around the injection well and the rock within this cooled region contracts, inducing a thermo-elastic stress which be calculated as:

$$\Delta\sigma^T = \frac{\alpha_T E \Delta T}{1 - \nu}$$

where  $E$  is Young's modulus,  $\nu$  is Poisson's ratio,  $\Delta T$  is the temperature difference between the formation and fluid ( $T_{surr} - T_{fluid}$ ), and  $\alpha_T$  is the coefficient of thermo-elasticity (Luo and Bryant 2010). Similar equations are presented in a number of other works (Paige and Murray 1994; Fjar et al. 2008; Hettema et al. 2004; Pepin et al. 2004; Maury & Idelovici 1995; Perkins & Gonzalez 1984). In some cases, a shape factor ( $\beta$ ) is included to account for the geometry of the cooled region (Paige & Murray 1994; Perkins & Gonzalez 1985). 'Typical' thermo-elastic stress changes for sandstones are calculated to be between 0.1 MPa/°C and 0.2 MPa/°C (Paige & Murray 1994; Fjar et al. 2008).

Luo and Bryant 2010 included the thermo-elastic stress term to calculate the formation 'breakdown pressure' (equivalent to fracture pressure as used in this document) at the well as:

$$P_b = 3S_{hmin} - S_{Hmax} - P_p - \Delta\sigma^T$$

Where  $S_{hmin}$  and  $S_{Hmax}$  are the minimum and maximum horizontal stresses, and  $P_p$  is pore fluid pressure. It is worth noting that these equations are based on a non-penetrating fluid (Haimson & Fairhurst 1967), and penetrating fluids could lead to different breakdown pressures

The symbols and sign conventions in the preceding equation are consistent with those in Luo & Bryant 2010. Zhang & Yin 2017 present similar equations but include a term representing the tensile strength of the rock. The magnitude of the change in breakdown pressure due to thermal effects ( $\Delta\sigma^T$ ) is, however, the same whether or not this term is included.

Kinik et al. 2016 considered the case where the minimum and maximum horizontal stresses were equal (i.e. isotropic), and indicate that the difference in the well breakdown pressure between isothermal and that resulting from thermally induced stress is given by:

$$\Delta\sigma_T = \frac{2E \cdot \alpha_T}{(1 - \nu)} \cdot (T_{ws} - T_{ei})$$

Where  $T_{ws}$  is the temperature of the drilling fluid,  $T_{ei}$  is the geothermal temperature, and  $E$ ,  $\alpha$  and  $\nu$  are the rock mechanical properties defined previously. This equation is presented exactly as in Kinik et al. 2016 to allow for comparison with the previous equation, as it appears to indicate the effect of temperature on breakdown pressure is doubled.

An additional challenge in modelling thermal effects of CO<sub>2</sub> injection, is determining the temperatures of the CO<sub>2</sub> and the reservoir, and how the cooled region grows away from the well, as CO<sub>2</sub> is injected. There will be some heat transfer between the CO<sub>2</sub> and formation as the CO<sub>2</sub> flows down the well, causing the temperature of the CO<sub>2</sub> at the bottom of the well to be higher than at surface. Previous works have shown that despite the warming of the CO<sub>2</sub> as it flows down the well, it will (almost certainly) not reach thermal equilibrium with the geothermal gradient, and thus is still cooler than the formation when it reaches the bottom of the well (Bissell et al. 2011). The magnitude of this effect is dependent on a number of factors, including injection rate and formation temperature. A (relatively) simple model for the temperature profile within a CO<sub>2</sub> injection well is presented by Luo and Bryant 2010. Using this model (with current best estimate of notional injection rates, and a mean specific heat capacity of the wellbore of 2,500 J/kg·K), it is estimated that the temperature of the CO<sub>2</sub> could be between approximately 25°C (assuming a winter time surface temperature, 5 Mtpa rate) and 50°C (assuming a summer time surface temperature, 0.5 Mtpa rate) as it enters the reservoir.

As CO<sub>2</sub> moves away from the well it cools the surrounding rock. This is an extremely complex process but attempts have been made to estimate the rate, extent (i.e. size and shape of cooled region) and magnitude of this cooling using simplified models. Perkins and Gonzalez 1985 considered a simplified case for cooling during water injection, where the area around the well was discretised into regions based on temperature and water saturation. The properties within each of these regions were considered uniform, allowing the volume of the cooled region to be determined using an energy balance, and accounting for conduction to and from the overlying and underlying formations using a method described in Marx and Langenheim 1959. While this appears to be a useful approach in water injection scenarios, it may be less useful when modelling CO<sub>2</sub> injection, where the upwards migration of CO<sub>2</sub> could cause more significant cooling near the caprock/seal. This is very sensitive to completion design (vertical, deviated, horizontal) and to assumptions of the ratio of vertical to horizontal permeability.

It is possible to use coupled (geomechanical/thermal) models to investigate cooling effects of CO<sub>2</sub> in reservoirs (Gor et al. 2013; Rutqvist et al. 2008; Vilarrasa et al. 2015), although this is extremely challenging, and attempts to history match these models appear to have had limited success (Bissell et al. 2011). Rodger et al. 2019a provides details on a range of models constructed to test the impact of thermal effects on stress and fracture pressures. There remains a high degree of uncertainty regarding the pressure at which fracturing would occur if relatively cool CO<sub>2</sub> was injected into the relatively warm Blocky Sandstone Reservoir. This is a combination of uncertainties regarding:

- The fracture pressure gradient (ignoring any thermal effects)
- The thermal properties of the reservoir and seal (i.e. how much the fracture pressure is reduced by cooling)
- The magnitude of cooling caused by CO<sub>2</sub> injection

The uncertainties surrounding the current fracture pressure and thermal properties of the formations should be reduced as part of an appraisal program if appropriate data is collected.

Due to the remaining high uncertainty, it is recommended that the bottomhole pressure of wells in dynamic models is varied as part of a sensitivity analysis. Three scenarios are suggested, which are intended to represent reasonable high-mid-low case estimates for bottomhole pressure in injection wells. These scenarios are summarised in Table 28.

**Table 28** Fracture pressure cases for SDAAP models

Case	Fracture Gradient (kPa/m)	Thermal Stress Effect (kPa/°C)	Temperature Reduction at perforations (°C)	Thermally Reduced Fracture Pressure @ 2350 m (kPa)	Injection BHP limit (kPa) or 90% FP
High	23.20	100	30	51,520	46,365
Mid	22.20	200	40	44,170	39,750
Low	21.20	300	50	34,820	31,340

#### 4.5.7 Water-CO<sub>2</sub>-rock reactive geochemistry

For carbon storage projects, as CO<sub>2</sub> is injected into geological formations it displaces some of the fluids (normally formation water) residing in the pore space. Water is, to a certain extent, soluble in supercritical CO<sub>2</sub> and supercritical CO<sub>2</sub> is soluble in water. This creates a complex dynamic area at the interface of the injected CO<sub>2</sub> and the indigenous formation water. The chemical effects of CO<sub>2</sub> on rocks and formation water may impact permeability and rock-strength of the rock-matrix or of fault zones, thereby potentially impacting containment risk. The analyses hereunder, suggest that risks to negative impacts on the injection reservoir are minor, analysis suggests beneficial trapping phenomena in the Transition Zone. Further uncertainty reduction is required from site-specific data.

As supercritical CO<sub>2</sub> dissolves in formation water it forms carbonic acid lowering the pH. This can result in its reactivity to minerals within the rock matrix, especially carbonate minerals. Calcite, for example, has the fastest dissolution kinetics. Dissolution and precipitation of minerals can modify the formation water chemistry, buffer the pH, and may modify for example porosity, permeability and geomechanical properties of the reservoir rock. Precipitation of carbonate minerals is a process that traps some of the injected CO<sub>2</sub> in mineral form. Precipitation in the reservoir or other related processes such as movement of fine particles if occurring too close to the injection well may scale or clog the reservoir and cause reduced injectivity. The potential CO<sub>2</sub> reactivity of various rock types is dependent on parameters such as mineral content. CO<sub>2</sub>-formation water- rock geochemical modelling requires data on the mineral content, porosity, temperature and water chemistry, therefore these

parameters were analysed for the UQ-SDAPP project in regions where data or core samples were available. Injection modelling results (Rodger et al. 2019 c, f) indicate that there is potential for minor volumes CO<sub>2</sub> to migrate into the Transition Zone and little potential for it to migrate out. Models also show limited lateral migration away from the injection wells.

However, geochemical modelling has been undertaken for the Blocky Sandstone Reservoir, Transition Zone and Ultimate Seal strata. This is not suggesting that CO<sub>2</sub> will migrate into the Ultimate Seal, but is considering the potential reactivity if CO<sub>2</sub> were to interact with the Ultimate Seal rocks. A range of possible lithologies were simulated so that findings may be generalised or give insights to other areas.

The report by Pearce et al. 2019 provides a detailed description of the mineralogy, geochemical CO<sub>2</sub>-water-rock reactions and associated characterisation in the UQ-SDAAP study area and how it is applied across study.

#### 4.5.7.1 Example of the geochemical modelling: Moonie Sector

Here one example of the reactive geochemical modelling and analysis of the Moonie sector. It is provided as it is located geographically close to the notional injection sector and it has good data control.

##### 4.5.7.1.1 Moonie 38 well

Five samples of drill core from the Moonie 38 well Blocky Sandstone Reservoir (called the 58 Sand in the well completion report) and Transition Zone (called the 56 Sand in the well completion report) were characterised for minerals (Figure 93, Figure 94). Only two samples were quantitatively characterised from the Blocky Sandstone Reservoir so limited conclusions can be drawn, however they contained less quartz content and more feldspar than those sampled from the Blocky Sandstone Reservoir of the MAR Sector area. The feldspar was often corroded/altered and quartz grains were sometimes fractured or compacted. The Moonie 38 well Blocky Sandstone Reservoir pore throat distributions represent a much broader range of values between 0.01 and 100 µm, whereas those published from the Blocky Sandstone Reservoir of the MAR Sector area wells (e.g. GSQ Chinchilla 4, West Wandoan 1, Woleebee Creek GW4) had mainly sharp distributions of large pore throats around 100 µm (Pearce et al. 2019; Pearce et al. 2019 in prep). This may indicate that the high porosities and permeabilities in the Moonie Sector area Blocky Sandstone Reservoir sands are partly fracture controlled.

**Figure 93** Mineral content with depth in the Moonie 38 well core for the Blocky Sandstone Reservoir (58 Sands, deeper two samples) and Transition Zone (56 Sands).

##### Moonie 38 mineral content

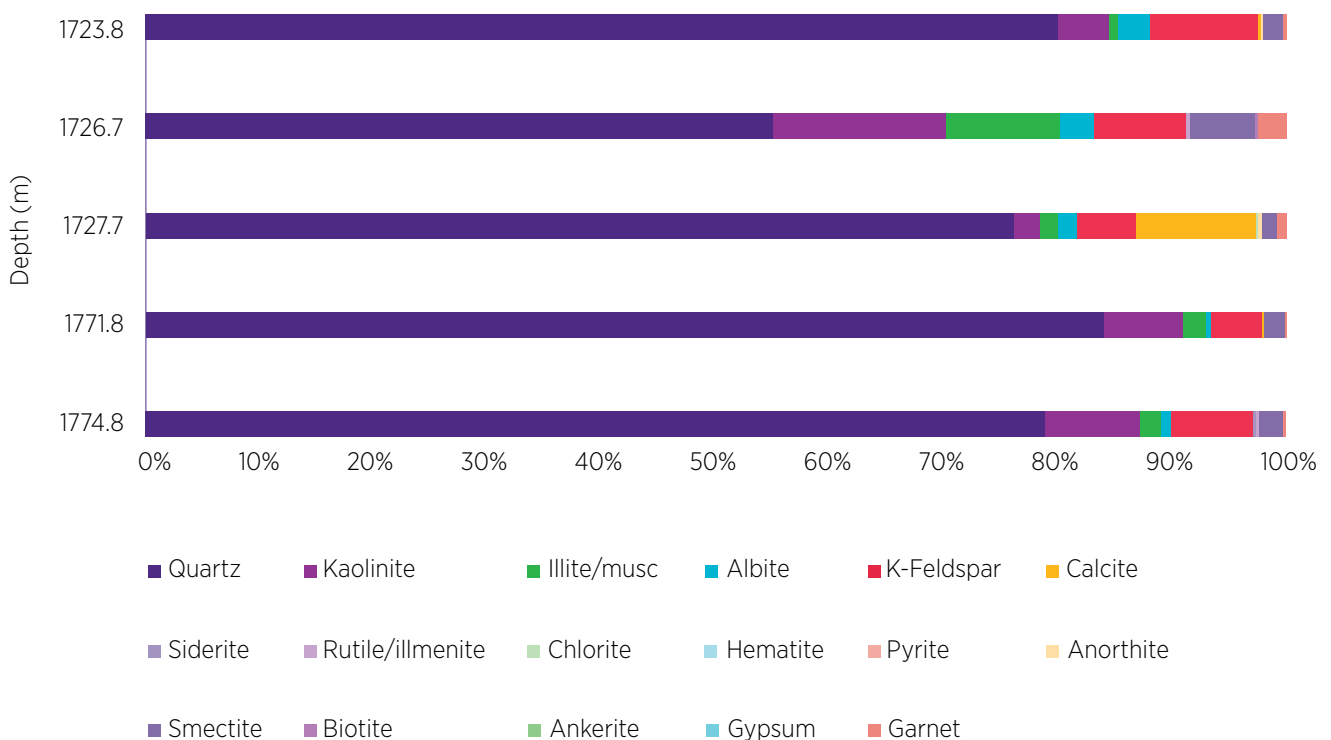
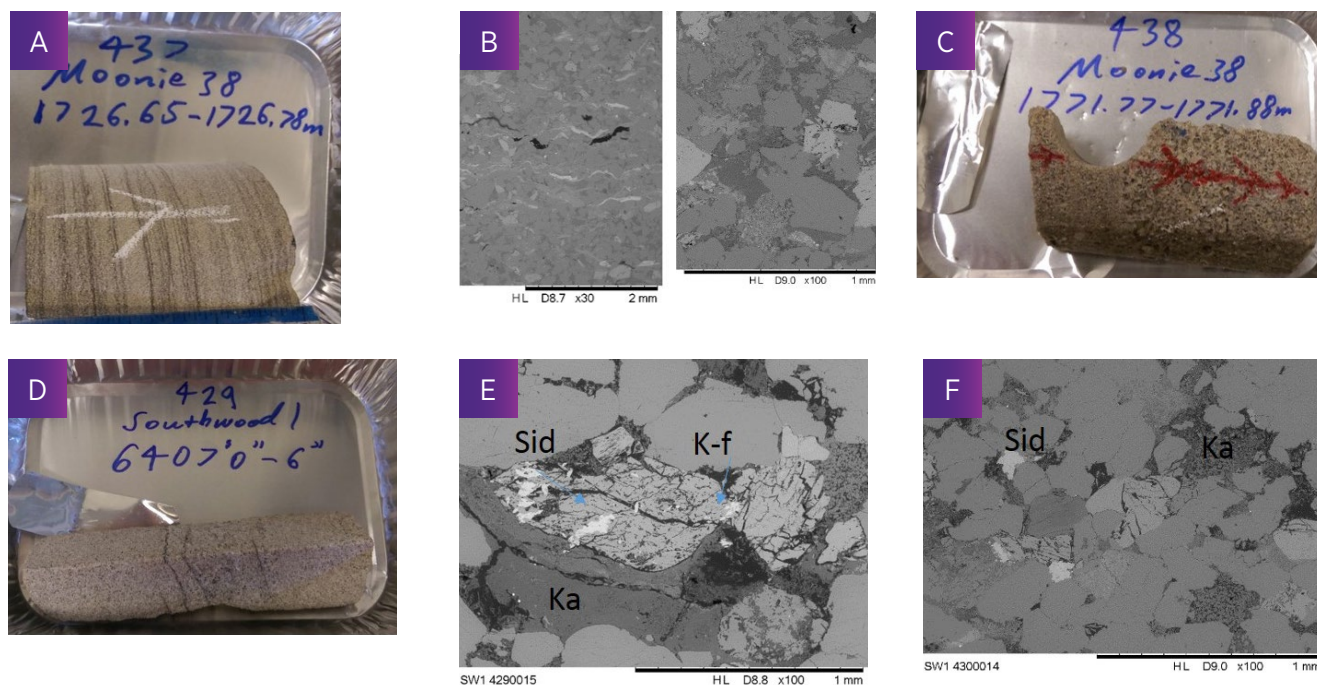




**Figure 94** Photos and SEM examples of sampled core from the Moonie 38 and Southwood 1 wells. (A) and (B) Moonie 38 Transition Zone (56 Sands) at ~ 1726.7 m. (C) Moonie 38 Blocky Sandstone Reservoir (58 Sands) 1771.8 m. (D) and (E) Southwood 1 Transition Zone 1952.9 m. (F) Southwood 1 Transition Zone 1955.0 m. Sid = siderite, K-f = K-feldspar, Ka=kaolinite.



Geochemical modelling of the Moonie 38 well Blocky Sandstone Reservoir sample from 1771.8 m resulted in a pH of 4.8 after 30 years simulation and 5.0 after 1000 years. For lower fugacity of CO<sub>2</sub> simulations e.g. the edges of the plume, the pH was 5.3 after 1000 years (Figure 95). The higher Na-bicarbonate content formation water in the Transition Zone (56 Sands) buffered pH to higher values along with dissolution of minerals. For the more reactive Transition Zone samples, the calcite cement dissolution at 1727.7 m quickly buffered pH to 4.9 after 30 years simulation, 5.0 after 100 years, and 5.3 after 1000 years. The low CO<sub>2</sub> fugacity model predicted a pH of 5.7 after 1000 y. The quartz rich 1723.8 m mineralogy (and the feldspar and clay rich 1726.7 m mineralogy) buffered pH to 4.9 after 30 y, 5.0 after 100 years, and 5.3 after 1000 years. The low fugacity model had a predicted pH of 5.6 after 1000 years.

#### 4.5.7.1.2 Moonie 22, Moonie 31 and Moonie 33 wells

Sandstones and mudstone core samples from the Moonie 22, 31 and 33 wells were additionally sampled primarily for MICP. The Moonie 22 well sample from 1772.0 m and the Moonie 31 well sample from 1786.0 m from the Blocky Sandstone Reservoir also appeared (via SEM characterisation) to contain a higher portion of K-feldspar and clay than the Blocky Sandstone Reservoir samples from the MAR wells in the north. They also had wider pore throat distributions than the MAR area wells, being more similar to those from Moonie 38 (Figure 96). Several Moonie 31 well mudstone core samples from between the 56 and 58 Sands Facies SM1 and SM2 of the Transition Zone, had very small pore throat radii, e.g. Moonie 31 1724.0 m, Moonie 31 1765.0 m, and Moonie 31 1768.0 m (Figure 96). Only the mineral content in Moonie 31 1724.0 m and Moonie 31 1768.0 m were quantified, they contained 36 - 50 % quartz and 40 % clays. Their pore throat distributions were similar to those measured from two Ultimate Seal samples from the West Wandoan 1 and GSQ Chinchilla 4 wells (Figure 96 lower panel).

**Figure 95** Predicted change in minerals and pH for the Moonie 38 well core samples over 1000 years simulation, with lower CO<sub>2</sub> fugacity (saturation) e.g. representing the edge of the plume. A)-B) Blocky Sandstone Reservoir (58 sands) 1771.8 m change in minerals and pH, C)-D) Transition Zone (56 Sands) 1727.7 m change in minerals and pH, and E)-F) Transition Zone (56 Sands) 1723.8 m change in minerals and pH.

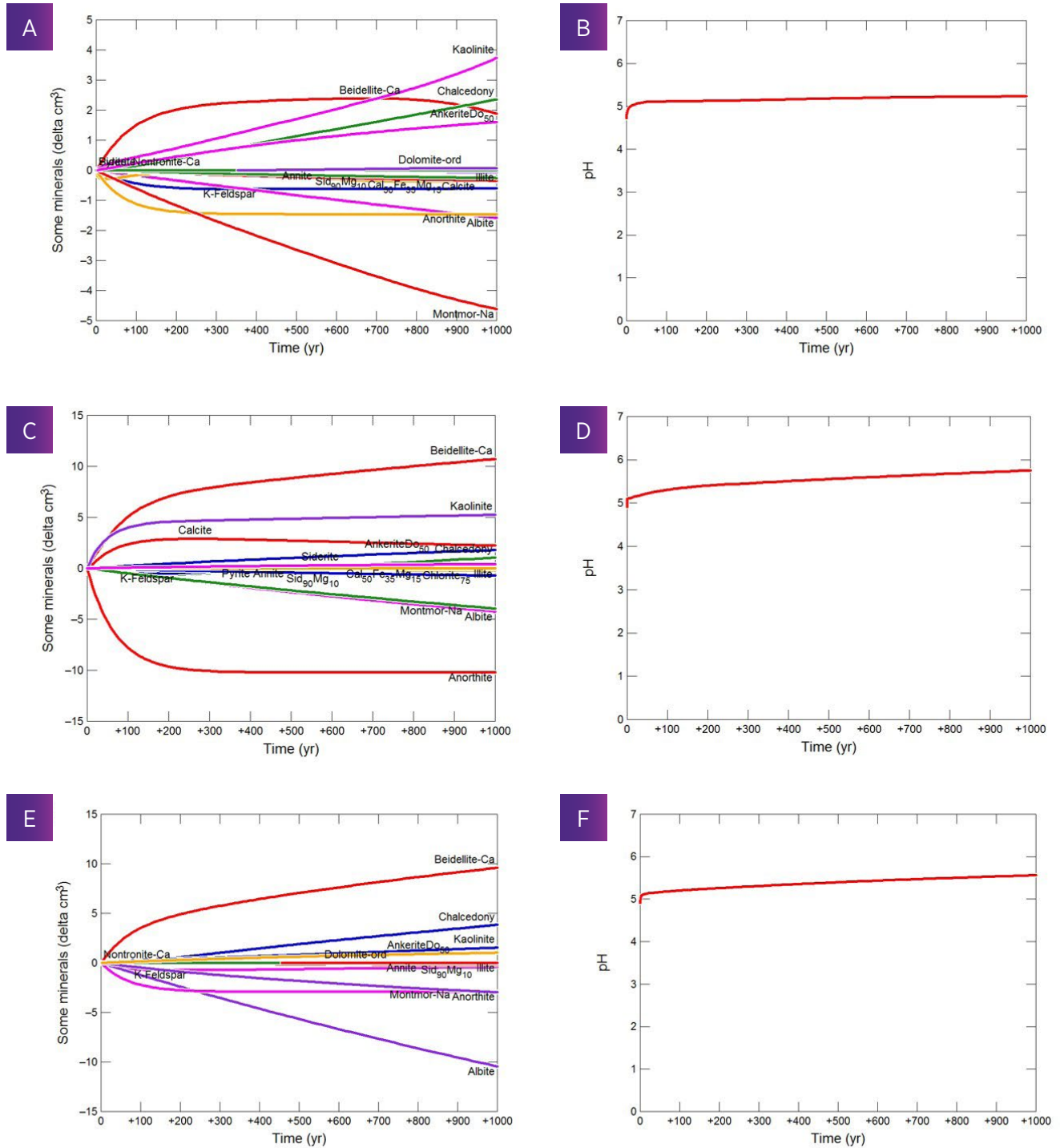
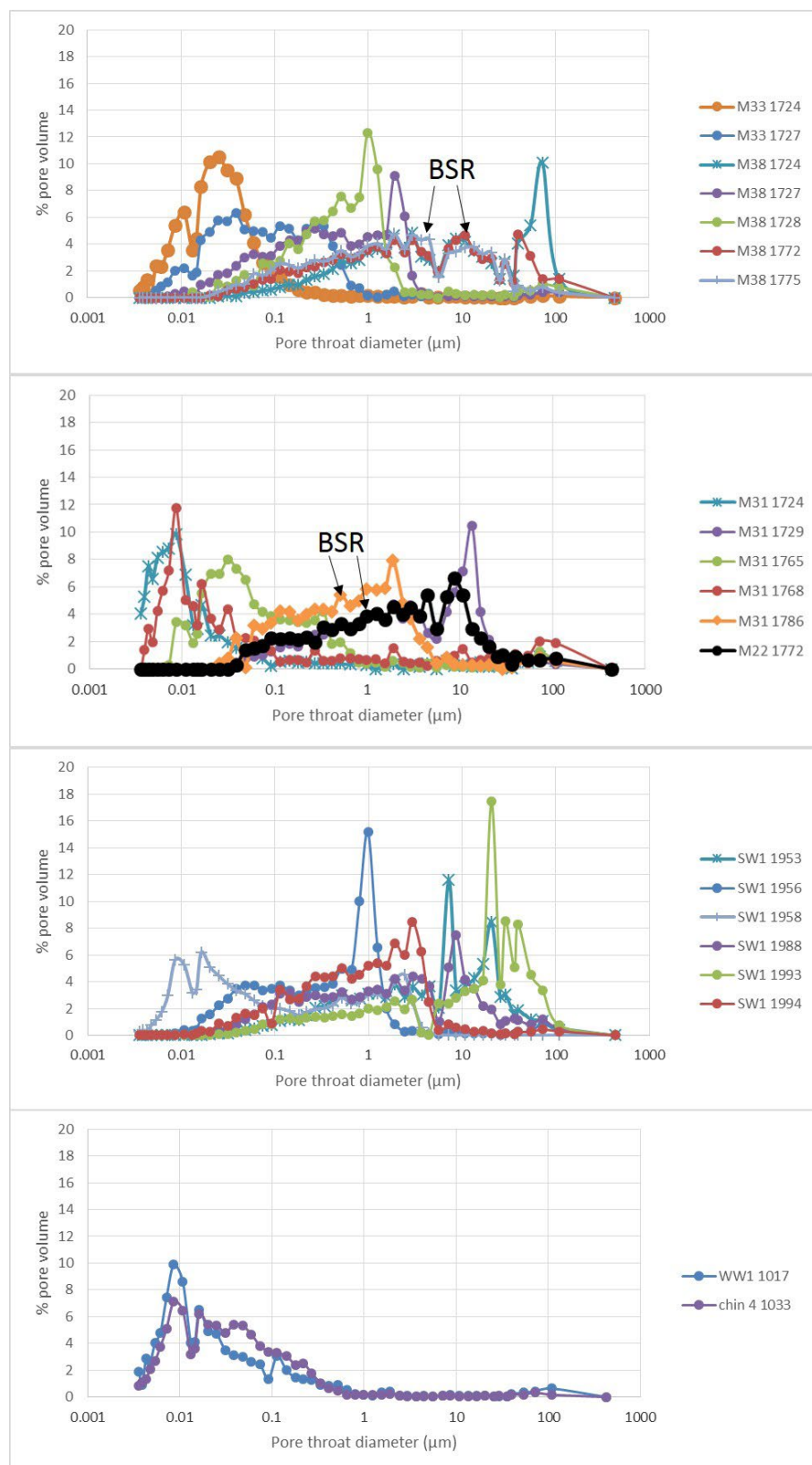


**Figure 96** MICP pore throat distributions measured for core samples from the Moonie 33, Moonie 38, Moonie 31, and Moonie 22 wells (labelled by M33 etc. and sample depth). Core samples are from the Transition Zone except those marked as the Blocky Sandstone Reservoir (BSR). Southwood 1 well samples (SW1) are from the Transition Zone, and two Ultimate Seal core samples from the West Wandoan 1 (WW1) and GSQ Chinchilla 4 (Chin 4) wells, labelled by depth in m (note-rounded to nearest m).



#### 4.5.7.2 Discussion and results

The results of the geochemical modelling are grouped according to the UQ-SDAAP project model sectors. These include:

- MAR Sector
- Moonie Sector
- Meandara Sector

The geological facies and stratigraphy referenced here are described in detail in La Croix et al. 2019a and 2019b (see section 4.3).

Overall, the drill core characterisation and geochemical CO<sub>2</sub>-water-rock modelling indicates that the Blocky Sandstone Reservoir has a low likelihood of plugging or scaling through mineral precipitation, however this is mainly based on the majority of data which was from the MAR sector.

The Transition Zone is variable in porosity and mineral composition and, where present, carbonate minerals can be dissolved. In modelling predictions, minerals such as plagioclase and chlorite were altered to ankerite and siderite that allowed mineral trapping of CO<sub>2</sub>. This is consistent with general natural analogue observations internationally (see Pearce et al. 2019 and references within). Regions with higher chlorite content for example have a higher mineral trapping potential. Smectites were also formed, and these have the potential to re-seal the pore space of the Transition Zone or Ultimate Seal, with overall no predicted significant net change in porosity. In addition, smectite may adsorb CO<sub>2</sub> and enhance trapping.

Formation water pH was predicted to be lowered by the dissolved CO<sub>2</sub>. However, the pH was in many cases subsequently buffered to higher values by mineral dissolution, especially in the presence of calcite, or additionally by the existing formation water chemistry in areas of higher buffering capacity (e.g. near the Condabri MB9-H well, or in the Moonie field). The generated predicted pH was in the range of 4-5 for the Blocky Sandstone Reservoir mineralogy at Reedy Creek MB3-H, GSQ Chinchilla 4, and the quartz rich Transition Zone of the Southwood 1 well, for example. The pH was more buffered in general in the Transition Zone (the northern MAR sector wells), which contained more reactive minerals than the Blocky Sandstone Reservoir. In the Condabri MB9-H and Moonie 38 well simulation results for the Blocky Sandstone Reservoir, the pH was in the range of 5-6, partly owing to the higher buffering capacity of the local formation water.

One uncertainty is the degree of cooling which will occur by CO<sub>2</sub> injection and how long it will last. This has been observed through downhole measurements in several field studies to be generally greater than predicted by injection modelling studies (e.g. the CO<sub>2</sub> CRC Otway projects, In Salah, Aquistore) (Bissell et al. 2011, Paterson et al. 2010, Vilarrasa et al. 2014). For example, at Otway CRC-1 after shut in the downhole temperature increased, 100 days after shut in it was still however 10°C below the original reservoir temperature. Further geochemical modelling to test the sensitivity of reactivity to different degrees of cooling is suggested.

Ultimate Seal characterisation data in the southern depositional centre remains lacking. Similarly, data for total concentrations of heavy metals (e.g. lead, arsenic) in drill core is limited. Where existing data was available or measured in the UQ-SDAAP project, heavy metal concentrations in core were variable by location and lithology. Core from the Reedy Creek MB3-H well had the highest concentrations of regulated metals including arsenic, chromium, zinc and mercury, which exceeded sediment trigger guidelines in the Blocky Sandstone Reservoir. The reason for this is hypothesised to be proximity to fractures/hydrothermal minerals, though this is not confirmed.

However, with respect to lack of data on “heavy metals”, the UQ-SDAAP geological review suggests a different provenance for a southern Blocky Sandstone Reservoir depo-centre (section 4.3); modelling shows limited lateral transport of CO<sub>2</sub> in the Blocky Sandstone Reservoir (sections 4.8 and 4.12); modelling further shows little opportunity for CO<sub>2</sub> to come into contact with minerals in the bulk of the Transition Zone and if it were to do so, migration out of the Transition Zone is also unlikely (above).

Furthermore, the site selection or screening approach has been to maximise distance from any faults (section 4.7).

In the context of site-specific characterisation, further studies would be undertaken to better constrain current uncertainty arising mainly from lack of data. The report by Pearce et al. 2019 provides a detailed description of the mineralogy, geochemical CO<sub>2</sub>-water-rock reactions and associated characterisation including core metal content in the UQ-SDAAP study area and how it is applied. Further studies are suggested in that report and allowed for in a suggested appraisal program in section 5.3.

## 4.5.8 Summary of evidence for containment potential

### The UQ-SDAAP project examined a number of lines of evidence regarding the likely seal performance of the Transition Zone and Ultimate Seal including:

- The facies analysis, stratigraphic correlations and depositional environment interpretations based on core, wireline petrophysical analysis and seismic interpretation suggest that the Transition Zone becomes less sandy (more mud prone) towards the centre of the basin and stratigraphically younger as part of an overall transgression and onset of marine conditions. This is corroborated with the petrophysical analysis calibrated with core analysis and DST well test interpretations of permeability. While the lateral continuity of the geobodies (both the sandy and muddy ones) in the Transition Zone are limited, the reverse is true for the Ultimate Seal where a marine transgression resulted in wide-spread deposition of the very low permeability Westgrove Ironstone Member and subsequent mud units
- The hydrocarbon systems analysis demonstrated commercial hydrocarbon accumulations on the eastern and western basin margin below the Ultimate Seal. These include the Moonie field as well as the hydrocarbon accumulations on the Roma Shelf. The accumulations that occur within various sandy units of the Transition Zone are generally isolated both vertically (i.e. not vertically continuous between stacked sands) and also laterally. This corroborates the facies analysis, stratigraphic correlations and depositional environment interpretations for the Transition Zone strata as being generally low permeability with both sandy/silty geobodies as well as low permeability muddy geobodies forming baffles and barriers, none of which are laterally continuous. The hydrocarbon migration indicators in the Hutton Sandstone generally are coincident with major fault zones suggesting that some fault segments may have transmitted hydrocarbons vertically across the Evergreen Formation over geological time
- The regional hydrogeological analysis identified that the Blocky Sandstone Reservoir and the Hutton Sandstone aquifers discharge to the Dawson River low topography boundary condition where the surface elevation is less than 200 m ASL. The Blocky Sandstone Reservoir may also discharge eastward into the Clarence Morton Basin to outcrop in the Lockyer Valley at surface elevations of less than 250 m ASL. This is supported by surface water and spring hydrochemistry and isotope chemistry. Finally, the Blocky Sandstone Reservoir may discharge to surface via up-fault hydraulic communication along certain segments of the Moonie-Goondiwindi fault system to surface topography less than 250 m ASL. There is, however, no hydrochemical indicators of this found in the current surface water (river drainage). Regionally there is generally a difference in hydraulic head between the Blocky Sandstone Reservoir and the Hutton Aquifer System of more than 5 m (see OGIA 2016 and this report) suggesting that the intervening Transition Zone and Ultimate Seal act regionally as a seal
- Fault seal analysis suggests that the faults in the Surat Basin are generally not critically stressed, with fault reactivation pressure threshold well above the formation breakdown pressures. Juxtaposition analysis of potential basin centred low offset strike-slip faults do not provide across fault leakage potential, however similar analysis of the Moonie fault segments suggest the potential for juxtaposition of Blocky Sandstone Reservoir against the Boxvale Sandstone Member (within the UQ-SDAAP Transition Zone)
- Historical oil and gas exploration wells and groundwater extraction bores provide a vertical leak age risk for carbon storage; however, the well density dramatically decreases towards the basin centre where notional injection sites have been identified. The site locations were selected using a philosophy of risk avoidance (i.e. staying a minimum lateral distance away from historical well locations and known faults)
- The reactive geochemistry analysis applied to predicting any changes to permeability suggest that the Transition Zone and Ultimate Seal would, if anything, promote precipitation of carbonate minerals such that would further reduce permeability
- Fracture analysis of core and image logs suggests that natural fractures occur in higher density near major faults such as the Moonie-Goondiwindi fault system. These also show evidence of paleo fluid flow events in the diagenetic history observed in thin section microscopy. This corroborates the hydrocarbon systems data of up fault fluid migration over geological history
- Mercury injection capillary pressure measurements on core samples from the Transition Zone indicate high capillary entry pressures well in excess of any anticipated CO<sub>2</sub> column height that might be generated by notions CO<sub>2</sub> injection. In the case of the Moonie oil field, the calculated seal capacity is well in excess of the observed oil column height suggesting that the Moonie oil field free water level is controlled by fault seal rather than top seal limitations

Collectively, the evidence would suggest that the Transition Zone is of generally low permeability but with contained sandstone geobodies of limited lateral continuity that will likely allow a small portion of vertical migration of injected CO<sub>2</sub> and pressure transmission. The overlying Ultimate Seal provides an ultra-low permeability regional sealing unit with lateral continuity. The locations where the Transition Zone and Ultimate Seal may have vertical seal capacity compromised, is at historical well locations and along certain fault segments. These features can be avoided in the notional site selection process (section 4.7).

## 4.6 Evidence for injectivity

There are significant and multiple lines of evidence that supports the development of secure, deep remote sites that could sustain materially high rates of injection with just 2-3 well pads, each with a small number of horizontal wells. Evidence includes, core data, drill stem tests, production tests, large-scale injectivity data and long-term oil field production data. There remains one “low case” reservoir scenario which might also support large-scale injection but would result in a much larger surface footprint (more and more widely spaced wells). The only way to reduce this residual uncertainty is to acquire additional data via drilling and testing (section 5.3 at the lowest risk sites identified by UQ-SDAAP (section 4.7). Notwithstanding this, current multiple lines of evidence supports a storage development with a minimum surface footprint, which can accommodate the majority of the emissions from the modern power plants region for a period of at least 20-30 years and probably longer (sections 4.8, 4.12 and 4.15).

The Blocky Sandstone Reservoir injectivity can be estimated through an integrated analysis of:

- Petrophysical properties calibrated with core analyses and DST well test data
- Evaluation of the reservoir geomechanics and fracture pressure corrected for thermal effects
- Reactive geochemistry (CO<sub>2</sub>-water-rock) evaluation (see previous section 4.2.3.8)
- Evaluation of the structural geology, *in-situ* stress and the likelihood of faults
- Inversion of the managed aquifer recharge monitoring well data pressure response
- History matching the dynamic simulation with Moonie oil field production data
- Well design and field lay-out
- Numerical simulation

However, there remains a lack of data in the centre of the basin near the notional injection sites. The UQ-SDAAP initially had the intent to piggyback off existing oil and gas field activity to opportunistically obtain new dynamic well test data that could be used to constrain the uncertainty around injectivity. This included a DST proposal to be included with the Armour Energy drilling activity near Myall Creek, well testing of the Daydream 1 and Fantome 1 wells of QGC/Shell in advance of their plug and abandonment, and instrumenting the Wandoan and Miles Town Bores (including the Glencore well) to record pressure transient data from normal pumping activities. For various reasons, none of these new data acquisition opportunities came to fruition, however, the well test design and predictive modelling are reported in detail by Honari et al. 2019a). This remaining uncertainty can only be reduced by data collection and site characterisation at the notional injection sites.

### 4.6.1 Production tests and drill stem tests

**Real flow-test and production data have been interrogated and used to calibrate deep basin injection models. All data are supportive of sustained, material, high rate injection potential and have helped frame the uncertainty bounds and guide new data acquisition requirements.**

Robust dynamic reservoir modelling highly depends on the quality of formation properties such as initial reservoir pressure, permeability and well productivity index (PI). The estimation of such properties, especially at large scales, has been one of the greatest challenges for petroleum engineers. To obtain an estimate of these properties, wells are tested by isolating an interval of a formation using a dual-packer assembly (or a single packer design if at the base of the well), pumping formation fluids out or injecting fluid into the formation at a constant rate for a short period (-10-30 min) and then shutting-in the assembly for an extended period (60-240 min) and recording the pressure change over time. To ensure reliability of data and provide opportunity for the reservoir to clean up, this sequence is usually repeated for each test (initial vs main flow/shut-in).

This procedure has been historically named a drill stem test (DST), however, there are many variations of well testing that accomplish similar results. DST data can be used to interpret formation fluid (PVT sampling) properties, reservoir pressure, reservoir temperature, formation permeability, PI, skin factor and an estimate of lateral distance to reservoir heterogeneity/ boundaries (Stewart 2011). PI defines the well deliverability, showing the flow rate of formation fluid that can be produced from the reservoir per unit pressure drawdown. Skin factor is a term introduced to account for any deviation from radial flow in the near well bore region and quantifies the pressure drop (positive skin) near the well bore due to formation damage induced during drilling operations, or flow improvement (negative skin) because of well stimulation such as acidisation.

During this study, well test analysis was undertaken by using a pressure transient analysis (PTA) software (IHS WellTest). The well test software estimates the permeability thickness product (k-h) and not absolute permeability. Section 4.3.8 summarises the interpretation performed on wireline logs to estimate contributing zone thickness (net pay) within the tested interval. There are three main elements in preparing and analysing test data for PTA:

1. Draw Down – Build Up rates and pressure versus time are imported into WellTest for any necessary data editing using the production editor tool in IHS WellTest software
2. Fluid properties are defined based on the reservoir fluid pressure and temperature
3. Conventional test analysis is conducted using both Horner (semi-log) and log-log derivative plots and the reservoir related properties (i.e. k-h, skin, reservoir pressure and any existing reservoir boundaries/characteristics) are estimated

Out of all wells with DSTs in the strata of interest, 79 DSTs from 60 wells had pressure-time data for the calculation of permeability, skin, (extrapolated) initial reservoir pressure and radius of investigation. The remaining wells had poor data quality rendering them inconclusive and the data needed to be disregarded. Of these 79 wells:

- 23 DSTs were conducted within the Blocky Sandstone Reservoir
- 40 DSTs were conducted in the Transition Zone
- 10 DSTs were conducted where the interval covered both the bottom of the Transition Zone and the top of the Blocky Sandstone Reservoir
- Four DSTs were conducted where the interval crossed the sub-Surat Unconformity (Blyth Creek 1, Marmadua 2, Paloma 1 and Wingnut 2 wells)
- One DST that was completed totally below the sub-Surat Unconformity (the Cherwondah 2 well)

There is also one DST analysed from the Colgoon1 well, however, it did not have the sequence stratigraphy picked and thus could not be used. Details of the well test and DST analysis are described in Honari et al. 2019a). Harfoush et al. 2019b and Honari et al. 2019a describe how the petrophysical analysis was calibrated with core laboratory measurements and DST analysis respectively.

## 4.6.2 Subsurface pressure constraints

**Injecting CO<sub>2</sub> (or any other fluid) increases the pressure in the subsurface over some period of time. This increase in pressure, or build-up, will be largest around the completion interval of the injection well, and decreases with distance (both horizontally and vertically) away from the wells completed interval. There are several pressure thresholds, which limit the injection of CO<sub>2</sub> (either limiting the total volume injected, the injection rate, or both). The discussion and analyses hereunder, describe the pressure thresholds and how they would be expected to impact CO<sub>2</sub> injection performance in the Surat Basin. There are no technical show-stoppers and a feasible injection scheme is possible well below safety limits and pressure constraints. Far-field pressure constraints e.g. set because of rising aquifer pressures in water users' bores, are unknown (section 4.13).**

### 4.6.2.1 Fracture pressure

If the pressure around the injection well is increased sufficiently, it is possible to mechanically break the rock, inducing fractures. The pressure at which this occurs is the fracture pressure<sup>16</sup> of the formation. In many cases fracturing the formation around the well while injecting, is acceptable, and is often beneficial as it improves permeability and increases injection rates. In other situations, it may be necessary to avoid fracturing, e.g. if there are concerns around fractures propagating into or through an overlying sealing formation. If this is the case, the bottomhole pressure (BHP) of the injection well should not be allowed to increase above the fracture pressure. In fact, a safety margin should be employed to ensure this does not occur, with BHP limited to some fraction of the estimated fracture pressure. In this case 90% of the fracture pressure will be used as the BHP limit of injection wells, as had been used in Canadian CO<sub>2</sub> injection operations (Bachu and Gunter 2005).

In order to estimate the fracture pressure for the Blocky Sandstone Reservoir identified as the notional target for CO<sub>2</sub> storage by the UQ-SDAAP, mechanical earth models (MEMs) were created for wells that had the required datasets (See Rodger et al. 2019a). MEM wellbore stability analysis for two representative Surat Basin wells with the required input datasets (i.e. Fantome 1 and Glen 1), indicated that isothermal formation fracture gradients are expected to be -22.20 kPa/m (0.98 psi/ft). This value will be used as the base case isothermal fracture gradient, with 21.20 kPa/m and 23.20 kPa/m being the low and high case values to allow some sensitivity analysis. Uncertainty in the fracture gradient, should be reduced by suitable testing (e.g. DFITs or XLOTs) during an appraisal program. Details of the Blocky Sandstone Reservoir geomechanical assessment can be found in Rodger et al. 2019a.

<sup>16</sup> Fracture pressure (or gradient) can be used to describe a number of different pressures. In this case it refers to the formation breakdown pressure, i.e. the pressure at which intact rock around the well breaks, creating new fractures.

### 4.6.2.2 Thermal effects and fault reactivation

Thermal effects of injecting relatively cold CO<sub>2</sub> in to a relatively hot reservoir can reduce the fracture pressure (described in the previous section). These effects are described in detail in section 4.2.3.7 previously. Similarly, if a fault exists that has a fault reactivation pressure less than the formation fracture pressure this may limit the allowable operational bottomhole injection pressure. Fault reactivation analysis is described previously in section 4.2.3.3 of this report where it describes the faults in the UQ-SDAAP as being relatively stable with a fault reactivation pressure well above the formation fracture pressure. Details of the thermal implications to the geomechanical assessment can be found in Rodger et al. 2019a and in section 4.5.

### 4.6.3 Large-scale injectivity data (MAR)

**Managed aquifer recharge (MAR) data are indicative of injection potential in the northern, Blocky Sandstone Reservoir depositional centre. The area is around 1 km shallower than the deep basin southern depositional centre and may be mineralogically different. However, the depositional and therefore fluid flow architecture is the same as the Blocky Sandstone Reservoir to the south. Inversion modelling of large-scale water injection confirms a highly heterogeneous desposition. There is no evidence for increased Blocky Sandstone Reservoir heterogeneity away from the injection sites, and therefore minimal risk of pressure increased caused by this. This is supportive of the feasibility of long term, sustained injection rates in the deep basin centre.**

Australia-Pacific LNG (APLNG – a joint venture between Origin, ConocoPhillips and Sinopec) produce Coal Seam Gas from several leases within the northern Surat Basin. Gas production targets both Permian coal-bearing strata in the Bowen Basin as well as the Jurassic aged Walloon Coal Measures in the Surat Basin. A by-product of CSG production is formation water produced with the gas and permeate from the reverse osmosis plant. A blend of these water streams is re-injected into the Blocky Sandstone Reservoir in a “managed aquifer recharge (MAR)” program since 2015 by APLNG at two sites: Reedy Creek (~17.5 ML/day average using 12 injection bores) and Spring Gully (~2 ML/day average using three injection bores). Observed hydraulic responses throughout the northern Surat Basin to MAR injection provide an opportunity to infer and better understand the Blocky Sandstone Reservoir hydraulic properties (primarily permeability), including their spatial distribution and uncertainty. These can be estimated through a process of inversion modelling. The full details of the MAR inversion modelling are described in Hayes et al. 2019a.

#### 4.6.3.1 Methodology

Hydraulic properties of the Blocky Sandstone Reservoir were estimated using a numerical model to invert the transient water level observations associated with APLNG MAR injection in the northern Surat Basin. The key components of the approach taken were:

- A simple three layer model was developed, based on the UQ-SDAAP’s Blocky Sandstone Reservoir roof/floor surfaces, and the following design elements:
  - The selected model code is MODFLOW-USG (Panday et al. 2013)
  - The model is focused on the Blocky Sandstone Reservoir northern depositional centre from the northern unconfined outcrop areas to the south around the latitude of the town of Chinchilla
  - The model mesh is locally refined around APLNG MAR injection bores, observation bores and other key hydrogeological features of the model
  - Prescribed boundary conditions include the MAR wells, town water and industrial supply bores, northern outcrop areas, and the southern model boundary
  - Temporal discretisation is dictated by the MAR injection, storage and recovery periods, and observed transient hydraulic responses
  - It is assumed that the overlying and underlying strata contribute little towards aquifer storage in comparison with the Blocky Sandstone Reservoir
- MAR injection and observation data sets were reviewed and incorporated into the model to constrain the inversion
- Aquifer hydraulic property measurement data were reviewed for ‘soft’ inclusion in the model inversion process where appropriate
- PEST-HP (Doherty 2018) was used with spatially-varying (pilot point) parameters for inversion of the hydraulic conductivity and compressibility (specific storage) fields
- Model inversion was repeated with varying interpolation schemes and parameters, both with and without kriging anisotropy
- A PEST utility (IDENTPAR; Doherty 2016) was used to assess parameter “identifiability” based on the available observation data
- PEST-HP (Doherty 2018) was used for model uncertainty analysis



#### 4.6.3.2 Inversion model set-up

The UQ-SDAAP geological characterisation as described by Gonzalez et al. 2019b was used as the underlying static geological model. The geological model was provided in z-map format and subsequently converted to ESRI ascii rasters. Regional Precipice Formation outcrop mapping was used in conjunction with a hydraulic head distribution for the Precipice Sandstone aquifer from Origin Energy 2017. Groundwater modelling was conducted in accordance with the Australian Groundwater Modelling Guidelines (Barnett et al 2012). An unstructured grid version of the industry standard MODFLOW code, called MODFLOW-USG-Transport v1.1 (MF-USG; Panday et al. 2013 and Panday 2017) was selected for this study.

The geological static model comprises three layers:

- The variable thickness and elevation of the Blocky Sandstone Reservoir (layer 2) top and base was defined by UQ-SDAAP
- Layers 1 and 3 are constant 20 m thick layers (except where layer 1 thins to a minimum of 1 m, due to the Blocky Sandstone Reservoir reaching land surface – as defined by Geoscience Australia's 1-second DEM)

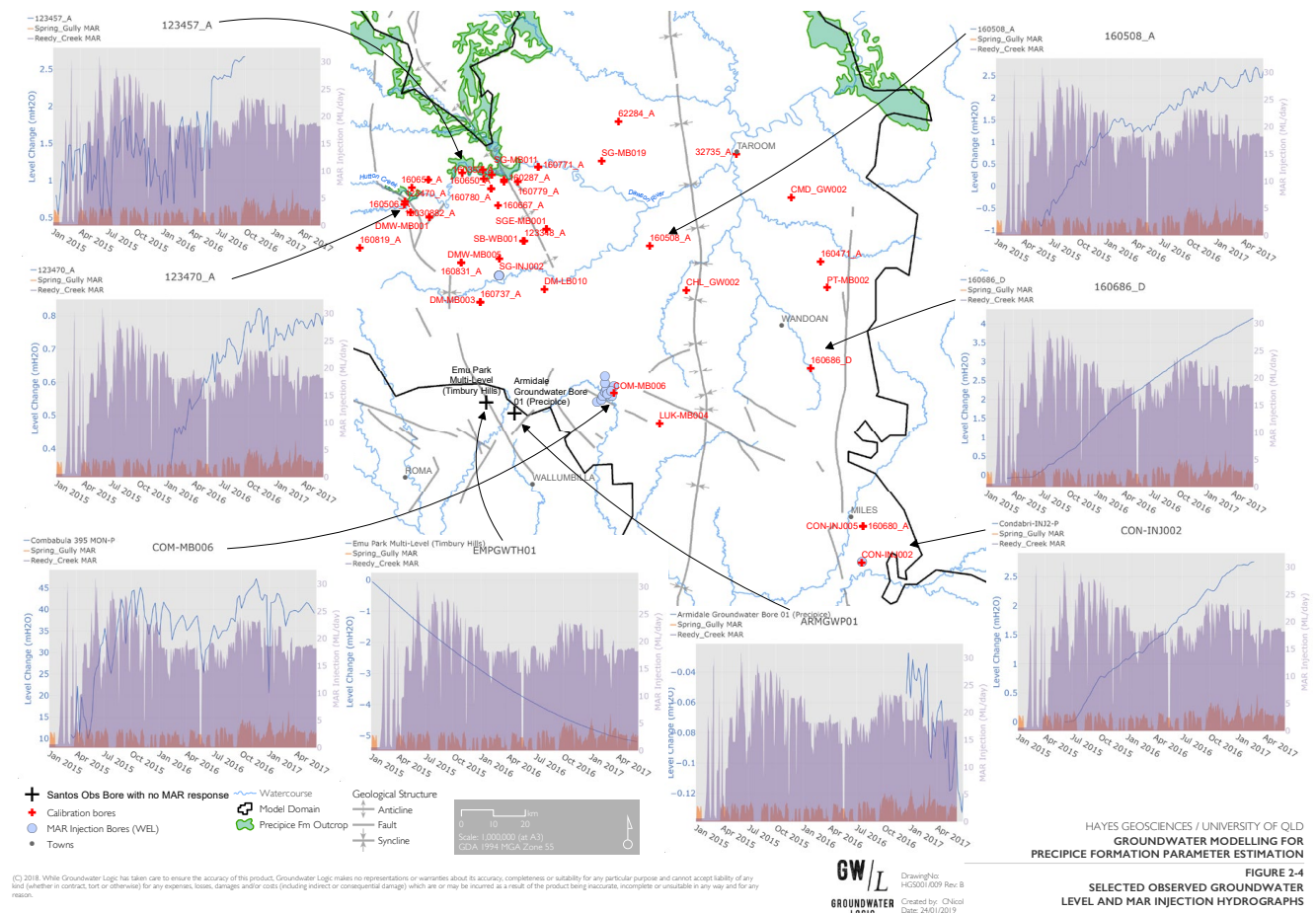
Layers 1 and 3 provide a representation of additional aquifer storage (compressibility) in the strata overlying and underlying the Blocky Sandstone Reservoir. They do not accurately represent the detailed geometry or properties of the overlying or underlying strata. This is justifiable on the basis that the MAR injection response data only cover a short time period (3 years), which is insufficient for injection responses to be significantly affected by storage in adjacent low permeability strata or model boundary conditions.

Blocky Sandstone Reservoir (Precipice Sandstone) groundwater pressure response data were collated for 45 bores from the following sources:

- The Queensland Government's Groundwater Database (GWDB)
- The Queensland Government's online Water Monitoring Information Portal (WMIP)
- OGIA 2016a; 2016b; 2016c groundwater data
- Origin 2016-17 Groundwater Assessment Report that itemises both the groundwater response level and total MAR scheme injection rate time series

A selection of observed pressure responses to MAR operations in the 2015-2017 period are shown in Figure 97. There has been approximately 40 m of hydraulic head rise near the Reedy Creek MAR operations, which diminishes with distance to only 3-4 m at the basin margins (north and east). In the far south of the model area, there is a declining trend (Figure 97) where the MAR effects have not reached or local water abstraction has overprinted those effects.

**Figure 97** The groundwater model inversion area for MAR with observation bore locations showing the water level over the same time period as the MAR injection.



There are differing water level response patterns between the eastern and northern basin margins, where the Blocky Sandstone Reservoir becomes unconfined in shallow subcrop and outcrop areas. There is evidence of a flattening of the water level response to MAR operations by 2016-2017 in the north, whereas there is an ongoing linear head rise to the east. This difference may reflect the MAR pressure response encountering the high storage of the unconfined Precipice Sandstone in the north.

Two Santos bores located 30-35 km west of APLNG's Reedy Creek MAR scheme monitor pressures in what has previously been termed the Precipice Sandstone but which falls to the west of the UQ-SDAAP zero pinch-out edge of the Blocky Sandstone Reservoir. The UQ-SDAAP stratigraphy would allocate these wells to the Transition Zone time equivalent to minor sands within the Lower Evergreen Formation. These two bores (EMPGWTH01 and ARMGWPD01; Figure 97), despite the EMPGWTH01 record being of low integrity<sup>17</sup>, show no response to the long-term MAR injection, and if anything, demonstrates a declining rather than rising trend over the primary recorded MAR injection period (2015-17). Therefore, it is concluded that there is no appreciable hydraulic connection between the Blocky Sandstone Reservoir and the sands within the overlying Transition Zone in this area. This conclusion supports the truncation of the MAR inversion model using a no flow boundary coincident with the western pinch-out edge of the Block Sandstone Reservoir between Reedy Creek and these two Santos bores.

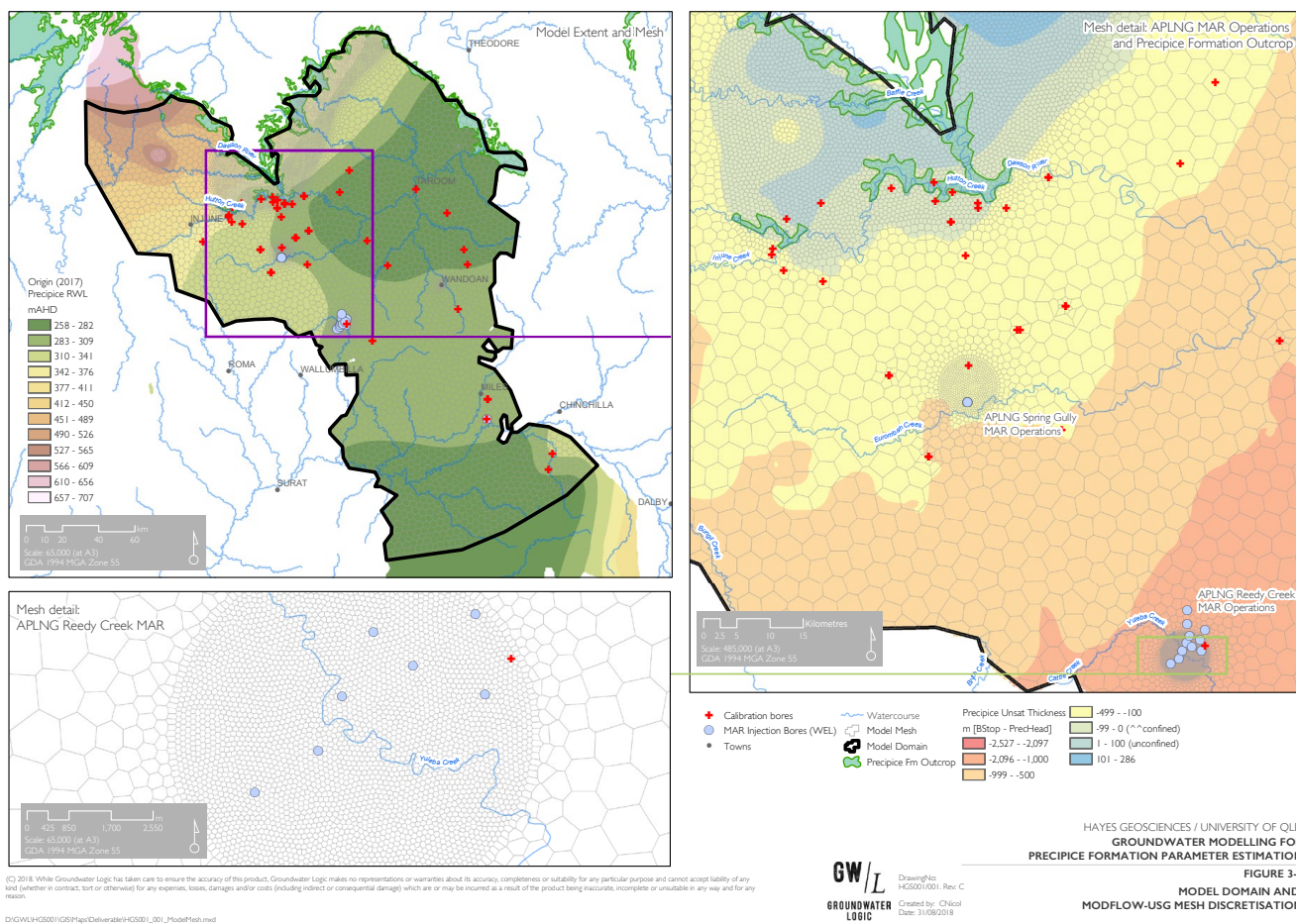
MF-USG WEL boundaries are used to simulate:

- The APLNG MAR (injection) bores at Reedy Creek and Spring Gully
- The APLNG trial MAR injection/abstraction bore at Condabri
- The licensed groundwater users: Miles and Wandoan town bores, and Lagoon Gully (Kogan Creek power station) water supply bore

<sup>17</sup> Communications with Santos have revealed that the recorded pressures in bore EMPGWTH01 are suspiciously low relative to groundwater pressures in other bores in the area and are therefore considered potentially erroneous.

General head boundaries are used to model lateral groundwater inflow and outflow around the edges of the model, where the APLNG potentiometric mapping (as shown in Figure 98) suggests that this inflow or outflow occurs. A 'no flow' boundary was assigned at the locations where the Blocky Sandstone Reservoir pinches. Modflow's Horizontal Flow Barrier (HFB) package was used to simulate the postulated hydraulic barrier effect of the Leichardt Burunga Fault System, a major north-south trending structure on the eastern side of the basin (Figure 99) that shows evidence of being a barrier to some degree (Ryan Morris, pers. comm. May 2018). Other known faults, such as the Hutton-Wallumbilla are not included, as there is no clear evidence of them influencing the propagation of the MAR injection pressure signal.

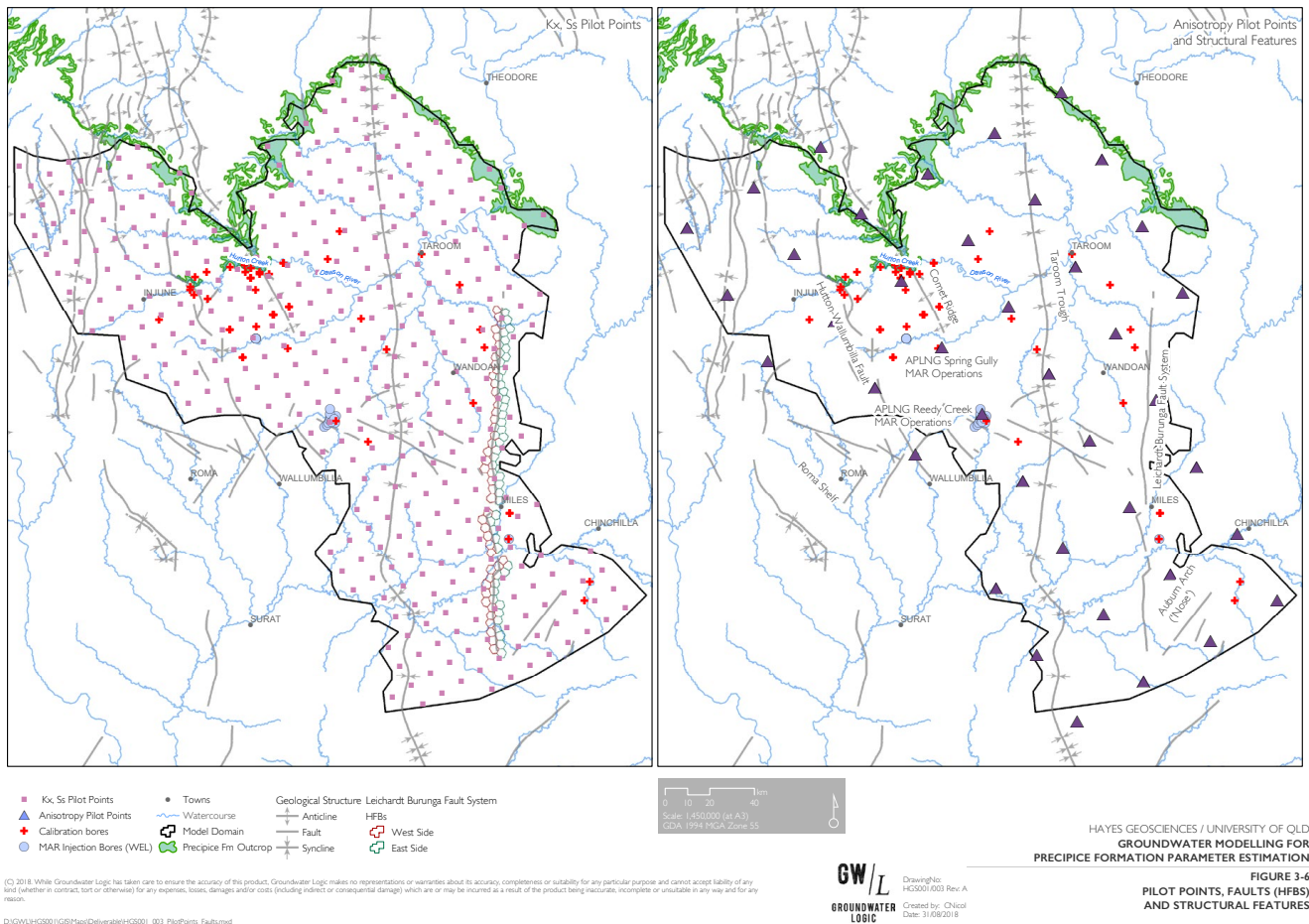
**Figure 98** The groundwater model inversion area for MAR (heavy black border), with the APLNG hydraulic head distribution (top left), grid refinement near injection wells (bottom left) and head boundaries (top right).



© 2018. While Groundwater Logic has taken care to ensure the accuracy of this product, Groundwater Logic makes no representations or warranties about its accuracy, completeness or suitability for any particular purpose and cannot accept liability of any kind (whether in contract, tort or otherwise) for any expenses, losses, damages and/or costs (including indirect or consequential damages) which are or may be incurred as a result of the product being inaccurate, incomplete or unsuitable in any way and for any reason.

D:\GWL\HCS001\GIS\Appl\Deliverables\HCS001\_001\_ModelTech.mxd

**Figure 99** The groundwater model inversion area for MAR with the discretisation highlighted near the Leichardt Burunga Fault System.



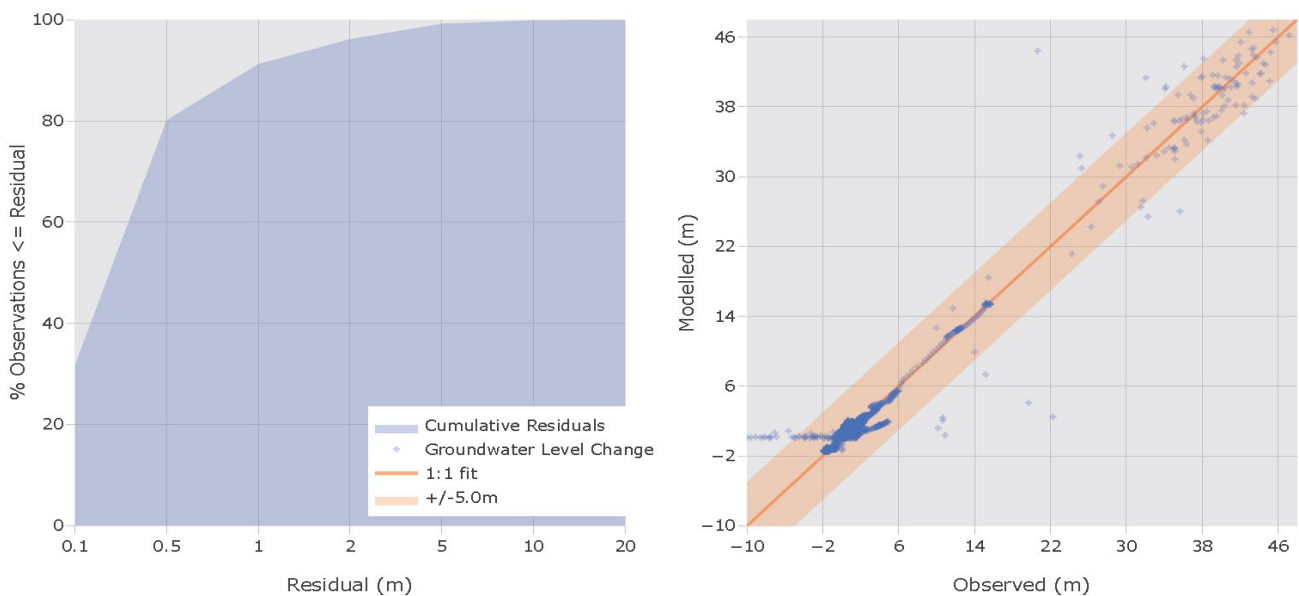
The calibration model consists of a single steady state stress period designed to provide stable initial heads for the subsequent transient stress periods. This is followed by 53 half-monthly transient stress periods, starting 1 January 2015 and terminating 16 March 2017. This period and its discretisation are defined based on the duration and temporal variability of available APLNG MAR injection rate data.

The groundwater model inversion was conducted using a combination of manual (trial and error) and automated techniques. A rough initial inversion was achieved using manual hydraulic conductivity parameter adjustments (up from an initial constant value of 1 m/day to a constant value of 5 m/day), at which point spatial variability was introduced and optimised using several applications and re-applications of PEST-HP (Doherty 2018). For the purposes of assessing uncertainty in the estimated hydraulic properties, the primary (minimum error variance) model was run using 1000 different randomly-generated parameter sets that calibrated the model to a 'reasonable degree'. Of the 1000 stochastic model runs, those with a MAR inversion quality within 33% of the primary (minimum error variance) model and with storage values closer to those derived from APLNG injection/abstraction tests, were retained (167 runs); the other 833 runs are discarded.

### 4.6.3.3 Results and discussion

Figure 100 provides a summary of inversion quality for the primary (minimum error variance) model. The key statistics show a normalised root mean square error<sup>18</sup> (nRMS) of 1.9% and a mean absolute error of 0.43 m in water level change forecast. The nRMS is well within typically acceptable ranges (Barnett et al. 2012). The cumulative residuals show no significant bias, and more than 90% of modelled groundwater level changes are within 1 m of their observed counterparts. A quantitative measure of inversion error on a per-bore basis is shown in Figure 101 with a range from 2-13% error from observed head changes. The simulated water balance for the transient period of the primary model (January 2015 to June 2017) is presented in Table 29. The major stress on the aquifer over this period is the MAR injection (17.7 ML/day on average). Injection is offset to a minimal degree (1.3 ML/day on average) by abstraction from the Blocky Sandstone Reservoir at other licensed groundwater users' bores; this results in a net storage increase of only 17.4 ML/day, slightly less than the MAR injection rate. The only other source of recharge to the model is regional groundwater inflow from the GHBs (33.2 ML/day gross inflow or 1.0 ML/day net).

**Figure 100** Modelled groundwater level calibration summary.



n Observations	Sum of squared residuals	Root Mean Square (RMS) residual (m)	Normalised RMS (nRMS) residual	Mean absolute residual (m)
4129	4826	1.08	1.9%	0.43

<sup>18</sup> Normalised root mean square error here represents a quality measure of forecast head changes over time, proportional to the observed head change range.

**Figure 101** Selected inversion hydrographs of better quality.

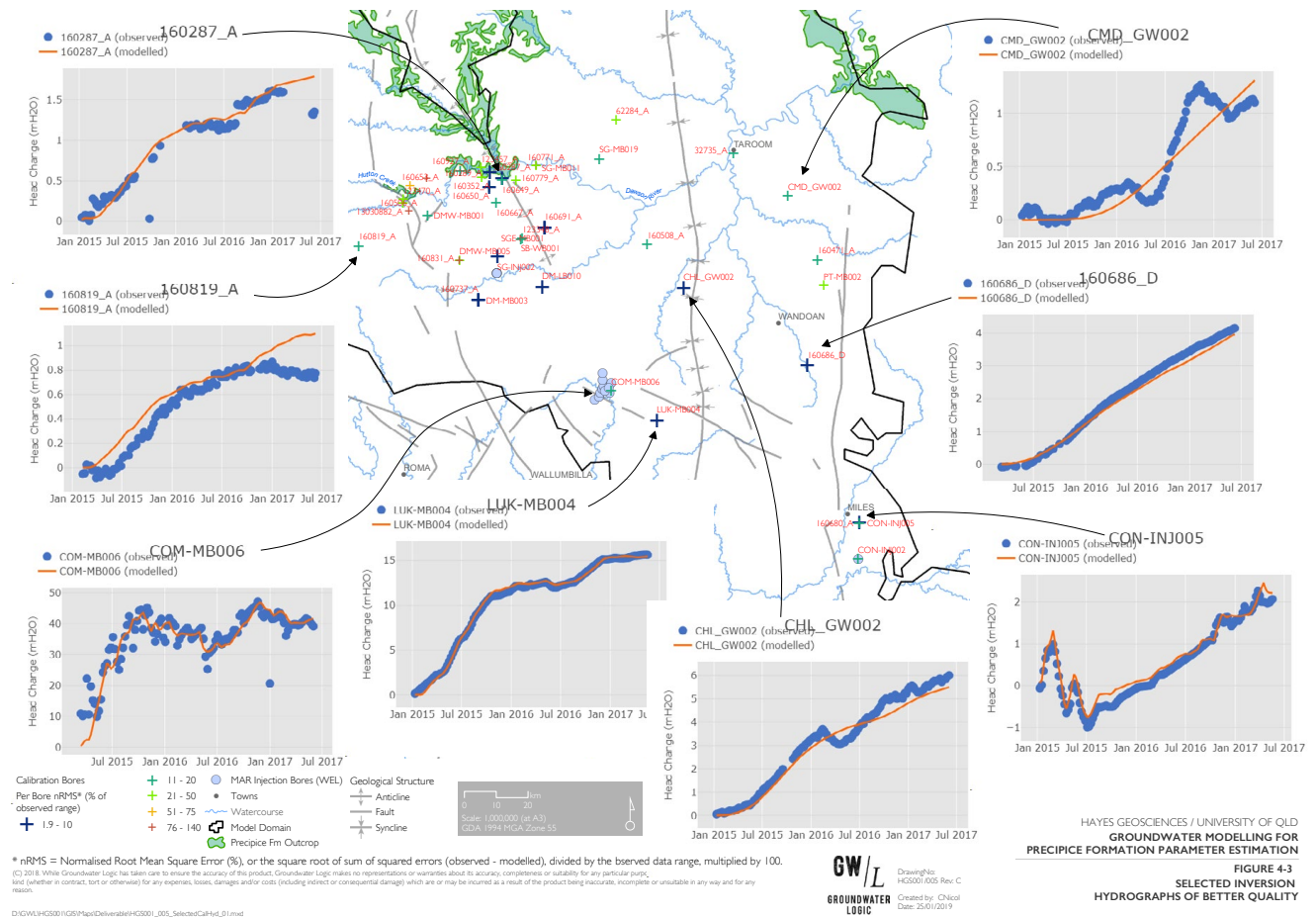


**Table 29** Transient historical water balance in MG/day –whole model

Component	In	Out	Net	Comment
Aquifer Storage	1.1	18.5	-17.4	Out of the model indicates water entering storage (e.g. due to MAR injection)
Injection / Abstraction Bores	17.7	1.3	16.4	MAR and other licensed groundwater bores
General Head Boundaries	33.2	32.2	1.0	Regional groundwater inflow / outflow
<b>TOTAL</b>	<b>52.0</b>	<b>52.0</b>	<b>0.0</b>	
ERROR	0%			
Units	ML/day			

Mapping of the pilot point-based hydraulic property parameters is provided in Figure 102 through Figure 106, and Figure 107 (minimum error variance hydraulic conductivity and storage, respectively).

Figure 102 and Figure 107 also present the permeability and storage estimates. Note that the inversion requires extremely high permeability (>190,000 mD) for the Blocky Sandstone Reservoir in order to converge on a solution that matches the observed monitoring bore water level responses.

Model inversion indicates that kriging anisotropy based on *in-situ* stress orientations, is not required to match the observed pressure responses to MAR injection. A qualitative comparison of kriging anisotropies was made with literature values of maximum *in-situ* stress orientations (Tavener 2018; and Flottman et al. 2013), however no consistent correlations were identified. Flottman et al. 2013 point out that dominant fracture orientations can occur at both high angles and low angles to the maximum stress direction and therefore comparison of kriging anisotropies from the MAR inversion with maximum horizontal stress directions is indeterminate.

**Figure 102** Blocky Sandstone Reservoir MAR hydraulic conductivity (minimum error variance).

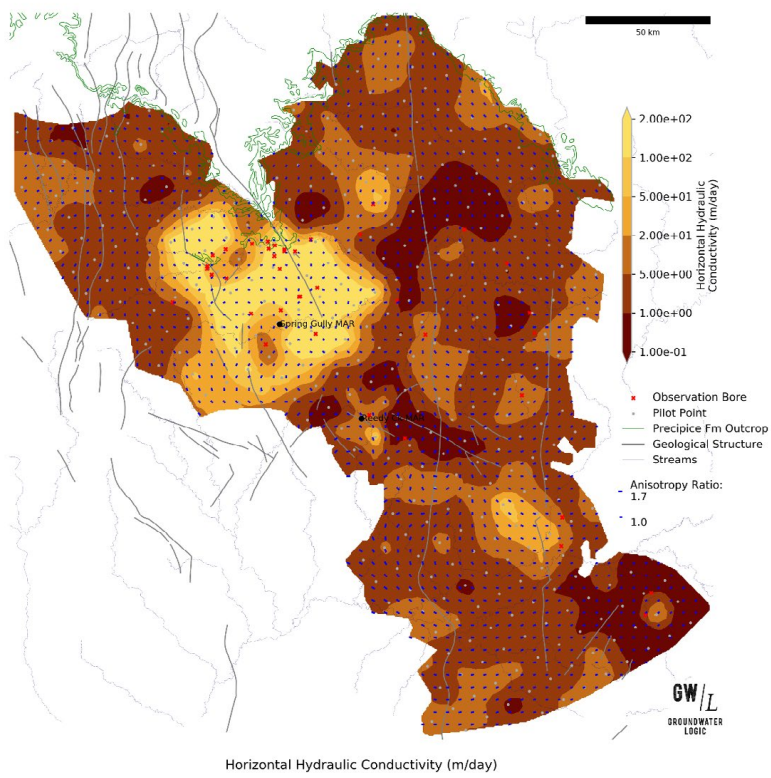


**Figure 103** Blocky Sandstone Reservoir MAR inversion aquifer thickness.

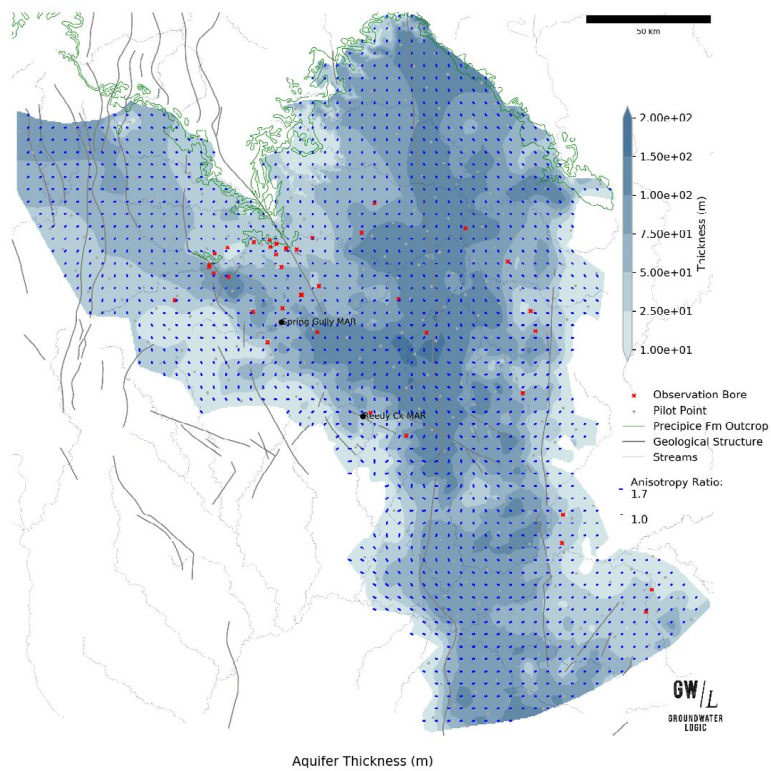


**Figure 104** Blocky Sandstone Reservoir MAR inversion transmissivity (minimum error variance).

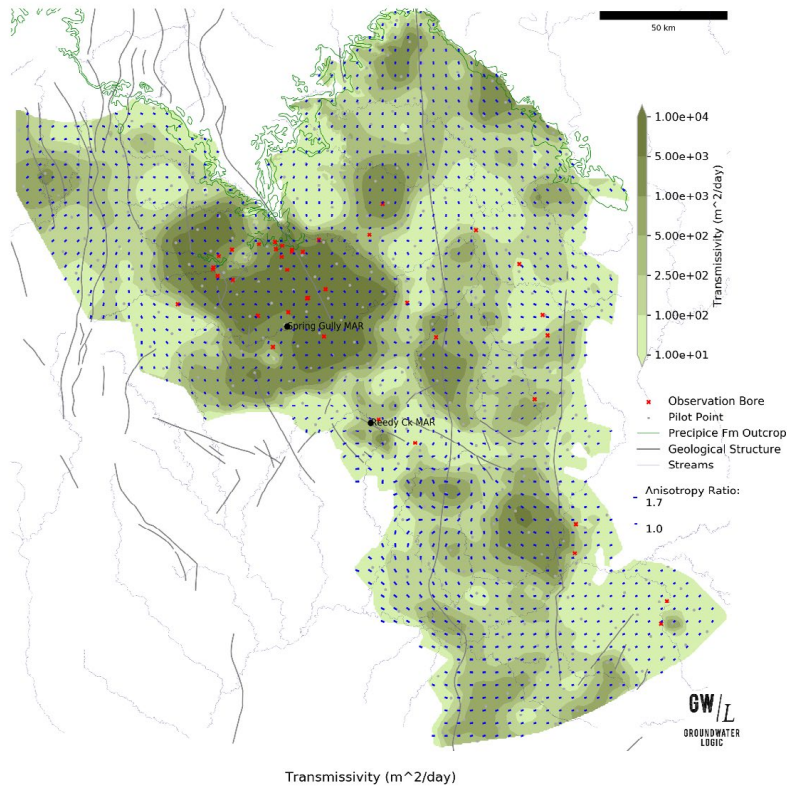


**Figure 105** Blocky Sandstone Reservoir MAR inversion intrinsic permeability (minimum error variance).

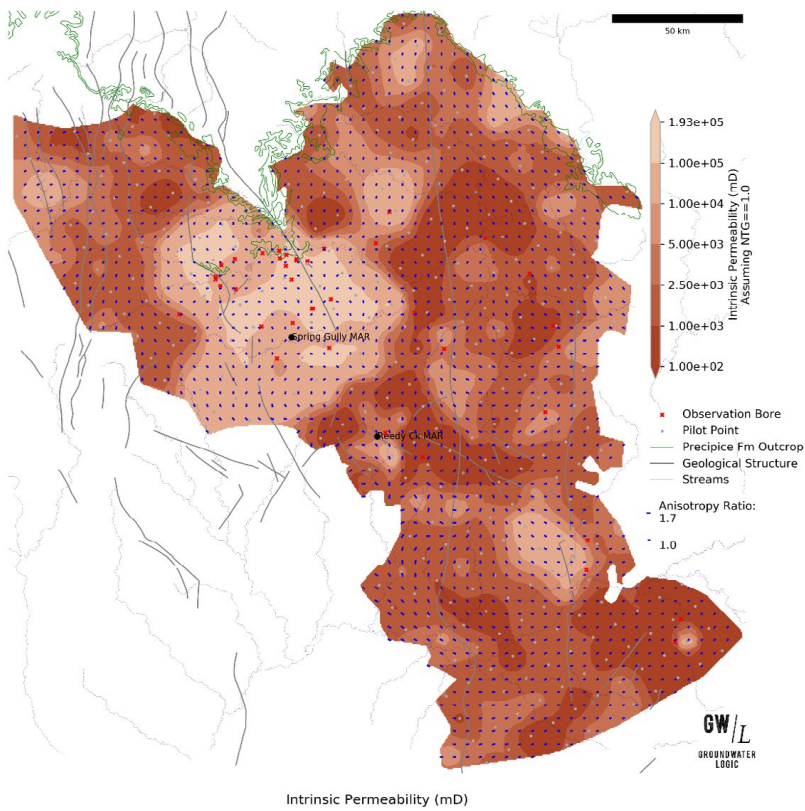




**Figure 106** Blocky Sandstone Reservoir MAR inversion storativity and compressibility (minimum error variance).

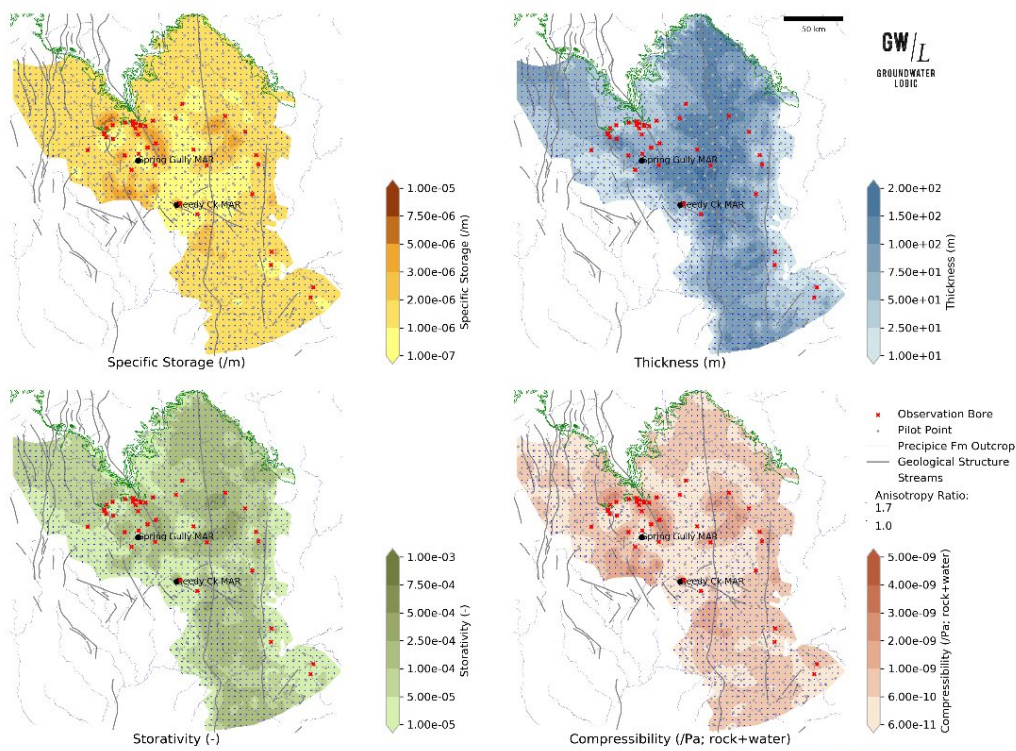
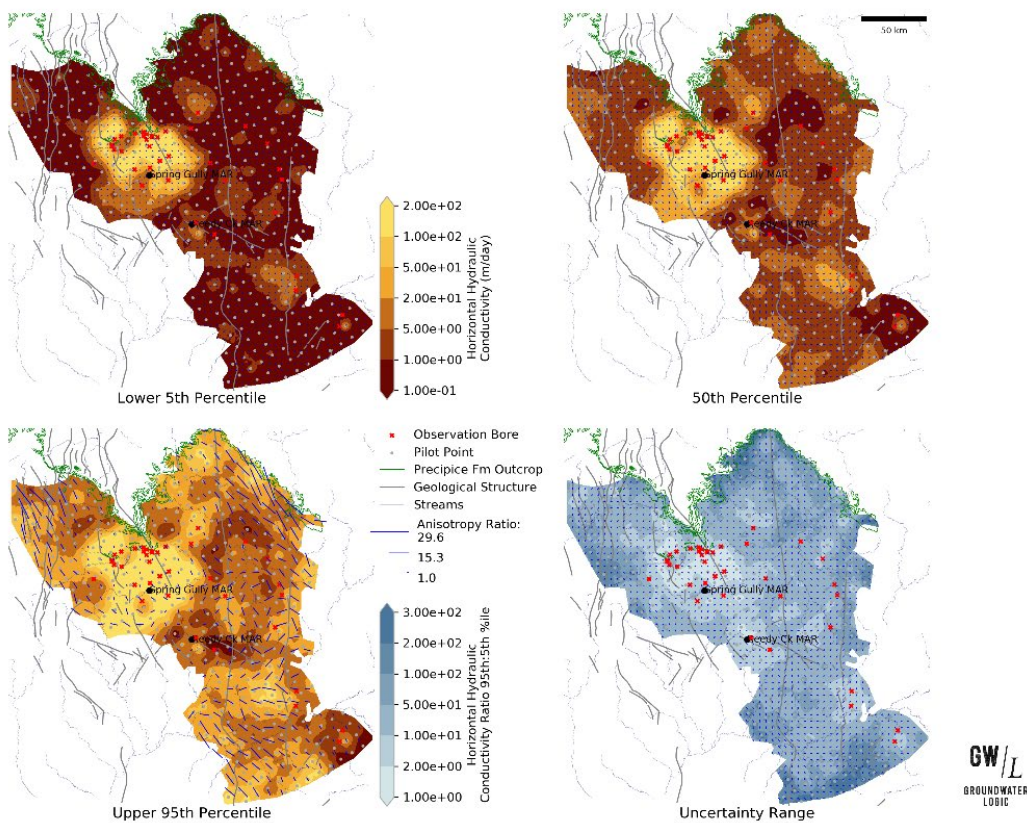


**Figure 107** Blocky Sandstone Reservoir MAR inversion hydraulic conductivity uncertainty.



A significant finding of the Manager Aquifer Recharge (MAR) inversion modelling is that the new UQ-SDAAP sequence stratigraphic framework and geological correlations are supported by observations in the monitoring well pressure response to MAR. Monitoring wells completed in the Blocky Sandstone Reservoir, show a pressure response to MAR up to 100 km away after only two years of injection. Two Santos monitoring bores on the Roma shelf completed in the UQ-SDAAP defined Transition Zone (historically considered to be Precipice Sandstone equivalent) only 25 km from the MAR injection, show no pressure response. This confirms that the UQ-SDAAP new geological correlation is predictive and has implications for the distribution of lateral and vertical hydraulic transmissivity. It also confirms that the Transition Zone is largely a baffle to upwards propagation of pressure of CO<sub>2</sub> migration.

#### 4.6.4 Large-scale production data: Moonie oil field

The Blocky Sandstone Reservoir in the Moonie oil field shares the same depo-centre as the deep basin centre though it is some 400-500 m shallower. The Transition Zone at Moonie contains oil and gas, but is expected to be more sand-prone than in the basin centre. Production data over decades, including evidence for strong aquifer support, supports the feasibility that material, sustained injection rates can be achieved in the basin centre. The Blocky Sandstone Reservoir is relatively homogenous and, in agreement with the seismic data (section 4.3.7), the Moonie fault is not a major, regional flow barrier. The data was critical to calibrating the deeper parts of the basin.

The Moonie field is located in the Surat Basin in southeast Queensland and was discovered by Union Oil in late 1961. It was the first commercial oil discovery in Australia and oil production began in 1964 with its highest oil production rate of ~9000 STB/day in 1966 (O'Sullivan et al. 1991). Oil production started declining since then and is currently producing oil at rate of about ~130 STB/day with over 99% water cut. The Moonie field has two oil bearing formations, The Evergreen Formation "56 Sand" that is equivalent to a sand within the UQ-SDAAP Transition Zone has limited production history. The Precipice Sandstone "58 Sand" that is roughly equivalent to the UQ-SDAAP Blocky Sandstone Reservoir is the main producing reservoir. A total of 44 wells have been drilled in this field of which 11 have been plugged and abandoned so far. There are currently 11 wells on production. Moonie wells 1-18 were drilled before the start of production and Moonie wells 19 onwards are drilled after production had begun. The total cumulative oil production for the field has been about 24 MMSTB oil which makes an approximate 38% recovery factor assuming STOOIP of 64 MMSTB (Barakat 2017). Bridgeport Energy (the current Moonie field operators) is currently undertaking a review on Moonie field to better estimate the remaining oil volume in the reservoir and the potential for future development such as infill drilling and CO<sub>2</sub> enhanced oil recovery (EOR).

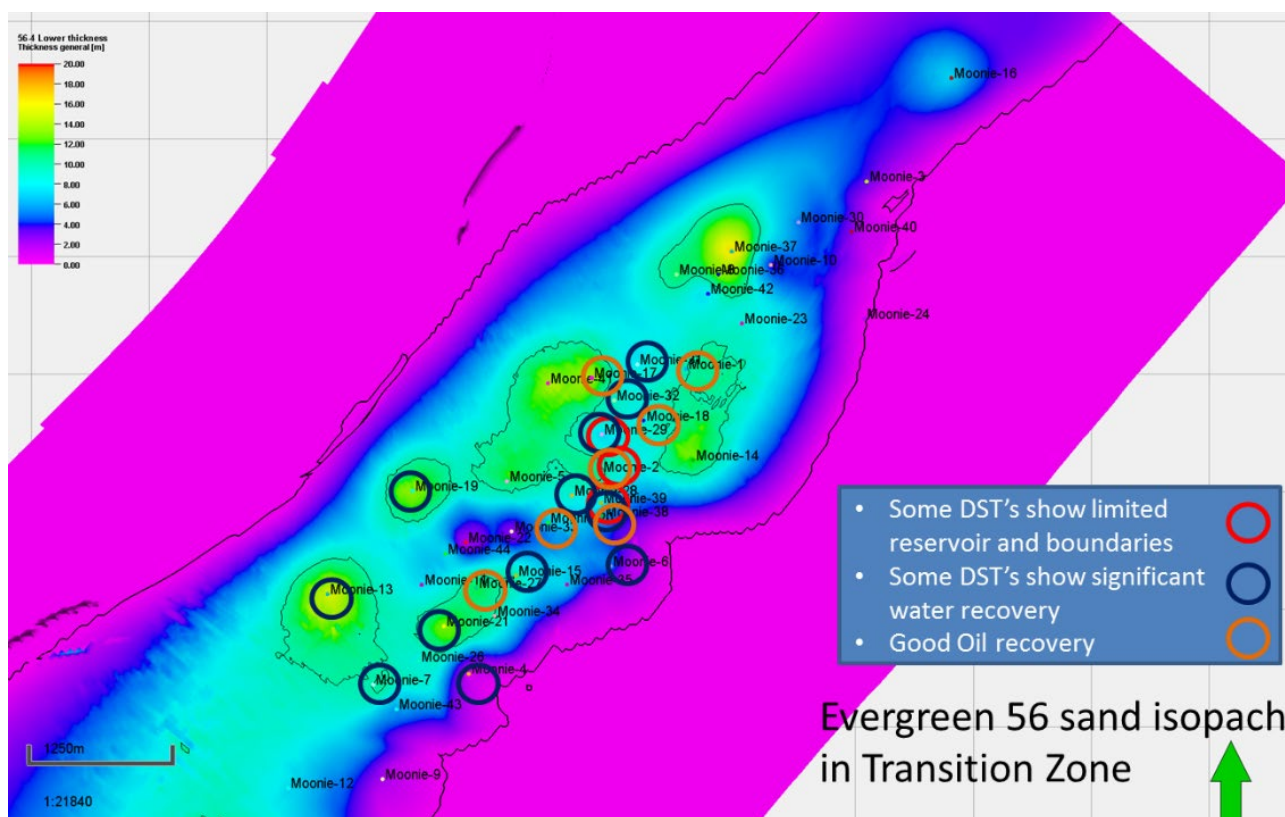
Bridgeport Energy provided the UQ-SDAAP project with full access to Moonie field data such as well completion reports (WCR), drill stem tests (DST), wireline logs, 50 years of production data from both the 56 and 58 Sands and the Bridgeport Energy static and dynamic models. The dynamic model was used to further review the history matching (HM) work done by Bridgeport Energy and to examine key uncertain parameters that could be modified for better HM results. The sensitivity analysis conducted in this study was mainly informed by historical Moonie data provided, as well as UQ-SDAAP new geological/geophysical findings.

The lessons learnt from this work was then incorporated into our model for the UQ-SDAAP notional injection site, in the south-central Surat Basin. Full details of the Moonie oil field analysis are presented in Honari et al. 2019b.

##### 4.6.4.1 Data and methodology

Production tests (PT) and/or DSTs were conducted historically in all 44 wells drilled to evaluate their productivity, fluid type and the free water level (FWL) for the 56 and 58 Sands. Figure 108 summarises the fluid type recovered during initial DST operations in wells testing the 56 Sand and used to estimate the FWL.

**Figure 108** Fluid type recovered during initial DST operations from wells testing the 56 Sand (UQ-SDAAP Transition Zone).



The UQ-SDAAP project analysed all DSTs that had interpretable pressure-time data for the Moonie field wells. The virgin FWL for the 56 Sand (UQ-SDAAP Transition Zone) estimated by Bridgeport Energy is around 1460 mSSTVD; however, our observation revealed that several Moonie wells showed initial oil production from DSTs with intervals below 1460 mSSTVD and also significant water recovery from DSTs with intervals above 1460 mSSTVD. In addition, pressure transient analysis of DSTs in the 56 Sand from some Moonie wells showed characteristics of no flow boundaries. In a similar context, large differences between the extrapolated reservoir pressures of nearby wells were noted from DSTs conducted in the same timeframe. **There is no clear lateral continuity of the oil saturation in the 56 (Transition Zone) Sand.**

The UQ-SDAAP project analysed all 58 Blocky Sand Reservoir sand well tests with sufficient pressure-time data to obtain an extrapolated formation pressure. Fluid recoveries from DSTs run on the 58 Sand in Moonie wells were reviewed with the results summarised in Figure 109. In this figure, Moonie 12 and 16 are located on the edges of the field and have calculated hydraulic heads of 252 m and 233 m, respectively.

In order to review the validity of the assumed 58 Sand FWL at -1515 mSSTVD, the DST extrapolated formation pressures are presented on a pressure-elevation plot in the context of hydraulic heads as illustrated in Figure 110.

The water pressure gradient lines (each representing various water hydraulic head values) were used to estimate various possible FWL values for the Blocky Sandstone Reservoir. The assumed FWL used by both Santos and Bridgeport Energy for field history matching was 1515 mSSTVD. Figure 110 demonstrates that the FWL of 1515 mSSTVD when matched with the oil pressure gradient for the 58 Sand would require a water leg hydraulic head of between 258 and 278 m (depending on the assumed representative oil pressure gradient).

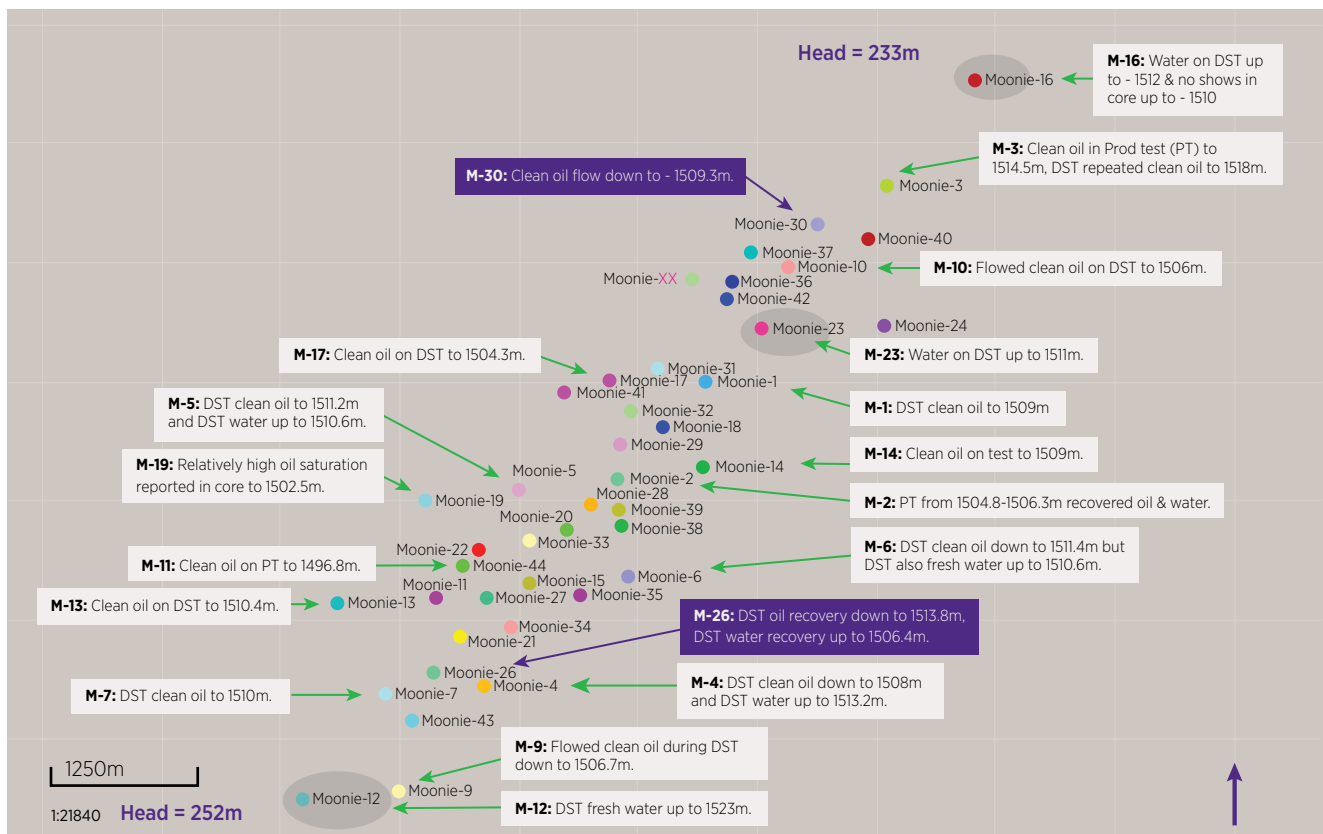
This range of hydraulic head is higher than other value observed in the region of the Moonie field (see section 4.3.2). The two hydraulic head values for water (corresponding to the two water pressure gradients could be interpreted as representing the north (233 m head) and south (252 m head) of the field with a hydraulic barrier such as a fault separating them. This would result in a different FWL in the north and south parts of the field. **The data does not support a compartmentalised field interpretation in the main Blocky Sandstone Reservoir.**

An alternative interpretation is that there is a continuous hydraulic head gradient across the field from south to north (high to low hydraulic head between Moonie 12 and 16) and a continuous hydrocarbon phase with a tilted FWL. To frame the range of possible FWL values for the Moonie field, the combination of the two water pressure gradients and two oil pressure gradients give four possible FWL estimates for the field (Figure 110) ranging between 1538 and 1735 mSS.

Additional production analysis in Honari et al. 2019b discusses further evidence for a tilted FWL.

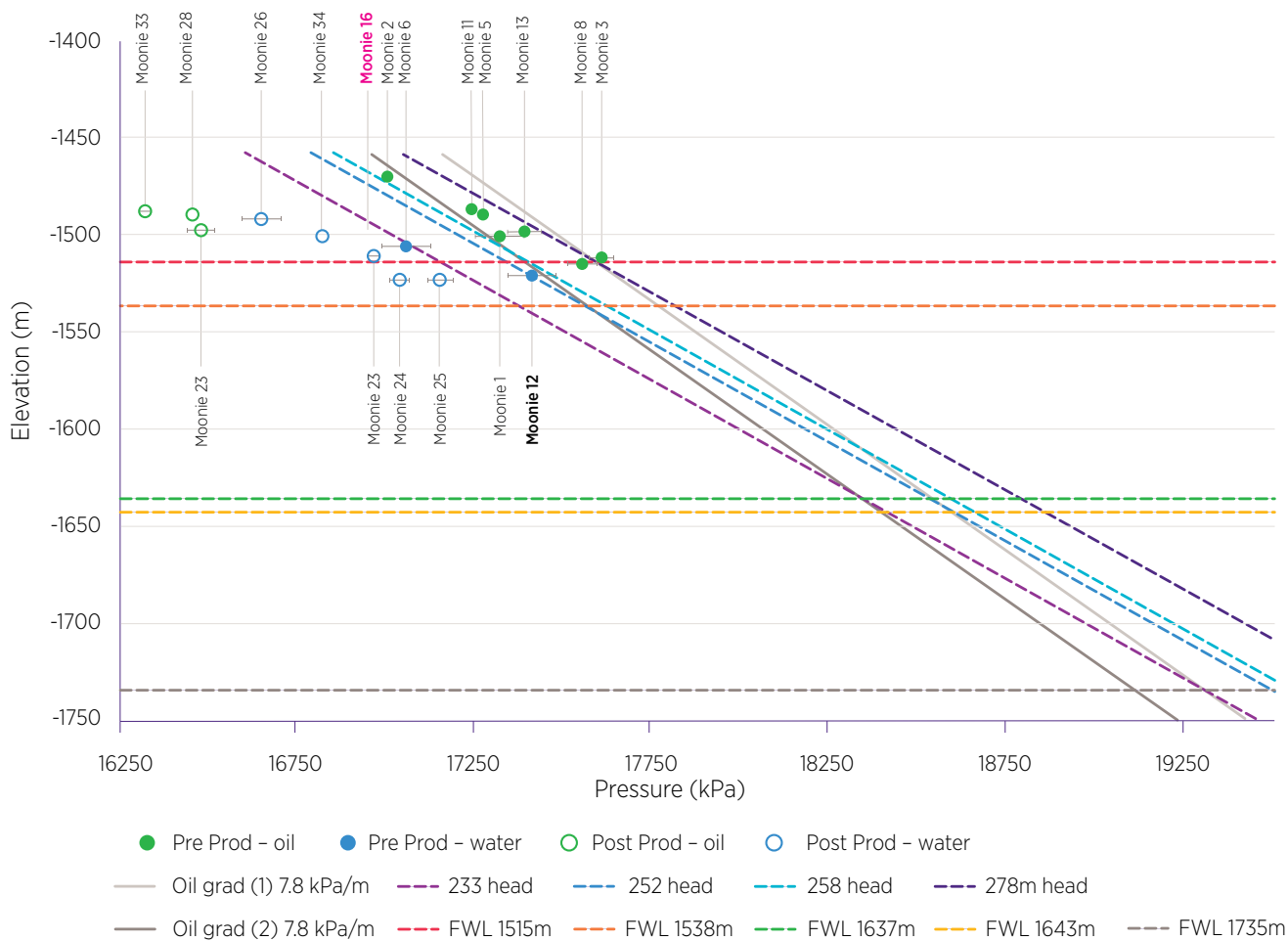
**The data supports a possible tilted FWL. Given the Blocky Sandstone Reservoir pinch-out to the east and south and the segmented Moonie Fault, this is supportive of a well-connected and extensive aquifer to the west which further supports a deep basin injection scenario with limited long-term pressure build up.**

**Figure 109** Fluid type recovery shown from DSTs that tested the 58 Sand in the Moonie field.



Highlighted in purple are postproduction tests.

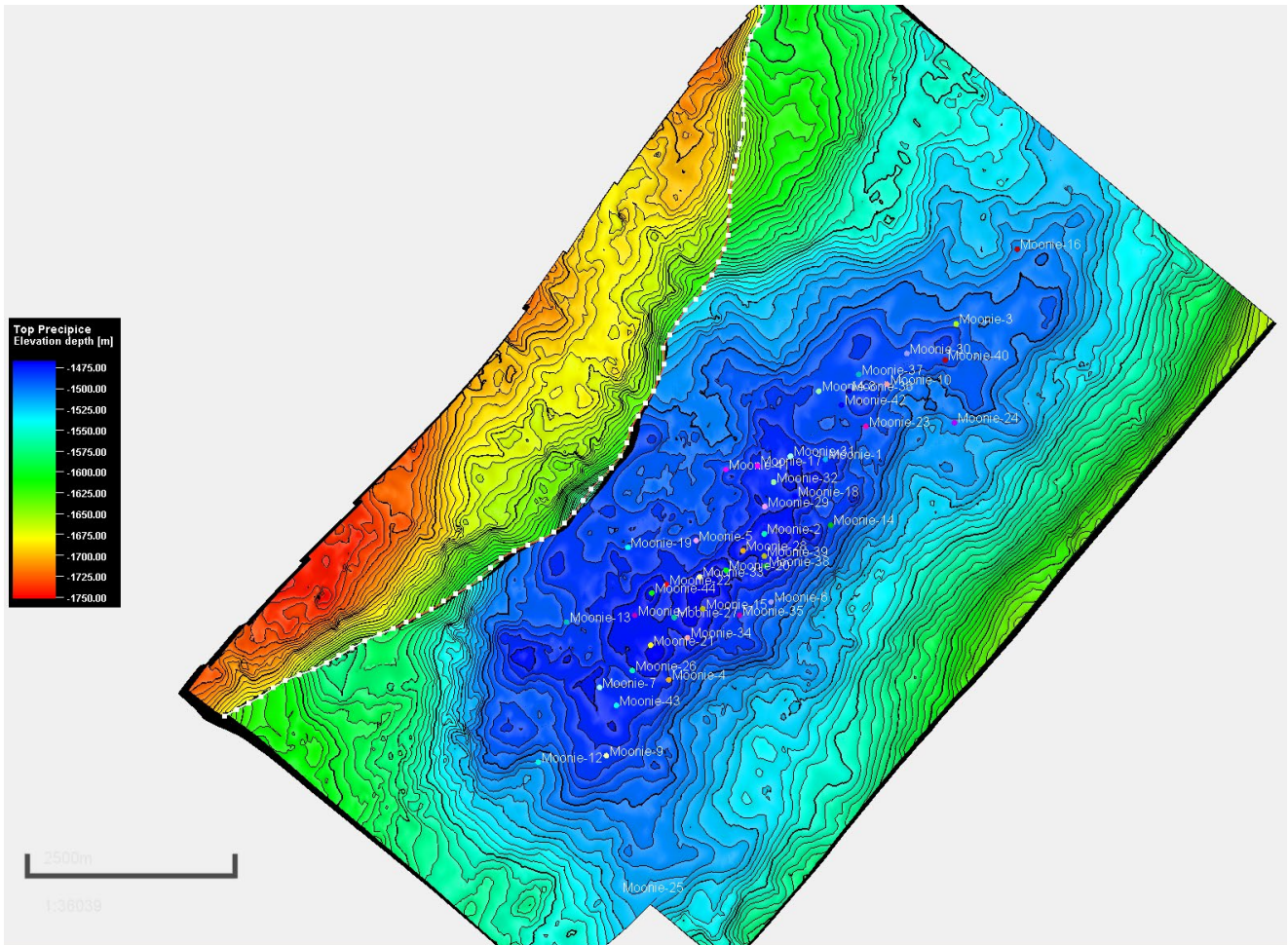
**Figure 110** Evaluation of FWL in Blocky Sandstone Reservoir using hydraulic heads calculated from DSTs in Moonie wells.



#### 4.6.4.2 Dynamic sector model and history match

The Bridgeport Energy static model has been reviewed by the UQ-SDAAP. The areal size of the model, as shown in Figure 111, is about 7 km wide and 11.5 km long roughly the size of the Moonie 3D seismic volume but with the actual Moonie wells distributed in a much narrower area of about 2 x 9 km. The original model consists of 72 layers in the equivalent of the UQ-SDAAP Blocky Sandstone Reservoir and 18 layers in the Transition Zone separated by a single impermeable shale layer. The grid cell sizes are 50 x 50 m in the X and Y directions with various thicknesses.

**Figure 111** Bridgeport Energy Moonie sector model area structure top of the 58 Sand depth map with inclusion of well locations and the Moonie fault.



The pressure measurements made in Moonie field over its production life indicate that the field pressure has dropped only about 1480 kPa over 50 years of production from its original value of -17450 kPa at reference depth of 1515 mSSTVD.

Analysis again suggests that there is a strong water drive mechanism operating in the Moonie field. UQ-SDAAP modelling also supports limited connection to any underlying (Bowen) aquifer system.

#### 4.6.4.3 Porosity and permeability

As described in Harfoush et al. 2019b and 2019c, the UQ-SDAAP project interpreted wireline logs for selected of Moonie wells (wells with sufficient quality and number of petrophysical logs) to calculate petrophysical properties such as net to gross (NTG), Sw, porosity and permeability. Several porosity-permeability transforms were developed for various facies or groups of facies as described in Table 30.

**Table 30** UQ porosity-permeability transform for Moonie area categorised based on facies or groups of facies.

Facies	Permeability Equation
SA	$KH \text{ CASE3\_LIN} = 10^{(-2.30 * VSH + 14.05 * PHIT\_V5 - 0.20)}$
DST comparison for SA	$KHMOONIE = 1.0354 * KH \text{ CASE3\_LIN}$
SB, SC, SD and SMA	$KHMOONIE = 10^{(-2.35 * VSH + 14.95 * PHIT\_V5 - 1.04)}$
Remaining facies	$KHMOONIE = 0.01 \text{ mD}$

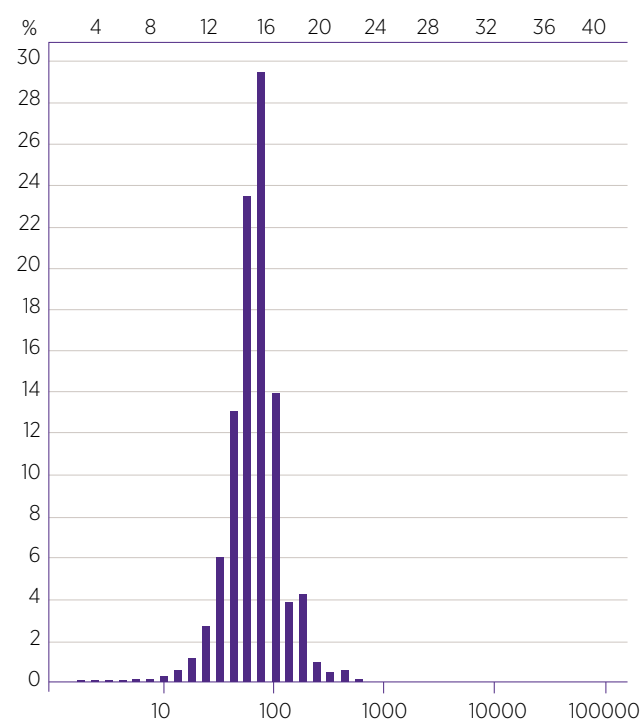
Applying UQ-SDAAP porosity-permeability transforms to the Moonie model significantly reduced the average horizontal permeability ( $k_h$ ) of the 58 Sand from -650 mD in the Bridgeport Energy model to -85 mD. Figure 112 illustrates the difference between horizontal permeability histograms in the Moonie field model. Our new porosity-permeability transform reduced STOOIP in the 58 Sand by 30% caused by our lower horizontal permeability in grid blocks which resulted in lower oil saturation defined by the saturation height function. Further study is needed to verify which petrophysical description would better represent 58 Sand parameterisation in the Moonie field.

Figure 113 illustrates the comparison between actual and simulated oil and water production data for a scenario that was run based on UQ-SDAAP horizontal permeability inputs. The model which was parameterised using UQ-SDAAP porosity-permeability transform showed significantly lower liquid production due to collectively low permeability values across the model and lower STOOIP. Some core observations have revealed the presence of (micro) fractures in the 58 Sand in the Moonie area (Pearce et al. 2019), which could partially explain the higher actual liquid production due to higher bulk permeability. Thus, the effect of (micro) fractures, which likely increase the horizontal permeability, would need to be captured in the Moonie static model. *This may be important for basin centre predictions, but this is currently unknown.*

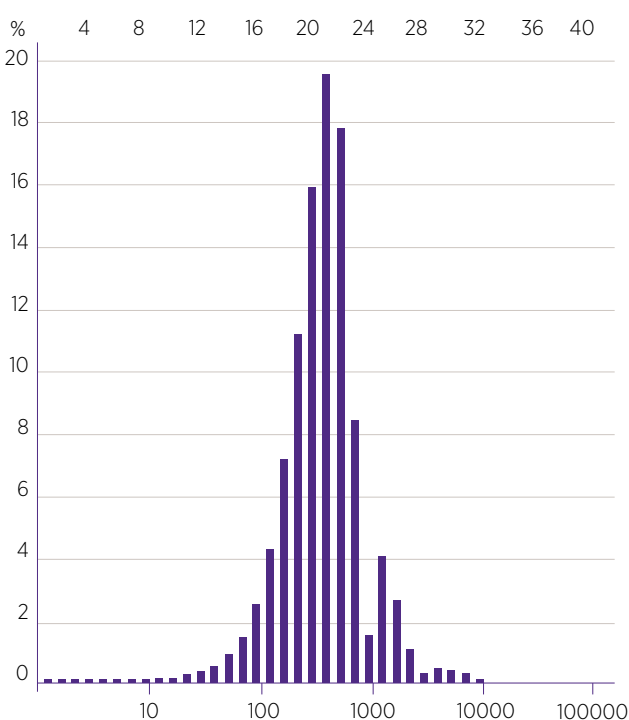
Uncertainty in permeability remains large for UQ-SDAAP. Three scenarios were constructed. New, site-specific data is required.

**Figure 112** Histograms of horizontal permeability for the 58 Sand of the Moonie model generated by the UQ-SDAAP porosity-permeability transform and the Bridgeport Energy original model (top) and their respective STOOIP values (bottom).

### UQ transform (DST corrected)

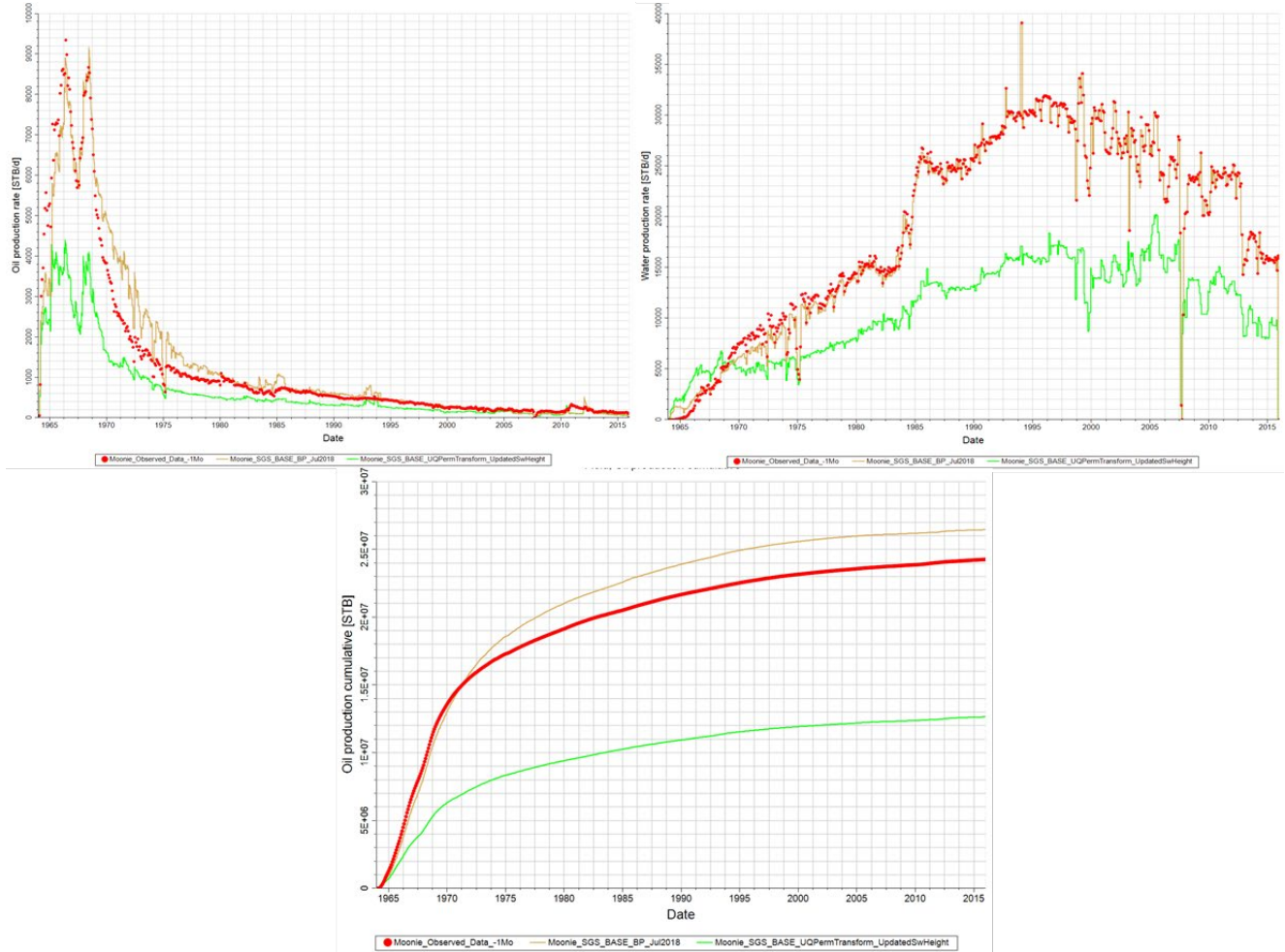


### Bridgeport model



Poro-perm transform used	STOOIP in Blocky Sand (*10 <sup>6</sup> sm <sup>3</sup> )
Bridgeport	10.33
UQ	7.11

**Figure 113** Moonie field oil production rate (top left), field water production rate (top left), field oil production cumulative (bottom). Red circles are historical data, light brown line and green line are for simulation runs with the Bridgeport Energy porosity-permeability model and UQ-SDAAP porosity-permeability transform, respectively.





## 4.6.5 Summary of evidence for injectivity

### UQ-SDAAP examined a number of lines of evidence regarding the likely Blocky Sandstone Reservoir injection performance including:

- The facies analysis, stratigraphic correlations and depositional environment interpretations based on core, wireline petrophysical analysis and seismic interpretation suggest that the Blocky Sandstone Reservoir represents a wide spread clean sandstone deposited in a large high energy braided plain depositional environment. This occurred in a northern and southern depositional centre each with different provenance. The northern depositional system is characterised by a “cleaner sandstone” with less clay content and higher matrix permeability. Conversely the southern depositional system has more clay and relatively lower permeability. Both are extensive and relatively homogenous
- The managed aquifer recharge groundwater inversion focused on the northern depositional centre confirms not only the high matrix permeability of the Blocky Sandstone aquifer but also a secondary fracture permeability resulting an extremely high bulk permeability (100’s of Darcy equivalent)
- Fractures in core have been observed in the vicinity of major fault systems of the southern depositional system. The Moonie oil field production history match requires a higher bulk permeability assumption than is justified from the petrophysical analysis. It is speculated that the difference is due to fracture permeability associated with a damage zone near the Moonie fault. This is corroborated by the strong aquifer support and the relatively low formation pressure drawdown that has occurred with ~30 years of Moonie oil field production
- The well test (DST) analysis, core and petrophysical analysis define a range of bulk permeability for the Blocky Sandstone Reservoir in the southern depositional centre that corroborates the facies analysis, stratigraphic correlations and depositional environment interpretations
- Moonie oil field data supports a well-connected Blocky Sandstone Reservoir with a strong, extensive aquifer connection to the west with minimised reservoir pressure loss over decades
- Thermal and geomechanical modelling of the notional injection locations in the Blocky Sandstone Reservoir of the southern depositional centre define formation breakdown pressure taking into account thermal cooling of relatively cool CO<sub>2</sub> being injected into relatively warm reservoir rocks
- The main uncertainty remaining is the degree of permeability degradation with depth in the basin centre

## 4.7 Notional injection site identification and sweet spot analysis

UQ-SDAAP has adopted an approach to notional site selection based on minimal containment risk and not on optimal economic grounds. The main approach has been to maximise the distance between possible injection sites and potential risk features and potential users of other resources; and to maximise depth. For clarity, sites discussed in this section, are **not** yet proposed for full scale injection, rather they are the key sites where further data is required *before* suitability can be confirmed and any final selection decision can be made. Extensive but fairly conventional data gathering is required at the next stage, similar to oil and gas exploration and appraisal phases. This will include, seismic, drilling, logging and testing; but will not require the injection of any CO<sub>2</sub> into the aquifer (and not any hydraulic stimulation).

The UQ-SDAAP CCS deployment scenario required the identification of hypothetical injection sites for reservoir and groundwater modelling, pipeline route identification and development of an illustrative field development plan. The project identified sites in the Blocky Sandstone Reservoir using, risk-minimising, multiple criteria decision-making methods and suitability analysis tools. A risk avoidance and minimisation approach was taken, selecting criteria that represent technical, social or environmental risks to a carbon capture and storage project. The suitability analysis involved three stages:

1. Analysis on sub-surface criteria
2. Analysis on surface criteria
3. Combining surface and subsurface analyses to form a final suitability map

Subsurface criteria focused on risks to CO<sub>2</sub> dynamic storage capacity and leakage from the geological Storage Complex, for example through groundwater bores or faults and injection pressure interference from third party operations or other geological factors. Surface criteria focused on risks to gaining regulatory approval and social licence to operate by having a negative effect on *perceived* social and environmental “values”. The final suitability map represents the combined subsurface and surface risks to locate “Sweet Spots” (lowest risk areas) for notional CO<sub>2</sub> injection sites. These locations are not precise – there is room for flexibility depending on local conditions.

### 4.7.1 Risk minimising and avoidance philosophy

Development of the Surat Basin for large-scale carbon capture and storage is currently in the pre-appraisal, “Greenfield stage”. More site-specific, appraisal data are therefore needed before confidence in whether a real, industrial scale CCS option exists. The aim of the UQ-SDAAP project was to identify the geographical location(s) that should be the target for the next stage of data gathering, and answers the question:

Given the current level of data and analysis, what is the area most likely to be suitable for CCS, on both a technical and non-technical basis, as the first site for industrial scale long-term injection and secure storage of CO<sub>2</sub>?

Based on the current UQ-SDAAP analyses, there is only one formation in the Surat Basin deeper than 800 m subsurface, which is likely to afford sustained (> 20 years), high rate (say, >5 million tpa), secure CO<sub>2</sub> storage potential. This is the “Blocky Sandstone Reservoir” (Precipice Sandstone). The total “technically injectable” area of the Blocky Sandstone Reservoir is, in principle, very large (the entire Blocky Sandstone Reservoir extent at a depth greater than 800 m). However, there are various surface and subsurface features that reduce the attractiveness of much of this region. The area for notional injection needs to be high-graded by some criteria, especially in the context of the CCS specific risks and potential for conflict with other resource development such as groundwater, oil and gas, coal mining, agriculture and other surface and subsurface activities in the area.

Considering the historical resource developments in the Surat Basin, for the purposes of UQ-SDAAP, the overall high-grading approach for identifying an initial, industrial-scale storage location has been designed to be **demonstrably the lowest, practicable risk** and with minimal groundwater impact (with no negative impact on water quality at depths which are economic for groundwater abstraction). This approach is in deliberate contrast to an approach, which could have optimised the economics or cost of notional injection and storage (minimal well depths, well counts, or permeability, and transport distance).

#### 4.7.1.1 Methodology

In line with a philosophy of *demonstrable* risk-minimisation, UQ-SDAAP high-graded or selected notional injection sites based on reducing both technical and non-technical risk factors (which overlap or coincide to some extent). Technical risk factors aim to select the *lowest overall injection and containment risk based on currently available data*. Non-technical risk factors aim to *maximise separation distance from other users and from any surface sensitivities or subsurface features that might cause stakeholder concern*.

The process followed in high-grading notional injection sites therefore involved common risk area or segment creation and analysis as follows:

1. Key subsurface features were characterised such as legacy oil and gas exploration wells, producing oil or gas wells, producing water bores from different formations and faults occurring at the storage complex level
2. Key surface features were defined; such as locations where people live, land use, areas with environmental values and Native Title

The research initially defined nominal minimum separation distances from any of these features, creating “grey zones”<sup>19</sup> within which injection wells and facilities would not be sited (in a first-pass analysis). Features representing the highest risk such as potential top seal penetrations (wells), potential pressure effects (wells and water bores) were marked as a grey zone with a 15 km radius. Features likely to cause less concern for stakeholders or with lower objective containment risk (e.g. active water wells completed in formations shallower than the storage complex) were assigned a smaller grey zone depending on the assigned relative risk. In the subsurface, grey zone radii were informed by plume spread modelling, so maximum separation distances were assigned to features within the Blocky Sandstone Reservoir (legacy wells and faults). Small distances were assigned to legacy wells completed above the Ultimate Seal.

The remaining areas “green to red zones”<sup>20</sup> were graded by structural dip of the seismic reflector at the Ultimate Seal (zero dip being most favourable). Other favourable parameters were the thickness of the reservoir (thicker is better), depth to the top of the reservoir (deeper is better), with green representing the most favourable areas and red representing least favourable, but still not within a “grey zone” area. Notional injection sites were therefore able to be selected, maximising the distance from known features that posed a hypothetical technical risk to CCS development. Surface environment and other non-technical risk factors were similarly graded: for example, in the surface criteria of land use, the research considered an area used for grazing native vegetation to be more suitable for an injection site than an area used for irrigated horticulture.

The result for notional site selection is considered a very low risk, very conservative approach. The grey zones should not be considered areas where no injection can take place, rather the green zones are the most attractive sites within the historic, social and geological context of the area and the philosophy of *demonstrably minimum risk* (for a first CCS development and therefore the next stage of data gathering).

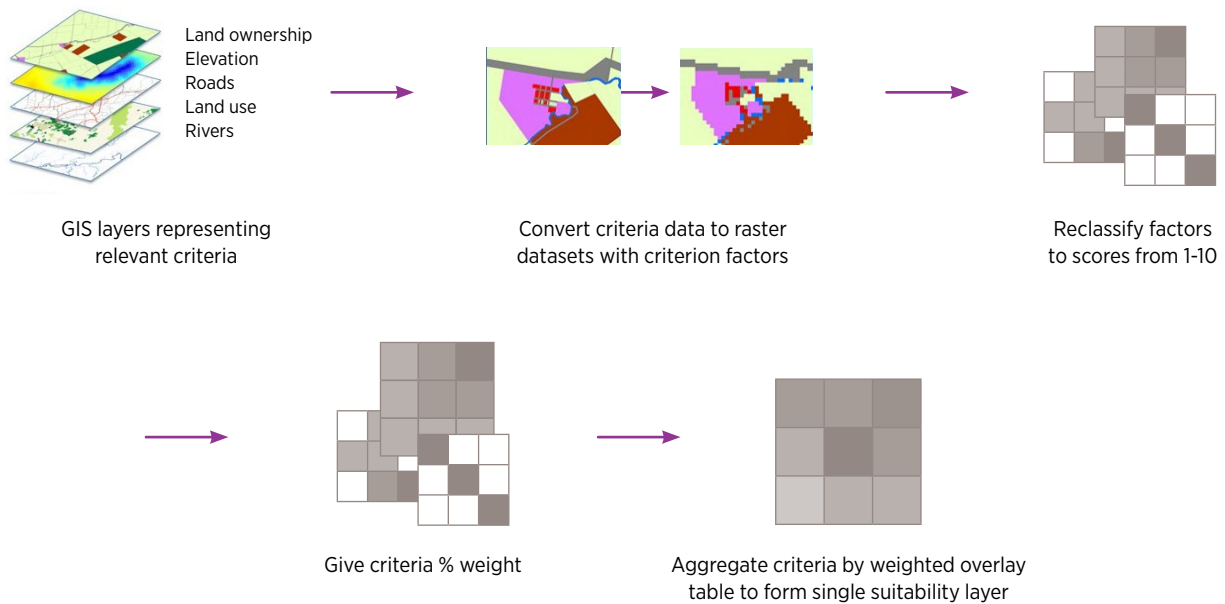
A geographic information systems (GIS) method known as “suitability analysis” was used to implement the notional injection site selection philosophy and linear weighted combination (Jiang and Eastman 2000, Beier, Majka et al. 2009; Malczewski 2006) to combine the information about relevant surface and subsurface features.

The report by Wolhuter et al. 2019a describes in detail the methodology and application of the *demonstrably minimum risk philosophy* is developing the ‘sweet spot’ locations for notional CCS.

Figure 114 describes the suitability analysis workflow. A scoring range of one to 10 was used, with 10 representing the most suitable factor and one representing the least suitable factor. Scores were assigned to criterion factors based on the *demonstrably minimum risk philosophy*, our knowledge of the risks represented by the factors and the distribution of the factor data.

<sup>19</sup> Grey zone: Areas not high-graded for the first tranche of industrial scale CO<sub>2</sub> injection i.e. not the *lowest demonstrable* containment risk or potential area of *least* stakeholder concern. For clarity, this does not indicate area where future injection will always be excluded; area risk assessment will need to be repeated on each cycle of new data gathering  
<sup>20</sup> Green to red zone: Areas that are high-graded for the first tranche of industrial scale CO<sub>2</sub> injection based on maximising distance from sensitive surface and sub-surface features and optimal containment factors. Green zones having the highest grade and red the lowest grade within the high-graded areas.

**Figure 114** Flow chart showing the UQ-SDAAP suitability analysis procedure.



## 4.7.2 Application of “rules” to subsurface features constraints

**By taking a conservative approach, based mainly on the avoidance of risk factors and features, a lowest risk injection and storage area has been scoped out for further investigation. The area is large enough to support a feasible, high sustained rate CCS scheme. More detailed field studies and local engagement with communities would be required to establish actual suitability.**

The criteria that UQ-SDAAP used in the subsurface suitability analysis represented technical requirements for CCS, CO<sub>2</sub> migration risks, risk of affecting the rights of a third party, or regulatory risks to the operator because of likely negative environmental impacts. As CO<sub>2</sub> migration out of the intended storage complex (consisting of the Blocky Sandstone Reservoir, Transition Zone and Ultimate Seal combined) and its effects on third party rights are a major factor in the viability of CCS, the nominal minimum separation distances were applied, indicated by grey zones to the criteria representing these risks. A restriction function was used to represent the grey zones. This had the effect of applying a very low suitability score (minimum suitability score minus one) to an area a set distance around features mapped for that criterion. Table 31 sets out the criteria used, what risks each criterion represents and the grey zone (restriction function) applied to each criterion.

For simplicity, for this study, each criterion was given the same weighting. The criteria used to determine subsurface suitability and the risks represented by each of the criteria and their associated restriction function are summarised in Table 31. Table 32 sets out the weighting for each of the criteria used in the subsurface analysis. *This does not negate the need for detailed field studies.*

**Table 31** Subsurface suitability criteria, risks represented and associated restriction function.

Criterion	Risks/Technical requirements	Grey zone
Depth of Transition Zone	Storage capacity	Minimum restriction applied to depths <800 m below ground level
Thickness of the Blocky Sandstone Reservoir (TS1 – J10)	Technical requirement	No restriction function, but thicker is better on injection and pressure grounds
Dip angle of the Blocky Sandstone Reservoir (TS1 – J10)	CO <sub>2</sub> flow direction and migration rate	No restriction function, but it is essentially parallel to the Ultimate Seal
Distance from petroleum lease boundaries	CO <sub>2</sub> migration and interference with 3 <sup>rd</sup> party rights	Minimum restriction applied to 5 km from Petroleum Lease boarders – a safety margin approach
Distance from the zero edge pinch-out and outcrop of the Blocky Sandstone Reservoir (TS1 – J10)	Technical requirement – pressure interference of the edge may limit injection based on BHP constraints	Minimum restriction applied to areas within 5 km of the edge – a safety margin approach
Distance from a fault (indication from seismic of possible fault) at the reservoir Storage Complex	CO <sub>2</sub> migration out of Storage Complex	Minimum restriction applied to areas within 5 km of the mapped fault – this would need revisiting after new data are acquired (data are sparse)
Groundwater bores/ex-petroleum wells that were drilled into the Ultimate Seal (J30) and are sourcing water from the Precipice Sandstone or Evergreen Formation or bores with no depth information or no information on water source or P&A methods. Springs sourcing water from the "Precipice Sandstone" Managed aquifer recharge wells	CO <sub>2</sub> migration risk & interference with groundwater levels and water chemistry	Minimum restriction applied to 15 km radius from bore/ex-petroleum well – this is 5 km more than the furthest model plume spread
Groundwater bores/petroleum wells that were drilled into the Ultimate Seal (J30) and are in use/sourcing water from a formation above the Evergreen Formation.	CO <sub>2</sub> migration risk & interference with groundwater levels and water chemistry	Minimum restriction applied to 10 km radius from bore/well (the Transition Zone in the MAR area does not transmit much pressure)
Petroleum wells drilled into the Ultimate Seal (J30) and plugged and abandoned.	CO <sub>2</sub> leakage risk out of the Storage Complex	Minimum restriction applied to 5 km radius from wells (the seal complex is tight)
Groundwater bores that did not go into the Ultimate Seal (J30) and are sourcing water from the Hutton Sandstone	Risk of interference with groundwater levels and water chemistry	Minimum restriction applied to 5 km radius from wells (the seal complex is tight)
Groundwater bores or petroleum wells that did not go through the Ultimate Seal (J30) and are not sourcing water from the Hutton Sandstone	Minor CO <sub>2</sub> leakage risk & interference with groundwater levels and water chemistry	Minimum restriction applied to 2 km radius from bore (the seal complex is tight)

**Table 32** Criteria weighting for subsurface analysis (initial weighting – a sensitivity analysis was undertaken and results in essentially the same high-graded sites).

Layer	% influence
Transition Zone (TS3/J20) depth	10
Blocky Sandstone Reservoir thickness	10
Blocky Sandstone Reservoir dip angle	10
Distance from petroleum leases	10
Distance from Blocky Sandstone Reservoir edge	10
Distance from faults at reservoir storage complex level	10
Distance from bores/wells/springs with 15 km restriction	10
Distance from bores/wells with 10 km restriction	10
Distance from bores/wells with 5 km restriction	10
Distance from bores/wells/springs with 2 km restriction	10

Table 33 to Table 40 set out the factors within each criterion and the factor scores applied, using a factor range of one to 10. A higher factor score indicates that the factor is more suitable for hosting notional CO<sub>2</sub> injection. Factor scores in the range of one to 10 were applied for each factor in the criteria, using our best estimate of the relative suitability of each factor for the location of an injection site. Arguments can however be made for different factor scores.

For Transition Zone depth, to ensure that the CO<sub>2</sub> would remain supercritical, any zone that may contain CO<sub>2</sub> would need to be below -800 m from ground level (Department of Mines, Industry Regulation and Safety 2013). The restriction function was used for any location with a depth above 600 m below sea level (surface elevation is between 1243 m and 195 m above sea level). For the remaining depth categories, higher suitability scores were given as the depth range increased with density of CO<sub>2</sub>, and therefore storage mass per volume increases with depth. Any location from 600 to 800 m below sea level was given the lowest possible value of one as the depth range is relatively close to the shallowest possible depth of 600 m below sea level. Depths of 800 to 1000 m below sea level a score of seven, and anything greater than 1000 m below sea level the maximum score of 10 (Table 33).

The thickness of the Blocky Sandstone Reservoir was used as it represents the primary storage capacity of the notional CO<sub>2</sub> Storage Complex, with thicker areas likely to have a higher theoretical storage capacity and injectivity. A reservoir thickness of over 100 m was considered to be best given an industrial storage volume scenario, so areas with a thickness of >100 m were given the maximum score of 10, while areas with a thinner Blocky Sandstone Reservoir were given lower scores based on the preliminary dynamic modelling results (Table 34).

The dip angle in the region of the notional CO<sub>2</sub> storage reservoir affects the estimated distance, rate and direction of the CO<sub>2</sub> plume spread. A flatter/lower dip angle would result a CO<sub>2</sub> plume with a smaller geographic footprint at any given time. GIS software was used to classify the dip angle range into five categories using natural breaks observed in the regional distribution where the flattest category was scored 10, the category with the highest slope a score of one, and intermediate values to the remaining dip angle categories based on the preliminary dynamic modelling results (Table 35).

The criteria of distance from the Blocky Sandstone Reservoir edge, distance from petroleum leases and distance from indications in seismic analysis of possible faults at the reservoir storage complex level was given. The same distance ranges and scores as the risk of pressure interference or CO<sub>2</sub> migration/leakage decreases with distance away from the criterion. The criteria were also all represented as linear features in ArcMap. Areas under 5 km from the edge of a Blocky Sandstone Reservoir edge/mapped fault/petroleum lease boundary were restricted. Areas 5 km to 10 km and 10 km to 20 km were given low scores of one and three respectively, while areas over 20 km were given the maximum score (Table 36). The distance ranges and scores were based on preliminary notional injection modelling that showed there would be significant pressure interference 5 km away, but a buffer of at 20 km would be suitable to reduce the likelihood of pressure interference.

A similar methodology was used based on the preliminary dynamic modelling results for assigning factor scores for all the criteria related to the distance from a bore, well or spring (Table 37, Table 38, Table 39, and Table 40) as risk of CO<sub>2</sub> leakage decreases the further away the injection site is from the bore/well. Each criterion was given four distance categories. The lowest distance category was the restriction distance related to the criteria. The distance categories then increases by 5 km, with a range of 5 km until the fourth distance category contains the maximum distance from any bore/well within the criteria.

**Table 33** Factor values for top of Transition Zone depth.

Top of Transition Zone depth from sea level (m)	Score
939 – -600	Restricted
-600 – -800	1
-800 – -1000	7
<-1000	10
No Data	No Data

**Table 34** Factor values for Blocky Sandstone Reservoir thickness.

Blocky Sandstone Reservoir thickness (m)	Score
<50.5	1
50.5 - 100	2
>100	10
No Data	No Data

**Table 35** Factor values for Blocky Sandstone Reservoir dip angle.

Blocky Sandstone Reservoir dip angle (deg)	Score
>7	1
3.4 – 7	3
1.8 – 3.4	5
0.9 – 1.8	9
<0.9	10
No Data	No Data

**Table 36** Factor values for distance from Blocky Sandstone Reservoir zero edge.

Distance from Blocky Sandstone Reservoir zero edge (m)	Score
0 – 5000	Restricted
5000 – 10000	1
10000 – 20000	3
>20000	10
No Data	No Data

**Table 37** Factor values for bores/wells with a 15 km radius restriction function.

Distance from bore/well (m)	Score
0 – 15000	Restricted
15000 – 20000	1
20000 – 25000	3
>25000	10
No Data	No Data

**Table 38** Factor values bores/wells with 10 km radius restriction.

Distance from bore/well (m)	Score
0 – 10000	Restricted
10000 – 15000	1
15000 – 20000	3
>20000	10
No Data	No Data

**Table 39** Factor values for bores/wells with 5 km radius restriction.

Distance from bore/well (m)	Score
0 – 5000	Restricted
5000 – 10000	1
10000 – 15000	3
>15000	10
No Data	No Data

**Table 40** Factor values for bores/wells with 2 km radius restriction.

Distance from bore/well (m)	Score
0 – 2000	Restricted
2000 – 5000	1
5000 – 10000	3
>10000	10
No Data	No Data

### 4.7.3 Application of “rules” to surface constraints

**A relatively large area has been identified in an illustrative manner only. Models based on these are support the technical feasibility if safe, secure storage. However, no definitive proposals are made for the “best” sites, only illustrative areas which were used to support further modelling. Considerably more engagement and local field-work is needed locally to investigate real on-the-ground suitability.**

The surface suitability analysis aimed to identify areas that are appropriate for notional CO<sub>2</sub> injection from a well construction and pipeline engineering perspective, as well as limiting the impacts on land use, the environment and people living in the area. Grey zones (restriction function) were not applied on surface criteria as the factors in the surface criteria did not represent risks to the *technical* viability of a CCS project to the same extent as subsurface criteria or the uncertainty of the data used for the factor made it impractical to apply grey zones. For example, grey zones could have been applied around dwellings, however a visual comparison of the data used to represent dwellings with satellite imagery suggested that not all dwellings were captured, or that the locations were not accurate (although a lot of the positional inaccuracy can be accounted for by different data projections). The radius of a grey zone placed around dwellings would have been at a similar scale the positional uncertainty of data. It was therefore determined it would be more appropriate to analyse the risks represented by the distance from dwellings within the red to green zone for this stage of the analysis. The following criteria was used to determine nominal surface suitability:

- Slope
- Distance from watercourses
- Distance from dwellings
- Land ownership (digital cadastral database)
- Land use
- Native Title
- Vegetation protected under the *Vegetation Management Act 1999*
- Areas to avoid (mining leases, areas where environmental surveys must be conducted)

See Wolhuter et al. 2019a for further discussion.

### 4.7.4 Sweet spot identification, description and remaining uncertainties

In order to amalgamate the subsurface and surface criteria, the suitability layers were combined using a weighted overlay table, with the surface and subsurface layers given equal (50%) weighting. ArcMap 10.6 was used to run the suitability analysis. The model boundary for the suitability analysis was the Blocky Sandstone Reservoir edge and the project projection was GDA94 MGA55 (EPSG 28355). The Blocky Sandstone Reservoir thickness raster was used to align raster cell extents in the subsurface analysis, and the reprojected digital elevation model to align raster cell extents in the surface analysis.

The results of the subsurface and surface analysis area is available in Wolhuter et al. 2019a. The combined suitability map (Figure 115) shows two “green to red zones” within which a notional injection site could be located. One scenario of a notional injection modelling showed that at least three well sites (pads), with three to four horizontal wells at each site could be required over the lifetime of a viable material-scale CO<sub>2</sub> injection project. The southernmost “green” area is the only area large enough to host three injection sites with enough distance between the sites to avoid pressure interference and provide an additional buffer of space with few intersecting risks around the wells.

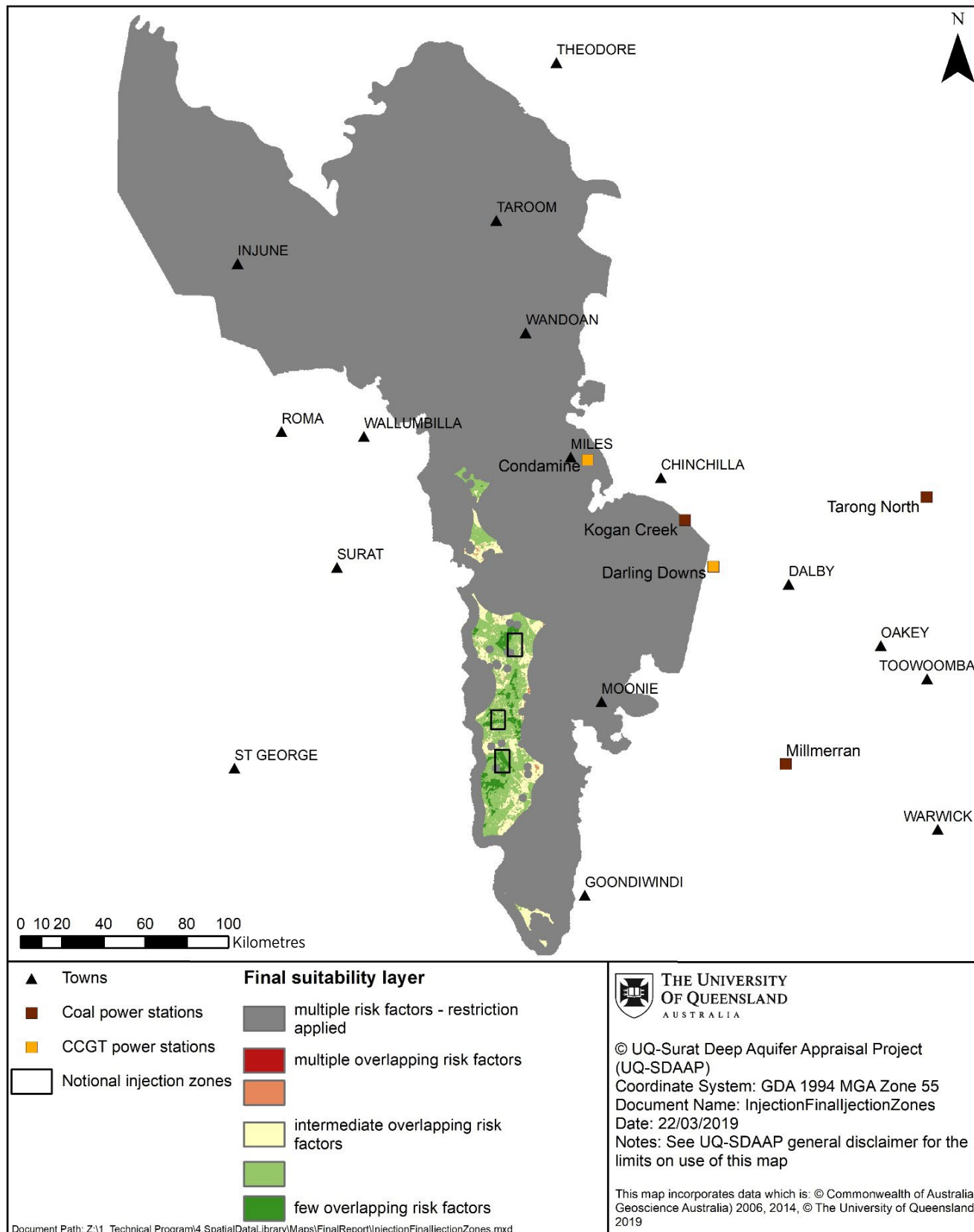
Three nominal locations were selected within the bottom green to red zone as locations for modelling. Proximity to power stations was included so that the length of the pipeline between the injection site and the power station could be estimated (Figure 115).

All green areas within the bottom green to red zone represent a location that, given current data, has our current *best guess of the lowest, practicable risk* for CO<sub>2</sub> injection.

There are several uncertainties associated with the source data used in the analysis to create risk overlays for the location of notional CO<sub>2</sub> injection sites. An appraisal program to reduce uncertainty in the data used for this analysis will be needed to progress a potential CCS project to determine whether a real, industrial scale CCS option exists.



Figure 115 Final suitability (low risk) map with notional injection locations and key power stations.



## 4.8 Notional injection site modelling and FDP – Reference case

There is a feasible field development plan which satisfies key elements of the development philosophy (e.g. minimum footprint and lowest containment risk) and can likely inject and safely store around 13 Mtpa for at least 20 years and a duration which is longer than the lifetime of the modern, supercritical coal plants. There is potential to extend this duration by a few decades.

### 4.8.1 UQ-SDAAP field development philosophy

Capture and transport “Hub” development philosophies are discussed in section 4.1.4. For the selection of notional sites (section 4.7) and engineering choices, the following “rules” were adopted:

1. The notional field development plan would be scoped out based on **lowest containment risk** considerations e.g. rather than lowest cost. *In addition to selecting, deep, basin centre sites, with flat lying geology, this resulted in horizontal wells to minimise temperature and pressure increases*
2. The development would aim for a **minimum surface footprint**. *This resulted in an avoidance of highest value land and an area which coincided with the basin centre and in a minimal number of well pads (2 to 3) from which all necessary wells*
3. The development would aim for **maximum separation from other subsurface resource users** (water, oil and gas, CSG)
4. The development would attempt to satisfy **material abatement of 5-10 Mtpa** for ~30 years. *In fact, a notional scheme for 12.7 Mtpa or more has been scoped out*
5. The development would **not consider late-life secondary or tertiary measures** which could further increase injection of cumulative storage (resource efficiency) e.g. in-fill drilling or pressure relief wells – this would impact items 1-3 above

### 4.8.2 Translating the revised geology and static models

A UQ-SDAAP regional static model (sections 4.3) served as a basis of running dynamic simulations to investigate the sustainability of large rate, long duration CO<sub>2</sub> injection and storage. It was also used as the basis for investigating the interaction of the storage process with regional groundwater systems, and with other anthropogenic activities in the same geology.

The regional model was modified to:

1. Reduce the number of cells to make the simulations less computationally expensive/time consuming, while still providing a reasonable representation of the fluid behaviour
2. Remove gridding issues, which would cause convergence problems within the numerical simulations
3. Add cells to allow more reasonable representation of the fluid behaviour at boundaries of the model in the north (where MAR injection could have some influence (section 4.3.9) and on the top/bottom boundaries of the model

The regional model has approximately 104 million cells over 47 layers between the top of the Ultimate Seal and bottom of the Blocky Sandstone Reservoir. While this granularity was required to develop confidence in the geological model (i.e. a model consistent with *all* data and key stratigraphic principles), it did not represent a pragmatic model for dynamic simulation.

Upscaling and area or sector selection was required to reduce the number of cells for dynamic modelling to make the simulations less computationally expensive and able to run on the UQ-SDAAP software/hardware.

Therefore, a “notional injection sector model grid” was used for multiphase models of notional CO<sub>2</sub> injection to be run in reservoir simulation software (CMG GEM). These models considered all the complications of multiphase flow in regions around the notional CO<sub>2</sub> injection where both formation water and CO<sub>2</sub> may occur over the time-scale of the simulation. This sector grid covered the area around the notional injection sites, albeit extending some distance away (65 x 115 km), and the cell count in this area was further reduced by “upgridding” (re-gridding parts of the model with larger cells) in parts of the model where high levels of detail occurred that were unnecessary for representing changes in fluid flow due to notional CO<sub>2</sub> injection. This process of reducing the cell count in these models involved 4 steps:

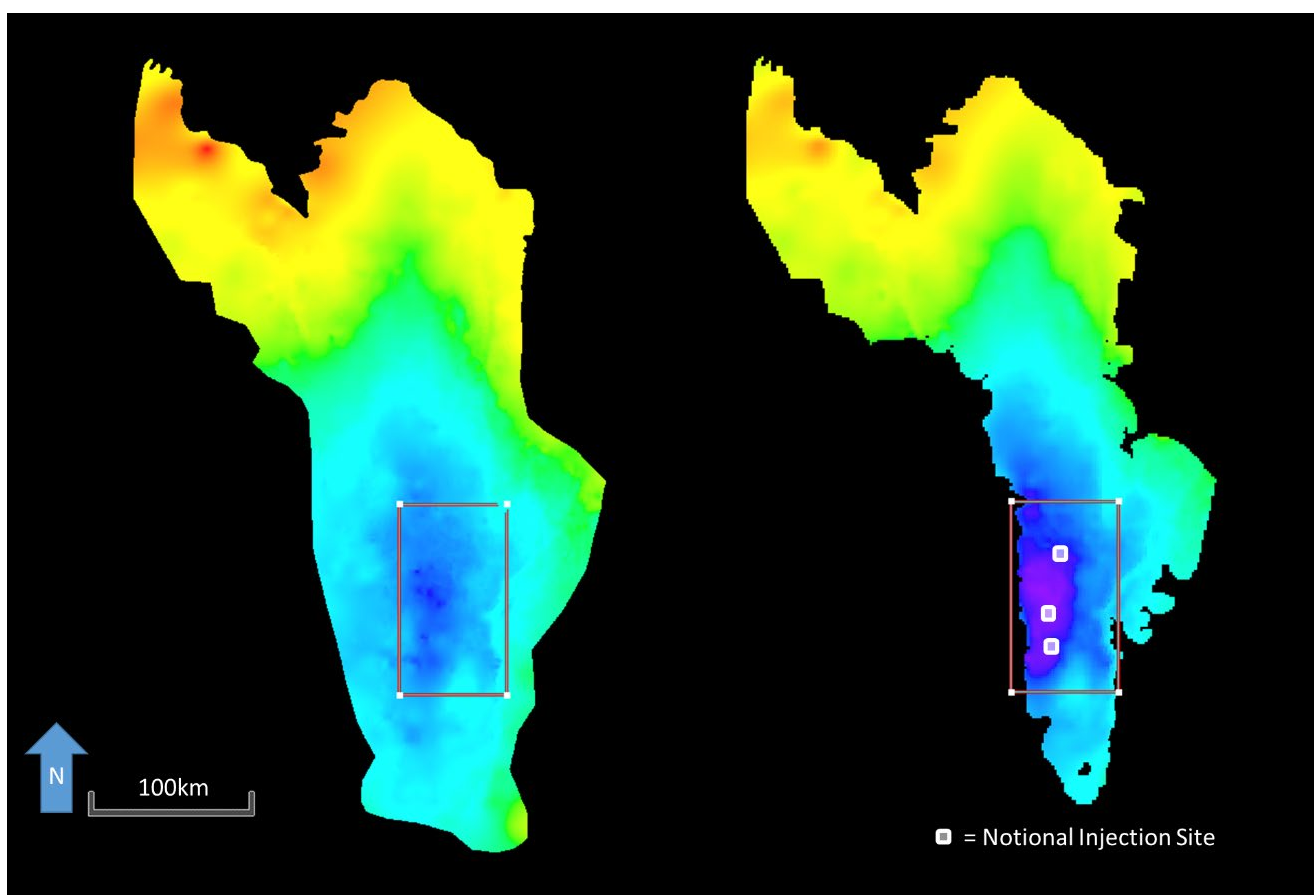
1. Clipping the regional static model to the area of interest
2. Upgridding the models using larger cells, based on the principle of maintaining detail in areas where multiphase (i.e. CO<sub>2</sub> and water) flow was likely to occur, while coarsening cells in parts of the model where single phase (water only) flow was expected
3. Upscaling the properties of the regional static model to the new grids, so the simulated behaviour of a dynamic model using the new grid would replicate the behaviour of an equivalent model using the original grid
4. Adjustment of gridding near faults to avoid convergence issues

Rodger et al. 2019 d and e presents a detailed description of how these four steps were implemented. The UQ-SDAAP project determined the boundary for the notional injection sector model based on the following criteria:

1. The notional injection sector model should include all notional injection sites (rather than modelling single injection locations in separate models) to allow for understanding any pressure interference between sites, and optimise injection rates between sites. This allows for several different roll-out scenarios to be tested (simulated) and more accurately represented. See Wolhuter et al. 2019 for more information on the notional injection sites
2. The notional injection sector model should be large enough that even in a credible worst-case scenario (i.e. most significant lateral migration of CO<sub>2</sub>), the simulated CO<sub>2</sub> plume would not reach the edge of the model area
3. The western boundary of the notional injection sector model should occur further west than the 'pinch-out' of the Blocky Sandstone Reservoir. This would allow the effects of increased pressure build-up caused by the proximity of the 'pinch-out' to be modelled in a more reasonable fashion than if a boundary condition mimicking this effect had to be specified for the western boundary of the model
4. The eastern boundary should extend beyond the Moonie and Goondiwindi fault systems, thus including them in the model area. This would allow the pressure build-up at these faults to be simulated, and allow testing various fault sealing scenarios (sealing, partially sealing or not sealing) and its impact on injectivity and pressure build-up

The resulting Notional Injection Sector model is illustrated in Figure 116.

**Figure 116** Location of the notional injection sector model (red box) relative to the top of the regional static model (left) and extent of Blocky Sandstone Reservoir (right). Colour indicates depth structure from sea level (blue/purple is deeper). notional injection sites shown as white squares.



### 4.8.3 Boundary conditions

**Lateral boundaries.** The boundary conditions used for the notional injection sector model were, for the most part, relatively straightforward for the south, east and west. For the reference case, these boundaries were defined as a number of ‘open’ boundaries (i.e. they would allow flow out of the model and into an assumed “aquifer” external to the model domain), using Carter-Tracy analytic (Carter and Tracy 1960) aquifers within CMG GEM functionality (CMG 2018). The defined external aquifers were connected to different zones within the model and had properties dependent on the zone they were connected to. For example, a ‘Blocky Sandstone Reservoir’ aquifer would be represented as having higher permeability than a “Transition Zone” aquifer.

**Top boundary.** To represent the boundary behaviour at the top (above the Ultimate Seal and bottom (below the Base Surat Unconformity) of the model, two layers were added. The top layer is a relatively thick (100 m), porous (20%) and permeable (100 mD) layer that sits directly on top of the Ultimate Seal. This layer represents a “dummy” Hutton aquifer, which sits directly above the Ultimate Seal. The properties and geometry of this layer are not actually representative of the complexity and heterogeneity of the Hutton. It was intended to allow flow of fluids, or transmission of pressure, which would be limited mainly by the extremely low permeability of the Ultimate Seal (and not by the assumed permeability of the Hutton). This layer was added because a closed boundary (no-flow) boundary above the Ultimate Seal would not be consistent with assumptions made in groundwater modelling elsewhere. The added dummy layer would allow a simple worst case assessment of (approximately) the volumes of fluid that could migrate from the Ultimate Seal into the Hutton as a result of CO<sub>2</sub> injection. A more sophisticated approach was not warranted by the data available for the Hutton in the area.

**Bottom boundary and pinch-out.** The UQ-SDAAP project also added a dummy layer at the bottom of the model. This layer is 20 m thick and has properties that were varied to allow scenario testing to represent any flow that might occur into, or along, the Base Surat Unconformity surface, at the base of the Blocky Sandstone Reservoir (whether due to weathering at the unconformity, or permeable sub-cropping porous formations). From well data in the general area, it is known that the sub-crop to the Surat is most often very tight Permian formations (the Moolayember). However, there are sometimes more porous Triassic formations which on occasion comprises of sandstones. A continuous permeable dummy layer is also likely a (probably unrealistic) worst case for this scenario. It was used to represent the base of the Blocky Sandstone Reservoir as more than a simple closed boundary condition. The addition of this dummy, substrate layer also allowed for testing the impacts of a ‘leaky’ Blocky Sandstone Reservoir pinch-out, where flow could occur along the unconformity, potentially creating a connection between the Blocky Sandstone Reservoir and other stratigraphically higher sands in the Transition Zone as they sequentially pinch-out against the Base Surat Unconformity surface towards the west.

**Northern, MAR boundary.** The final modification to the notional injection sector model grid was required to represent the MAR injection occurring more than 134 km away in the northern parts of the Surat Basin into the Blocky Sandstone Reservoir. This injection increases the pressure the Blocky Sandstone Reservoir in the north part of the basin, and could impact on the injectivity in the notional injection sites locations in the south part of the basin. While dynamic modelling suggests that this effect would be relatively small based on current MAR volumes, it was still considered appropriate to create a boundary condition in the north that would allow us to represent the MAR injection *under various future scenarios at different volumes*.

To achieve this, a ‘pseudo-boundary’ was created by stretching the second, third and fourth last rows of cells at the far north of the notional injection sector model so their total combined length (N-S) was approximately 100 km (Figure 117). This was intended to represent the volume of rock and fluid between the MAR injection location and the north of the UQ-SDAAP Notional Injection Sector model. The facies characterisation (La Croix 2019a), definition of the sequence stratigraphic framework (La Croix et al. 2019b), definition of paleodepositional environments (La Croix et al. 2019c) and the Petrophysical analysis (Harfoush et al. 2019a; 2019b; 2019c) suggest that there are two, probably interleaved, depositional centres for the Blocky Sandstone Reservoir (northern and southern) with separate sediment provenance and with resulting different petrophysical characteristics such as higher clay content and generally lower permeability in the southern depositional centre. As such each of the two depositional centres had their rock properties characterised independently. Note that Figure 117 shows a sharp boundary between relatively high permeability in the northern depositional centre and the relatively low permeability in the southern depositional centre for the Blocky Sandstone Reservoir. *This is an artefact*. The changes would be gradational. Large cells on the northern side of the boundary were assigned with bulk reservoir properties representing the northern depositional centre, i.e. a very high permeability (4 Darcies) analytic aquifer was defined as the northern boundary condition for these cells to represent the Blocky Sandstone Reservoir in that area (Hayes et al. 2019b).

After stretching the grid, a single well was placed in the final row of cells and was used to control injection of water into the Blocky Sandstone Reservoir at rates based on the MAR injection to date. The parameters (including porosity, permeability and volume modifiers) of these ‘stretched’ cells were manually adjusted until the pressure response in these cells was similar to that predicted by groundwater models of MAR injection to date (e.g. section 4.3.9 and Hayes et al. 2019a). The resulting horizontal permeabilities for the Blocky Sandstone Reservoir in the notional injection sector model ‘pseudo-boundary’ area are shown in Figure 118.

While the stretched cells do not accurately represent the geometry or properties of the Surat Basin and Blocky Sandstone Reservoir in the area north of the notional injection sector model, they should act as a reasonable ‘pseudo-boundary’ that mimics and equivalent of the MAR injection in the UQ-SDAAP Notional Injection Sector models. In the forward models of CO<sub>2</sub> injection, the ‘MAR’ well at the north of the pseudo-boundary area will inject water until 2054 at the estimated rates for the MAR scheme per OGIA (OGIA 2016a and 2016b).

The ‘pseudo-boundary’ cells are not shown in the subsequent results of dynamic simulations.

**Figure 117** The scale of the ‘Pseudo- Boundary’ area created by stretching three rows of cells in the notional injection sector model, shown overlain on the horizontal permeability distribution used in the groundwater model grid. The difference in permeability between the north and south parts of the groundwater model is due to two depo centres that are hypothesised by the UQ-SDAAP team. (Hayes et al. 2019a; Gonzalez et al. 2019b).

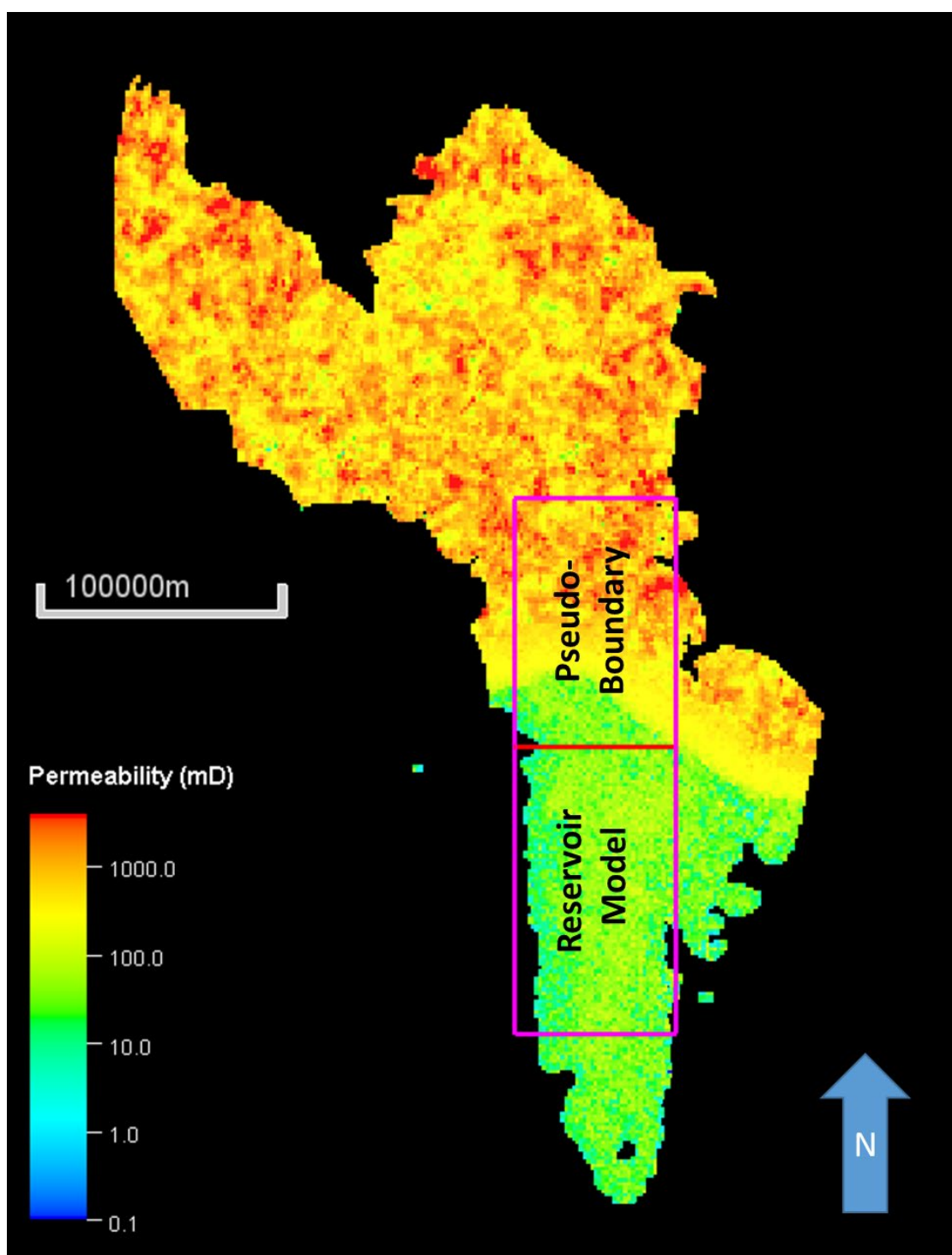
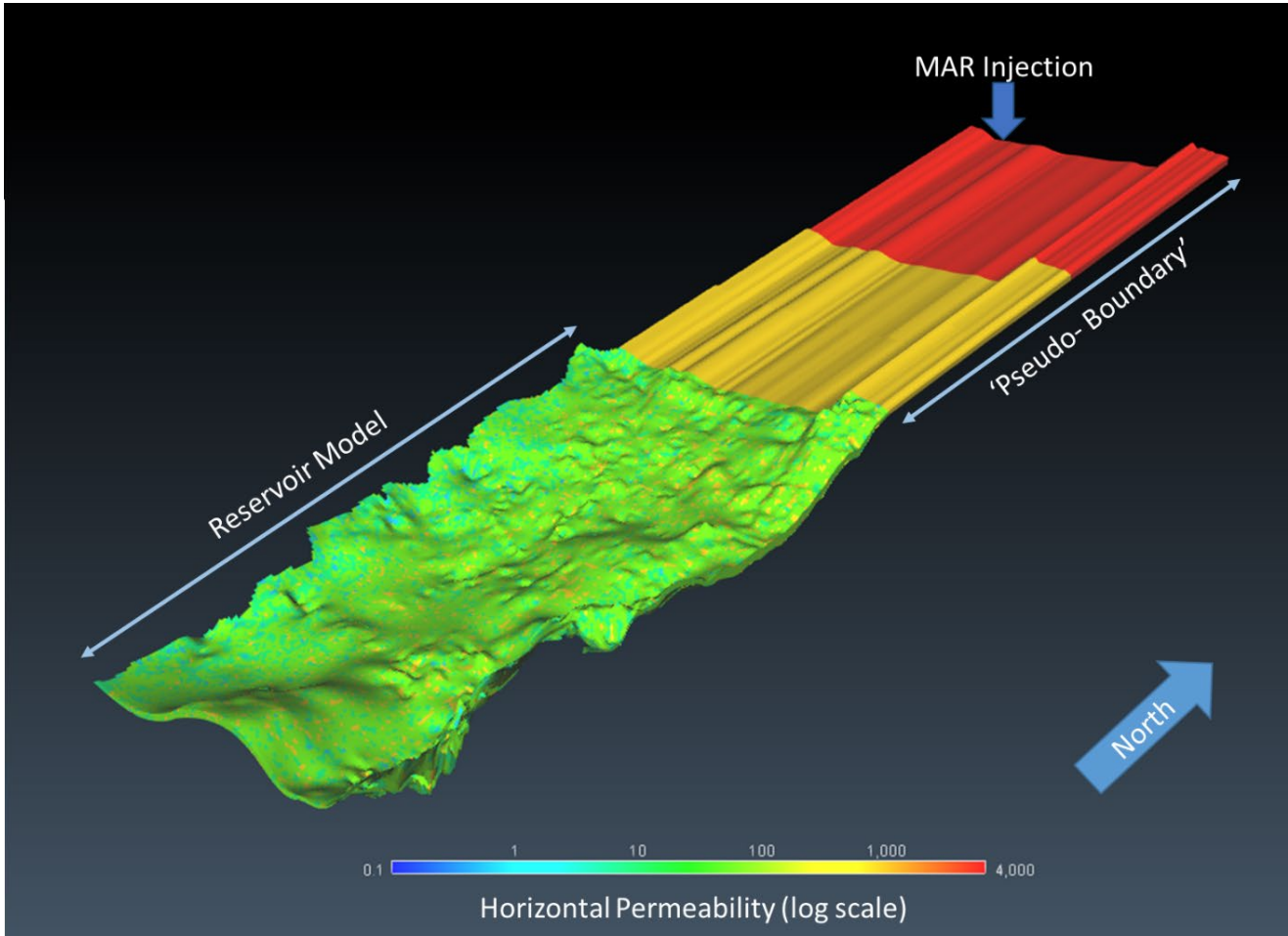


**Figure 118** The structure and horizontal permeability of the Blocky Sandstone Reservoir in the notional injection sector reservoir model and 'pseudo-boundary'. Note that the permeability in the 'pseudo boundary' has similar trend to the groundwater model grid shown in Figure 117.



#### 4.8.4 Fluid model

When CO<sub>2</sub> is injected via an injection well and into an aquifer, it goes through different physical processes. From top to bottom of the well, CO<sub>2</sub> is heated due to friction, compression, and conduction from the surrounding environment and the pressure rises with depth reaching its supercritical state, at which its density increases by some orders of magnitude. Details of the fluid model characterisation can be found in Ribeiro et al. 2019a.

As injected CO<sub>2</sub> flows from the wellbore into the reservoir, it may be heated again and increase in volume if it is cooler than the reservoir. Given its higher compressibility, it is further compressed when displaced by subsequent injected volumes. At the same time, the injected CO<sub>2</sub> is cooling the reservoir with this effect being greatest near the injection well. These transient variations in CO<sub>2</sub> density may result in some vertical migration due to buoyancy and could, at least in theory, generate thermal convective currents in the reservoir.

At the same time, small portions of the injected CO<sub>2</sub> can dissolve in formation water (up to 1.8 moles per kilogram of water or 8% CO<sub>2</sub>-to-water mass ratio, for up 50,000 kPa) and increase the water density (Appelo, Parkhurst & Post 2014; Akinfiyev & Diamond 2010; Duan et al. 2006). Any resulting convective currents would enhance the mixing of fluids and increase the dissolution.

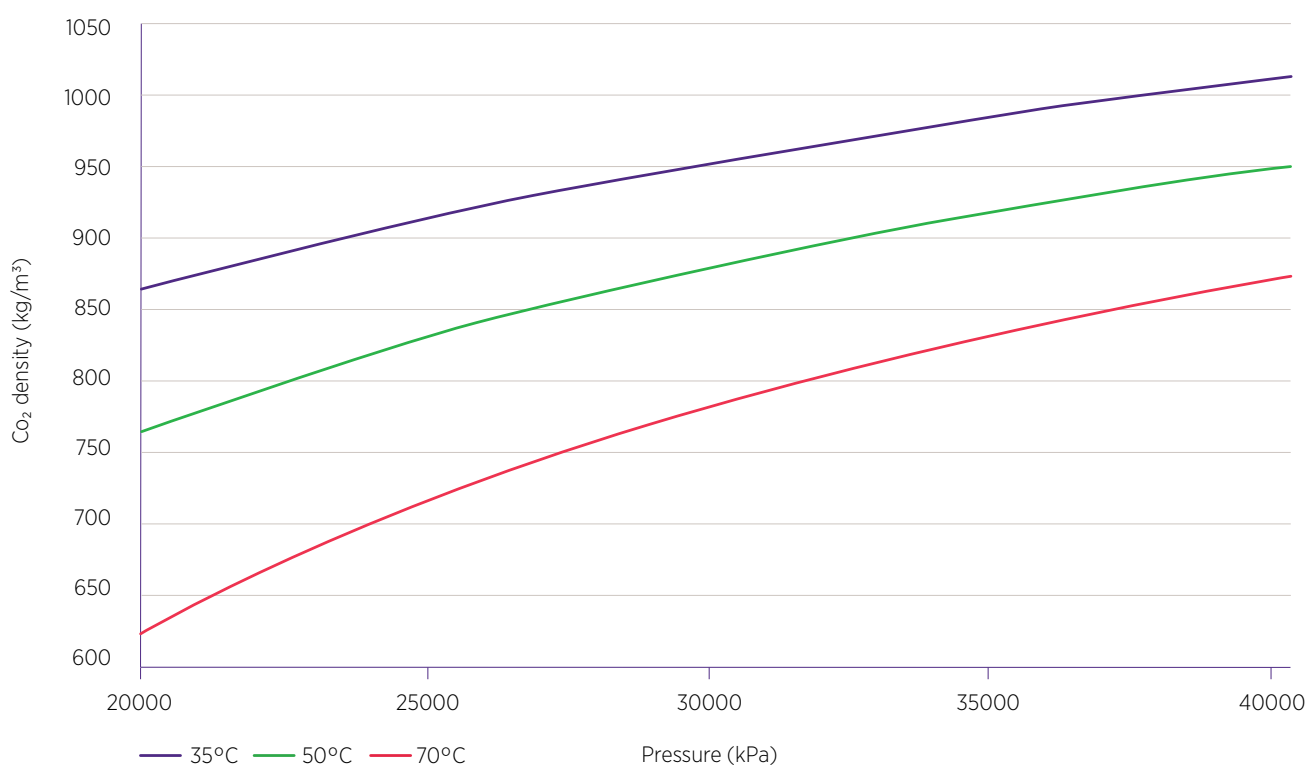
To calculate the properties and interactions of water and CO<sub>2</sub>, most of the default models in GEM were used, adding some constraints related to the specific reservoir conditions including:

1. **Components:** CH<sub>4</sub> and CO<sub>2</sub> were included as components and the Peng-Robinson equation-of-state was chosen to model their fugacities and volumes, with all input parameters set to default (e.g. specific gravity, critical temperature, acentric factor, etc.). Including CH<sub>4</sub> is a numerical condition to control the initial content of CO<sub>2</sub> in the reservoir, since GEM requires the sum of mole fractions of gaseous component to be equal to unity. In this way, a reservoir with negligible CO<sub>2</sub> content could be initialised by setting 0.999 and 0.001 to CH<sub>4</sub> and CO<sub>2</sub> mole fractions, respectively. Moreover, the viscosities using the correlations of Jossi, Stiel, and Thodos, were modelled with default coefficients

2. **Water properties:** Water compressibility was set to the default value ( $4.35E-7$  1/kPa at 101.3 kPa), while density and viscosity was calculated via Rowe-Chou and Kestin correlations, respectively. Water salinity was set at 3000 ppm of NaCl as Moonie produced water varies between 1000 and 5000 ppm. Water was not allowed to vaporise
3. **CO<sub>2</sub> Solubility:** CO<sub>2</sub> solubility in water was modelled using Henry's Law with Henry's constant determined by the Harvey correlation, making the solubility a function of pressure, temperature and salinity. The CO<sub>2</sub> solubility in water is calculated in terms of molality (moles of dissolved gas per kilogram of water)
4. **Thermal option:** Heat exchange calculations between fluid components and reservoir rock were enabled. Enthalpies were calculated using a polynomial function of temperature for each fluid component and rock thermal properties were set to default values

To justify the use of the more advanced (also more computationally intensive) non-isothermal simulation (Thermal option turned on), 10 years of CO<sub>2</sub> injection was simulated using a horizontal well operated with a wellhead pressure of 15,000 kPa. Three simulation runs were performed, each with different injecting temperature: 70°C (isothermal), 50°C and 35°C. Figure 119 shows that the CO<sub>2</sub> density variations at reservoir conditions may be more than 10% when heat exchange is considered and this may affect the pressure build-up around the wellbore, as well as the fluid flow.

**Figure 119** CO<sub>2</sub> density from 20,000 to 40,000 kPa at 35, 50 and 70°C.



In Figure 120, the pressure map after 10 years of injection under isothermal flow is shown. The black rectangular window was selected to analyse profiles of pressure and densities around the well for all this and the non-isothermal simulations. By looking at Figure 121, Figure 122 and Figure 123 one can see that not only the pressure build up is lower when heat exchange is considered but also the density oscillation profile has a higher amplitude for both water and CO<sub>2</sub> phases. As said before, these larger density differences generate more convective currents and enhance the CO<sub>2</sub> mixing and dissolution within the aquifer.

**Figure 120** Pressure map after 10 years injecting CO<sub>2</sub> at 70°C (isothermal flow). The horizontal well trajectory is located at 775 m oriented north-south and the black rectangle sets the observation window for analysing profiles of pressure and densities.

**Injected fluid at 25°C – Pressure (kPa) after 10 years**

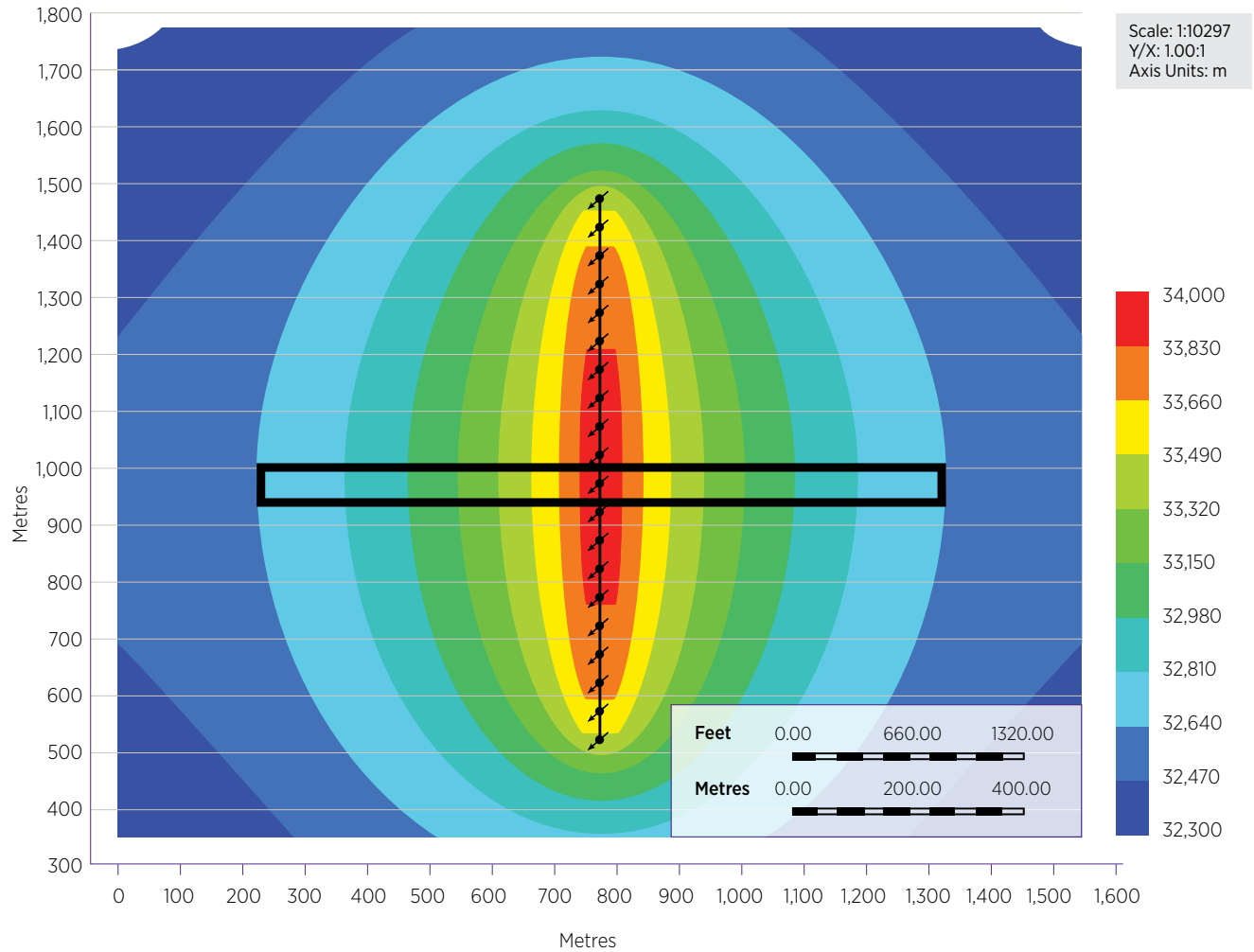




**Figure 121** Pressure and density of CO<sub>2</sub> and water for injecting CO<sub>2</sub> at 70°C (isothermal flow). This 2D cross section view of pressure and density within the injection reservoir, runs perpendicular to the horizontal well trajectory with the well located at 775 m on the horizontal axis.

#### Injected fluid at 70°C

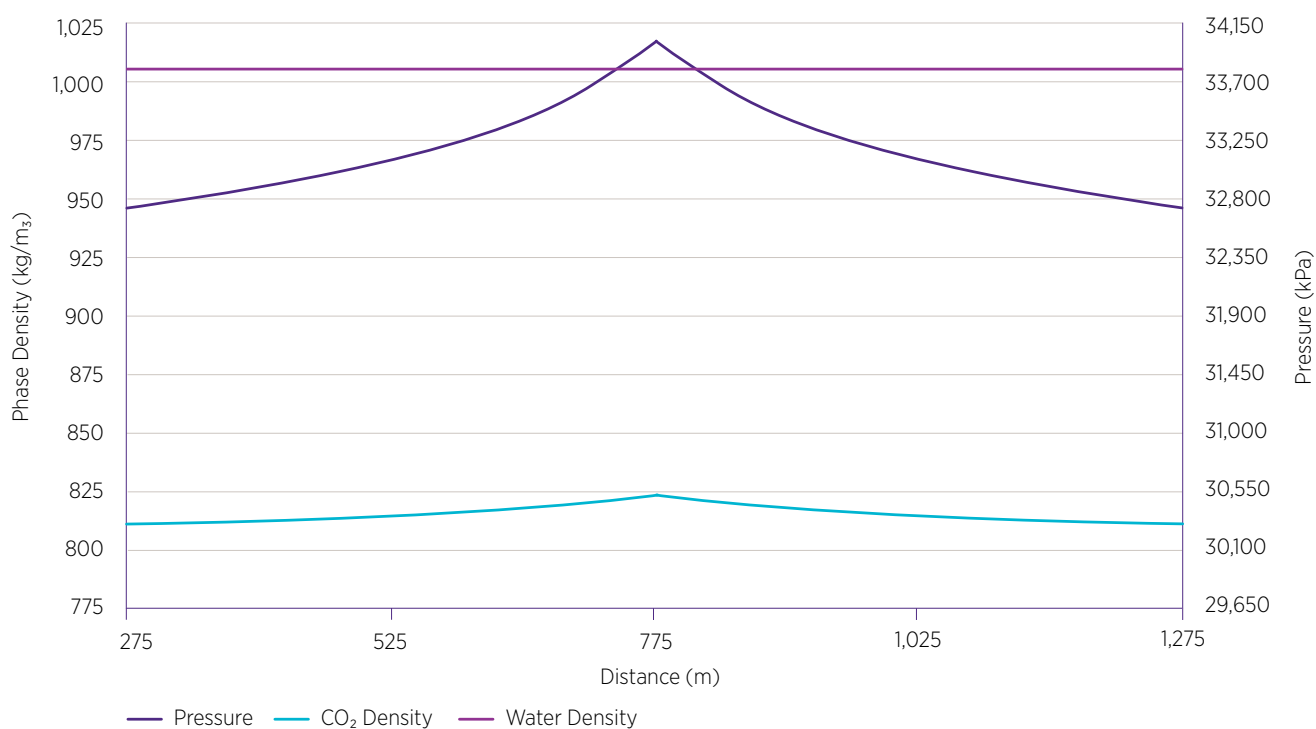


**Figure 122** Pressure and density of CO<sub>2</sub> and water for injecting CO<sub>2</sub> at 50°C (non-isothermal flow). This 2D cross section view of pressure and density within the injection reservoir, runs perpendicular to the horizontal well trajectory with the well located at 775 m on the horizontal axis.

#### Injected fluid at 50°C

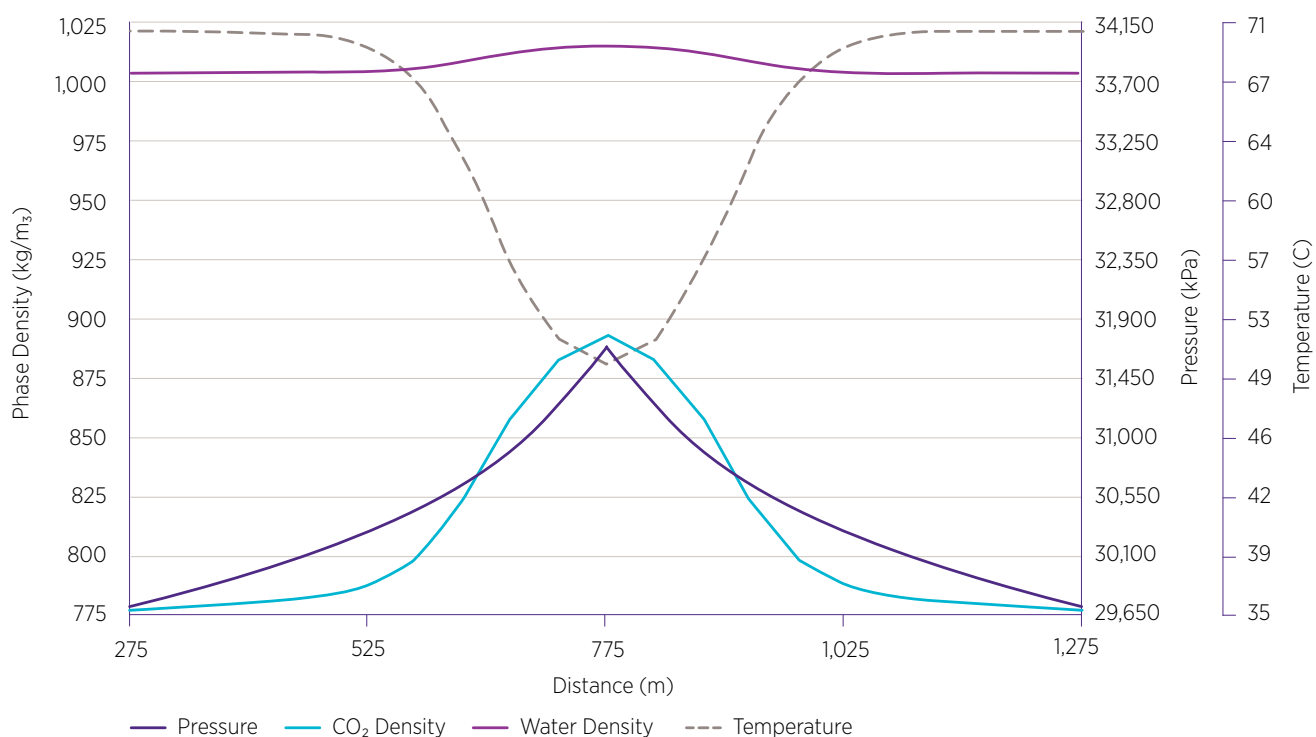


**Figure 123** Pressure and density of CO<sub>2</sub> and water for injecting CO<sub>2</sub> at 35°C (non-isothermal flow). This 2D cross section view of pressure and density within the injection reservoir, runs perpendicular to the horizontal well trajectory with the well located at 775 m on the horizontal axis.

**Injected fluid at 35°C**

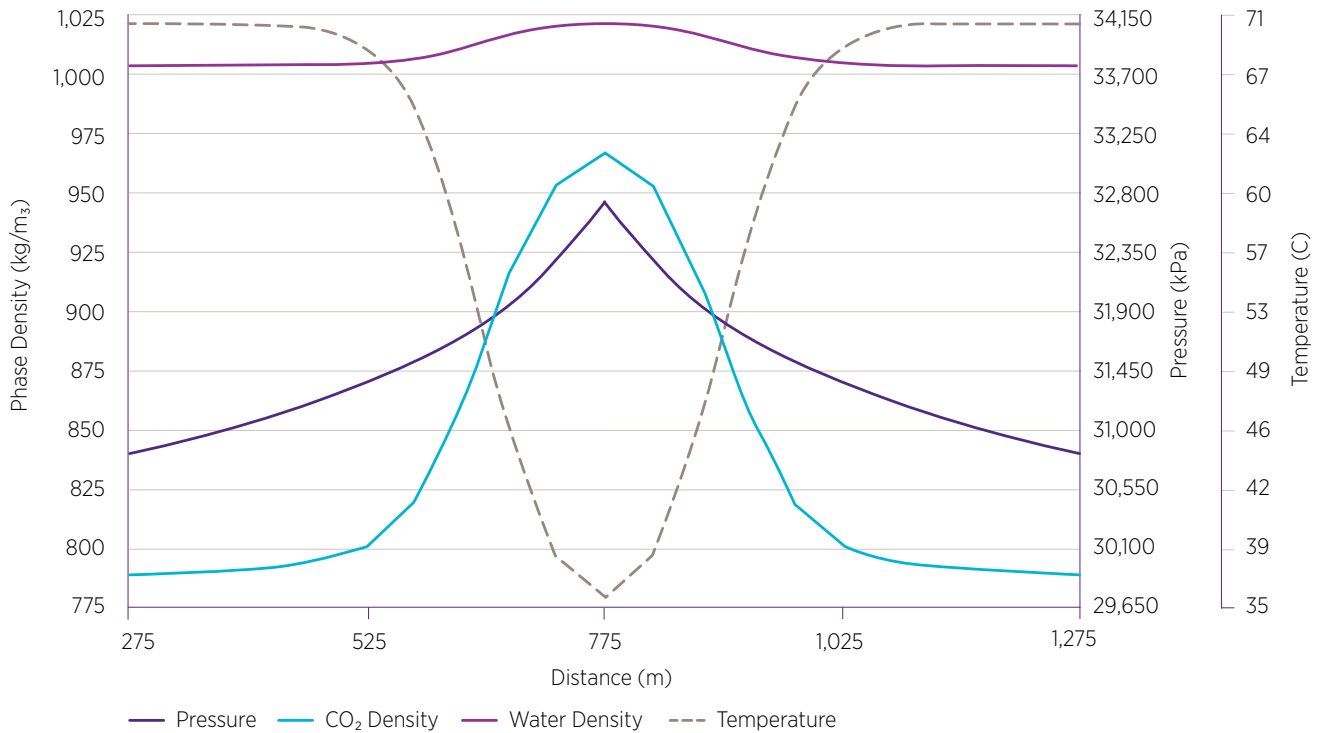


Table 41 shows that the ultimate CO<sub>2</sub> stored is slightly less for non-isothermal simulations, which is explained by the higher CO<sub>2</sub> density in the cooler zone around the wellbore. However, since the pressure build up is lower, injectivity is higher and the injection period (before reaching the bottomhole pressure constraint) may be longer.

**Table 41** Well performance after 10 years of injection for isothermal and non-isothermal simulations.

10 years of Injection	Isothermal (70 °C)	50 °C	35 °C
Cum CO <sub>2</sub> INJ (Mt)	32.7	31.4	32.1
Cum CO <sub>2</sub> INJ (Mm <sup>3</sup> )	42.6	36.9	34.9
BHP (kPa)	35861	34469	35572
BHF (m <sup>3</sup> /day)	3376	5207	4183
Mass rate (t/day)	2801	4678	4069
Injectivity (m <sup>3</sup> /day/kPa)	0.094	0.151	0.118
Injectivity (t/day/kPa)	0.078	0.136	0.114

## 4.8.5 Transition Zone investigations

**Several injection models, including ‘worse case’ scenarios, confirm that the Transition Zone is a robust element of the seal complex with minimal flow and penetration of CO<sub>2</sub> into it. There were no scenarios in which CO<sub>2</sub> reaches the Ultimate Seal.**

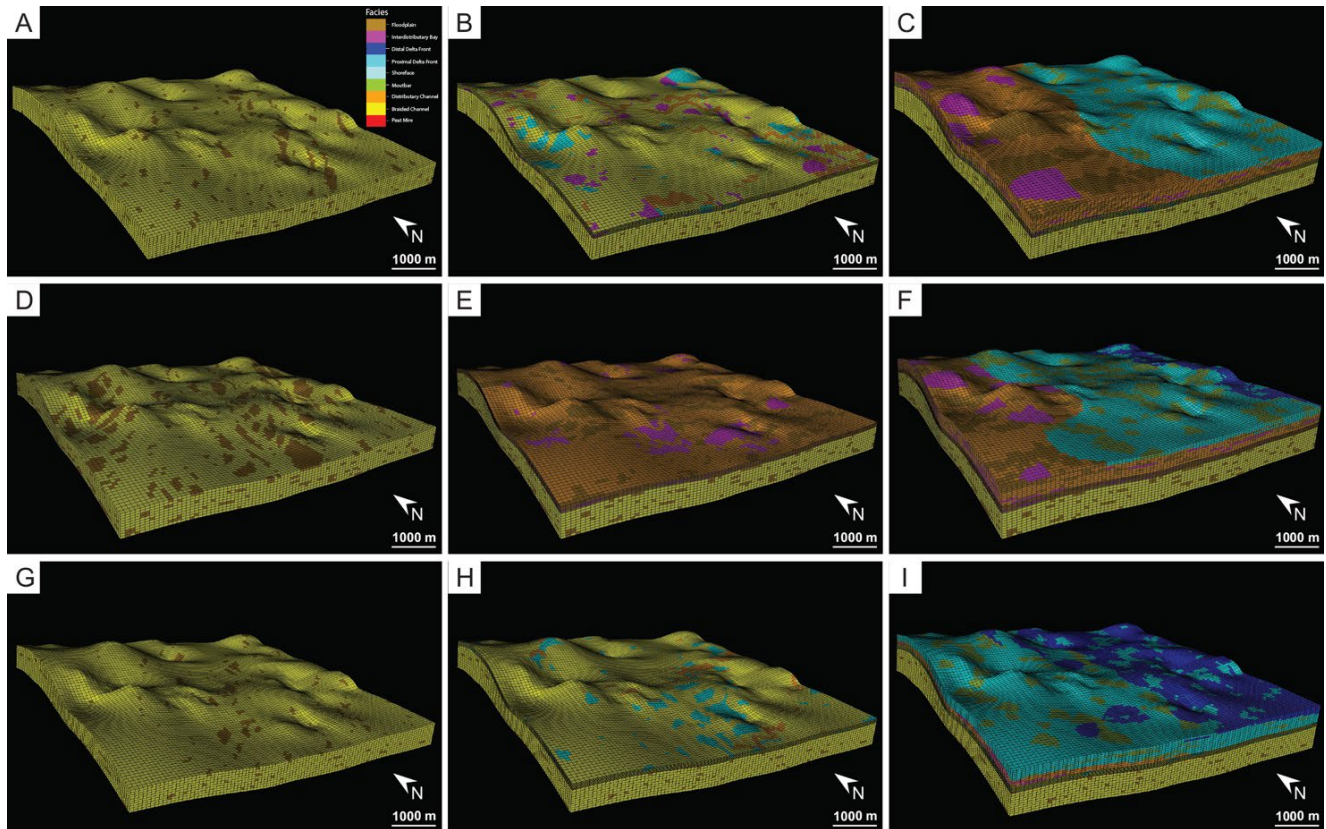
The Transition Zone is the lithologically heterogeneous interval between the top of the Blocky Sandstone Reservoir and bottom of the Ultimate Seal. In general, the majority of the Transition Zone appears to be low permeability (<1 mD). Some extremely low permeability (or tight) parts of the Transition Zone would likely act as localised seals, but these may not be thick or laterally continuous enough to be considered as the continuous seals across the area of a plume for commercial-scale CO<sub>2</sub> containment. Other sandier parts have sufficient porosity and permeability to be considered reservoirs (sections 4.5.1, 4.5.2, 4.5.5). The overall flow behaviour of the Transition Zone, in any area, is largely dependent on the presence, connectedness and lateral extent of any high permeability strata. Evidence in this research suggest that this is limited.

Sector scale static models of three various possible Transition Zone stratigraphic conceptualisations were constructed to capture the range of uncertainty in Transition Zone flow characteristics (section 4.5.5 and the detailed sector static model report: La Croix et al. 2019e).

The dynamic numerical simulations that were used to ‘test’ these different Transition Zone conceptualisations are described below. These models also assess the likely temperature reduction in the Transition Zone caused by CO<sub>2</sub> injection (important due to the thermal effects on fracture pressures – section 4.5.6, and Rodger et al. 2019a).

Static models of the three Transition Zone conceptualisations were named after “type-wells” which were considered to best represent each: Moonie (most sandy and permeable), Meandarra (base case), and Woleebee Creek (least sandy and permeable) (Figure 124). These models covered a 10 x 10 km area, extending from the top of the Ultimate Seal to the base-Surat Unconformity at the base of the Blocky Sandstone Reservoir (approximately 190 m total thickness). They were created on structurally identical 100 x 100 x 55 cell grids, but with properties constrained by the different facies for each conceptualisation (La Croix et al. 2019e).

**Figure 124** Differences in the facies distribution between the three type areas for sector models. (A–C) show the facies evolution from the lower Blocky Sandstone Reservoir to the upper Blocky Sandstone Reservoir and then the lower Transition Zone in the Moonie sector. (D–F) shows the same progression for the Meandarra sector. Finally, (G–I) shows the facies progression for the Woleebee Creek sector.



As the aim of these simulations was to test the Transition Zone only, the Blocky Sandstone Reservoir was repopulated as a homogenous volume with an effective porosity of 12.8%, a horizontal permeability ( $k_h$ ) of 43 mD and a vertical permeability ( $k_v$ ) of 6.5 mD (i.e.  $k_v/k_h$  is 0.15). This was intended to approximately represent a reference of ‘mid-case’ Blocky Sandstone Reservoir to allow direct comparison of the different Transition Zone types without variations in the Blocky Sandstone Reservoir affecting the results.

These conceptual models were then set up for the larger scale sector model used for CO<sub>2</sub> injection modelling at the field scale. The same fluid model, rock properties (including thermal properties), relative permeability curves and capillary pressure J-functions were used – see Rodger et al. 2019b and Ribeiro et al. 2019b for details. A large analytic (Carter-Tracy) aquifer was defined as a boundary condition connected to all sides of the Blocky Sandstone Reservoir. Another analytic aquifer was defined on the top of the model to represent a ‘Hutton-like’ formation overlying the seal.

A single 1 km-long horizontal well was defined 10 m above the base of the Blocky Sandstone Reservoir, and set up to inject CO<sub>2</sub> at a rate of 0.75 Mtpa for 30 years, then shut-in. The well was also limited by a wellhead pressure of 15 MPa (150 barsa) and a bottomhole pressure limit of 40.5 MPa (405 barsa), although these pressures were not reached during the simulation, and the well injected at the predefined rate throughout. An alternate case (described below) was run with the well limited by these pressure constraints only.

After testing the effect of the differing Transition Zone types on fluid movement, two additional cases were run using the Moonie-type static model (the model that resulted in the most flow into the Transition Zone). Both had zero capillary pressure throughout, representing CO<sub>2</sub> wet relative permeability cases and thus no membrane seal effects. In these cases, the flow rate of CO<sub>2</sub> through the Transition Zone is limited only by permeability, not by capillary effects.

In the second of these cases, the well was controlled to inject while limited by wellhead pressure at 15 MPa. A bottomhole pressure limit at 40.5 MPa (405 barsa) was also defined, but this limit was not reached. This final case represented a worst-case scenario for vertical CO<sub>2</sub> migration, where the pressure around the well would be high during injection (and thus increase viscous flow), but capillary effects would not limit the vertical migration of CO<sub>2</sub>.

In all cases, simulations were for a nominal 30-year injection period and continued for 30 years post-injection.

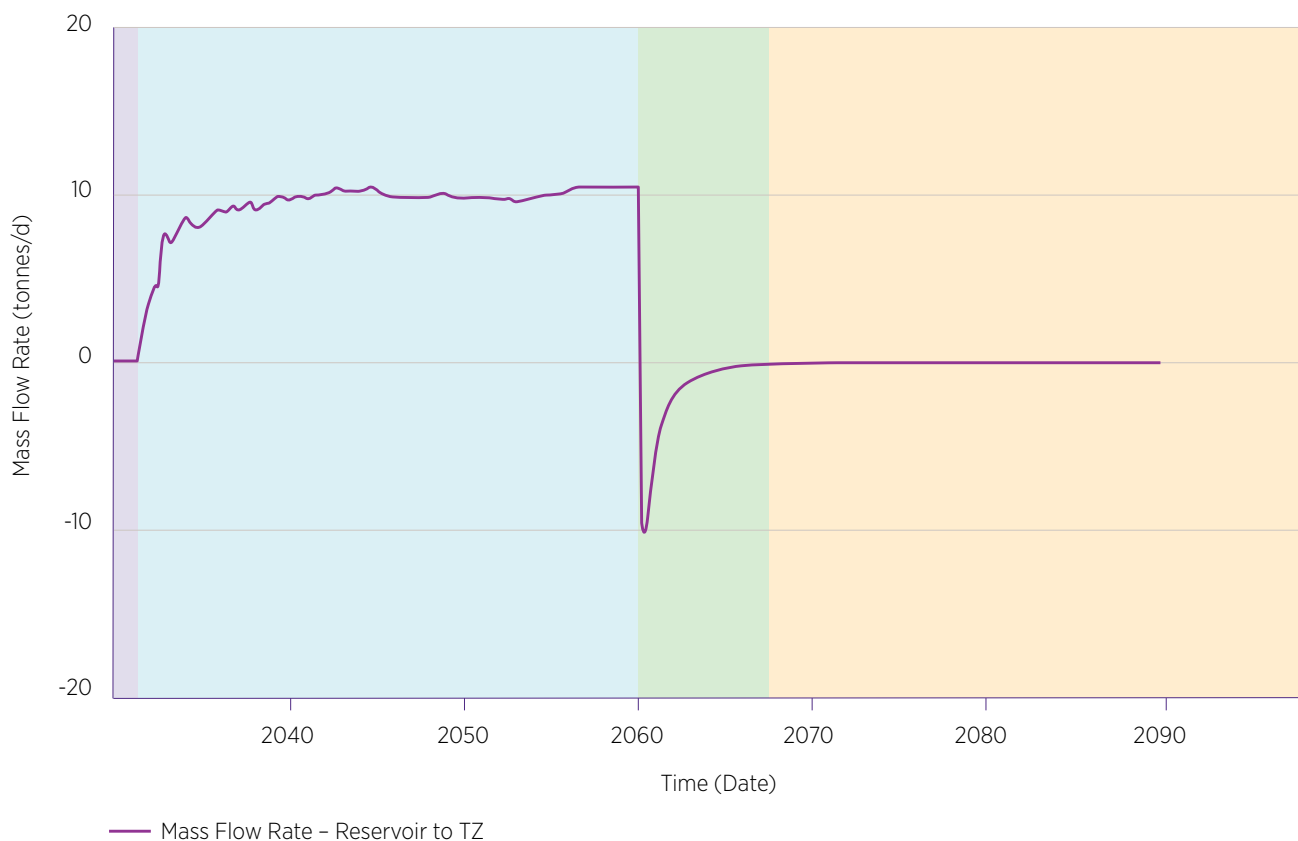
#### 4.8.5.1 Meandarra model results

Figure 125 shows the mass flow of supercritical CO<sub>2</sub> from the Blocky Sandstone Reservoir into the lower part of the Transition Zone, and from the mid Transition Zone into the upper Transition Zone for the Meandarra model. CO<sub>2</sub> flow rates into the Transition Zone during injection were relatively steady at around 10.5 tonnes/d (12 m<sup>3</sup>/d at reservoir conditions). For comparison, the CO<sub>2</sub> injection rate was over 2000 tonnes/d; almost 200 times the flow rate into the Transition Zone. The ratio of the cumulative flow from the Blocky Sandstone Reservoir into the Transition Zone to the cumulative injected CO<sub>2</sub> is shown in Figure 126. Throughout the injection period, only 0.45% of the total injected CO<sub>2</sub> flowed into the Transition Zone, with some flowing back into the reservoir post-injection.

The CO<sub>2</sub> did not enter the Transition Zone uniformly. It instead migrated into parts that have lower capillary pressures – likely also to be those with higher permeability. This uneven migration of CO<sub>2</sub> can be seen in the cross-section in Figure 127.

While some supercritical CO<sub>2</sub> did move into the Lower Transition Zone, it remained in the lowest 8 m. The saturation of CO<sub>2</sub> in the column of cells where CO<sub>2</sub> migrated furthest through the Transition Zone is shown in Figure 128. **No CO<sub>2</sub> flowed into the upper Transition Zone at any point in the Meandarra model (or, in fact, in any of the simulations).**

**Figure 125** Mass flow rates of CO<sub>2</sub> from the Blocky Sandstone Reservoir into the Transition Zone. Positive values indicate upwards flow, negative values are downwards flow. For comparison, well injection rate was >2000 tonnes/d. Coloured background indicates periods discussed in text.



**Figure 126** Ratio of cumulative flow of CO<sub>2</sub> into Transition Zone to cumulative injected CO<sub>2</sub>.

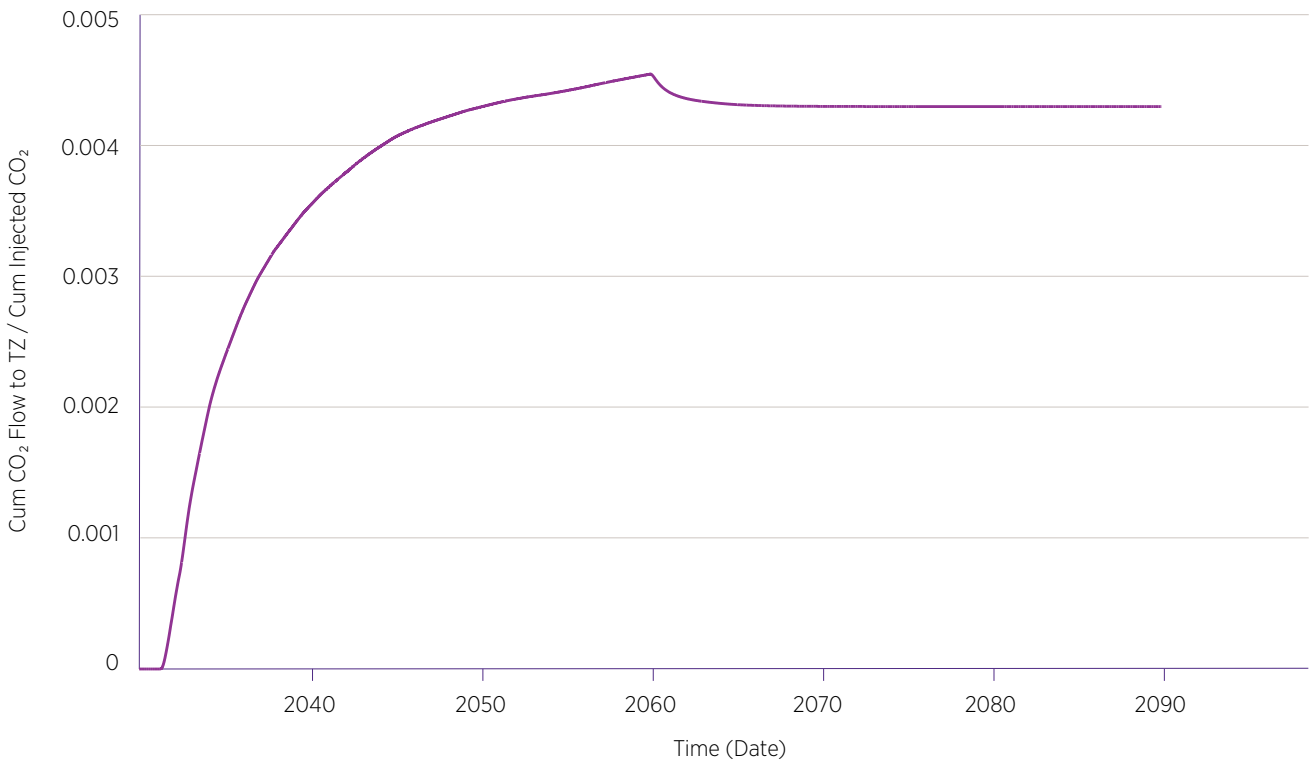


**Figure 127** Saturation of supercritical CO<sub>2</sub> at the end of 30 years of injection for the Meandarra model. Horizontal well is in centre of model, running perpendicular to page. Red indicates higher CO<sub>2</sub> saturation. The boundary between the Transition Zone and Blocky Sandstone Reservoir is relatively clear across most of the model as the boundary between high CO<sub>2</sub> saturation below (orange) and low CO<sub>2</sub> saturation above (blue). In some more permeable areas near the centre of the model, capillary pressures are overcome and supercritical CO<sub>2</sub> is able to enter the Transition Zone (green patches higher in model).

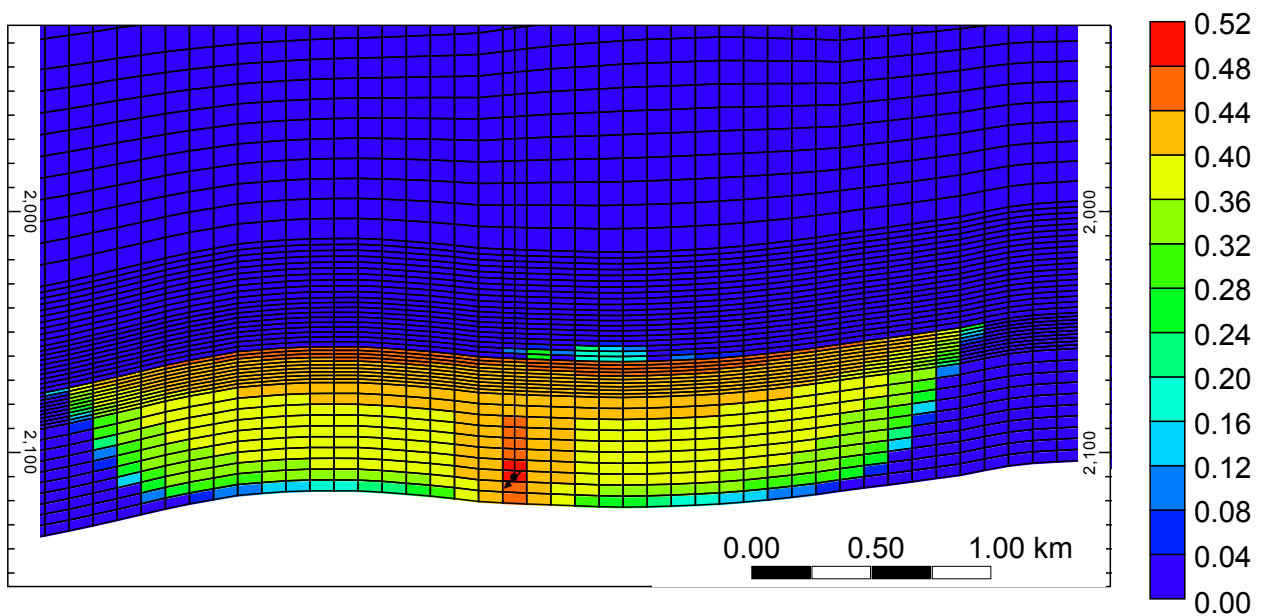


**Figure 128** Vertical profiles of supercritical CO<sub>2</sub> saturation in the column of cells where CO<sub>2</sub> migrated furthest vertically in the Meandarra model (approximately 300 m from the well completion). Shown at end of 30-year injection period (red) and 30 years after injection stops (green). Note that CO<sub>2</sub> saturation actually decreases in the Transition Zone after injection stops.

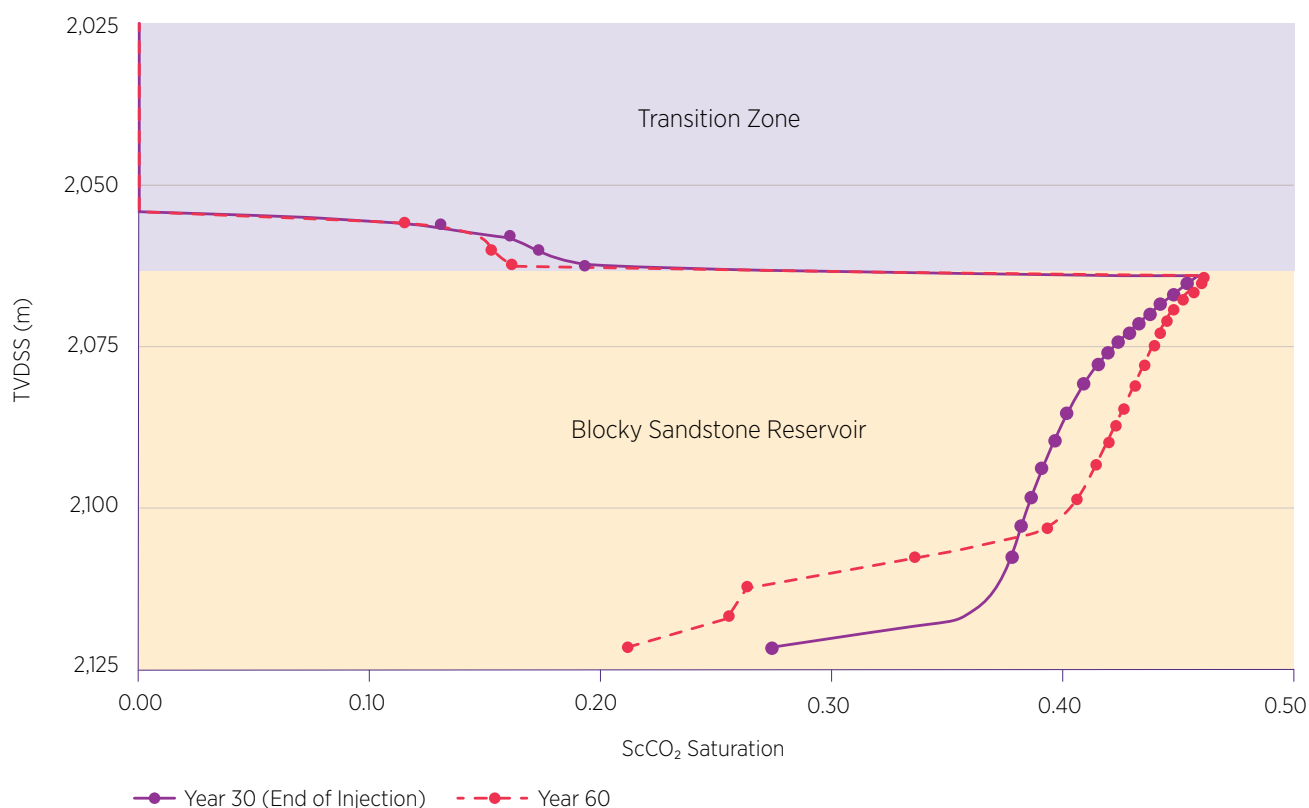


Figure 125 has been coloured to highlight four periods which occur during and after injection. The first period (purple Figure 125) occurs after injection has started, but before CO<sub>2</sub> has migrated from the well completion to the boundary between the Blocky Sandstone Reservoir and Transition Zone. During this period, no CO<sub>2</sub> flows into the Transition Zone. Water does flow vertically due to the increased pressure in the Blocky Sandstone Reservoir – see Figure 128.

The second period (blue in Figure 125) starts when CO<sub>2</sub> reaches the Transition Zone, and continues until the well is shut in. Due to the high pressure in the area around the injecting well it is likely that capillary threshold pressures will be overcome in areas near the well, and CO<sub>2</sub> will begin to move into, and through, the lower parts of the Transition Zone, albeit at low rates relative to the injection rate.

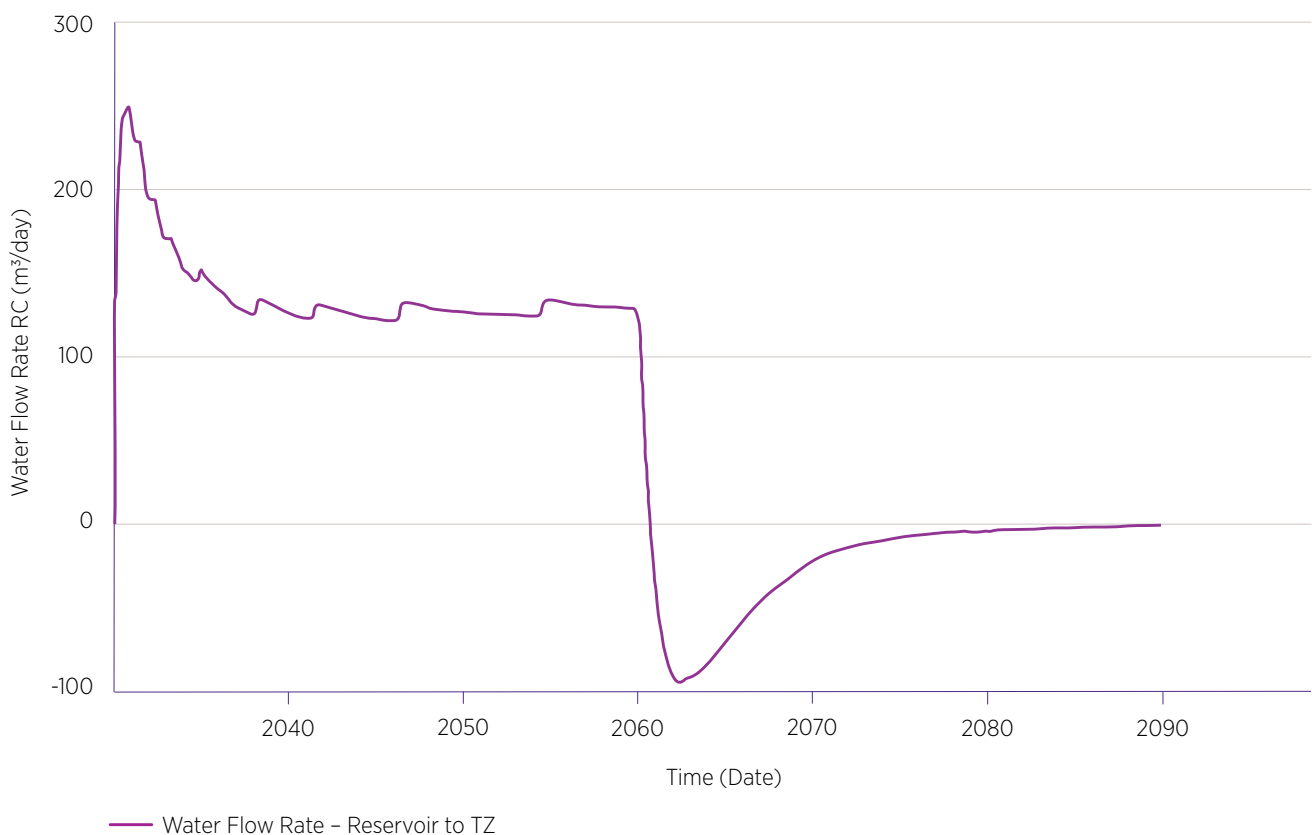
The third period (green in Figure 125) begins after 30 years, when the injection well is shut in. At this point, the pressure around the well drops as fluids (water and supercritical CO<sub>2</sub>) move due to the pressure gradient around the well. As the horizontal permeability of the Blocky Sandstone Reservoir (43 md) is much higher than the vertical permeability in the Transition Zone (typically <<0.1 md), the pressure in the Blocky Sandstone Reservoir quickly reduces due to horizontal flow, while parts of the Transition Zone remain relatively over-pressured. Buoyancy acts on the supercritical CO<sub>2</sub> during this period, but the overall flow in the Meandarra model is dominated by the pressure gradient, which causes downwards flow of both water and CO<sub>2</sub> back into the Blocky Sandstone Reservoir. The CO<sub>2</sub> in the Blocky Sandstone Reservoir further from the well remains trapped in the Blocky Sandstone Reservoir by the Transition Zone, which is acting as a membrane seal. The rate of downwards flow decreases over time as the Blocky Sandstone Reservoir and Transition Zone move closer to hydrostatic equilibrium.

The final period (yellow) is not as well defined as the previous three periods, but instead represents the period post-injection when the Blocky Sandstone Reservoir and Transition Zone have very nearly returned to hydrostatic equilibrium. During this period, depending on capillary pressures, CO<sub>2</sub> may be able to move upwards into the Transition Zone driven by buoyancy forces. In the Meandarra model this effect was minimal with no net flow of CO<sub>2</sub> into the Transition Zone in the 30 years post-injection. However, other models did indicate net upwards flow of CO<sub>2</sub> when buoyancy forces become dominant in the longer term (sections 4.8.7 and 4.12).

Figure 129 shows the flow of water from the Blocky Sandstone Reservoir into the lower Transition Zone for the Meandarra model. Water began to move from the Blocky Sandstone Reservoir into the Transition Zone almost as soon as injection started. The rate declined gradually, before levelling out at approximately 120 m<sup>3</sup>/d. When injection stopped, water began to flow back into the Blocky Sandstone Reservoir from the Transition Zone, although the change in the direction of net flow was not as abrupt as for supercritical CO<sub>2</sub>. This is because all of the CO<sub>2</sub> in the Transition Zone was in the area immediately around the well, and was therefore affected more quickly by the well being shut in. In areas further from the well, water could continue to flow from the Blocky Sandstone Reservoir into the Transition Zone for a period after injection stops. The net rate of water flow back into the Blocky Sandstone Reservoir peaked, then declined as the Blocky Sandstone Reservoir and Transition Zone moved towards hydrostatic equilibrium.

**The flow rate of water from the lower Transition Zone into the upper Transition Zone was very low throughout the simulation.**

**Figure 129** Flow rates of water (volumetric, reservoir conditions) from the Blocky Sandstone Reservoir to the Transition Zone. Positive values indicate flow upwards, negative values are flow downwards.



The Meandarra model represents the Transition Zone ‘type’ considered most likely to occur in the notional injection areas (see La Croix et al. 2019e). The results of the numerical simulations for this study indicate that in this case, vertical CO<sub>2</sub> migration is likely to be limited to the lowest 8 m of the Transition Zone, due to a combination of low permeability and high capillary pressures. While some slightly higher permeability parts of the Transition Zone did allow flow of CO<sub>2</sub>, these parts are not well-connected throughout the Transition Zone. At the end of injection, less than 0.5% of the total injected CO<sub>2</sub> had migrated into the Transition Zone.

The generally low permeability in the Transition Zone, and the lack of connectivity between the higher permeability parts, also limited water flow, and very little pressure build up was seen anywhere above the lowest 30 m of the Transition Zone.

Thermal effects occur further through the Transition Zone, with the region up to 75 m above the top of the Blocky Sandstone Reservoir cooled by 1°C at the end of the simulations, but only in the immediate vicinity of the injection well.



#### 4.8.5.2 Model comparisons between the Transition Zone scenarios

Dynamic simulations indicate that, in any of the Transition Zone case scenarios, the Transition Zone acts as an effective barrier, limiting vertical migration of CO<sub>2</sub>. It seems that, even for the sandiest and most permeable Transition Zone types, the Transition Zone is likely to have such low vertical permeability that any flow (of CO<sub>2</sub> or water) through it will be limited. Even in a worst-case scenario, which combined the most permeable and most sandy Transition Zone type, zero capillary pressure and high injection rates, only 3.6% of the injected CO<sub>2</sub> entered the Transition Zone in the 30-year injection period and 30 years post injection. Even in this worst case, the CO<sub>2</sub> did not migrate beyond the lowest 10m of the Transition Zone during the simulation period.

In all cases, the lowest part of the Transition Zone was cooled by up to 15°C during the simulation, which caused an apparent reduction in pressure in parts of the Transition Zone where the permeability was low and fluid flow was near zero. These findings also allow for the sensible vertical discretisation of the notional injection model where fine grid detail is only required in the lower part of the Transition Zone. For the details of all the Transition Zone scenario modelling see Rodger et al. 2019c.

These models indicate that the Transition Zone is an effective barrier to vertical CO<sub>2</sub> migration. However, future efforts should focus on reducing uncertainty in model parameters through an appraisal plan that can provide additional information on the depositional setting and petrophysical properties (including wettability and capillary pressure) of the Transition Zone. This would most reasonably be achieved by drilling a well to the base-Surat unconformity, and collecting core.

#### 4.8.6 Injection well design

**A horizontal injection well design is feasible with current, proven technology within established well integrity standards. The design reduces surface footprint, minimises injection pressure and allows for sustained high-rate, material injection/abatement. This type of well significantly minimises pressure and temperature effects in the seal complex and thus minimises any risk of inducing fractures. It also allows for effective “pad” drilling (only 2 or 3 pads are needed in the reference development scenario).**

As part of the UQ-SDAAP assessment, *notional* development plans have been created that are intended to represent technically feasible options for a large-scale CO<sub>2</sub> injection project. These notional plans are based on the current understanding of the geology and flow characteristics of the Blocky Sandstone Reservoir, as well as the overlying Transition Zone and Ultimate Seal (La Croix et al. 2019a, 2019b; Gonzalez et al. 2019a, 2019b; Harfoush et al. 2019a). They remain subject to important uncertainties, which are unlikely to be reduced without further appraisal of the subsurface at the notional injection sites.

Carbon storage scenarios for UQ-SDAAP (section 4.8.7) involve capture of CO<sub>2</sub> from (up to) 3, modern coal fired power stations – Millmerran, Kogan Creek, and Tarong North. In these hypothetical scenarios, the captured CO<sub>2</sub> would be transported by pipeline to any or all (notional) injection sites, then injected into the Blocky Sandstone Reservoir in the deepest parts of the Surat Basin. For the purpose of investigating well design, a scenario that involved capture and storage of CO<sub>2</sub> from all three power stations over a ~40-year period was considered. This would result in the injection of approximately 380 Mt of CO<sub>2</sub> in total, with a peak rate of 12.7 Mt/yr (total across all sites/wells) for around 18 years. **Note that this reference scenario includes a longer period than the currently estimated life-time of those plant** (sections 4.8.7, 4.14 and 4.15).

The research assumed high purity (>99.8%) dehydrated CO<sub>2</sub> will arrive at the well sites in a dense phase (i.e. as a liquid or supercritical fluid), and at a pressure of 15,000 kPa (150 bar). The arrival pressure may increase to 20,000 kPa (200 bar) if required to sustain injection rates as the reservoir pressure increases. To ensure the CO<sub>2</sub> remains in a dense phase, the minimum wellhead pressure at any time during normal injection will be 8000 kPa (80 bar), 10% higher than the critical pressure of CO<sub>2</sub>. The temperature of the CO<sub>2</sub> is expected to vary seasonally, with wellhead temperatures that vary between 5° C and 40° C. A reference case of 25°C is assumed for steady-state operation.

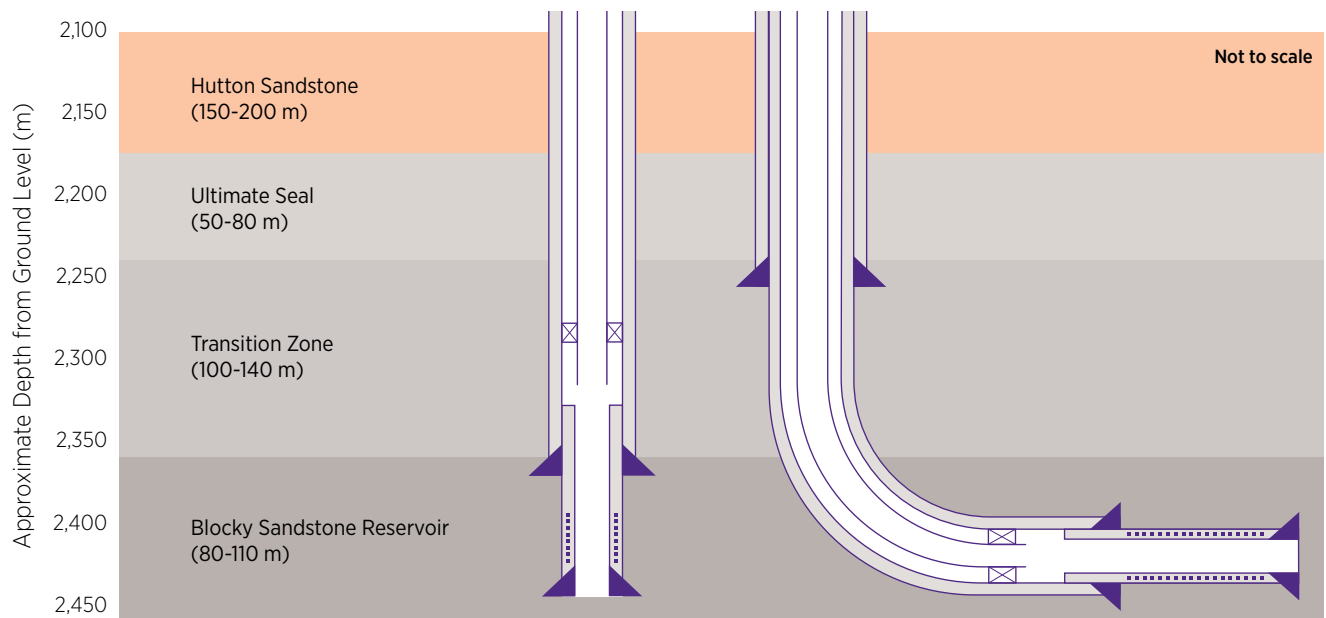
Any of these notional development plans would require a number of injection wells. A well design is described here, which is considered a credible option for industrial scale CO<sub>2</sub> injection in the Blocky Sandstone Reservoir. The decisions leading to this design are based on the current best estimates of the reservoir properties and behaviour, which are subject to significant uncertainty. A more detailed study, including economic assessment of the available options, would be required post-appraisal, when these uncertainties (particularly those regarding injectivity and geomechanics) will have been reduced.

CO<sub>2</sub> injection wells for any carbon capture and storage (CCS) project must fulfil a number of safety and economics-related criteria. Overall, the UQ-SDAAP notional well design work was based on two key principles:

1. In accordance with the overall development philosophy (section 4.8.1), the surface footprint of the wells and associated infrastructure should be minimised, and within this
2. Well placement, design and construction should minimise containment risk and *within this constraint*, maximise injectivity

The notional injection well design is in consideration of maintaining well integrity and ensuring operability with little planned maintenance and minimum human intervention. The U.S. EPA's Class VI<sup>21</sup> Well Construction Guidelines (US EPA 2012) were used as a guide to design despite these guidelines being considered "conservative". UQ-SDAAP presumed that minimum surface footprint is important, thus focused on horizontal injection wells, however, a scenario using vertical injection wells was also run. A schematic of the horizontal and vertical injection well concepts is shown in Figure 130. Well design aspects include a selection of: well trajectory, tubing size, casing sizes and depths, cementing, metallurgy/materials and downhole equipment selection. Rodger et al. 2019d presents details of the analysis and choices in the overall well design.

**Figure 130** Illustrative vertical and horizontal well design. Horizontal well length could be several kilometres, and could kick off (i.e. become deviated) at shallower depth, depending on achievable build-up rates, extended reach requirements, and wellbore stability.



Surface facilities, designs and costs are discussed in section 4.10 in and Advisian 2019.

<sup>21</sup> Class VI refers to CO<sub>2</sub> injection wells for CCS projects

#### 4.8.6.1 Injection well design notes

A notional design for a CO<sub>2</sub> injection well suitable for injecting in the Blocky Sandstone Reservoir has been developed, based on the current best estimates regarding the reservoir properties and development options. The notional design involves a horizontal well, with a 3 km to 4 km long horizontal section. The use of a horizontal well would allow CO<sub>2</sub> injection at lower bottomhole pressure, and targeted at the base of the Blocky Sandstone Reservoir, reducing containment risk. Horizontal wells would also reduce the well count, and surface footprint. The main disadvantage of horizontal wells is that they would be more technically challenging to drill, and may require expertise and equipment which is not widely available in Australia. However, the notional design discussed herein is well within the limits of current technology.

The notional wells would be completed with a pre-slotted 7" liner, with injection through 7" tubing to allow for high rates. Chrome steel (e.g. 13Cr or Super 13Cr) could be used for the tubing, and other well components that would be exposed to wet CO<sub>2</sub>, with carbon steel a suitable material for other parts of the well.

Based on the U.S. EPA's guidelines for class VI wells (U.S. EPA 2012), the notional well design features a 9 $\frac{5}{8}$ " casing run across the ultimate seal to provide an additional barrier protecting the Hutton Sandstone, with shallower 13 $\frac{3}{8}$ " and 20" casing strings as required. Per the same EPA guidance, the notional designs have all strings cemented to surface. This conservative approach may not be required, or even be beneficial, for wells targeting the Blocky Sandstone Reservoir. A more detailed study into the most effective means of minimising the risk of CO<sub>2</sub> migration along the wellbore (and protecting overlying aquifers) would be required post-appraisal, when more information regarding the likely behaviour of the Transition Zone and Ultimate Seal in the notional injection areas would be available.

The design discussed herein is feasible and conservative rather than optimal. It intended to represent a feasible option for injection of CO<sub>2</sub> into the Blocky Sandstone Reservoir, based on the current best estimates of the reservoir properties, and an assumed CO<sub>2</sub> delivery schedule. If different reservoir properties are encountered, or if an alternate delivery profile is required, the design would be expected to change to be fit for purpose. For example, a lower quality reservoir might require more/longer wells, but perhaps with slimmer tubing (due to the reduced injection rate per well). If the reservoir quality was determined to be better than the current estimates, then fewer wells might be required, and vertical wells may become a feasible option.

Overall, the research showed that it is possible to design CO<sub>2</sub> injection wells that fulfil the criteria of achieving high CO<sub>2</sub> injection rates while minimising containment risk, *and which are well within the limits of current technology.*

#### 4.8.7 CO<sub>2</sub> injection scenarios and well lay-out

**In all scenarios modelled in this and subsequent chapters, the scale of the capture assumed built has been driven by improved estimates of the rate at which the geology can safely accept and retain CO<sub>2</sub>.**

The highest rate scenario modelled has considered the partial sequential retrofitting of Millmerran, then Kogan Creek, then Tarong North, Millmerran and finally Kogan Creek (the MKTMK scenario). For this scenario, the simulations and field development plan (FDP) scenarios include rates up to around 12.7 million tonnes pa. For the reference case reservoir model, after ramp up, these rates can be sustained probably some years beyond the assumed technical life of the plants. This is the rate has been used to inform the high-level capture and roll out scenarios (Gamma Energy Technology 2019).

Detailed field optimisation may enable higher rates to be safely reached and/or these rates to be sustained for longer. However, such optimisation is not justified based on the data available. It would be a key outcome of a field appraisal and testing program.

**In most reservoir cases, the potential for sustained, high rate injection is for a longer duration than the current estimates of the life-time of the power plants.**

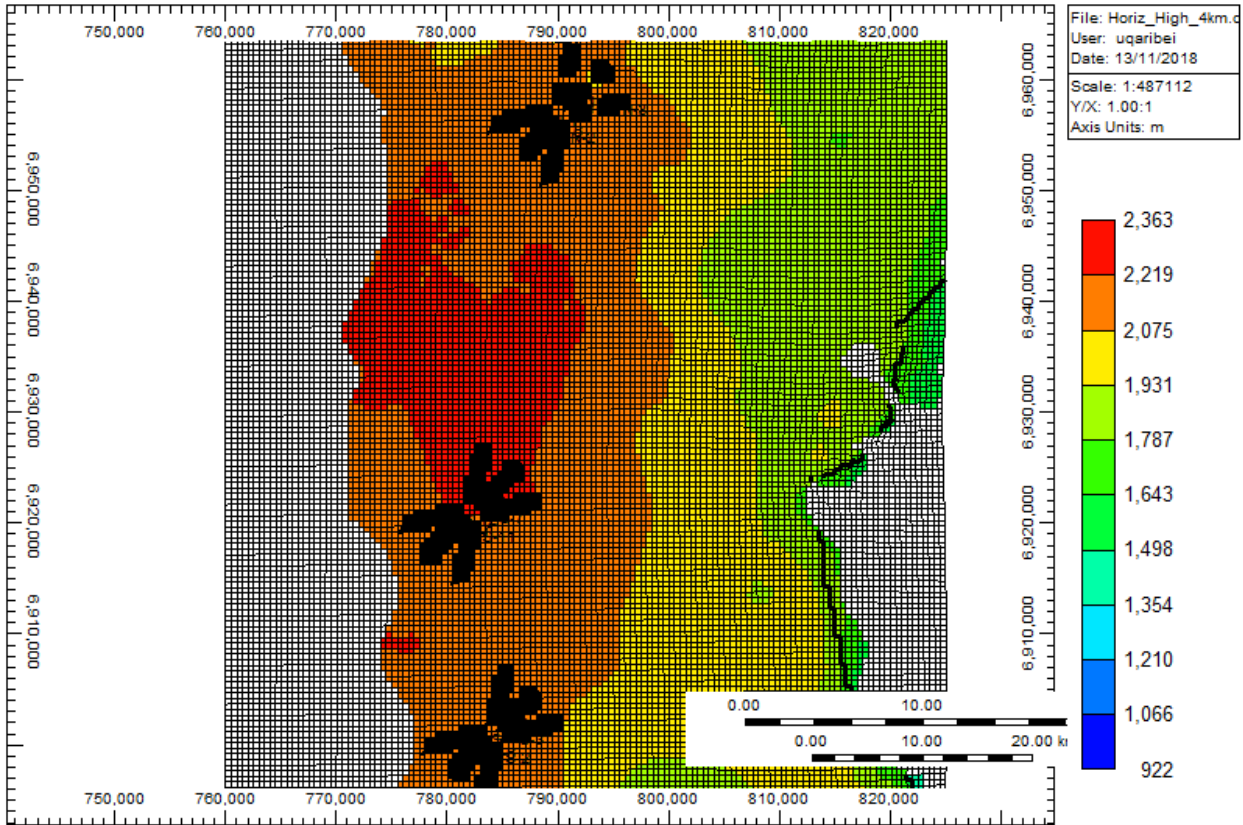
A horizontal well pattern was designed by putting two wells in opposing northeast and southwest directions and four more wells around them each at 30 degrees between them for a total of six wells per pad. One set of six wells was placed in the northern injection site, while for the southern region, one set of wells was placed in each of two different locations that are 20 km apart along the north-south direction (see Figure 131).

In most reservoir cases, the potential for sustained, high rate injection is for a longer duration than the current estimates of the life-time of the power plants.

**Figure 131** Six-well horizontal patterns for each injection site (North, South A and South B). Grid refinements were performed for each well grid blocks and its neighbour. From north to south, the injection centres (each with multi well pads) are called: 1) North, 2) South A and 3) South B.

**High case**

**Grid Top (m) 2016-01-01 K layer: 15**



The perforation interval length in the horizontal wells was set at 4 km and then, as a sensitivity analysis of the simulations were repeated at either 2 or 3 km intervals. In this way, it could be determined for different permeability fields (shown in Table 42) how many wells of a given length are needed to meet the various injection target scenarios defined below.

**Table 42** Permeability fields used in the simulation scenarios.

Geological scenario	Reservoir Permeability	Transition Zone Permeability
High Res	High Case	Reference Case
Mid Res	Reference Case	Reference Case
Low Res	Low Case	Reference Case
High Tz	Low Case	High Case

Scenarios with vertical injection wells RE also described in Ribeiro et al. 2019. These could result in a 2.3 times increase in cumulative injected CO<sub>2</sub> with a plateau injection extending to ~38 years. This is at the expense of a larger surface footprint i.e. 48 wells in total with an individual spacing of 3 km and associated pipelines, power and access tracks.

UQ-SDAAP has developed *injection* test scenarios for CO<sub>2</sub> storage based on hypothetical supply (section 4.8.7 and 4.14) of CO<sub>2</sub> from the Millmerran (M), Kogan Creek (K) and Tarong North (T) power stations. Injection scenarios run for >30 years which is longer than capture scenarios. Capture scenarios are assumed to be limited by the estimated life-time of the power stations (section 4.15).

## Test scenarios

- Scenario MKMK represents an injection schedule for CO<sub>2</sub> coming from Millmerran and Kogan Creek, with two increasing stages of supply each. This schedule was used to check the sensitivity of well-type and well count to the reservoir permeability case
- MKTMKT was created by adding Tarong North supply to the north injection site. Building on the well-type and count sensitivity, this was used for investigating how the results changed when additional pressure is imposed in the north
- MKTMK (extended) was another scenario developed to test the duration of high rate, sustainable injection – it roughly matched the reference capture scenario (scenario #1, section 4.14); however, in this combination, plant life-time limitations were ignored, a higher supply from all power stations and the peak injection rate of almost 13 Mtpa was extended to 38 years. This could result in a notional storage of 634 Mt of CO<sub>2</sub>, which is more than double the MKMK scenario

**Conservative, lowest risk, reference case injection scenario can likely inject and securely store the estimated rates available from the retrofit operations hypothesised herein.**

**There is significant potential for field development optimisation which would increase the dynamic capacity of the container and associated field development plan. This would be at the cost of an increased surface footprint and increased unit technical cost of injection. The degree of optimisation is uncertain and requires site specific data.**

For more discussion of the injection scenarios and modelling output see Ribeiro et al. 2019b.

### 4.8.7.1 MKMK injection scenario – well count required

The results of the 12 combinations of injection modelling scenarios for the MKMK injection schedule assumptions are summarised in Table 43. The results reveal the impact of porosity and permeability on well performance as well as degree of CO<sub>2</sub> migration into the Transition Zone. The results show the technical feasibility of different well patterns.

**The results indicate the importance of site specific reservoir data to discount the “Low Reservoir” permeability scenario, before any material capture decisions can be made.**

**Table 43** MKMK development scenarios. Wells reached the injectivity limit for low reservoir permeability cases (LowRes and HighTZ) – well redundancy not included (add at least one per site).

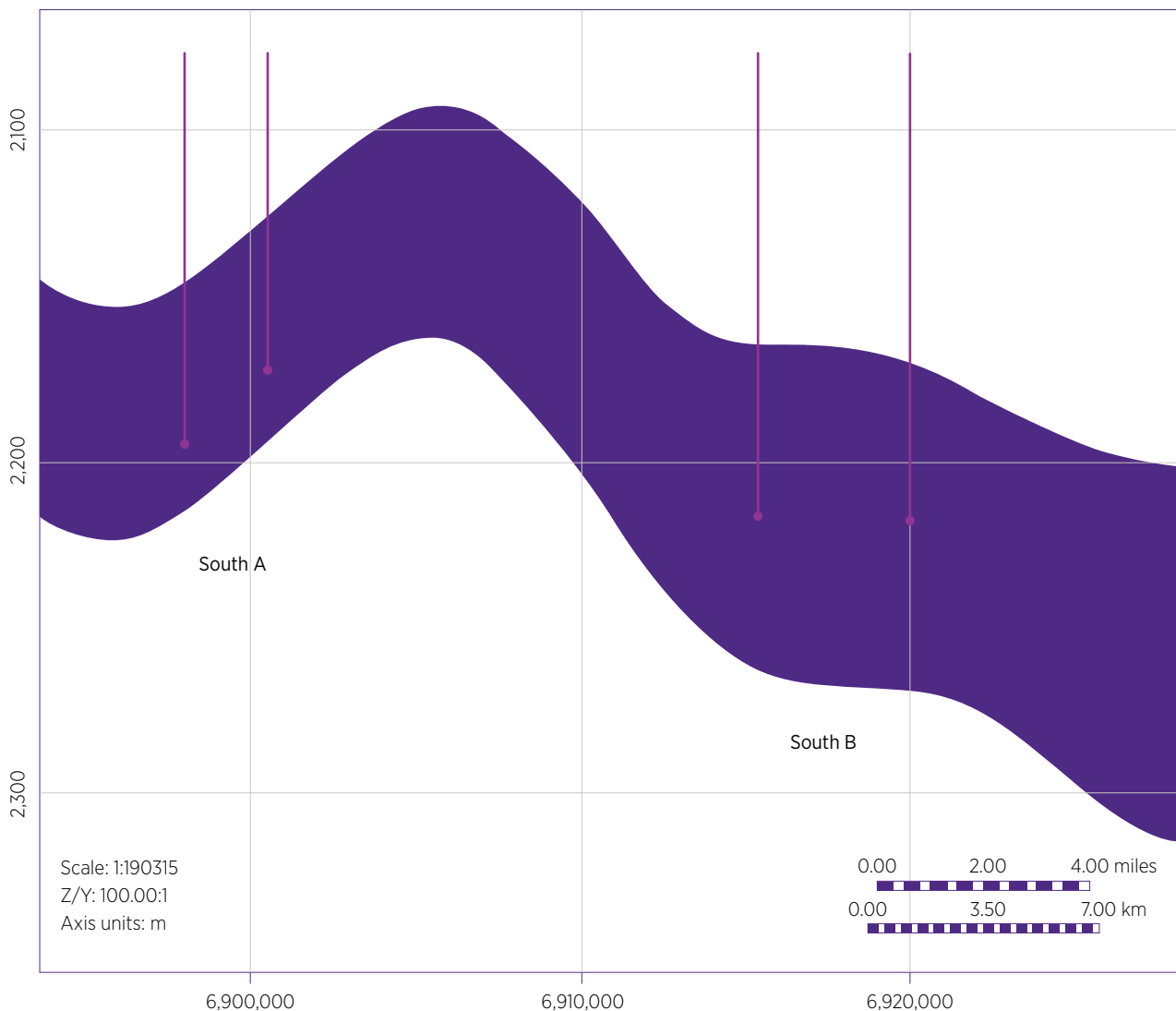
Reservoir Scenario	Well Type	Number of wells in North	Number of wells in South A	Number of wells in South B	Total Number of Wells	Target Met?
HighRes	4 km, horiz.	2	2	0	4	Yes
HighRes	3 km, horiz.	2	2	0	4	Yes
HighRes	2 km, horiz.	2	3	0	5	Yes
HighRes	Vertical	5	5	5	15	Yes
MidRes	4 km, horiz.	3	6	0	9	Yes
MidRes	4 km, horiz.	3	0	5	8	Yes
MidRes	3 km, horiz.	3	6	0	8	No, 98.5% of South
MidRes	3 km, horiz.	3	0	5	8	Yes
MidRes	Vertical	14	5	7	26	Yes
LowRes	4 km, horiz.	6	3	3	12	No, 99.8% of North
LowRes	3 km, horiz.	6	3	5	14	No, 98% of North
LowRes	Vertical	17	17	17	51	No, 82%
HighTZ	3 km, horiz.	6	3	4	13	No, 99.5% of North
HighTZ	Vertical	17	17	17	51	No, 84%

Apparently “better” performance was modelled when injecting at South B because the reservoir is predicted to be thinner around South A (see Figure 132). For 3 km wells, injection at South A reaches the injectivity limit (WHP at 15 000 kPa).

**Poorly constrained reservoir data means that a “low permeability” reservoir scenario is plausible. Reservoir quality is predicted to deteriorate to the south. The sites need appraisal wells and extended well test.**

**Figure 132** North-South Cross-section of the reservoir layers around south A and B. Injection performance is modelled as “better” for South B because it is predicted to have a greater thickness. Note that the vertical axis scale is 100 times larger than the horizontal scale to clearly display the variations in thickness.

**Reference case – North-South Cross-section (1 Layer 43)**



In the higher permeability scenarios (HighRes), lower pressure build-up was modelled and thus fewer wells would be needed to meet the injection target. In this case, since the increase in reservoir pressure was lower, the resulting water and gas inflow into the Transition Zone during the injection period is also lower. Higher permeability would also allow a faster depressurisation in the post-injection period, which would also contribute to a faster decrease in the water inflow rate to the Transition Zone.

Vertical wells result in higher pressure, more cooling of the Transition Zone and more penetrations of the Ultimate Seal. They are not a “lowest risk” design concept. If used, a larger plume area would result at the top of the reservoir, because of a higher build up pressure at each well and a larger number of wells (larger geographic area) needed for the injecting well patterns. The migration to the Transition Zone is initially higher since the distance between the top of the perforations and the base of the Transition Zone is less than for horizontal wells.

For “worst-case” injectivity scenarios (LowRes or lowest reservoir permeabilities; and, HighTz or highest Transition Zone permeabilities), the injection target volume could not be met for the north site using horizontal wells. It could not quite be met for any site using vertical wells, but the shortfall is probably not significant given large uncertainties in the models.

#### 4.8.7.2 MKTMKT injection – well count required

Simulation results show that when the Tarong North power station is added to the injection schedule in the north site, more wells are required to meet the target for HighRes and MidRes scenarios (1 and 2 additional wells, respectively). For the LowRes and HighTZ scenarios, the injection targets could not quite be met (only making ~90% of the target volume) even with the maximum number of wells (see Table 44). However, uncertainties are large and a 10% shortfall may not be significant.

**Table 44** MKTMKT development scenarios. Injectivity limits are similar to MKMK scenarios.

Scenario	Wells	#North	#South A	#South B	#Total	Target Met?
HighRes	4 km, horiz.	3	2	0	5	Yes
MidRes	4 km, horiz.	5	2	2	9	Yes
LowRes	4 km, horiz.	6	3	4	13	No, 91.3%
HighTZ	3 km, horiz.	6	3	3	13	No, 93.2%

#### 4.8.7.3 MKTMK injection – well count required

The considerably higher injection target imposed by the MKTMK extended schedule injection scenario is easily met for the HighRes case with only seven horizontal wells operating with maximum wellhead pressure of 15,000 kPa. On the other hand, if reservoir properties of the MidRes case are assumed, all 18 wells are required to meet 96% of the target. Allowing a higher wellhead pressure limit of 20,000 kPa for the MidRes scenario leads to a number of required wells being eight (see Table 45). The LowRes, High TZ, and vertical well scenarios were not run as they would clearly not meet the injection targets.

**Table 45** MKTMK extended development scenarios. Higher wellhead pressure is required to meet the injection target for MidRes.

Scenario	Wellhead Pressure	#North	#South A	#South B	#Total	Target Met?
HighRes	15,000 kPa	3	2	1	6	Yes
MidRes	15,000 kPa	6	6	6	18	No, 96%
MidRes	20,000 kPa	4	2	2	8	Yes

### 4.8.8 Injection sector test cases – upside and uncertainties

We investigated a number of notional field development plans, intended to represent technically feasible (and reasonable) options for such a development. A reference case has been chosen, which is constrained by a conservative, minimum risk development philosophy (section 4.8.1).

There is considerable upside for longer plateau injection rates. There is some upside for higher plateau rates (at some cost to duration). There is some downside risk if poor reservoir quality is encountered. There is very little risk to a scheme being “less than 5 Mtpa, 20 year” i.e. the UQ-SDAAP definition of “material abatement”.

One of the main challenges affecting UQ-SDAAP was the lack of subsurface data available from the areas identified as notional sweet-spots for injection. As proposed in the original project plan, this has been largely compensated for extensive dynamic calibration data sets applied to a fundamental geological revision.

Many uncertainties remain. We used two main approaches for addressing these uncertainties. The first involved creating a range of static reservoir models with properties that envelop the expected variation in porosity and permeability. These were in turn used in dynamic simulations and allowed us to identify notional development plans that appear to be technically feasible in the circumstances represented by each of the models (Ribeiro 2019b).

A second approach described hereunder, involves simulating the notional injection using the base case reservoir properties, but modifying key parameters one at a time for each simulation. This task was performed using CMG's CMOST software (CMG 2018a). Simulation results were analysed to assess the impacts of changes in reservoir properties on two key subsurface criteria for such a project:

1. Injectivity – If different reservoir properties were encountered, injection rates, and thus the number of wells required to achieve the desired injection volume would change, which would therefore impact the cost of the notional CCS project. As some of the cases were unable to achieve the desired injection, the results are presented in terms of tonnes of CO<sub>2</sub> injected per well, where higher values would typically be associated with lower cost per tonne.
2. Containment – One concern that often surrounds CO<sub>2</sub> injection projects is migration of the CO<sub>2</sub> plume after injection. The supercritical CO<sub>2</sub> plume area (km<sup>2</sup>) is presented for each simulation to indicate the parameters that most significantly impact CO<sub>2</sub> movement within the Blocky Sandstone Reservoir (i.e. lateral containment). In addition, the percentage of the injected CO<sub>2</sub> that migrates vertically from the Blocky Sandstone Reservoir into the Transition Zone is used as a measure of the impact of each parameter on vertical containment.

Comparisons of these results for the various simulations are intended to help identify the parameters that would be expected have the most significant impacts on likely success of a CCS project in the Surat Basin, and thus inform a data appraisal program.

Two different injection scenarios were used as reference cases for the subsequent sensitivity study. Both used the base case UQ-SDAAP notional injection sector model (Gonzalez et al. 2019b), but with different CO<sub>2</sub> delivery schedules. Details of the notional injection sector reference case can be found in Rodger et al. (2019d and 2019f). Details of a modular, sequential approach to capture and retrofit can be found in Gamma Energy Technology 2019 and section 4.14.

For model and grid parameters and boundary conditions refer to earlier sections and Gonzalez et al. (2019), Rodger et al. (2019c and 2019f). The area outline is given in Figure 133.

There is considerable upside for longer plateau durations. There is some upside for higher plateau rates (at some cost to duration). There is some downside risk if poor reservoir quality is encountered. There is little risk that the storage potential is immaterial i.e. little risk that it is “less than 5 Mtpa for 20 years”.

#### 4.8.8.1 Parameterisation

The UQ-SDAAP regional static model was upscaled as described in more detail in (Rodger et al. 2019c). Histograms of the resulting grid properties in the Blocky Sandstone Reservoir and Transition Zone/Ultimate Seal are shown in Figure 135 and Figure 136 respectively.

In the Blocky Sandstone Reservoir, mean porosity was 12.7%, while horizontal permeability was typically between 1 md and 100 md (with an arithmetic mean of 44 md). The vertical permeability in this interval was around 0.15 times the horizontal permeability.

In the Transition Zone and Ultimate Seal, the porosity and permeability were generally much lower (mean of 6%) than in the Blocky Sandstone Reservoir, while the horizontal permeability was typically two to three orders of magnitude lower than in the Blocky Sandstone Reservoir. Vertical permeability in these intervals was very low, typically 10<sup>-6</sup> to 10<sup>-3</sup> md.



**Figure 133** Map indicating extent of notional injections sector model (red) relative to Blocky Sandstone Reservoir structure (black) and the three notional injection sites (green).

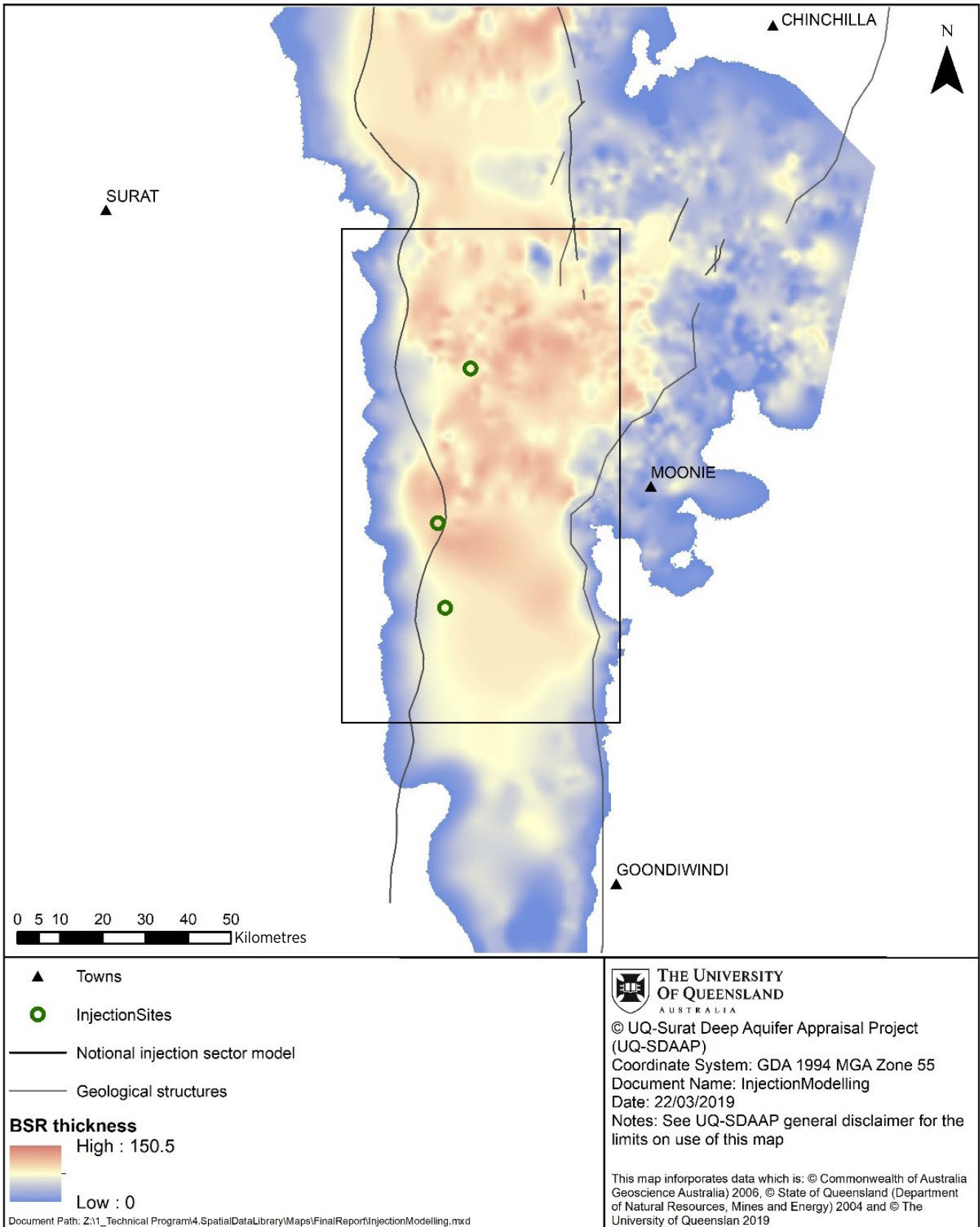


**Table 46** Notional injection sector model layers. The colour column refers to Figure 133.

Layer(s)	Description	Total Thickness (m)	Colour
1	“Hutton Sandstone” (Top Boundary Condition)	100	Blue
2	Ultimate Seal	35 - 115	Green
3 - 11	Transition Zone	80 - 150	Yellow
12 - 20	Blocky Sandstone Reservoir	0 - 125	Orange
21	“Below Unconformity” (Bottom Boundary Condition)	20	Dark Orange

**Figure 134** West-east cross section indicating layering in notional injection sector model. Colours indicate parts of model as outlined in Table 46. Left side scale shows depth in meters (True Vertical Depth Subsea). The dark area at the top of the Blocky Sandstone Reservoir (yellow) in the deeper part of the model is the area where cells have been refined to more accurately model CO<sub>2</sub> plume migration. Also note the fault near the east of the figure.

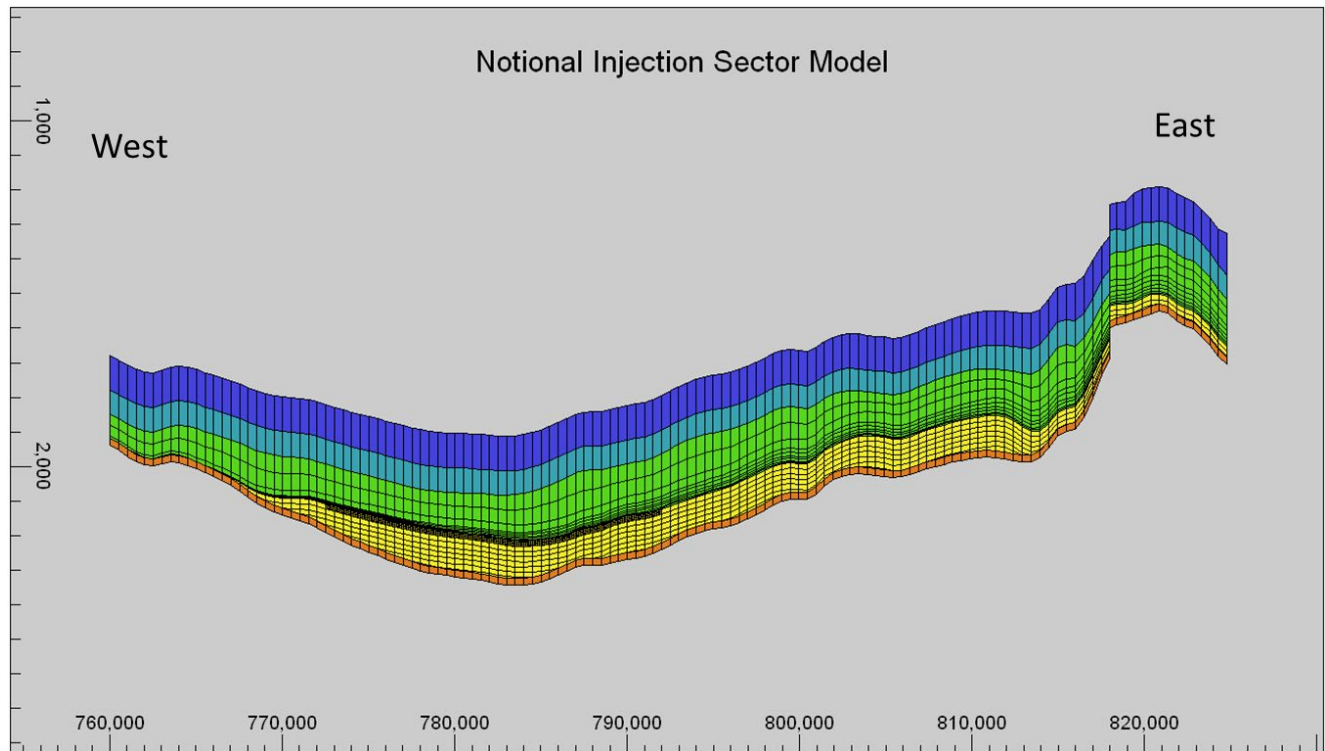


**Figure 135** Histograms of grid properties for Blocky Sandstone Reservoir cells in the base case notional injection sector model. Note x axis scales for horizontal (left) and vertical (centre) permeability are different. Vertical permeability is typically around 0.15 times horizontal permeability for cells in this model.

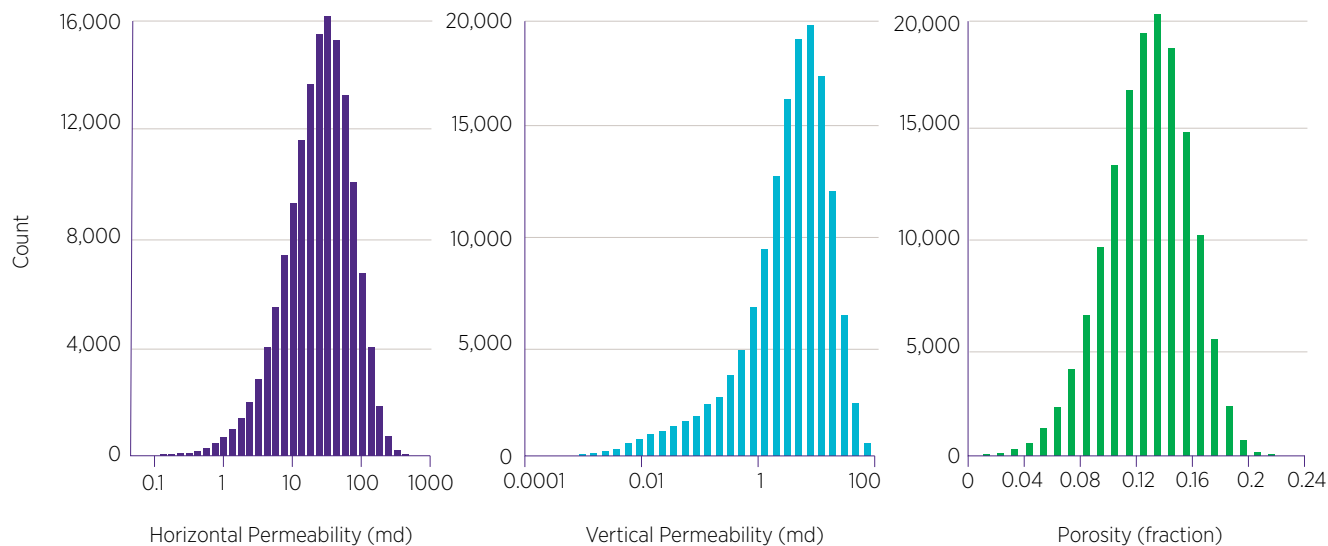
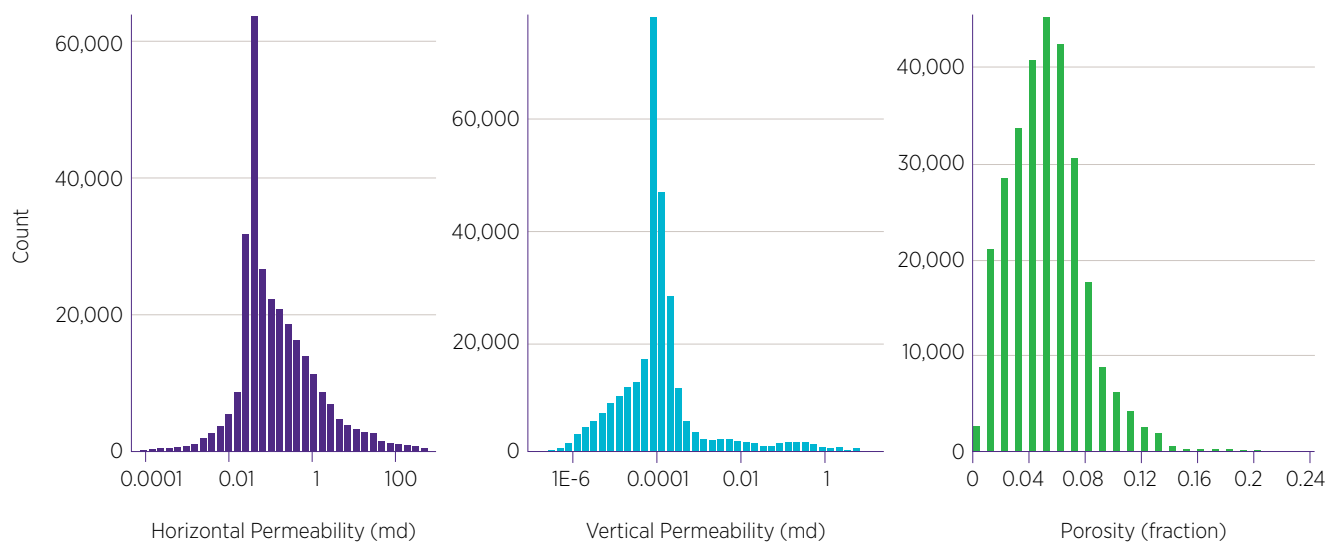
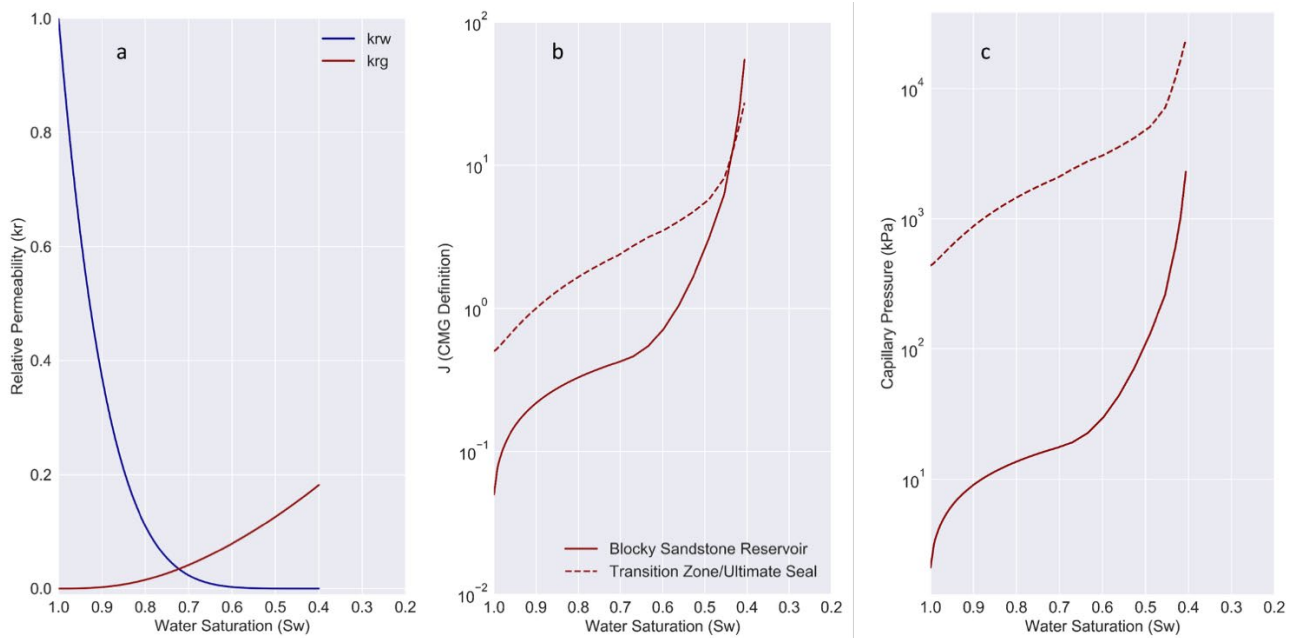


**Figure 136** Histograms of grid properties for Transition Zone and Ultimate Seal cells in the base case notional injection sector model. Note x axis scales for horizontal (left) and vertical (centre) permeability are different, and also different from the equivalent histograms in Figure 135.



The fluid model is described briefly in section 4.8.4 and in detail by Ribeiro 2019a. Relative permeability curves were created based on core analysis from the West Wandoan 1 well (Rodger 2019a). The base case relative permeability curves, which have a residual water saturation ( $S_{wr}$ ) of 40% and a maximum relative permeability to  $\text{CO}_2$  ( $kr_g$ ) of 0.18, are shown in Figure 137a. These are the drainage (i.e.  $\text{CO}_2$  displacing water) curves. Imbibition curves were not defined. Instead, the maximum residual saturation of  $\text{CO}_2$  was defined as a parameter in the GEM input. This allows GEM to evaluate imbibition curves that leave the drainage curve at any saturation (i.e. even if  $S_{wr}$  is not reached). A value of 0.35 was input as the base case value for the residual saturation of  $\text{CO}_2$ .

**Figure 137** (A) Drainage relative permeability curves used for all cells in the base case notional injection sector model, (B) J-function curves for the Blocky Sandstone Reservoir (solid line) and Transition Zone/Ultimate Seal (dashed line), and (C) Capillary pressure curves calculated using the curves in 'b', and typical porosity/permeability values from the Blocky Sandstone Reservoir (solid line,  $\Phi=0.12$ ,  $k=44\text{md}$ ) and Transition Zone/Ultimate Seal (dashed line,  $\Phi=0.06$ ,  $k=0.05\text{md}$ ).



Rather than defining capillary pressure curves, J-functions were used to model variations in capillary pressure caused by heterogeneity, particularly in the Transition Zone as described briefly in section 4.8.5 and in detail by Rodger 2019a.

## 4.8.9 Field development simulations – testing rates and durations

Two CO<sub>2</sub> delivery schedules were used in the sensitivity analysis. These schedules involved delivery of CO<sub>2</sub> from up to three power stations: Millmerran (M), Kogan Creek (K) and Tarong North (T). Both schedules *nominally* start injection around 2030 (referred to as “injection year” 0 in the schedules in Table 47 and Table 48).

More details of the Field development concept can be found in Rodger et al. 2019f.

### 4.8.9.1 Discussion of MKMK limited test injection cases

Refer to section 4.14 for a discussion on sequencing and roll-out of capture. The step-wise increase in the injection scenario below, is roughly in line with this sequencing.

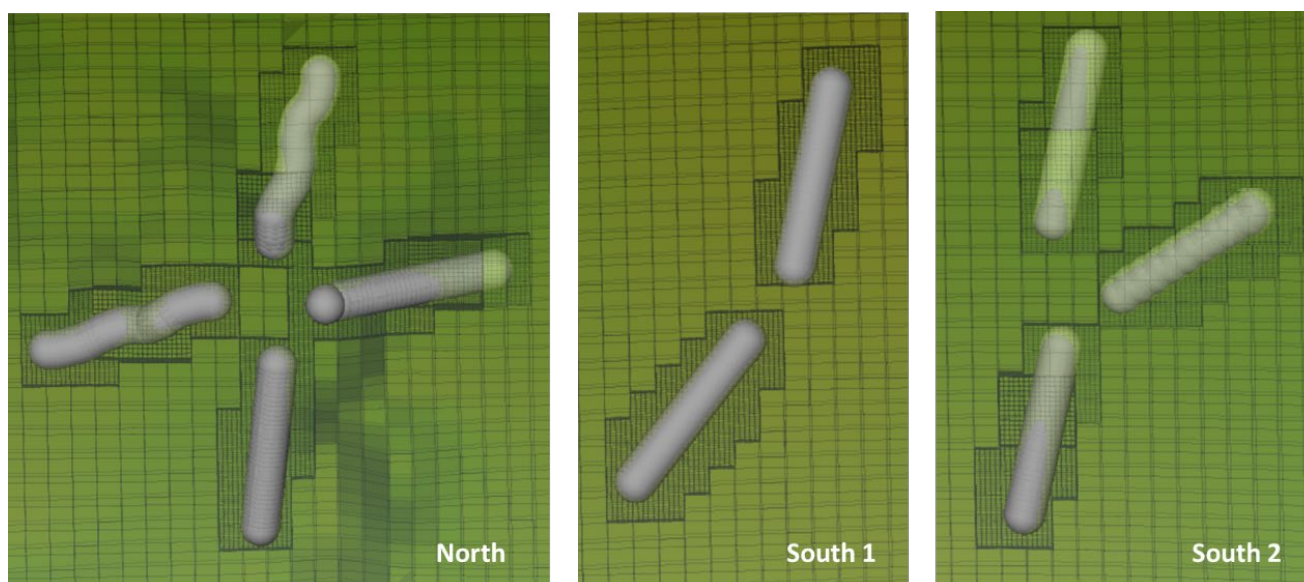
Injection commences in the south first supplied from Millmerran, a second capture retrofit is built on Kogan Creek and comes on line in year 3. The second Millmerran and Kogan Creek retrofits follow at 3 year intervals.

For injection modelling purposes, the injection durations were not limited to the plant life (estimated to end in the mid 2050s), rather injection was run for slightly longer (30 years), before the injection rates were stepped down, eventually stopping completely in year 39. This resulted in a total peak injection rate of 9.2Mtpa for 21 years, in this scenario. This is a slightly lower peak rate than the maximum indicated in the capture deployment section (4.14) representing a lower percentage retrofit or reduced availability outcome. In any case, a robust and expandable development can be accommodated.

**Table 47** Mass rates for MKMK schedule

Inj. Year	0	3	6	9	...	30	33	36	39
North Injection Rate (Mtpa)	0	2.2	2.2	4.4	...	4.4	2.2	2.2	0
South Injection Rate (Mtpa)	2.4	2.4	4.8	4.8	...	2.4	2.4	0	0
<b>Total</b>	<b>2.4</b>	<b>4.6</b>	<b>7.0</b>	<b>9.2</b>	<b>...</b>	<b>6.8</b>	<b>4.6</b>	<b>2.2</b>	<b>0</b>

For the MKMK schedule (Table 47), a wellhead pressure constraint of 15,000 kPa (150 bar) for all wells was used as the reference case. Excluding the need for well redundancy, notional development plan for this scenario required three horizontal wells at the north notional injection site, and two horizontal wells at each of the south notional injection sites. Generally speaking we have assumed an N+1 redundancy philosophy at each site. Therefore, nine wells were needed for all MKMK simulations (Figure 138), although not all wells were opened in every simulation.

**Figure 138** Well layouts for the MKMK schedule. Refined cells are visible around each well. The apparent “wobbling” of some of the north wells is due to these refined cells, but is not expected to affect the results of this particular study.

#### 4.8.9.2 Discussion on MKTMK extended test case

The MKTMK *injection* scenario involves hypothetical capture and injection of CO<sub>2</sub> from all three power stations; CO<sub>2</sub> from Millmerran (M) into the two sites in the south, and CO<sub>2</sub> from Kogan Creek (K) and Tarong North (T) into the site in the north. This scenario also featured a longer injection period (50 years for each stage, and 62 years in total), as well as higher estimates for the CO<sub>2</sub> capture rates from the individual power stations (Table 48).

**Table 48** Mass rates for MKTMK extended schedule

Inj. Year	0	3	6	9	12	...	50	53	56	59	62
North Injection Rate (Mtpa)	0	2.5	3.69	3.69	6.5	...	6.5	4.0	2.81	2.81	0
South Injection Rate (Mtpa)	2.54	2.54	2.54	6.18	6.18	...	3.64	3.64	3.64	0	0
<b>Total</b>	<b>2.54</b>	<b>5.04</b>	<b>6.23</b>	<b>9.87</b>	<b>12.68</b>	<b>...</b>	<b>10.14</b>	<b>7.64</b>	<b>6.45</b>	<b>2.81</b>	<b>0</b>

As in the MKMK scenario, injection from Millmerran started in the south in 2030, 3 years before injection from Kogan Creek. Three years further on, the rate at the north notional injection site was increased to represent injection of CO<sub>2</sub> captured at Tarong North. The schedule then progressed, with the rates at each site increasing as the second stages of CO<sub>2</sub> capture at Millmerran and Kogan Creek are added in years 9 and 12 respectively. Each “stage” lasted 50 years, before the injection rates were stepped down, eventually stopping completely in year 62. This resulted in a total peak injection rate of 12.68 Mtpa for 38 years.

A different approach was used to assess the injectivity and CO<sub>2</sub> plume spread when considering the MKTMK scenario. Rather than only defining wells that had been required for the base case, a total of 18 wells spread between three notional injection sites (North, South1 and South 2) were defined for all cases, although not all wells would become active in every case. The sites were each set up with six 3.75 km long horizontal wells extending approximately radially from a notional well pad, but avoiding running in a NW-SE direction, to avoid limitations from in-situ stress (Figure 139).

CMG’s AUTODRILL feature (CMG 2018) was used to simulate bringing wells online as required to achieve the pre-defined injection rates without breaching any other constraints. An N+1 redundancy scheme was assumed, and thus two wells (one north, one south) would need to be added to the totals required in each simulation. The results are presented in terms of the wells *required* for injection, not including the redundant wells (Figure 140).

**Figure 139** Well layout at South 1 notional injection site for all MKTMK simulations. The same layout was used at the other two notional injection sites. This figure shows one layer of cells only, which can be seen to “pinch-out” at the bottom left of the figure. Also note the refined cells around the wells. For reference large grid blocks are approximately 500 x 500 m, and well completions are approximately 3.75 km long.

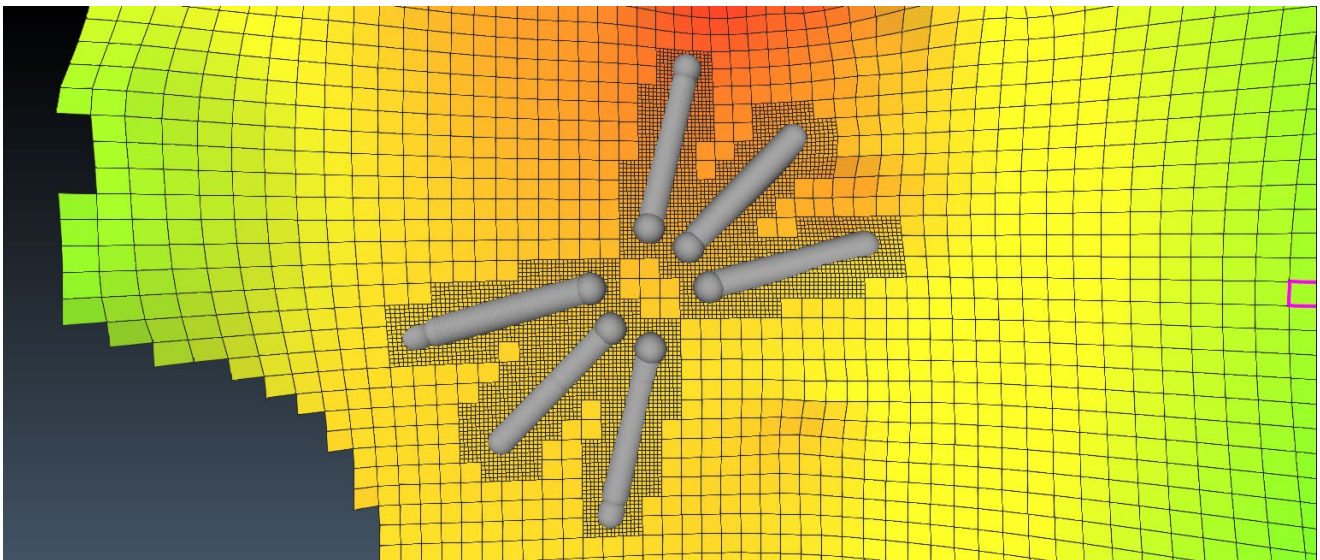
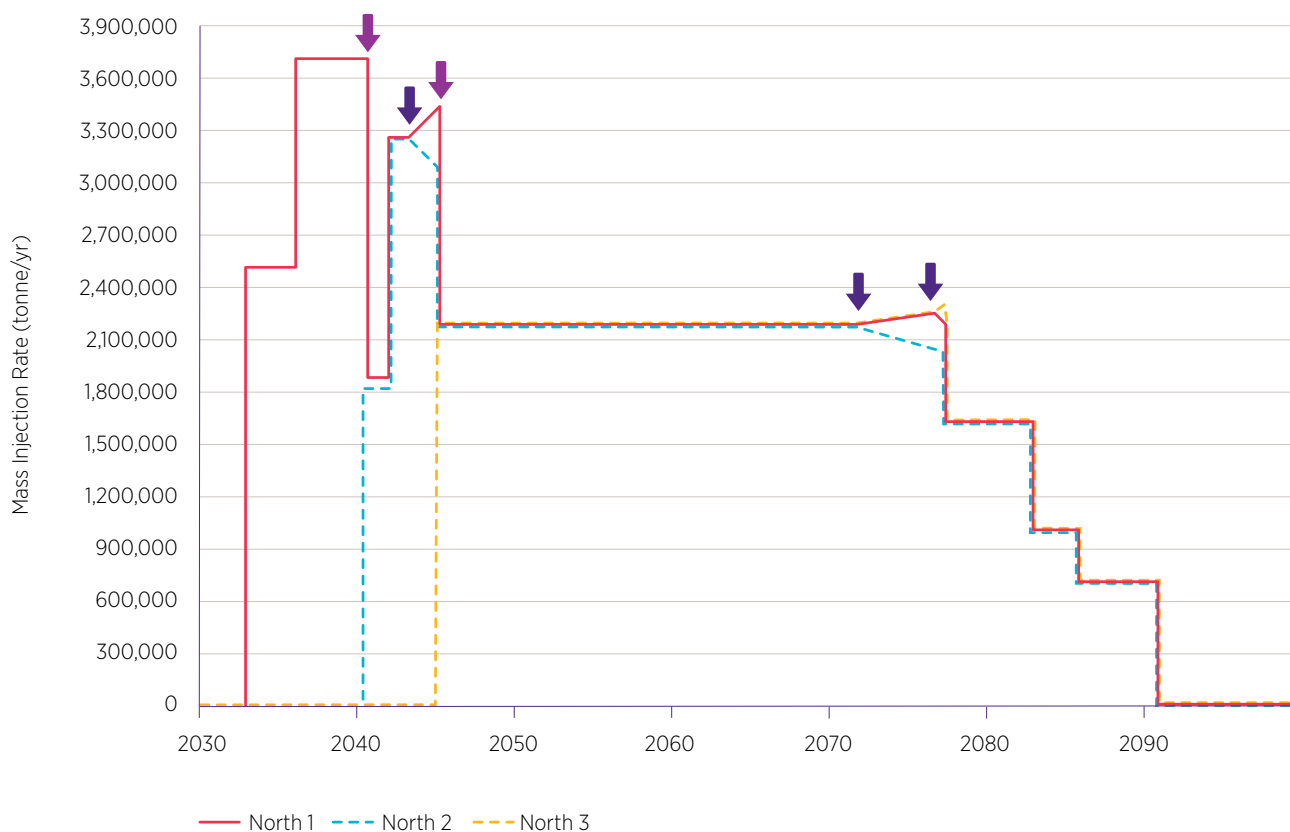


**Figure 140** An example of CMG GEMs AUTODRILL control for wells at the north notional injection site and MKTMK extended delivery schedule. Most of the time, all wells inject at the same rate. Arrows indicate points where wells become limited by wellhead pressure and either; (A) Injection is redistributed to other wells (blue arrows), or (B) All currently open wells are pressure limited, so the next well in the queue is opened and starts injection (red arrows).

#### Northern Site Mass Injection Rates



For the extend MKTMK case, a wellhead pressure constraint of 20,000 kPa (200 bar) for all wells was used as the reference case for simulations, which had been determined to be a suitable method of achieving the required injection rate in previous simulations (Ribeiro 2019b). The effect of the lower wellhead pressure limit of 15,000kPa on the number of wells required for this schedule is tested as part of this sensitivity study. The higher wellhead pressure meant several wells became constrained by bottomhole pressure limits, which had been calculated as 90% of the estimated thermally reduced fracture pressure (Rodger et al. 2019a).

## 4.8.10 Summary of site modelling test cases

**Site selection has been described previously as being driven by “lowest containment risk” considerations. There would be additional development costs (well depths and pipeline distances) imposed in this approach, these are considered essential for a first of a kind development in a sensitive area.**

Injection modelling has also been constrained, conservatively with respect to maximum allowed pressures (managed to be well below any critical containment pressures) and has been further constrained to minimise surface footprint.

A development scenario has been investigated in which a single northern injection well pad accepts CO<sub>2</sub> from Kogan Creek (and possibly a Tarong North retrofit). Maximum operating pressures have been constrained in line with geological limitations.

Modelling shows that the Transition Zone concept as a buffer or baffle between injection reservoir and ultimate seal is valid.

A given well pad will have 4-6 wells. Significant benefits can be gained in terms of both risk reduction and rate enhancement by selecting horizontal wells.

Emplaced CO<sub>2</sub> plumes do not move more than 10 km from the injection sites, though groundwater pressures are raised over a very large area.

### **Notwithstanding the need for site specific drilling and testing data.**

Generally speaking, the sites can sustain a rate of injection equal or greater than the rate captured from retrofit of the three plants and can probably sustain this as a plateau for longer than estimated life-time of these plants.

A single-pad development of 4-6 wells can likely accommodate safely at least 30 years of captured emissions (this includes redundant wells to eliminate operational venting). The southern area has been modelled with two well pads, separated by around 19.8 km, because of poorer predicted reservoir properties (which needs to be confirmed). These southern sites can also likely accept at least 30 years' worth of captured emissions from the Millmerran plant.



## 4.9 Pipeline network – a scoping investigation

Detailed pipeline network design and planning was outside the scope of this project. However, the feasibility of material carbon abatement through CCS relies on the ability to find and licence suitable transport routes from sources to sinks. To discover whether there are any potential show-stoppers, or major cost-inducing route detours, required a scoping study and sensitivity analysis of several pipeline routes to investigate the main likely variables and options. The analysis described below concluded that for various combinations of environmental values, there are likely to be reasonable options for pipeline routing which can minimise disturbance of higher value land and make maximum use of existing easements. However, to progress concepts further requires detailed in-field studies and considerable community and regulatory engagement.

The project investigated the notional pipeline routes using multiple criteria decision-making methods and geographic information systems (GIS) suitability analysis and least cost pathway tools. A linear weighted combination method (Jiang & Eastman 2000) was used to combine information about relevant surface features to determine whether an area was more or less suitable for hosting a notional CO<sub>2</sub> pipeline. Least-“cost” pathway tools were then used to determine the pipeline route between a power plant and the notional injection sites. A simple linear weighted combination was used for the suitability analysis as it is easy to implement in ArcMap and is suitable for the analyses using several criteria, as well as criteria with many factors. In contrast, methods such as Analytical Hierarchy Process (AHP) can be difficult to implement when attempting pairwise comparisons between many criteria, or factors within a criterion (Malczewski 2006). Fuzzy membership does not allow for criteria to be weighted according to their relative importance in determining suitability (Esri 2017), and so is not reflective of how different factors may contribute to determining a suitable route.

In linear weighted combination, any features relevant to determining suitability are represented by criteria (e.g. rate of change of elevation or land use) that vary spatially. The spatial variation for each criterion is represented by factors. Each factor within a criterion is given a score that represents that factor’s *suitability* to host a notional pipeline, or the *relative* “cost” of locating a pipeline over that area. For example, in land use, an area used for grazing native vegetation was considered to be more suitable/less costly for laying a CO<sub>2</sub> pipeline than an area used for irrigated horticulture. The research considered “cost” in a broad sense in this analysis, with cost referring to social and environmental costs, such as the loss of endangered species’ habitat as well as monetary costs. A preliminary suitability analysis method used to determine the notional pipeline routes is similar to the method used to determine the notional injection sites (Wolhuter et al. 2019a).

This study is only an *exploratory* analysis once where criteria weights and factor scores were assigned using values that reflected the relative effect of different factors and criteria on the cost of constructing a CO<sub>2</sub> pipeline. Factors within each criterion were simply given a score of one to 10, with a lower score indicating a lower cost/better suitability for CO<sub>2</sub> pipeline construction. Criteria weighting was then assigned, with the sum of the weights adding to 100 to fulfil the requirements of the weighted overlay tool. The criteria weights used were an attempt to balance technical, environmental and social considerations along with relevant regulatory requirements. This analysis formed a reference or base case pipeline route.

**This is not a substitute for detailed in-field investigation nor for engagement with communities and regulators.**

A sensitivity analysis was conducted, where factor scores and criteria weighting were assigned values that prioritised environmental, social/human centred concerns or technical constraints. Finally, the base case pipeline route was compared with the routes created in the sensitivity analysis. The pipeline routes were compared using the metrics of pipeline length, and number of roads, railway lines, powerlines and pipelines crossed. Figure 141, shows the process used for the analysis.

### 4.9.1 Methodology

Our analysis involved connecting up to five power stations: three supercritical coal plants, Kogan Creek, Tarong North and Millmerran; and two CCGTs, Condamine, Darling Downs, to three notional injection locations. Kogan Creek, Tarong North, Condamine, Darling Down would be connected to the northern notional injection location, while Millmerran would be connected to the two southern locations (Figure 142 and Figure 143).

An iterative approach was used to connect the power stations to the northern site as the CO<sub>2</sub> injection from the power stations and building of the CO<sub>2</sub> pipelines would be phased i.e. **the whole network would grow organically and not be built as one**. As the Kogan Creek power station was the closest source to a notional site, it was connected first. The pipeline connecting Kogan Creek to the notional injection location then became the connection location for the next “least cost” path analysis to connect Tarong North, Condamine and Darling Downs.

The criteria used in the route investigation (described further in Wolhuter et al. 2019b) were selected to represent technical, social and environmental factors. The datasets also represented criteria that varied at the appropriate scale for analysis and would therefore have some effect on the pipeline route. Datasets that did not vary, or barely varied across the extent of the analysis, were not used. For example, the Australian Geological Survey Organisation’s 2000 earthquake risk dataset shows the same range of earthquake risk across the entire analysis area. Only government and publicly available spatial datasets were used.

The criteria used in the analysis included:

- Rate of change of elevation
- Distance from watercourses
- Distance from buildings
- Distance from roads pipelines and railways
- Distance from powerlines
- Land ownership
- Land use
- Native Title
- Easements
- Vegetation regulated under the *Vegetation Management Act*
- Areas to avoid (e.g. military bases, mines, areas requiring extra survey)

Figure 141 Flow chart showing analysis methods.

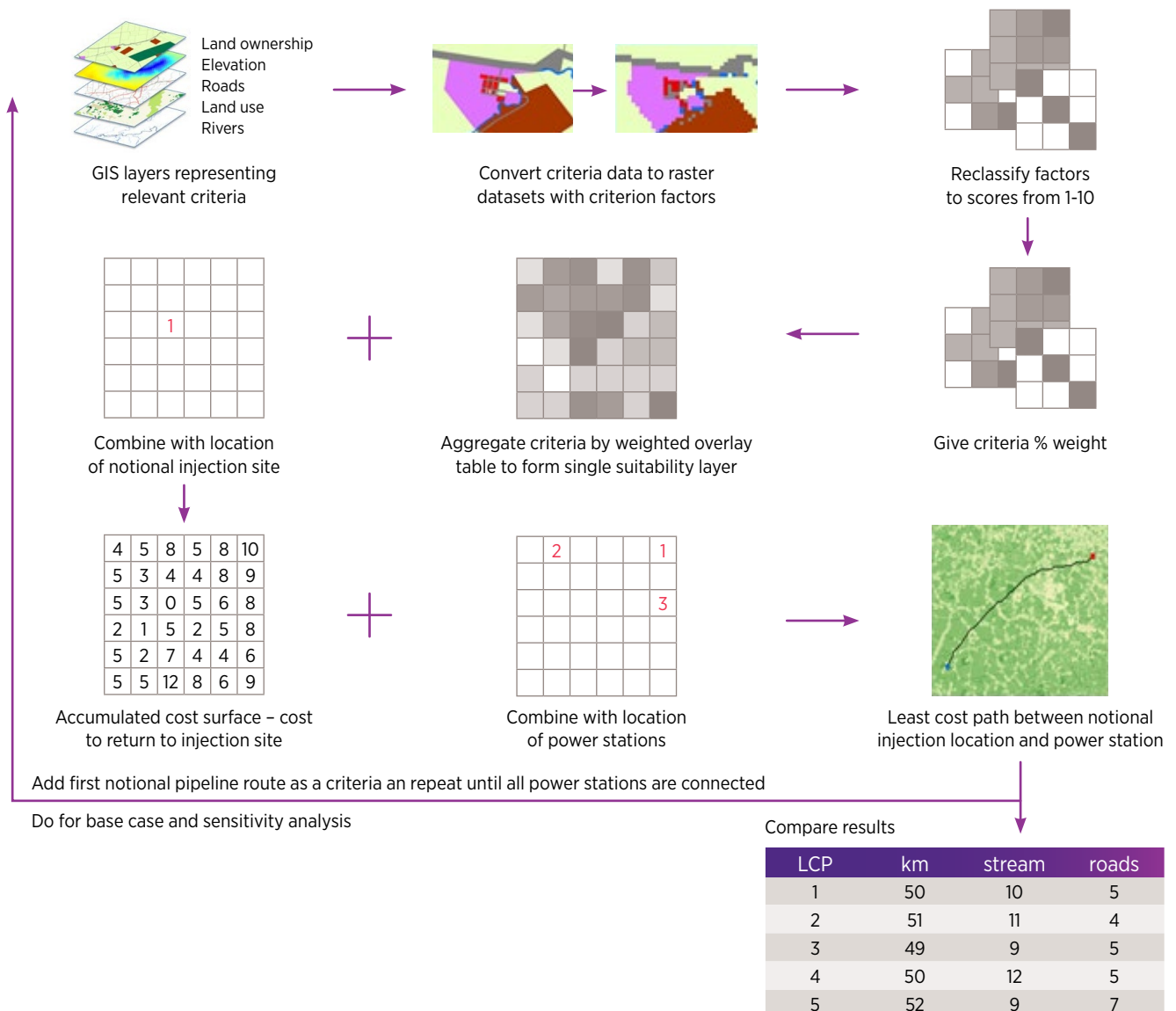


Table 49 sets out an exploratory example of weightings for each of the criteria that were used as the base case. For the sensitivity analysis, where factors were not entirely relevant to the concerns being prioritised (not the top priority), they were put in the same relative position or order as the base case. The weightings investigated are an attempt to show the impact of balancing many interests e.g. people living near the injection site, indigenous interests, environmental values and practical considerations related to construction. Further details of the data used for each of these criteria, any changes made to the data, the factors within each criterion and the factor scores applied for the base case and sensitivity analysis can be found in Wolhuter et al. 2019b.

**Table 49** Weighting for each criteria in the base case and sensitivity analysis for the pipeline route selection.

Layer	% influence base case	% influence environment	% influence social	% influence technical
Slope	14	6	5	14
Easements	13	8	11	13
Distance from buildings	12	4	14	9
Distance from watercourses	11	12	8	12
Distance from powerlines	10	5	4	11
Distance from roads, pipelines & railway	9	8	6	10
Land ownership	8	10	13	8
Land Use	8	14	10	8
Native Title	6	9	12	5
Regulated vegetation (VMA)	5	13	9	6
Areas to avoid	4	11	8	4

## 4.9.2 Pipeline network final routing and sensitivities

The UQ-SDAAP project used ArcMap 10.6 to run the suitability analysis. The model boundary for the suitability analysis was as shapefile that defined an area around the notional injection locations and power stations used in the analysis. GDA94 MGA Zone 55 (EPSG 28355) was used as the coordinate system.

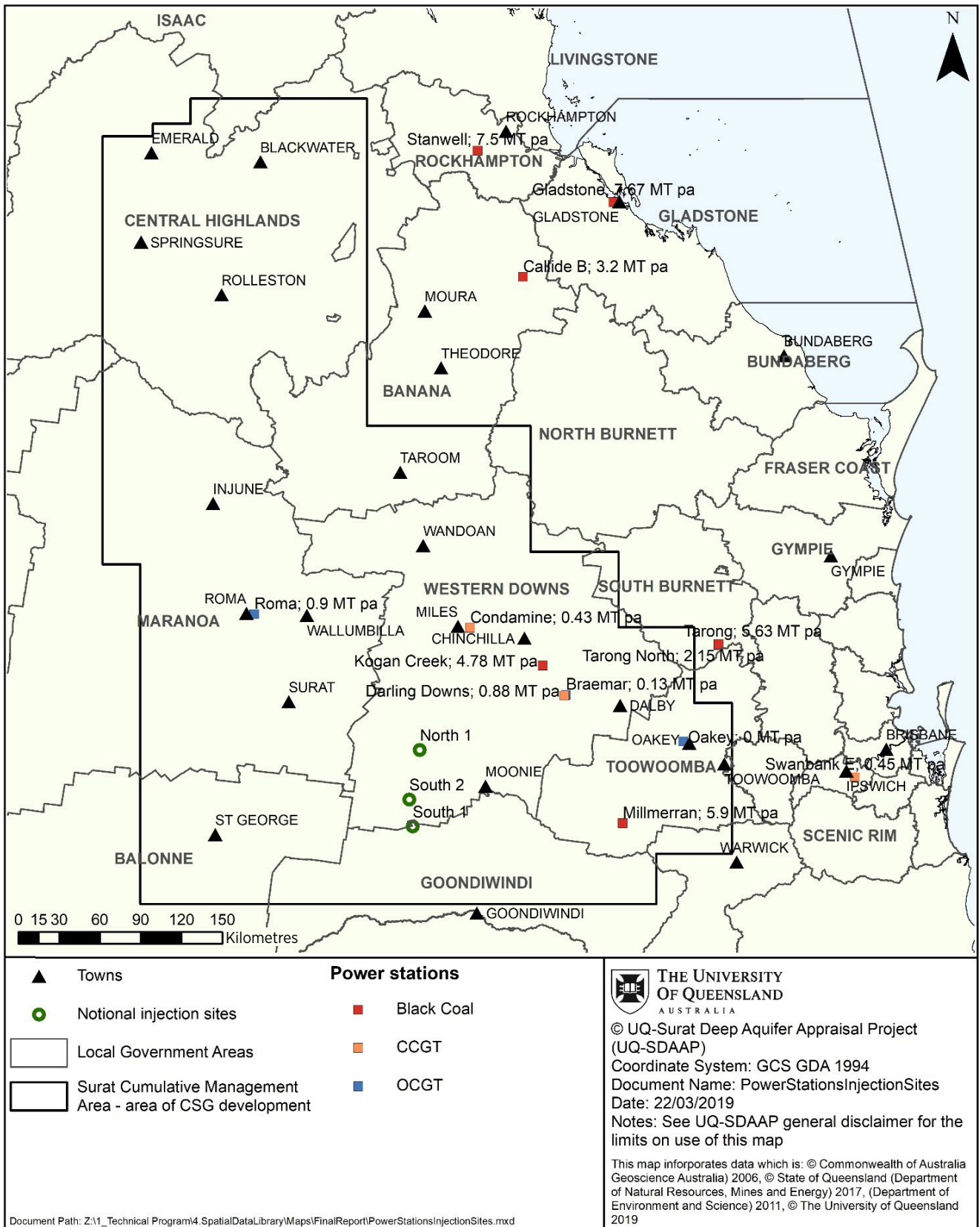
The surface criteria represent a set of sometimes competing factors that can be traded against each other to show whether a location is more or less suitable for hosting a pipeline in comparison to another location. Wolhuter et al. 2019b describes the data used to represent the criteria in the analysis, including the source of the dataset and a description of possible sources of error or uncertainty in the data.

Figure 143, shows the notional pipeline routes produced by an exploratory base case analysis, Figure 144 shows alternative pipeline routes produced by prioritising environmental variables, Figure 145 shows the notional pipeline routes produced by a more social-interaction analysis.

Table 50 to Table 53 compares the notional pipeline route lengths, stream crossings, road crossings, pipeline crossings, rail crossings and power line crossings for the four pipeline route selection analyses.

Importantly, routes are achievable in each case with a very small range of pipeline lengths, depending on the combination of parameters used. Since length is a major cost driver, this means that uncertainty in pipeline cost from this source will be minimal. There are other cost-driving factors, such as stream crossings, which vary between routes. **Optimisation would be required in the context of a detail EIS and community engagement process.**

Figure 142 Selected power stations in the study area and notional injection locations.



**Figure 143** Pipeline routes: example from a “base case” analysis (note use of existing pipeline easements in the south near Moonie).

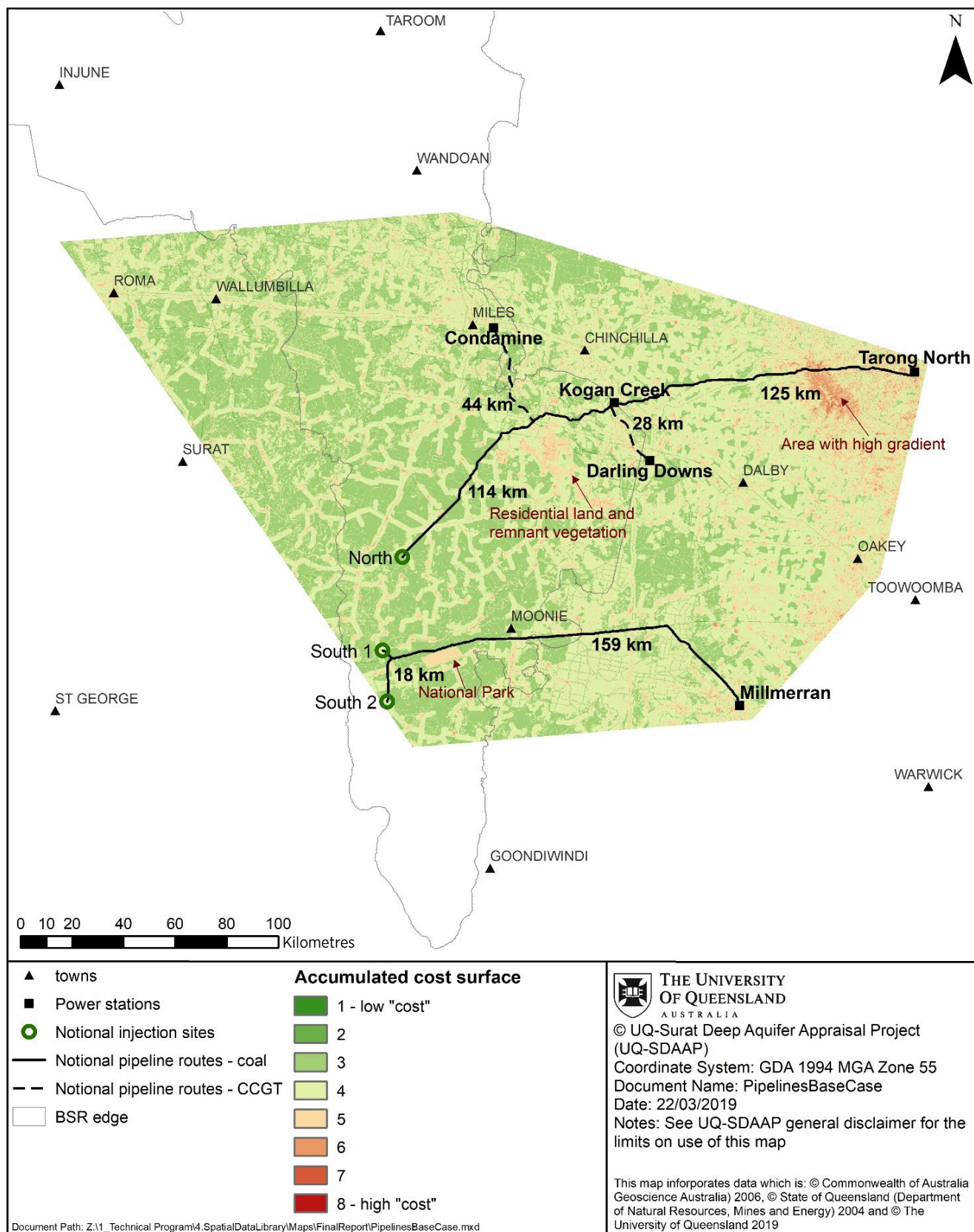


Figure 144 Pipeline routes; example from environment analysis.

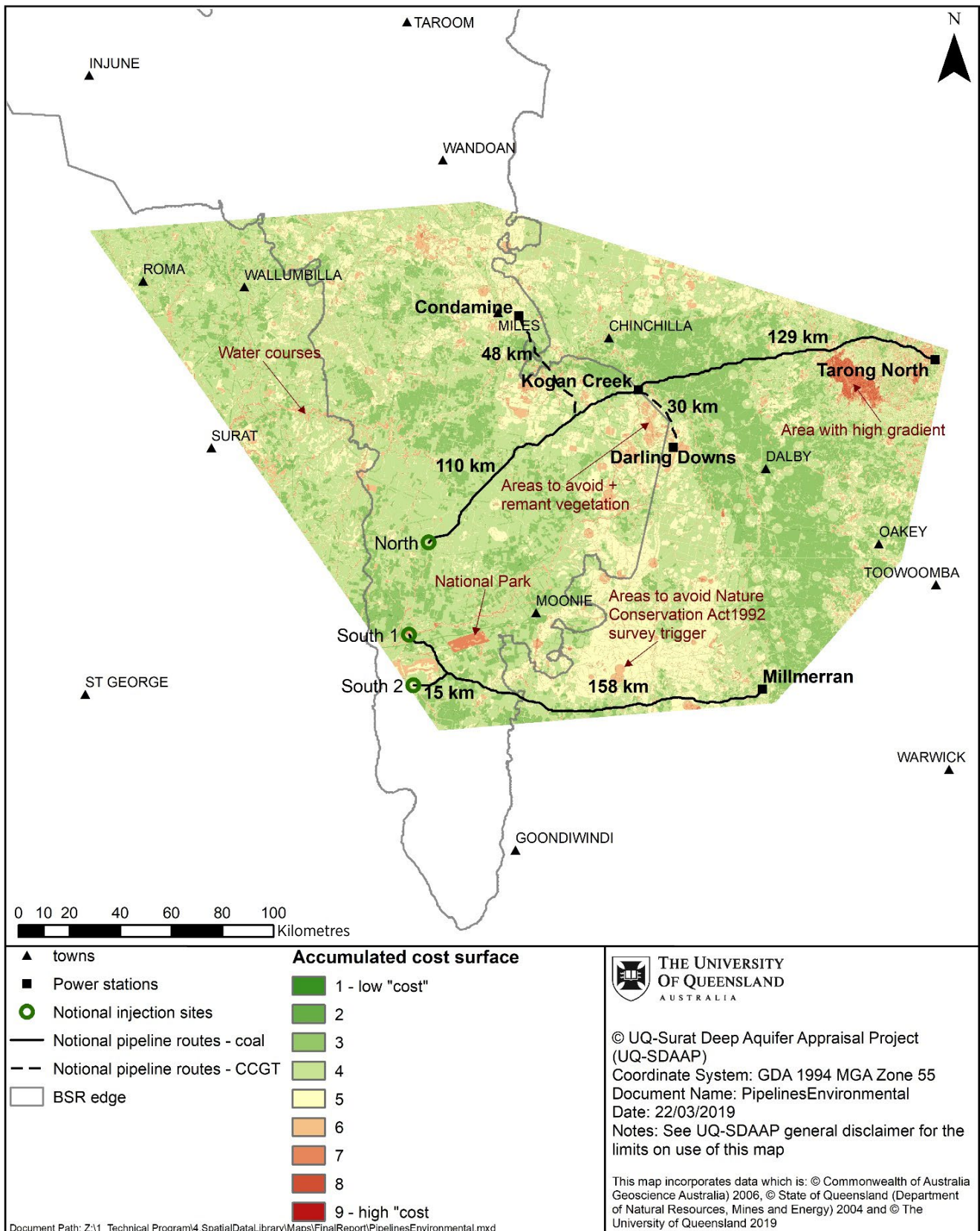


Figure 145 Pipeline routes from social analysis.

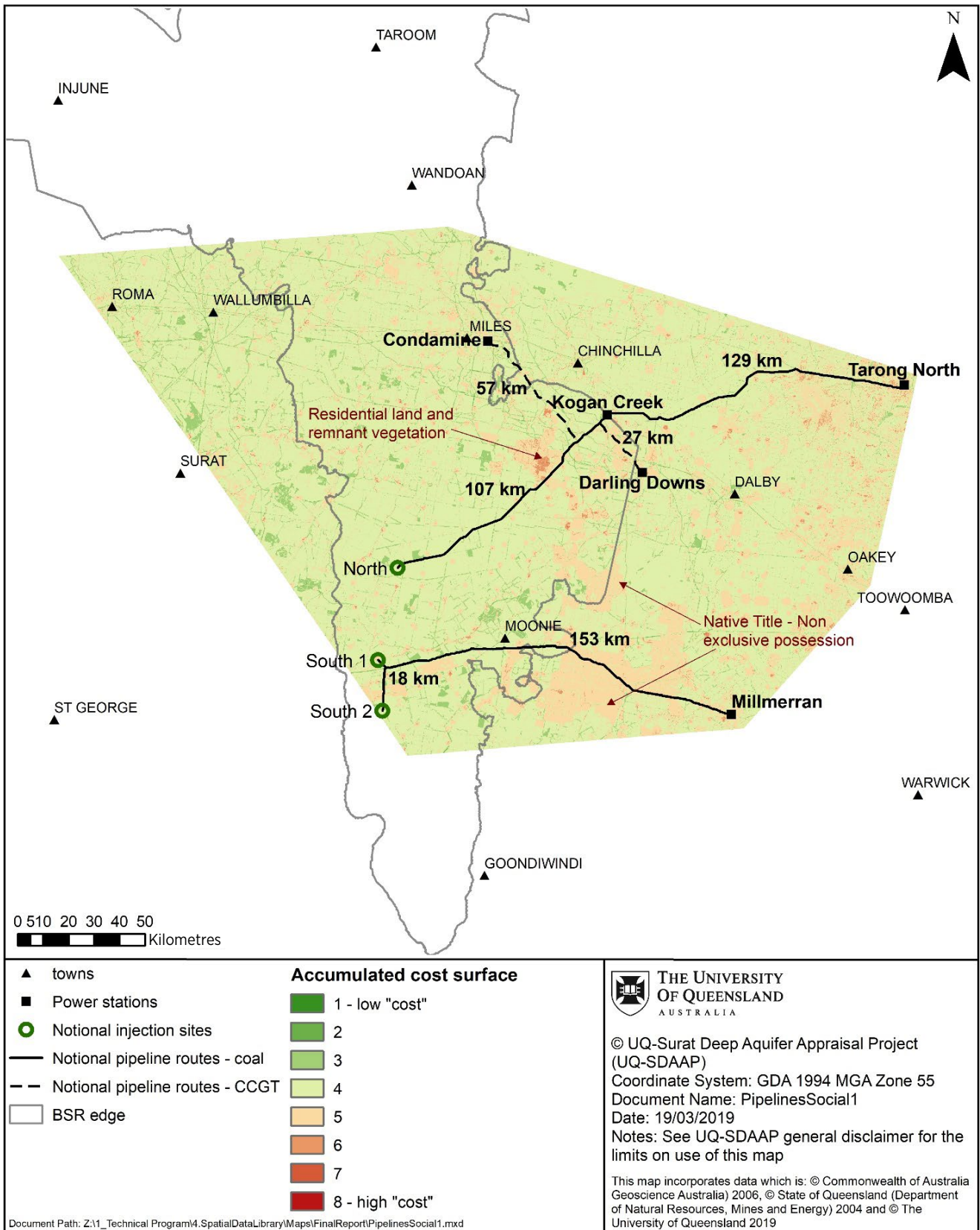
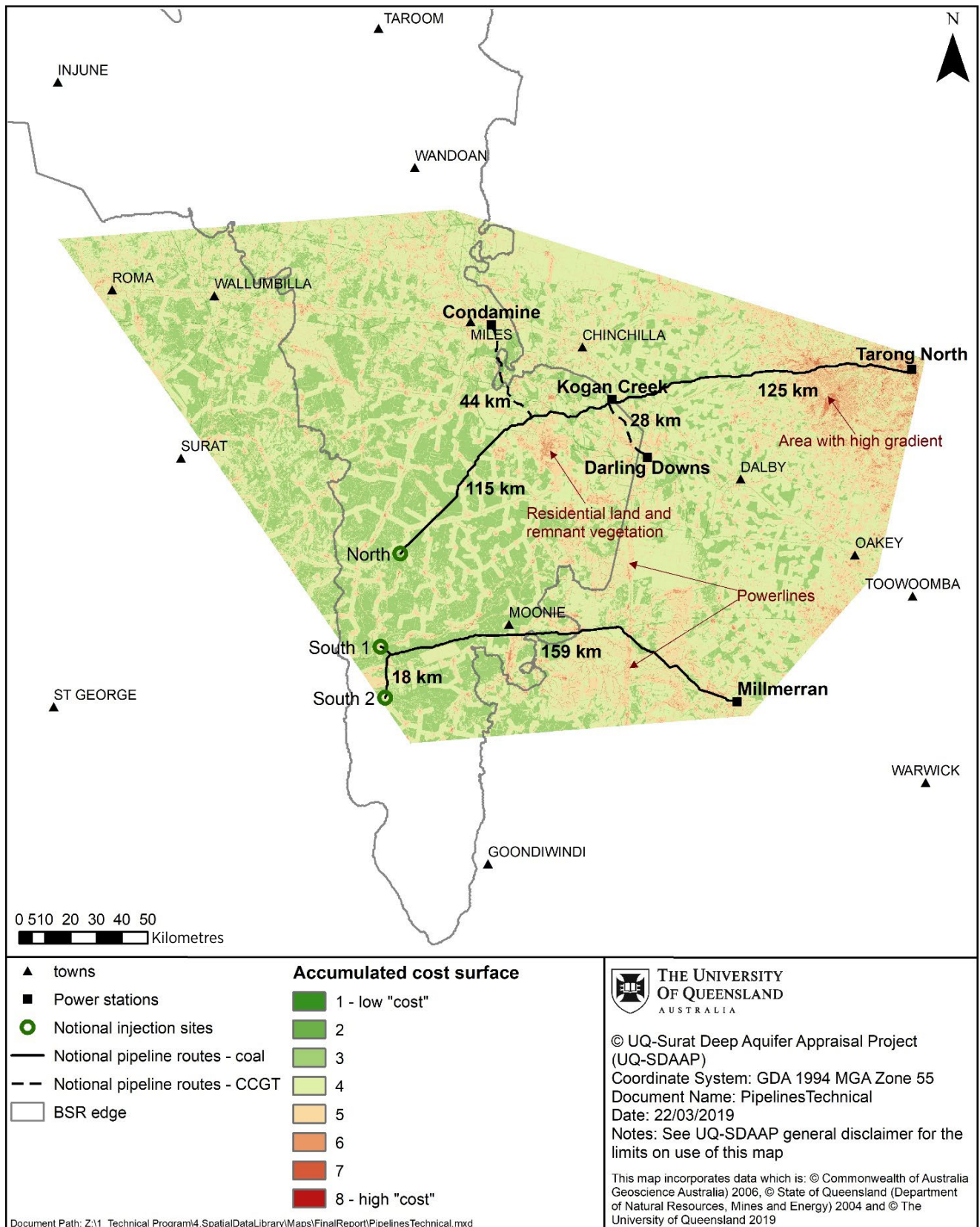


Figure 146 Pipeline routes from 'environmental' analysis.





**Table 50** Pipeline route length (km).

Pipeline route	Base Case	Environment	People-centred	Technical
Kogan Creek to notional northern injection location	114.4	110.4	107.5	114.5
Condamine to Kogan Creek pipeline	44.2	48.4	56.7	43.8
Darling Downs to Kogan Creek pipeline	27.8	29.8	27.2	28.3
Tarong North to Kogan Creek	124.8	128.5	128.6	125.2
Millmerran to notional southern injection site 1	159.1	158.4	152.5	158.8
Connection between southern injection sites	17.7	15.3	17.5	18.0
<b>Total length</b>	<b>488</b>	<b>490.8</b>	<b>490</b>	<b>488.6</b>

**Table 51** Pipeline route stream crossings.

Pipeline route	Base Case	Environment	People-centred	Technical
Kogan Creek to notional northern injection location	19	21	27	18
Condamine to Kogan Creek pipeline	17	19	23	17
Darling Downs to Kogan Creek pipeline	17	8	14	17
Tarong North to Kogan Creek	93	66	111	79
Millmerran to notional southern injection site 1	40	54	46	42
Connection between southern injection sites	3	0	3	3
<b>Total crossings</b>	<b>189</b>	<b>151</b>	<b>224</b>	<b>176</b>

**Table 52** Pipeline route road, pipeline and rail crossings.

Pipeline route	Base Case	Environment	People-centred	Technical
Kogan Creek to notional northern injection location	24	31	29	23
Condamine to Kogan Creek pipeline	10	11	11	7
Darling Downs to Kogan Creek pipeline	7	13	7	6
Tarong North to Kogan Creek	34	43	29	34
Millmerran to notional southern injection site 1	32	47	42	32
Connection between southern injection sites	5	1	5	4
<b>Total crossings</b>	<b>112</b>	<b>146</b>	<b>123</b>	<b>106</b>

**Table 53** Pipeline route powerline crossings.

Pipeline route	Base Case	Environment	People-centred	Technical
Kogan Creek to notional northern injection location	6	6	6	6
Condamine to Kogan Creek pipeline	2	4	6	2
Darling Downs to Kogan Creek pipeline	4	4	4	4
Tarong North to Kogan Creek	13	16	17	13
Millmerran to notional southern injection site 1	4	9	4	3
Connection between southern injection sites	2	1	2	2
<b>Total crossings</b>	<b>31</b>	<b>40</b>	<b>39</b>	<b>30</b>

Underlying data used in the criteria also change and change at different time scales. While drastic changes in the data used for the surface suitability analysis are unlikely to occur in the short term, the project recommends ground-truthing of the underlying data and analysis results if a similar pipeline route selection procedure is used for a CCS project in future.

**Following site-specific appraisal, real, in-field investigations would be required as well as community and regulator engagement.**

## 4.10 Surface facilities concepts

UQ-SDAAP worked with Advisian (a Worley Parsons Group company) on a preliminary engineering concepts study for wellhead and well pad facilities. The intent was to investigate whether there were any potential show-stoppers for maintaining very high rate injection at a few remote sites. More detail can be found in Advisian 2019.

The overall project evaluation and development philosophy adopted by UQ-SDAAP has been to demonstrably identify and assess the lowest risk configurations (rather than lowest cost for example), in recognition of what would be a first of a kind deployment.

In line with this overall ethos, the operating philosophy for this study considered several key factors. First and foremost is safety, particularly given that CO<sub>2</sub> can be hazardous. This issue helped to inform the project's approach to venting and well sparing, for example. Another key factor is that the notional well pad's siting would be in a relatively remote location and as such, operation would be expected to be not normally attended and might not be connected to the national power grid. This means that supervisory oversight would be provided from a remote location with local control and shutdown capability. A concept design and costing of surface facilities is based upon Class 1500 equipment and piping to manage the pressures required for the project and at this early stage of design eliminate pressure protection issues at the well pads.

### 4.10.1 General configuration

The overall notional development considered includes two pipelines, three well pads and a total of 8 to 12 wells configured as described below:

- A northern pipeline from Kogan Creek and Tarong North power stations would feed a single well pad with 4 to 6 wells
- A southern pipeline from Millmerran power station would feed initially one, and in future, two well pads each with up to 4 wells

Power supply is not available reliably and is expected to be locally generated to support the facilities at each well pad.

The facilities shall be designed at a concept level only with recognition that future work would look at the assessment of optimal approaches to the design. Cost estimate is to be prepared to AACE Class 5 level (i.e. +50% / -40%).

The carbon dioxide is extracted from combustion exhaust. For the purposes of this study the gas is assumed to be liquid free and dehydrated with a composition of 95% CO<sub>2</sub> and 5% nitrogen. Overall fluid properties are not sensitive to minor variations in composition although actual design would need to take these into account. Nominal process conditions for the CO<sub>2</sub> exiting the pipeline are as shown in Table 54.

**Table 54** Basis of design (BoD) process conditions for pipeline CO<sub>2</sub> fluid.

Property	Min.	Max.
Temperature	10°C	30°C
Pressure	10 MPag	20 MPag
Pipeline Flow	2000 tpd	17,800 tpd
Injection Well Flow	2000 tpd	9000 tpd

If the fluid is maintained between these maximum and minimum conditions of pressure and temperature the CO<sub>2</sub> stream exiting the pipeline would be in the liquid phase. If temperatures are higher than the nominated range the fluid would change from liquid phase to supercritical.

Dehydration at the source of carbon dioxide capture is critical. At the wellhead pressure range, if water is present hydrates would form in the liquid phase once the temperature reduces below 10°C to 13°C depending on pressure. Formation of hydrates would cause severe blocking of equipment, piping and valves.

## 4.10.2 Well pad facilities basis of design – working assumptions

The relatively remote location of the notional sites indicates that they would require their own utilities and power supply. Options considered included solar with batteries and diesel generation. Given the average demand of the facility and the key consideration that the facility must have reliable power supply to safely inject CO<sub>2</sub>, diesel generation was selected as the preferred option at this early stage. Advisian 2019 engaged with equipment vendors to ascertain the availability of the equipment required for the project and its cost. No “showstoppers” were identified for the majority of equipment required for the project. Some bespoke design work would be required for the filters, but this would not pose a significant risk.

A Class 5 capital cost estimate summary was prepared for this component of the project based on January 2019 Australian dollars. Given this, the estimated total installed cost (excluding wells) is \$24.2 million for a standard four well pad set (-\$31.6 million for six wells). Reservoir modelling discussed in section 4.8, indicates that between three and six wells are needed per well pad. This includes at least one redundant well which avoids the need for on-site venting in the case that a work-over is required. The capital costs and this design scale mainly with by aggregate rate received and number of wells. The aggregate rate assumptions for the facilities costs and for the reservoir injection modelling is essentially the same (within the accuracy possible in this stage of the project).

The largest component of this includes piping, pipe fittings, spooling and valves (14%). Indirect costs were also estimated and the highest component of this were contingency (25%) and engineering, procurement, construction and management (EPCM) costs (18%). Some additional studies will be required in future should the notional injection proceed to an actual project, including dispersion analysis, a hazard identification study and alternative power supply options. For full details of the wellhead design see Advisian 2019.

## 4.10.3 Well pad facilities high level operating philosophy

The design principle and operating philosophy incorporated in this study is first and foremost predicated on safety. A well pad operation would be expected to be not normally attended, with supervisory oversight from a remote location with local control and shutdown capability.

The operational approach to the well pad considered in this study is to manage the conditions in the delivery pipeline while also managing the conditions in the injection wells. At this stage the understood parameters are as follows:

- Pipeline pressure to be maintained within a preferred envelope and ensure that pressure does not drop below critical pressure
- Control the flow rate to each well where practical, in line with expected allocations
- Control of the pressure into the well to prevent exceedance of fracturing pressure inferred from flowline pressure
- Control of the pressure into the well to prevent exceedance of fracturing pressure as measured downhole

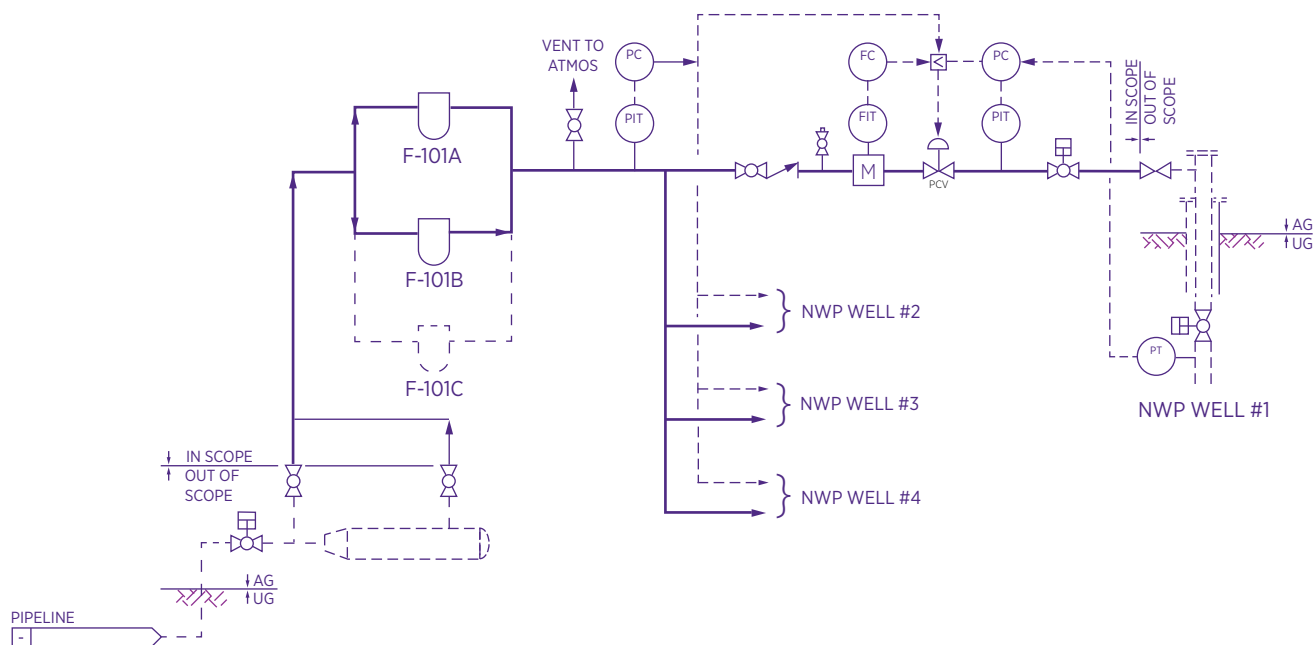
Normal operational control and shutdown/start-up situations would need to be managed to ensure that the rate of closure/opening of valves do not cause over or under pressure issues in the pipeline or well pad piping.

## 4.10.4 Description of surface and well site process facilities

The description of facilities is for a single well pad and this is expected to be replicated for each well pad – a four well concept is shown in Figure 147, below.

The scope of facilities described in this study is defined in the sketch below and includes those facilities from the end of the pipeline through to the wing valve on the injection wellheads. A more comprehensive schematic is provided in Advisian 2019: Appendix B & C.

**Figure 147** Surface facilities schematic.



The pressure range for operation requires the use of Class 1500 piping, resulting in heavy wall pipe and vessels and significant valve actuator sizing.

Pipeline pressure is generated by compression at the extraction/treatment site while the backpressure in the pipeline would be controlled at the well site.

**Well site process facilities.** The main header from the pipeline to the process facilities would be 400 NB (the same diameter as the pipeline). The well site facilities would include 2 X 50% filters (5 micron particle removal) with space allowance made for a third filter if required when the overall pipeline and injection system is at full capacity. The filter units would be skid mounted. Downstream of the filters the piping would divide from the main header into four separate wellhead lines each of DN 250 in diameter. The wellhead lines would have a check valve, measurement, control systems on each wellhead flow stream. Each well is expected to have surface safety valve and subsurface safety valve installed.

The liquid CO<sub>2</sub> stream would transition to dense phase above approximately 30°C. At a pressure of 20 MPag and 10°C, the density of the liquid phase is 949 kg/m<sup>3</sup>. At a pressure of 10 MPag and 30°C the density of the supercritical dense phase CO<sub>2</sub> reduces to 601 kg/m<sup>3</sup> with a consequent increase in piping velocities. Pressures need to be maintained in piping above the critical pressure to prevent two phase or potential solid formation.

**Utilities.** As the well sites are expected to be remote and also need to be highly reliable, it is expected that they would have their own utilities and power supply. These are currently modelled to consist of the following:

- Power supply consisting of diesel generator (two off) for local power generation. In addition to lighting and electrical cabinet cooling, this would also drive the hydraulic power pack for the subsurface safety valves (SSSV). See Section 8 “Electrical Power Generation” below for further details
- Diesel fuel storage tank
- UPS for critical functions and control system to provide for suitable control duration in case of power interruption
- Instrument air package with 2 x 100% compressors with integrated dryer packages for control systems
- Interception and separation of oily water for offsite disposal
- CO<sub>2</sub> vent secured by a derrick structure. A vent stack has been included given a preliminary elevation of 50 m for the purposes of this cost estimate. This is not intended as a suggestion or ideal design, rather it has been included to focus efforts at subsequent design stages on operational and emergency control of venting. (the primary risk-management of interruptions to flow at the well-pad has been to include redundant wells, such that failure in one could still be safely handled by others)

## 4.10.5 Venting

The overall concept assumes **no routine or 'operational' venting**. Redundant wells and injection capacity would be installed in order to manage flow interruptions in injection wells. Venting is only considered as non-routine or emergency occurrence.

There may however be occasions when the blowdown of the pipeline as well as filters and associated piping for change-out of filter elements is required. In these instances, for safety reasons, a vent stack would be necessary. The vent would have to be of sufficient height to mitigate the possibility of a CO<sub>2</sub> cloud descending to ground level.

Further detailed design may result in the conclusion that no pipeline blowdown capability through the vent is required. In this case, the vent stack size and height should be able to be reduced and have minimal visual impact. The venting configuration should be further reviewed and optimised, taking into account: process, safety, operational, environmental and social considerations.

The potential safety zone around the pipeline facilities, well pad and vent is site specific (at present there are only 'notional' sites). It is recognised that offsets would need to be carefully controlled and managed. This also has implications for land access and ownership and would need to be resolved early in any project.

## 4.10.6 Communications and control

Each well pad would be able to act independently but with setpoint and supervisory oversight from the remote operating centre. A separate safety system would be used to monitor key parameters and implement shutdowns. The well pad control systems provide three key functions, namely:

1. Control backpressure in the pipeline to maintain CO<sub>2</sub> in the correct phase for transport
2. To limit the maximum pressure per well to prevent formation damage
3. To split flow of carbon dioxide across wells according to predetermined philosophy and record the flow to each well for reservoir management purposes

To achieve this each wellhead injection line requires flow measurement, a control valve and shutdown valve in addition to the manual and check valves and surface safety valve.

Pneumatic actuation has been suggested at this stage of assessment because of ease of maintenance and lower incremental costs if additional actuated valves are included in the design during project development. As a result, an instrument air package has been incorporated to drive the control and shutdown valves.

The control and communication systems required consist of the following all housed in a suitably cooled building:

- Main switchboard
- Control and safety shutdown system
- Communication panel, including CCTV converters
- Uninterruptible power supply/ battery charger

A SCADA system would communicate all information back to the main control centre at the capture facilities and this is expected to be via an armoured fibre optic cable. This cable could be laid with the pipeline which connects the CO<sub>2</sub> capture facilities to the wellhead facilities to save construction costs and would be more reliable than microwave communication.

Advisian 2019 describes, in more detail, options for redundant systems and emergency back-up in a number of control functions. No showstoppers have been found.

For example; an allowance of 3 x line-of-sight CO<sub>2</sub> detectors has been allowed for each well pad and this would require further assessment in future phases of the project. In addition, an allowance of 3 x infrared CCTVs with zoom, pan and tilt functions has been allowed for in the estimate. The number required would be determined in future phases of the project.

### 4.10.7 Electrical power generation

At the notional well sites considered in this study, grid supply (distribution network service provider) for electrical power is not available and there are no nearby permanent fuel facilities such as gas distribution.

Given the site is expected to be not normally manned (NNM), the power generation system requires a high degree of reliability/availability with redundant generation.

Power generation options considered include:

- Solar and batteries
- Diesel generation

Expected average demand is approximately 5 to 7 kVA. Solar power for stand-alone power systems is typically limited to loads less than 1 kW due to the high CAPEX incurred and large area needed for the panels. Preliminary sizing indicates that 2 x 9 kVA diesel powered generation units would be suitable (1 x duty; 1 x standby). An uninterruptible power supply or battery charger would be provided for critical loads.

Clearly the selection of diesel fuelled generation would need to be revisited after site selection is finalised, but the **simple solution here again indicates no “show stoppers”**.

### 4.10.8 Cost estimate summary

A Class 5 capital cost estimate has been prepared for surface facilities scope for each four well pads. The scope of estimate is within the defined battery limits which are downstream of the valves on the pig traps to the upstream face of the wing valves on the wellheads. Estimate accuracy is +50%/-40%.

The summarised P50 CAPEX is presented in Table 55 and the detail of the estimate is provided in Advisian 2019.

**Table 55** Summary P50 CAPEX estimate – 4 well configuration (\$2019, excludes owners' costs and escalation).

Description	Total Cost (\$)	% of TIC
A. SITE DEVELOPMENT	454,191	2%
B. EARTHWORKS	207,651	1%
C. CONCRETE	659,011	3%
D. STRUCTURAL STEEL	1,065,615	4%
F. BUILDINGS	79,400	0%
M. MECHANICAL EQUIPMENT	1,370,911	6%
P. PIPING, PIPE FITTINGS, SPOOLING & VALVES	3,350,943	14%
U. ELECTRICAL EQUIPMENT	1,589,815	7%
V. INSTRUMENTATION EQUIPMENT	3,139,941	13%
W. ELECTRICAL BULKS	497,000	2%
X. INSTRUMENTATION BULKS	205,637	1%
<b>TOTAL DIRECT COSTS</b>	<b>12,620,116</b>	<b>52%</b>
COMMON DISTRIBUTABLES	1,213,473	5%
EPCM COSTS	4,368,502	18%
OWNERS COSTS	-	-
CONTINGENCY	6,067,363	25%
ESCALATION	-	-
<b>TOTAL INDIRECT COSTS</b>	<b>11,649,337</b>	<b>48%</b>
<b>TOTAL INSTALLED COSTS</b>	<b>24,269,453</b>	<b>100%</b>

## 4.10.9 Summary of surface facilities

The high-level study of the surface facilities did not identify any technical showstoppers.

The functionality required to move 5-13 million tonnes pa of CO<sub>2</sub> is well within existing proven technology and risks can be well understood and managed. Developments are modular and could be expanded by extending plant lives or building additional boilers.

Some additional studies are recommended should the project proceed beyond further subsurface appraisal and onto the next engineering stage. These include further definition of the project's business case, dispersion analysis, a hazard identification study and alternative power supply options, for example.

## 4.10.10 FDP Concept M&V for long term operations

The notional storage sites have been screened on the basis of minimising containment risk. They are selected so as to be inherently safe. However, monitoring and verification will be prerequisite requirements of a project receiving an injection permit. Unterschultz et al. 2017, Stalker et al. 2015, Boreham et al. 2011, Jenkins et al. 2011, Michael et al. 2010, Freifeld et al. 2009, Stalker et al. 2009, White 2009, Benson 2006 and Oldenburg et al. 2003 represent a few examples of a vast literature on the topic of various M&V for various carbon storage applications.

Injection modelling to date shows minimal plume movement (Rodger 2019d) though a wide-spread pressure inflation in the Blocky Sandstone Reservoir (Ribeiro 2019b; Rodger 2019d) is anticipated. Modelling also shows little chance for material flow of CO<sub>2</sub> from the Blocky Sandstone Reservoir into the Transition Zone and, to date, no scenarios show flow of CO<sub>2</sub> reaching the base of the Ultimate Seal.

More site-specific data is required, particularly data which informs the large-scale, lateral flow structure of the Blocky Sandstone Reservoir and the ability of the Transition Zone to transmit pressure and fluids. A detailed appraisal program is described in section 4.15 and in (Honari et al. 2019c). Importantly, this will include both long-term well tests (flow structure) and vertical inference tests across the Transition Zone and Ultimate Seal. After these data are gathered, along with the suggested seismic data, a detailed M&V program can be more thoroughly designed.

Monitoring for operating leakage and venting will form a standard part of later engineering studies and is likely to include accurate fiscal (flow) metering from capture, through pipeline, boosters and well-pad facilities as well as leak detection in these sites (e.g. Advisian 2019 and Shell 2017). Similarly, period mechanical well integrity testing, corrosion logs and casing/cement sonic surveys will likely form part of standard operating procedures along with other standard well measurements such as casing pressure, WHT, WHP and injection rates. There are also options for distributed sensors along the well bore such as temperature sensing – though serious consideration needs to be given to the impact of such sensors on cement bond integrity.

Baseline measurements will also be required which evaluate the natural levels and variation of CO<sub>2</sub> flux in the atmosphere, biosphere and geosphere. Other than the proposed appraisal program itself (section 4.15), baseline studies are not suggested until after further storage confidence is achieved.

Nevertheless, some basic principles and components can be suggested which would form part of “*A site-specific, risk-based and adaptive measurement, monitoring and verification (MMV) plan*” (Shell 2017). Building on the cited work, a monitoring and verification (M&V) concept is required which manages two main risks (i) loss of containment i.e. ensuring that CO<sub>2</sub> is not moving outside the defined container (section 4.4); and, (ii) loss of conformance – showing that the development of pressure inside the container is within modelled, predicted bounds; and, using these data to update and improve predictive models (*ibid*).



## 4.10.11 Subsurface M&V for loss of containment

Analysis of seismic response to increasing CO<sub>2</sub> saturations indicates that seismic techniques are unlikely to detect or resolve movements of CO<sub>2</sub> within the container or through the Ultimate Seal (Harfoush et al. 2019d). This is because of relatively low porosities (~13%) in the Blocky Sandstone Reservoir and relatively high density of CO<sub>2</sub> at depth (~0.95 kg/m<sup>3</sup>). Seismic techniques may be revisited when new data is acquired for the sites. It may be that vertical seismic profile technology can be used for plume monitoring in the near well bore but this can only be ascertained after new data are analysed.

The primary subsurface monitoring technology for M&V would therefore be pressure monitoring. Techniques relying on pressure are the mainstay of underground natural gas storage sites and are mature and can provide very accurate resolution of small pressure changes within and outside the container.

An M&V scheme would focus on the higher risk locations (close to injection well pads) and also focus on higher risk features (legacy wells and faults).

The well site, where pressures are highest, would likely include the following:

- The horizontal injection wells (lateral offset 3-4 km) will monitor flowing bottomhole and wellhead pressures and temperature
- A “Hutton Sandstone” monitoring well will be situated on the well pad. This well will be completed above the Ultimate Seal and will monitor pressure in the lowermost sands of the Hutton Sandstone aquifer. This, together with data acquired in the appraisal phase, will enable reliable monitoring of pressure transition
- A Blocky Sandstone Reservoir monitoring well. The current intent would be to convert the proposed vertical appraisal well into a Blocky Sandstone Reservoir pressure and temperature monitoring well. This would be in the centre of the injection pattern

After more seismic data is acquired, any major faults that are close to the prognosed plume area may also be monitored by a pressure monitoring well above the Ultimate Seal. Such a well might also sample water quality periodically to investigate whether there is evidence for water mixing. Surface sampling (soil, atmosphere water) for CO<sub>2</sub> or other changes in gases might also inform predictive models.

Legacy, abandoned wells, depending on their completion status and proximity to the operation, surface sampling might be required at these locations to monitor potential changes.

Additionally, remote, far-field pressure monitoring bores (say 8-10) could be drilled into the Blocky Sandstone Reservoir 15-20 km to the north, east and west of the injection sites. Pressure from these wells, along with the wells above, would allow for reliable history matched models of plume and pressure evolution and for greater confidence in “conformance” and within a reasonable period of time.

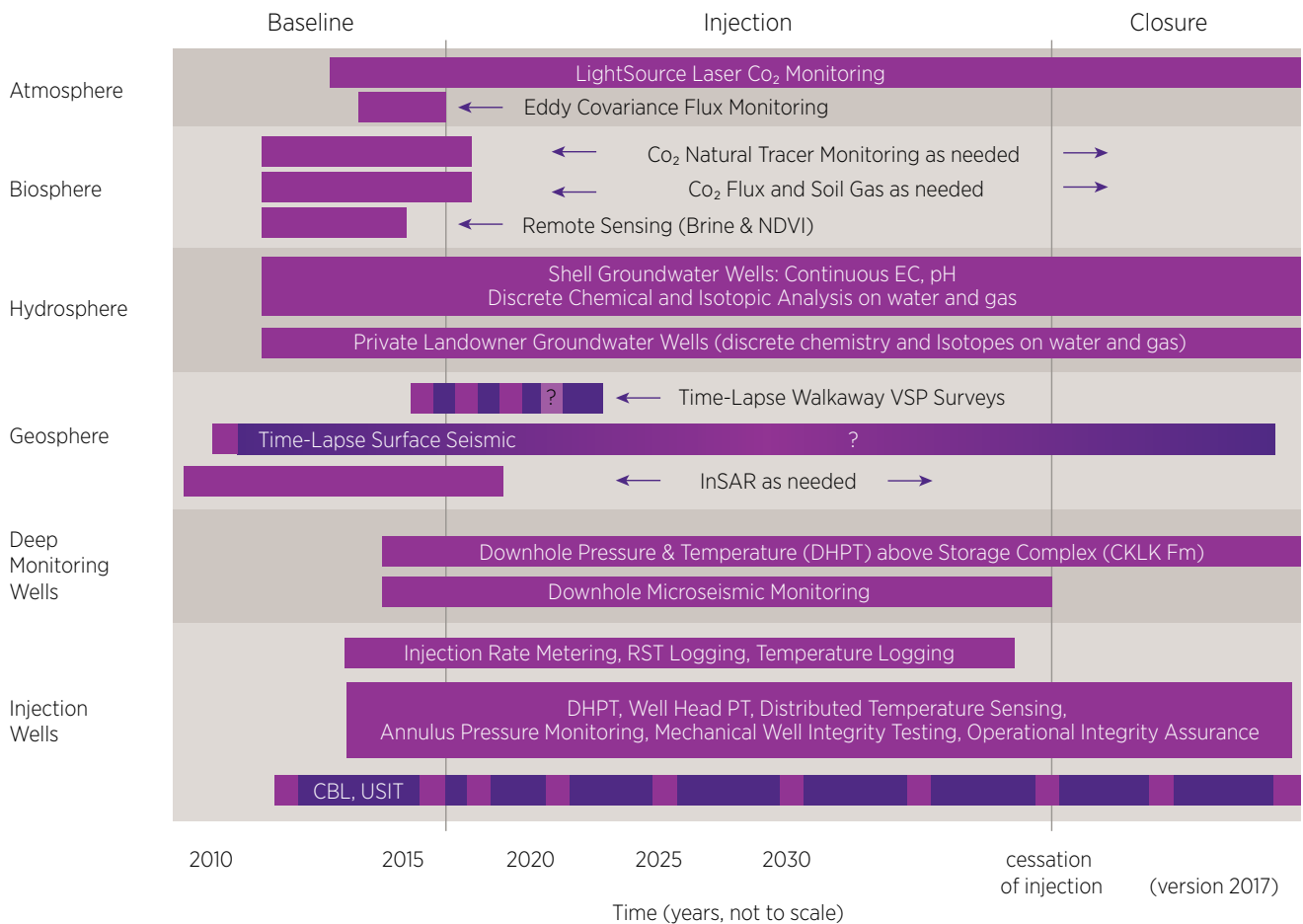
To the west of the injection well pads, additional monitoring wells could be drilled beyond the prognosed Blocky Sandstone Reservoir “pinch-out” edge (Gonzalez 2019b). These would confirm the sealing concept of the pinch-out, as well as provide a direct measurement of lateral transmission of pressure through the Transition Zone or along the sub-Surat Unconformity surface.

Dedicated monitoring wells allow not only for continuous pressure monitoring but also for periodic groundwater sampling and lab analysis.

While aquifer pressure monitoring through *dedicated* wells would likely form the backbone of any monitoring scheme, additional data sources can also be accessed e.g. via a campaign of monitoring land-holder bores or through ground movement monitoring with InSAR technology etc. An illustration of options is shown in Figure 148 below.

The primary subsurface monitoring technology for M&V would therefore be pressure monitoring.

**Figure 148** Illustration of M&V options and concepts (Shell 2017).



For the most part, the formation pressure, groundwater chemistry and other monitoring and sampling systems will have to be put in place well before the start of injection and form part of the pre-FID investment for baseline conditions. Ten M&V wells have been included in section 4.14 and section 5.6. In most scenarios they would be installed 6-7 years before start of injection.

In addition to more conventional Environmental Impact Statement (EIS) processes, this period or baseline monitoring would be essential to understand natural background variability and to inform trigger events and detection thresholds for reporting and for intervention (response planning).

#### 4.10.12 Summary of M&V

**Progressing M&V for this abatement option in more depth still requires considerable site-specific data (ref. Section 5.3). Following this detailed baseline and M&V programs can be designed. Subsurface pressure monitoring will most likely be the dominant M&V technique. Its use is well established in oil and gas field developments as well as in underground gas storage operations.**

UQ-SDAAP modelling and analysis are consistent with a view that a low risk site can be selected, monitoring technologies exist which can detect material loss of containment and well-established techniques exist which, along with appraisal, operation and M&V data, can be used to verify conformance of CO<sub>2</sub> movements within a specified container.

## 4.11 Notional injection modelling and FDP reference cases – groundwater impact

Groundwater modelling of the notional field development plan (FDP) reference case predicts that significant groundwater pressure increases due to CO<sub>2</sub> injection, in excess 100 m of groundwater head, will occur in the Blocky Sandstone Reservoir (Precipice Sandstone aquifer equivalent) in the deep southern depositional centre of the Surat Basin.

CO<sub>2</sub> injection will cause groundwater pressure increases in the Precipice Sandstone and Hutton Sandstone aquifers, and this will extend to existing water bores. At some locations, remedial wellhead or downhole works may be required to ensure old bores can control induced artesian conditions. Due to the depth and relative isolation of the Blocky Sandstone Reservoir in the deepest part of the Surat Basin, the number of significantly, potentially impacted wells (> 100 m of groundwater head) is very small. A larger number of wells, including wells drilled as water bores, in the Precipice Sandstone and Hutton Sandstone aquifers are predicted to experience smaller pressure increases of 10 to 30 m of groundwater head. The smaller pressure increases predicted over a large portion of the Surat Basin will provide a beneficial use by helping re-pressurise otherwise declining Great Artesian Basin aquifers and lowering (or even eliminating) pumping costs.

The transmission of pressure increases occurs over a much larger area than the footprint occupied by injected supercritical CO<sub>2</sub>. The footprint of CO<sub>2</sub> extends less than 10 km from the injection sites after 100 years, whereas the 10 m groundwater head increase extends some 90 km from the injection sites after 100 years. Pressure increases vertically within and through the Transition Zone, Ultimate Seal and potentially the Hutton Sandstone. This does not imply any loss of CO<sub>2</sub> containment.

### 4.11.1 UQ-SDAAP groundwater modelling philosophy

The objective of groundwater modelling is to characterise the range of *possible* impacts on groundwater pressures (or equivalent in metres of groundwater head) in the Precipice Sandstone aquifer, the Transition Zone and Ultimate Seal as well as the overlying Hutton Sandstone aquifer across the Surat Basin from CO<sub>2</sub> injection. The groundwater modelling focuses on pressure propagation, with full fluid physics of CO<sub>2</sub> injection and FDP development addressed by the multiphase notional injection site model, detailed in 4.8. With this characterisation, we can also then consider and assess impacts of fault stability, groundwater dependant ecosystems, discharge, water quality variation geographically and interaction with other major groundwater sources and sinks such as managed aquifer recharge.

The philosophy adopted for the groundwater modelling is to closely follow the geometry and layering of the notional injection site reservoir model (section 4.8), so that appropriate comparisons can be made, whilst extending the domain to the spatial extent of the Surat Basin regional geological static model (section 4.3.11). The predictive modelling is also kept relatively simple and conservative, including the sensitivity analysis. This befits the current level of knowledge of reservoir and seal parameters at the notional injection sites, and a conservative approach helps to clearly identify risks from groundwater pressure increases. In terms of the Australian Groundwater Modelling Guidelines (Barnett et al. 2012), the groundwater model is a Class 1 model, meaning that in the area high-graded for deep injection studies, it is uncalibrated against historical injection data, but is a starting point capable of providing initial impact estimates.

Groundwater models solve equations of flow based on the same principals as multi-phase reservoir models but make many simplifying assumptions about fluid and reservoir properties that include a single iso-density fluid and constant temperature. A groundwater model cannot, therefore, represent the physics of compressible liquid CO<sub>2</sub> in its supercritical state, and CO<sub>2</sub> injection is approximated by an equivalent volume of water injection. The approximation of CO<sub>2</sub> injection with an equivalent water volume at reservoir temperature and pressure has been demonstrated by Nicot et al. 2011. These three regions develop: a “drying” region next to the well in which CO<sub>2</sub> injectate occupies 100% of the pore space; a brine region away from the injection well in which 100% of the pores are saturated with brine; and a two-phase region in which water and CO<sub>2</sub> coexist. Several papers describe the speeds at which those two fronts progress outward using the Buckley-Leverett fractional flow (BLFF) to provide reasonable and slightly conservative responses at distance from the injection site, both during and after injection.

## 4.11.2 Translating static and GEM model into a groundwater model

The groundwater model is developed using the Modflow-6 code (Langevin et al. 2017). Modflow-6 is the most recent version of Modflow, one of the groundwater industry's standard codes that has been continually developed by the US Geological Survey since the late 1970s. It represents 3D fluid flow of a single water phase, with a wide variety of boundary condition options available. Modflow-6 is from the same family of codes as Modflow-USG, the code adopted by the Office of Groundwater Impact Assessment for modelling the Surat Cumulative Management Area.

Groundwater model construction uses a coarser grid than the multi-phase notional injection site model (section 4.8) due to the scale of the Surat Basin, and its objective of predicting pressure changes away from injection. This means that *accurate* predictions of pressures at injection wells is not the focus (this information is provided by the, two phase, notional injection site model). Mesh refinement at injection sites is not necessary. The grid adopted has 1.5 x 1.5 km cells in plan view, with a uniform orthogonal mesh. The model domain extends 480 km north-south and 280 km east-west from the outcrop of the Precipice Sandstone in the north to the limit of the Surat Basin in the south. The domain of the groundwater model compared to the notional injection site model is show in Figure 149.

The 47-layer regional static geology model (Gonzalez et al. 2019b) is reduced to a 16-layer representation for the groundwater model by “upgridding”. The reduction in the number of layers was based on modelling of the smaller 10 x 10 km notional injection sector models which tested the behaviour of fluids in the Transition Zone (Rodger et al. 2019c). This showed that it was unlikely that any liquid CO<sub>2</sub> would migrate further vertically than the lowest -10 m of the Transition Zone (even in the worst-case scenario of the sensitivity analysis), and that layering could be simplified to represent single phase flow. The “upgridding” therefore reduces the number of layers representing the Transition Zone and Ultimate Seal whilst maintaining detail in the Blocky Sandstone Reservoir. For the groundwater model, the upgridding process provided outputs on an approximately 1.5 x 1.5 km grid as described by Rodger et al. 2019e. Minor deviations from a square mesh occurred around faults, including the Moonie fault on the eastern side of the southern Surat Basin. These deviations were smoothed to a uniform regular grid in the translation from Petrel to Modflow-6 (Hayes et al. 2019b).

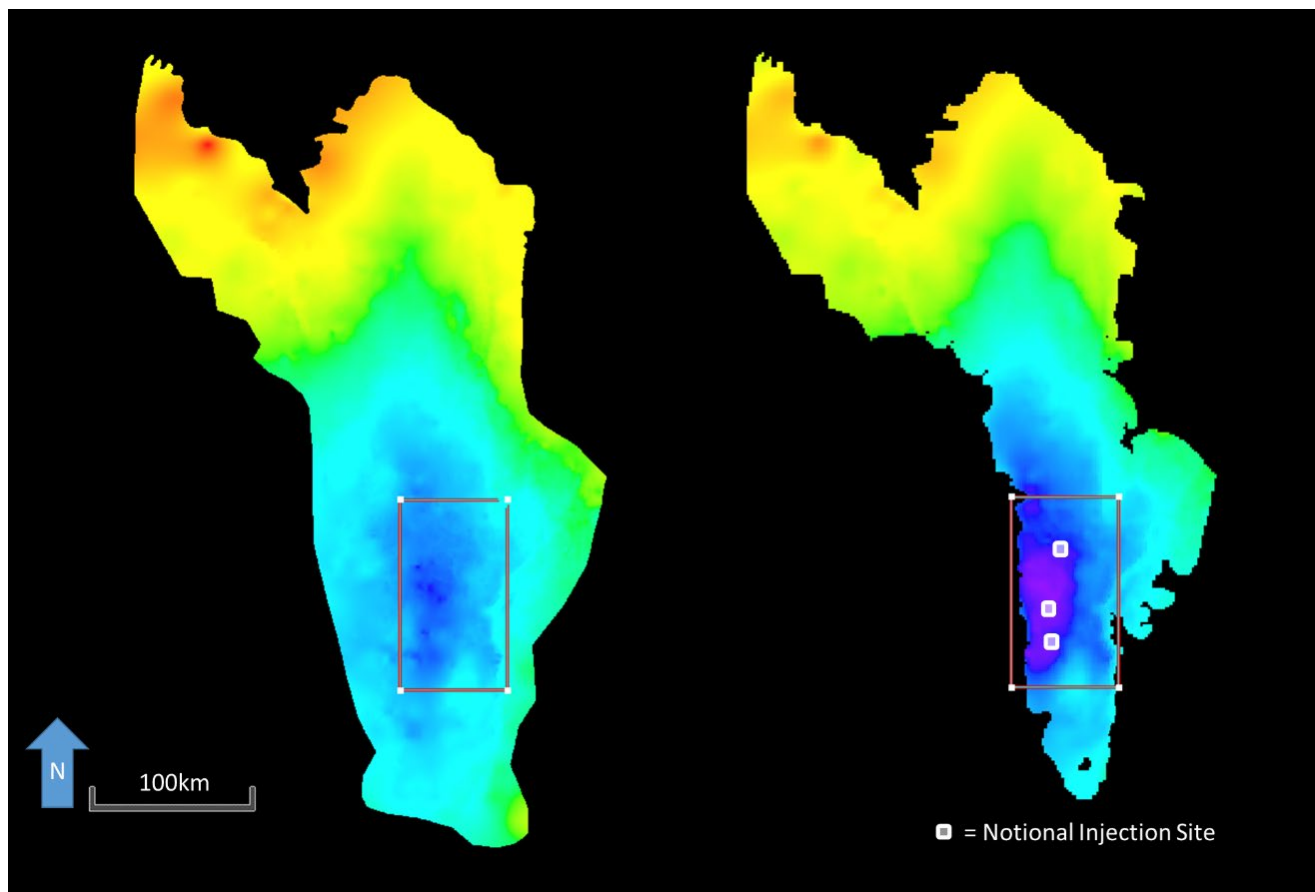
The groundwater model also includes a layer above the Ultimate Seal and another below the Blocky Sandstone Reservoir, such that pressure impacts to the overlying Hutton Sandstone and underlying Moolayember Formation may be estimated.

**Table 56** Layering of the groundwater model compared to geological static and notional injection models.

Interval	Geological Static Model Layer numbering	Notional Injection Sector Model Layer numbering	Groundwater Model Layer numbering
Hutton	n/a	1	1
Ultimate Seal	1 to 8	2	2
Transition Zone	9 to 35	3 to 11	3 to 4
Blocky Sandstone Reservoir	36 to 47	12 to 20	5 to 15
Moolayember	n/a	21	16

The upscaling procedure produced permeability, in X, Y, and Z principal directions, and porosity on a 1.5 x 1.5 km grid (Rodger et al. 2019e) and were converted to equivalent hydrogeological parameters of hydraulic conductivity and specific storage (see Hayes et al. 2019b). The conversion to hydrogeological parameters takes account of viscosity changes with temperature due to the geothermal gradient.

**Figure 149** Domain of the groundwater model (left) compared to the notional injection sector model (red box) and extent of Blocky Sandstone Reservoir (right). Colour indicates depth structure from sea level (blue/purple is deeper). Notional injection sites are shown as white squares.



### 4.11.3 Model boundary conditions and time discretisation

To follow the philosophy of a relatively simple and conservative modelling approach, the groundwater model has straightforward boundary conditions applied. No-flow or closed impermeable boundary conditions are applied at the lateral extends of the static geological model and the same closed conditions are applied above and below the top and bottom model layers. This means that the water injection represents the equivalent volume of CO<sub>2</sub> that can be accommodated only by pressure increase and changing aquifer storage.

This simple approach is also *conservative* in that impermeable boundaries permit no interaction with material outside the active model domain. In the southern depositional centre of the Surat Basin, the Precipice Sandstone is deeply buried and confined between the Moolayember and Evergreen Formations, with no known active recharge or discharge points. In the northern depositional centre of the Surat Basin, the Precipice is unconfined close to the outcrop, having interaction with surface water in the Dawson River and its tributaries. The application of closed no-flow conditions in the northern depositional centre (section 4.3) enables the groundwater model to be kept simple and means **predictions will tend to overestimate impacts**, particularly once pressure propagates further north at later times.

Note that the groundwater model boundary conditions are somewhat simpler than those applied in the notional injection sector modelling (section 4.8) due to the groundwater model domain covering the whole Surat Basin. The notional injection sector model includes boundary conditions to approximate the effects of the connected Blocky Sandstone Reservoir and Transition Zone material outside its domain (which is much smaller). These areas are included in the areal extent of the groundwater model and therefore additional boundary conditions are not needed.

## 4.11.4 CO<sub>2</sub> injection scenarios

The notional injection sector model simulates up to 18 injection locations using horizontal wells (section 4.8.9 and Ribeiro et al. 2019b). The 3D coordinates of the heel, toe and mid points of the horizontal wells defined by Ribeiro et al. 2019b are included in the groundwater model as injection locations within the lower Blocky Sandstone in model layers 7, 8 and 9. Section 4.8.7 describes three notional injection sites: North, South A and South B. These are shown on Figure 149 to Figure 151. The notional injection site model reference case and the groundwater model consider injection at the North and South B injection sites only.

As described in section 4.8.9.1, the FDP injection scenario test cases include the successive retrofitting of CO<sub>2</sub> capture to Millmerran (M) and Kogan Creek (K) power stations to create a so-called 'MKMK' scenario that injects ~275 Mt of CO<sub>2</sub> over around 39 years. Notionally, injection starts in modelled year referred to as 2030 and is labelled as "Injection Year 0" on figures and continues to a nominal shut-off date in 2069. This is longer than required by the presumed capture plant lifetime (section 4.14). The impact is that modelled pressure rises resulting from groundwater modelling analyses are higher than those which would be produced in scenarios that would be perfectly matched retrofit, deployment scenarios. The intention throughout has been to remain conservative.

The boundary conditions representing injection in the groundwater model are taken from the notional injection sector modelling, by recording the volume rate during injection modelling to ensure that the temperature and pressure dependencies of liquid CO<sub>2</sub> volume are accounted for by the notional injection sector model, rather than using an approximation such as a fixed density conversion. The volume of CO<sub>2</sub> injected at each well in the notional injection sector modelling is used as the basis for the equivalent volume of water injected in the groundwater model. In the groundwater model, the base injection scenario has a total injection of 327 Mm<sup>3</sup> of water to represent 276 Mt of CO<sub>2</sub> injection.

Sensitivity analysis of the groundwater model is described in section 4.13.

### 4.11.4.1 Spatial changes in groundwater pressure

Predictions of pressure changes due to injection are plotted as contours of increased groundwater head (m) in the upper layer of the Blocky Sandstone Reservoir and the Hutton Sandstone (groundwater model layers 5 and 1 respectively). Figure 150 shows simulated pressure increases for these layers after injection for 39 years. The contours in Figure 150A for the Blocky Sandstone Reservoir show increases in pressure in excess of 600 m of groundwater head at the northern and southern notional injection sites and increases in excess of 100 m occurring over ~7,800 km<sup>2</sup> up to 45 km from injection sites. The area of high groundwater head increase includes the location of legacy oil and gas exploration wells, such as Cabawin 1, Pring 1 and the Moonie oil field.

With large increases in groundwater head at some wells, there is a risk of increasing pressure exceeding artesian conditions causing flowing wells and potential loss of groundwater resources. It may be necessary to manage impacts, for example by remedial well works including artesian well headworks. Due to the depth and relative isolation of the reservoir in the deepest part of the Surat Basin, the number of significantly and potentially impacted wells is considered small. Investigation of the nearest Precipice and Hutton Sandstone wells shows that all wells that are predicted to experience more than 100 m of groundwater head increase were drilled as oil and gas wells. Generally speaking, these are drilled to higher zonal isolation and cementing standards than water bores. Furthermore, the vast majority, if not all, of these have been plugged and abandoned, or plugged at the depths of the Precipice and Hutton Sandstones, and left as water wells abstracting from shallower formations.

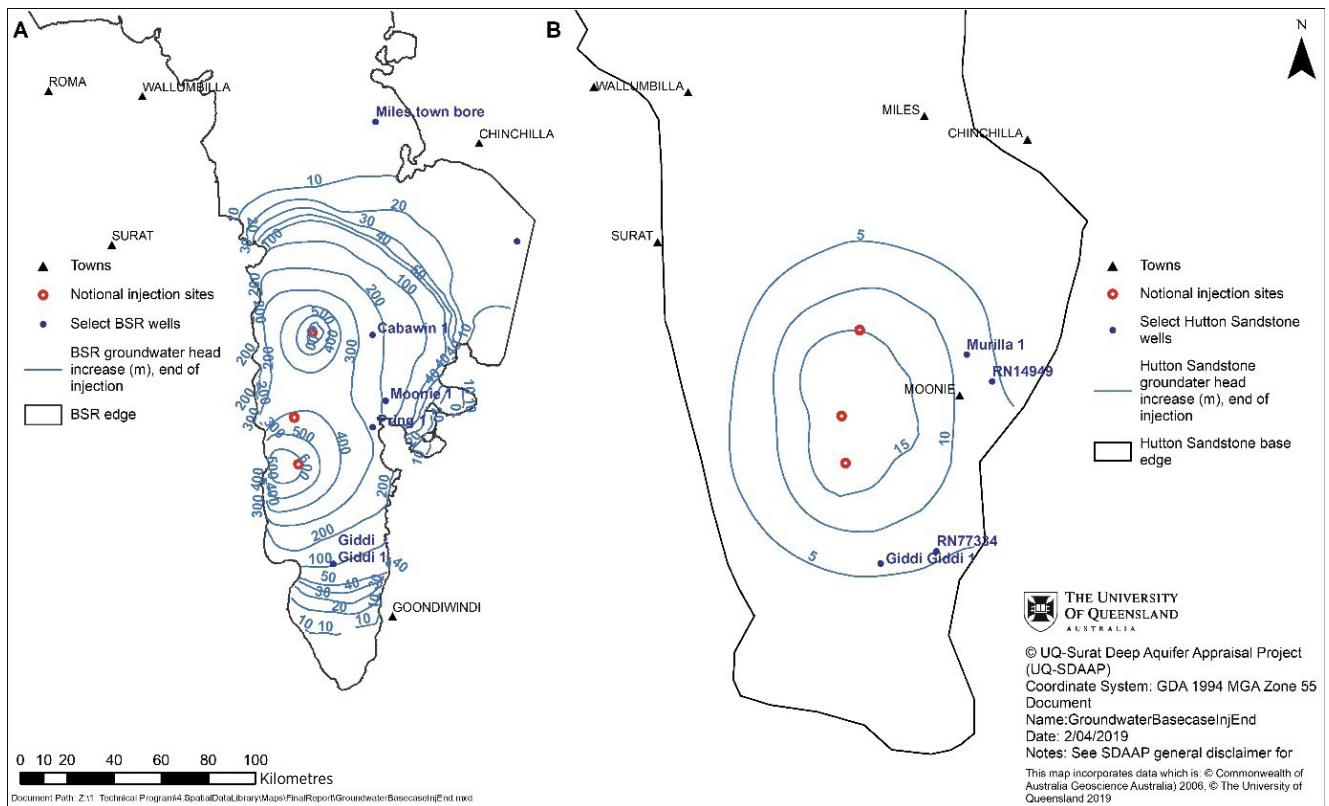
A larger number of wells in the Precipice Sandstone and Hutton Sandstone aquifers would experience smaller pressure increases of 10 to 30 m. This scale of head increase is less likely to cause wellhead containment issues from artesian conditions.

High pressure increases in excess of 100 m are confined to the Blocky Sandstone Reservoir in the southern depositional centre of the Surat Basin. Propagation of pressure further north does occur, and pressure increases of 5 to 10 m are predicted at Precipice Sandstone water wells such as Kogan Creek and Miles Town Bore.

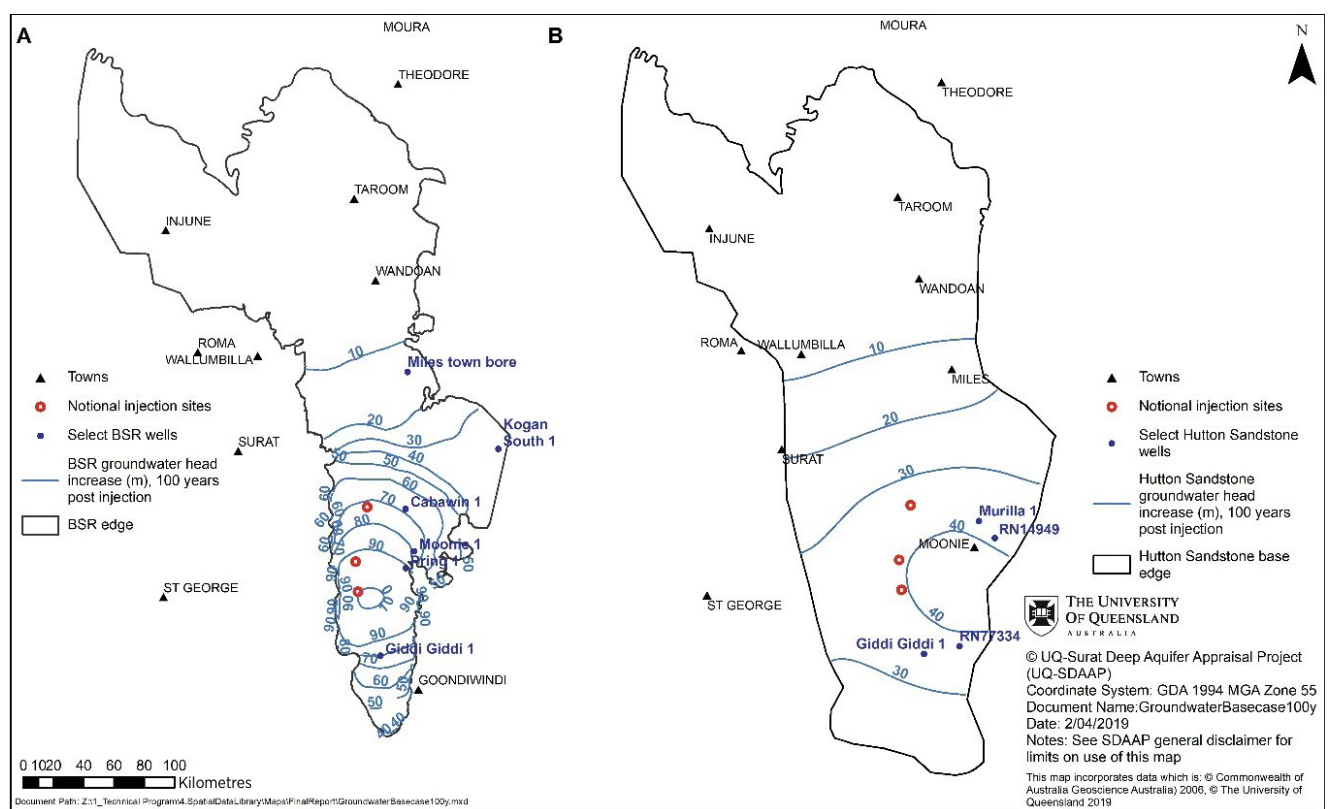
In model layer 1, representing the Hutton Sandstone, Figure 150 (B) shows pressure increases in the range 1 to 17 m after 39 years of injection. The area with more than 5 m of pressure increase includes four known bores and covers an area of ~13,000 km<sup>2</sup>.

Figure 151 shows the pressure increase 100 years after injection ceases. In the upper Blocky Sandstone Reservoir, Figure 151 (A), pressure increases at the injection well locations diminish from a maximum at the end of injection to around 100 m, whilst the area of pressure rise has propagated northward. At this time, pressure increases of > 10 m occur across the entire southern depositional centre and extends northwards to locations such as Miles. At Kogan Creek and Miles Town Bore, pressure increases reach 35 and 11 m respectively, after 100 years. Figure 151 (B) shows the pressure increase in the Hutton Sandstone after 100 years. The pattern is similar but subdued to that in the Precipice Sandstone. At the notional injection sites, pressure increases are 30 to 40 m and the area with greater than 10 m rise covers the southern depositional centre and northwards to Miles. The pressure boosts to a large region of the Hutton Sandstone Aquifer, what is considered to be a generally over-allocated aquifer in pressure decline, may be considered a considerable benefit.

**Figure 150** Predicted groundwater head increase contours (A) in the top of Blocky Sandstone Reservoir and (B) Hutton Sandstone at the end of injection, after 39 years.



**Figure 151** Predicted groundwater head increase contours (A) in the top of Blocky Sandstone Reservoir and (B) Hutton Sandstone 100 years after injection ceases.



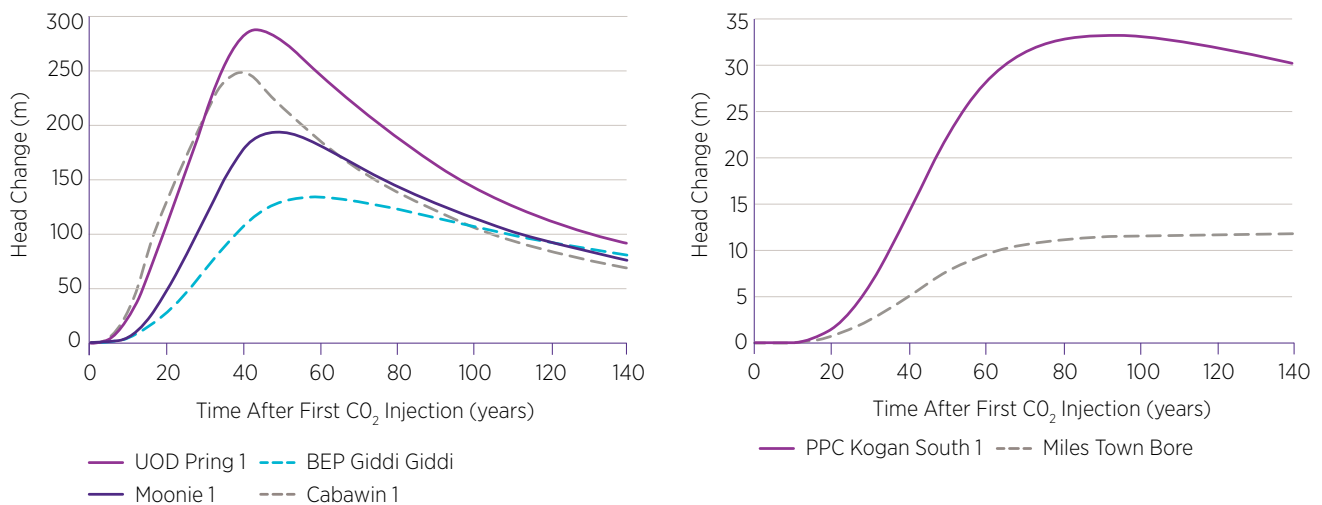
#### 4.11.4.2 Temporal pressure changes at known wells due to injection

Figure 152 presents hydrographs of groundwater head increase over time for selected Precipice Sandstone wells. Figure 152 (A) shows that at wells closest to the notional injection site have predicted pressure rises that start 5 to 10 years after injection commences and peak approximately 10 years after injection ceases. These wells are located 20 to 45 km from injection, at locations shown on Figure 150. Whilst the majority<sup>22</sup> of these wells are reported to have been plugged and abandoned, if any wells still exist, they could be included in the M&V program as useful monitoring bores (section 4.10). Maximum pressure increase at the four well locations is 130 to 280 m of head. Figure 152 (B) shows pressure increases at Kogan Creek and Miles Town Bore. These are selected as indicative wells drilled for groundwater extraction and lie some 90 km from the northern notional injection site and more than 80 km beyond the maximum CO<sub>2</sub> plume extent after 100 years. These wells show an initial pressure rise 20 to 30 years after injection commences, with maximum pressure increase occurring approximately 40 years after injection ceases. Maximum pressure increases are 34 and 11 m respectively.

Figure 153 presents hydrographs of pressure increase over time for selected Hutton Sandstone wells. It shows that wells closest to the notional injection site encounter pressure rises starting 20 years after injection commences, with increasing pressures seen through to 100 years post injection. These wells are located 45 to 55 km from notional injection sites, at locations shown on Figure 150. Maximum pressure increase at the four wells is 35 to 40m of head.

The hydrograph plots show that the response to injection is different between the Precipice Sandstone and Hutton Sandstone aquifers, with high impacts in the Precipice Sandstone largely during injection that diminish once injection ceases. In the Hutton Sandstone, the low vertical permeability of the Transition Zone and Ultimate Seal delay and broaden the propagation of the injection signal such that maximum pressure changes are not seen until many decades after injection ceases.

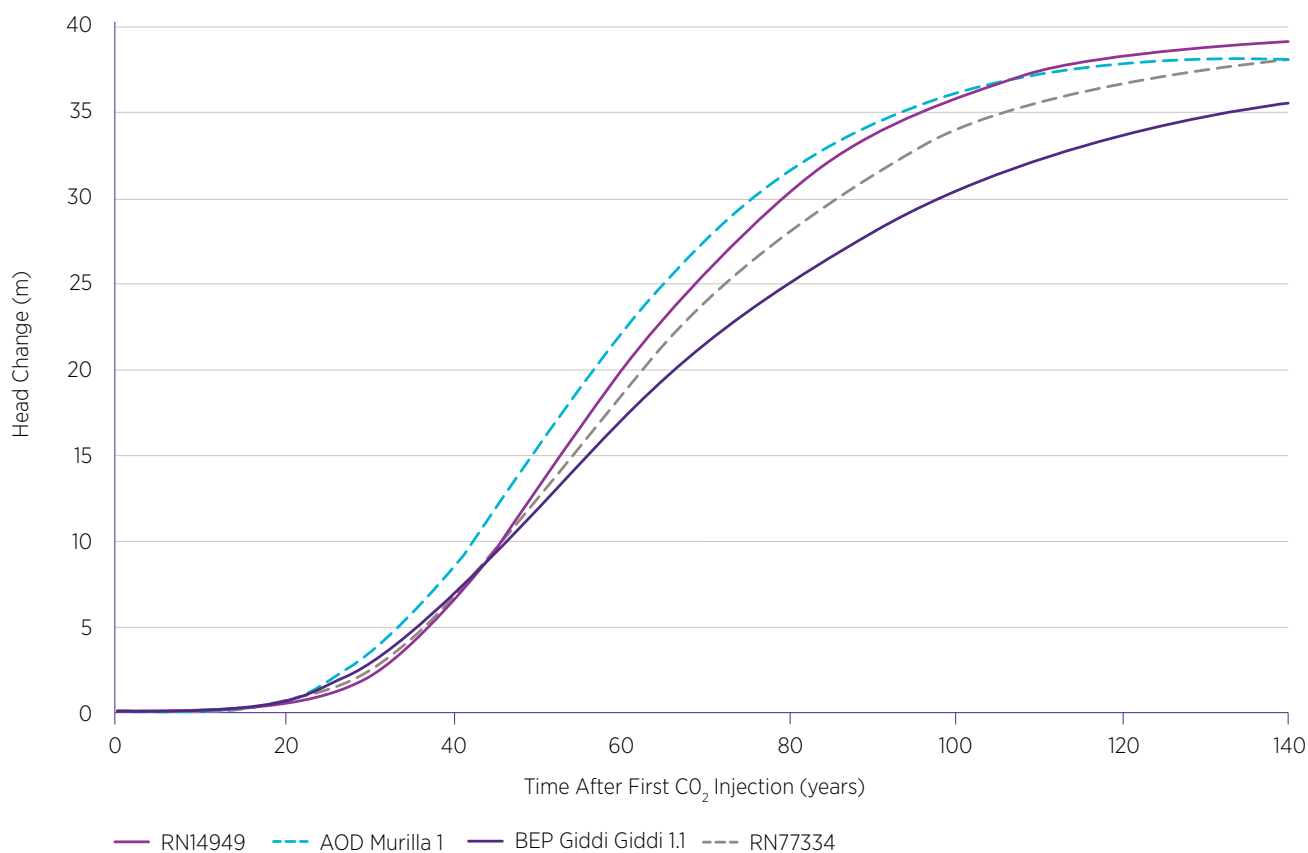
**Figure 152** Predicted groundwater head increase in the top of the Blocky Sandstone Reservoir during and after injection for: (A) Precipice wells closest to notional injection sites; (B) Selected wells located further north.



<sup>22</sup> Some inconsistencies in the current databases make us refrain from stating with 100% confidence that "all" these wells have been P&A'd.



**Figure 153** Predicted groundwater head increase in the Hutton Sandstone during and after injection for Hutton wells closest to notional injection sites.



#### 4.11.4.3 Groundwater fluxes due to injection

Beside pressure increases, another potential impact of CO<sub>2</sub> injection on groundwater resources is to cause changes in water quality (degradation or improvement) by forcing migration of poorer quality groundwater into higher quality areas or vice versa. The low permeability rocks that comprise the Ultimate Seal and upper Transition Zone are conceptualised to contain poorer quality groundwater than aquifers such as the overlying Hutton Sandstone that are used for groundwater extraction. There exists a risk that vertical gradients induced by CO<sub>2</sub> injection could promote flow (leakage) of poorer quality (higher TDS) water from the Ultimate Seal (upper Evergreen Formation) into the overlying Hutton Sandstone.

Mass balances from the groundwater model show that the maximum flux through the Transition Zone peaks approximately 20 years after injection ceases. At this point in time an area of over 35,000 km<sup>2</sup> has groundwater head increases of 1 m or more. The maximum flux of water induced by vertical gradient over this area through the Ultimate Seal and into the Hutton Sandstone is equivalent to 0.05 to 0.1 mm/year. As this flow rate is low, the risk is also considered low. However, it remains on the project risk register (Honari et al. 2019e) as this assessment depends on the nature of the vertical seal, and groundwater quality in the southern depositional centre, both of which are currently poorly constrained.

Most of the wells in the southern depositional centre of the Surat Basin were originally drilled for oil and gas exploration. Some of these exploration wells have been converted to water bores and several are known to be completed in multiple aquifers. For example, well Giddi Giddi-1 is listed as being completed in Precipice and Hutton sandstones (see Figure 150 to Figure 151), although other information in the well completion reports suggests these formations have been plugged. Whether plugged or not, Giddi Giddi-1 illustrates that there is an unquantified risk or possibility that increases in groundwater head due to injection in the Blocky Sandstone Reservoir could cause cross-formation flow to be induced in wells with multi-aquifer completions. This risk could, in principle, require remedial well works, although due to the depth and relative isolation of the reservoir in the deepest part of the Surat Basin, the number of significantly impacted wells is considered small.

#### 4.11.5 Summary of groundwater modelling

Groundwater modelling of the notional field development plan reference case shows that significant groundwater pressure increases due to CO<sub>2</sub> injection will occur in the strata between the Blocky Sandstone Reservoir and Hutton Sandstone aquifer in the deep southern depositional centre of the Surat Basin. At existing wells (drilled for oil and gas exploration) near the notional injection sites, pressure increases are predicted to exceed 250 m of groundwater head. During injection, the increased pressure will continue to propagate horizontally in the Blocky Sandstone Reservoir and vertically through the Transition Zone and Ultimate Seal into the overlying Hutton Sandstone. This propagation and spreading of pressure increases continues post-injection away from the injection sites whilst pressures diminish somewhat at the notional injection sites themselves. At some locations, remedial well headworks or downhole works may be required to manage pressure increases. Due to the depth and relative isolation of the Blocky Sandstone Reservoir in the deepest part of the Surat Basin, the number of significantly affected wells is small. A larger number of wells in the Precipice and Hutton aquifers are predicted to experience smaller pressure increases of 10 to 30 m. The predicted pressure increases over a large portion of the Surat Basin is considered a positive impact, helping re-pressurise otherwise declining Great Artesian Basin aquifers and lowering pumping costs. This pressure benefit to both the Precipice Sandstone and the Hutton Sandstone aquifers is projected to occur across some 25,000 km<sup>2</sup>, while the CO<sub>2</sub> plume itself remains within less than ~10km of the injection locations (~300 km<sup>2</sup> in area) in the Blocky Sandstone Reservoir.

Some deep wells are known or suspected to be completed across multiple formations, such as the Hutton and Precipice Sandstones. These wells are many tens of kilometres outside the predicted footprint of the CO<sub>2</sub> plume, but they represent a potential pathway through which pressure can more rapidly propagate and flow could therefore be induced to occur between formations of differing water quality. Remedial well works may be necessary to eliminate this potential communication pathway.

The increased pressure induced in the Blocky Sandstone Reservoir is predicted to propagate through the Transition Zone and Ultimate Seal into the Hutton Sandstone. The new vertical pressure gradients will induce some increase in the flux of formation water between these units. If the water quality of the Upper Evergreen in the southern depositional centre of the Surat Basin is poor (this is currently unknown), for example with high TDS there is a risk that pressure gradients and inter-formation vertical flow could cause water quality degradation in over, or underlying formations. Current modelling shows this risk to be small because the increase in flux is small given low bulk permeability of the Ultimate Seal and the reservoir volume of the Hutton Sandstone aquifer is relatively large. As further information regarding formation water quality and vertical permeability becomes available, further assessment of this risk is required.

## 4.12 Notional injection modelling and FDP – sensitivity analysis

While the UQ-SDAAP study has significantly reduced many key uncertainties, the remaining main technical uncertainties relate to the degree to which porosity and permeability have been degraded by greater burial depth at the notional injection locations compared to offset data. There is relatively little variation of lateral plume spread distances and so there is a low risk of migration, up dip, and movement out of the defined container. There is, however, a low-case permeability scenario in which rates may not be sustained within the set pressure limits. This scenario would not allow for a minimal surface footprint development because significantly more well pads would be required. Site specific data is required. It will be important to collect months of production data for each proposed site to help calibrate potential pressure build up. The Transition Zone looks likely to perform the function required, however, it needs to be directly sampled and the possibility of transmitting pressure or fluids across it could be directly tested.

Current estimates and sensitivity analysis support the view that material high rate, secure storage will be achievable and will likely be able to accept around 90% of the emissions from the three most modern, supercritical coal-fired power plants in the region, and possibly more. It is also likely that the formations can accept these rates for the lifetime of the plants and probably longer.

The notional injection sector reference case was altered by changing individual parameters, one at a time, using CMG's CMOST software. These parameters are listed in Table 57. The high and low values are estimates based on the understanding of the Blocky Sandstone Reservoir gained by the UQ-SDAAP team throughout the project. The aim of these simulations was to test which of these parameters were likely to most significantly impact the success of a CCS project, by assessing how the injectivity and containment change as each parameter is varied.

The aim of this work was not to test the full multivariate “parameter space”. The behaviour of different combinations of these parameters would lead to a much wider range of outputs than are presented here. This could be tested as part of a more detailed study when further data (e.g. gathered during an appraisal program) allows improved estimates of the properties of the subsurface in the notional injection locations.

For the properties which varied spatially, such as the porosity and permeability, multipliers were used to modify the property for every cell in the relevant layers of the grid. This retained the spatial variation of the parameters, while scaling the mean value. Most of the other parameters were altered by changing the relevant term in the CMG input files. The only minor exceptions to this were the terms relating to the relative permeability and capillary pressure curves. The relative permeability curves were altered using terms for the end points of the curves, that is; the residual saturations of water and CO<sub>2</sub>, and the maximum relative permeability to CO<sub>2</sub>. The values used for these endpoints were based on the data collated in Rodger et al. 2019b. GEM scales the previously defined relative permeability curves to these end points. Example drainage relative permeability curves scaled to the high and low case residual water saturations, and high and low relative permeability to CO<sub>2</sub> are shown in Figure 154. The imbibition curves were not defined, but were scaled to the residual saturation of CO<sub>2</sub>.

**Figure 154** (A) Drainage relative permeability curves used for all cells used in the high and low residual water saturation cases. (B) Drainage relative permeability (to CO<sub>2</sub>) curves as used in the high and low relative permeability to CO<sub>2</sub> cases.

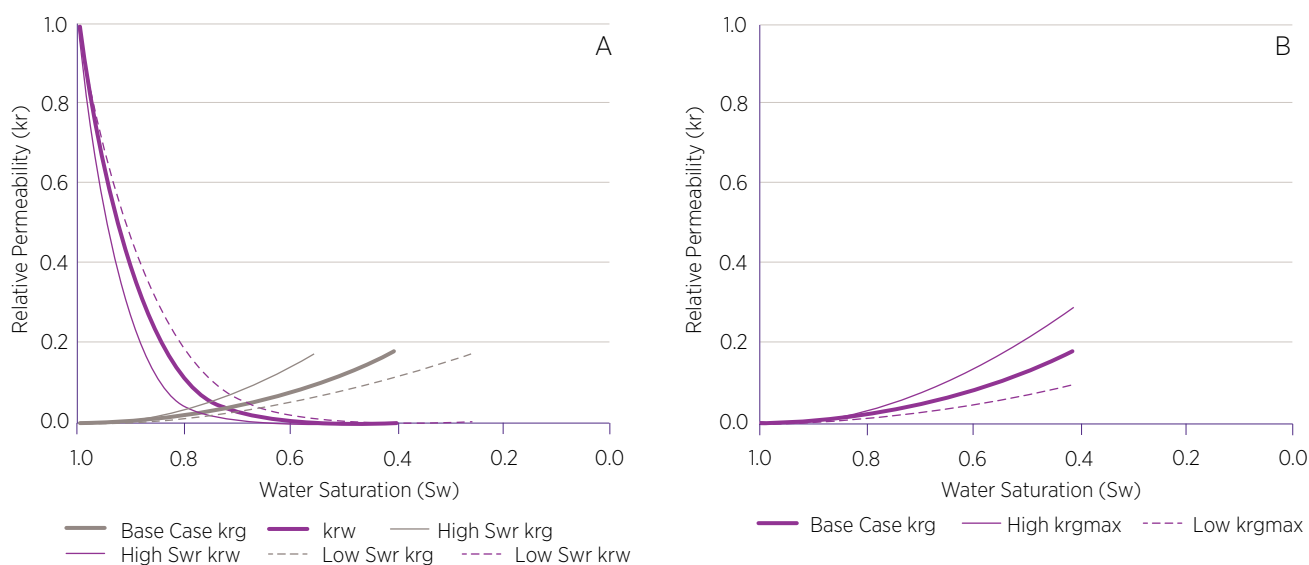


**Table 57** Parameters tested in the sensitivity studies. \*indicates mean/typical values are shown in this table. Reference case in bold.

Parameter	Low	Mid	High	Comment
Blocky Sandstone Reservoir Effective Porosity	8.7%	<b>12.7%*</b>	16.7%	From Petrophysics (Harfoush et al. 2019). Modified using multiplier in CMG GEM
Blocky Sandstone Reservoir Horizontal Permeability ( $k_h$ )	22 md	<b>43 md*</b>	87 md	From Petrophysics (Harfoush et al. 2019). Modified using multiplier in CMG GEM
Rock Compressibility	$2.6 \times 10^{-7} \text{ kPa}^{-1}$	<b><math>4 \times 10^{-7} \text{ kPa}^{-1}</math></b>	$5.2 \times 10^{-7} \text{ kPa}^{-1}$	From Petrophysics (Harfoush et al. 2019)
Blocky Sandstone Reservoir Permeability Anisotropy ( $k_v/k_h$ )	0.12	<b>0.15*</b>	0.3	From Petrophysics (Harfoush et al. 2019). Tested for MKMK schedule only. $k_v$ Modified using multiplier in CMG GEM
Transition Zone Vertical Permeability ( $k_v$ )	0.2x	<b>Varies</b>	50x	$k_v$ modified using multiplier in CMG GEM
Maximum Relative Permeability to $\text{CO}_2$ ( $k_{rgmax}$ )	0.1	<b>0.18</b>	0.3	Based on previous core analysis – see Rodger et al. 2019
Capillary Pressure Curve SRTNFG factor	0 and 12.5	<b>25</b>	30	Modified by altering SRTNFG in CMG GEM (factor for J function – section 4.5.5.1)
Residual Water Saturation ( $S_{wr}$ )	0.25	<b>0.4</b>	0.55	Based on previous core analysis – see Rodger et al. 2019
Residual $\text{CO}_2$ Saturation	0.2	<b>0.35</b>	0.5	Based on previous core analysis – see Rodger et al. 2019
Temperature	80°C	<b>85°C</b>	90°C	Temperature at 2100 m (TVDSS) in the model. From Petrophysics (Harfoush et al. 2019)
Salinity	1000 ppm	<b>3000 ppm</b>	5000 ppm	Based on salinity of produced water from Moonie oil field
BHP Limit	32,500 kPa	<b>39,500* kPa</b>	n/a	From Geomechanics (Rodger et al. 2019). <i>Note that high BHP limit from Rodger et al. (2019) cannot be reached, even with high WHP</i>
WHP Limit	<b>15,000 kPa</b>	<b>20,000 kPa</b>		Reference case was 15,000 kPa for the MKMK schedule, and 20,000 kPa for the MKTMK schedule
Skin	-2	<b>0</b>	10	Based on range of values from well tests in ZeroGen (2012)
Tubing Radius	0.05 m	0.06 m	<b>0.076 m</b>	Only tested in MKTMK models. See Rodger et al. 2019b for discussion on tubing sizes

Capillary pressure curves were modelled using J-functions. To test cases where the capillary pressures were higher or lower (representing changes in the wettability of the system), alternate values were used for the SRTNFG term used in GEMs capillary pressure calculations. This does not change the shape of the curves, but simply scales them. For example, using a value of 12.5 in place of the base case 25 would halve the capillary pressure. An additional “low” case with zero capillary pressure was also tested, representing a case where the Transition Zone rocks are  $\text{CO}_2$  wet (Rodger et al. 2019b).

## 4.12.1 Sensitivity analysis results

The sensitivity analysis results are presented in terms of their impact on: a) injectivity, and b) containment.

### 4.12.1.1 Injectivity

The impact of each parameter on injectivity was assessed by comparing the mass of CO<sub>2</sub> injected per well for each simulation. For clarity, this is the total cumulative mass of CO<sub>2</sub> injected, divided by the total number of wells required. For the MKMK reference case this was a total of 279 Mt across seven wells, giving an average of 39.8 Mt per well. The results for the other MKMK simulations are presented as a percentage of this reference case in Figure 155.

For the MKTMK extended reference case a total of 631 Mt was injected, again through seven wells. This was made possible due to the higher wellhead pressure constraint in this case, giving an average of 90.1 Mt per well. The results for the other MKTMK extended simulations are presented as a percentage of this reference case in Figure 156.

**Figure 155** Mass of CO<sub>2</sub> injected per well for MKMK cases, presented as a percentage of reference case value (39.8 Mt/well).

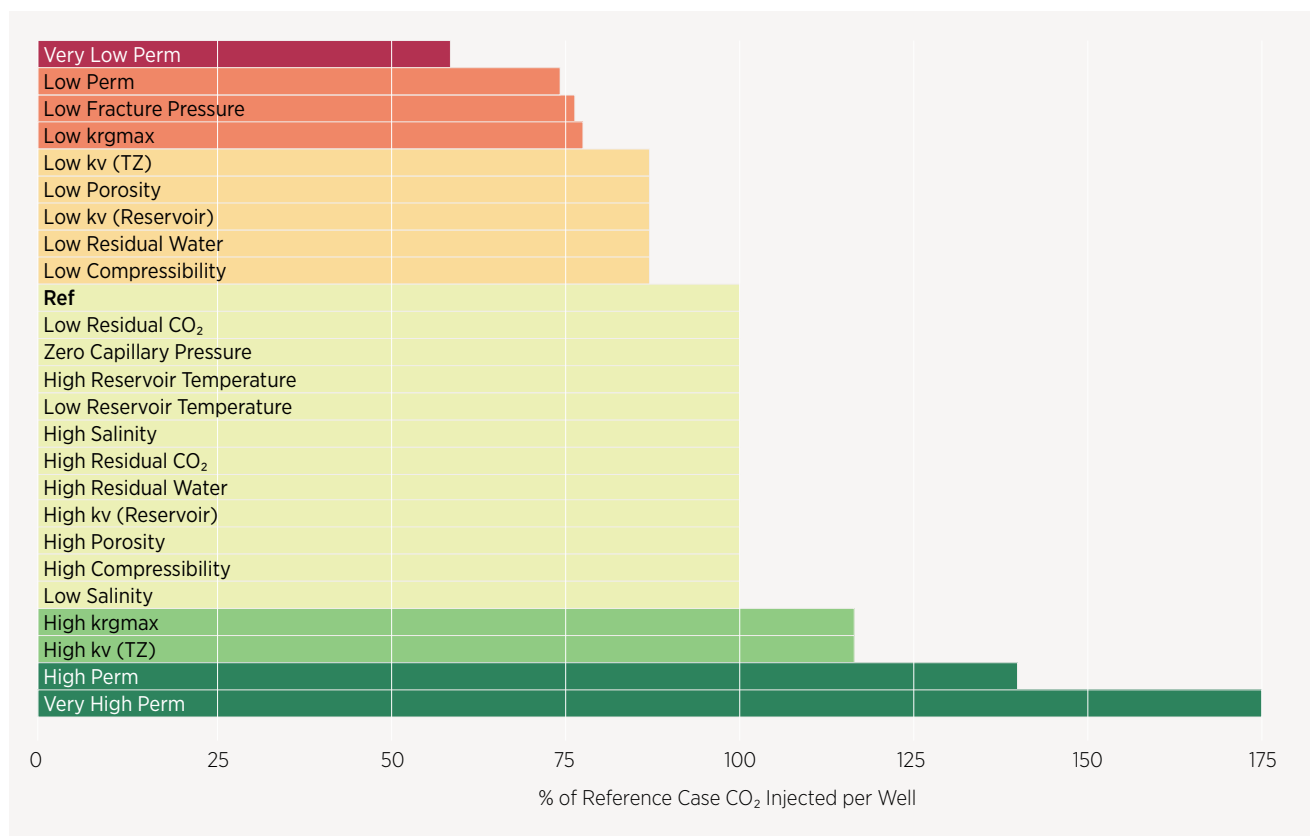
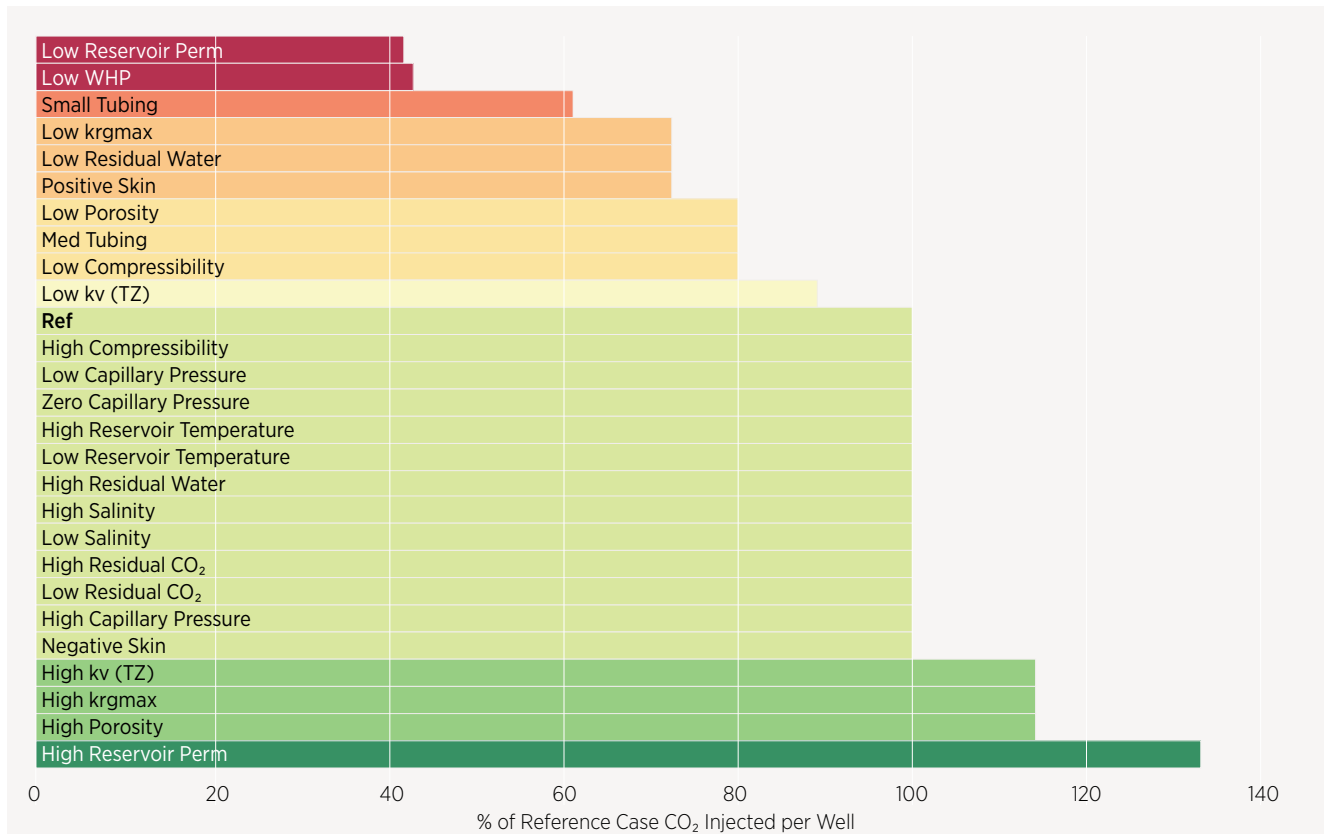


**Figure 156** Mass of CO<sub>2</sub> injected per well for MKTMK extended cases, presented as a percentage of reference case value (90.1 Mt/well).



One potential issue with this comparison is that the actual impact of each parameter may not be represented fairly, due to the discretisation caused by opening one extra well. To demonstrate this, the cumulative injection for northern wells in the “MKMK – Low Reservoir  $k_v$ ” case is shown in Figure 157.

**Figure 157** Cumulative Mass of CO<sub>2</sub> injected for north notional injection site wells in the “MKMK – Low Reservoir k<sub>v</sub> case”. Note that the last well to start injecting (pink line) only injects for five years, and its cumulative injected CO<sub>2</sub> is just over 3 Mt, compared to 35 Mt for the previous well.

#### Low reservoir kv

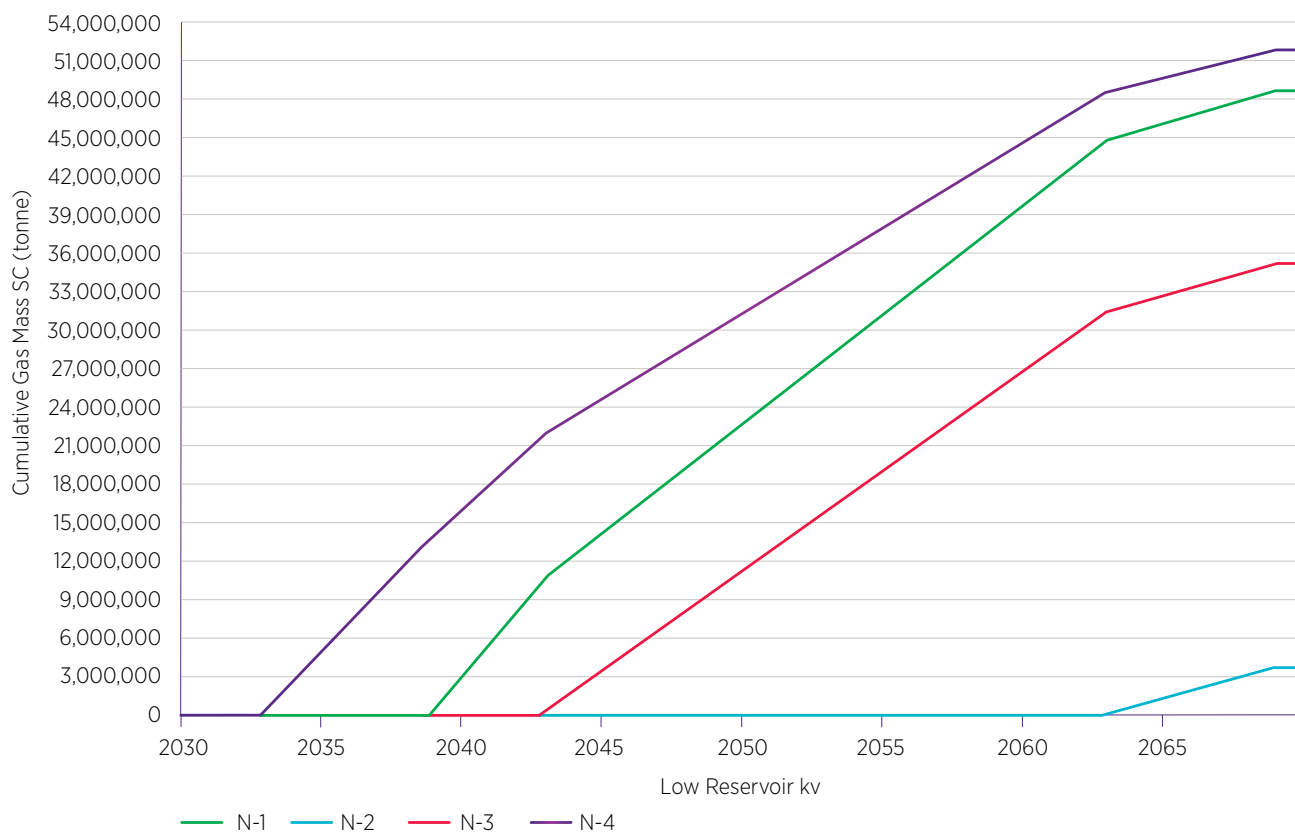
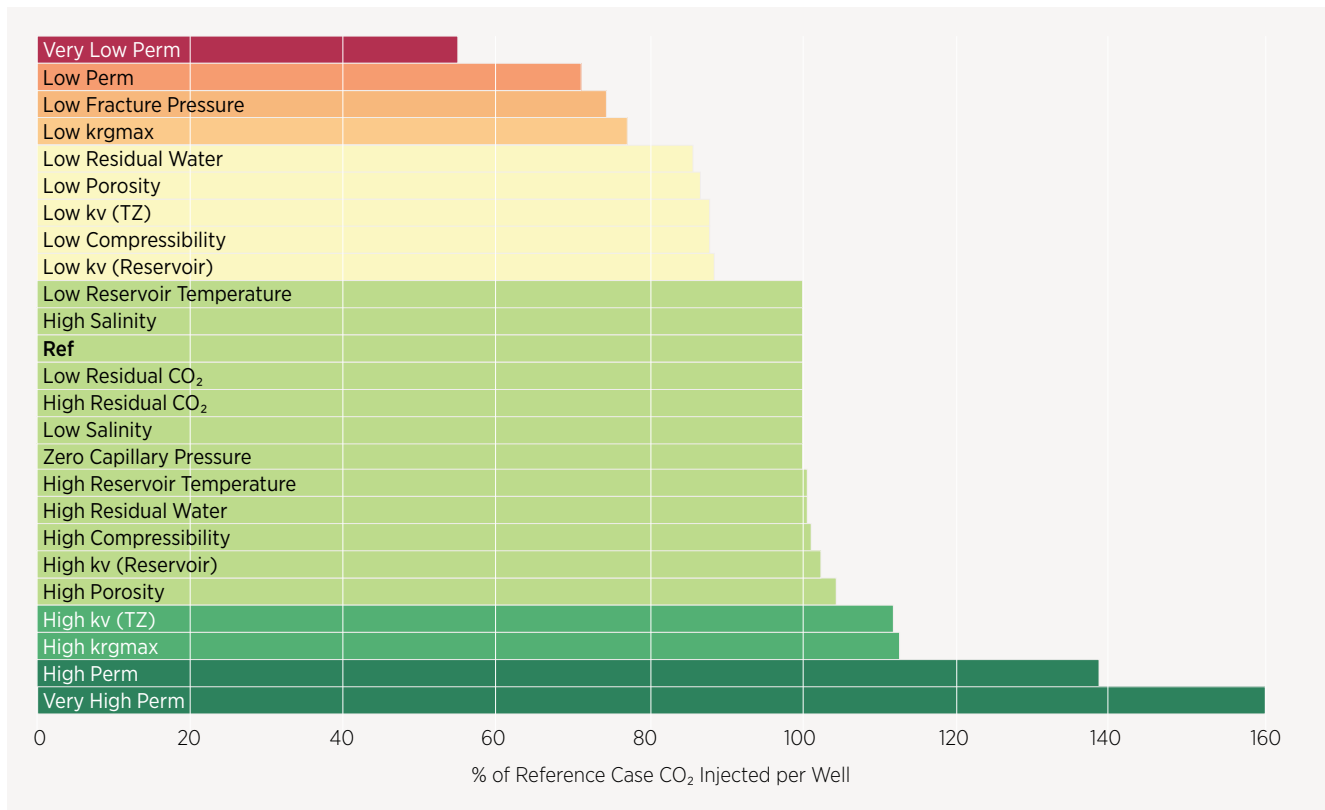


Figure 157 shows an example of a case where the final well is required to maintain the required injection rate, but only at the very end of the injection period. This additional well creates a step decrease in the apparent mass of CO<sub>2</sub> injected per well, regardless of the mass injected by the last well. To account for this an additional comparison, is presented where the lowest injecting well (the last well to start injecting) was removed from the analysis. The mass injected by this well was subtracted from the total mass injected, and the mass of CO<sub>2</sub> injected per well was recalculated using this lower mass, and with one less well. For the MKMK reference case, this resulted in an adjusted value of 44.5Mt per well. For the MKTMK extended case the new value was 102.5 Mt per well. These reference case values were used as the basis for the comparisons shown in Figure 158 and Figure 159.

As an alternative method of assessing the impact of the various parameters on “cost”, the number of wells per Mt of injected CO<sub>2</sub> was also calculated (in essence, the opposite of the previous analysis). Again, this was repeated excluding the final well. The results for the MKMK and MKTMK extended cases are shown in Figure 160 and Figure 161 respectively, with the results excluding the last well (as described above) shown in Figure 162 and Figure 163.

Of the reservoir properties tested, the permeability terms – including the vertical permeability in the Blocky Sandstone Reservoir and Transition Zone, and maximum relative permeability to CO<sub>2</sub> (“kr<sub>gmax</sub>”) – have the most significant impact on injectivity. A low reservoir permeability (half of the reference case) could more than double the number of wells required for a larger project, such as a project based on the MKTMK extended schedule. The effect appears less significant for the smaller MKMK project, where even a four-fold reduction in reservoir permeability (“Very Low Perm”) only increases the required wells per Mt injected to 1.85 of the reference case.

**Figure 158** Mass of CO<sub>2</sub> injected per well for MKMK cases, excluding the well with the lowest injection, presented as a percentage of reference case value (44.5 Mt/well).



**Figure 159** Mass of CO<sub>2</sub> injected per well for MKMK extended cases, excluding the well with the lowest injection, presented as a percentage of reference case value (102.5 Mt/well).

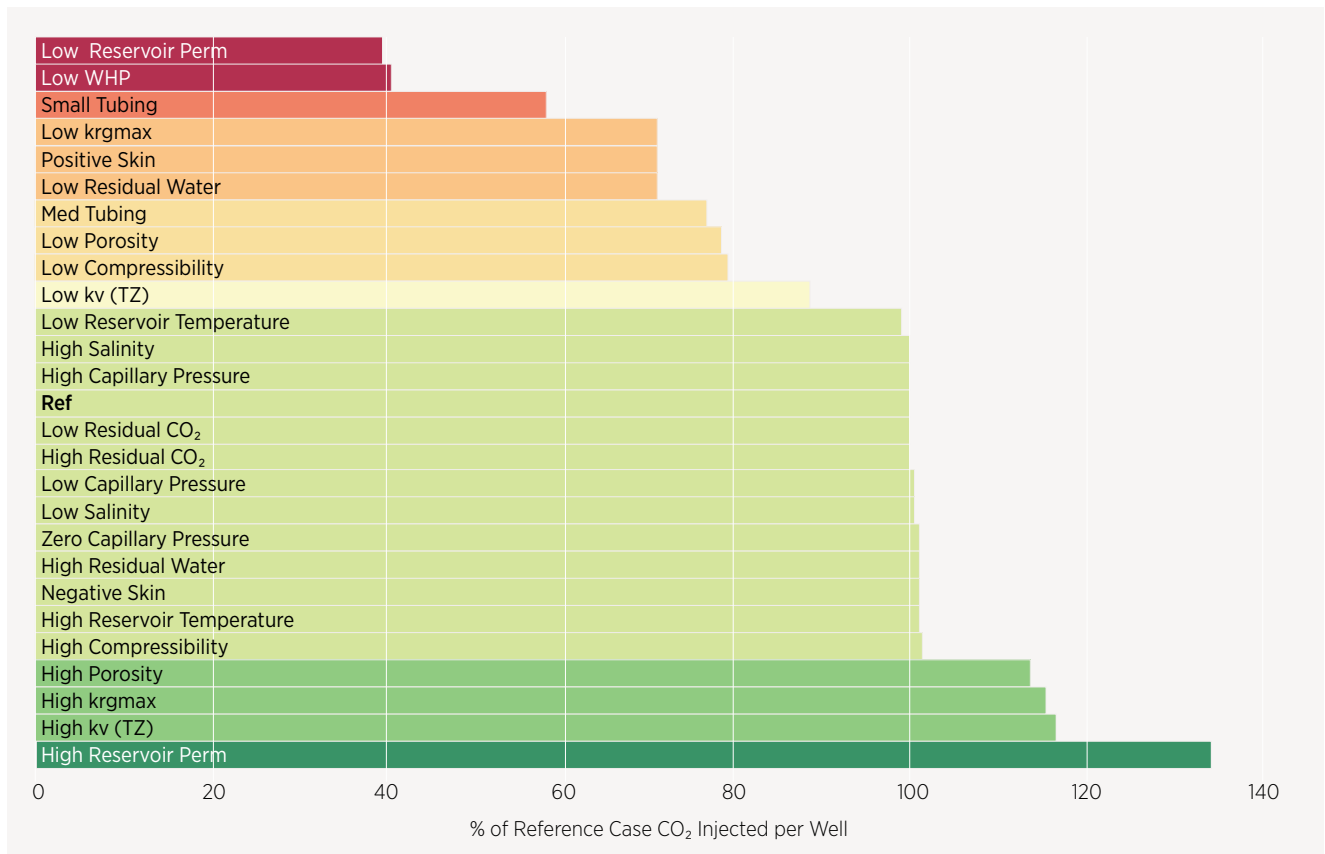




Figure 160 Wells required per Mt of CO<sub>2</sub> injected for MKMK cases.

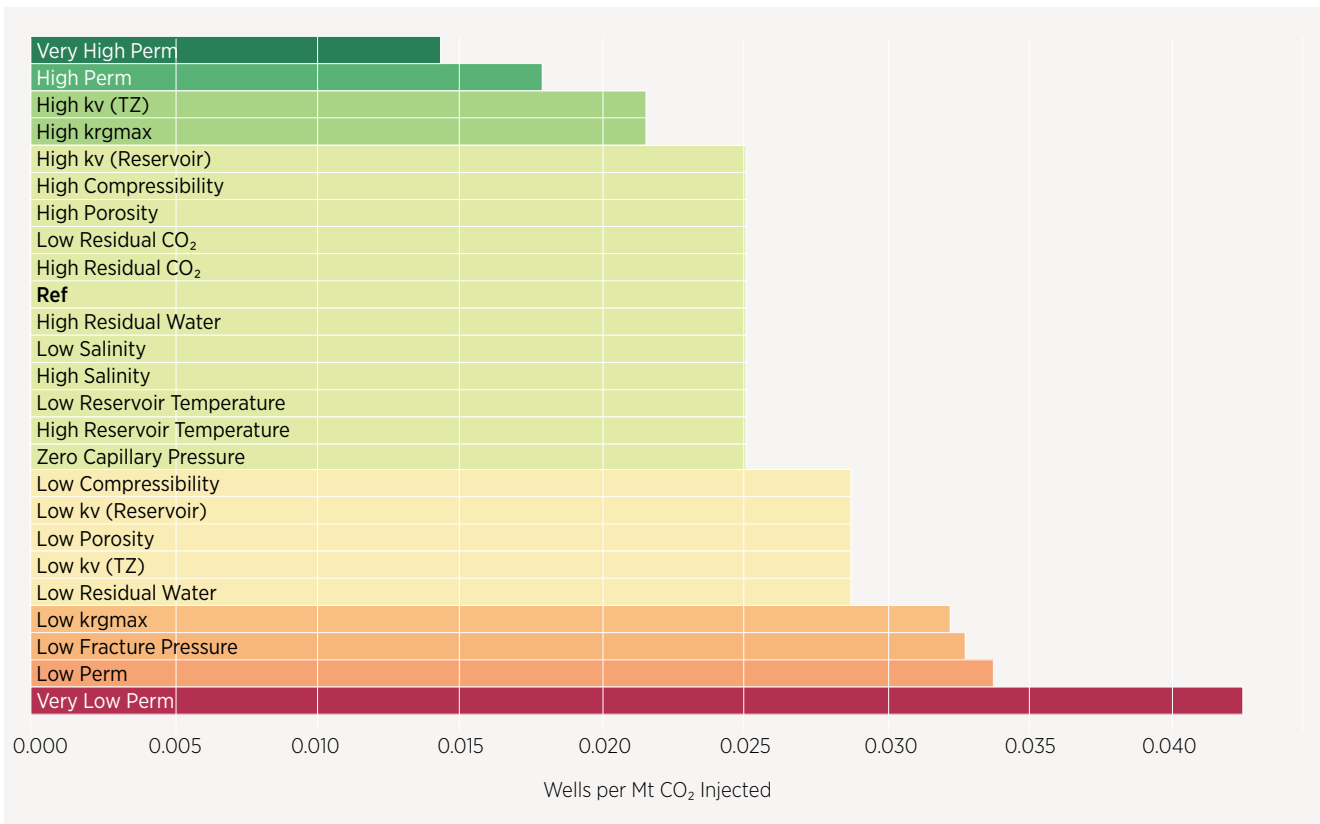
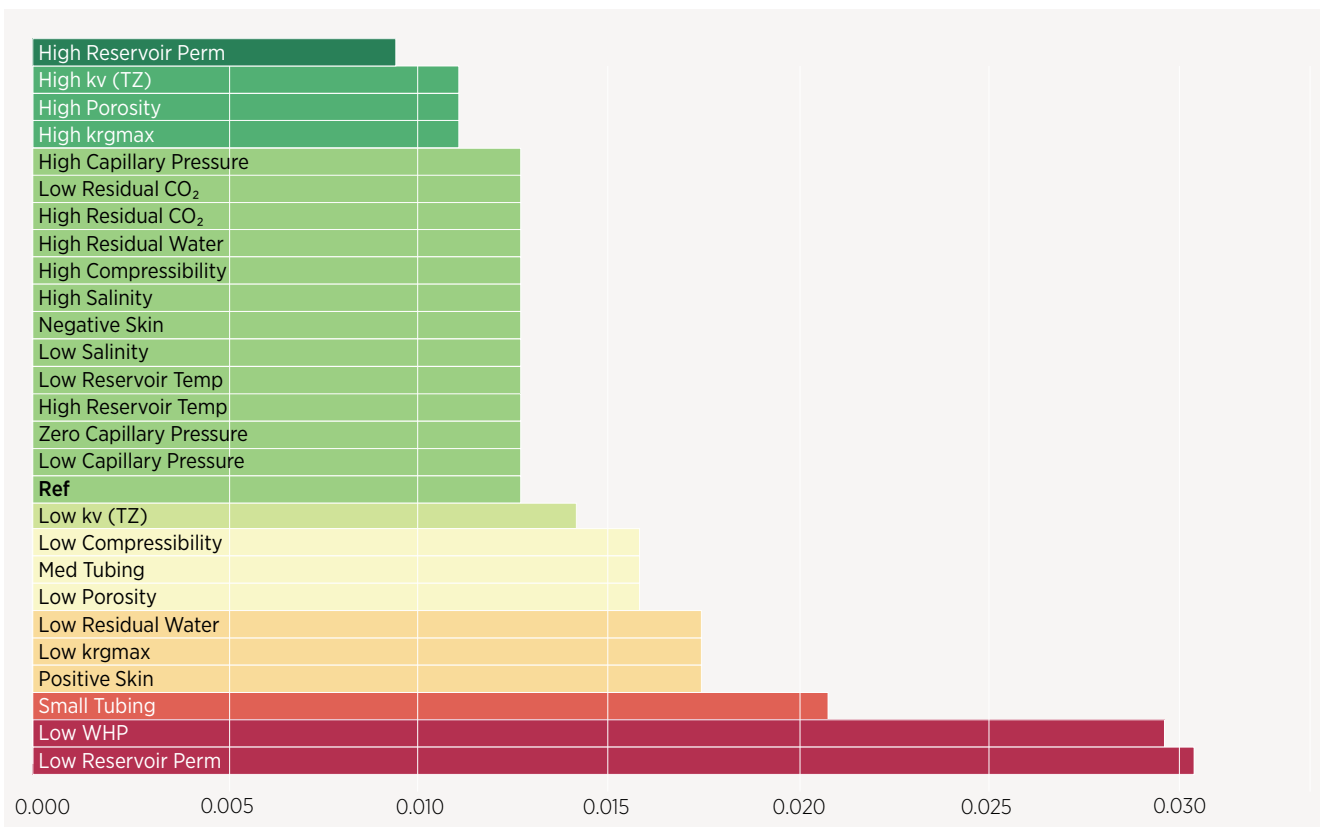
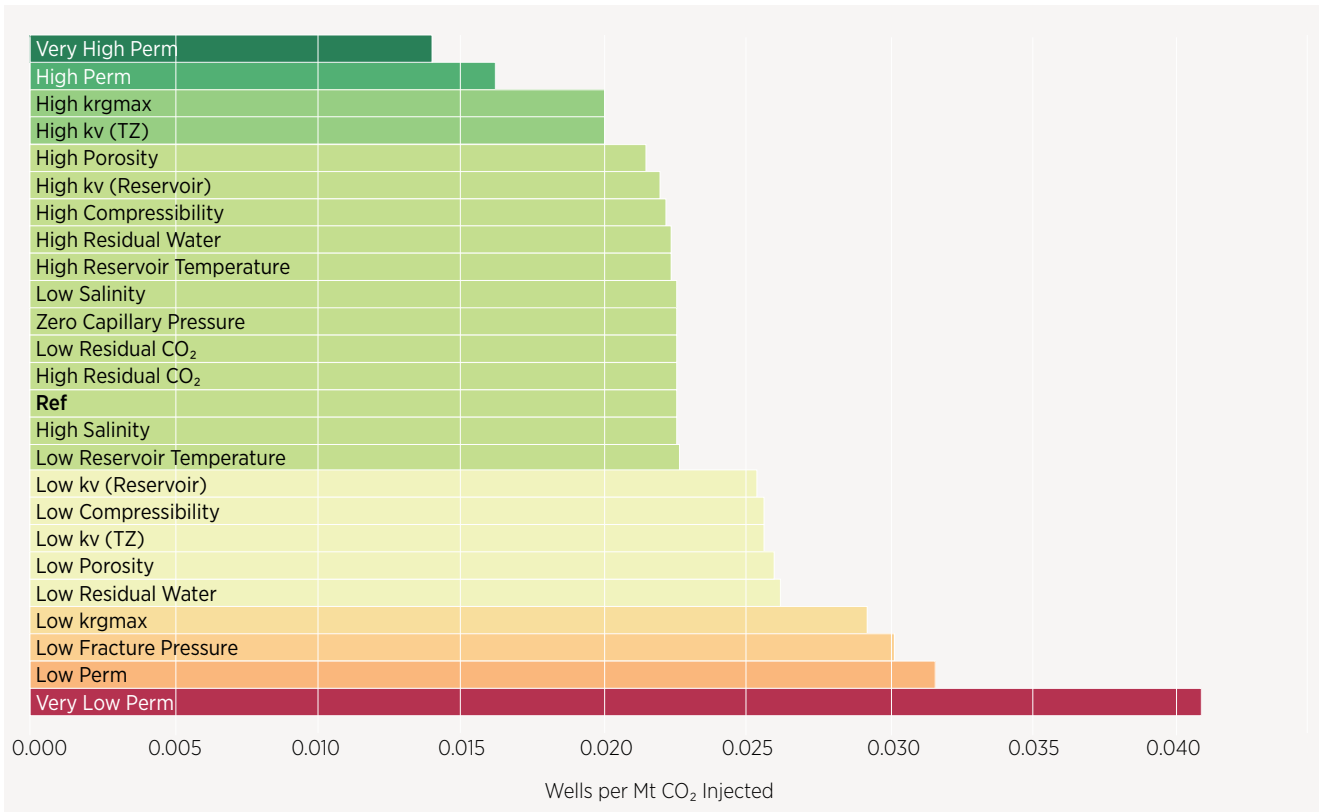


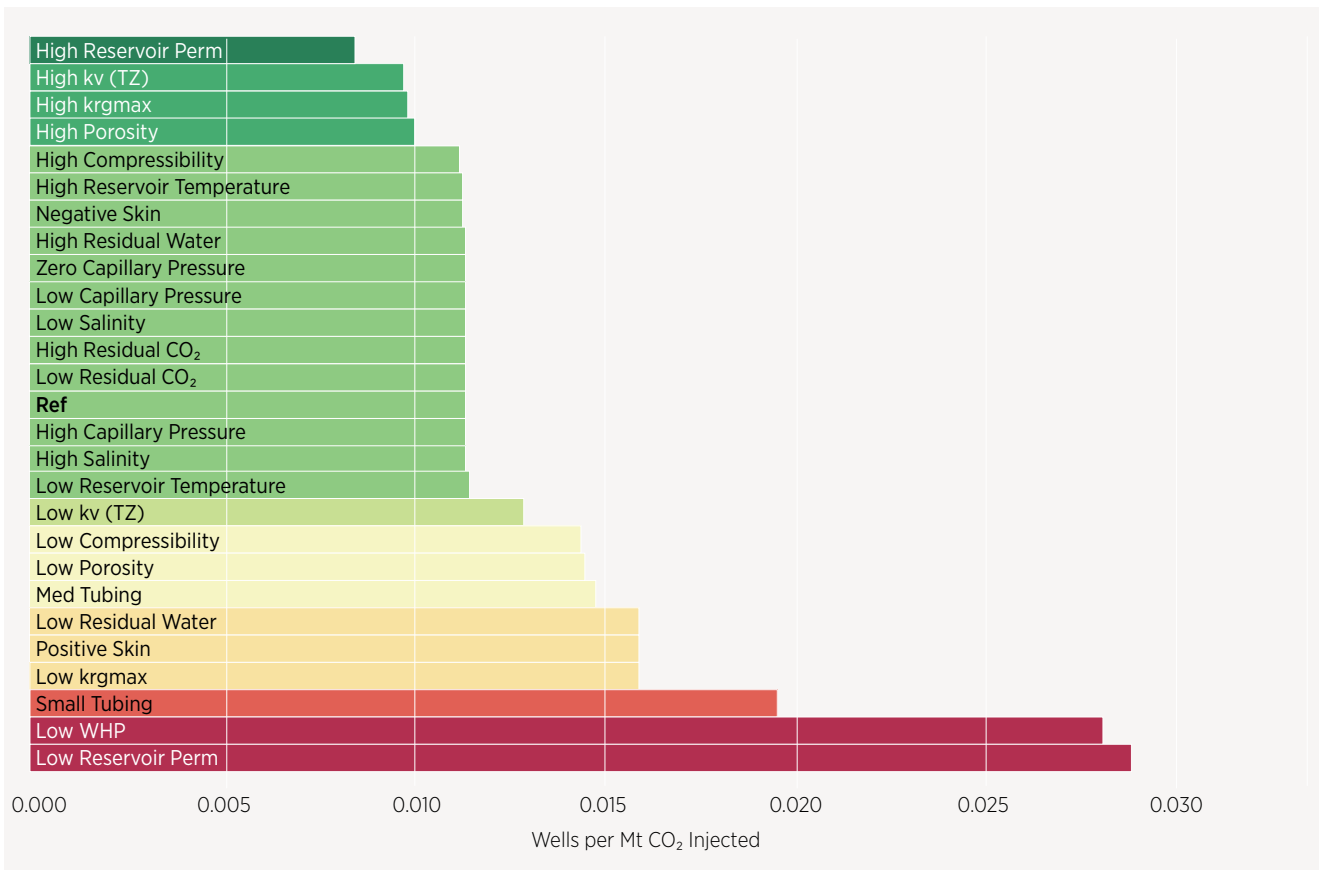
Figure 161 Wells required per Mt of CO<sub>2</sub> injected for MKTMK cases.



**Figure 162** Wells required per Mt of CO<sub>2</sub> injected for MKMK cases, excluding the well with lowest injection.



**Figure 163** Wells required per Mt of CO<sub>2</sub> injected for MKTMK cases, excluding the well with lowest injection.

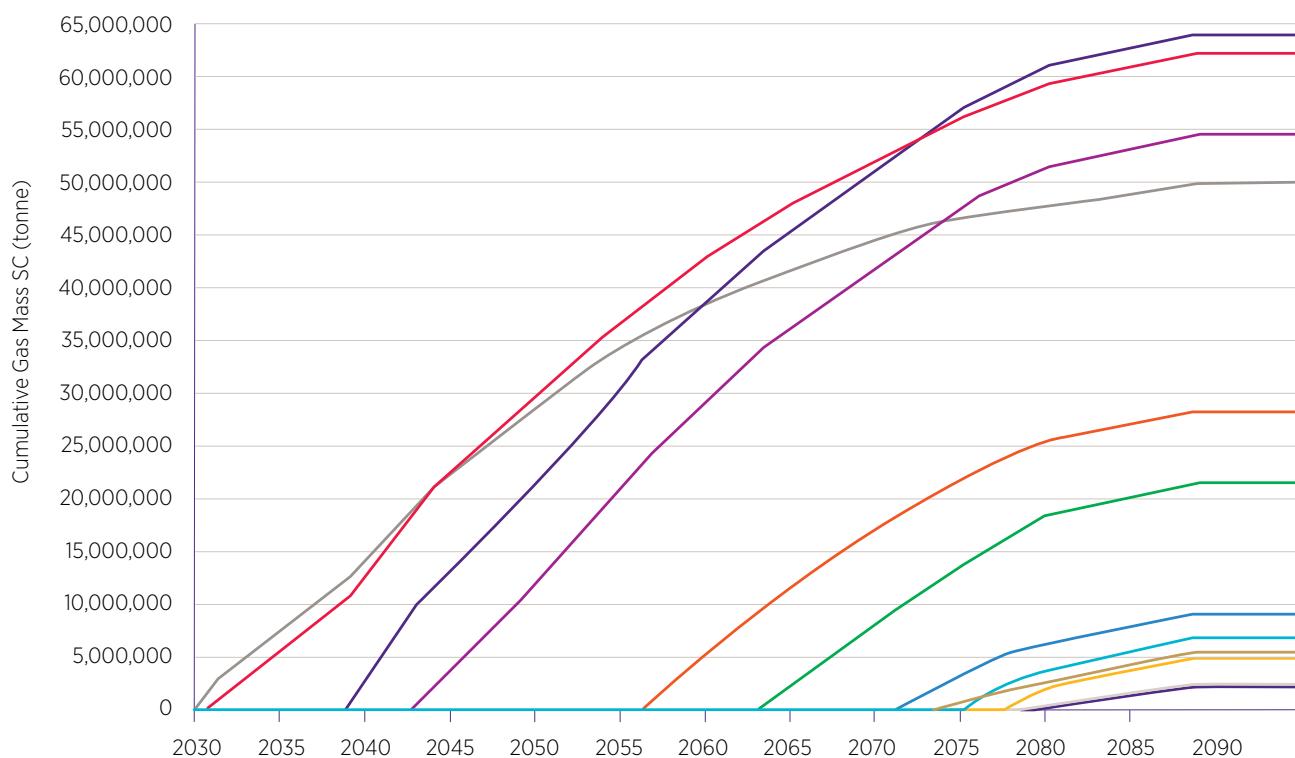


It is important to note that this lesser effect is likely due to the fact that only nine wells in total were defined in the MKMK cases. This meant that the three MKMK cases with poor injectivity (the low and very low permeability cases, and the low fracture pressure case) were unable to meet the desired injection rate, but were not able to open more wells. If these wells had opened, they would be less efficient (i.e. would inject less CO<sub>2</sub> in total) than the early wells due to the increased reservoir pressure caused by previous injection, and the limited time they would be open. Thus, opening these additional wells would reduce the overall average CO<sub>2</sub> injected per well, and increase the wells required per Mt of injected CO<sub>2</sub>. In the MKTMK cases, more wells were defined, and could therefore be opened to attempt to maintain injection over the prolonged injection period. Figure 164 shows the cumulative injected CO<sub>2</sub> for the 12 wells in the two southern notional injection sites in the MKTMK extended low reservoir permeability case. This reveals the last six wells to start injecting account for only 10% of the total mass of CO<sub>2</sub> injected. While these issues regarding “inefficient” wells, may impact the magnitude of the effect on “cost”, the relative ranking of each parameter should remain the same (as the inefficient wells only open in cases where injectivity is poor anyway).

Porosity and compressibility also impact injectivity by changing how the pressure builds up in the Blocky Sandstone Reservoir, and in the Transition Zone and Ultimate Seal. Lower porosity or compressibility is associated with a larger pressure increase and thus poorer long term injectivity. The effect appears less significant than for the permeability terms, despite the high and low porosity values in this study appearing to represent more extreme values than the permeability estimates.

Poorer injectivity was also associated with lower residual water saturation. This effect can be explained by considering the relative permeability curves in Figure 137. Reducing the residual water saturation in the simulations “stretches” the curve. This means the relative permeability to CO<sub>2</sub> remains lower for longer (as the saturation increases) and thus the effect appears similar to the case with lower relative permeability to CO<sub>2</sub>.

**Figure 164** Cumulative injection versus time for the 12 wells across the two southern notional injection sites in the MKTMK extended — low reservoir permeability case. Note that six of the 12 wells inject for less than 20 years (injection ends in 2088), and inject less than 30 Mt in total, or around 10% of the total injection for all 12 wells.



Other parameters that have significant impact on injectivity were those associated with the wells and how they were controlled. Reducing the injection pressure, whether by reducing the wellhead pressure for the MKTMK extended case, or by reducing the bottomhole pressure (fracture pressure) in the MKMK case, reduced the mass of CO<sub>2</sub> injected per well. The simulated injected mass per well for the MKTMK extended case with low wellhead pressure constraint (15,000 kPa) was around 40% of the reference case value, which had a wellhead pressure constraint of 20,000 kPa. Reduced tubing sizes (equivalent to 4.5" and 5.5" tubing) were also associated with reduced injection rates and increased well counts compared to the reference case (7" tubing).

Aside from a reduced bottomhole pressure limit, which would be dependent on the fracture pressure determined during appraisal, the other well design and control parameters would need to be investigated as part of an optimisation process once the properties of the subsurface, and the project constraints, are better understood.

Overall, this sensitivity study highlights the importance of permeability, including relative permeability, in relation to the well counts required for any large-scale CCS project targeting the Blocky Sandstone Reservoir. The vertical permeability of the Transition Zone is also very important, as increased permeability in this interval allows fluids (mainly water) to migrate into the Transition Zone, reducing the pressure increase in the Blocky Sandstone Reservoir around the injection wells and allowing wells to inject at higher rates.

#### 4.12.1.2 Containment (plume spread)

To assess the impact of each parameter on plume spread, the area of the plume of supercritical CO<sub>2</sub> in the top model layer of the Blocky Sandstone Reservoir was calculated at each time step, using a cut off of 0.1% saturation of CO<sub>2</sub> to define the limit of the plume. Example plots indicating the smallest (high porosity) and largest (low porosity) supercritical CO<sub>2</sub> plumes at the northern notional injection site 100 years after injection ends are shown in Figure 165 for the MKMK cases, and in Figure 166 for the MKTMK extended cases. A comparison of the overall smallest and largest plumes is shown in Figure 167. To give some sense of scale, Figure 168 shows the plumes at all three notional sites for the MKMK reference case, relative to the Blocky Sandstone Reservoir and model boundaries. For reference, the largest total plume area across all three notional injection sites for any of the cases was around 490 km<sup>2</sup>, which is just over 1% of the total area of the Blocky Sandstone Reservoir (48,815 km<sup>2</sup>).

In all cases, the plume of supercritical CO<sub>2</sub> spread around the wells, but didn't migrate away, remaining in the area around the notional injection sites throughout the simulated injection period, and 100 years post-injection. This is likely due to the relatively high density of CO<sub>2</sub>, and low dip around the notional injection sites (which was one of the criteria used to select the sites), reducing migration due to buoyancy effects.

**Figure 165** Supercritical CO<sub>2</sub> plumes at the northern notional injection site, 100 years after injection ends for MKMK-high porosity and MKMK-low porosity cases. Colour in first two plots indicates gas saturation, with grey indicating areas with saturations below the 0.1% cut off.

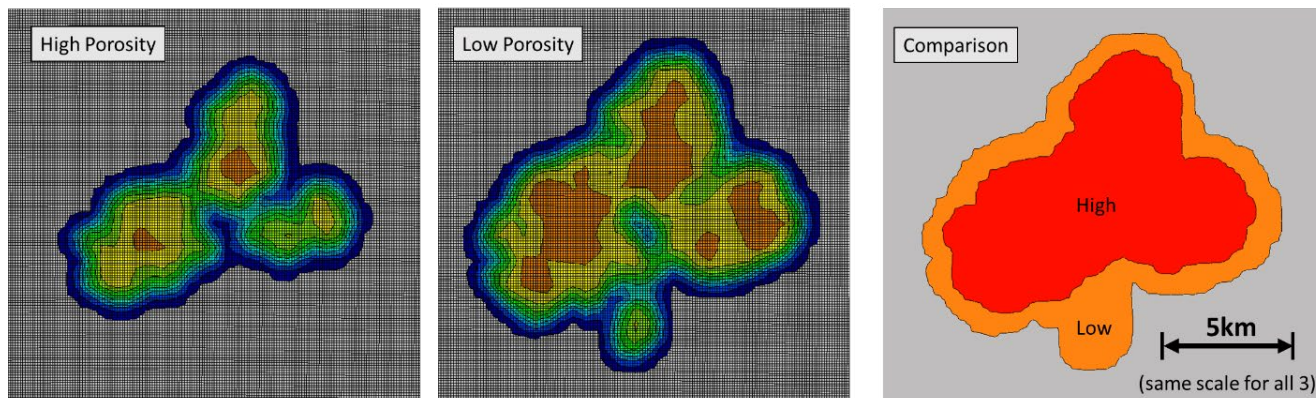


**Figure 166** Supercritical CO<sub>2</sub> plumes at the northern notional injection site, 100 years after injection ends for MKTMK-high porosity and MKTMK-low porosity cases. Colour in first two plots indicates gas saturation, with grey indicating areas with saturations below the 0.1% cut off.

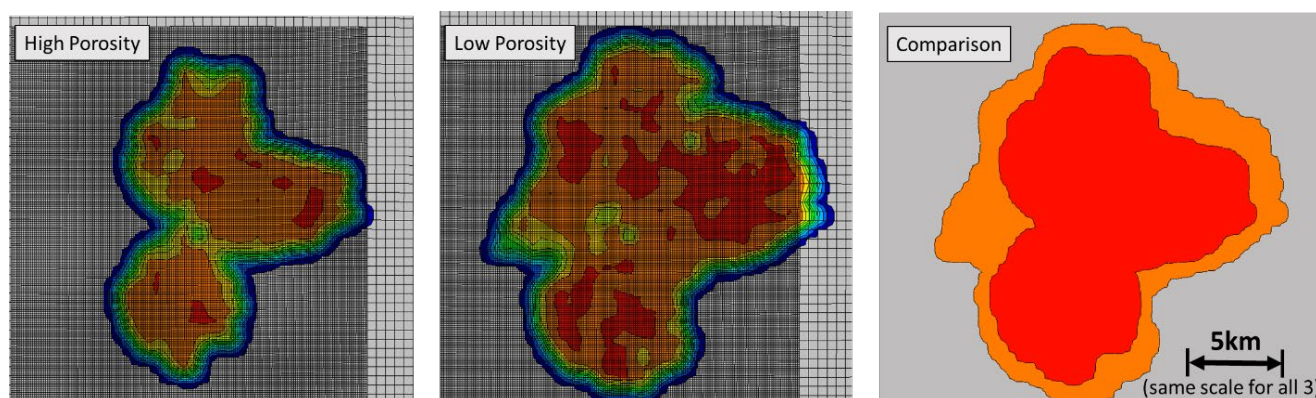


**Figure 167** Comparison for the Supercritical CO<sub>2</sub> plumes at the northern notional injection site, 100 years after injection ends for MKMK-high porosity and MKTMK-low porosity cases. These were the smallest and largest plume sizes respectively. Colour in first two plots indicates gas saturation, with grey indicating areas with saturations below the 0.1% cut off.

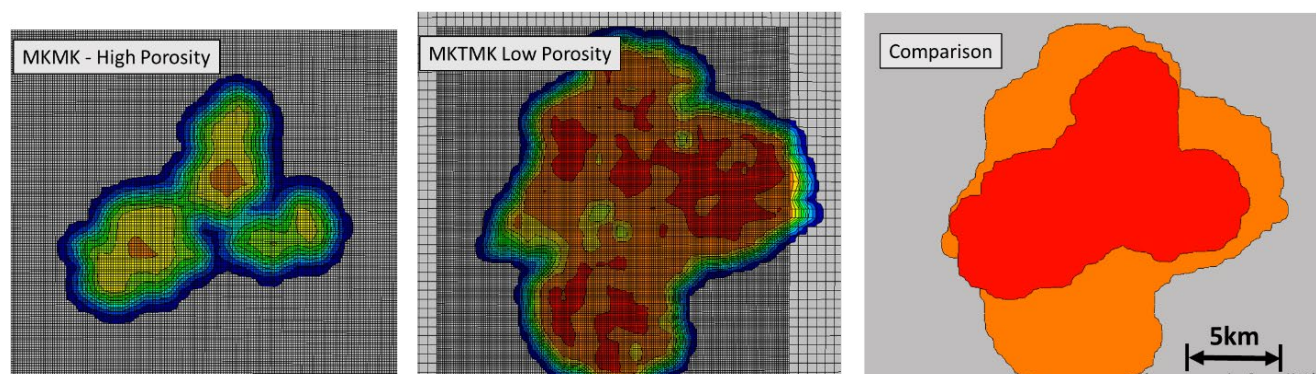
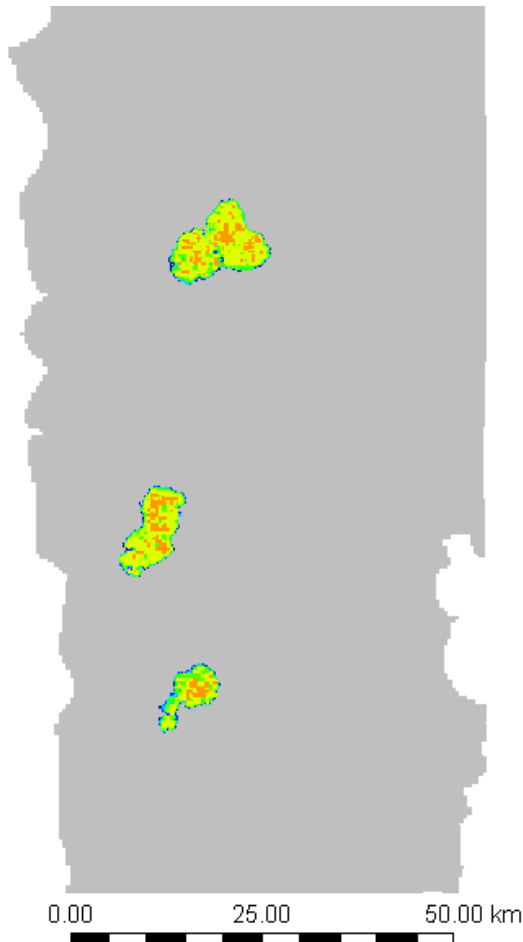


**Figure 168** MKMK — reference case, supercritical CO<sub>2</sub> plume 100 years after injection ends compared to Blocky Sandstone Reservoir in the UQ-SDAAP notional injection sector model to give indication of scale. The plume around the northern notional injection site in this figure is somewhere between the plume sizes shown in Figure 165.



The total supercritical CO<sub>2</sub> plume area across all three notional injection sites was plotted against time to give some indication of how the various parameters impact not only the plume size, but also the plume growth during and after injection. Figure 169 and Figure 170 show these plots for all notional injection sites combined for the MKMK and MKTMK extended cases respectively. Figure 171 shows the equivalent plot for only the northern notional injection site in the MKTMK cases. To give some perspective on the scale of the plumes, the right-hand axis in Figure 171 indicates the equivalent radius of a circular plume with the same area as those simulated.

These results indicate that the pore space available for CO<sub>2</sub> to occupy, which is affected by porosity and residual water saturation, has the most significant impact on the simulated plume area. The overall plume area at the top of the Blocky Sandstone Reservoir was simulated to be 1.4 times larger for the low porosity case than the reference case model, and nearly 1.7 times larger than the high porosity case.

The other properties which most significantly impacted plume area were the maximum relative permeability to CO<sub>2</sub>, and the reservoir temperature. Lower reservoir temperatures would be associated with smaller plume areas as the higher density of CO<sub>2</sub> under these conditions means the same mass of CO<sub>2</sub> would take up less total volume in the reservoir. The higher density of the CO<sub>2</sub> would also mean there was less buoyancy acting to drive CO<sub>2</sub> towards the top of the reservoir, or up-dip.

**Figure 169** Supercritical CO<sub>2</sub> plume areas versus time for the MKMK cases. Darker grey area indicates injection period. Black line is reference case. Dashed lines are those where desired injection rate could not be achieved due to poor injectivity and thus less CO<sub>2</sub> was injected in total (e.g. very low permeability case). Key parameters (those with most significant impact on plume area) are indicated, along with area of plume as a percentage of reference case. Swr is residual water saturation. Krgmax is the maximum relative permeability to CO<sub>2</sub>.

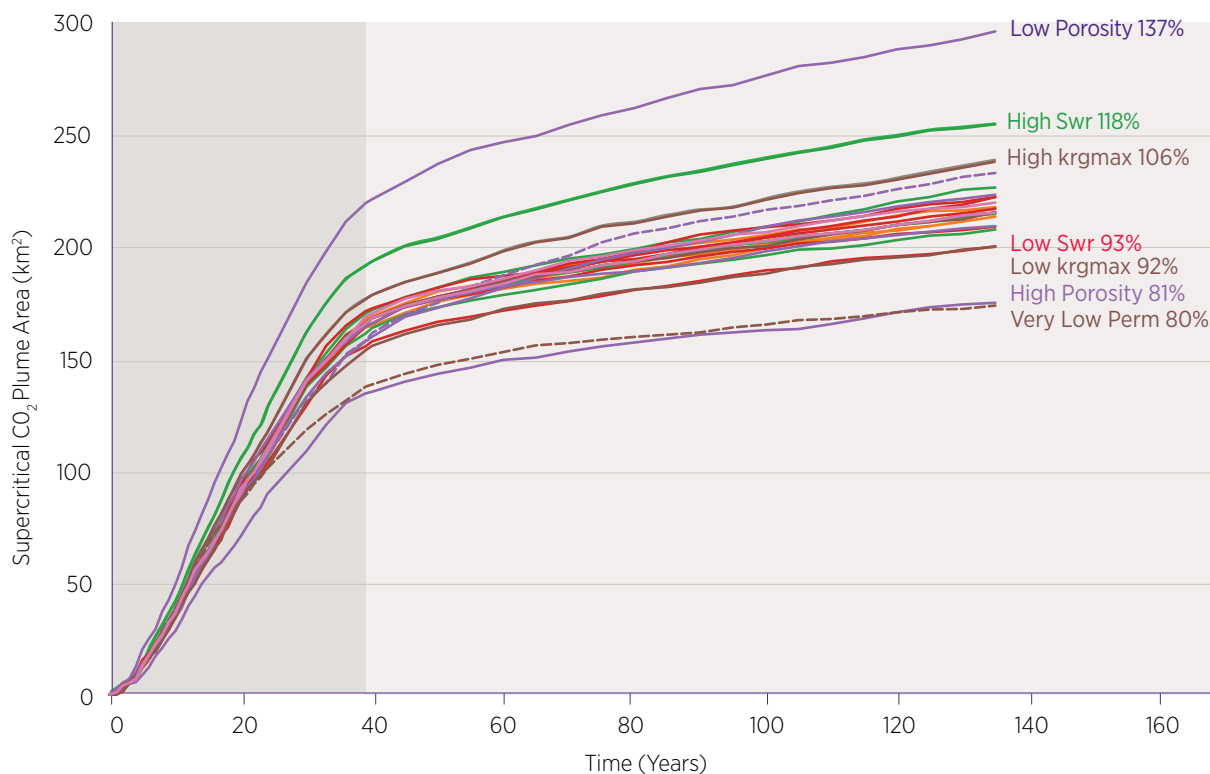


**Figure 170** Supercritical CO<sub>2</sub> plume areas versus time for the MKTMK cases. Darker grey area indicates injection period. Black line is reference case. Dashed lines are those where desired injection rate could not be achieved due to poor injectivity and thus less CO<sub>2</sub> was injected in total. Key parameters (those with most significant impact on plume area) are indicated, along with area of plume as a percentage of reference case. Swr is residual water saturation. Krgmax is the maximum relative permeability to CO<sub>2</sub>.

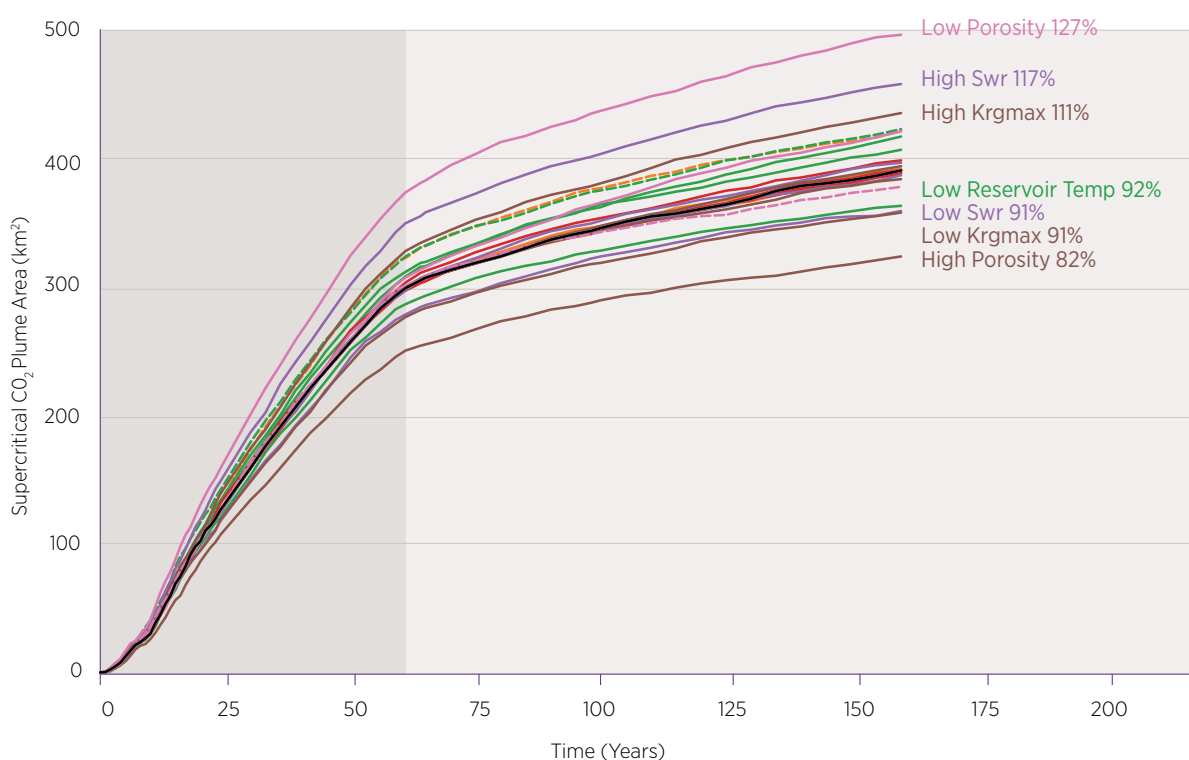
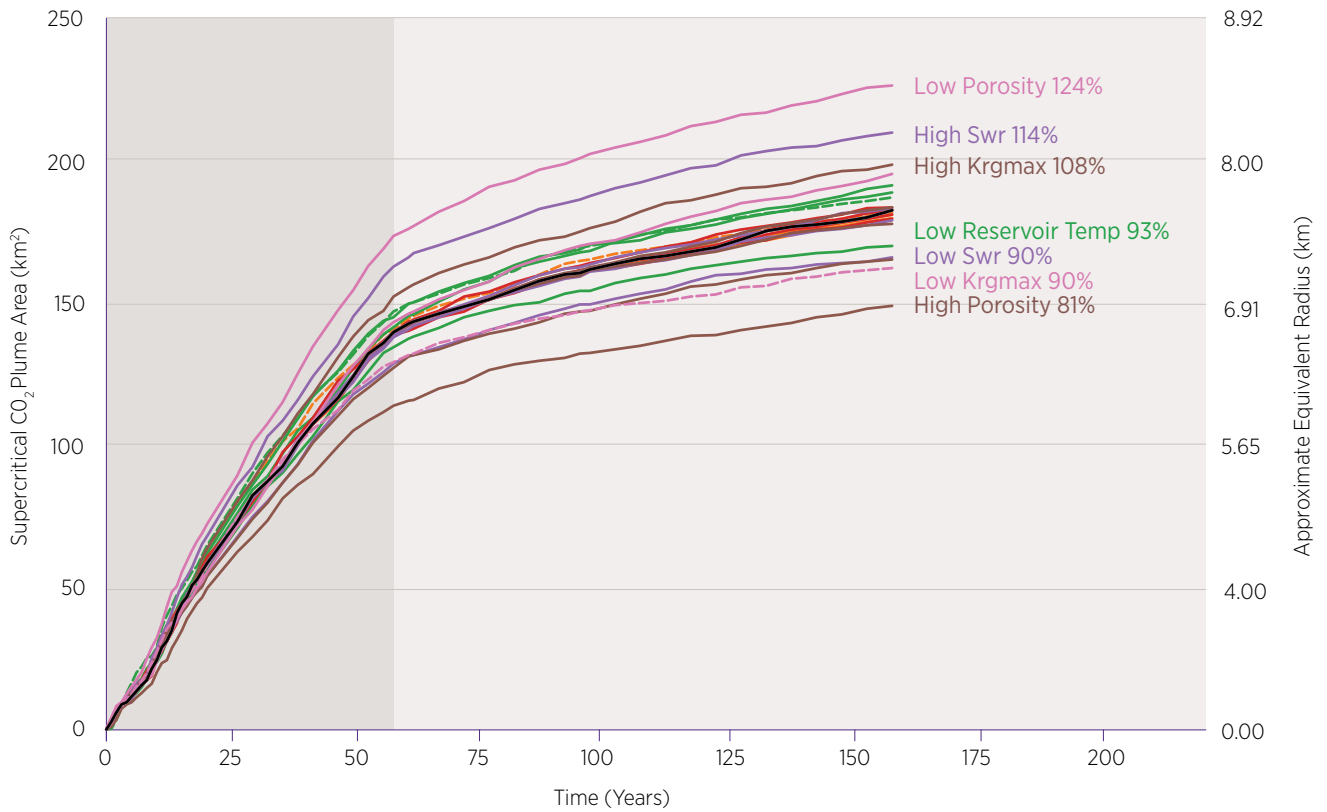


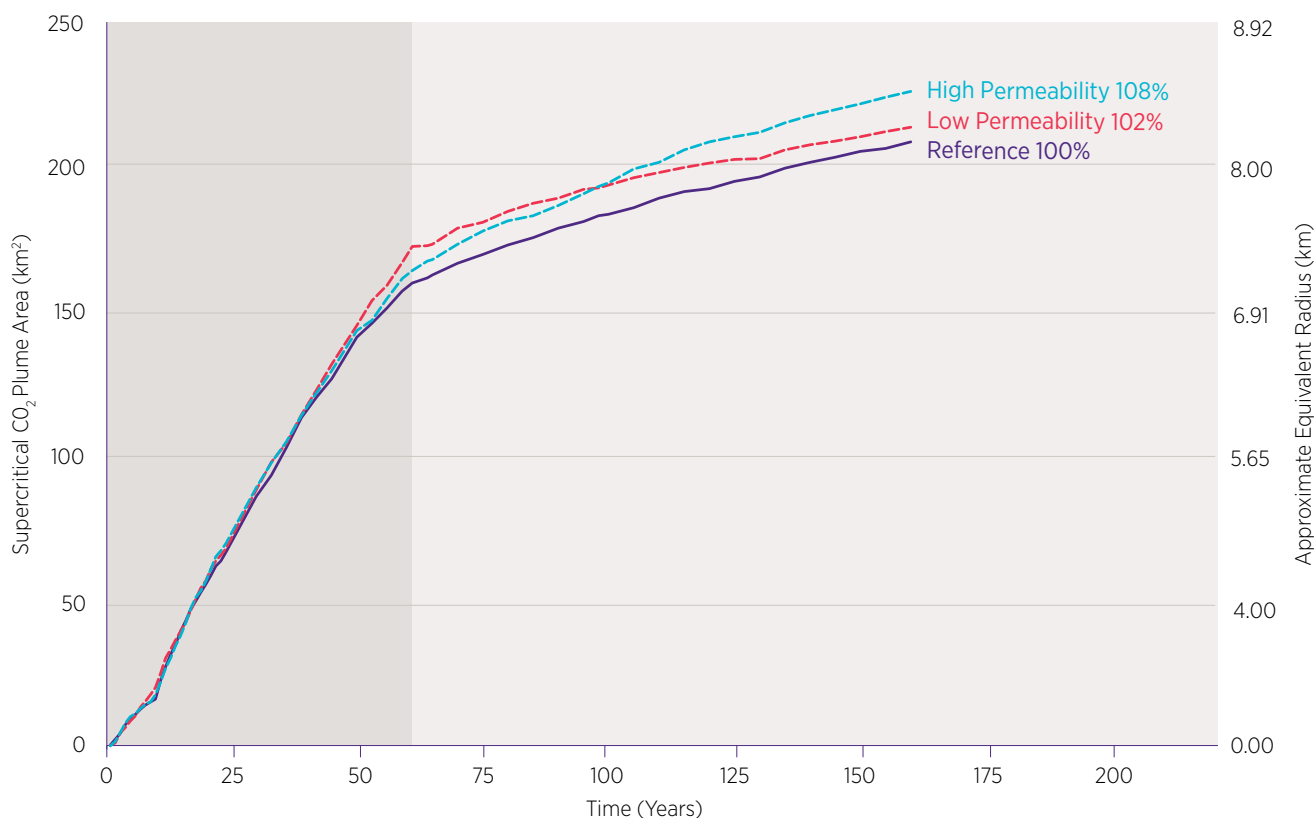
**Figure 171** Supercritical CO<sub>2</sub> plume areas at the northern notional injection site versus time for the MKTMK cases. Darker grey area indicates injection period. Black line is reference case. Dashed lines are those where desired injection rate could not be achieved due to poor injectivity and thus less CO<sub>2</sub> was injected in total. Key parameters (those with most significant impact on plume area) are indicated, along with area of plume as a percentage of reference case. Swr is residual water saturation. Krgmax is the maximum relative permeability to CO<sub>2</sub>.



Predictably, given the highly homogenous nature of the Blocky Sandstone Reservoir, permeability appears to have little impact on plume area, apart from in the low permeability cases where injectivity is limited so much that the total mass of injected CO<sub>2</sub> is decreased and thus the plume area also decreases. However, permeability does have an important impact on plume behaviour, particularly after injection ends. Figure 172 shows the combined plume area around both southern notional injection sites for the high and low permeability, and reference cases for the MKTMK schedule.



**Figure 172** Supercritical CO<sub>2</sub> plume areas at the southern notional injection site versus time for the MKTMK permeability cases. Darker grey area indicates injection period. Note that the low permeability case has the largest plume area at end of injection (due to higher well count), in but the high permeability case, the plume grows more quickly after injection stops.



Both the high and low permeability cases resulted in larger CO<sub>2</sub> plumes around the southern notional injection site than the reference case. For the low permeability case, this seems to be due to the higher number of wells, while for the high permeability case the CO<sub>2</sub> is more mobile, migrating further from the wells that are injecting. After injection stops, the effect of permeability becomes clear. The plume in the low permeability case does continue to grow, but more slowly than the high permeability case. The plume area was similar at the end of the simulations (100 years). This variation in plume growth rates after injection stops indicates the important role that permeability plays in longer term plume stability.

There would also be slightly larger areas around the notional injection sites where water would have increased levels of dissolved CO<sub>2</sub> (Figure 173). Using a cut-off for molality of 0.002 mol/kg, the area at the top of the Blocky Sandstone Reservoir with elevated levels of dissolved CO<sub>2</sub> was calculated. Figure 174 shows this area versus time for the MKTMK cases. This indicates that porosity is again the key parameter, due to its effect on the available pore space. Aside from porosity, the area with increased CO<sub>2</sub> molality appears to be most significantly affected by changes in the well count. For this reason, cases where more wells were required, such as cases with low wellhead pressure and smaller tubing, had larger areas with increased molality.

**Figure 173** Comparison of the supercritical CO<sub>2</sub> plume (red) with molality (green/blue colours) around the northern injection site in the MKTMK-high porosity case. The supercritical CO<sub>2</sub> plume is the same as that shown on the left in Figure 166. The minimum contour for the molality plume is at 0.002 mol/kg, and the darkest blue outside this indicates areas where CO<sub>2</sub> levels have not increased during injection.

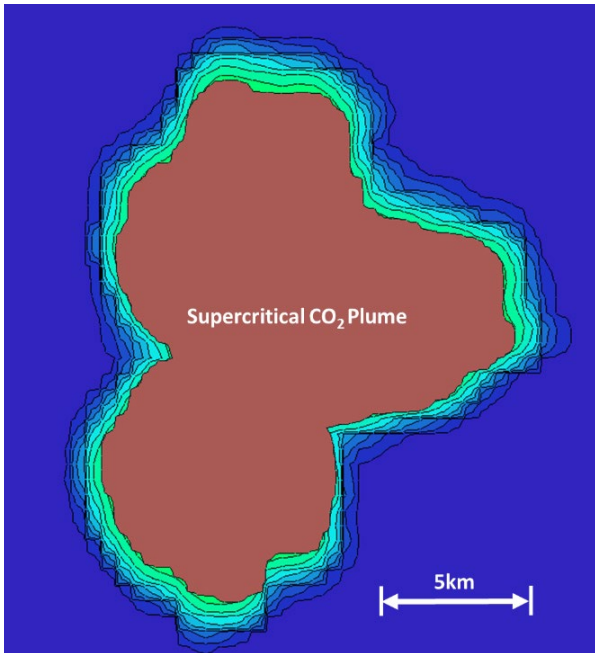
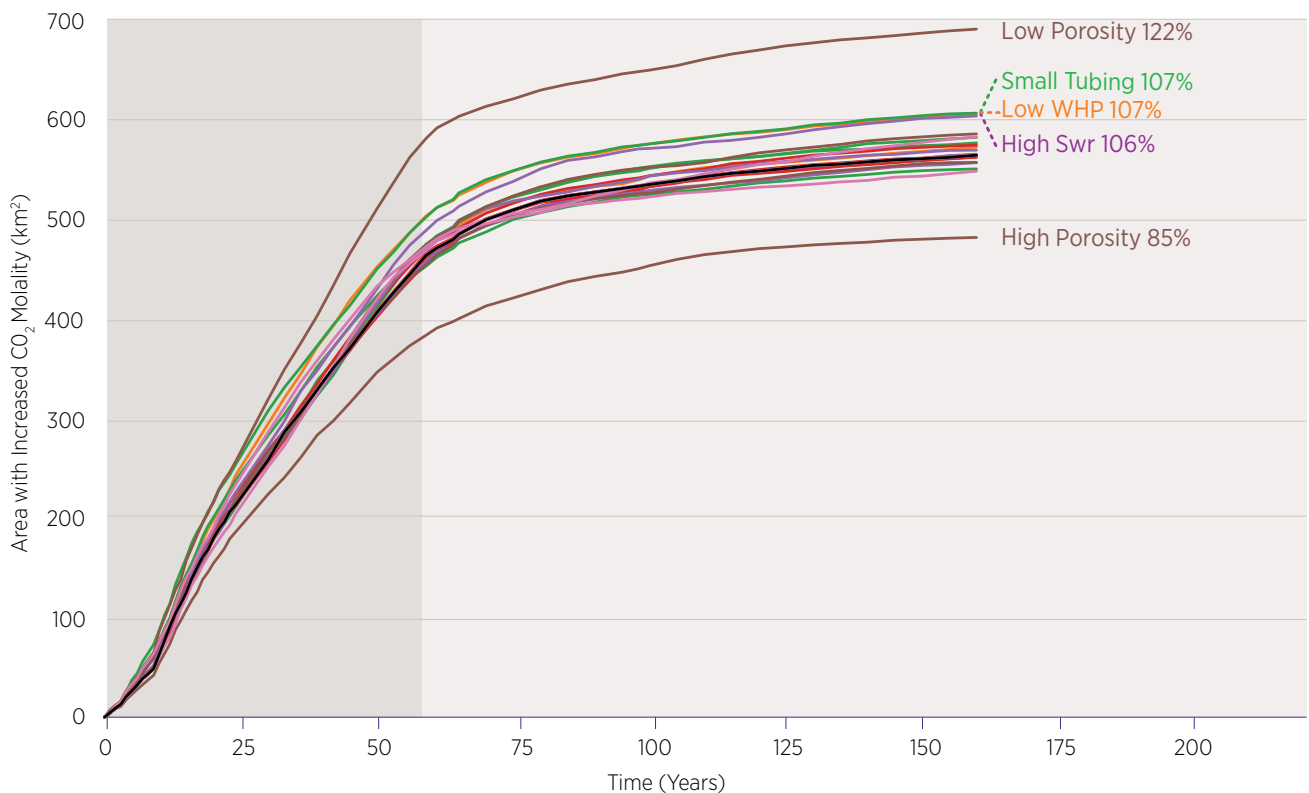


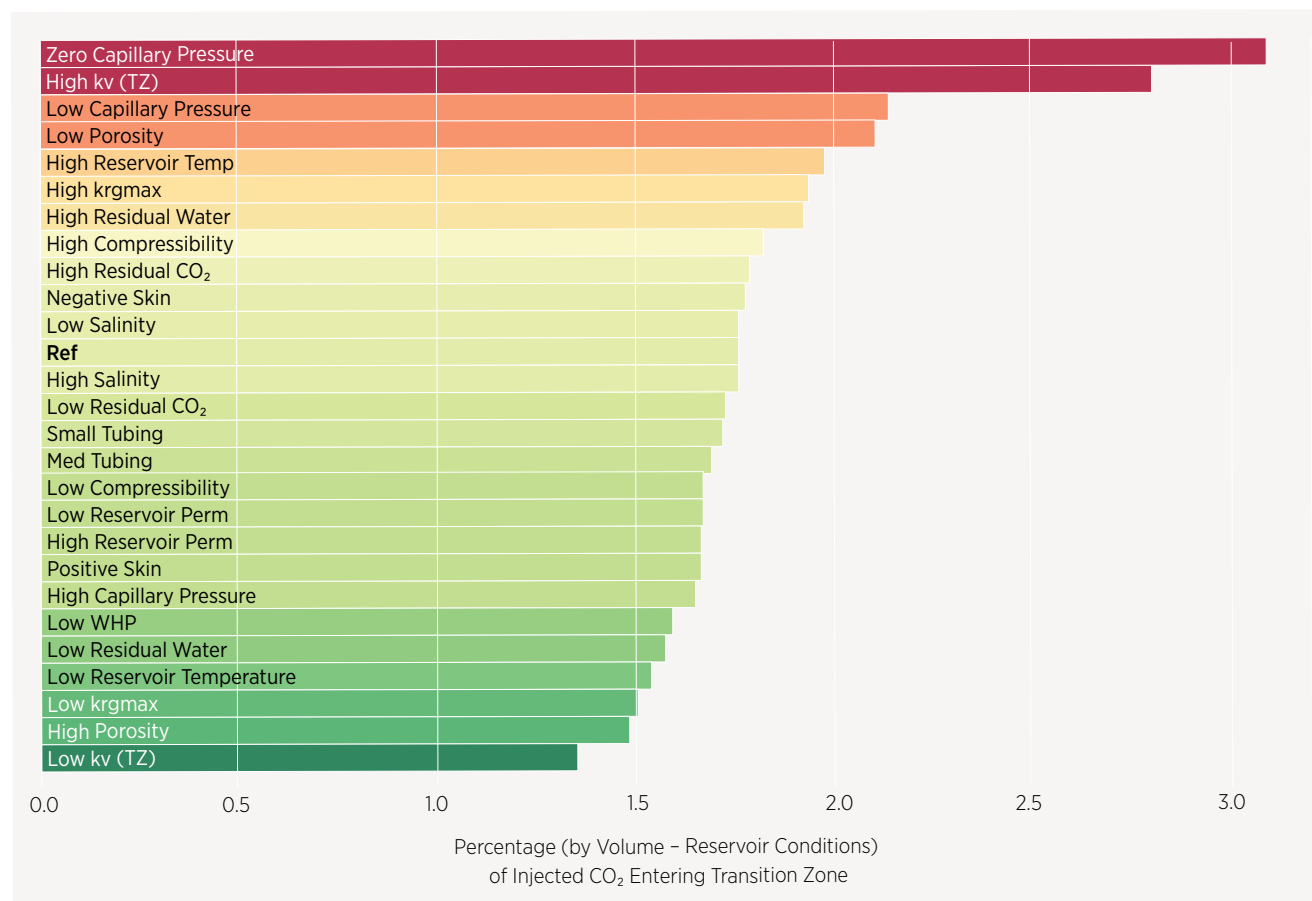
**Figure 174** Total area of increased molality in the top layer of the Blocky Sandstone Reservoir, plotted versus time for the MKTMK cases. The dark grey colour indicates the injection period. Key parameters (those with most significant impact on the area) are indicated, along with area of plume as a percentage of reference case.



The MKMK scenario simulations using the reference case properties, resulted in a plume of supercritical CO<sub>2</sub> which reached a maximum distance of 8.2 km from the northern notional well pad, 100 years after injection stopped. Simulation results showed water with increased levels of dissolved CO<sub>2</sub> approximately 500 m beyond the supercritical plume, at a distance of 8.7 km from the well pad. It is important to note that these are the distances from the well pad, not from the completion. In the models, the toe of each horizontal well was around 5.5 km from the location of the notional well pad and the supercritical CO<sub>2</sub> plume extended only 2.7 km beyond the end of one of the wells. For the MKMK reference case, the simulated plume of supercritical CO<sub>2</sub> reached a maximum distance of 10.4 km from the well pad 100 years after injection stopped, with increased levels of dissolved CO<sub>2</sub>, 12.3 km from the well pad.

As well as the lateral containment, the impact of the various parameters on vertical containment was assessed by comparing the percentage (by volume at reservoir conditions) of the injected CO<sub>2</sub> that entered the Transition Zone by the end of the simulations, 100 years after injection ended (Figure 175). This value for the MKMK cases varied between 1.3%, for the low vertical permeability in the Transition Zone, and 3.1%, for the case with zero capillary pressure. For comparison, the more detailed Transition Zone test models presented in Rodger et al. 2019c resulted in between 0.45% and 3.6% of the injected CO<sub>2</sub> entering the Transition Zone. The slight differences between these values from the two studies may be because the models in Rodger et al. 2019c had higher (and homogenous) permeability in the Blocky Sandstone Reservoir, and included a case with *both* higher permeability in the Transition Zone *and* zero capillary pressure.

**Figure 175** Percent by volume at reservoir conditions of injected CO<sub>2</sub> that migrates into the Transition Zone for the MKMK cases.



While the cases with zero capillary pressure and high vertical permeability in the Transition Zone resulted in similar percentages (2.8% and 3.1% respectively) of the injected CO<sub>2</sub> entering the Transition Zone, there were important differences in this behaviour. In the case with high vertical permeability in the Transition Zone, more CO<sub>2</sub> migrated into the Transition Zone during the injection period when pressures are high enough to overcome capillary threshold pressures, but after injection stops the flow rate of CO<sub>2</sub> declines rapidly, limited by capillary pressures. In the case with zero capillary pressure, there is less migration during the injection period (limited by the lower permeability), but buoyancy driven migration continues after injection stops, ultimately resulting in a higher percentage of the injected CO<sub>2</sub> entering the Transition Zone.

The distance the supercritical CO<sub>2</sub> migrates vertically is also different in these cases. In the case with zero capillary pressure, CO<sub>2</sub> enters the Transition Zone across a larger area around the injection wells, but the very low permeability in the Transition Zone limits the vertical migration, and the CO<sub>2</sub> does not migrate beyond the lowest 15 m of the Transition Zone throughout the simulation. This is again consistent with the models presented in Rodger et al. 2019c. In the case with high vertical permeability in the Transition Zone, supercritical CO<sub>2</sub> flowed around 28 m into the Transition Zone, albeit only in very small areas. It is important to note that this was still 80 m below the base of the Ultimate Seal.

## 4.12.2 Summary of sensitivity analysis

The results of several simulations have been presented, with the intention of identifying parameters that would most affect the likelihood of success for a large-scale CCS project targeting injection in the Blocky Sandstone Reservoir, particularly in relation to two key criteria: injectivity and containment.

These simulations indicate the horizontal permeability in the Blocky Sandstone Reservoir is the most important factor influencing injectivity. Halving the permeability meant that even by using twice as many wells, it was not possible to sustain the required injection rates throughout the injection period. The maximum relative permeability to CO<sub>2</sub>, and the vertical permeability in both the Blocky Sandstone Reservoir and Transition Zone also affected injectivity, but less so.

Porosity had the most significant effect on the plume spread, both of supercritical CO<sub>2</sub> and water containing elevated levels of dissolved CO<sub>2</sub>. Residual water saturation, which can be considered to reduce the pore volume available to CO<sub>2</sub>, and reservoir temperature, alters the density, and thus total volume and buoyancy of CO<sub>2</sub> in the reservoir. One other key result from these simulations was that the plume of supercritical CO<sub>2</sub> did spread around the wells, but didn't migrate away, remaining in the area around the notional injection sites throughout the simulated injection period, and 100 years post-injection. This is likely due to the relatively high density of CO<sub>2</sub> and low dip around the notional injection sites (which was one of the criteria used to select the sites), reducing migration due to buoyancy effects.

The effect of each parameter on vertical containment was assessed by comparing the percentage of the injected CO<sub>2</sub> that managed to migrate upwards into the Transition Zone during the simulations. This revealed that, unsurprisingly, the Transition Zone vertical permeability and wettability/capillary pressure were the most significant parameters. However, it is important to note that only 3.1% of the total injected CO<sub>2</sub> had migrated into the Transition Zone 100 years after injection stopped, even in the worst-case (zero capillary pressure) simulated. The CO<sub>2</sub> did not manage to migrate beyond the lowest 25 m of the Transition Zone in any of the simulations.

It must be pointed out that these models did not test the full parameter space, and it may be that different combinations of parameters could lead to results outside of those presented here. There is also a possibility that the effects of reservoir heterogeneity were not captured in this large-scale model, and it would seem sensible to re-assess plume spread, and vertical CO<sub>2</sub> migration, using more detailed models when more information is available regarding the reservoir properties. It would also seem beneficial to investigate the longer-term behaviour of the CO<sub>2</sub> plume post-injection. Even 100 years after injection, the plume was still growing (but slowly).

Another limitation of this study is that it does not address any of the uncertainties regarding the structure of the Blocky Sandstone Reservoir, Transition Zone and Ultimate Seal. The grid in all the simulations was the same, and thus could not be used to test the impacts of changes in dip, reservoir thickness, or the location of the pinch-out of the Blocky Sandstone Reservoir. These are all subject to uncertainties, such as those relating to seismic depth conversions and seismic resolution, particularly in areas where there is limited well control.

Overall, this study suggests permeability, both in the Blocky Sandstone Reservoir and Transition Zone, are extremely important in terms of both injectivity and containment, and should be tested as part of any appraisal plan. Multiphase behaviour (i.e. relative permeability and capillary pressure curves) also plays a very important role in both key criteria. It would seem prudent to take core samples from the Blocky Sandstone Reservoir and Transition Zone to test these behaviours. These core samples would also allow porosity (the key factor when considering plume spread) to be constrained.

The other parameters which would appear to most significantly impact a large-scale CCS project were the engineering/design aspects of the project, such as tubing sizes and wellhead pressure constraints. These would need further investigation as part of a detailed optimisation study post appraisal. Details of the sensitivity analysis can be found in Rodger et al. 2019f.

#### The results of the sensitivity analysis indicates that:

1. Porosity had the most significant effect on the plume spread, both of supercritical CO<sub>2</sub> and water containing elevated levels of dissolved CO<sub>2</sub>
2. The plume of supercritical CO<sub>2</sub> did spread around the injection wells up to 10 km, but didn't migrate away, remaining in the area around the notional injection sites throughout the simulated injection period, and 100 years post-injection. This is likely due to the relatively high density of CO<sub>2</sub>, and low dip around the notional injection sites, thus reducing migration due to buoyancy effects
3. The rim of dissolved CO<sub>2</sub> in formation water characterised by reduced pH is between 500 m and 2 km at the end of the 100 year modelling period, depending on the injection scenario
4. Transition Zone vertical permeability and wettability/capillary pressure were the most significant parameters to vertical migration of CO<sub>2</sub>. However, only 3.1% of the total injected CO<sub>2</sub> migrated into the Transition Zone 100 years after injection stopped, even in the worst-case (zero capillary pressure) simulated. In the worst-case scenario, the CO<sub>2</sub> did not migrate beyond the lowest 25 m of the Transition Zone, well below the base of the Ultimate Seal

## 4.13 Notional injection modelling and FDP sensitivity analysis – groundwater impacts

**Sensitivity analysis of predicted impacts to groundwater pressures shows that for the parameter ranges considered, the timing of impact is affected significantly, but the overall magnitude of impact changes relatively little.**

The groundwater model sensitivity analysis follows the low and high permeability ranges explored by the notional injection sector model (section 4.8). The notional injection sector model considers average low, reference (mid) and high horizontal intrinsic permeabilities to be 22, 43 and 87 mD respectively. The low and high cases are therefore effectively multipliers 0.5 and two times the reference case.

The groundwater model adopts a simple reproduction of this range, and extends the sensitivity analysis to include the vertical and horizontal hydraulic conductivity components of the Blocky Sandstone Reservoir, Transition Zone, Ultimate Seal and the under and overlying layers representing the Hutton Sandstone and Moolayember Formation. For the low case, reference hydraulic conductivities are multiplied by a factor of 0.5. For the high case they are multiplied by a factor of 2.

### 4.13.1 Sensitivity analysis results

Sensitivity results are presented in terms of hydrographs at key well locations of increased groundwater head due to injection. The low and high permeability cases are plotted together with the reference groundwater model results presented in section 4.11. Figure 176 and Figure 177 present hydrographs for known wells in the Precipice Sandstone (upper Blocky Sand Reservoir) and Hutton Sandstone aquifers.

These plots show:

- High permeability leads to injection pressure increases propagating more quickly within the Blocky Sandstone Reservoir to the locations of known bores
- In the high permeability case and for wells within approximately 50 km of the injection sites, the maximum pressure increases are reduced slightly due to more rapid propagation of pressure beyond the wells, and pressures decline more quickly after injection. At wells further away (Kogan Creek and Miles Town Bore), maximum pressure changes are similar between the high and reference permeability cases
- In the low permeability case, it takes longer for pressure increases to reach the known well locations. Maximum impacts are higher at well locations with 50 km of injection sites, and lower at a further distance
- Whilst the timing of maximum pressure rise varies between the sensitivity scenarios, the absolute magnitude of pressure increase is similar
- In the Hutton Sandstone, the permeability sensitivity cases change the timing of pressure increases, but the overall magnitude of impact remains similar

**Figure 176** Sensitivity of predicted groundwater head increase to low, reference and high permeability cases in the upper Precipice Sandstone (upper Blocky Sandstone Reservoir) during and after injection for select wells.

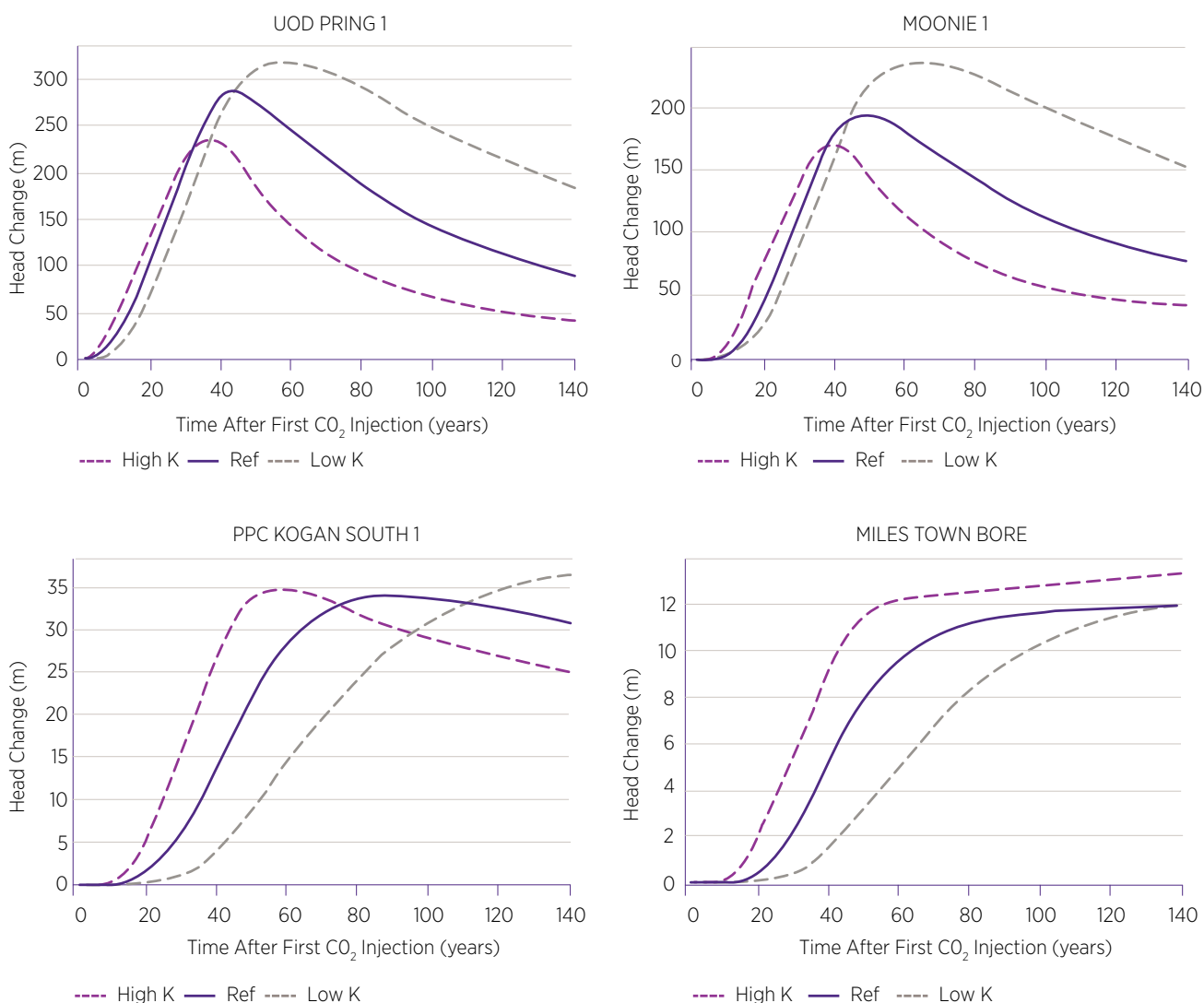
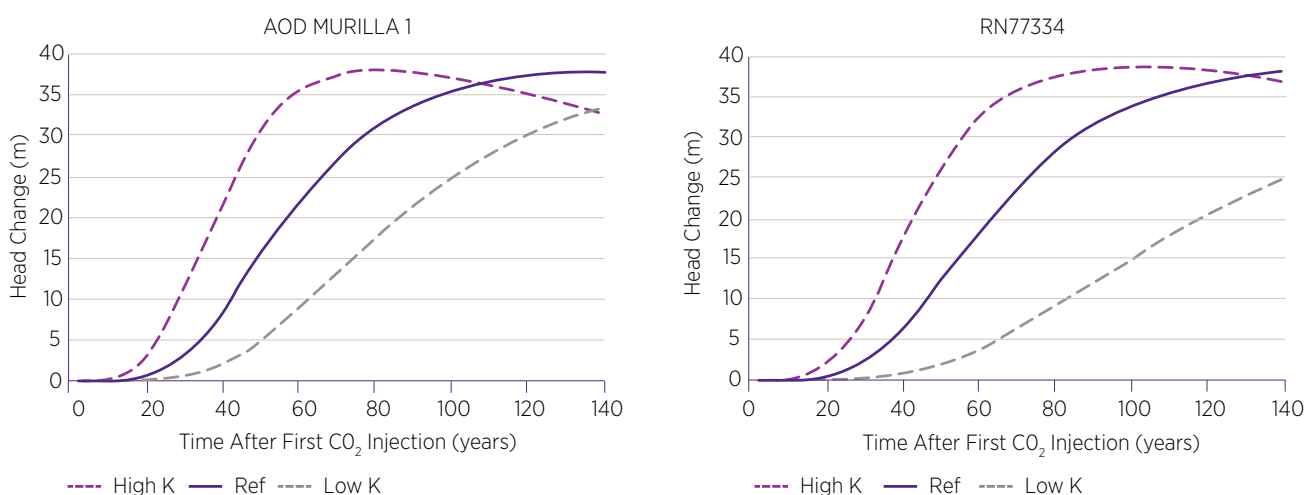


**Figure 177** Sensitivity of predicted groundwater head increase to low, reference and high permeability cases in the Hutton Sandstone (layer 1), during and after injection for selected wells.



## 4.13.2 Summary of sensitivity analysis and conclusions

The groundwater modelling completed for the UQ-SDAAP project provides predictions of the impact on groundwater heads due to CO<sub>2</sub> injection. This approach is adopted to most clearly demonstrate the predicted propagation, magnitude and timing of groundwater head changes caused by the project. The modelling to date does not show the impacts in context of the natural flow systems within the Precipice and Hutton Sandstone aquifers and other units, or the influence of other known stresses on the system including: water extraction for industrial, agricultural and town water supplies; water extracted at the Moonie oil field; or the influence of managed aquifer recharge in the northern Surat Basin.

In May 2019, OGIA is due to release an updated Underground Water Impact Report based on their 2019 groundwater model of the Surat CMA that will provide a current understanding of the whole Surat Basin hydrogeological system. OGIA's work and a recently started University of Queensland project characterising the hydrochemistry of the Precipice Sandstone in the southern Surat Basin should provide the next steps in system understanding.

If CCS is to be developed in the deep southern depositional centre of the Surat Basin, the next groundwater modelling steps are to include the new information described above, the natural groundwater fluxes and the anthropogenic stresses of extraction and injection on the system. These will provide a more accurate distribution of hydraulic head with known major stressors representing the initial conditions for the carbon storage forward model.

**Site-specific data to better inform groundwater impact assessment is a key part of the recommended appraisal program (section 5.5). The groundwater model sensitivity analysis shows that the low and high permeability cases mainly change the timing of impacts propagating to known wells, without substantially altering the maximum pressure changes predicted.**

The overall assessment of groundwater impact modelling, including the sensitivity analysis, suggests the following conclusions and observations:

- The supercritical CO<sub>2</sub> plume remains within ~10 km radius of the injection sites after 100 years (~300 km<sup>2</sup> in area) within the Blocky Sandstone Reservoir
- The supercritical CO<sub>2</sub> plume migrates up to ~10 m vertically into the Transition Zone (even in a worst-case scenario), but remains ~80 m below the base of the Ultimate Seal after 100 years
- The pressure footprint defined by the area of 10 m or more groundwater head increase is approximately 90 km from the injection sites for both the Blocky Sandstone Aquifer and the Hutton Aquifer (an area of ~25,000 km<sup>2</sup>) after 100 years
- The pressure increase near the notional injection sites in the Blocky Sandstone Aquifer dissipates post-injection, and at 100 years the maximum pressure increase remains at ~100 m groundwater head in the Blocky Sandstone Reservoir and possibly ~40 m groundwater head in the overlying Hutton Sandstone
- The pressure increase continues to build and lasts longer further away from the injection sites in the Blocky Sandstone Reservoir and in the overlying Hutton Sandstone
- The pressure benefits to groundwater resources occur over a considerable geographic area (~25,000 km<sup>2</sup>) and last over a considerable period of time (>100 years) in both the Precipice Sandstone and Hutton Sandstone aquifers
- The maximum pressure increase in the vicinity of the Moonie Fault is ~200 m of groundwater head (~2,000 kPa) and the fault reactivation analysis suggested reactivation at ~30,000 kPa pressure increase. The fault reactivation risk is therefore low (section 4.5)
- The estimated change in flux across the Ultimate Seal is low and presents an equivalently low risk of low water quality leakage from the Ultimate Seal into the overlying Hutton Sandstone
- Future work should examine the location of Precipice Sandstone and Hutton Sandstone aquifer related groundwater dependant ecosystems (GDE's) and evaluate them in relation to the modelled pressure increase at 100 years, and the associated increased discharge
- The risk of lateral changes of water quality within the Precipice Sandstone aquifer remains untested due to a lack of high confidence water quality data at the nominal sites. A current project by ANLEC R&D is gathering this data over the next two years and once achieved this risk could be evaluated in the future. A well is required fully to inform this risk (section 5.5)
- The previous work on inverse modelling of MAR (section 4.6.3) would indicate a roughly 1 m groundwater head increase at the northern boundary of the southern depositional centre. The risk of significant pressure interference between MAR in the northern depositional centre and carbon storage in the southern depositional centre is considered low
- A future work package could take the groundwater model outcomes for the pressure distribution in the Precipice Sandstone and Hutton Sandstone aquifers at 100 years and evaluate the degree of ground heave expected. This could prove to be a useful monitoring tool of CO<sub>2</sub> plume distribution using InSAR



## 4.14 Retrofit deployment, hub scenarios, costs and cash-flow

Retrofit options have been investigated for the three modern supercritical coal-fired power plants in the region. These were high level scoping studies. Deployment has been modelled in which the plants are partially retrofitted in sequence. This minimises disruption to baseload power generation, shares the disruptive load across plants/owners, allows for maximum learning between retrofits and also allows for a large investment to be broken down into several smaller incremental decisions points, each of which could see either the full deployment, halt, pause or continue. A series of plausible scenarios exist with significant opportunity to accelerate deployment if required.

Given the injection rate constraints discussed earlier, a conservative, lowest risk, minimum footprint storage development could safely accept around 13 million tonnes pa (reference case reservoir). Therefore, it is feasible to capture and store the majority of the CO<sub>2</sub> emissions from these plants, starting from around 2032 up to (and beyond) their estimated technical lifetime. There is a possibility of significant injection potential remaining for 20-30 years beyond this date allowing for either extensions or for new builds or for capture from CCGT gas plants in the area. This would be pending the observed injection reservoir performance during initial stages.

### 4.14.1 Introduction

UQ-SDAAP is part of the ongoing development of carbon capture and storage (CCS) to help reduce emissions from fossil fuel in Australia. Detailed engineering studies of capture and transport options are beyond the scope of the UQ-SDAAP project. This chapter provides information and a high-level analysis on the post combustion capture elements of carbon capture and storage in the Surat Basin. Within an overall project development philosophy established for the project, this section also develops possible capture, retrofit roll-out sequencing options. Note that literature on Australian CCS costs were briefly reviewed early in this project (Ampofo and Garnett 2019). Wide ranges of input assumptions have been used in previous literature (ibid) and most cost or economic analyses have been very context specific or are too generic. However, for this section, useful and credible information was mostly sourced from more recent industry and government reports for capture plants (Gamma Energy Technology 2019). Transport costs were adapted (ibid) from Surat-specific estimates made for ZeroGen (Garnett et al. 2012). Storage costs were estimated based on recent, high level market information (Honari and Garnett 2019a) with surface facilities costs estimated by Advisian 2019.

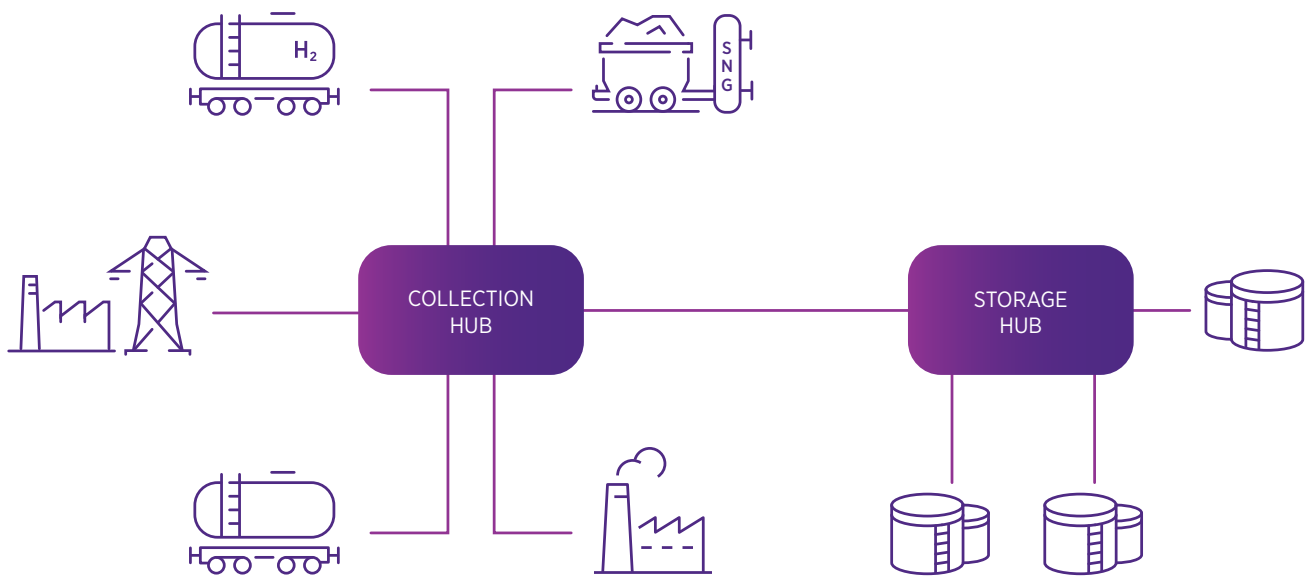
While many CCS applications do not have a strong commercial incentive currently, CCS is not an experimental technology. At scale, it has the capability to provide a competitive, carbon reduction option for reliable, high volume, 24-7 electricity from gas and coal-fired power plants. CCS is also suitable to decarbonise a number of existing and prospective emissions-intensive industries including natural gas and LNG production, iron and steel making, cement production, fertilisers, bio-ethanol, chemicals and textiles. CCS is also required in three of the four postulated hydrogen production mechanisms. Finally, the systematic retrofitting of CCS on the three modern power coal-fired plants in Queensland could both safeguard existing jobs as well as create new jobs during the construction and operations phases.

### 4.14.2 What is a hub and how does development start?

CCS hubs are central collection or storage distribution systems for CO<sub>2</sub>. A simplified concept schematic is shown in Figure 178 (GCCSI 2016). Collection and storage hubs provide point-to-point transportation for compressed/supercritical CO<sub>2</sub>, thereby reducing the risk and cost of transport infrastructure between the individual point-source emitters and individual points of injection into geological storage.

Hubs are very common in the natural gas distribution industry, where pipeline networks interconnect in order to bring together gas from many different production fields, or to distribute gas to dispersed markets. There are also many existing CO<sub>2</sub> hubs in the USA (Wallace, Goudarzi, Callahan and Wallace 2015) and Canada where mainly, but not solely, natural sources of CO<sub>2</sub> feed into enhanced oil recovery (EOR) developments (Peletiri, Rahmanian, and Mujtaba 2018).

**Figure 178** A CO<sub>2</sub> hub system, showing a collection and storage hub (GCCSI 2016).



The overall design of a CO<sub>2</sub> hub system needs to consider interaction of capture and the trade-offs in pipeline and injection design and operation (Greig, Bongers, Stot and Byrom 2016). Most importantly, the flow rate and operating pressure constraints required to inform the basis of (capture) design for any such hub are governed by the ability of the storage site(s) safely to receive CO<sub>2</sub> at sustained rates, and not by a target or *desired* capture rate. Overall, a hub is a rate constrained physical system, where the constraints are set by the natural (storage) resource. Until these storage characteristics are confidently known, the sizing of the capture elements cannot be properly designed.

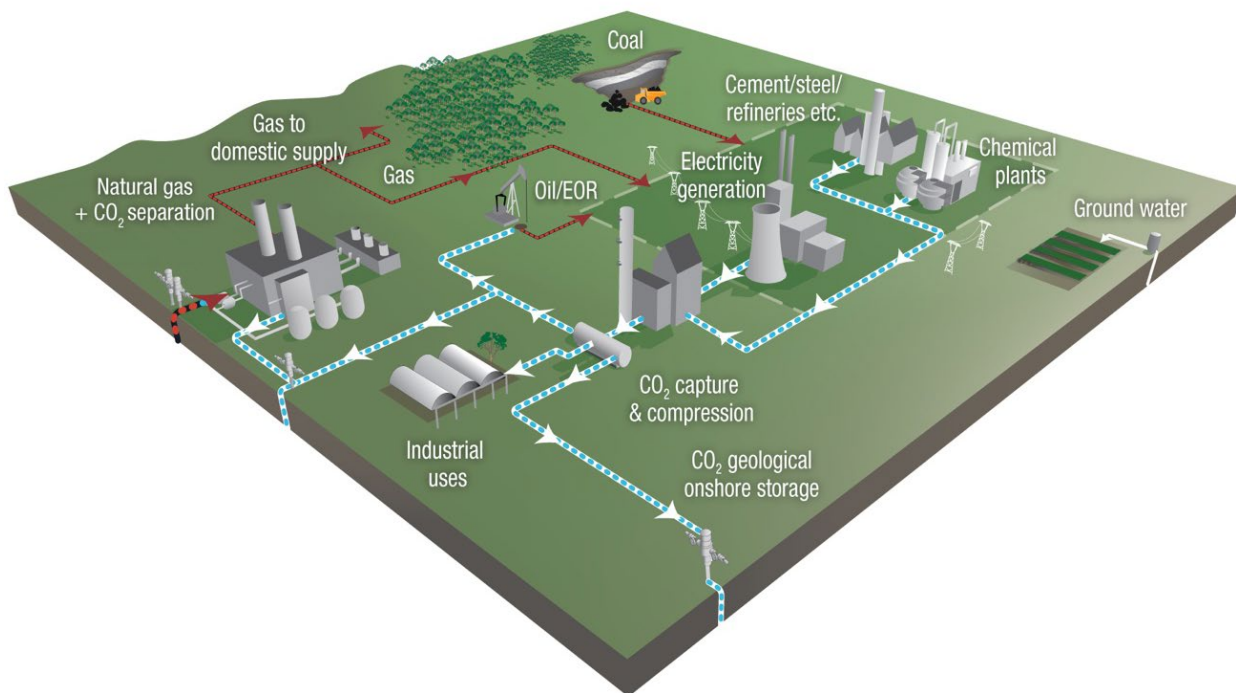
The establishment of a collection hub, such as the one conceptualised in Figure 179 (Bongers, Byrom, Malss and Constable 2017) is likely to occur over time. First, storage sites which can sustain large rates over many years need to be found and appraised or characterised with sufficient confidence to enable larger investment decisions in capture and transport. In other words, confidence in large sustained rate storage sites is required as a first step to enable and to size a hub.

Sections 4.5 to 4.12 indicate that safe storage may be attainable in the order of 10-13 million tonnes per year of CO<sub>2</sub> over a period of 30-40 years. Those assessments also indicate that impacts on groundwater quality are localised and wide-ranging pressure impacts could be managed and even beneficial.

However, additional technical confidence is required via further site-specific investment. This has been estimated (section 5.5) to be in the order of \$100 million of “at risk” investment over 3-4 years. There is also a scenario in which either the geology is found to be unsuitable and/or where a regulatory pathway cannot be clarified.

Notwithstanding this, if current assessments hold, the Surat Basin could enable a 30-40 year low emissions future for Queensland’s industry as a CO<sub>2</sub> storage hub. The region includes three modern coal-fired power stations, and a diverse number of other existing CO<sub>2</sub> sources, existing pipeline easements and a range of potential new projects that would be able to utilise the collection or storage hub.

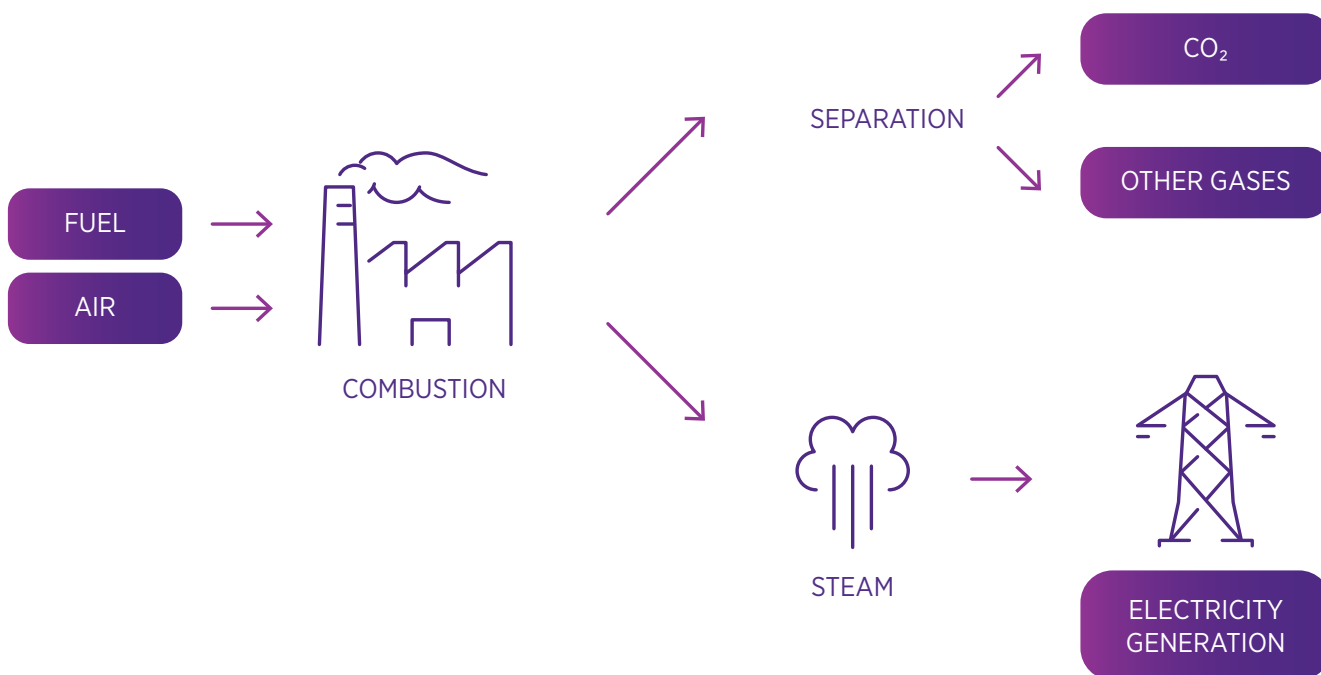
Figure 179 CCS hub concept (Bongers et al. 2017).



### 4.14.3 Retrofit and post combustion capture

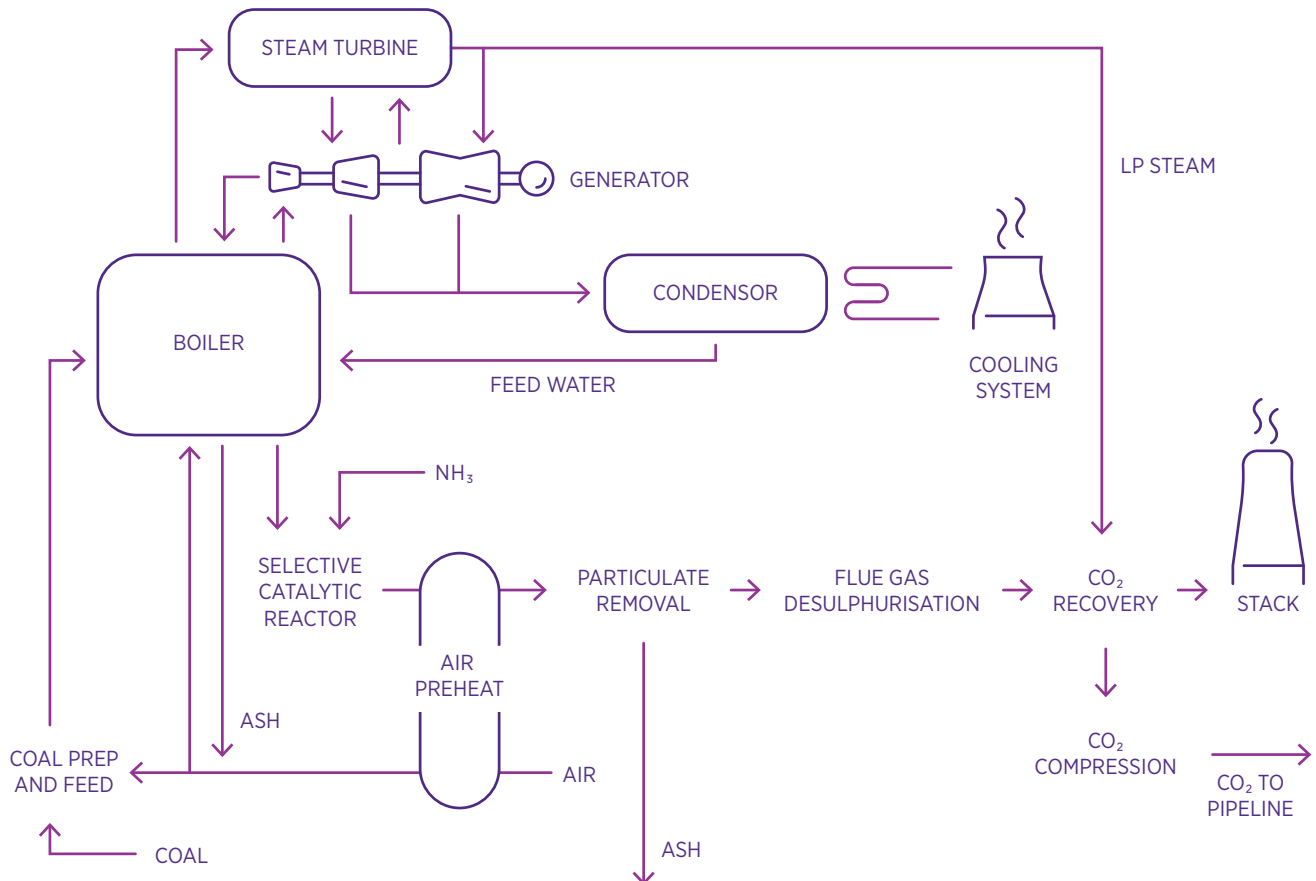
Post combustion capture (PCC), refers to the separation of CO<sub>2</sub> from flue gas derived from the combustion of carbon-based fuel (a simplified process concept is shown in Figure 180, see Bongers G, Byrom S, Oettinger M & Malss S 2018). This typical PCC is considered for either coal or natural gas-based power systems, but the technology is also applicable to biomass and oil-based systems.

Figure 180 PCC simplified process (Bongers et al. 2018).



The PCC process most frequently used is based on monoethanolamine (MEA), an amine solvent. The process principle is based on the thermally reversible reaction between components in the liquid absorbent and CO<sub>2</sub> present in the flue gas. A typical flow sheet of CO<sub>2</sub> recovery using chemical absorbents is shown in Figure 181 (Bongers, Kinaev, and Pregeli 2018).

**Figure 181** Typical black coal electricity power plant configuration with conventional SO<sub>x</sub> and NO<sub>x</sub> removal prior to CO<sub>2</sub> recovery (Bongers et al. 2018).



#### 4.14.4 CO<sub>2</sub> hub scenarios

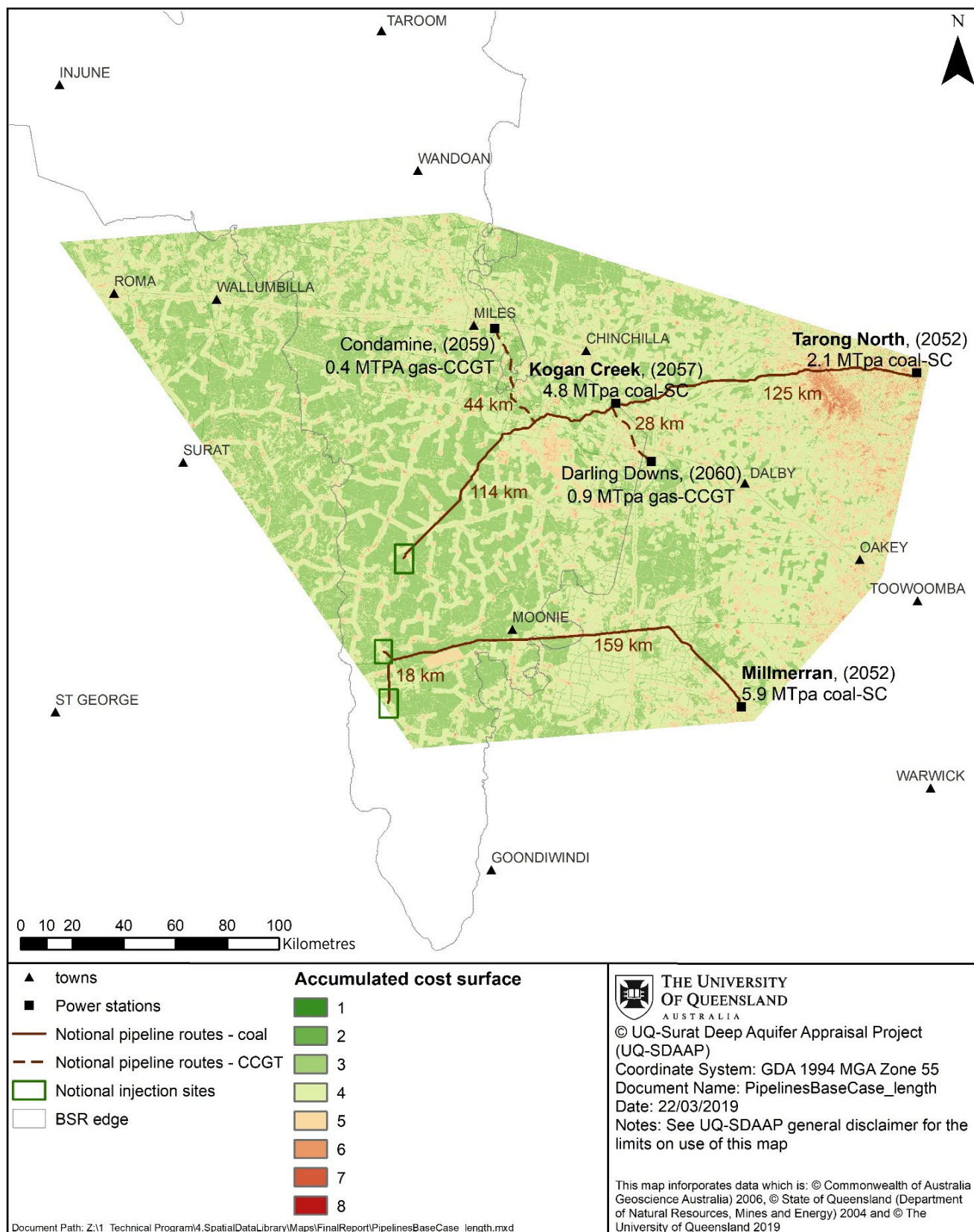
There are three elements that are critical to scoping a potential hub scenario. These need to be established as follows:

1. Suitable (and possibly multiple) CO<sub>2</sub> sinks need to be established with a high degree of site-specific confidence (i) that there is secure, long term containment, as well as (ii) a forecast, sustained high injection rate over the required period of emissions
2. Viable pipeline routes are needed that can connect these sinks to stationary sources. The pipelines are designed to deliver sustained CO<sub>2</sub> supply at rates and pressures matched to the injection or storage sites
3. Multiple CO<sub>2</sub> sources – existing or potential, to which “capture” technology can be fitted to produce high concentration CO<sub>2</sub> streams which can then be plumbed-in to a suitably sized pipeline distribution and storage system

#### Sinks and pipelines

As discussed in earlier sections, the possible storage locations comprise one small well pad per location, each with 4-6 horizontal wells reaching a depth of over 2.3 km. These sites are shown in Figure 182 along with illustrative pipeline routes (section 4.9). The illustrative site location and pipeline routes have been selected based on risk-minimisation considerations, rather than on any economic or cost optimisation. These are not “proposed” locations at this time but are suitable for additional data gathering and study.

Figure 182 Notional injection sites and pipeline routes based on risk minimisation algorithms.



## Emissions sources

The Surat Basin has three of Australia's four supercritical black coal power stations within a 250 km radius; Millmerran, Kogan Creek and Tarong North Power Stations. The estimated retirement dates for these plants is between 2052 and 2057 i.e. over 30 years of baseload power generation and associated GHG emissions.

Today, these power plants together emit over 16 million tonnes of CO<sub>2</sub> pa. The typical emissions intensity of these plants is around 960 - 1000 kg CO<sub>2</sub> per MWh with around 13% CO<sub>2</sub> in the flue gas.

In contrast, the six small gas fired power plants in the area emit less than 2 million tonnes pa with an emissions intensity of ~650 kg CO<sub>2</sub> per MWh for open cycle (OGGT) plants and ~400 kg CO<sub>2</sub> per MWh for closed (or combined) cycle plants (CCGT), with only around 8% CO<sub>2</sub> in the flue gas.

Clearly, the three supercritical black coal power stations in the region offer the greatest emissions reduction potential, the richest CO<sub>2</sub> streams and the most concentrated overall footprint.

Other potential CO<sub>2</sub> sources also exist in the region including gas production and biofuels manufacturing. Depending on the availability of rate-matched storage, the Surat Basin may be well positioned to enable a low emissions future for Queensland's industry as a CO<sub>2</sub> Storage Hub.

## Deployment assumptions and modelling rules

This study considers the following assumptions and rules to determine scale and sequence:

- As informed by studies of potential storage sites and the sustainable rates suggested therein and the project aims for material abatement, the *first* hub scenario considers only the three modern supercritical power stations in the area
- Individual power stations/sites will have modular, partial, sequential capture fit-out and commissioned per plant. The sequential retrofit continues to the next plant once commissioning for the previous partial conversion is complete. There would likely be further optimisation possible in a real deployment
- Implementation across power stations will be aimed at minimal reduction in supply availability (work on one part of one plant at a time). This implies an approximate 50% boiler conversion per retrofit stage
- Capture is assumed to be using proven technology, i.e. amine solvents
- The PCC units are 175MW modules
- To maximise on-site learning, conversions will be limited at first to 50% incremental within a power station (i.e. 50% of a boiler, allowing it to load follow to its minimum stable generation level pre-capture retrofit)
- During construction, a six-month period with no output is assumed per boiler to allow for tying the PCC to plant and during commissioning. Assume both boilers at Millmerran are shut during the same six-month period. In reality, the plant would likely run during commissioning, however zero output is a simplifying assumption
- Generation output is indicative and does not represent precise scheduling
- A key decision is materiality which drives pipeline sizing, hence the conversion of two or three supercritical coal plants would be in advance of the two CCGT plants. Capture and injection from the CCGT plants has not been modelled in this study because the three supercritical coal plants utilise most of the storage injection potential. The OCTG plants have not been considered
- The Millmerran Pipeline and Kogan Creek Pipeline decisions are independent. The Kogan Creek decision requires consideration of Tarong North capture
- In these UQ-SDAAP scenarios Tarong North would be a 50% retrofit only (a simplifying assumption not intended to limit actual retrofit options)
- Capital expenditure has been split evenly across the construction phase – this is illustrative only
- Land availability for the PCC plant has not been investigated
- Class 5 (Sanchez 2011) cost estimate has been utilised
- Financial assumptions are detailed in Table 58.

**Table 58** Financial assumptions (Gamma Energy Technology 2019).

		Input
Nominal cost of equity	%pa	11.5%
Nominal cost of debt	%pa	8.0%
Percentage debt	%	70.0%
Inflation	%pa	2.5%
Company tax rate	%pa	30.0%
Property tax / Insurance	%pa	2.0%
Analysis year		2018
Currency		AUD
Asset book life		30
Asset tax life		30
<b>SC Black Coal Plant Costs</b>		
Capital cost of retrofit	\$/kW	2700 - 2900
Fixed O&M	\$/kW/yr	82
Variable O&M	\$/MWh	9.5
<b>Gas Plant Costs (CCGT)</b>		
Capital cost of retrofit	\$/kW	1700 - 1900
Fixed O&M	\$/kW/yr	27
Variable O&M	\$/MWh	9.5

#### 4.14.5 Activities and decisions on capital phasing

Given three supercritical plants (and two possible, later CCGT plants), there are a number of sequences in which they could be refitted. The sequences studied in this project are not optimised, but along with the general approach, are constructed in a way in which capital exposure would be managed in an incremental way and interruption to power generation from the main plants would be minimised. Several scenarios are discussed in a supplementary UQ-SDAAP report (Gamma Energy Technology 2019). The scenario described in this section assumes the following sequential, partial rolling retrofit (Table 59).

**Table 59** Roll out scenario #1: cumulative installed capture rate and sequence.

Roll-out scenario	1 <sup>st</sup> retrofit job	2 <sup>nd</sup> retrofit job	3 <sup>rd</sup> retrofit job	4 <sup>th</sup> retrofit job	5 <sup>th</sup> retrofit job
#1	Millmerran	Kogan Creek	Tarong North	Millmerran	Kogan Creek
Cumulative CO <sub>2</sub> capture rate on completion Mtpa	2.54	5.04	6.23	9.88	12.68

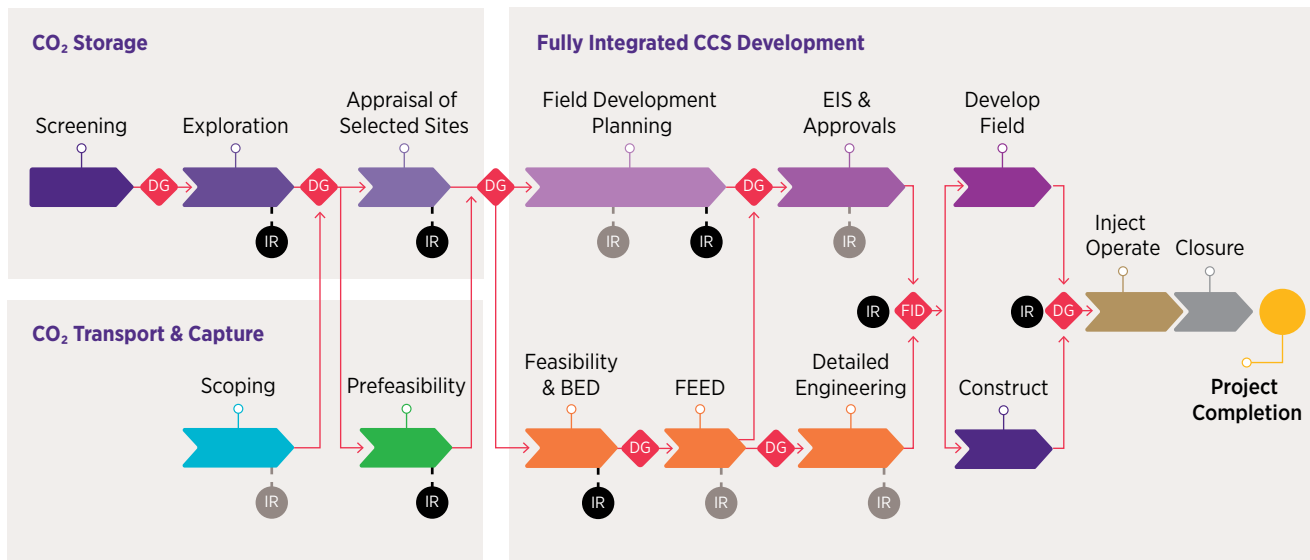
As discussed above, in advance of taking major investment decisions on capture (and transport) engineering, additional site-specific investment is required (section 5.5).

Importantly, the deployment and roll-out scenarios developed in UQ-SDAAP are designed to enable an incremental, stage-gated project development approach. Capital investments can be spread-out over time, incremental decisions can be delayed (e.g. to take advantage of lessons learned or to wait for data from the storage operation), and the decision to retrofit one part of one power plant does not oblige investors to complete all, or even the next, retrofit.

A generalised decision sequence, including Decision Gates (DG), is shown in Figure 183 below. The sequence shows the importance of developing high levels of confidence in sustained high rate injection before taking (larger) investment decisions in capture and transport specific engineering studies (the basis of design for scale and rate is informed by the subsurface).

The diagram also suggests that there is flexibility in timing for when studies (spend) can be undertaken. The contingent factors are tolerance to risk and urgency which might guide a decision whether to implement various activities in parallel.

**Figure 183** Generalised CCS decision framework (Garnett & Grieg 2014a pp 49).



Note that the *CO<sub>2</sub> Transport and Capture Prefeasibility* stage may also be delayed until after the *Storage Appraisal of Selected Sites*, depending on the residual post-Exploration risk and the estimated cost of the Prefeasibility Study.

Mandatory stage gate review
  Mandatory review upon a significant unfavourable report
  Optional technical review

Deployment in the Surat Basin is still at the earliest stages. Transport and capture are only at the scoping (pre-DG2) stages. By incorporating extensive new geological analysis and all available dynamic data (e.g. from the Moonie oil field, managed aquifer recharge etc.), the subsurface studies are also at the pre DG-2 stage. The next step is to appraise the high-graded sites, though is not clear which parties would invest in this stage. In the following tables, all investment values are estimated as **undiscounted, real term, 2018 dollar values**.

Decision Gate 2	Investment at DG around ~\$100 million	Time to next DG, DG-3
<b>Year 1</b> UQ-SDAAP proposed work program should start ASAP	Investment amount is dependent on whether one or all sites are appraised. "All sites" is recommended.  Major uncertainty in geological appraisal. A "poor case" geology could result in an early halt after approximately \$30 million spent in years 1-2 on the first stage of appraisal (section 5.6.5). Early and firm views from the regulator may also remove the incentive to invest.	<b>3-4 years</b>

This decision is discussed in further detail in Garnett 2019a and in section 5.6.

DG2 is the decision to address regulatory and social challenges *and* to appraise the site. Environmental approvals (EAs) and various permits are required to undertake field activities, for simplicity, these are not shown on the decision sequence. There would also be the option to undertake pre-feasibility studies for pipeline routes and capture (common to all plants) or to delay this step until more site-specific data are acquired and the regulations are clearer. The main risk at this time is that the regulatory pathway does not mature and the project halts or stalls. It is possible to invest additional amounts in this phase e.g. on more extensive, plant-specific, engineering studies pre DG3. This is simply more financial exposure and a greater chance that designs need to be repeated. During the pre DG3 phase, decision criteria for subsequent decisions need to be agreed (refer to lessons learned from ZeroGen - Garnett et al. 2012). More importantly a project consortium and appropriate agreements need to be in place with private and government entities to support further investment.



<b>Decision Gate 3-6</b> <b>Year 3 or 4</b> Should start ASAP	<b>Investment required at DG-3 ~\$113 million</b> Investment amount is largely dependent on duration and to a lesser extent the degree of plant-specific engineering on plants other than Millmerran. This phase also sees the installation of extensive aquifer monitoring bores.	<b>Time from DG 3 to FID on first retrofit execution</b> <b>3 to 6 years</b> Major uncertainty on the duration of required consultation and EIS processes for first of a kind (FOAK)
---	--	--

At DG-3, there should be confidence that the regulatory *pathway* (not full consent) to large-scale injection is clear, and that the constraining injection rates and pressures are known with sufficient confidence. Based on this, relative confidence levels for sustained rate and for unit technical costs of development should be known and inform DG3. This is a significant strategic decision and might well commence a “*project of state significance*” or similar high profile. Pre-DG3 also needs to see activity in the forming of appropriate joint ventures and engineering supply contracts, as well as environmental screening and initial studies.

Decision gates 4, 5 and 6, show that detailed field development planning (including monitoring and verification) may be required to feed into an EIS. In fact, an EIS process is likely to take 2-3 years with field development and engineering studies being undertaken in parallel. The commencement of an EIS process is described here as a major, strategic decision (DG5). It can be taken, for example before FEED is “complete”. The EIS process could therefore commence at DG4, DG5 or DG6, with the main contingencies being an assessment of social acceptance (a key pre DG3 activity), the position of State and Federal regulators, the status of key agreements, and a set of competencies available to the main project proponent. It is expected that a large element of engineering studies will be common to all plant conversions. The decision to undertake detailed engineering design for the first, or for all plants to be retrofitted, can be taken in this period, but does not need to be.

<b>Decision Gate 7 &amp; 8</b> <b>Year 8 to 11</b> FID on the first retrofit – leading to execution	<b>Investment required at DG-7 ~\$1.06 billion</b> Investment amount is largely dependent on duration and to a lesser extent the degree of plant-specific engineering on remaining plants (Kogan Creek and Tarong North).	<b>Time from DG 7 to next retrofit FID</b> <b>3-4 years</b> Period will see injection, pipeline and capture construction and system commissioning.
---	--	--

This is the main final investment decision (FID) for the first plant retrofit (the first “job” the scenario table above). Capital exposure on plant retrofits is limited to the first job. However, a decision is required at that time on pipeline size i.e. whether to size for the first job or for the full re-fit (Millmerran in the South and Kogan Creek & Tarong North in the North).

<b>Subsequent retrofit FIDs</b> <b>Year 13 to onward.</b> FID on the first retrofit – leading to execution	<b>Investment decisions</b> Kogan Creek (part a) ~ \$1.20 billion Tarong North (part a) ~ \$652 million Millmerran (part b) ~ \$905 million Kogan Creek (part b) ~ \$787 million	<b>Typically 2-3 years between investment decisions. None are “locked in”.</b> A degree of learning-by-doing has been assumed (Gamma Energy Technology 2019)
--	--	---

## Comment on parallel activities and synergies

It is assumed that a large amount of the prefeasibility and FEED studies would be applicable for all power plants, but that detailed engineering design, and of course site preparation, would be site specific. Detailed engineering for plants could be undertaken during construction and commissioning of the preceding retrofit job, allowing for learnings to be captured. The development of this roll-out scenario is summarised in Table 60.

**Table 60** Summary of deployment sequence, retrofit jobs and cumulative capture rate installed.

<b>Pre-execution.</b> Site appraisal, project set-up, funding/financing, consents and approvals, project co-venture agreements, environmental baseline studies, aquifer monitoring wells in place. Public engagement continuous throughout. All engineering studies complete.		
Job	Cumulative capture installed	Description of main activities
First retrofit	2,540,000 t CO <sub>2</sub> /pa	Southern site drilled up and facilities installed. Two PCC modules built at Millmerran Power Station. Pipeline built from plant to southern injection site (decision to size for full Millmerran)
Second retrofit	5,040,000 t CO <sub>2</sub> /pa	Northern site drilled up and facilities installed. Two PCC modules built at Kogan Creek Power Station. Pipeline built from plant to northern injection site (decision to size pipeline for Kogan Creek <i>and</i> Tarong North).
Third retrofit	6,230,000 t CO <sub>2</sub> /pa	One PCC module built at Tarong North Power Station. Pipeline extended from Kogan Creek Power Station to Tarong North Power Station
Fourth retrofit	9,870,000 t CO <sub>2</sub> /pa	Two additional PCC modules built at Millmerran Power Station and plumbed in to existing pipeline and southern site
Fifth retrofit	12,680,000 t CO <sub>2</sub> /pa	Two additional PCC modules built at Kogan Creek Power Station and plumbed in to existing pipeline and northern site

Figure 184, shows the impact on power generation and CO<sub>2</sub> captured/stored during the progressive implementation of retrofit. A significant amount of engineering works can likely be undertaken without disruption to baseload power generation and dispatch. However, some reduction has been assumed while final integration and commissioning are undertaken. This leads to the “saw-tooth” appearance on the figures as, while reductions are probably for a number of weeks or months, annualised data is shown.

The sequence shown assumes a period of commissioning before construction on subsequent plants.

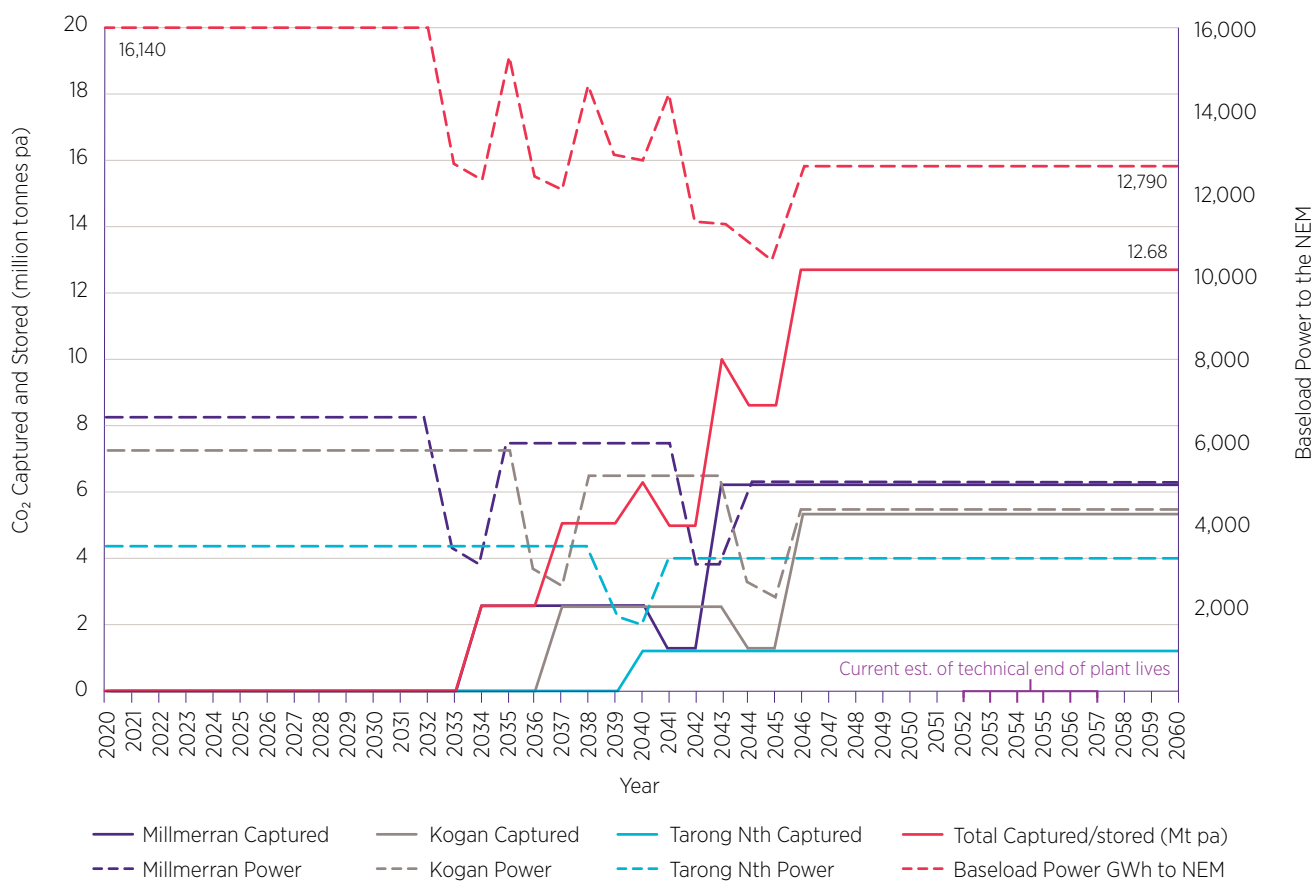
The timeline is considered to be very conservative with many options of sequence optimisation remaining un-explored. It is important to note there are major uncertainties on financing and approvals timeframes.

The **emissions intensities** achieved in this scenario are of the order of:

- A reduction from ~1,000 to 135 kg CO<sub>2-eq</sub> / MWh for the *fully* retrofit plants
- A reduction from ~ 960 to 690 CO<sub>2-eq</sub> / MWh for the *partial* retrofit
- The weighted average for this mixed scenario is ~270 kg CO<sub>2-eq</sub> / MWh (a value of ~135 kg / Mwh results from all full retrofits)

**Figure 184** Deployment scenario 1, impact on power generation and CO<sub>2</sub> captured/stored throughout sequential, partial retrofit.

**Scenario 1: MKTMK (full retrofit on ML & KC, partial on TN). CO<sub>2</sub> Captured and Stored & Baseload Power to NEM**



With reference to the discussion above and Figure 185, the figures show the main investment decisions or commitments to be made. In essence, deployment from the date of this report consists of a series of discrete decisions which do not commit investors to invest in a full roll-out.

Securing funding and financing for the investments would be one of the main tasks of the project entity which takes this forward. However, the source of the next (appraisal phase) investment of around \$100 million is not clear. This is essentially an exploration decision with a downside risk of around \$50 million i.e. if either the geology proves unsuitable or if a regulatory route can't be found in Queensland. This is discussed further in section 5.5 and 5.6 and in Garnett 2019a.

Nevertheless, it is clear from complementary work done in parallel with this UQ-SDAAP study (Boston, Bongers, Byrom & Garnett 2019a), that a significant amount of CCS (*more than identified in this study*) is required for deep decarbonisation of the NEM.

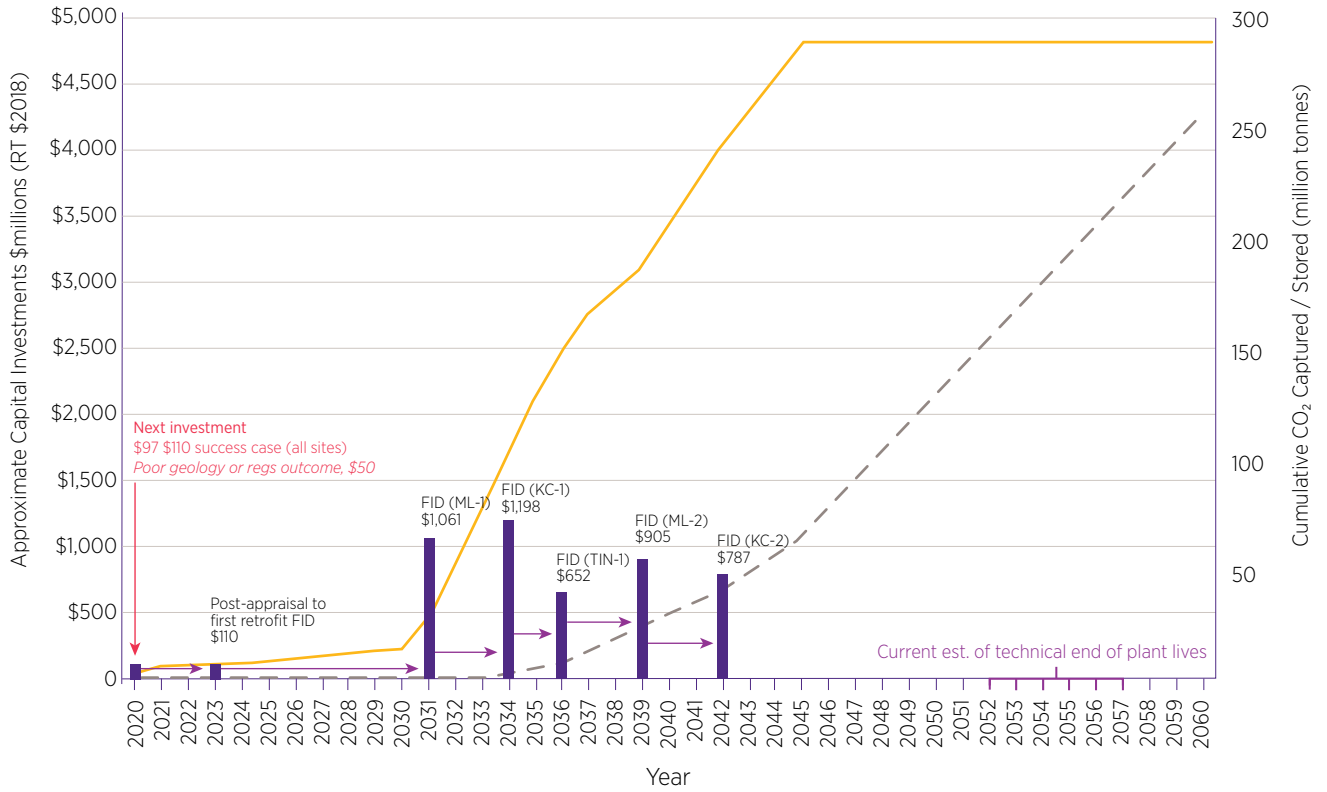
With the absence of any commercial incentive to invest in CCS, and the clear need for low carbon baseload power generation in the context of Australian COP21 commitments and beyond, as well as requirements of a future NEM with an increasing penetration of "intermittents", it is suggested that government investment is the main source for this 'higher risk' phase. This could include potentially partnering with industries who have a strategic interest (e.g. power generators and the coal and gas industries).

However, it is also suggested that a special purpose vehicle is created with a corporate governance and structure working under a suitable industry-experienced board.

Corporate structure and venture set-up are beyond the scope of UQ-SDAAP. However, important requirements and lessons relevant to appropriate structures and issues are included in Garnett et al. 2012, chapter 2; Greig et al. 2016a; Greig et al. 2016b; Berly & Garnett 2018; Garnett, Undersultz & Ashworth 2018.

**Figure 185** Illustration of discrete investment (stop/go/review) decisions and cumulative capex and CO<sub>2</sub> captured/stored for roll-out scenario 1 (MKTMK).

**Scenario 1: MKTMK Cumulative Capex and Cumulative CO<sub>2</sub> Captured/Stored (line chart)**  
**Main, sequential, discretionary, investment decisions (bar chart)**



## 4.14.6 Implications for regional employment

A CCS hub development project, as described in this study, represents a major industrial enterprise. In addition to generating jobs during the design phase, a significant number of regional jobs would be created through the lengthy, sequential, retrofit construction phase.

In addition to this, the emplacement of CCS infrastructure and a reduction in emissions intensity may safeguard existing jobs related to generating power or providing fuel for the three power plants (and the many 'multiplier' jobs in the regional communities).

This could create around 250 new regional jobs in the retrofit and construction phase, as well as either safeguarding, or even extending the need for, approximately 500 existing regional jobs in the power plants and adjacent mines. Indirect employment multipliers in the local economy have not been assessed in this study, however previous work has suggested this would be statistically significant (Fleming & Measham 2014), and in the range of 1 to 6 (Knights & Hoods 2009; Rolfe, Lawrence & Rynne 2011).

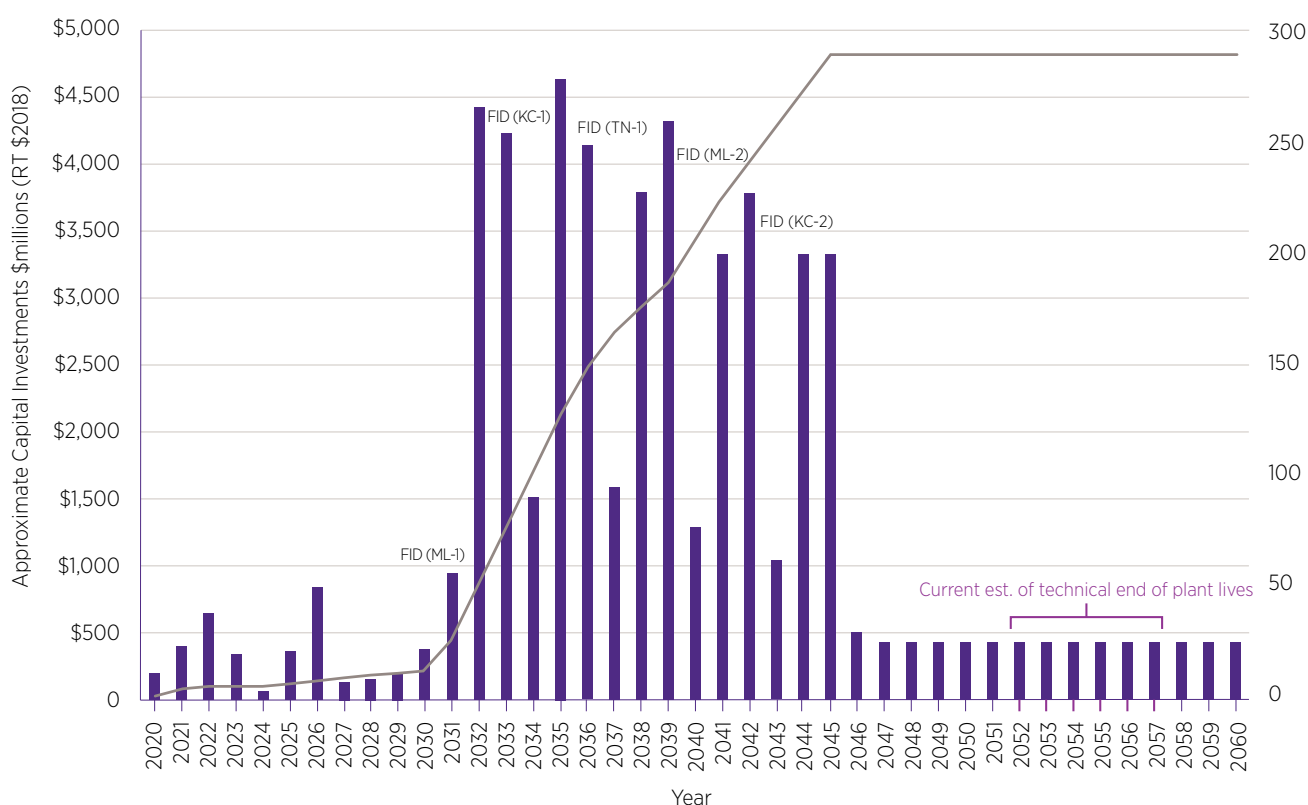
Gamma Energy Technology 2019 has produced *high level* estimates of job creation, with the majority of jobs during the construction phase being in the region.

**Figure 186** High level estimate of employment and regional construction jobs generated by a large scale, CCS retrofit project.

### Scenario 1: MKTMK

#### Cumulative Capex (line chart)

#### High level estimate of jobs (bar chart)



## 4.14.7 Post-retrofit, power and emissions reductions and unit costs

Assuming appraisal and regulatory development are successful, the remainder of the deployment can be considered an *incremental* project. Table 61, shows some key performance outcomes.

Project capital costs, emissions reductions and operating costs can be considered compared to either a business-as-usual, “no retrofit” case, or to some alternative development. For example an early closure of these plants and a valid functional (baseload) replacement with either gas, gas with CCS, or with a generation “usual case” which offers a different intermittent service e.g. solar or wind generation.

For the purpose of this discussion, benefits and performance are compared to a business as usual case i.e. it is not assumed that the plants are retired before their estimated technical life. It is also assumed that the parasitic loss of power output to the NEM caused by power-needs of CCS is compensated for by other low or zero carbon sources, such that scoping estimates of the unit costs of CO<sub>2</sub> are roughly the same for ‘avoided’ as for ‘stored’.

Excluding individual project cost sensitivities and excluding appraisal costs (section 5.6 and Garnett 2019a), indicative total unit technical costs of CO<sub>2</sub> abatement<sup>23</sup> are in the range of \$57-75/tonne depending on the scenario, though considerably more engineering work is required to crystallise these estimates.

Storage and transport costs are in the range \$10-20/tonne, limited by the lifetime of the retrofit assets rather than the ability to continue to accept high rate injection. Extending the injection period at similar rates for say, 30 years could reduce these values by around \$2-3/tonne.

**Table 61** Comparison of scoping-level performance outcomes for three different retrofit scenarios.

Scenario	Millmerran only	Scenario 1 MKTMK (4)	Scenario 1a MKMK (4)
Incremental capital (excluding storage appraisal) Undiscounted Σ (RT \$2018)	\$113 million + \$ 1.97 billion	\$113 million + \$4.83 billion	\$113 million + \$4.17 billion
Cumulative reduction (1) Mt CO <sub>2</sub> to 2060	132	256	256
Emissions rate before and after retrofit Mtpa CO <sub>2</sub>	6.87 → 0.69	16.18 → 3.50	12.77 → 1.28
Power GWh out before and after retrofit	6,720 → 5,110	16,140 → 12,790	12,590 → 9,570
Emissions intensity before KgCO <sub>2</sub> /MWh	1,020 → 135	1,002 → 270	1,014 → 134
UTC - \$ per tonne CO <sub>2</sub> captured (2)	\$39.60	\$50.40	\$46.70
UTC - \$ per tonne CO <sub>2</sub> transport (2)	\$3.70 to \$4.50	\$5.60 to \$6.70	\$4.10 to \$4.90
UTC - \$ per tonne CO <sub>2</sub> storage (2) (3) (excl. appraisal costs)	\$7.30 to \$11.60	\$6.40 to \$10.40	\$7.00 to \$10.60

Notes:

1. The cumulative emissions reduction for MKTMK and MKMK scenarios is approximately the same because the conversion of two larger plants can happen sooner in the latter scenario, and thus they capture and store for longer before nominal end of life. A full retrofit on Tarong North would address this, if it were able to run longer
2. The high-level estimates of unit technical costs (UTC), dollars per tonne CO<sub>2</sub> captured, transported and stored (not ‘avoided’). These exclude the first 3-4 years of (appraisal) costs which are required to confirm the option. This is because, appraised storage rates and volumes associated with the appraisal costs are not those limited by the development scenario (unit appraisal costs are not additive to the unit technical costs in this table). UTCs are calculated as the sum of discounted *incremental* capex and incremental (CCS related) opex, divided by the sum of the discounted injection or capture rate. These are roughly equivalent to a constant in real terms, pre-tax payment per tonne of carbon which, if received by a capture, transport or storage provider, would lead to a break-even
3. The unit storage costs for a “Millmerran only” scenario is higher because two well pads may be needed in this scenario and proportionally less CO<sub>2</sub> is stored
4. The difference between the MKTMK and MKMK scenario shows a trade-off between unit costs, total emissions captured and availability of capital. If capital is limited a partial retrofit can make material emissions reductions, though a full retrofit has lower unit CCS unit costs

<sup>23</sup> “Abatement” assumes that in a generally decarbonising grid that generation lost by parasitic load to enable CCS is replaced by low carbon sources (or is not needed). The emissions from this load are captured and stored. Abated is not necessarily avoided.

## 4.14.8 LCOE and capital cost sensitivity analyses

The high-level scoping costs discussed in this section are conservative and there are significant opportunities for cost reductions. Detailed capture engineering studies are outside the remit of this study. However, with reference to Gamma Energy Technology 2019, some sensitivity analyses for Scenario 1 (MKTMK) are described below, to show an indication of the potential for improvements.

### 4.14.8.1 Capacity Factor

By changing the capacity factor to 80% (sensitivity 3B) or 70% (sensitivity 3A) from the base case of 90%, the levelised cost of electricity (LCOE) changes. The results are presented in Table 62.

**Table 62** LCOE sensitivity to capacity factor assumptions (\$/MWh).

Capacity factors ->	Base Case – 90%	3A – 70%	3B – 80%
Millmerran	\$62.10	\$73.10	\$93.40
Kogan Creek	\$67.20	\$80.90	\$73.20
Tarong North	\$87.50	\$101.10	\$93.40

From the perspective of a levelised cost of electricity, and therefore maintaining a limit on price increases, it is important for CCS retrofitted baseload plants to operate at stable and high capacity factors.

This, in addition to (a) engineering factors which require capture plants to be run at as much possible at steady rate; and (b) the intent to minimise emissions, indicate that **a new market position and dispatch rules will likely be needed for retrofitted CCS plants** (this in agreement with extensive work previously done on an IGCC plant with CCS in Queensland, Garnett et al. 2012 and as further discussed in Greig et al. 2016b).

### 4.14.8.2 Learning by doing

The base case capital cost estimate (RT \$2018, undiscounted) for the capture plants, is of the order of \$4.72 billion, a learning-by-doing assumption of 5% has been applied. This may be conservative but is thought to be appropriate for Australian conditions. Operators of the Boundary Dam power station in Canada have estimated that they could reduce capital costs by 20-30% on a subsequent retrofit units<sup>24</sup>.

With relatively little learning by doing (1%), the capital costs for scenario 1 capture would be ~\$4.34 billion, while with a 10% rate of improvement, capital costs would be ~\$3.46 billion.

In addition to minimum impact on availability and power prices, a partial retrofit and sequential roll-out concept has the potential to realise savings of over RT \$1 billion compared roll out which is less coordinated.

### 4.14.8.3 New technology (solvent)

Sensitivity 1A tests a new solvent that has the potential to reduce the cost of a plant retrofit through removing the need for NO<sub>x</sub> and SO<sub>x</sub> treatment of the flue gas. This assumes that by the time of FID (~10 years from now), a new solvent will be commercially available that does not require this treatment. As these processes, which are essential when using an amine capture solvent, represent approximately half of the retrofit capital cost, the first sensitivity case tests what happens when this cost is removed.

Sensitivity 1B shows the case if a new solvent has the potential to decrease the parasitic load the capture plant requires. The second sensitivity study tests this increase in performance.

Sensitivity 1C combines 1A and 1B showing a new solvent that can improve cost and performance simultaneously. Results are summarised in Table 63.

<sup>24</sup> See: [www.sequestration.mit.edu/tools/projects/boundary\\_dam.html](http://www.sequestration.mit.edu/tools/projects/boundary_dam.html)

**Table 63** Sensitivity of capital cost and parasitic loss to new technology (solvent).

		New Technology (solvent)			
		Base Case	Sensitivity 1A	Sensitivity 1B	Sensitivity 1C
Capital Cost	\$/kW	\$2,800	\$1,400	\$2,800	\$1,400
Retrofit loss	%	24%	24%	19%	19%

#### 4.14.8.4 Sensitivities to cost of capital

There is currently no sound economic rationale for private funding of CCS projects. For the purposes of this scenario discussion, Gamma Energy Technology 2019 have assumed a real weighted average cost of capital (WACC) of the order of 9.1% assuming some mixture of low cost (public) debt.

Varying the WACC can have a significant impact on the total capital cost of a project. The base case has a 9.1% real WACC. Sensitivity 5A assumes a lower cost of capital, with a 5% WACC. Sensitivity 5B assumes a higher cost of capital, with a 12.5% WACC. See Table 64.

**Table 64** Impact on LCOE on funding source (WACC).

	Base Case 9.1%	Sensitivity 5A 5%	Sensitivity 5B 12.5%
Millmerran	\$62.10	\$49.60	\$75.40
Kogan Creek	\$67.20	\$54.70	\$80.50
Tarong North	\$87.50	\$75.00	\$100.80

Again, with a view to minimising pressure on upward prices, while striving for material carbon abatement, it is essential that attractive financing be secured. At that low cost, finance is likely to require government funding of some kind.

However, Herzog 2017 describes several government mechanisms to finance carbon capture “demonstration” projects. He noted that reliance on government subsidies is a “*risky business*” noting that major demonstrations, analogous to the UQ-SDAAP hub, take years to develop and have been cancelled at late stages when government schemes have been halted. The author notes that “... *a more secure path forward for CCS is to have government create the regulatory environment to create business drivers*” but adds that “... *For initial projects, direct government support will probably still be required to overcome first mover costs*” (*ibid* p 5698).

Major hub development will rely on public financing to a large degree, however, this is, in itself a major risk factor (Greig et al. 2016b).

“ Finally, we agree largely with Kepetaki & Scowcroft 2017, who concluded in their review of business models, risk and enablers that “... successful CCS project development depends on multiple factors, such as (i) clarity of regulatory frameworks, (ii) efficiency of permitting processes, and (iii) early and sustained stakeholder engagement for public acceptance. However, project finance remains the most challenging piece”  
(*ibid*, p.6623).

We would only add “and environmental permitting” to this.



## 4.15 The calibrated *dynamic capacity* of the Surat Basin

### 4.15.1 Typical capacity concepts

Discussions on storage “capacity” have traditionally centred on the quantification of static, corrected pore volume calculations for certain basin or plays or segments thereof (e.g. Bachu et al. 2007; DOE 2007; Bradshaw et al. 2011; and Bachu et al. 2008). Capacity in this paradigm is a function of pore space with some discount defined by a storage efficiency factor. More recently this has been modified to be analogous to resource and reserves definitions to the petroleum resources management system (e.g. SPE 2016).

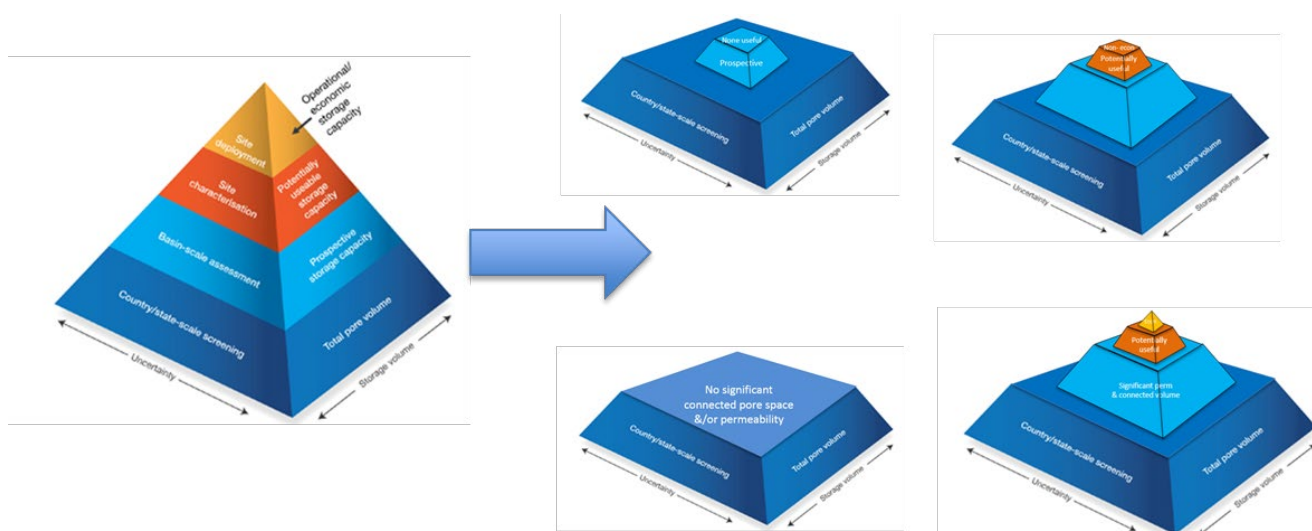
However, it has been noted that static-based capacity calculations have limited benefit in estimating dynamic ‘practical capacity’ (e.g. Garnett et al. 2012 pp 353, 441; Allinson et al. 2014).

The historic, static approach represents largely a fallacy of construction. For any proposed sequestration site or sites, the challenge at hand is not to sequester a given *volume* of CO<sub>2</sub> but to sequester a given *rate* for a sustained, defined period. Static methods either fail to recognise that mitigation is a rate-governed challenge and/or make implicit assumptions that large static capacities can support a large sustained injection rate and that somehow sustainable injection rate is mainly a function of capacity.

Kaldi & Gibson-Poole 2008, building on Bachu et al. 2007, suggested a now commonly used “resource-reserves” pyramid (refer left pyramid in Figure 187). While this has been a useful communication tool to explain that rate “matched” capacities are significantly lower than “theoretical capacities”, the model can be misleading in that it appears to suggest that there is some scaled relationship between different resource levels. This can lead to a significant over estimation and overconfidence in the available, useful storage.

A more nuanced view of the relationship between theoretical (static) capacities and “useful” or rate-matched capacities can be represented as in Figure 187.

**Figure 187** Modified view of storage resource pyramid (Garnett 2017, modified after Kaldi & Gibson-Poole 2018).



When evaluating a “rate matched” (dynamic capacity) requirement, the size of a theoretical static capacity is not indicative of the dynamic potential.

The pyramid model is limited. A new language and set of concepts is required to discuss dynamic capacities.

## 4.15.2 Dynamic capacity – concepts and communicating uncertainty

While not capturing the full complexity, for the purposes of communication, dynamic capacity can be usefully discussed in terms of **a rate that can be sustained over a defined period of time** (rather than a simple cumulative volume or mass).

As noted by previous authors (e.g. Allinson et al. 2014) and demonstrated by others (Garnett et al. 2012) this dynamic capacity is a function of geology and an engineered field development plan (FDP).

It is *constrained* by geology (e.g. rate and pressure constraints); and by the developable area (e.g. surface constraints, cross-well interference, interference with other subsurface users; and by regulatory limits such as licence boundaries and pressure build-up limits).

It may also be economically constrained. For example, if optimised on unit technical cost (UTC)<sup>25</sup>, more injection might be possible in a given FDP, but there are diminishing incremental sustainable-injection returns (lower rates and durations) for incremental capital investment (drilling more wells). UQ-SDAAP sought to establish technical rather than economic feasibility of large-scale injection and therefore has not applied an economic limit. However, such a limit or UTC target is recommended as a decision test (e.g. Garnett et al. 2012 pp 346) at the end of field appraisal. Further discussion on unit costs can be found in Garnett 2019a, Ampofo & Garnett 2019 and Garnett & Greig 2014b.

To estimate dynamic capacity, therefore, constraints and geology need to be evaluated (sections 4.3, 4.5 and 4.6), a container defined (section 4.4), specific sites identified (section 4.7) and a development philosophy set (section 4.8.1). Within this, it is then possible to evaluate the impact of different injection scenarios in the 'high graded sites (sections 4.7 and 4.11). These evaluations then inform engineered FDP options (sections 4.8, 4.10 and 4.11) which lead to a holistic estimate.

Any calculated dynamic capacity is then specific to these parameters, constraints, definitions and engineering solutions. Additionally, any assessment of dynamic capacity, carries uncertainty. This is especially true of early stage assessments such as those undertaken by this research.

Communicating uncertainty is important because when designing capture plants and deciding on their capacity (Mtpa), the ideal would be to retrofit a capture-rate that can be utilised to its maximum extent, but so that it does not become limited by declines in storage injection potential during its useful lifetime. To install too much capture is to waste significant capex, and the capex required for capture is very much greater than the cost of establishing greater confidence in sustainable injection rates.

The basis of design (BoD) for capture rate in a CCS hub is constrained by confidence in storage potential its plateau rate and how long it can be sustained.

Three models for discussing dynamic capacity uncertainty are discussed herein.

Figure 188, show a schematic of confidence in sustaining different plateau rates (Mtpa) for different durations. These can be estimated from FDP specific models for a given play, location, development philosophy and constraints.

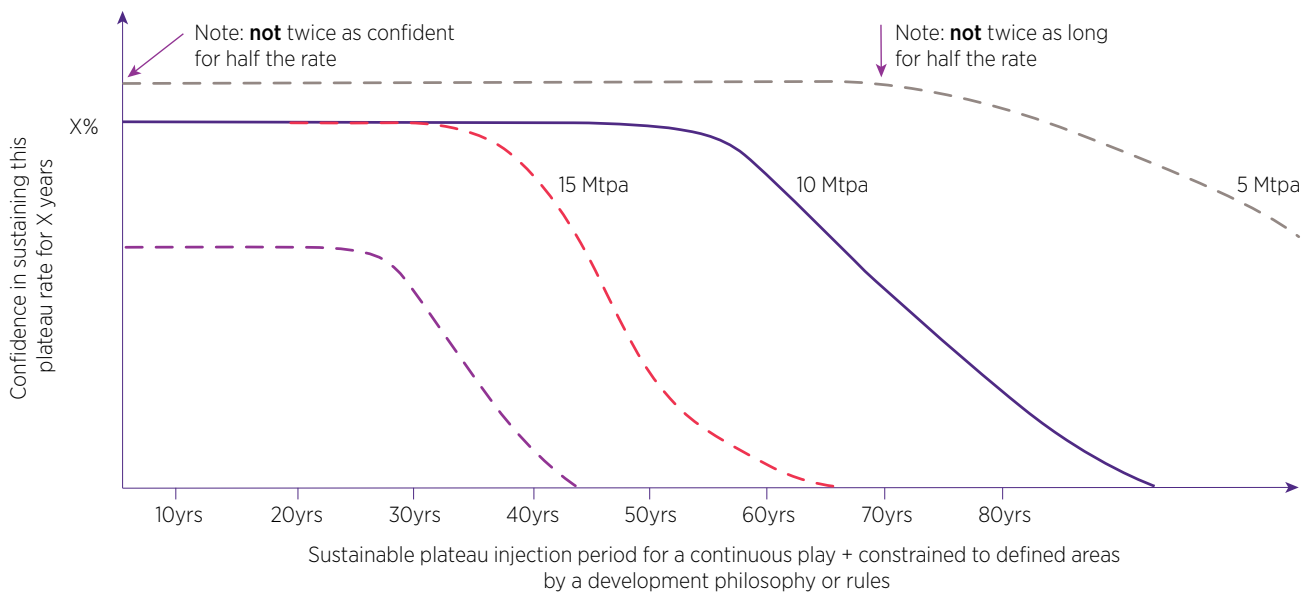
Clearly, there is a higher confidence level for lower rates in general. Furthermore, for higher plateau rates, confidence in sustainable plateau time is lower. **Confidence is lower for higher plateau rates and also confidence decreases for longer sustained plateaus.**

In such a discussion, for given play and area constraints, the differences between the sustainable rate curves are caused by different field development choices (mainly well count, type and spacing). Higher rates and longer durations would lead to higher costs and unit costs.

The basis of design (BoD) for capture rate in a CCS hub is constrained by confidence in storage potential its plateau rate and how long it can be sustained.

<sup>25</sup> Unit technical cost, UTC = discounted sum of capex + opex divided discounted sum of injection rates. This is an estimate of a constant real terms, pre-tax, carbon price which a storage operator would need to receive to break-even.

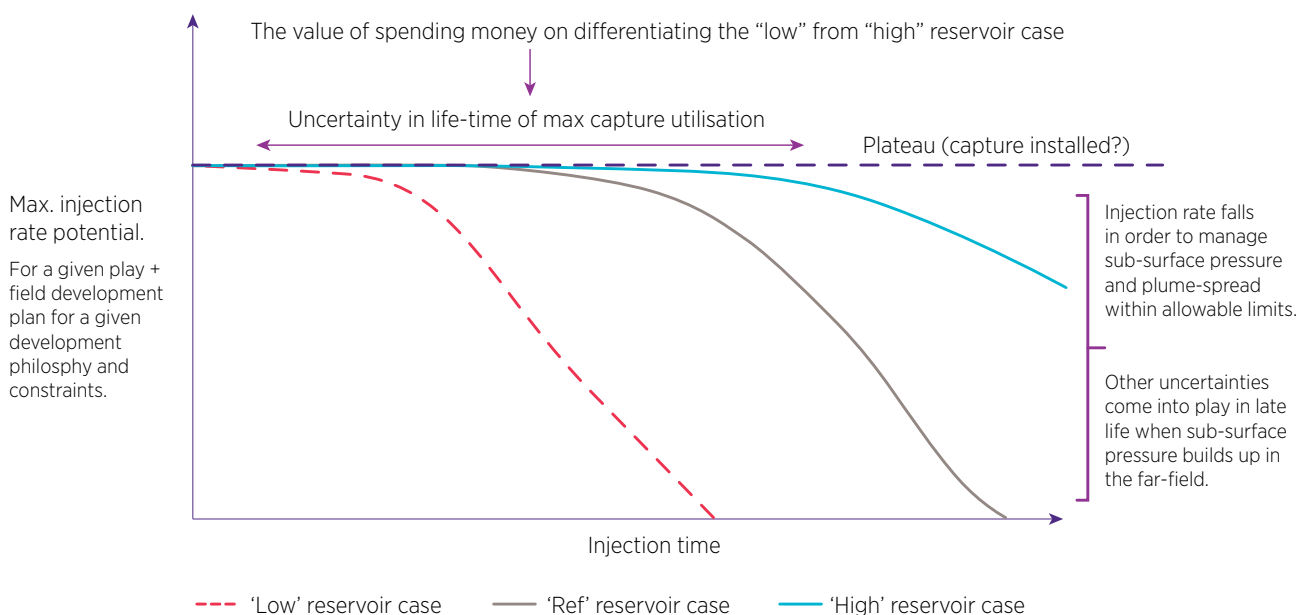
**Figure 188** Model for discussing confidence in dynamic capacity.



An alternative way of considering uncertainties, especially in an early stage development that requires further site appraisal, is shown in Figure 189. In this figure, different subsurface realisations (all consistent with the data) result in different plateau durations when developed with a given FDP. There are several reasons that the injection rate can fall off, ranging from; physical limits, to reservoir pressure at the well, to regulatory restrictions, to allowed plume area, to far-field pressure rises. The main uncertainty in this illustration is geological. The impact on basis of design for capture can be significant, with the risk of long periods of time when installed capture capacity is under-utilised.

**Even when a field development plan can be constructed that can attain the required injection rate, significant uncertainty in the onset of injection decline is driven by the (uncertain) reservoir case.**

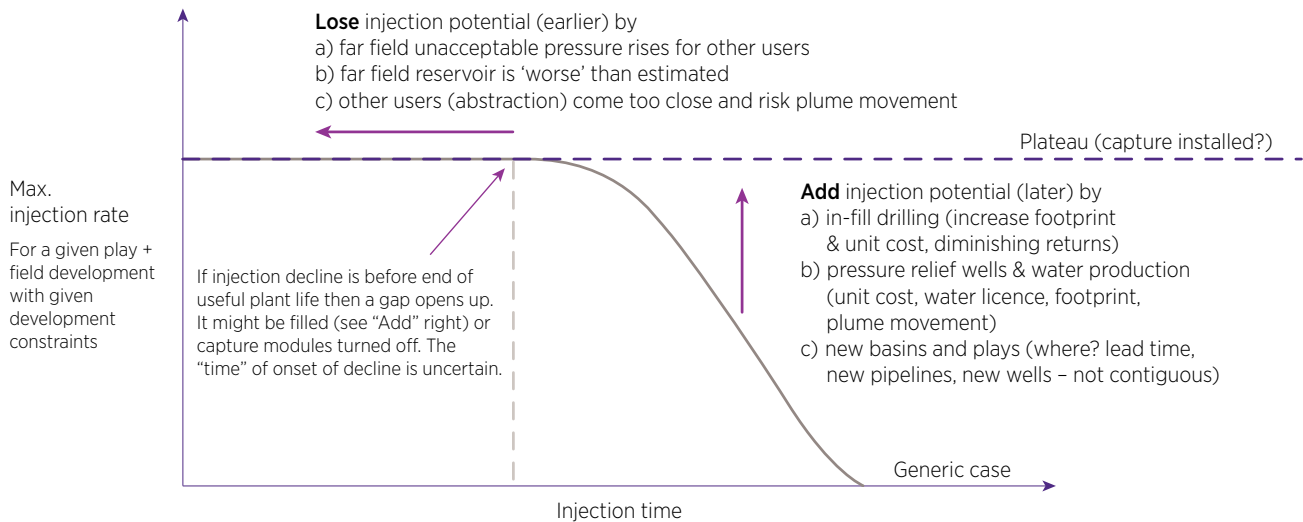
**Figure 189** Model for discussing uncertainty in dynamic capacity.



Finally, development options may exist which in later field life can extend a plateau and similarly, other factors at these times could act to reduce plateau times and cause early onset decline. Figure 190 shows factors that can influence plateau duration. There are secondary and tertiary measures which can increase or “add” injection potential (with some influence on footprint and cost). There may also be an option to move to non-contiguous storage locations in different basins and plays. Similarly, unforeseen future events can cause injection potential to be “lost”, thus reducing plateau durations.

**For a given reservoir case and FDP, there are additional technical and non-technical uncertainties which also impact onset of decline and rate of decline, both positively and negatively.**

**Figure 190** Model for discussing late-life uncertainties in dynamic capacity.



### 4.15.3 UQ-SDAAP calibrated, risked dynamic capacities and uncertainties

**What is considered to be “material” abatement?** UQ-SDAAP aimed to establish whether or not material carbon abatement was feasible in the Surat Basin in southern Queensland via large-scale CCS. “Material” was taken to mean *at least* the emissions of the remaining technical lifetime of one of the large supercritical power stations (nominally greater than 5 Mtpa for more than 20 years); and if possible the majority of emissions of all three modern supercritical plants in the area. A working plateau rate of -13 Mtpa has been used as a reference case, representing the full retrofit of Millmerran and Kogan Creek and a partial retrofit at Tarong North, with assumed technical retirement dates in the mid-2050s (full-bore injection period of 20+ years, assuming a ~2030 start-up). All reservoir models were run for longer than this indicating surplus dynamic capacity.

**What are the risks of it not being “material”?** There remains a finite probability that the play and selected sites are found not to be suitable. This cannot be established without further site-specific appraisal (section 5.5). The *main* geotechnical risks are:

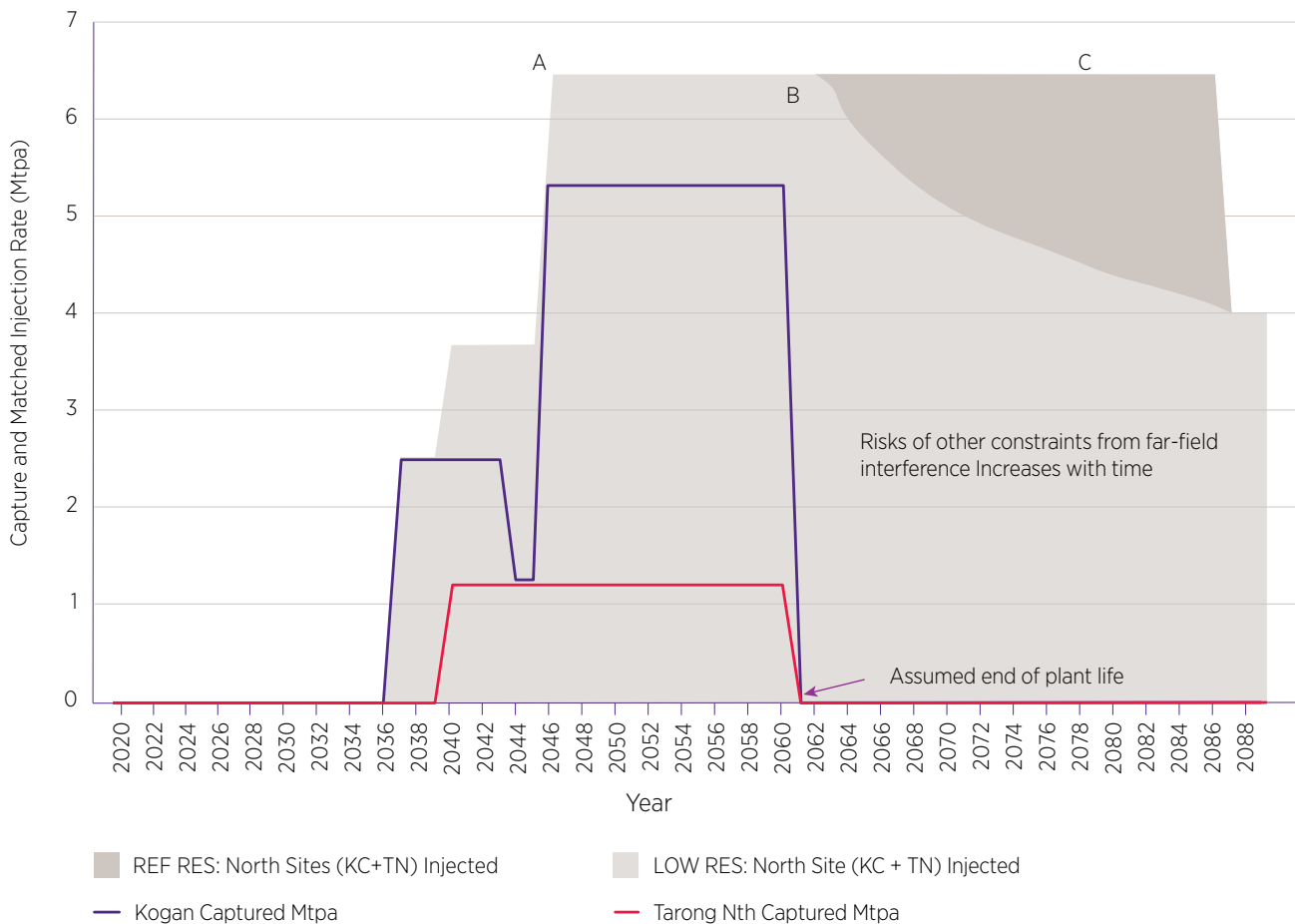
1. That there are fault barriers or leaking faults in the area
2. That the reservoir is poorer than the “low case” e.g. due to depth-induced diagenesis
3. That the Transition Zone and Ultimate Seal are found to be more sand-prone than modelled

If the chance of these occurrences are independent but low, say 20%, 10% and 10% respectively, then the combined chance of failure is 35% and the a-priori probability of technical success is 65%, where “success” then has a range of “material” outcomes, (all bigger than the minimum “materiality” criteria of 5 Mtpa for 20 years). This is discussed hereafter.

With reference to Figure 189 and Figure 190 (plateau rate vs. time uncertainties), a UQ-SDAAP illustration of time-limited retrofit capture and current estimates of injection potential are shown in Figure 191 and Figure 192.

**Figure 191** Injection potential, uncertainty and capture profiles for northern site (scenario 1, nominal dates).

**Northern Injection Site Capture and Dynamic Capacity Estimates**



**Northern site.** With reference to Figure 191, the roll-out scenario discussed in section 4.14, leads to a ramp-up of injection rate matched to the capture development. The FDP and capture have been *engineered* to match at a maximum rate operated at maximum flowing bottomhole pressure (point A). It may be possible to modify the reference case FDP within the set philosophy and constraints to support a slightly higher rate (e.g. to complete the retrofit of Tarong North or to add CCGT emissions), but this *may* be at the cost of reduced plateau durations. The solid, injection potential profiles in the figure, represent a “low” or poor reservoir case (light blue) and a “ref” or reference reservoir case (dark blue). If the low case is encountered, then the site could accommodate the captured emissions (> 6 Mtpa) just beyond the assumed end of plant life (point B). If the reference reservoir case is encountered, then there would be potential to continue injection at high rate for around 25 years extra (point C).

**There may be sufficient storage injection potential to support significant plant extensions, new builds or the later “plumbing in” of CCGT plants in the high-graded area.**

**Figure 192** Injection potential, uncertainty and capture profiles for southern 2 sites (scenario 1, nominal dates).

**Southern Injection Sites (x2) Capture and Dynamic Capacity Estimates**



**Southern sites.** With reference to Figure 192, a capture deployment ramp up is shown. Again, the FDP and capture have been *engineered* to match at a maximum rate operated at maximum flowing bottomhole pressure (point A). In the south, it is more difficult to attain a -6 Mtpa rate. Two injection pads are required due to poorer reservoir quality in the reference case than in the north (though this could give some potential for additional wells within the footprint constraint). The solid, injection potential profiles represent a “low” or poor reservoir case (green). A reference reservoir case is not shown in this figure because low and reference case reservoirs are similar in this area. In this low case, the FDP has included additional wells on the same pads. Beyond this, options for in-fill drilling to manage decline would be limited under the development constraints, and expansion to the south is thought to be limited due to increasing seal risk. Nevertheless, even in the low reservoir case, there is still potential for a major plant emissions abatement for around 20 years *beyond* the assumed life of existing plants (point B).

Towards the end of the plateau (point C), the reservoir dynamic is influenced by interference between the two pads and decline would be relatively rapid. Note that the apparent levelling off of injection potential at point D is an artefact.

## 4.16 Conclusion (technical feasibility)

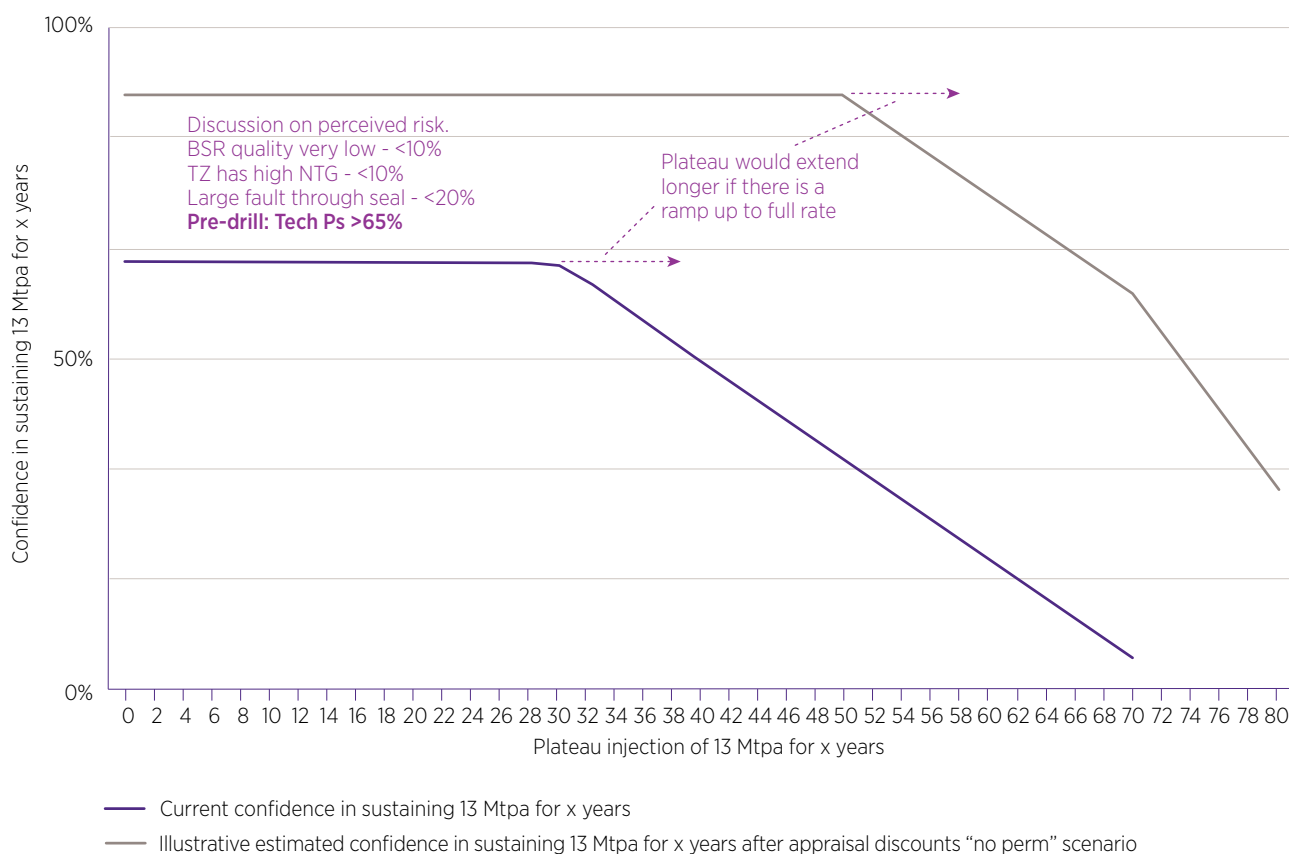
The research set out to produce a dynamically calibrated estimate of for the Precipice-Evergreen play in the Surat Basin. UQ-SDAAP adopted a lowest risk, site selection and development philosophy, with minimum surface and subsurface footprint. The study aimed to inform a decision as to whether to continue to invest in site appraisal by evaluating whether or not material carbon abatement was likely to be technically feasible. It is.

Notwithstanding the need for site-specific data, the following observations can be made:

- It is feasible that material injection rates (i.e. well over 5 Mtpa) can be sustained for more than 20 years and possibly 40+ in each of the northern and southern sites. In this study 12.7 Mtpa was supportable.
- This would accommodate capture from the three modern supercritical power stations, as described in scenario 1, as well as the other scenarios (Gamma Energy Technology 2019)
- High rate injection potential is probably achievable for around 20 years more than (beyond) the currently estimated technical of the three plants
- There are discrete technical risks that require appraisal before a full project can be sanctioned (section 5.5)

As a whole, the dynamic capacity constructed in this research is approximately 13 Mtpa for at least 20 years, and possibly up to 40 years or even longer. With reference to Figure 188, an illustration of current views and confidence levels is given in Figure 193.

**Figure 193** Illustration: confidence in ~12.7 Mtpa now and (est.) after appraisal (20 to 40 years). It is expected that confidence in longer plateau periods would be influenced by early operations and M&V.



A summary of critical success factors to progress the options is given in section 5.

# 5. Next steps: actions required to progress CCS

UQ-SDAAP summarises the next stage of actions to progress CCS in four themes:

**Theme 1: Clarify regulatory pathways.**

**Theme 2: Continue and deepen community and stakeholder engagement.**

**Theme 3: Acquire site-specific subsurface data.**

**Theme 4: Setting up and growing a suitable venture company or entity.**

## 5.1 Discussion

Section 3 of this report summarises an updated understanding of public perceptions and options on future energy choices (with CCS as one of a mix of options). It also summarises current ambiguities in Queensland regulations which need to be addressed. Two action themes arising from this are:

**Theme 1. Clarify regulatory pathways.**

**Theme 2. Continue and deepen community and stakeholder engagement.**

Section 4 of the report then investigates the potential for carbon abatement through CCS in particular to establish what the rate potential is, and for how long CO<sub>2</sub> can be safely injected. For this, a complete revision of the lowermost basin geology was required. Additionally, the project accessed a significant amount of large-scale, dynamic calibration data courtesy of the oil and gas industry. A lowest risk (not lowest cost) philosophy to site-screening and CO<sub>2</sub> storage development was created. This resulted in the demarcation of an area of the deepest parts of the Surat Basin (>2.3 km depth) where a high rate of CO<sub>2</sub> can be injected, with few containment risk features and minimal lateral migration of the emplaced plume.

Sections 4.8 to 4.13 show that it is likely that around 12.7 Mtpa of CO<sub>2</sub> can be injected and securely contained for at least 20-30 years within manageable and large areas, with beneficial groundwater impacts. There are “dynamic capacity” uncertainties which need to be carefully discussed (section 4.15). However, there seems to be a reasonable chance of this extending out to 40 years. It is further possible, but not *knowable* on existing data, that this could extend out even as far as 60 years. It is finite, but the maximum duration is uncertain. These magnitudes could accommodate the majority of emissions from the three existing, modern supercritical power plants for their remaining lifespan as well as additional abatement from other sources.

To better define opportunities and possibilities as required to enable lowest *total system costs of decarbonisation*, as demonstrated by Boston et al. 2019, another crucial action theme arises. This is by far the most extensive and expensive.



### Theme 3. Acquire site-specific subsurface data.

Finally, section 4.14 has also investigated a roll-out and deployment scenario which would have minimal reduction to baseload power availability, maximum learning, plant disruption shared across locations and owners/operators, and manages overall risk by disaggregating one very large “hub” investment to several smaller investments, each of which is stage-gated and at each a decision to “halt” can be made.

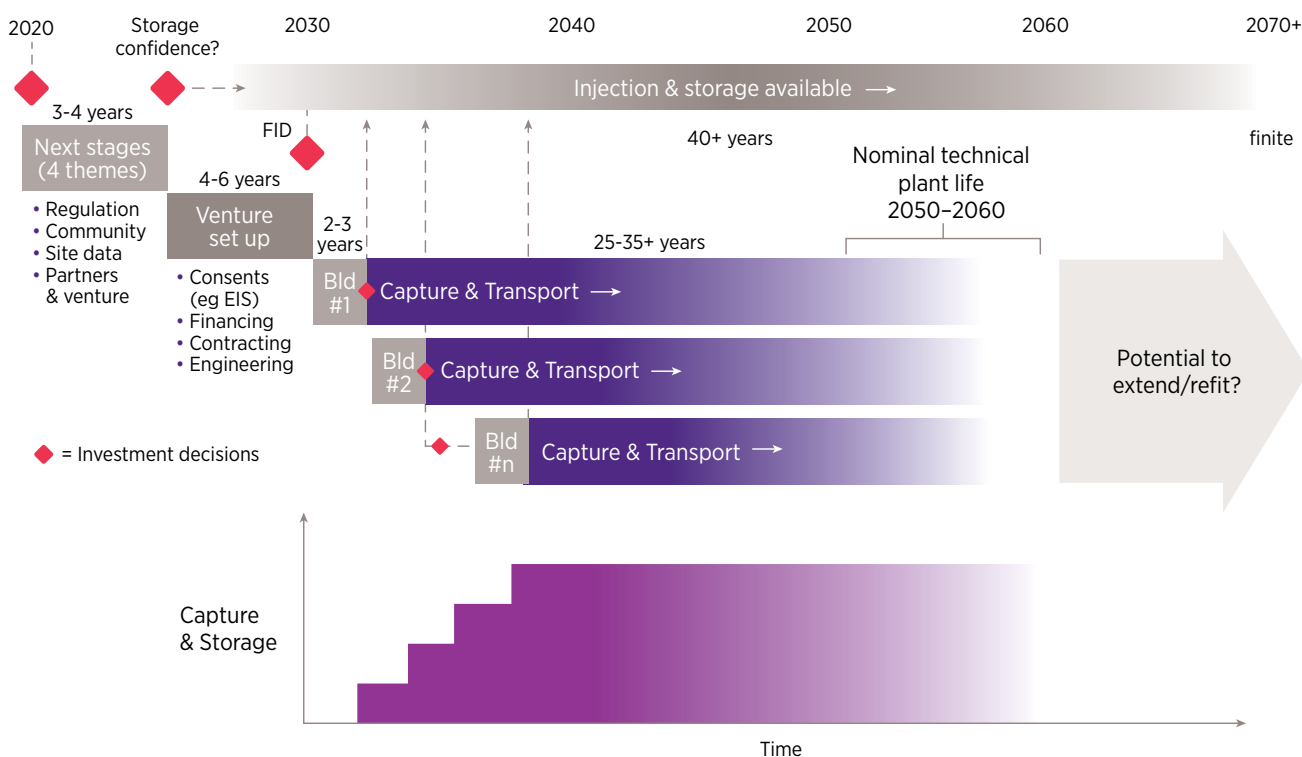
Previous work has highlighted the organisational challenges in progressing large scale CCS project e.g. Garnett et al. 2012 chapter 2; Greig, Baird & Zervos 2016b, Herzog 2017, Kapetaki & Scowcroft 2017 and Berly & Garnett 2018.

Not least of these challenges relates to raising finance, securing large engineering contracts and undertaking complex EIS processes, while at the same time progressing the three action themes above. This leads to:

### Theme 4. Setting up and growing a suitable venture company or entity.

A high-level timeline is shown in Figure 194 and the action themes are further described.

**Figure 194** High level timeline to carbon abatement through retrofit.



## 5.2 Overview – project forward risk assessment

The project has identified and explored (and in many case reduced) the deployment risks associated with material scale CCS, hub deployment. These risks arise from the various analyses described in section 3 and 4, and are summarised further in Honari et al. 2019e. A summary is shown in Figure 195.

**Figure 195** UQ-SDAAP risk matrix (forward progress) appraisal and contingent deployment stages.

### Technical risks

Consequences	5				R51 (Maturity of assessment)	
	4	R8, 9, 10, 11, 12, 13, 15 & 41	R18 & 43	R20	R34 (also an opp)	
	3	R22, 23, 39, 40 & 42	R3, 7, 19 & 21			
	2	R1, 2 & 4	R5, 16 & 24		R17	
	1	R6				
		1	2	3	4	5
Probability or Likelihood						

### Non-technical risks

Consequences	5	R33	R27	R25, 26 & 49	R30 & 31	R28 & 32
	4	R46	R29	R36, 37 & 38	R34 (also an opp)	R35
	3	R47 & 48				
	2					
	1					
		1	2	3	4	5
Probability or Likelihood						

With reference to Figure 195, the main risk (R51) relates to the maturing of **site-specific** measurements assessments. This is a compounded risk in that it highlights the importance of a better evidentiary base to underpin any decision to deploy (or not).

If not addressed (through UQ-SDAAP the proposed appraisal plan, theme), it is scored as highly consequential in the technical, economic, social and political domains. It will not be possible to progress other regulatory and community based risks, nor to adequately plan for a Hub deployment without these data. It is deemed almost certain that failure to acquire these data would prevent any project being defined adequately.

Note that **the majority of the “High” risks are non-technical** (though they are dependent on improved assessment of specific sites. They are generally speaking related to regulatory pathways and community engagement (Honari et al. 2019e).

The highest non-technical risks are listed below, though there are many others which are significant and to be addressed through the proposed action themes in stage 1 (Figure 194).

- R28 Legal & Reg: Environmental Protection Regulations prevent injection of CO<sub>2</sub> as “waste”
- R30 Legal & Reg: Complexity of water allocations impacted under Water Act
- R31 Legal & Reg: CO<sub>2</sub> injection is “interfering with water” (including pressure beyond tenement)
- R32 Legal & Reg: GABORA (nor EPBC) does not yet consider large scale injection impacts
- R35 Social: resistance to further appraisal works and possibly subsequent development works (though they are contingent)

The four action themes have been constructed with a view to addressing the uncertainties from the social and technical analyses and with reference to actions included in the Project Risk Register (*ibid*).

## 5.3 Regulatory pathways (theme 1)

**The large-scale implementation of CCS requires the development, adaptation or modification of Queensland's existing Green House Gas (GHG) and environmental and water regulations. A regulatory roadmap needs to be constructed with the Queensland Government. Furthermore, interaction (if any) with the federal *Environment Protection and Biodiversity Conservation Act 1999* needs to be defined.**

The UQ-SDAAP study found that it would be important to conduct early engagement with the regulator in five key areas:

1. Whether a waste stream of CO<sub>2</sub> would be classified as an 'end of waste' product
2. Whether deep aquifer storage of CO<sub>2</sub> could be considered a public amenity. It is important to note that managed aquifer recharge (MAR), as practiced by coal seam gas operator APLNG, is considered "beneficial use"
3. Whether remote pressure inflation or water level increases off-tenement would be recognised as a benefit and can be allowed through some appropriate instrument
4. Whether this benefit and/or GHG emissions mitigation could be argued to trade off against what might be classed as environmental 'harm' or changes to localised groundwater quality
5. Whether water licences currently held by some extractors (mining, petroleum and gas resource extractors and, to a lesser extent, stock and domestic users and Aboriginal and Torres Strait Islander people) need to be curtailed from the injection reservoir in the local injection area to prevent interference with an emplaced CO<sub>2</sub> plume

The Queensland Government needs to be engaged initially on these regulatory questions. Sometime into the exercise, the Australian Government will also need to be engaged.

A clear regulatory pathway would be needed to progress beyond the appraisal stage. UQ-SDAAP suggests a taskforce approach.

## 5.4 Community and stakeholder engagement (theme 2)

Further engagement with key stakeholders is required to inform and explore the nature of benefits and trade-offs associated with the establishment of a large-scale CCS hub in the area. This needs to be set within the broader context of long-term decarbonisation of the energy sectors. It is expected that a period of at least 24 months will be required to deepen the discussion and establish ongoing dialogue with a range of key stakeholders and other community members on the topic of CCS. It will be important to include mine and power plant employees as a key group to engage about CCS and its associated implications.

There are a number of clear activities that will be required to overcome the low levels of knowledge about CCS that exist in the general public, particularly, in regional areas across the Surat Basin if the CCS hub project was to go ahead. Some of these activities are outlined below, in no order of priority.

### 5.4.1 Engaging with local communities

- Clearly, there is a need to continue the **engagement in local communities** and explore in more detail individual concerns that arise from discussions around injecting CO<sub>2</sub> into the Great Artesian Basin. The project recommends using the large group process designed by Ashworth, as it has already successfully trialled across Australia, and subsequently in Canada, Scotland and the Netherlands. The process provides a way to maximise time and engage a larger group of individuals together. This allows the opportunity for everyone to hear a variety of views
- **Influential stakeholders across the region**, local council representatives, small business owners, and other community groups should be engaged in a more targeted fashion. Depending on the final potential sites, this could be through establishing community interest and advisory groups that serve as a reference point into communities
- **Local employees of power plants and associated mines** – there is no doubt these are an important stakeholder group that needs to understand the risks of power plant shut downs to them, and what opportunities could arise from investment in a CCS hub. This could be a mix of face-to-face as well as print material that is openly shared across the region
- **Schools** also form a good vehicle to raise awareness about CCS and where it fits in the portfolio of mitigation options. Different materials have already been developed that could be easily adapted and implemented over the school year

### 5.4.2 Awareness raising at the national level

- While the **media coverage** has dropped considerably and is almost non-existent, there is an opportunity to provide **more active blogs about CCS** in the portfolio of responses to climate mitigation. However, the focus of the blogs should centre on the need for baseload power, the jobs and services that would be sustained in the region, and economics over time. Ideally moving the discussion away from an us versus them discussion, to one focussed on the tangible practicalities would be helpful
- It will be important to **engage influential stakeholders**, politicians, journalists and financiers on the opportunities presented by following on the UQ-SDAAP project and just what it entails. This would take consistent and repeated engagement, but should not be overlooked
- **Policy makers, both state and federal**, will need to be included on the discussions about latest requirements and changes around regulatory requirements and how this can be managed
- Build on the lessons learned from experimental research as it is rolled out

### 5.4.3 Monitoring of attitudes

The national survey, with an over-emphasis on regional Australia, provides good insights into ongoing knowledge and awareness of CCS. This should continue with a replication of the 2019 survey to allow comparisons over time. It can also allow testing of whether any of the targeted community engagement is increasing knowledge and awareness over time.

## 5.5 Site-specific appraisal data gathering (theme 3)

Seismic surveys, deep well drilling and non-CO<sub>2</sub> well tests are required to finalise whether or not the potential, lowest risk sites prove suitable. If after additional data gathering, technical suitability is confirmed, then designs, costs and risk mitigation can be finalised (d, below). This could require immediate investment of around \$100 million to appraise all sites and undertake the additional necessary pre-project works (themes 1, 2 & 4). This range also assumes that early engineering work can be commenced because the wells find the geology to be as promising as expected. If it turns out to be poorer quality, this program might be halted and the total spend might then be around \$50 million. Environmental permitting and contracting are also required in the short-term for the appraisal data-gathering phase.

This project has focussed on the Surat Basin as it had previously been identified for its high-grade, lowest risk, high rate storage potential. However, **to maximise the potential for CCS in future Australian carbon abatement and industry development (e.g. hydrogen) it is essential to appraise other Queensland basins by drilling and testing new, dedicated wells to obtain dynamic data.**

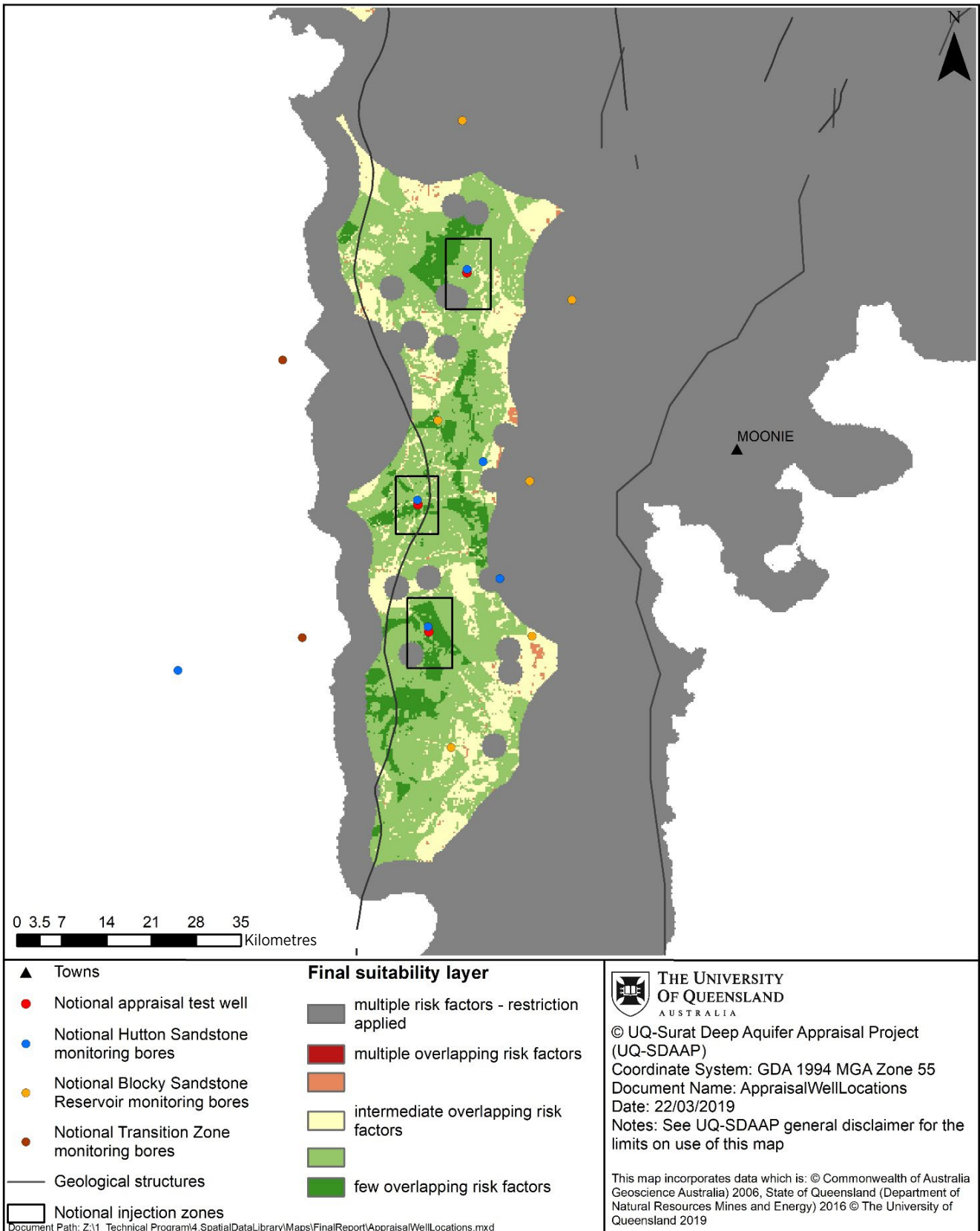
While UQ-SDAAP analyses to date suggest that industrial-scale CCS development in the Surat Basin is technically feasible, the concept remains at a pre-appraisal, almost “greenfield” stage. With limited well control and limited seismic control, the notional injection sites lack data and thus have remaining uncertainty – too high for a financial investment decision (FID) of >\$ 1 billion on a commercial-scale storage project. Further technical appraisal work is needed to confirm the feasibility of developing a CCS carbon abatement option.

The sole purpose to undertake such a CCS project would be to achieve *material* abatement. Therefore, any activities, risks and disturbances that do not inform and lead to this, are not supportable and may decrease the chances of development. It is essential that all appraisal work can demonstrably and convincingly be shown to minimise risk, minimise footprint and minimise negative groundwater impact and lead to a material environmental gain. UQ-SDAAP has identified three notional injection sites based on surface and subsurface selection criteria anchored in risk avoidance philosophy, and these three sites form the basis of appraisal plan development, assuming that commercial storage with a material climate impact is the objective. Details of the notional injection site appraisal plan and data acquisition can be found at Honari et al. 2019.

### 5.5.1 Technical storage project risks

Three notional injection sites are located mainly within the EPQ-10 permit area with one site in a northern region of EPA-A10 (N1) located approximately 45 km to the north-west of the Moonie oil field and two sites in the southern region (S1 and S2) of EPQ-10A approximately 45 km south-west of the Moonie oil field. Figure 196 describes the notional injection sites including the N1, S1 and S2 locations.

**Figure 196** Location map of the proposed notional injection sites in Surat Basin in Queensland, Australia.



Over 50 individual opportunities and risks have been identified by UQ-SDAAP. These include the technical, environmental and legal risks relating to a notional commercial-scale CCS project in the Surat Basin as well as opportunities such as enhanced water recovery and greenhouse gas mitigation. The full list can be found in detail in Alan et al. 2019. The remaining technical uncertainties to be addressed by an appraisal program can be prioritised based on the sensitivity analysis conducted through dynamic simulation. Some of these key uncertainties can be collectively reduced by data acquisition relevant for all three sites and others require specific data acquisition at each site individually.

**High priority uncertainties:**

1. The thickness, porosity and bulk permeability distribution of the Blocky Sandstone Reservoir
2. The lateral continuity of the bulk permeability in the Blocky Sandstone Reservoir away from the notional injection sites
3. The location of the western pinch-out edge of the Blocky Sandstone Reservoir
4. The existence (or not), location, throw and orientation of faults in the area of the three notional injection sites

**Moderate priority uncertainties:**

- The dip of the strata and quality of the seismic depth conversion within a 10 km radius of each of the notional injection sites
- The detailed nature of the stratigraphy and geobody geometry in the Transition Zone within a 10 km radius of the notional injection sites
- The in-situ stress and geomechanical properties of the storage complex stratigraphy
- The geology and rock properties of the strata beneath the sub-Surat Unconformity in the vicinity of the three notional injection sites

A more complete list of subsurface uncertainties and risks is discussed in Honari et al. 2019e and 2019b.

All three notional injection sites are in the southern depositional centre and share common “stratigraphic/depositional risks” where new data from any one of the sites would inform the others. Uncertainties in reservoir and seal properties arise from extrapolation from areas with data control to deeper areas without. Hence, uncertainty generally increases with both depth and with distance from well control. Therefore, new stratigraphic/depositional data obtained through a data well from the deeper, more remote sites would reduce uncertainty the most.

A well-based appraisal program at one site location will address stratigraphic/depositional uncertainties across all sites with some advantage of placing a new well at one of the two southern sites first. However, while stratigraphic data from any one site will inform certain risk categories on the other sites as well, structural data (presence or absence of faults and the location of the Blocky Sandstone Reservoir pinch-out) at one site would not inform likelihood of structures at the other sites. While the high-graded areas are considered to have low chance of major faulting (from structural narratives) seismic data density in these areas is low and ‘demonstration’ of lack of faults is not possible with the current data. Site-specific 2D seismic acquisition would increase confidence in optimal appraisal well siting and would provide evidence that significant faults structures were absent.

## 5.5.2 Appraisal strategies

Appraisal activities are designed based on a minimum work requirement for uncertainty reduction. The main critical risks identified within the UQ-SDAAP evaluation include: (i) the potential presence of significant faults or boundaries (Blocky Sandstone Reservoir pinch-out) which should be avoided in the optimal selection of final injection sites; and (ii) the potential for a significant reduction in reservoir quality (permeability and heterogeneity).

In all appraisal scenarios, both surface seismic data and new well data and testing is required. However, a priority assessment can determine the most appropriate sequence of data acquisition (seismic data acquisition or drilling of the appraisal well first). There are pros and cons to each choice of sequencing and the best approach comes down to a determination if reservoir quality ( $k_r$ ) or the location of thus far undetected faults presents the higher risk. This decision can also be impacted by the urgency to reach a final investment decision (FID) and finalise deployment design.

**Discussion on risk, pace and sequence:** Technically, it would be possible to commence an appraisal drilling and testing program based on current seismic data in N1 or S1 rather than wait for new seismic data to be acquired. If a well was drilled that confirms adequate or inadequate permeability, this result would apply all three (N1, S1 and S2) notional injection sites (see geology conclusions of La Croix et al. 2019a and 2019b). In this case a negative result can kill the play for all sites without having to invest in seismic. However, if the appraisal well indicated favourable rock properties, it may be located in a sub-optimal position for well testing with respect to subsequently discovered faults or the reservoir pinch-out boundary with the benefit of a subsequent seismic acquisition program. If this was the case, the appraisal well might usefully be converted into a monitoring well with a new injection well being drilled in an optimised location based on the new seismic.

The appraisal program generally can be defined in two ways:

1. The **idealised appraisal case** for any one of the three notional injection locations therefore starts with acquisition of a new in-fill 2D seismic grid that will be tied to key wells in the area. This is a data driven program to mitigate risks of the key uncertainties. The new in-fill 2D seismic acquisition has a suggested line spacing of ~4 km and orientation that will reduce possible aliasing of faults with strikes expected to be present in the area (Gonzalez et al. 2019a). After processing and interpretation of the seismic data, this will be followed by the drilling of an appraisal well. A basic well appraisal program would comprise a pair of wells per site. The 'main' appraisal well would be drilled to a depth beneath the base-Surat Unconformity. A second well could be drilled to the base of the Hutton Sandstone and completed in a suitable high permeability zone above the Ultimate Seal. The two well configuration allows for a vertical interference test (VIT) by applying pressure to one and monitoring a pressure response in the other, with the two completions separated by the Ultimate Seal and Transition Zone. The main well would also be the site of a specifically designed dynamic, production and injection extended well test (EWT) (e.g. draw-down / build up or similar), which will investigate a wide radius of investigation (ROI) into the reservoir, preferably sufficient to confirm the nearest mapped possible baffle or barrier
2. An **'accelerated' case** is essentially the same as the 'idealised' one, but it would start with a staged seismic and well data together. Rather than increase the odds of selecting an optimum well site location (away from faults), an early decision can be made on existing data with the selection for drilling of the "best" location(s) based on existing seismic data. *The risk run by this approach is that subsequent seismic data acquisition shows that the location is not optimal for injection.* In that case the well could be completed as a monitoring bore or plugged and abandoned. A poor result relating to reservoir permeability would negate the need for any extra spend on drilling, testing or on seismic data as it would kill the prospective for all three sites (N1, S1 and S2). The likelihood of a poor reservoir quality is considered low compared to the risk of unrecognised faults being located near any of the three sites. This is not the recommended program

Since the lack of structures at one site does not lead to a de-risking of the other in this regard, the possibility of a phased seismic program that matures one drilling site in advance of another could be implemented.

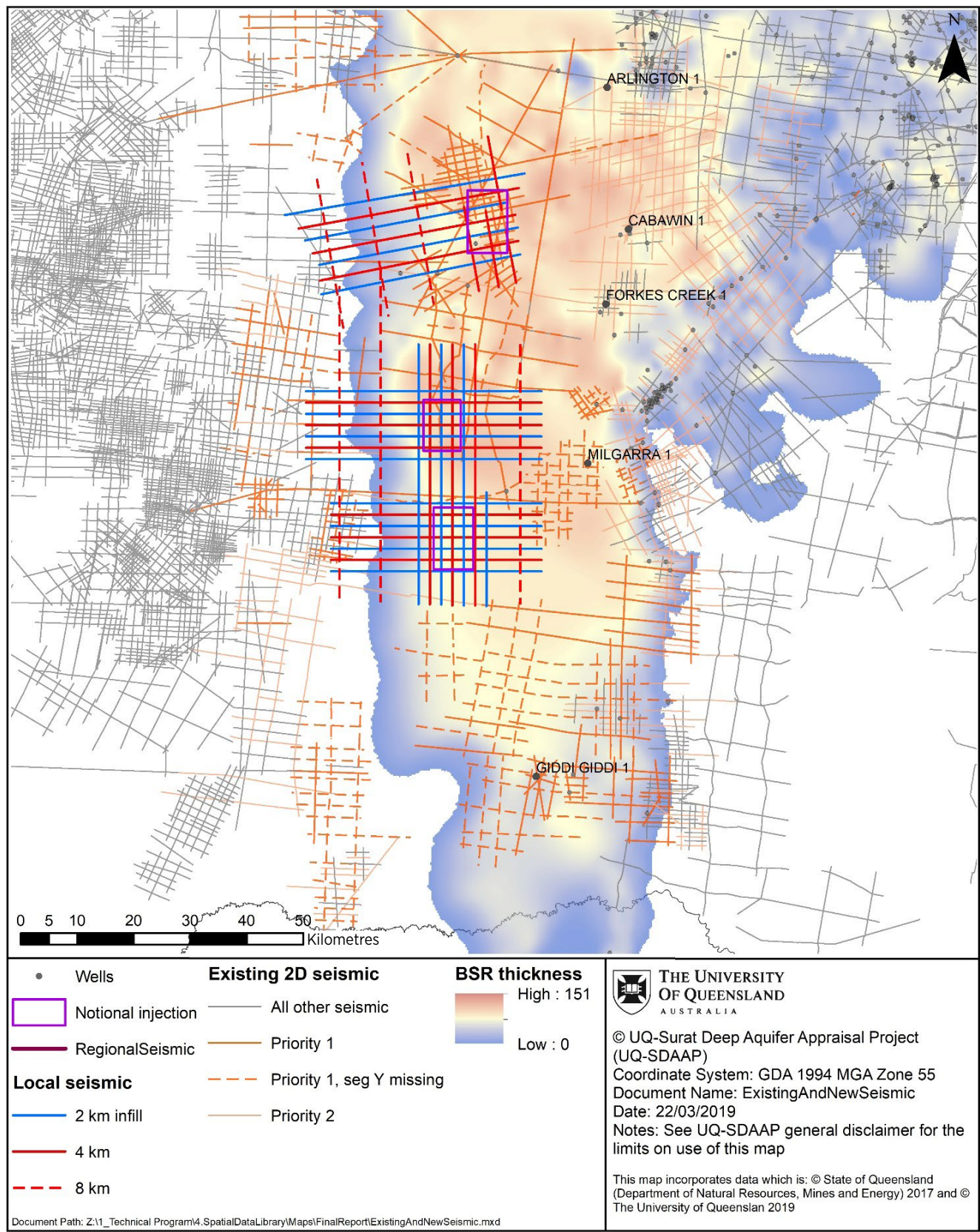
**To minimise ambiguity for later decisions, it is important first to acquire site-specific 2D seismic data and optimise the first appraisal well location (i.e. ensure maximum separation from faults); and also to optimise well test design (i.e. to ensure that the radius of investigation of the EWT would reach any faults in the vicinity and to ensure that a Hutton VIT could be optimally placed).**

The first site can then be tested with a well(s), while a seismic program continues to cover the other areas sequentially. It is also possible that any appraisal of the second or third site could be postponed (to reduce the pace of appraisal spend). This however leaves open the chance that there is insufficient data available on the second or third sites to assess storage options required for a full hub development (rather than a single source-sink development) and thus insufficient information to assess the financial benefits of optimised surface equipment design (particularly the pipeline size) of a wide deployment roll-out.

For the purposes of this document and the UQ-SDAAP project, it is assumed that the south location (S1) becomes the first drilling and testing target for appraisal followed by the other two sites N1 and S2. All three would be covered by the initial N-S and W-E, 4 x 4 km 2D seismic acquisition program (Figure 197).



Figure 197 Overview of suggested appraisal program.



### 5.5.3 Appraisal well Blocky Sandstone Reservoir testing program

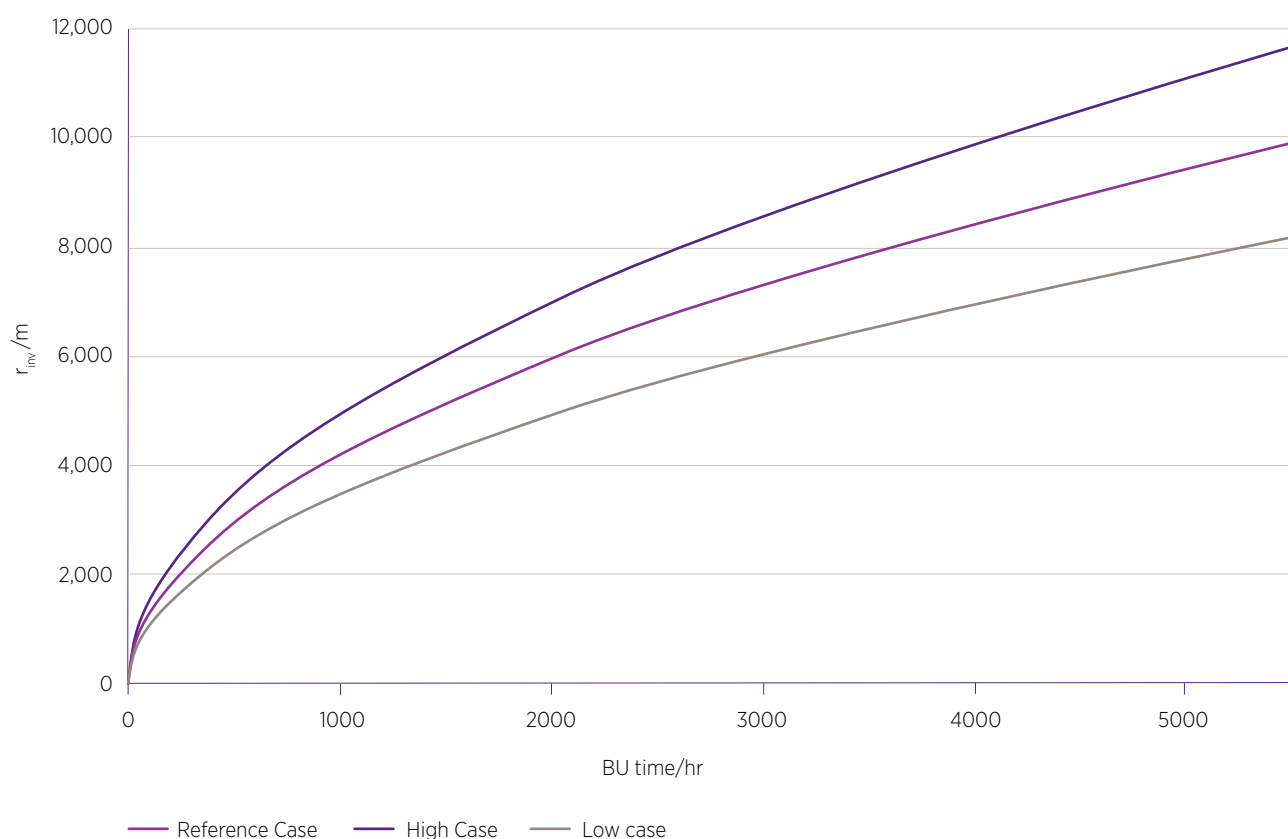
A wireline formation testing tool is proposed to be run prior to the extended well test in order to estimate permeabilities of different formations (Blocky Sandstone Reservoir, Transition Zone, Ultimate Seal and Hutton Sandstone) and their virgin pressure. This would potentially assist the operator to design the EWT based on new acquired data. Production testing of the main appraisal wells are required to understand reservoir dynamic properties and any barriers in terms of faults or the Blocky Sandstone Reservoir pinch-out distance away from the wellbore.

Table 65 summarises relevant modelling parameters defined for low, mid and high cases to estimate production rate, production time and shut-in times required during the dynamic production testing for the appraisal plan. Three scenarios were considered to design draw down – build up (DD-BU) well test and the parameters shown in Table 65 was utilised to evaluate the well testing sequences required for low, mid and high cases. Based on these reservoir parameters, the radius of investigation (ROI) were plotted versus build-up time shown in Figure 198. It is noteworthy that the ROI illustrated in Figure 198 does not take into account the gauge resolution.

**Table 65** Modelling parameters for well testing design for notional injection site in south-central Surat.

Parameter	Low Case	Reference Case	High Case
Reservoir Porosity	8.7	12.7	16.7
Reservoir Permeability (mD)	22	43	87
Rock Compressibility (kPa <sup>-1</sup> )	2.6 x10 <sup>-7</sup>	4 x10 <sup>-7</sup>	5.2 x10 <sup>-7</sup>
Max. Rel Perm to CO <sub>2</sub> (krgmax)	0.1	0.18	0.3
Capillary Pressure Curves (TZ)		Base	
Residual Water Saturation	0.25	0.4	0.55
Residual CO <sub>2</sub> Saturation	0.2	0.35	0.5
Temperature (°C)	65	87.5	90
Salinity (ppm)	1000	3000	5000
BHP Limit (kPa)	32500	39500	46000
WHP Limit (bar)	80	150	200
k <sub>v</sub> /k <sub>n</sub> – Reservoir	0.12	0.15	0.3
k <sub>v</sub> /k <sub>n</sub> – TZ	0.2	Varies	50
Skin	-2	0	10

**Figure 198** Radius of investigation for the testing well located in notional injection site calculated at various build up periods in a low, mid and high case.



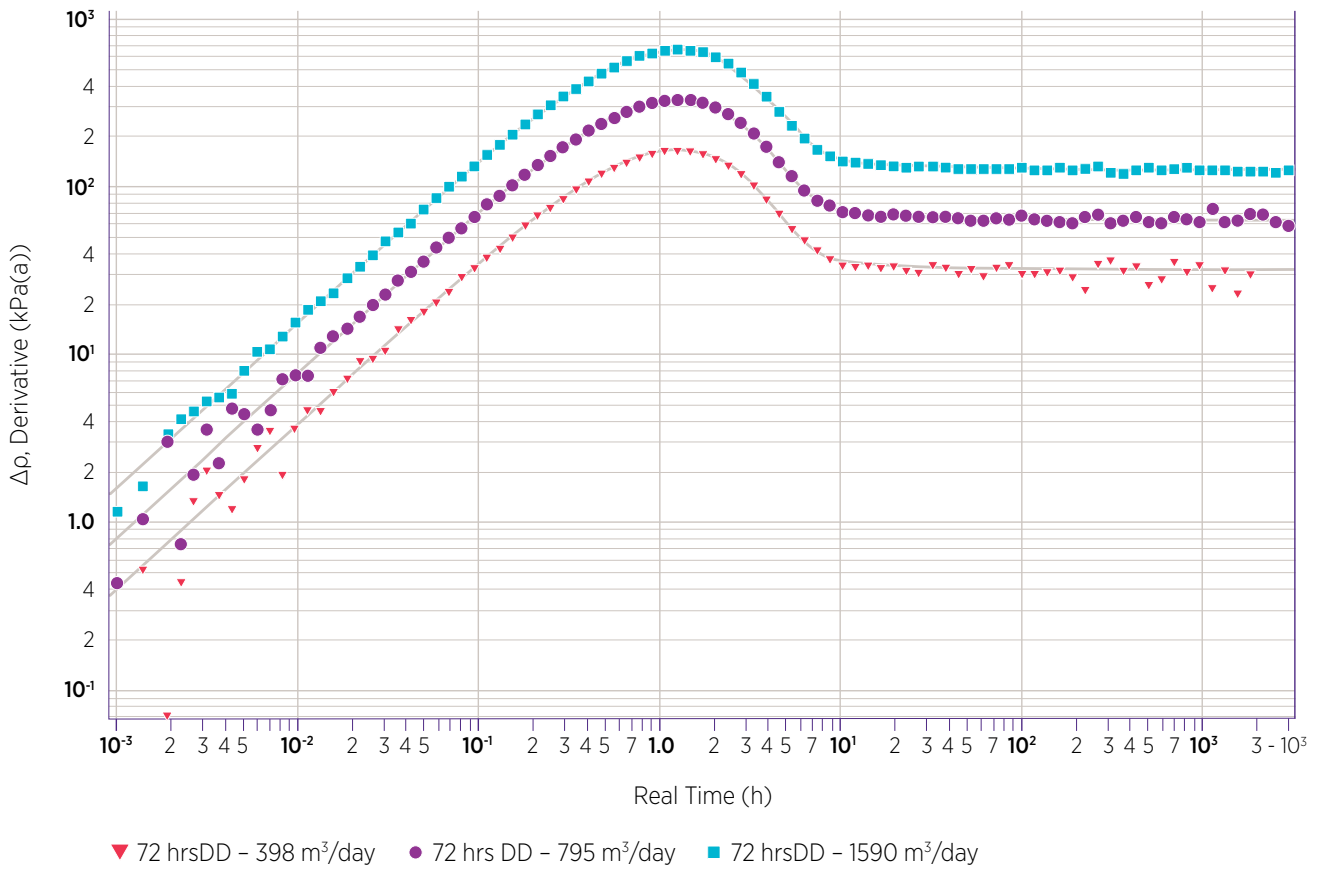
Results from the dynamic model have indicated that CO<sub>2</sub> plume will remain within 2 km from the injecting well (depending on assumed rates and period of injection). In addition, the Basal Sandstone Reservoir is estimated pinch-out ~9000 m away from the S2 notional injection site. Therefore, a ROI of ~9000 m was considered to be *adequate at this stage of modelling* in order to de-risk/evaluate the storage capacity of Blocky Sandstone Reservoir in the south-central Surat Basin. **This needs to be revised after site specific data is acquired.**

Draw down and build up periods and rate for the reference case in Table 66 were used as the basis of well testing scenarios, obtaining a maximum ROI of approximately 9.3 km. Table 66 indicates that the largest test duration is 203 days and the maximum water produced during the test is about 5,000 m<sup>3</sup>. The log-log derivative plots for the testing well located at the notional injection site are illustrated in Figure 199. It indicates that flow rates of 398 m<sup>3</sup>/day and 795 m<sup>3</sup>/day could reach a ROI of about 1.6 km and 3.5 km, respectively, prior to the data becoming noisy. Thus, a higher flow rate would be required in order to confidently achieve the ROI of about 9 km. The draw down time required to achieve interpretable data was estimated based on gauge noise/resolution of ±4 kPa.

**Table 66** Well testing sequences for the reference case in notional injection site.

Well Test Scenario at NIS	Reference Case		
Flow rate (m <sup>3</sup> /day)	398	795	1590
Total produced water (m <sup>3</sup> )	1194	2385	4770
DD duration (days)	3	3	3
BU duration (days)	200	200	200
r <sub>inv</sub> (m)	1600	3500	9300

**Figure 199** Log-log derivative response for the testing well in notional injection site at different pumping rates.

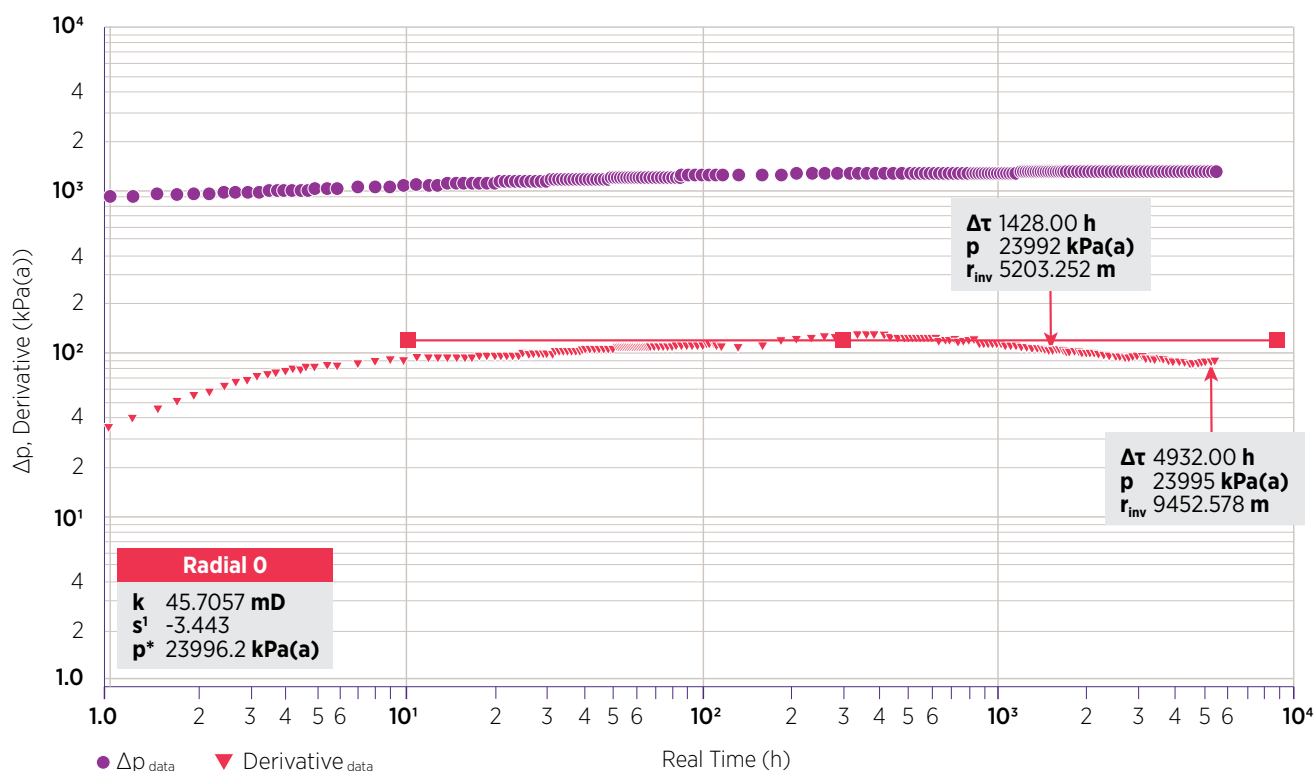


The notional injection site model was used to run a scenario with the reference case reservoir parameters and draw-down period of 3 days, a build-up period of 200 days and pumping rate of 1590 m<sup>3</sup>/day. A vertical well fully perforated over the Blocky Sandstone Reservoir interval and located in the S2 notional injection site was used to perform the well test modelling. Figure 200 shows the log-log plot of pressure response generated by reservoir simulation software package (CMG) and indicates that there would be an interpretable dataset over the whole build-up period. The permeability calculated from the log-log plot is 46 mD with a ROI of 9.5 km. As shown in Figure 200, the pinch-out on western side of the S2 notional injection site starts effecting the log-log pressure derivative where the derivative deviates from the horizontal line (at build-up time of ~1500 hours).

**A significant component and cost of the site appraisal will be to conduct a well test with a draw-down and build-up of sufficient duration to appraise a large reservoir volume for pressure boundaries including the location of the Blocky Sandstone Reservoir pinch-out distance or the location of unknown faults that are acting as barriers. To achieve a radius of investigation of say, >9 km for the assumed reservoir conditions at the S2 injection site and a fully penetrating and perforated vertical well, a draw-down period of 3 days, a build-up period of 200 days and pumping rate of 1590 m<sup>3</sup>/day could be required. In the event, the extended well test (EWT) should be designed with reference to the proposed new seismic data. It will be important for the ROI of the EWT to investigate if the nearest faults act as baffles or boundaries.**

**Figure 200** The log-log pressure derivative of an EWT generated by CMG reservoir simulation software and analysed by IHS WellTest software. The pumping rate of 1590 m<sup>3</sup>/day, 3 days DD and 200 days BU were used during this EWT design.

### Typecurve



## 5.5.4 Vertical interference test

A vertical interference test (VIT) is proposed for this appraisal program to investigate the vertical connectivity between the Blocky Sandstone Reservoir and Hutton Sandstone through the Transition Zone and Ultimate Seal. The main appraisal well and the Hutton Sandstone monitoring well can be utilised to conduct a VIT. Two approaches are considered in Honari et al. 2019d – one of which is discussed hereunder.

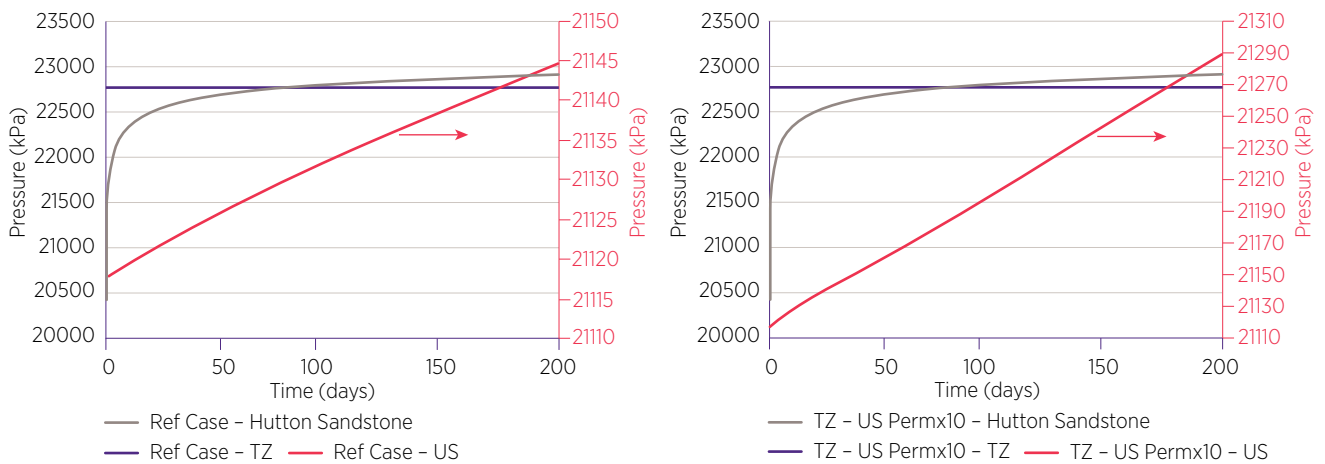
Water is injected into Hutton Sandstone and the pressure change is observed in the Blocky Sandstone Reservoir, main appraisal well. The notional injection site model with the reference case reservoir properties was initially used. Bottomhole pressure (BHP) was chosen as the modelling constraint where the maximum BHP was set to 27,324 kPa which was 90% of Hutton Sandstone fracture pressure taking into account the temperature effect (injecting at 30°C from surface into the Hutton Sandstone at a temperature of 78°C). This BHP constraint allowed an average water injection rate of 9660 m<sup>3</sup>/day (though Hutton permeability is very poorly constrained and Hutton Sandstone continuity is expected to be very low).

As described in Table 67, a scenario was run where the Ultimate Seal and Transition Zone permeability increased by an order of magnitude. Figure 201, shows the modelled pressure response. The results show that the pressure increase in the Hutton Sandstone is about 2620 kPa at the end of the injection period (200days). Both cases showed pressure increase in Ultimate Seal layer and no pressure change in the Transition Zone even with such a large injection rate and duration. Any pressure signal transmitted across the seal-complex would be indicative of either an un-imaged, sub-seismic resolution fault or unexpectedly high connectivity of Transition Zone sands. Seeing no pressure increase in the Blocky Sandstone Reservoir would give a direct measurement of seal potential.

**Table 67** Parameters used during VIT scenarios in which water is injected into Hutton Sandstone and pressure changes observed in the Blocky Sandstone Reservoir.

Water injection into Hutton Sandstone and observe pressure in BSR									
	kh (mD)				kv (mD)				Average Injection rate (m <sup>3</sup> /day)
	BSR	TZ	US	Hutton	BSR	TZ	US	Hutton	
Reference case	43	0.03	0.03	100	6.5	1E-04	1E-04	10	9660
TZ-US Permeability x10	43	0.3	0.3	100	6.5	0.001	0.001	10	9660

**Figure 201** The pressure change in Blocky Sandstone Reservoir, Transition Zone and Ultimate Seal is generated by CMG reservoir simulation software when water is injected at 9660 m<sup>3</sup>/day for 200 days: (top) reference case and (bottom) one order of magnitude increase of permeability in the Transition Zone and Ultimate Seal.



Modelling and regional geology indicates that the Ultimate Seal probably has sufficiently low permeability and is sufficiently thick that even in the worst-case scenario, a vertical interference test (VIT) should not generate an observable pressure response within a reasonable testing timeframe if the sealing hypothesis and estimations are sound. A pressure build-up on an appraisal VIT would indicate that the site is not suitable. Modelling of commercial scale inject of CO<sub>2</sub>, suggests that eventually the Hutton Sandstone could have a pressure increase in the geographic vicinity of the injection wells. Therefore, a Hutton Sandstone appraisal well serves two purposes (i) to uncover any fatal flaws in the current seal-complex hypothesis through a VIT; and, (ii) as an effective M&V well during later large-scale injection.

### 5.5.5 Costs and notional plans schedules

Cost estimates for the N1, S1 and S2 appraisal programs are summarised in Table 68. These figures are current as the date of this report, using UQ's market sources and local service companies in Australia. A schematic schedule is shown in Figure 203.

The cost estimates are considered to be conservative. The nature of the operating entity is unknown and important (theme 4). In order for it to operate, it will need to have access to significant additional funds to enable any board or similar governance structure to carry and respond to typical risks and exposures.

This high-level estimate excludes the following cost relating to this and other themes:

- Typical establishment and 'owners' costs (could be up to 10%)
- High operational contingencies for drilling and extended testing (allow up to 20%)
- Costs for early engineering studies (promising results from drilling and testing would enable acceleration of prefeasibility engineering)
- Costs for pre-EIS environmental studies or baselines (as above, promising results would open this opportunity if funds were available)
- Costs for community outreach
- Costs for regulator engagement

For the purposes of scoping economics, an assumption has been carried that spend could be up to \$97 million over a 3-4 year appraisal period.

**Table 68** High level cost estimates (all costs are before market testing) for proposed appraisal program of both the north and south notional injection sites.

Activity	Description	N (\$1000)	S1 & S2 (A\$1000)	Total (A\$1000)	Notes
Technical Study Costs	G&E (Geological, Engineering), admin and technical management fees	\$5,000	\$5,000	\$10,000	Early work and during the appraisal program
Planning & Application Cost	High level tenement and land applications	\$300	\$300	\$600	Early work program and permit application cost (includes allowance for NT & CH clearance and EA preparations)
Seismic Reprocess	Re-process good quality existing 2D data for target depth close or inside the area to locate new wells	\$650	\$950	\$1,600	Refer to section Honari et al. 2019d and appendix A about the details of existing lines that require re-processing at the rate of \$400 per km
Drill three vertical appraisal Wells (in N1, S1 & S2 notional injection sites)	Land access	\$100	\$150	\$250	Allowance for contracts and land compensations to the local land owners for large well sites and access tracks.
	Rig mob-demob per site	\$550	\$1,100	\$1,650	Total rig mob-demob of \$1.65 million (potentially from Cooper basin) and assuming all appraisal and Hutton monitoring wells drilled during <b>one</b> campaign
	Drill and core	\$4,525	\$9,050	\$13,575	Drill to ~2500 m TVD and core mid Hutton to TD
	Log & well test (drill pipe/wire line)	\$2,300	\$4,600	\$6,900	Full suite of logs (super combo, dipole sonic, image). Perform frac initiation FI, DST, fluid sampling
	Laboratory testing (geomechanics/geochemistry)	\$300	\$600	\$900	Geomechanics (rock mechanics, stress) /Geochemistry
Drill three Hutton monitoring bores (paired with appraisal wells)	Land access	\$50	\$100	\$150	Contracts and land compensations to the local land owners
	Drill & log to TD	\$2,900	\$5,800	\$8,700	Drill to ~2100 m TVD and log from surface to TD
	Complete the wells (install monitoring gauges in Hutton)	\$600	\$1,200	\$1,800	Create baseline pressure and water quality before/ after injection
	Perform vertical interference test (water injection into Hutton Sandstone)	\$850	\$1,700	\$2,550	Identify any vertical connectivity between the Blocky Sandstone Reservoir and Hutton Sandstone
New Seismic Acquisition (North & South)	2D Acquisition & processing + land access and approvals	\$6,100	\$15,000	\$21,100 +\$4,000 of regional Seismic	Refer to Honari et al. 2019d and 2019e, details of new lines that are proposed at the rate of \$12,600 per km
<b>Total (AUD)</b>				<b>\$73,775</b>	



**Figure 202** Schematic of the completion diagram for the appraisal wells.

**Appraisal Wells (Future monitoring) – Not to scale**

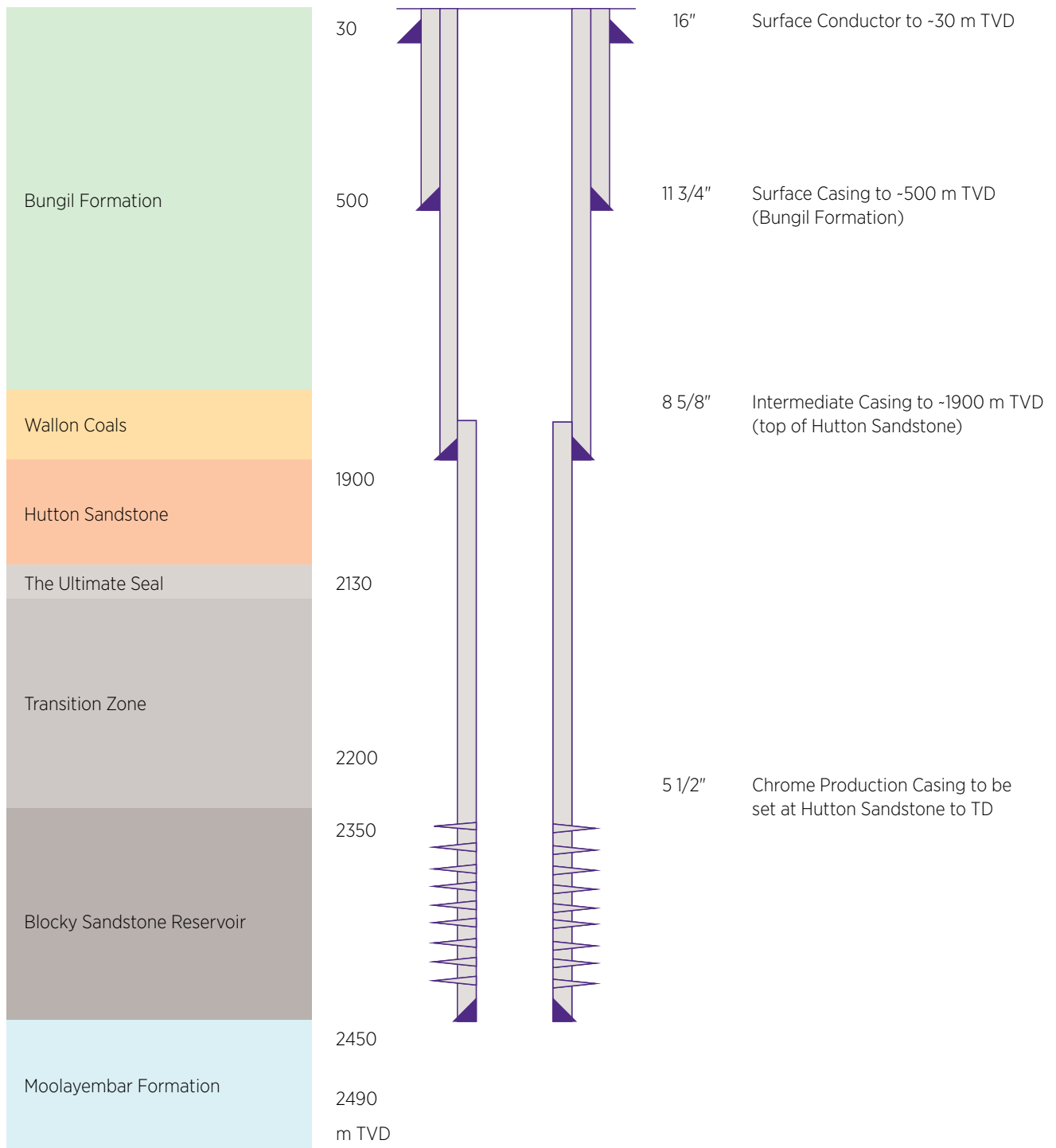
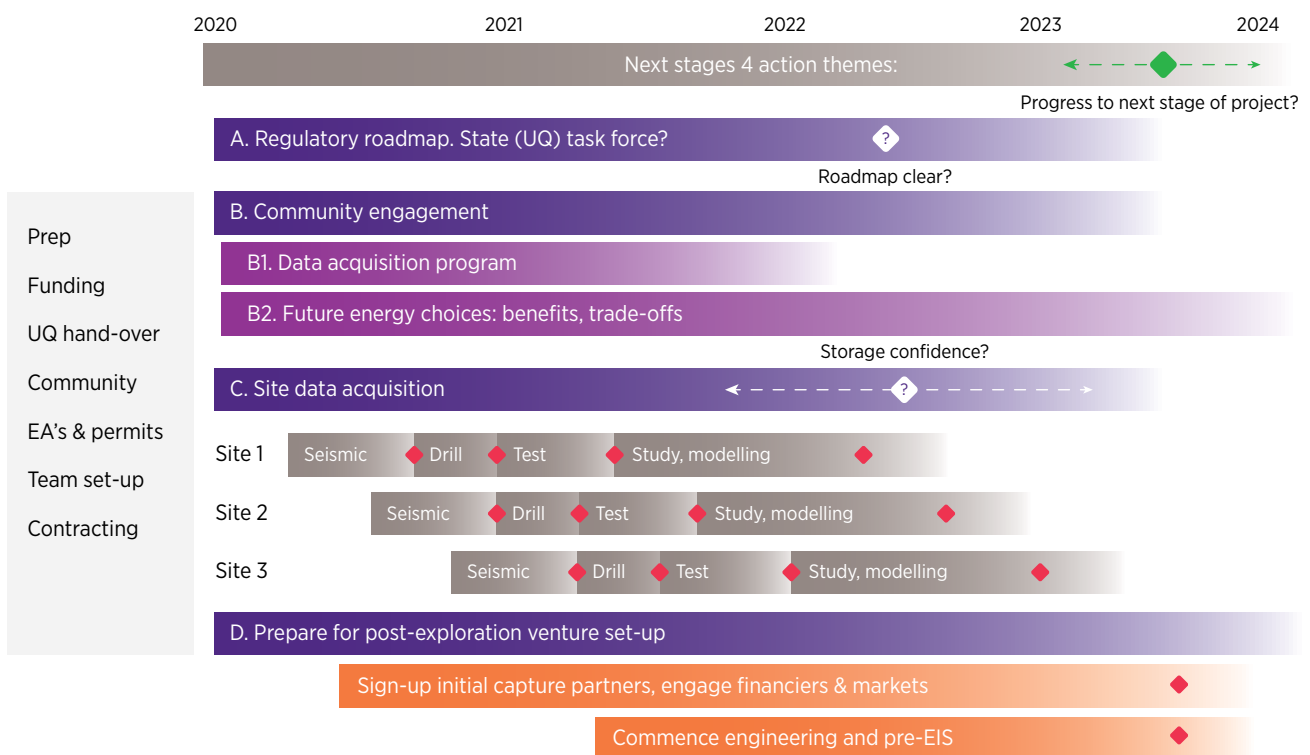


**Table 69** Schematic of logging, coring and downhole testing program requirements.

Assumed Formation Unit			Log	Core	DST/IFT	Fluid Sample	DFIT	LOT
Age	Common Name for Unit	UQ-SDAAP Unit	Y					
Cretaceous	Wallumbilla FM		Y					
	Bungil		Y					
	Orallo		Y					
	Gubberamunda		Y					
Jurassic	Westbourne		Y					
	Springbok		Y					
	Walloon		Y					
	Hutton Sandstone		Y		Y	Y	Y	
	Evergreen	The Ultimate Seal Complex	Y		Y	Y	Y	Y
	Upper Precipice	Transition Zone	Y		Y	Y	Y	Y
	Lower Precipice	The Blocky Sandstone Reservoir	Y		Y	Y	Y	Y
Triassic	Moolayember		Y		Y			
	Snake Creek		TD (40 m from top of Moolayember (rat-hole))					
	Showgrounds		N/A					

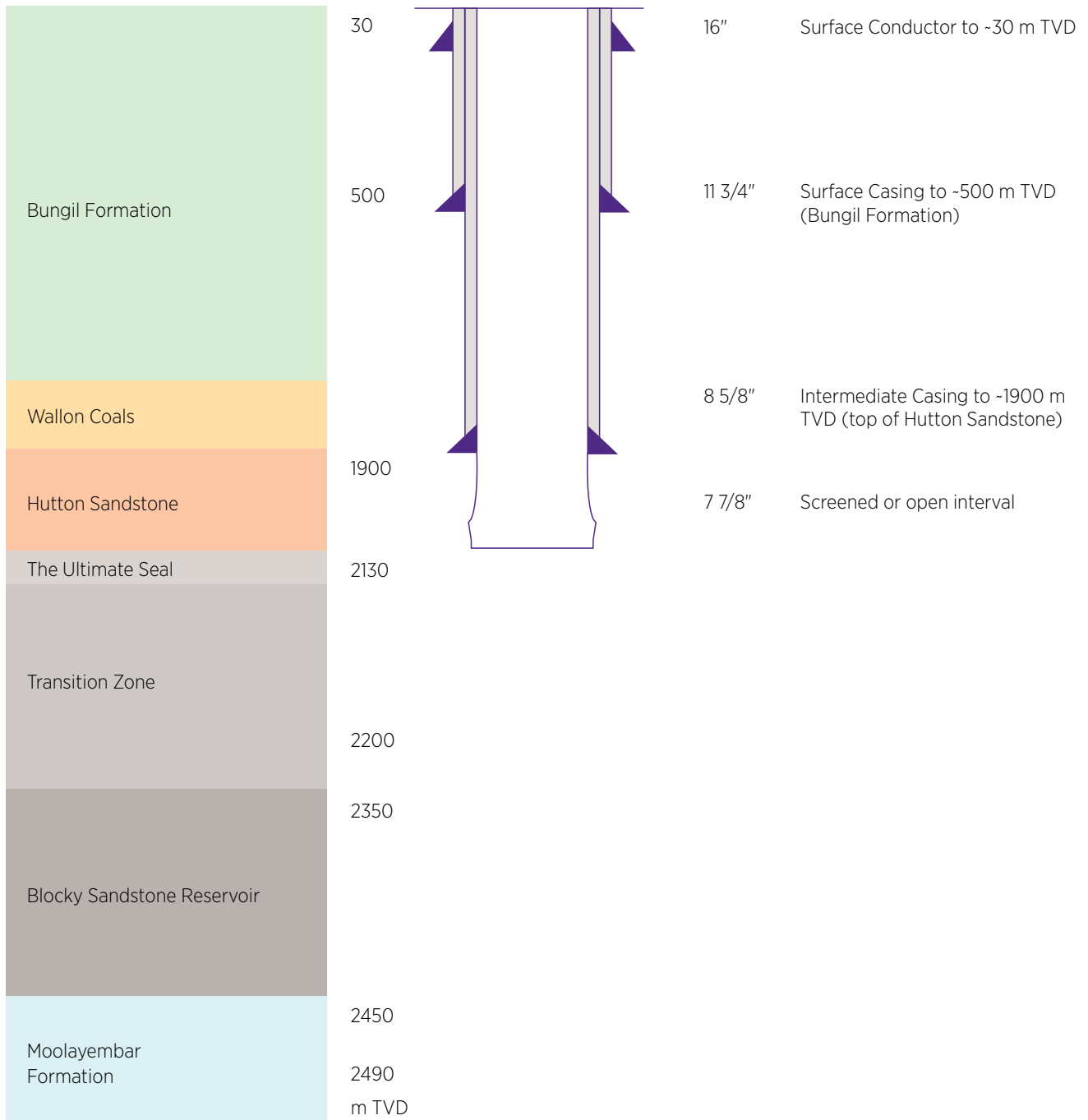
**Figure 203** Schematic of the appraisal program (with the other required action themes).



◆ = Key information and decision points for stop/review/continue

**Figure 204** Schematic of the completion diagram for the Hutton Sandstone pressure monitoring bore.

**Hutton Sandstone (pressure monitoring bore) – Not to scale**



## 5.6 Unit costs and discussion of the value of investment in appraisal

Detailed discussions about appraisal and storage costs and about justification for an investment of “at risk” funds on appraisal activities are in Garnett 2019a.

In essence, if there is confidence that the value of carbon in the 2030–2060 timeframe will be in the region of \$80/tonne, then the appraisal spend is justified. As a point of reference, the simple mean of the European Investment Bank’s “central” carbon price scenario between 2030 and 2050 is around \$150/tonne. As an alternative way of conceptualising the decision, if the Present Value of the first built retrofit asset (plus pipeline and injection sites) is deemed to be of the order of \$440 million, then the costs of appraisal (and other ‘Action Themes’) can also be justified. Importantly, the decision analyses, on which these judgements are formed, do not adequately account for all of the benefits identified by this study.

**Significant benefits and trade-offs for a CCS hub development have been discussed elsewhere. Site appraisal per se has little or no adverse impact, but it requires that funds be put “at risk” to mature the option to an investable point.**

In the absence of an agreed way to value carbon and/or forecast the value of carbon in the 2030–2060 timeframe, there is no classical way economically to justify either appraisal or subsequent development investment at this time. Two approaches are described herein to inform the discussion (i) a modification to a typical ‘exploration-type’ expected monetary value or EMV analysis; and (ii) a discussion on what dollar value a CCS asset would need to create to justify appraisal investment.

Section 4.14 and Gamma Energy Technology 2019, describe high-level studies of CCS hub deployment and roll out scenarios which could be supported by the new dynamic storage calibration.

This section discusses unit costs per tonne of CO<sub>2</sub> (appraised and developed) for three simplified roll-out scenarios. It also discusses the value of investment in appraisal and how this might be conceptualised.

Boston et al. 2019 demonstrates the value of understanding, with confidence, the CCS (rate) potential as soon as possible. To do this in Queensland requires investment of up to \$100 million over the next 3–4 years. The challenge remains to justify this at least in a narrative sense.

### 5.6.1 Scoping level unit technical costs (scenario or project specific)

Unit costs (per tonne CO<sub>2</sub>) for deployment discussed and estimated in this report are unit technical costs (UTCs). These are representative of an equivalent, pre-tax, constant, real terms, unit price which a hypothetical capture, transport and storage “venture” would need to receive in order to break-even. They are therefore indicative of a minimum price or value which would need to be put on CO<sub>2</sub> in order for the venture to ‘work’. Details of how to calculate these values and the background data and assumptions are discussed in Garnett 2019. UTCs refer to post-appraisal expenditure only. UTCs are therefore linked to a specific project deployment scenario and can vary significantly depending on the scenario. Appraisal costs are a different class of expenditure (*ibid*) as briefly mentioned below.

All assessments UTCs in this report are high level scoping estimates only and give indicative ranges relative to specific roll-out scenarios. Importantly, capture-related UTCs in this report **do not include opportunity costs for the plants such as “loss of sales” due to the reduced power output.**

UTCs refer to the following scenarios (Gamma Energy Technology 2019 and Garnett 2019a).

**Table 70** Summary of example deployment scenarios for unit cost discussions.

Roll out scenario Notes ->	Low carbon baseload after retrofit (GWh pa) [1]	Emissions intensity after retrofit (t/MWh) [2]	Nominal injection period [3]	Plateau Rate (Mtpa) [4]	Year plateau rate attained [5]	Cumulative captured/injected (Mt) to 2060 [6]	Cumulative capital investment (RT\$2018, mln) [7]
MKTMK	12,790	0.270	2034 - 2060	12.68	2046	256.31	\$4,720
MKMK	9,570	0.130	2034 - 2060	11.49	2043	250.67	\$4,060
MIL only	5,110	0.140	2034 - 2060	6.18	2037	156.06	\$2,080

Notes on Table 70:

1. The loss of baseload, dispatchable power loss after full retrofit is approximately 20%.
2. The emissions reduction is approximately 90% for a full retrofit (Millmerran and Kogan Creek). The emissions intensity reduction on these plants is around 87%. The table illustrates the impact on overall emissions intensity of a partial retrofit only on Tarong North.
3. The start date for injection is conservative and not optimised. It assumes a 3-4 year appraisal period commencing 2020 which results in a firm storage option and then “project” definition. A further 6-8 years is then assumed to complete, financing, venture agreements, community engagement, baseline monitoring and extensive, first-of-a-kind, environmental impact assessments *before* the Final Investment Decision (FID) on the first partial retrofit. A further 2-3 years is then assumed for construction and commissioning of the first capture plant and the associated pipeline and storage infrastructure with subsequent FIDs taken in this period. The nominal end-date, 2060, is based on the current estimate of the technical life of the power plants (range 2053-2057). There remains some storage injection potential beyond this date.
4. The plateau rate is achieved after sequential deployment of the whole set.
5. The time to plateau attainment is **not optimised**, no learning has been included for the construction and commissioning times of the  $n^{\text{th}}$  plant.
6. The relatively small difference in cumulative volume captured between the MKTMK and MKMK scenarios, results from the faster completion (longer duration) of the full retrofit on these two largest emitters.
7. The cumulative capital cost is a high level, scoping estimate and is stated in, undiscounted, real terms 2018 Australian dollars. It excludes the appraisal costs incurred in the first 3-4 years on establishing whether there is an investable option.

## 5.6.2 Accounting for appraisal costs.

In essence, the dynamic capacity (sustainable rate and duration; see section 4.15) evaluated by an appraisal program is not inherently the same as that developed by a given hub scenario. In fact, they are likely (in the case of UQ-SDAAP) to establish more rate and/or a longer duration than the Hub scenario requires (sections 4.8 to 4.15). Unit cost of appraisal are *not* inherently additive to unit technical costs. Davis (1965) discusses some of the relevant complexities which apply to cost allocation for pre-resource development costs.

Appraisal costs may be defined as follows:

1. **Unit resource finding costs (URFC).** Unit costs of appraising a certain resource “volume”, which is calculated as the integral of the maximum injection rate over time modelled with given pressure constraints and undiscounted rates over time. This is not additive to UTC.
2. **Unit project appraisal costs (UPAC).** Unit costs of appraisal *for a specific project* (which may not “use” the entire dynamic capacity appraised), limited by the project lifetime, with the denominator as *discounted* injection rates. This *could be* additive to UTC, but the capital spent has likely appraised more storage than the project has ‘used’. It has benefited other future investors.
3. **Unit play segment appraisal costs (UPSAC).** Unit costs for a specific plateau rate which probably uses the majority of the dynamic capacity appraised and is not limited by the project lifetime, again with the denominator as *discounted* injection rates. This could also be additive to UTC and assumes that, at some future point, additional sources of CO<sub>2</sub> are found to “use up” all of the storage resource.

Simple comparisons are shown in Table 71.

**Table 71** Indicative unit appraisal costs for storage resources.

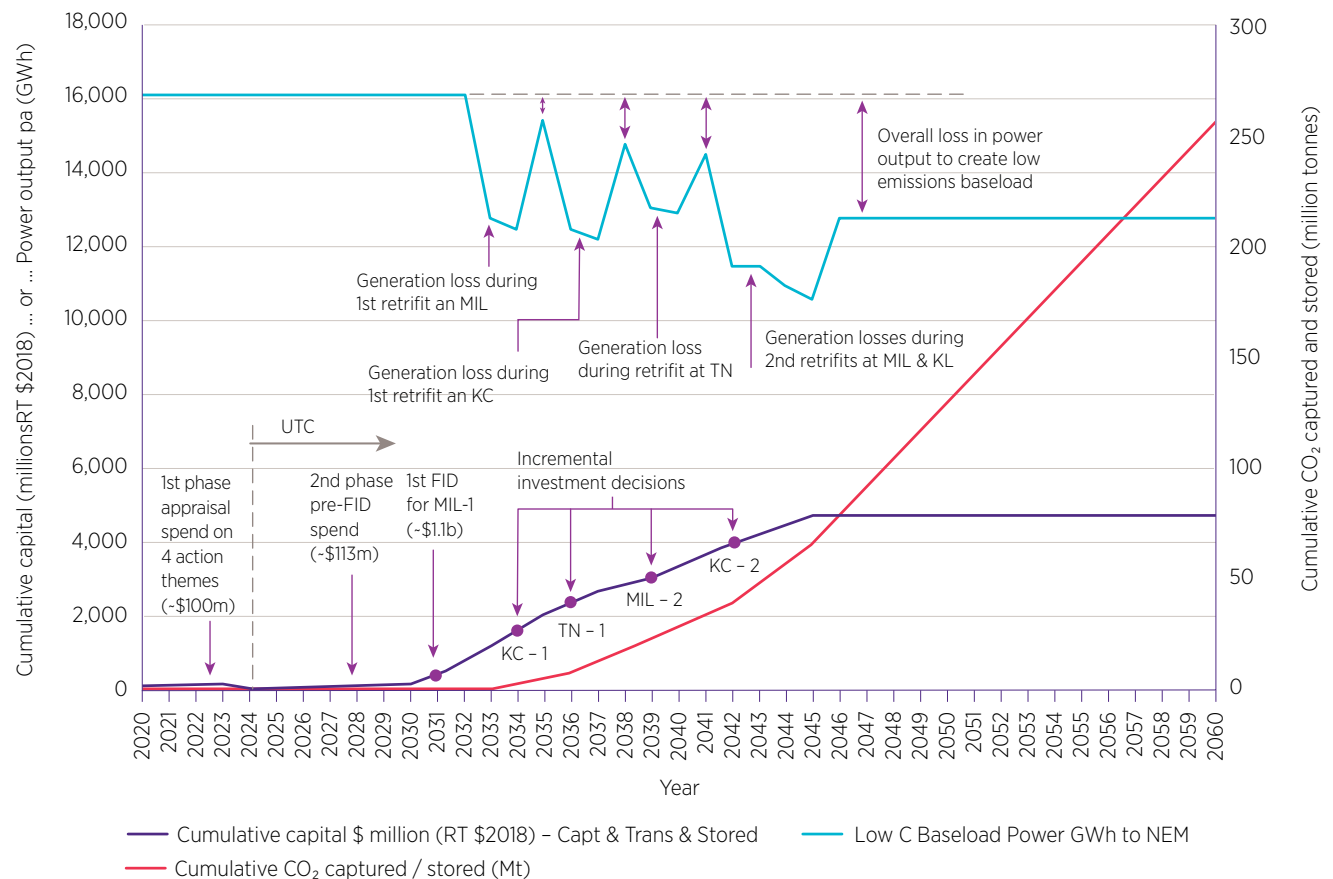
Unit Costs → Scenario	Undiscounted resource volume (at ~13 Mtpa)	Unit resource finding cost – URFC (based on 636 Mt)	Unit project appraisal costs UPAC (to 2060)	Unit play segment appraisal costs UPSAC (to ~620 Mt)
MKTMK 256 Mt cum. inj.	<b>Low:</b> 590 Mt	\$0.12 / tonne	\$4.00 / tonne	\$3.40 / tonne
MKMK 250 Mt cum. inj.	<b>Med:</b> 636 Mt		\$3.90 / tonne	\$3.40 / tonne
MIL only 156 Mt cum. inj.	<b>High:</b> un-evaluated (e.g. in-fill or pump-off or other late-life injection schemes)		\$5.40 / tonne	\$4.80 / tonne

### 5.6.3 Unit costs discussion leading to value of appraisal discussion

Figure 205, shows a typical cash-flow, CO<sub>2</sub> reduction/injection and power output scenario (MKTMK), illustrating the main investment timing as well as optionality for incremental investments for each subsequent retrofit. It assumes that full appraisal and pre-FID costs are common to all scenarios.

**Figure 205** Illustrative scenario (MKTMK) time series for investment, CO<sub>2</sub> reduction and power generation

#### Overview of MKTMK Retrofit Scenario



Applying uncertainty ranges to the main expenditure classes (except capture, see section 4.14 and Gamma Energy Technology 2019), the unit cost ranges in Table 72 were estimated (Garnett 2019a).

**Table 72** Summary of high-level unit technical costs (UTCs) of 3 scenarios.

Unit costs (RTBEPs) in discounted RT \$2019 / tonne	UPAC – Unit project appraisal cost (to 2060) \$/t	Project specific UTC storage \$/t	Project specific UTC transport \$/t	Project specific Mid value of UTC capture only \$/t	Project specific Mid value of total scenario UTC (excl. appr) \$/t
MKTMK	\$3.20 - \$4.80	\$6.40 - \$10.40	\$5.60 - \$6.70	\$50.40	\$64.40
MKMK	\$3.20 - \$3.90	\$7.00 - \$10.60	\$4.10 - \$4.90	\$46.70	\$59.30
MIL only	\$4.30 - \$6.40	\$7.30 - \$11.60	\$3.70 - \$4.50	\$39.60	\$52.70

Based on this table, a RT \$2018, carbon value of around \$65/tonne (with a wide range of uncertainty), applied from 2030 to 2060 would be required for the full MKTMK scenario to “break-even”.

**However, this does not include the appraisal costs required to establish the option.**

#### 5.6.4 The impact of “at risk” appraisal costs on UTC (break-even) considerations

Classical, expected monetary value, EMV-type, exploration economics are used to establish “risk coverage for an investment (Garnett 2019a). However, these cannot be used directly to CCS appraisal investments because:

- × there is no foreseeable success-case net present value or other quantified value added (only extra cost and loss of sales): **unless either:**
  - × there is a real or implicit (high enough) price or value on carbon, say over \$65/tonne (as above)
  - × there is a mechanism for valuing low carbon, grid stabilising, dispatchable baseload; and related to this
  - × there is a clear mechanism for a CCS retrofit plant to operate in the current NEM market structure – no agreed way to estimate changes (increases?) in power prices

However, a minimum required earned carbon price or effectively earned carbon price can be estimated if UTC and unit costs or project appraisal (UPAC) can be estimated, along with an estimate of a priori risk – the chance of a successful appraisal (Ps).

A minimum real terms unit price earned (RTUPE), which would risk-cover the appraisal costs can be calculated. From Garnett 2019a, this is:

$$\text{RTUPE} > \text{UPAC} / P_s + \text{UTC}$$

With reference to the MKTMK reference scenario and mid-case unit project appraisal costs (to 2060):

- ✓ UTC = \$64.40 / tonne
- ✓ UPAC = \$4.00 / tonne

#### Accounting for Technical Risks:

Considering **technical risks only**; UQ-SDAAP have suggested a current probability of success (Ps) of the order of at least 65%, with uncertainties mainly related to lack of site-specific data (section 4.15).

Using the RTUPE equation above, this chance factor raises the *required* value of carbon by over \$6/t, to:

- ✓ RTUPE = \$70.60 / tonne

## Accounting for Non-Technical Risks:

If we also consider *nominal, subjective non-technical risks*, we might derive a non-technical probability of success to be *around 50%*, as follows:

- ✓ Chance of success with regulatory changes = 80%
- ✓ Chance of community acceptance = 80%
- ✓ Chance of establishing suitable commercial conditions = 80%

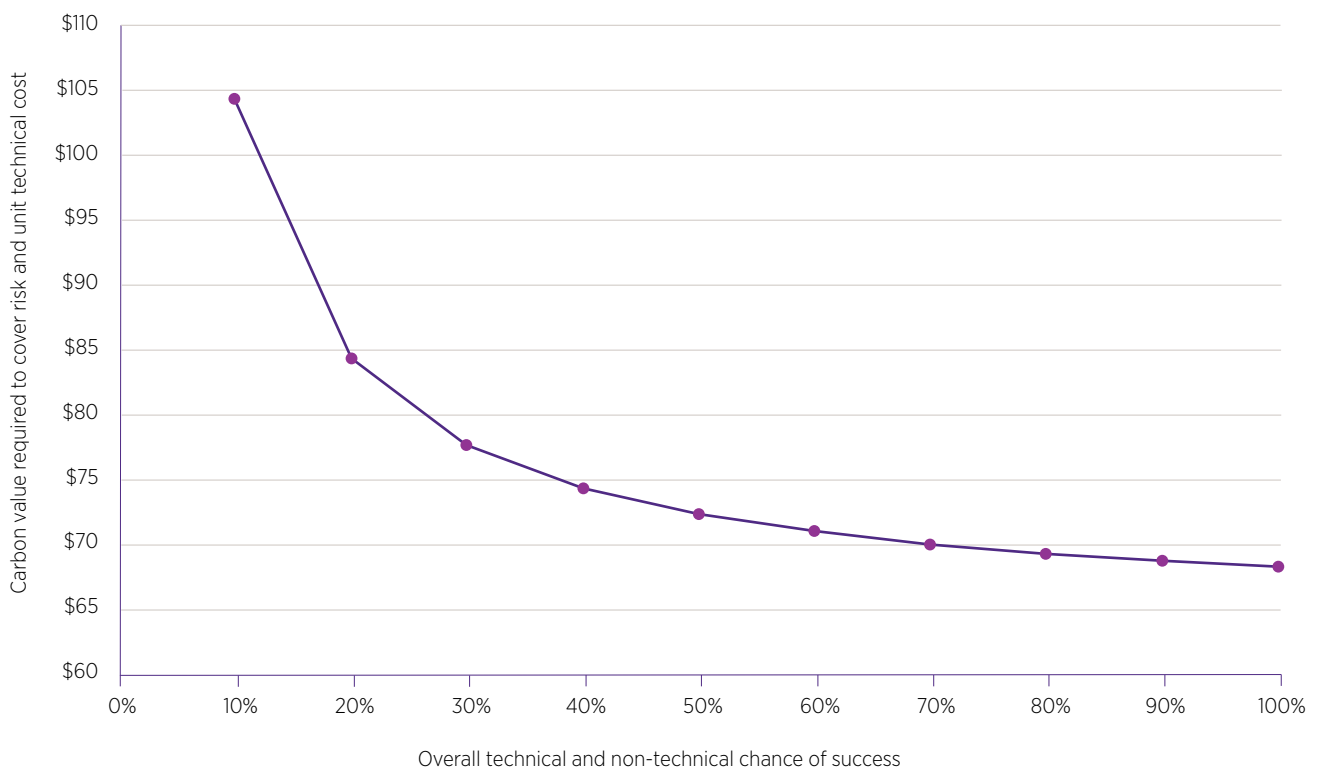
Then the overall chance of success would be *around 33%* (technical + non-technical). Therefore:

- ✓ RTUPE = \$76.50 / tonne (say ~\$80 / tonne)

**The forward view or assumption on the unit value or price of CO<sub>2</sub> that is required to justify the whole venture (including appraisal spend) is highly risk-dependent.**

This is summarised in Figure 206, below.

**Figure 206** Sensitivity of carbon value or price required vs. overall perceived project risk (for MKTMK scenario).

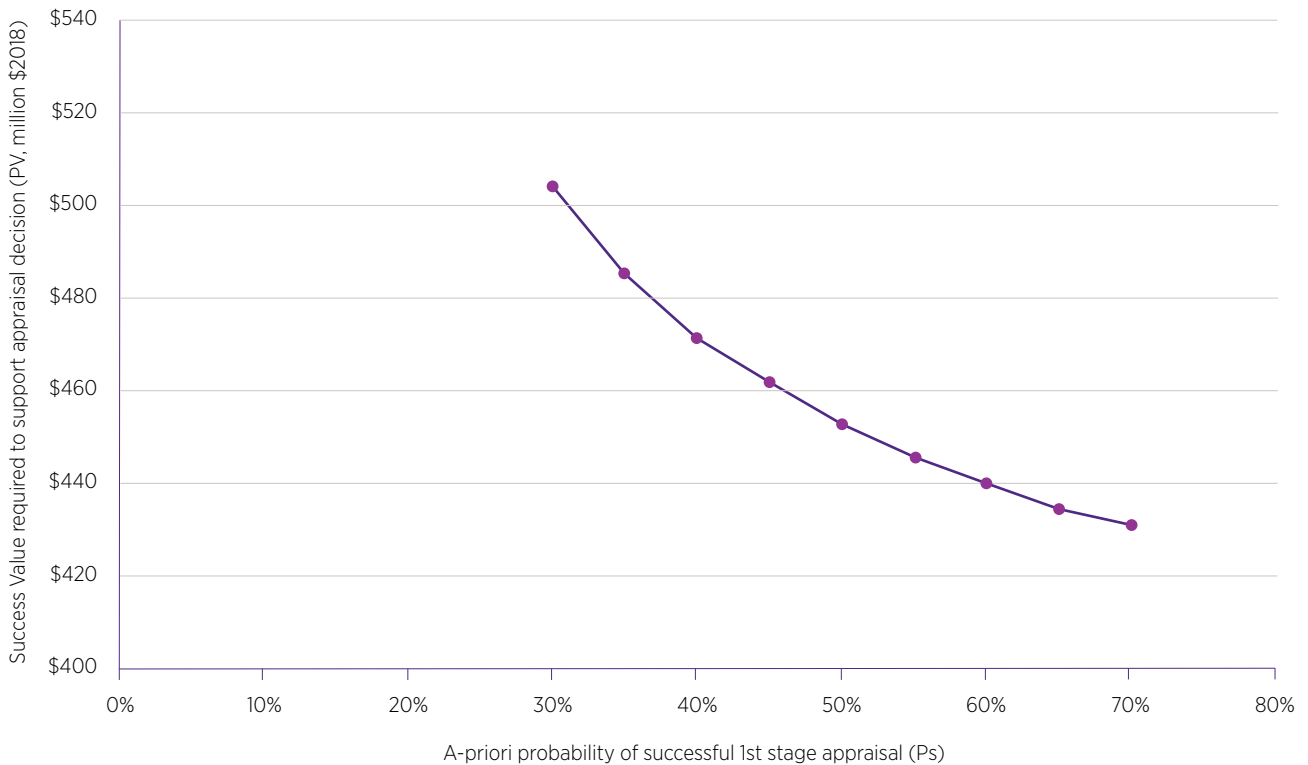


The decision to invest in appraisal is very sensitive to perceived technical AND non-technical risk; high risk perceptions require higher “carbon price” outlooks.





**Figure 208** Impact of appraisal risk on required CCS retrofit success value.



## 5.6.6 Conclusions

As expected, there is no simple, conventional economic justification to invest in the required next stage of appraisal. However, there is significant value identified if not quantified (emissions obligations, low carbon baseload grid services, regional jobs and raised groundwater levels).

Appraisal can be divided into two stages. The first stage (seismic + well + test at one site + progress on the other action themes) significantly polarising the chance or success if the site is chosen in line with section 5.5.2. The undiscounted, funds at risk for this stage 1 appraisal decision could be as low as (undiscounted) ~\$30 million over 1-2 years (section 4.14.5 and Garnett 2019a). This could get to a “do not progress” decision, if it is promising additional appraisal would be required to cover the three sites.

Appraisal *could* be justified, either:

1. If it assumed that CO<sub>2</sub> will have an *effective* value or price **of the order** of \$80<sup>26</sup>/tonne across the 2030-2036 time frame
2. If it is assumed that the value added by building and operating the first CCS retrofit asset would be of the order of \$440 million (present value, \$2018)

Given lack of carbon pricing policy in Australia at the present time, the basis for judgement of future value is challenging.

For simple comparative purposes, the European Investment Bank (EIB), has suggested previously that they carry 3 forecasts for their “shadow prices” of CO<sub>2</sub> on which they base their investment decisions. The meaning and critiques of these price scenarios have been discussed by several parties (for a simple discussion see, Carbon Pulse 2015).

The simple mean of the 2015, EIB “central” price scenario between 2030 and 2050 translates<sup>27</sup> to around A\$150/tonne, with a simple mean “low” price scenario around A\$65/tonne.

<sup>26</sup> Constant RT \$2018

<sup>27</sup> EIB scenarios given in year 2015 Euros: translation assumes EU inflation at 3% and an exchange rate of A\$1.58 to Eu1.00.

## 5.7 Venture set-up (theme 4)

Details of “how” to progress towards full deployment are beyond the scope of UQ-SDAAP, however, many risks and uncertainties have been highlighted which will require a suitably competent, resourced and governed entity to carry forward.

**An entity capable of accepting operator liability and holding appropriate GHG Storage permits is required. Such an entity must be able to access significant financial resources and must also access high quality technical, commercial and community outreach skills. It must be able to operate (contract, procure, enter agreements, manage finances etc.) in a similar way to a private company in the upstream oil and gas market.**

Detailed venture set-up, financing and organisational design are beyond the scope of UQ-SDAAP. However, important requirements and lessons relative to appropriate structures and issues are included in Garnett et al. 2012: chapter 2; Greig et al. 2016a; Greig et al. 2016b; Berly & Garnett 2018; Garnett, Underschultz & Ashworth 2018.

The UQ-SDAAP study highlighted the lowest risk storage sites are likely in the deepest parts of the basin, mostly with GHG Exploration Permit, EPQ 10. Since this is the prime ‘real estate’, the government will need to assure within the licence term: (i) that work plans deliver an “FID-ready” storage assessment; (ii) that progress on technical work is adequate; (iii) that there is progress on forming suitable partnerships and contracts, including next-stage funding; and (iv) that the community are engaged and kept up to date.

The Queensland Government would also need to be responsible for ensuring that a regulatory pathway is available by the end of the exploration period (section 5.2).

Partnerships and contracts need to be formed between various power plant owners, engineering contractors and storage operators. Financing/funding is required for the site-appraisal stage (section 5.5) as well as for the subsequent stages required to get to a Final Investment Decision (FID).

Longer lead time work needs to be started to inform an environmental impact assessment and for follow-up engineering works, e.g. front end engineering design (FEED).

The project would require large-scale funding/financing for incremental, sequential roll-out. Detailed financial modelling and project financing were beyond the scope of this project. It is worth reflecting on lessons from the ZeroGen project (Garnett et al. 2012). That project concluded that while some private financing might be achievable, deployment of a first-of-a-kind CCS plant would require significant public support, including grant funding and a special power purchase agreement (PPA), covering the key additional expenses as well as some form of market positioning that recognised the value of (low-carbon) baseload. These issues are further discussed by later work by Greig et al. 2016a and 2016b.

The ultimate market positioning would have to be negotiated with state and federal regulators prior to major investments and as part of the business case. This UQ-SDAAP study suggests that this should be done in parallel with the other three immediate action themes outlined above.

A clear funding pathway and commercial model would be required to progress beyond the appraisal stage.

## 5.8 Summary of critical success factors in moving beyond the next appraisal stage

The appraisal phase requires an investment of possibly up to \$100 million over 3-4 years (assuming all sites are appraised and all four action themes addressed). A subsequent 4-6 year \$113 million phase would be required before FID, with the major schedule uncertainties relating to the time required for financing and funding, collaborative venture agreements and for environmental approvals.

To progress through these stages, the following critical success factors will need to be in place:

1. A clear regulatory roadmap to consents for large scale injection of CO<sub>2</sub> captured from industrial processes (e.g. flue gas) into the precipice aquifer. Clear support and cooperation from the Queensland Government. Clarity on federal government requirements
2. Site-specific technical data and analyses which give a high level of confidence (say better than 85%) that a high-rate injection plateau of over 6 Mtpa can be sustained for more than 30 years; and that this can be attained within a unit storage cost limit (to be defined)
3. A suitable project entity with a GHG storage lease (initially an exploration permit), with a clear route to convert this to a storage lease - with no show-stoppers
4. An ongoing and active process of community engagement, with an *increased understanding* of the trade-offs and benefits of CCS in the context of other energy options
5. A suitable partnership agreement with current CO<sub>2</sub> source or sources (power plant(s)) with conditional commitment to supply and support for necessary investment in pre-FID, site specific engineering and environmental assessments
6. Funding agreements for the next stage to FID
7. An outline commercial model for the ultimate operation of the capture, transport and storage operations
8. A new PPA or power dispatch model for a new type of entity in the NEM which produces low carbon baseload power
9. A public-private funding/financing concept for the major post-FID retrofit costs
10. A suitably qualified entity to continue all action themes, environmental approvals, engineering studies, financing and commercial agreements and contracts

These factors form the basis of pre-determined storage decision criteria, which are yet to be crystallised, as recommended in Garnett et al. 2012 p 457.

## 6. References

- Advisian (2019), *Well-pad concept definition study*, Report for The University of Queensland Surat Deep Aquifer Appraisal Project – Supplementary Detailed Report, The University of Queensland.
- Agusta AU (2017), Surat/Bowen conventional gas field post mortem analysis: Borah Creek Field, UQ MS research project report, pp 124.
- Ahmed U, Crary SF & Coates GR (1991), Permeability estimation: the various sources and their interrelationships, *Journal of Petroleum Technology*, vol 43(05), pp 578-587.
- Akinfiev NN & Diamond LW (2010), Thermodynamic model of aqueous CO<sub>2</sub>-H<sub>2</sub>O-NaCl solutions from -22 to 100 °C and from 0.1 to 100 MPa, *Fluid Phase Equilibria*, vol 295, pp 104-124.
- Allinson WD, Nguyen & Bradshaw J (2003), Dealing with carbon dioxide - Threat or opportunity - The economics of geological storage of CO<sub>2</sub> in Australia, *APPEA Journal-Australian Petroleum Production and Exploration Association*, vol 43(1), pp 623-636.
- Allinson WG, Neal PR, Kaldi J & Paterson L (2014), CO<sub>2</sub>-Storage Capacity--Combining Geology, Engineering and Economics. *SPE Economics & Management*, SPE-133804-PA, January 2014. doi.org/10.2118/133804-PA.
- Allmendinger RW, Zapata T, Manceda R & Dzelalija F (2004), Trishear Kinematic Modeling of Structures, with Examples from the Neuquen Basin, Argentina: in KR McClay eds, *Thrust tectonics and hydrocarbon systems: American Association of Petroleum Geologists Memoir*, vol 82, pp 356-371.
- Andersen ST (1974), Wind conditions and pollen deposition in a mixed deciduous forest: Wind conditions and pollen dispersal, *Grana*, vol 14, pp 57-63.
- ANLEC (2016), Milestone 1.4 Final report of RCA and SCAL data on plugs from West Wandoan-1 Well. Lithicon, Canberra.
- Ampofo K & Garnett A (2019), *Reviews of previous work on costs in Australian CCS*, The University of Queensland Surat Deep Aquifer Appraisal Project – Supplementary Detailed Report, The University of Queensland.
- Appelo CAJ, Parkhurst DL & Post VEA (2014), Equations for calculating hydrogeochemical reactions of minerals and gases such as CO<sub>2</sub> at high pressures and temperatures, *Geochimica et Cosmochimica Acta*, vol 125, pp 49-67.
- APLNG (2013), *Australia Pacific LNG Upstream Phase 1. Reedy Creek Aquifer Injection Management Plan - Precipice Sandstone*, Report Q-4255-95-MP-004.
- Ashworth P, Dowd A-M, Rodriguez M, Jeanneret T, Mabon L & Howell R (2013), *Synthesis of CCS social research: Reflections and current state of play in 2013*, EPI34303, CSIRO, Australia.
- Ashworth P, Jeanneret T, Gardner J & Shaw H (2011), *Communication and climate change: What the Australian public thinks*, EP112769 CSIRO, Pullenvale.
- Ashworth P, Pisarski A & Thambimuthu K (2009a), Public acceptance of carbon dioxide capture and storage in a proposed demonstration area, *Proceedings of the Institution of Mechanical Engineers, Part A: Journal of Power and Energy*, vol 223(3), pp 299-304.
- Ashworth P, Carr-Cornish S, Boughen N & Thambimuthu K (2009b), Engaging the public on carbon dioxide capture and storage: Does a large group process work?, *Energy Procedia*, vol 1(1), pp 4765-4773.
- Australian Geological Survey Organisation (2000), *Geohazard Risk Contour Map (National Geoscience Dataset)*, Canberra.
- Babaahmadi A & Rosenbaum G (2014), Late Mesozoic and Cenozoic wrench tectonics in eastern Australia: Insights from the North Pine Fault System (southeast Queensland), *Journal of Geodynamics*, vol 73, pp 83-99.
- Bachu S (1995), Flow of variable-density formation water in deep sloping aquifers: review of methods of representation with case studies, *Journal of Hydrology*, vol 164, pp 19-38.
- Bachu SD, Bonijoly J, Bradshaw R, Burruss S, Holloway NP, Christensen & Mathiassen OM (2007), CO<sub>2</sub> storage capacity estimation: methodology and gaps, *International Journal of Greenhouse Gas Control*, vol 1(4), pp 430-443.
- Bachu S (2008), *Comparison between Methodologies Recommended for Estimation of CO<sub>2</sub> Storage Capacity in Geological Media by the CSLF Task Force on CO<sub>2</sub> Storage Capacity Estimation and the USDOE Capacity and Fairways Subgroup of the Regional Carbon Sequestration Partnerships Program-Phase III Report*. Available online at [www.cslforum.org/publications/documents/PhaseIIIReportStorageCapacityEstimationTaskForce0408.pdf](http://www.cslforum.org/publications/documents/PhaseIIIReportStorageCapacityEstimationTaskForce0408.pdf)

- Bachu S & Celia MA (2009), Assessing the potential for CO<sub>2</sub> leakage, particularly through wells, from geological storage sites, vol 183, pp 203-216.
- Bachu S & Watson TL (2009), Review of failures for wells used for CO<sub>2</sub> and acid gas injection in Alberta, Canada, *Energy Procedia*, vol 1(1), pp 3531-3537.
- Baker JC & de Caritat P (1992), Postdepositional history of the Permian sequence in the Denison Trough, Eastern Australia, *American Association of Petroleum Geologists Bulletin*, vol 76(8), pp 1224-1249.
- Barnett B, Townley LR, Post V et al (2012), Australian groundwater modelling guidelines, National Water Commission, Canberra.
- Barnett et al. (2012), Australian groundwater modelling guidelines, Waterlines report, National Water Commission, Canberra.
- Batten RJ (1974), Wealden palaeoecology from the distribution of plant fossils, *Proceedings of the Geological Association*, vol 85, pp 433-458.
- Baublys KA, Hamilton SK, Golding SD, Vink S & Esterle J (2015), Microbial controls on the origin and evolution of coal seam gases and production waters of the Walloon Subgroup; Surat Basin, Australia. *International Journal of Coal Geology*, pp 147-148, 85-104.
- Beier PDR, Majka & Newell SL (2009), Uncertainty analysis of least-cost modeling for designing wildlife linkages, *Ecological Applications*, vol 19(8), pp 2067-2077.
- Benson SM (2006), Monitoring carbon dioxide sequestration in deep geological formations for inventory verification and carbon credits, *SPE Annual Technical Conference and Exhibition*, Society of Petroleum Engineers, January.
- Berggren WA, Kent DV, Swisher CC & Aubry MP (1995), A revised Cenozoic geochronology and chronostratigraphy. In: Berggren WA, Kent DV, Swisher CC & Aubry MP (eds.) *Geochronology, Time scales and global stratigraphic correlation*, SEPM.
- Berly T & Garnett A (2018), Scaling up CO<sub>2</sub> transport and storage infrastructure. Proceedings of the 14th International Conference on Greenhouse Gas Control Technologies, GHGT-14, 21-25 October 2018, Melbourne, Australia.
- Bernauer T & McGrath L (2016), Simple reframing unlikely to boost public support for climate policy, *Nature Climate Change*, vol 6, pp 680-684.
- Bethke CM & Yeakel S (2012), The Geochemist's Workbench (Version 9.0), Reaction modeling guide, pp 96 ed. Aqueous Solutions, LLC, Champaign, Ill. pp 96.
- Bianchi M, Kearsley T & Kingdon A (2015), Integrating deterministic lithostratigraphic models in stochastic realizations of subsurface heterogeneity: Impact on predictions of lithology, hydraulic heads and groundwater fluxes, *Journal of Hydrogeology*, pp 531, 557-573.
- Bianchi V, Zhou F, Pistellato D, Martin M, Boccardo S, Esterle J (2018), Mapping a coastal transition in braided systems: an example from the Precipice Sandstone, Surat Basin, *Australian Journal of Earth Sciences*, vol 2, pp 1-20.
- Bissell RC, Vasco DW, Atbi M, Hamdani M, Okwelegbe M & Goldwater MH (2011), A full field simulation of the in Salah gas production and CO<sub>2</sub> storage project using a coupled geo-mechanical and thermal fluid flow simulator, *Energy Procedia*, vol 4, pp 3290-3297.
- Birks HJB (1981), Long-distance pollen in late Wisconsin sediments of Minnesota, U.S.A.: a quantitative analysis, *New Phytologist*, vol 87, pp 630-661.
- Bolsen T, Druckman JN & Cook FL (2014), How frames can undermine support for scientific adaptations: Politicization and the status-quo bias, *Public Opinion Quarterly*, vol 78(1), pp 1-26.
- Bolsen T & Druckman JN (2018), Do partisanship and politicization undermine the impact of a scientific consensus message about climate change?, *Group Processes & Intergroup Relations*, vol 21(3), pp 389-402.
- Bongers GD, Byrom S, Malss S & Constable T (2017), Surat Basin CCS Hub – Helping secure a low carbon future, CO<sub>2</sub>CRC Limited, Victoria, Australia.
- Bongers G, Byrom S, Oettinger M & Malss S (2018), Post Combustion Capture Technology Review. Gamma Energy Technology, Brisbane, Australia.
- Bongers GB, Kinaev NK & Pregeli Z (2018), Method for Improving Power Efficiency of Coal Fired Power Plants Fitted with CCUS, 2018 International Pittsburgh Coal Conference Manuscript Submission.
- Boot-Handford ME, Abanades JC, Anthony EJ, Blunt MJ, Brandani S, Mac Dowell N & Fennell PS (2014), Carbon capture and storage update, *Energy & Environmental Science*, vol 7(1), pp 130-189.
- Boreham CJ (1994), Origin of petroleum in the Bowen and Surat basins: Implications for source, maturation and migration, Australian Geological Survey Organisation, Canberra, pp. 112.

- Boreham CJ (1995), Origin of petroleum in the Bowen and Surat Basins: geochemistry revisited. *Australian Petroleum Exploration Association Journal*, vol 35, pp 33.
- Boreham CJ (1999), Predicting the quantities of oil and gas generated from Australian Permian coals, Bowen Basin using pyrolytic methods, *Marine and Petroleum Geology*, vol 16(2), pp 165-188, doi: 10.1016/S0264-8172(98)00065-8.
- Boreham CJ, Korsch R & Carmichael D (1996), The significance of mid-Cretaceous burial and uplift on the maturation and petroleum generation in the Bowen and Surat Basins, eastern Australia, Paper presented at the Mesozoic Geology of the Eastern Australia Plate conference, Brisbane.
- Boreham C, Underschultz J, Stalker L, Kirste D, Freifeld B, Jenkins C & Ennis-King J (2011), Monitoring of CO<sub>2</sub> storage in a depleted natural gas reservoir: Gas geochemistry from the CO<sub>2</sub> CRC Otway Project, Australia, *International Journal of Greenhouse Gas Control*, vol. 5(4), pp1039-1054.
- Boston, A., Bongers, G., Byrom, S. and Garnett, A. (2019) Net Zero Emissions Electricity. A total system cost approach for Queensland. Gamma Energy Technology P/L. Brisbane, Australia. A special report for Coal21.
- Bradshaw JB, Bradshaw G, Allinson A, Rigg V, Nguyen & Spencer L (2002), The potential for geological sequestration of CO<sub>2</sub> in Australia: preliminary findings and implications for new gas field development, *APPEA journal*.
- Bradshaw BE, Spencer LK, Lahtinen A-L, Khider K., Ryan DJ., Colwell JB, Chirinos A, Bradshaw J, Draper JJ, Hodgkinson J & McKillop M (2011), An assessment of Queensland's CO<sub>2</sub> geological storage prospectivity – The Queensland CO<sub>2</sub> Geological Storage Atlas, *Energy Procedia*, vol 4, pp 4583-4590.
- Bruine de Bruin W & Wong-Parodi G (2014), The role of initial affective impressions in responses to educational communications: The case of carbon capture and sequestration (CCS), *Journal of Experimental Psychology: Applied*, vol 20(2), pp 126.
- Bruine de Bruin W (2011), Framing effects in surveys: How respondents make sense of the questions we ask, in G Keren (ed), *Perspectives on framing*, Taylor & Francis, London, pp 303-324.
- Brunsting S, Upham P, Dütschke E, de Best-Waldhober M, Oltra C, Desbarats J, Riesch H & Reiner D (2011), Communicating CCS: Applying communications theory to public perceptions of carbon capture and storage, *International Journal of Greenhouse Gas Control*, vol 5, pp 1651-1662.
- Bureau of Resources and Energy Economics (2014), Australian energy resource assessment, Bureau of Resources and Energy Economics, Canberra, pp 364.
- Burke K (2011), Plate tectonics, the Wilson Cycle, and mantle plumes: geodynamics from the top, *Annual Review of Earth and Planetary Sciences*, vol 39, pp 1-29.
- Buscheck TA, Sun Y, Chen M, Hao Y, Wolery TJ, Bourcier WL & Aines RD (2012), Active CO<sub>2</sub> reservoir management for carbon storage: Analysis of operational strategies to relieve pressure buildup and improve injectivity, *International Journal of Greenhouse Gas Control*, vol 6, pp 230-245.
- Cadman SJ, Pain L & Vuckovic V (1998), Bowen and Surat basins, Clarence-Morton Basin, Sydney Basin, Gunnedah Basin and other minor onshore basins, QLD, NSW and NT. *Australian petroleum accumulations Report*, Bureau of Resource Sciences, Canberra, vol 11, pp 810.
- Calf GE & Habermehl MA (1984), Isotope hydrology and hydrochemistry of the Great Artesian Basin, Australia, *Isotope Hydrology 1983*, pp 397-413.
- Carbon Pulse (2015). *Carbon Pulse website: News and intelligence on carbon markets, greenhouse gas pricing and climate policy*. <<http://carbon-pulse.com/7699/#!prettyPhoto>> (last accessed 20/02/2019)
- Carey JWM, Wigand SJ, Chipera G, WoldeGabriel R, Pawar PC, Lichtner SC, Wehner MA, Raines & Guthrie GD (2007), Analysis and performance of oil well cement with 30 years of CO<sub>2</sub> exposure from the SACROC Unit, West Texas, USA, *International Journal of Greenhouse Gas Control*, vol 1(1), pp 75-85.
- Carle SF & Fogg GE (1996), Transition probability-based indicator geostatistics, *Mathematical Geology*, vol 28, pp453-476.
- Carle SF & Fogg GE (1997), Modeling spatial variability with one and multidimensional continuous-lag Markov Chains, *Mathematical Geology*, vol 29, pp 891-918.
- Carman PC (1956), *Flow of gases through porous media*, New York: Academic Press.
- Carmichael D. & Boreham CJ (1997), Source rock evaluation in the southern Taroom Trough. In Green PM (ed), *The Surat and Bowen Basins, south-east Queensland, Queensland Minerals and Energy Review Series*, Brisbane: Queensland Department of Mines and Energy, Brisbane, pp 193-228.
- Carter RD & Tracy GW (1960), An Improved Method for Calculating Water Influx, *Society of Petroleum Engineers*, vol 3.
- Chadwick RA, Marchant BP & Williams GA (2014), CO<sub>2</sub> storage monitoring: leakage detection and measurement in subsurface volumes from 3D seismic data at Sleipner. *Energy Procedia*, vol 63, pp 4224-4239.

- Chmura GL (1994), Palynomorph distribution in marsh environments in the modern Mississippi Delta plain, *Geological Society of America Bulletin*, vol 106, pp 705-714.
- CMG (2018), *GEM 2018.10 User Guide*, Computer Modelling Group Ltd, Calgary, Alberta, Canada.
- Cook AG, Bryan SE, Draper JJ (2013), Post-orogenic Mesozoic basins and magmatism. In: Jell P. A. ed. *Geology of Queensland*, Geological Survey of Queensland, pp 515-576.
- Cooper RA, Crampton JA, Raine JI, Gradstein FM, Morgans HEG, Sadler PM, Strong CP, Waghorn D. & Wilson GJ (2000), Quantitative biostratigraphy of the Taranaki Basin, New Zealand: A deterministic and probabilistic approach, *AAPG Bulletin*, vol 85, pp 1469-1498.
- Cope JCW (1995), High resolution biostratigraphy. In: Hailwood EA & Kidd RB (eds.), *High Resolution Stratigraphy*, Geological Society.
- Copley J, Mukherjee S, Babaahmadi A, Zhou F, Barbosa K, Hurter S & Tyson S (2017), Faults and Fractures in the Surat Basin Relationships with Permeability, The University of Queensland Centre for Coal Seam Gas (confidential report).
- Corcoran DV & Dore AG (2005), A review of techniques for the estimation of magnitude and timing of exhumation in offshore basins, *Earth Science Reviews*, vol 72(3), pp 129-168.
- CSA Z741 (2012), Canadian Standards Association, Standard CSA Z741-12 Geological storage of carbon dioxide: Mississauga, Ontario, Canada.
- Czarnecki JM, Dashtgard SE, Pospelova V, Matthewes RW & Maceachern JA (2014), Palynology and geochemistry of channel-margin sediments across the tidal-fluvial transition, lower Fraser River, Canada: Implications for the rock record. *Journal of Marine and Petroleum Geology*, vol 51, pp 152-166.
- Dalrymple RW (2010), Interpreting sedimentary successions: facies, facies analysis and facies models, in James NP & Dalrymple RW, (ed) *Facies Models 4: St. John's, Newfoundland and Labrador*, Canada, Geological Association of Canada, pp 3-18.
- Darrell JHI (1973), Statistical evaluation of palynomorph distribution in the sedimentary environments of the modern Mississippi River Delta, PhD, Louisiana State University.
- Davis MB (1968), Pollen grains in lake sediment: redeposition caused by seasonal water circulation, *Science*, vol 162, pp 796-799.
- Davis MB (1973), Redeposition of pollen grains in lake sediment, *Limnology and Oceanography*, vol 18, pp 44-52.
- Davis WB (1965). *The Enigma of Oil and Gas Finding Costs*, Society of Petroleum Engineers. doi:10.2118/1094-MS.
- Deichmann N, Mai M, Bethmann F et al. (2007), Seismicity induced by water injection for geothermal reservoir stimulation 5 km below the city of Basel, Switzerland, *AGU Fall Meeting Abstracts*.
- de Best-Waldhober M, Dancker D, Ramirez A, Faaij A, Hendriks C & de Visser E (2009), Informed public opinions on CCS in comparison to other mitigation options, *Energy Procedia*, vol 1, pp 4795-4802.
- de Coninck H & Benson SM (2014), Carbon dioxide capture and storage: Issues and prospects, *Annual Review of Environment and Resources*, vol 39, pp 243-70.
- de Marsily G, Delay F, Goncalves J, Renard P, Teles V & Violette S (2005), Dealing with spatial heterogeneity, *Hydrogeology Journal*, vol 13, pp 161-183.
- Delany JM, Lundeen SR (1989), The LLNL thermodynamic database. Lawrence Livermore National Laboratory Report, UCRL-21658.
- Deutsch CV (2006), A sequential indicator simulation program for categorical variables with point and block data: BlockSIS, *Computers and Geosciences*, vol 32, pp 1669-1681.
- Deutsch CV & Journel AG (1992), *GSLIB: Geostatistical Software Library and user's guide*, New York, Oxford University Press.
- de Vernal A (2009), Marine palynology and its use for studying nearshore environments, *IOP Conference Series: Earth and Environmental Science*, no 5.
- DOE (2007), Carbon Sequestration Atlas of the United States and Canada, U.S. Department of Energy/NETL, pp 88
- Doherty J (2016), PEST, Model-Independent Parameter Estimation User Manual, Brisbane: Watermark Numerical Computing, ver 6.
- Doherty (2018) PEST HP: PEST for Highly Parallelized Computing Environments: Manual for Version 15. Watermark Numerical Computing.
- DRNM (2015), Queensland Government Water Monitoring Portal, [www.water-monitoring.information.qld.gov.au](http://www.water-monitoring.information.qld.gov.au) <accessed 19/2/2019>.



- Druckman JN (2015), Eliminating the local warming effect, *Nature Climate Change*, vol 5, pp 176-177.
- Druckman JN, Levendusky MS & McLain A (2018), No need to watch: How the effects of partisan media can spread via interpersonal discussions, *American Journal of Political Science*, vol 62(1), pp 99-112
- Duan Z & Sun R (2003), An improved model calculating CO<sub>2</sub> solubility in pure water and aqueous NaCl solutions from 273 to 533 K and from 0 to 2000 bar, *Chemical Geology*, vol 193(3-4), 257-271.
- Duan Z, Sun R, Zhu C & Chou I (2006), An improved model for the calculation of CO<sub>2</sub> solubility in aqueous solutions containing Na<sup>+</sup>, K<sup>+</sup>, Ca<sup>2+</sup>, Mg<sup>2+</sup>, Cl<sup>-</sup>, and SO<sub>4</sub><sup>2-</sup>, *Marine Chemistry*, vol 98(2-4), pp 131-139.
- Dütschke E, Wohlfarth K, Höller S, Viebahn P, Schumann D & Pietzner K (2016), Differences in the public perception of CCS in Germany depending on CO<sub>2</sub> source, transport option and storage location, *International Journal of Greenhouse Gas Control*, vol 53, pp 149-159.
- Ennis-King J, Dance T, Xu J, Boreham C, Freifeld B, Jenkins C, Paterson L, Sharma S, Stalker L & Underschultz J (2011), The role of heterogeneity in CO<sub>2</sub> storage in a depleted gas field: history matching of simulation models to field data for the CO<sub>2</sub>-CRC Otway Project, Australia, *Energy Procedia*, vol 4, pp 3494-3501.
- Esri (2017), Applying fuzzy logic to overlay rasters, ArcMap 10.5, retrieved 14/02/2018 from [desktop.arcgis.com/en/arcmap/10.5/tools/spatial-analyst-toolbox/applying-fuzzy-logic-to-overlay-rasters.htm](http://desktop.arcgis.com/en/arcmap/10.5/tools/spatial-analyst-toolbox/applying-fuzzy-logic-to-overlay-rasters.htm).
- Exon NF (1976), Geology of the Surat Basin in Queensland, Bureau of Mineral Resources, Geology and Geophysics, Canberra, Australia, pp 160.
- Exon NF & Burger D (1981), Sedimentary cycles in the Surat Basin and global changes in sea level, *BMR Journal of Australian Geology and Geophysics*, vol 6, pp 153-159.
- Exon NF & Senior BR (1976), The Cretaceous of the Eromanga and Surat basins. *BMR Journal of Australian Geology and Geophysics*, vol 1, pp 33-50.
- Farley MB (1990a), Palynological facies fossils in nonmarine environments in the Paleogene of the Bighorn Basin, *Palaios*, vol 4, pp 565-573.
- Farley MB (1990b), Vegetation distribution across the early Eocene depositional landscape from palynological analysis, *Palaeogeography, Palaeoclimatology, Palaeoecology*, vol 79, pp 11-27.
- Farquhar SM, Pearce JK, Dawson GKW, Golab A, Kirste D, Biddle D, Golding SD (2015), A fresh approach to investigating CO<sub>2</sub> storage: Experimental CO<sub>2</sub>-water-rock interactions in a freshwater reservoir system, *Chemical Geology*, vol 399, pp 98-122.
- Feitz AJ, Ransley TR, Dunsmore R, Kuske TJ, Hodgkinson J, Preda M, Spulak R, Dixon O & Draper J (2014), Geoscience Australia and Geological Survey of Queensland Surat and Bowen Basins Groundwater Surveys Hydrochemistry Dataset (2009-2011).
- Ferguson F, Witt K, Nisa C & Ashworth P (2019), *Effects of message framing on the support for carbon capture and storage (CCS) and alternative energy technologies*, The University of Queensland Surat Deep Aquifer Appraisal Project – Supplementary Detailed Report, The University of Queensland.
- Ferguson M, Witt K & Ashworth P (2019), *Managed aquifer recharge focus groups*, The University of Queensland Surat Deep Aquifer Appraisal Project – Supplementary Detailed Report, The University of Queensland.
- Ferguson M, Witt K & Ashworth P (2019), *Five country survey*, The University of Queensland Surat Deep Aquifer Appraisal Project – Supplementary Detailed Report, The University of Queensland.
- Fielding CR (1996), Mesozoic sedimentary basins and resources in eastern Australia – a review of current understanding, Mesozoic Geology of the Eastern Australia Plate Conference, Geological Society of Australia, Brisbane, Queensland, pp 180-185.
- Fielding CR, Gray ARG, Harris GI, Saloman JA (1990), The Bowen Basin and overlying Surat Basin, in: Finlayson DM (ed), *The Eromanga–Brisbane Geoscience Transect: A Guide to Basin Development Across Phanerozoic Australia in Southern Queensland*, Australian Government Publishing Service, Canberra, ACT.
- Fielding CR, Sliwa R, Holcombe RJ & Jones AT (2001), *A new palaeogeographic synthesis for the Bowen, Gunnedah and Sydney basins of eastern Australia*, Paper presented at the Eastern Australasian Basins Symposium.
- Fjar E, Holt RM, Raen A et al. (2008), *Petroleum related rock mechanics*: Elsevier.
- Fleming DA & Measham TG (2014), Local job multipliers of mining, *Resources Policy*, vol 41, 2014, pp 9-15, ISSN 0301-4207, <https://doi.org/10.1016/j.resourpol.2014.02.005>.
- Flottman T, Brook-Barnett S, Trubshaw R, Naidu S, Kirk-Bumnan E, Pau P, Buseti S, Hennings P (2013), Influence of In-Situ Stresses on Fracture Stimulations in the Surat Basin, SPE Unconventional Resources Conference and Exhibition-Asia Pacific, Brisbane, Australia, 11-14 November 2013, SPE International. SPE167064.
- Frederiksen NO (1985), Review of early Tertiary sporomorph paleoecology. *American Association of Stratigraphic Palynologists Contribution Series*, vol 15, pp 1-92.

- Freeze RA & Cherry JA (1979), *Groundwater*, Englewood Cliffs, New Jersey, Prentice-Hall.
- FU Y (2014), *Leak-off test (LOT) models*. Master of Science in Engineering, The University of Texas, Austin.
- Freifeld BM, Daley TM, Hovorka SD, Hennings J, Underschultz J & Sharma S (2009), Recent advances in well-based monitoring of CO<sub>2</sub> sequestration, *Energy Procedia*, February 2009, vol 1(1), pp 2277-2284.
- Gaina RD, Muller J-Y, Royer J, Stock J, Hardebeck P, Symonds (1998), The tectonic history of the Tasman Sea: a puzzle with 13 pieces, *Journal of Geophysical Research*, vol 103(1998), pp 12413-12433.
- Gardezi M & Arbuckle JG (2018), Techno-optimism and farmers' attitudes toward climate change adaptation, *Environment and Behavior*, <https://journals.sagepub.com/doi/10.1177/0013916518793482>, retrieved 10/07/2018)
- Galloway WE (1989), Genetic stratigraphic sequences in basin analysis, I. Architecture and genesis of flooding-surface bounded depositional units, *American Association of Petroleum Geologists Bulletin*, vol 73, pp 125-142.
- Gallagher K, Dumitru TA, Gleadow AJW (1994), Constraints on the vertical motion of eastern Australia during the Mesozoic, *Basin Research*, vol 6, pp 77-94.
- Gamma Energy Technology (2019), *Hub development: Industrial-scale deployment via retrofitting sequencing and pipeline development*, Report for The University of Queensland Surat Deep Aquifer Appraisal Project – Supplementary Detailed Report, The University of Queensland.
- Garnett AJ, Greig CR & Oettinger M (2012), *ZeroGen IGCC with CCS: A Case History*. The University of Queensland, ISBN: 978-0-646-91501-2, [www.uq.edu.au/energy/docs/ZeroGen.pdf](http://www.uq.edu.au/energy/docs/ZeroGen.pdf) (last retrieved 9/3/19).
- Garnett AJ & Greig CR (2014a), What lies in store for CCS?, International Energy Agency Insights Series, chapter 3, pp 44-53. [www.iea.org/publications/insights/insightpublications/Insight\\_CCS2014\\_FINAL.pdf](http://www.iea.org/publications/insights/insightpublications/Insight_CCS2014_FINAL.pdf)
- Garnett AJ and Greig CR (2014b), *CCS Mitigation – A Discussion on Forecasting Storage Costs and Learning Effects*, The University of Queensland.
- Garnett AJ (2017), *Defining and Classifying CO<sub>2</sub> Storage Resource*. A presentation to the IEA CCS Transport and Storage Infrastructure Workshop, Paris, 16-17 May, 2017.
- Garnett AJ, Underschultz J & Ashworth P (2018), Accelerating Commercial-Scale Carbon Storage Assessment by “Piggybacking” on Oil & Gas Industry Development, Proceedings of the 14th International Conference on Greenhouse Gas Control Technologies, GHGT-14, 21 - 25 October 2018, Melbourne, Australia.
- Garnett A (2019), *Estimates of unit costs and discussion of the value of investment in appraisal*, The University of Queensland Surat Deep Aquifer Appraisal Project – Supplementary Detailed Report, The University of Queensland.
- Garnett A (2019), *Experiences in adapting legacy oil and gas wells for CCS-related well testing*, The University of Queensland Surat Deep Aquifer Appraisal Project – Supplementary Detailed Report, The University of Queensland.
- Garnett A & Underschultz J (2019), *Methodology for assessment of dynamic capacity*, The University of Queensland Surat Deep Aquifer Appraisal Project – Supplementary Detailed Report, The University of Queensland.
- Gasda SES, Bachu & MA Celia (2004), Spatial characterization of the location of potentially leaky wells penetrating a deep saline aquifer in a mature sedimentary basin, *Environmental Geology*, vol 46(6-7), pp 707-720.
- GCCSI (2016), *The Global Status of CCS. Special Report: Understanding Industrial CCS Hubs and Clusters*, Global CCS Institute, Australia.
- Golding SD, Boreham CJ & Esterle JS (2013), Stable isotope geochemistry of coal bed and shale gas and related production waters: A review, *International Journal of Coal Geology*, vol 120, pp 24-40. doi: 10.1016/j.coal.2013.09.001.
- Golding SD, Dawson GKW, Pearce JK, Farrajota F, Mernagh T, Boreham CJ, Hall LS, Palu TJ, Sommacal, S (2016), ANLEC Project 7-1011-0189, Great Artesian Basin Authigenic carbonates as natural analogues for mineralisation trapping, UQ, GA, ANLEC R&D and CO<sub>2</sub>CRC, Manuka, ACT, Australia, pp 47.
- Gonzalez S, He J, Underschultz J & Garnett A (2019), *Seismic interpretation - geophysics*, The University of Queensland Surat Deep Aquifer Appraisal Project – Supplementary Detailed Report, The University of Queensland.
- Gonzalez S, Harfoush A, La Croix A, Underschultz J & Garnett A (2019), *Regional static model*, The University of Queensland Surat Deep Aquifer Appraisal Project – Supplementary Detailed Report, The University of Queensland.
- Gonzalez S, Harfoush A, La Croix A & Underschultz J (2019), *Seismic files: data set*, The University of Queensland Surat Deep Aquifer Appraisal Project – Supplementary Detailed Report, The University of Queensland.
- Gor GY, Elliot TR and Prévost JH (2013), Effects of thermal stresses on caprock integrity during CO<sub>2</sub> storage, *International Journal of Greenhouse Gas Control*, vol 12, pp 300-309.

- Green PM, Carmichael DC, Brain TJ, Murray CG, McKellar JL, Beeston JW, Gray ARG (1997), Lithostratigraphic units in the Bowen and Surat Basins, Queensland, Green PM (ed) *The Surat and Bowen Basins, South-east Queensland*. Queensland Department of Mines and Energy.
- Green PM, Hoffmann KL, Brain TJ, Gray ARG (1997), *The Surat and Bowen Basins, south-east Queensland: Queensland Minerals and Energy Review Series*, Queensland Department of Mines and Energy, Brisbane, Queensland, pp 244.
- Greig C, Bongers G, Stot C & Byrom S (2016a), Overview of CCS Roadmaps and Projects. The University of Queensland, Brisbane. ISBN 978-1-74272-178-1.
- Greig C, Baird J & Zervos T (2016b), Financial Incentives for the Acceleration of CCS Projects, The University of Queensland, Brisbane, ISBN 978-1-74272-177-4.
- Grigorescu M (2011), Mineralogy of the north-eastern Bowen Basin and north-eastern Surat Basin, Queensland. Queensland Geological Record.
- Habermehl MA (1980), The Great Artesian Basin, Australia, *BMR Journal of Australia Geology and Geophysics*, vol 5(1), pp 9-38.
- Haese R, Frank A, Grigorescu M, Horner KNM KD, Schacht U, Tenthorey E (2016), Geochemical impacts and monitoring of CO<sub>2</sub> storage in low salinity aquifers, 3-1110-0088, CO<sub>2</sub>CRC report RPT15-5328 for ANLEC R&D.
- Haimson B & Fairhurst C (1967), Initiation and extension of hydraulic fractures in rocks, *Society of Petroleum Engineers Journal*, vol 7, pp 310-318.
- Hallam A & Wignall PB (1999), Mass extinctions and sea level changes, mass extinctions and their aftermath, *Earth-Science Reviews*, vol 48, pp 217-250.
- Hamilton SK, Golding SD, Baublys KA & Esterle JS (2014), Stable isotopic and molecular composition of desorbed coal seam gases from the Walloon Subgroup, eastern Surat Basin, Australia. *International Journal of Coal Geology*, vol 122, pp 21-36. doi: 10.1016/j.coal.2013.12.003.
- Hammond J & Shackley S (2010), Towards a public communication and engagement strategy for carbon dioxide capture and storage projects in Scotland, Working Paper 2010-08, Scottish Centre for Carbon Capture, Edinburgh.
- Haq BU, Hardenbol J & Vail PR (1987), Chronology of fluctuating sea levels since the Triassic, *Science*, vol 235, pp 1156-1166.
- Harfoush H, Altaf I & Wolhuter A (2019), *Wireline log analysis*, The University of Queensland Surat Deep Aquifer Appraisal Project – Supplementary Detailed Report, The University of Queensland.
- Harfoush A, Pearce J & Wolhuter A (2019), *Core data analysis*, The University of Queensland Surat Deep Aquifer Appraisal Project – Supplementary Detailed Report, The University of Queensland.
- Harfoush A, Hayes P, La Croix A, Gonzalez S & Wolhuter A (2019), *Integrating petrophysics into modelling*, The University of Queensland Surat Deep Aquifer Appraisal Project – Supplementary Detailed Report, The University of Queensland.
- Harfoush A, Gonzalez S, Ribeiro A & Wolhuter A (2019), *Fluid substitution for seismic detection of plume*, The University of Queensland Surat Deep Aquifer Appraisal Project – Supplementary Detailed Report, The University of Queensland.
- Hayes P, Nicol C & Underschultz J (2019), *Precipice sandstone hydraulic property estimation from observed MAR responses*, The University of Queensland Surat Deep Aquifer Appraisal Project – Supplementary Detailed Report, The University of Queensland.
- Hayes P, Nicol C & Underschultz J (2019), *Regional groundwater model*, The University of Queensland Surat Deep Aquifer Appraisal Project – Supplementary Detailed Report, The University of Queensland.
- HE X, Koch J, Sonnenborg TO, Jorgensen F, Schamper C, & Refsgaard JC (2014), Transition probability-based stochastic geological modeling using airborne geophysical data and borehole data. *Water Resources Research*, vol 50, pp 3147-3169.
- Helby R, Morgan R & Partridge AD (2004), *Updated Jurassic – Early Cretaceous Dinocyst Zonation: NWS Australia*, Geoscience Australia Publication.
- Herczeg AL, Torgersen T, Chivas AR & Habermehl MA (1991), Geochemistry of ground waters from the Great Artesian Basin, Australia, *Journal of hydrology*, vol 126(3-4), pp 225-245.
- Herzog H (2017), Financing CCS Demonstration Projects: Lessons Learned from Two Decades of Experience, *Energy Procedia*, doi.org/10.1016/j.egypro.2017.03.1708, vol 114, pp 5691-5700.
- Hettema M, Bostrøm B & Lund T (2004), Analysis of lost circulation during drilling in cooled formations, *SPE Annual Technical Conference and Exhibition*, Society of Petroleum Engineers.
- Higgs KE, Funnell RH, Reyes AG (2013), Changes in reservoir heterogeneity and quality as a response to high partial pressures of CO<sub>2</sub> in a gas reservoir, New Zealand, *Marine and Petroleum Geology*, vol 48, pp 293-322.
- Hillis RR, Enever JR & Reynolds SD (1999), In situ stress field of eastern Australia, *Australian Journal of Earth Sciences*, vol 46, pp 813-825.

- Hitchon B. & Hays J (1971), Hydrodynamics and hydrocarbon occurrences, Surat Basin, Queensland, Australia, *Water Resources Research*, vol 7(3), pp 658-676.
- Hobman EV & Ashworth P (2013), Public support for energy sources and related technologies: The impact of simple information provision, *Energy Policy*, vol 63, pp 862-869.
- Hodgkinson J, Hortle A & McKillop M (2010), The application of hydrodynamic analysis in the assessment of regional aquifers for carbon geostorage: preliminary results for the Surat Basin, Queensland, *The APPEA Journal*, vol 50(1), pp 445-462.
- Hodgkinson J & Grigorescu M (2013), Background research for selection of potential geostorage targets—case studies from the Surat Basin, Queensland, *Australian Journal of Earth Sciences*, vol 60(1), pp 71-89.
- Hoffmann KL, Totterdell JM, Dixon O, Simpson GA, Brakel AT, Wells AT, Mckeller JL (2009), Sequence stratigraphy of Jurassic strata in the lower Surat Basin succession, Queensland, *Australian Journal of Earth Sciences*, vol 56, pp 461-476.
- Hofstede Insights. (n.d.) Country comparison: India. Retrieved on 27 March 2019: [www.hofstede-insights.com/country-comparison/india/](http://www.hofstede-insights.com/country-comparison/india/)
- Holloway S (2001), Storage of fossil fuel-derived carbon dioxide beneath the surface of the earth, *Annual Review of Energy and the Environment*, vol 26(1), pp 145-166.
- Honari V, Harfoush A, Underschultz J & Wolhuter A (2019), *DST Analysis*, The University of Queensland Surat Deep Aquifer Appraisal Project – Supplementary Detailed Report, The University of Queensland.
- Honari V, Gonzalez S, Underschultz J & Garnett A (2019), *Moonie oil field history match and re-evaluation*, The University of Queensland Surat Deep Aquifer Appraisal Project – Supplementary Detailed Report, The University of Queensland.
- Honari V, Underschultz J & Garnett A (2019), *Appraisal well test designs*, The University of Queensland Surat Deep Aquifer Appraisal Project – Supplementary Detailed Report, The University of Queensland.
- Honari V, Gonzalez S & Garnett A (2019), *Site appraisal plan*, The University of Queensland Surat Deep Aquifer Appraisal Project – Supplementary Detailed Report, The University of Queensland.
- Honari V, Garnett A & Underschultz J (2019), *Risk register report*, The University of Queensland Surat Deep Aquifer Appraisal Project – Supplementary Detailed Report, The University of Queensland.
- Horsfield B, Schenk HJ, Mills N & Welte DH (1991), An investigation of the in-reservoir conversion of oil to gas: compositional and kinetic findings from closed-system programmed-temperature pyrolysis, *Advances in Organic Chemistry*, vol 19(1-3), pp 13.
- Hu LY & Chugunova T (2008), Multiple-point geostatistics for modeling subsurface heterogeneity: a comprehensive review, *Water Resources Research*, vol 44, W11413.
- International Energy Agency (2013), *Technology Roadmap – Carbon capture and storage*, OECD/IEA, Paris.
- International Energy Agency (2019). *World Energy Outlook 2018*. OECD/IEA, Paris: ISBN: 978-92-64-24365-1
- Intergovernmental Panel on Climate Change (IPCC) 2018, Global warming of 1.5 °C: An IPCC special report on the impacts of global warming of 1.5 °C above pre-industrial levels and related global greenhouse gas emission pathways, in the context of strengthening the global response to the threat of climate change, sustainable development, and efforts to eradicate poverty. Summary for policy makers, IPCC, Geneva, Switzerland, viewed 17 January 2019, [www.ipcc.ch/report/sr15/](http://www.ipcc.ch/report/sr15/) and [www.report.ipcc.ch/sr15/pdf/sr15\\_spm\\_final.pdf](http://www.report.ipcc.ch/sr15/pdf/sr15_spm_final.pdf).
- Itaoka K, Dowd A-M, Saito A, Paukovic M, de Best-Waldhober M & Ashworth P (2013), Relating individual perceptions of carbon dioxide to perceptions of CCS: An international comparative study, *Energy Procedia*, vol 37, pp 7436-7443.
- Jacome MCS (2016), Bowen/Surat basin hydrocarbon field assessments Kincora Field, UQ MS research project report, pp 98.
- Jeanneret T, Muriuki G & Ashworth P (2014), Energy technology preferences of the Australian public: Results of a 2013 national survey, EP145414, CSIRO, Pullenvale.
- Jenkins CR, Cook PJ, Ennis-King J, Undershultz J, Boreham C, Dance T, de Caritat P, Etheridge DM, Freifeld BM, Hortle A, Kirste D, Paterson L, Pevzner R, Schacht U, Sharma S, Stalker L & Urosevic M (2011), Safe storage and effective monitoring of CO<sub>2</sub> in depleted gas fields, *Proceedings of the National Academy of Science*, 1107255108, pp 7.
- Jiang H & Eastman JR (2000), Application of fuzzy measures in multi-criteria evaluation in GIS, *International Journal of Geographical Information Science*, vol 14(2), pp 173-184.
- Journal AG & Alabert FG (1988), Focusing on spatial connectivity of extreme valued attributes: stochastic indicator models of reservoir heterogeneities, *SPE*, paper 18324.
- Journal AG & Issaks EH (1984), Conditional indicator simulation: application to a Saskatchewan uranium deposit, *Mathematical Geology*, vol 16, pp 685-718.

- Kahneman D & Frederick S (2002), Representativeness Revisited: Attribute Substitution in Intuitive Judgment, in Gilovich T, Griffin D & Kahneman D (eds), *Heuristics and biases: The psychology of intuitive judgment*, Cambridge University Press, New York, pp 49-81.
- Kaldi JG & Gibson-Poole C. M (2008), Storage capacity estimation, site selection and characterization for CO<sub>2</sub> storage projects, CO<sub>2</sub> CRC Report No. RPT08-1001. 2008.
- Kapetaki Z & Scowcroft J (2017), Overview of Carbon Capture and Storage (CCS) Demonstration Project Business Models: Risks and Enablers on the Two Sides of the Atlantic. *Energy Procedia*, doi.org/10.1016/j.egypro.2017.03.1816, vol 114, pp 6623-6630.
- Kashoob AAS (2018), Bowen/Surat basin hydrocarbon field assessments – Newstead Gas Fieldm UQ MS research project report.
- Kaufmann B (2006), Calibrating the Devonian Time Scale: A synthesis of U-Pb ID-TIMS ages and conodont stratigraphy, *Earth-Science Reviews*, vol 76, pp 175-190.
- Kelson R (2017), Brownfield review – Colgoon, Didgeridoo & Digger fields in the Surat Basin, UQ MS research project report, pp 37.
- Ketzin, Germany—Design, results, recommendations, *International Journal of Greenhouse Gas Control*, vol 15, pp 163-173.
- Kinik K, Wojtanowicz AK & Gumus F (2016), Probabilistic Assessment of the Temperature-Induced Effective Fracture Pressures, *SPE Drilling & Completion*, vol 31, pp 40-52.
- Knights P & Hoods M (eds) (2009), Coal and the Commonwealth - The greatness of an Australian resource, The University of Queensland; DEEWR (2010) "Resourcing the future national resource sector employment task force report", at [www.deewr.gov.au/Skills/Programs/National/nrset/Documents/FinalReport.pdf](http://www.deewr.gov.au/Skills/Programs/National/nrset/Documents/FinalReport.pdf).
- Köhler SJ, Dufaud F, Oelkers EH (2003), An experimental study of illite dissolution kinetics as a function of ph from 1.4 to 12.4 and temperature from 5 to 50°C, *Geochimica et Cosmochimica Acta*, vol 67, pp 3583-3594.
- Korsch RJ, O'Brien PE, Sexton MJ, Wake-Dyster KD & Wells AT (1989), Development of Mesozoic transtensional basins in easternmost Australia, *Australian Journal of Earth Sciences*, vol 36, pp 13-28.
- Korsch RJ, Boreham CJ, Totterdell JM, Shaw RD & Nicoll MJ (1998), Development and petroleum resource evaluation of the Bowen, Gunnedah and Surat basins, Eastern Australia, *APPEA Journal*, vol 38(1), pp199-237.
- Korsch RJ, Totterdell JM (2009), Subsidence history and basin phases of the Bowen, Gunnedah and Surat Basins, eastern Australia. *Australian Journal of Earth Sciences*, vol 56, pp 335-353.
- Korsch RJ, Totterdell JM, Fomin T & Nicoll MG (2009), Contractional structures and deformational events in the Bowen, Gunnedah and Surat Basins, eastern Australia, *Australian Journal of Earth Sciences*, vol 56(3), pp 477-499.
- Koltermann CE & Gorelick SM (1996), Heterogeneity in sedimentary deposits: a review of structure-imitating, process-imitating, and descriptive approaches, *Water Resources Research*, vol 32, pp 2617-2658.
- La Croix A, Wang J & Underschultz J (2019), *Integrated facies analysis of the Precipice Sandstone and Evergreen Formation in the Surat Basin*, The University of Queensland Surat Deep Aquifer Appraisal Project – Supplementary Detailed Report, The University of Queensland.
- La Croix A, Wang J, Gonzalez S, He J, Underschultz J & Garnett A (2019), *Sequence stratigraphy of the Precipice Sandstone and Evergreen Formation in the Surat Basin*, The University of Queensland Surat Deep Aquifer Appraisal Project – Supplementary Detailed Report, The University of Queensland.
- La Croix A, He J, Wang J & Underschultz J (2019), *Facies prediction from well logs in the Precipice Sandstone and Evergreen Formation in the Surat Basin*, The University of Queensland Surat Deep Aquifer Appraisal Project – Supplementary Detailed Report, The University of Queensland.
- La Croix A, Hannaford C & Underschultz J (2019), *Palynological analysis of the Precipice Sandstone and Evergreen Formation in the Surat Basin*, The University of Queensland Surat Deep Aquifer Appraisal Project – Supplementary Detailed Report, The University of Queensland.
- La Croix A, Hannaford C & Underschultz J (2019), *Palynological analysis of the Precipice Sandstone and Evergreen Formation in the Surat Basin*, The University of Queensland Surat Deep Aquifer Appraisal Project – Supplementary Detailed Report, The University of Queensland.
- Langevin CD, Hughes JD, Banta ER, Niswonger RG, Panday, Sorab, Provost AM (2017), Documentation for the MODFLOW 6 Groundwater Flow Model: U.S. Geological Survey Techniques and Methods, book 6, chap A55, pp 197, doi.org/10.3133/tm6A55.
- Lee SY, Carle SF & Fogg GE (2007), Geologic heterogeneity and a comparison of two geostatistical models: Sequential Gaussian and transition probability-based geostatistical simulation, *Advances in Water Resources*, vol 30, pp 1914-1932.
- Li G, Lorwongngam A & Roegiers J-C (2009), Critical review of leak-off test as a practice for determination of in-situ stresses, *43rd U.S. Rock Mechanics Symposium*, Asheville, North Carolina: American Rock Mechanics Association.
- Liao E (2015), Bowen/Surat basin hydrocarbon field assessments - Carbean Field. UQ MS research project report, pp 51.

- Liebscher A, Möller F, Bannach A, Köhler S, Wiebach J, Schmidt-Hattenberger, C & Zemke J. (2013), Injection operation and operational pressure-temperature monitoring at the CO<sub>2</sub> storage pilot site.
- L'Orange S, Arvai J, Dohle S & Siegrist M (2014), Predictors of risk and benefit perception of carbon capture and storage (CCS) in regions with different stages of deployment, *International Journal of Greenhouse Gas Control*, vol 25, pp 23-32.
- Loydell DK (1993), Worldwide correlation of Telychian (Upper Llandovery) strata using graptolies, *In: Hailwood EA & Kidd RB (eds.), High Resolution Stratigraphy*. Geological Society.
- Lowson RT, Comarmond MCJ, Rajaratnam G, Brown PL (2005), The kinetics of the dissolution of chlorite as a function of pH and at 25°C, *Geochimica et Cosmochimica Acta*, vole 69, pp 1687-1699.
- Luo Z and Bryant SL (2010), Influence of thermo-elastic stress on CO<sub>2</sub> injection induced fractures during storage, *SPE International Conference on CO<sub>2</sub> capture, storage, and utilization*, Society of Petroleum Engineers.
- Malczewski J (2006), GIS-based multicriteria decision analysis: a survey of the literature, *International Journal of Geographical Information Science*, vol 20(7), pp 703-726.
- Mahlbacher A (2019), Hydrogeochemical investigation of the Precipice Sandstone aquifer in the Moonie Area, Southern Surat Basin, Australia: Assessing up-fault discharge potential, Masters of Science Thesis, The University of Queensland Surat Deep Aquifer Appraisal Project – Supplementary Detailed Report, The University of Queensland.
- Mallants D, Underschultz J & Simmons C (2018) Integrated analysis of hydrochemical, geophysical, hydraulic and structural geology data to improve characterisation and conceptualisation of faults for use in regional groundwater flow models, prepared by the Commonwealth Scientific and Industrial Research Organisation (CSIRO) in collaboration with University of Queensland (UQ) and Flinders University of South Australia (FUSA).
- Mallet JL (2002), *Geomodelling*, New York, Oxford University Press.
- Manceau JC, Trémosa J, Audigane P, Lerouge C, Claret F, Lettry Y & Nussbaum C. (2015), Well integrity assessment under temperature and pressure stresses by a 1: 1 scale wellbore experiment, *Water Resources Research*, vol 51(8), pp 6093-6109.
- Marshall JP (2016), Disordering fantasies of coal and technology: Carbon capture and storage in Australia, *Energy Policy*, vol 99(C), pp 288-298.
- Martin M. Wakefield, M. Bianchi, V. Esterle, J. and Zhou, F. 2018. Evidence for marine influence in the Lower Jurassic Precipice Sandstone, Surat Basin, eastern Australia. *Marine and Petroleum Geology*, 65, 75-91.
- Marx J & Langenheim R (1959), Reservoir heating by hot fluid injection.
- Mathieson A, Midgely J, Wright I, Saoula N & Ringrose P (2011), In Salah CO<sub>2</sub> Storage JIP: CO<sub>2</sub> sequestration monitoring and verification technologies applied at Krechba, Algeria, *Energy Procedia*, vol 4, pp 3596-3603.
- Maury V & Idelovici J (1995), Safe drilling of HP/HT wells, the role of the thermal regime in loss and gain phenomenon, SPE/IADC Drilling Conference, Society of Petroleum Engineers.
- McKellar JK (1998), Late Early to Late Jurassic palynology, biostratigraphy and palaeogeography of the Roma Shelf area, north western Surat Basin, Queensland, Australia, PhD The University of Queensland, Brisbane, Australia, pp 620.
- Miall AD (2010), *The Geology of Stratigraphic Sequences*, Berlin Heidelberg, Springer-Verlag.
- Michael KA, Golab V, Shulakova J, Ennis-King G, Allinson, Sharma S & Aiken T (2010), Geological storage of CO<sub>2</sub> in saline aquifers - a review of the experience from existing storage operations, *International Journal of Greenhouse Gas Control*, vol 4(4), pp 659-667.
- Middleton GV (1978), Facies, *in Fairbridge RW & Bourgeois J. (eds), Encyclopedia of Sedimentology: Stroudsbury, Pennsylvania*, Dowden, Huchison, and Ross, pp 323-325.
- Moock I, Kwiatak G & Zimmermann G (2009), Slip tendency analysis, fault reactivation potential and induced seismicity in a deep geothermal reservoir, *Journal of Structural Geology*, vol 31, pp 1174-1182.
- Morgan RP, Hooker N & Ingram B (2002), Towards higher palynological resolution in the Australian Mesozoic.
- Neele F, Nepveu M, Hofsee C & Meindertsmas W (2011), CO<sub>2</sub> storage capacity assessment methodology. TNO report TNO-060-UT-2011-00810, pp 45.
- NETL (2008), Methodology for development of Geological Storage Estimates for carbon dioxide, US Department of Energy report, pp 37.
- Nicot J-P, Hosseini SA, Solano SV (2011), Are single-phase flow numerical models sufficient to estimate pressure distribution in CO<sub>2</sub> sequestration projects?, *Energy Procedia*, vol 4, pp 3919-3926. doi: 10.1016/j.egypro.2011.02.330.

- Nisa C, Witt K, Ferguson M, Hodson A & Ashworth P (2018), *Australian Energy Preferences and the place of Carbon Capture and Storage (CCS) within the energy mix*, The University of Queensland Surat Deep Aquifer Appraisal Project – Supplementary Detailed Report, The University of Queensland.
- Nordbotten, Celia JMMA & Bachu S (2005), Injection and storage of CO<sub>2</sub> in deep saline aquifers: Analytical solution for CO<sub>2</sub> plume evolution during injection, *Transport in Porous media*, vol 58(3), pp 339-360.
- OGIA (2016a), Hydrogeological conceptualisation report for the Surat Cumulative Management Area. Department of Natural Resources and Mines, Office of Groundwater Impact Assessment, Brisbane.
- OGIA (2016b), Underground Water Impact Report for the Surat Cumulative Management Area, Department of Natural Resources and Mines, Office of Groundwater Impact Assessment, Brisbane.
- OGIA (2016c), Groundwater modelling report for the Surat Cumulative Management Area, Department of Natural Resources and Mines, Office of Groundwater Impact Assessment, Brisbane.
- OGIA (2016d), Springs in the Surat Cumulative Management Area, DNRME, pp 67.
- Oldenburg CM, Lewicki JL & Hepple RP (2003), *Near-surface monitoring strategies for geologic carbon dioxide storage verification*, No. LBNL-54089, Lawrence Berkeley National Lab.(LBNL), Berkeley, CA (United States).
- Oldendick RW (2008), Question order effects, in PJ Lavrakas (ed), *Encyclopedia of Survey Research Methods*, Sage Publications Inc. Thousand Oaks, CA, pp 663-665.
- Owen DDR, Shouakar-Stash O, Morgenstern U & Aravena R (2016), Thermodynamic and hydrochemical controls on CH<sub>4</sub> in a coal seam gas and overlying alluvial aquifer: new insights into CH<sub>4</sub> origins, *Scientific Reports*, vol 6, pp 32407.
- Oz SEEBASETM (2005), Public domain report to Shell Development Australia by FrOG Tech Pty Ltd. Brisbane.
- Paige R & Murray L (1994), Re-injection of produced water-Field experience and current understanding, *Rock Mechanics in Petroleum Engineering*, Society of Petroleum Engineers.
- Palandri JL, Kharaika YK (2004), A compilation of rate parameters of water-mineral interaction kinetics for application to geochemical modelling, USGS Open File Report 2004-1068, pp 64.
- Panday S, Langevin CD, Niswonger RG, Ibaraki M & Hughes JD (2013), MODFLOW-USG version 1: An unstructured grid version of MODFLOW for simulating groundwater flow and tightly coupled processes using a control volume finite-difference formulation: U.S. Geological Survey Techniques and Methods, book 6, chap A45, pp 66.
- Panday S (2017), USG-Transport v1.1.0: The Block-Centered Transport (BCT) Process for Modflow-USG. GSI-Environmental, [www.gsi-net.com/en/software/free-software/modflow-usg-software.html](http://www.gsi-net.com/en/software/free-software/modflow-usg-software.html).
- Paterson L, Ennis-King JP, Sharma S (2010), Observations of Thermal and Pressure Transients in Carbon Dioxide Wells, SPE Annual Technical Conference and Exhibition, Society of Petroleum Engineers, Florence, Italy, pp 12.
- Pearce JK, Kirste DM, Dawson GKW, Farquhar SM, Biddle D, Golding S, Rudolph V (2015), SO<sub>2</sub> Impurity Impacts on Experimental and Simulated CO<sub>2</sub>-Water-Reservoir Rock Reactions at Carbon Storage Conditions, *Chemical Geology*, vol 399, pp 65-86.
- Pearce JK, Dawson GKW, Law ACK, Biddle D, Golding SD (2016), Reactivity of micas and cap-rock in wet supercritical CO<sub>2</sub> with SO<sub>2</sub> and O<sub>2</sub> at CO<sub>2</sub> storage conditions, *Applied Geochemistry*, pp72, 59-76.
- Pearce JK & Dawson G (2018b), Experimental Determination of Impure CO<sub>2</sub> Alteration of Calcite Cemented Cap-Rock, and Long Term Predictions of Cap-Rock Reactivity, *Geosciences*, vol 8(7), pp 241; <https://doi.org/10.3390/geosciences8070241>.
- Pearce JK, Dawson GKW, Golab A, Knuefing L, Sommacal S, Rudolph V, Golding SD (2019), A combined geochemical and  $\mu$ CT study on the CO<sub>2</sub> reactivity of Surat Basin reservoir and cap-rock cores: Porosity changes, mineral dissolution and fines migration, *International Journal of Greenhouse Gas Control*, vol 80, pp 10-24.
- Pearce et al. Long term CO<sub>2</sub> reactivity of low salinity sandstone reservoir, transition zone and seal lithologies, 2019, in prep.
- Pearce J, Unterschultz J & La Croix A (2019), *Mineralogy, geochemical CO<sub>2</sub>-water-rock reactions and associated characterisation*, The University of Queensland Surat Deep Aquifer Appraisal Project – Supplementary Detailed Report, The University of Queensland.
- Peletiri SP, Rahmanian N & Mujtaba IM (2018), CO<sub>2</sub> Pipeline Design: A Review, *Energies*, vol 11, page 2184.
- Pepin G, Gonzalez M, Bloys JB et al. (2004), Effect of Drilling Fluid Temperature on Fracture Gradient: Field Measurements and Model Predictions, Gulf Rocks 2004, the 6th North America Rock Mechanics Symposium (NARMS), American Rock Mechanics Association.
- Perkins T & Gonzalez J (1984), Changes in earth stresses around a wellbore caused by radially symmetrical pressure and temperature gradients, *Society of Petroleum Engineers Journal*, vol 24, pp 129-140.

- Perkins T & Gonzalez J (1985), The effect of thermoelastic stresses on injection well fracturing, *Society of Petroleum Engineers Journal*, vol 25, pp 78-88.
- Perrin M, Zhu X, Rainaud J & Schneider S (2005), Knowledge-driven applications for geological modelling. *Journal of Petroleum Science and Engineering*, vol 47, pp 89-104.
- Pol D & Norell MA (2006), Uncertainty in the Age of Fossils and the Stratigraphic Fit to Phylogenies, *Systematic Biology*, vol 55, pp 512-521.
- Power PE & Devine SB (1970), Surat Basin, Australia – subsurface stratigraphy, history, and petroleum. *American Association of Petroleum Geologists Bulletin*, vol 54, pp 2410-2437.
- Price PL (1997), Permian to Jurassic palynostratigraphic nomenclature of the Bowen and Surat basins, *In: Green PM (ed), The Surat and Bowen Basins, southeast Queensland*, Queensland Department of Mines and Energy, Brisbane.
- Prommer H, Rathi B, Donn M, Siade A, Wendling L, Martens E, Patterson B (2016), Geochemical Response to Reinjection, Final Report for GISERA, CSIRO, Australia.
- Raiber M, Lewis S, Cendón DI, Cui T, Cox ME, Gilfedder M & Rassam DW (2019), Significance of the connection between bedrock, alluvium and streams: A spatial and temporal hydrogeological and hydrogeochemical assessment from Queensland, Australia, *Journal of Hydrology*, vol 569, pp 666-684.
- Refsgaard JC, Christensen S, Sonnenborg TO, Seifert D, Hojberg AL & Troldborg L (2012), Review of strategies for handling geological uncertainty in groundwater flow and transport modelling, *Advances in Water Resources*, vol 36, pp 36-50.
- Raza A, Hill KC & Korsch RJ (2009), Mid-Cretaceous uplift and denudation of the Bowen and Surat Basins, eastern Australia: relationship to Tasman Sea rifting from apatite and fission-track and vitrinite-reflectance data, *Australian Journal of Earth Sciences*, vol 56, pp 501-531.
- Ribeiro A, Rodger I & Underschultz J (2019), *Fluid model*, The University of Queensland Surat Deep Aquifer Appraisal Project – Supplementary Detailed Report, The University of Queensland.
- Ribeiro A, Rodger I, Underschultz J & Garnett A (2019), *Notional injection sites – injection scenarios*, The University of Queensland Surat Deep Aquifer Appraisal Project – Supplementary Detailed Report, The University of Queensland.
- Ringrose PS & Bentley M (2015), *Reservoir Model Design - a Practitioner's Guide*, Dordrecht Heidelberg New York London, Springer.
- Robertson & Garnett (2018), *Discussion document - A regulatory review of greenhouse gas storage - governance of pressure impacts in the GAB, Queensland*, The University of Queensland Surat Deep Aquifer Appraisal Project – Supplementary Detailed Report, The University of Queensland.
- Rodger I, Altaf I, Underschultz J & Garnett A (2019), *Pressure constraints on injection*, The University of Queensland Surat Deep Aquifer Appraisal Project – Supplementary Detailed Report, The University of Queensland.
- Rodger I, Sedaghat M & Underschultz J (2019), *Multiphase behaviour – relative permeability and capillary pressures*, The University of Queensland Surat Deep Aquifer Appraisal Project – Supplementary Detailed Report, The University of Queensland.
- Rodger I, La Croix A, Underschultz J & Garnett A (2019), *Transition Zone behaviour test models*, The University of Queensland Surat Deep Aquifer Appraisal Project – Supplementary Detailed Report, The University of Queensland.
- Rodger I, Garnett A & Underschultz J (2019), *Notional injection well design*, The University of Queensland Surat Deep Aquifer Appraisal Project – Supplementary Detailed Report, The University of Queensland.
- Rodger I, Gonzalez S & Underschultz J (2019), *Sector model for carbon dioxide injection simulations – gridding and upscaling*, The University of Queensland Surat Deep Aquifer Appraisal Project – Supplementary Detailed Report, The University of Queensland.
- Rodger I, Harfoush A & Underschultz J (2019), *CO<sub>2</sub> injection sensitivity study*, The University of Queensland Surat Deep Aquifer Appraisal Project – Supplementary Detailed Report, The University of Queensland.
- Rolfe J, Lawrence R & Rynne D (2011), The Economic Contribution of the Resources Sector, *Regional Areas in Queensland. Economic Analysis and Policy*, March, vol 41(1).
- Babaahmadi A, Tonguç U, Rosenbaum G (2019), Late Jurassic intraplate faulting in eastern Australia: A link to subduction in eastern Gondwana and plate tectonic reorganisation, *Gondwana Research*, February, vol 66, pp 1-12. <https://www.sciencedirect.com/science/article/pii/S1342937X18302521?via%3Dihub-bbb0305>.
- Rosenbaum G (2018), The Tasmanides: Phanerozoic tectonic evolution of eastern Australia, *Annual Review of Earth and Planetary Sciences*, vol 46, pp 291-325.



- Rutqvist J, Birkholzer J & Tsang C-F (2008), Coupled reservoir–geomechanical analysis of the potential for tensile and shear failure associated with CO<sub>2</sub> injection in multilayered reservoir–caprock systems, *International Journal of Rock Mechanics and Mining Sciences*, vol 45, pp 132-143.
- Samuelson W & Zeckhauser R (1988), Status quo bias in decision making, *Journal of Risk and Uncertainty*, vol 1, pp 7-59.
- Sanchez R (2011), *Cost Estimating Guide*, U.S. Department of Energy, Washington D.C. United States of America.
- Schintie R, Pinetown KL, Underschultz JR, Vink S, Peters CA & Midgley D (2018), Occurrence and fate of natural total petroleum hydrocarbons and other organic compounds in groundwater from coal-bearing basins in Queensland, CSIRO, Australia.
- Sedaghat M, Pearce J, Underschultz J & Hayes P (2019), *Flow modelling of the managed aquifer recharge areas*, The University of Queensland Surat Deep Aquifer Appraisal Project – Supplementary Detailed Report, The University of Queensland.
- Shackleton NJ, Hall MA, Raffi I, Tauxe L & Zachos J (2000), Astronomical calibration age for the Oligocene-Miocene boundary, *Geology*, vol 28, pp 447-450.
- Shaw RD, Korsch RJ, Boreham CJ, Totterdell JM, Lelbach C & Nicoll MG (2000), Evaluation of the undiscovered hydrocarbon resources of the Bowen and Surat Basins, southern Queensland, *AGSO Journal of Australian Geology and Geophysics*, vol 17(5-6), 23. <https://open.alberta.ca/dataset/00bafb16-6e20-407b-9752-77acec295ff7/resource/c91323e1-55b2-4182-913a-cc360963e3f9/download/quest-monitoring-measurement-and-verification-plan-update.pdf> (accessed 10/02/2019).
- Shell (2017), Shell Quest Carbon Capture and Storage Project. Measurement, Monitoring and Verification Plan, February 2017, revised 5 May 2017.
- SPE (2016), CO<sub>2</sub> Storage Resources Management System [www.spe.org/industry/CO<sub>2</sub>-storage-resources-management-system.php](http://www.spe.org/industry/CO2-storage-resources-management-system.php) (accessed 11/2/2019).
- Stalker L, Boreham C, Underschultz J, Freifeld B, Perkins E, Schacht U & Sharma S (2009), Geochemical monitoring at the CO<sub>2</sub>CRC Otway Project: tracer injection and reservoir fluid acquisition, *Energy Procedia*, vol 1(1), pp 2119-2125.
- Stalker L, Boreham C, Underschultz J, Freifeld B, Perkins E, Schacht U & Sharma S (2015), Application of tracers to measure, monitor and verify breakthrough of sequestered CO<sub>2</sub> at the CO<sub>2</sub>CRC Otway Project, Victoria, Australia, *Chemical Geology*, vol 399, pp 2-19.
- Steeffel CI (2001), GIMRT, version 1.2: Software for modeling multicomponent, multidimensional reactive transport, User's Guide, UCRL-MA-143182, Livermore, California: Lawrence Livermore National Laboratory.
- Steg L, Dreijerink L, Abrahamse W (2005), Factors influencing the acceptability of energy policies: a test of VBN theory, *Journal of Environmental Psychology*, vol 25(4), pp 415-425.
- Stoker G, Evans M & Halupka M (2018), Trust and democracy in Australia: Democratic decline and renewal, Report No. 1, December 2018, Museum of Australian Democracy and UC-IGPA. <https://www.democracy2025.gov.au/documents/Democracy2025-report1.pdf>
- Subhi ZA (2018), Bowen/Surat basin hydrocarbon field assessments – Yarrabend Gas Field, UQ MS research project report, pp 111.
- Suckow A, Deslandes A, Meredith K, Raiber M, Taylor A & Gerber C (2018), Environmental tracer studies to characterise and quantify groundwater flow and recharge in aquifers of the Surat Basin, Queensland, Australia. In *EGU General Assembly Conference Abstracts*, April, vol 20, pp 12219.
- Tang H, Meddagh WS, Toomey N (2011), Using an artificial-neural-network method to predict carbonate well log facies successfully, *SPE Reservoir Evaluation & Engineering*, vol 14(01), pp 35-44.
- Tavener E, Flottman T, Brooke-Barnett S (2018), In situ stress distribution and mechanical stratigraphy in the Bowen and Surat basins, Queensland, Australia. From: Turner JP, Healy D, Hillis RR & Welch MJ (eds) (2017), *Geomechanics and Geology*, Geological Society, London, Special Publications, vol 458, pp31-47.
- Terra Sana Consultants (2019), *Methane survey over Surat Basin seismic anomaly*, Report for The University of Queensland Surat Deep Aquifer Appraisal Project – Supplementary Detailed Report, The University of Queensland.
- Terwel BW, Harinck F, Ellemers N, Daamen DD & de Best-Waldhober M (2009), Trust as predictor of public acceptance of CCS, *Energy Procedia*, vol 1(1), pp 4613-4616.
- Torgersen T, Habermehl MA, Phillips FM, Elmore D, Kubik P, Jones GB & Gove HE (1991), Chlorine 36 dating of very old groundwater: 3. Further studies in the Great Artesian Basin, Australia, *Water Resources Research*, vol 27(12), pp 3201-3213.
- Taylor AM & Goldring R (1993), Descriptions and analysis of bioturbation and ichnofabric, *Journal of the Geological Society*, London, vol 150, pp 141-148.
- Tehseenullah (2015), Yellowbank - Bowen/Surat basin hydrocarbon field assessments, UQ MS research project report, pp 72.
- Timur A (1968), An investigation of permeability, porosity and residual water saturation relationships for sandstone reservoirs, *The Log Analyst*, vol 9(04).

- Totterdell JM, Moloney J, Korsch RJ, Krassay AA (2009), Sequence stratigraphy of the Bowen-Gunnedah and Surat basins in New South Wales, *Australian Journal of Earth Sciences*, vol 56, pp 433-459.
- Turner AK (2006), Challenges and trends for geological modelling and visualization, *Bulletin of Engineering Geology and the Environment*, vol 65, pp 109-127.
- Underschultz J (2007), Hydrodynamics and membrane seal capacity, *Geofluids* 7, pp 148-158.
- Underschultz JR, Rifkin W, Pasini P, Grigorescu M & de Souza TL (2015), Bowen/Surat Hydrocarbon Systems Analysis, The University of Queensland Centre for Coal Seam Gas (confidential report), pp 79.
- Underschultz J & Vink S (2015), Emerging complexity of the GAB Aquifer Systems in the Surat Basin. APPG/SEG International Conference and Exhibition, PESA Eastern Australian Basins Symposium. 13-16 September 2015, Melbourne.
- Underschultz JR, Pasini P, Grigorescu M & de Souza TL (2016), Assessing aquitard hydraulic performance from hydrocarbon migration indicators: Surat and Bowen basins, Australia, *Marine and Petroleum Geology*, vol 78, pp 712-727.
- Underschultz J, Dodds K, Michael K, Sharma S, Wall T & Whittaker S (2017), Chapter 23 Carbon Capture and Storage, in ed. Devasahayam S, Dowling K & Mahapatra M, *Sustainability in the Mineral/Energy Sectors*. CRC press, pp 730.
- Vail PR, Mitchum RMJ, Thompson S (1977), *Seismic stratigraphy and global changes of sea level, part four: global cycles of relative changes of sea level*. American Association of Petroleum Geologists Memoir, vol 26, pp 83-98.
- Van der Kuip, Benedictus MDCT, Wildgust N & Aiken T (2011), High-level integrity assessment of abandoned wells, *Energy Procedia*, vol 4, pp 5320-5326.
- Van Wagoner JC, Posamentier HW, Mitchum RM Jr, Vail PR, Sarg JF, Loutit TS & Hardenbol J (1988), An overview of sequence stratigraphy and key definitions. In *Sea Level Changes—An Integrated Approach* C.K. Wilgus CK, Hastings BS, Kendall CG, St C, Posamentier HW, Ross CA & Van Wagoner JC, (eds.), SEPM Special Publication 42, pp 39-45.
- Verly G (1993), Sequential Gaussian Simulation: A Monte Carlo Method for Generating Models of Porosity and Permeability. In: Spencer AM (ed.), *Generation, Accumulation and Production of Europe's Hydrocarbons III*, Berlin, Heidelberg: Springer.
- Vilarrasa V, Olivella S, Carrera J, Rutqvist J (2014), Long term impacts of cold CO<sub>2</sub> injection on the caprock integrity, *International Journal of Greenhouse Gas Control*, vol 24, pp 1-13.
- Vilarrasa V, Rutqvist J and Rinaldi AP (2015), Thermal and capillary effects on the caprock mechanical stability at In Salah, Algeria, *Greenhouse Gases: Science and Technology*, vol 5, pp 449-461.
- Wainman CC, McCabe PJ, Crowley JL & Nicoll RS (2015), U-Pb zircon age of the Walloon Coal Measures in the Surat Basin, southeast Queensland: implications for paleogeography and basin subsidence, *Australian Journal of Earth Sciences*, vol 62, pp 807-816.
- Wallace M, Goudarzi L, Callahan K & Wallace R (2015), A Review of CO<sub>2</sub> Pipeline Infrastructure in the US. DOE/NETL-2104/1681.
- Wallquist L, Visschers VH, Dohle S & Siegrist, M (2012), The role of convictions and trust for public protest potential in the case of carbon dioxide capture and storage (CCS), *Human and Ecological Risk*.
- Walsh III FR & Zoback MD (2016), Probabilistic assessment of potential fault slip related to injection-induced earthquakes: Application to north-central Oklahoma, USA. *Geology*, vol 44, pp 991-994.
- Watson MN, Zwingmann N, Lemon NM (2004), The Ladbroke Grove-Katnook carbon dioxide natural laboratory: A recent CO<sub>2</sub> accumulation in a lithic sandstone reservoir, *Energy*, vol 29, pp 1457-1466.
- Waschbusch P, Korsch RJ, Beaumont C (2009), Geodynamic modelling of aspects of the Bowen, Gunnedah, Surat and Eromanga Basins from the perspective of convergent margin processes, *Australian Journal of Earth Sciences*, vol 56, pp 309-334.
- White AF (1995), Chemical weathering rates of silicate minerals in soils, *Reviews in Mineralogy and Geochemistry*, vol 31, pp 407-461.
- White D (2009), Monitoring CO<sub>2</sub> storage during EOR at the Weyburn-Midale Field, *The Leading Edge*, vol 28(7), pp 838-842.
- Whittaker S, Rostron B, Hawkes C, Gardner C, White D, Johnson J & Seeburger D (2011), A decade of CO<sub>2</sub> injection into depleting oil fields: monitoring and research activities of the IEA GHG Weyburn-Midale CO<sub>2</sub> Monitoring and Storage Project, *Energy Procedia*, vol 4, pp 6069-6076.
- Wolhuter A, Garnett A & Underschultz J (2019), *Notional injection site identification report*, The University of Queensland Surat Deep Aquifer Appraisal Project – Supplementary Detailed Report, The University of Queensland.
- Wolhuter A, Garnett A & Underschultz J (2019), *Notional pipeline route analysis*, The University of Queensland Surat Deep Aquifer Appraisal Project – Supplementary Detailed Report, The University of Queensland.
- Wong PM, Henderson DJ & Brooks LJ (1998), Permeability Determination Using Neural Network in the Ravva Field, Offshore India, *SPE Reservoir Evaluation & Engineering*, vol 1(2), pp 90-104.
- Wu B (2015), Bowen/Surat basin hydrocarbon field assessments – Sandy Creek, *UQ MS research project report*, pp 82.

- Wye D (2019), *The Lockyer Valley; Great Artesian Basin groundwater discharge to the east of the Great Dividing Range*, Masters of Mineral Resources Thesis, The University of Queensland Surat Deep Aquifer Appraisal Project – Supplementary Detailed Report, The University of Queensland.
- Xu C & Dowd PA (2003), Optimal construction and visualisation of geological structures, *Computers and Geosciences*, vol 29, pp 761-773.
- Yang L, Zhang X & McAlinden KJ (2016), The effect of trust on people's acceptance of CCS (carbon capture and storage) technologies: Evidence from a survey in the People's Republic of China, *Energy*, vol 96, pp 69-79.
- Yousafi Y (2018), New approach to quantitative estimation of CO<sub>2</sub> leakage through abandoned wells, UQ PhD confirmation report, pp 46.
- Zhang J & Yin S-X (2017), Fracture gradient prediction: an overview and an improved method, *Petroleum Science*, vol 14, pp 720-730.
- Ziolkowski V, Hodgkinson, Mckillop J, Grigorescu M & McKellar JL (2014), Sequence stratigraphic analysis of the Lower Jurassic succession in the Surat Basin, Queensland – preliminary findings, Queensland Minerals and Energy Review Series, Queensland Government Department of Natural Resources and Mines, Queensland, 30 pp.

## 7. UQ-SDAAP: project reports listing

Ferguson et al. 2019a	Ferguson F, Witt K, Nisa C & Ashworth P (2019), <i>Effects of message framing on the support for carbon capture and storage (CCS) and alternative energy technologies</i> , The University of Queensland Surat Deep Aquifer Appraisal Project – Supplementary Detailed Report, The University of Queensland
Ferguson et al. 2019b	Ferguson M, Witt K & Ashworth P (2019), <i>Managed aquifer recharge focus groups</i> , The University of Queensland Surat Deep Aquifer Appraisal Project – Supplementary Detailed Report, The University of Queensland
Ferguson et al. 2019c	Ferguson M, Witt K & Ashworth P (2019), <i>Five country survey</i> , The University of Queensland Surat Deep Aquifer Appraisal Project – Supplementary Detailed Report, The University of Queensland
Nisa et al. 2018	Nisa C, Witt K, Ferguson M, Hodson A & Ashworth P (2018), <i>Australian Energy Preferences and the place of Carbon Capture and Storage (CCS) within the energy mix</i> , The University of Queensland Surat Deep Aquifer Appraisal Project – Supplementary Detailed Report, The University of Queensland
La Croix et al. 2019a	La Croix A, Wang J & Underschlutz J (2019), <i>Integrated facies analysis of the Precipice Sandstone and Evergreen Formation in the Surat Basin</i> , The University of Queensland Surat Deep Aquifer Appraisal Project – Supplementary Detailed Report, The University of Queensland
La Croix et al. 2019b	La Croix A, Wang J, Gonzalez S, He J, Underschlutz J & Garnett A (2019), <i>Sequence stratigraphy of the Precipice Sandstone and Evergreen Formation in the Surat Basin</i> , The University of Queensland Surat Deep Aquifer Appraisal Project – Supplementary Detailed Report, The University of Queensland
La Croix et al. 2019c	La Croix A, He J, Wang J & Underschlutz J (2019), <i>Facies prediction from well logs in the Precipice Sandstone and Evergreen Formation in the Surat Basin</i> , The University of Queensland Surat Deep Aquifer Appraisal Project – Supplementary Detailed Report, The University of Queensland
Gonzalez et al. 2019a	Gonzalez S, He J, Underschlutz J & Garnett A (2019), <i>Seismic interpretation - geophysics</i> , The University of Queensland Surat Deep Aquifer Appraisal Project – Supplementary Detailed Report, The University of Queensland
La Croix et al. 2019d	La Croix A, Hannaford C & Underschlutz J (2019), <i>Palynological analysis of the Precipice Sandstone and Evergreen Formation in the Surat Basin</i> , The University of Queensland Surat Deep Aquifer Appraisal Project – Supplementary Detailed Report, The University of Queensland
Pearce et al. 2019	Pearce J, Underschlutz J & La Croix A (2019), <i>Mineralogy, geochemical CO<sub>2</sub>-water-rock reactions and associated characterisation</i> , The University of Queensland Surat Deep Aquifer Appraisal Project – Supplementary Detailed Report, The University of Queensland
Harfoush et al. 2019a	Harfoush H, Altaf I & Wolhuter A (2019), <i>Wireline log analysis</i> , The University of Queensland Surat Deep Aquifer Appraisal Project – Supplementary Detailed Report, The University of Queensland
Harfoush et al. 2019b	Harfoush A, Pearce J & Wolhuter A (2019), <i>Core data analysis</i> , The University of Queensland Surat Deep Aquifer Appraisal Project – Supplementary Detailed Report, The University of Queensland
Honari et al. 2019a	Honari V, Harfoush A, Underschlutz J & Wolhuter A (2019), <i>DST Analysis</i> , The University of Queensland Surat Deep Aquifer Appraisal Project – Supplementary Detailed Report, The University of Queensland
Harfoush et al. 2019c	Harfoush A, Hayes P, La Croix A, Gonzalez S & Wolhuter A (2019), <i>Integrating petrophysics into modelling</i> , The University of Queensland Surat Deep Aquifer Appraisal Project – Supplementary Detailed Report, The University of Queensland
Sedaghat et al. 2019	Sedaghat M, Pearce J, Underschlutz J & Hayes P (2019), <i>Flow modelling of the managed aquifer recharge areas</i> , The University of Queensland Surat Deep Aquifer Appraisal Project – Supplementary Detailed Report, The University of Queensland
La Croix et al. 2019e	La Croix A, Harfoush A, Rodger I & Underschlutz J (2019), <i>Sector-scale static reservoir modelling of the basin-centre in the Surat Basin</i> , The University of Queensland Surat Deep Aquifer Appraisal Project – Supplementary Detailed Report, The University of Queensland
Gonzalez et al. 2019b	Gonzalez S, Harfoush A, La Croix A, Underschlutz J & Garnett A (2019), <i>Regional static model</i> , The University of Queensland Surat Deep Aquifer Appraisal Project – Supplementary Detailed Report, The University of Queensland
Gonzalez et al. 2019c	Gonzalez S, Harfoush A, La Croix A & Underschlutz J (2019), <i>Seismic files: data set</i> , The University of Queensland Surat Deep Aquifer Appraisal Project – Supplementary Detailed Report, The University of Queensland

Terra Sana Consultants 2019	Terra Sana Consultants (2019), <i>Methane survey over Surat Basin seismic anomaly</i> , Report for The University of Queensland Surat Deep Aquifer Appraisal Project – Supplementary Detailed Report, The University of Queensland
Rodger et al. 2019a	Rodger I, Altaf I, Underschultz J & Garnett A (2019), <i>Pressure constraints on injection</i> , The University of Queensland Surat Deep Aquifer Appraisal Project – Supplementary Detailed Report, The University of Queensland
Rodger et al. 2019b	Rodger I, Sedaghat M & Underschultz J (2019), <i>Multiphase behaviour – relative permeability and capillary pressures</i> , The University of Queensland Surat Deep Aquifer Appraisal Project – Supplementary Detailed Report, The University of Queensland
Rodger et al. 2019c	Rodger I, La Croix A, Underschultz J & Garnett A (2019), <i>Transition Zone behaviour test models</i> , The University of Queensland Surat Deep Aquifer Appraisal Project – Supplementary Detailed Report, The University of Queensland
Hayes et al. 2019a	Hayes P, Nicol C & Underschultz J (2019), <i>Precipice sandstone hydraulic property estimation from observed MAR responses</i> , The University of Queensland Surat Deep Aquifer Appraisal Project – Supplementary Detailed Report, The University of Queensland
Honari et al. 2019b	Honari V, Gonzalez S, Underschultz J & Garnett A (2019), <i>Moonie oil field history match and re-evaluation</i> , The University of Queensland Surat Deep Aquifer Appraisal Project – Supplementary Detailed Report, The University of Queensland
Rodger et al. 2019d	Rodger I, Garnett A & Underschultz J (2019), <i>Notional injection well design</i> , The University of Queensland Surat Deep Aquifer Appraisal Project – Supplementary Detailed Report, The University of Queensland
Wolhuter et al. 2019a	Wolhuter A, Garnett A & Underschultz J (2019), <i>Notional injection site identification report</i> , The University of Queensland Surat Deep Aquifer Appraisal Project – Supplementary Detailed Report, The University of Queensland
Wolhuter et al. 2019b	Wolhuter A, Garnett A & Underschultz J (2019), <i>Notional pipeline route analysis</i> , The University of Queensland Surat Deep Aquifer Appraisal Project – Supplementary Detailed Report, The University of Queensland
Rodger et al. 2019e	Rodger I, Gonzalez S & Underschultz J (2019), <i>Sector model for carbon dioxide injection simulations – gridding and upscaling</i> , The University of Queensland Surat Deep Aquifer Appraisal Project – Supplementary Detailed Report, The University of Queensland
Ribeiro et al. 2019a	Ribeiro A, Rodger I & Underschultz J (2019), <i>Fluid model</i> , The University of Queensland Surat Deep Aquifer Appraisal Project – Supplementary Detailed Report, The University of Queensland
Ribeiro et al. 2019b	Ribeiro A, Rodger I, Underschultz J & Garnett A (2019), <i>Notional injection sites – injection scenarios</i> , The University of Queensland Surat Deep Aquifer Appraisal Project – Supplementary Detailed Report, The University of Queensland
Hayes et al. 2019b	Hayes P, Nicol C & Underschultz J (2019), <i>Regional groundwater model</i> , The University of Queensland Surat Deep Aquifer Appraisal Project – Supplementary Detailed Report, The University of Queensland
Advisian 2019	Advisian (2019), <i>Well-pad concept definition study</i> , Report for The University of Queensland Surat Deep Aquifer Appraisal Project – Supplementary Detailed Report, The University of Queensland
Rodger et al. 2019f	Rodger I, Harfoush A & Underschultz J (2019), <i>CO<sub>2</sub> injection sensitivity study</i> , The University of Queensland Surat Deep Aquifer Appraisal Project – Supplementary Detailed Report, The University of Queensland
Honari et al. 2019c	Honari V, Underschultz J & Garnett A (2019), <i>Appraisal well test designs</i> , The University of Queensland Surat Deep Aquifer Appraisal Project – Supplementary Detailed Report, The University of Queensland
Honari et al. 2019d	Honari V, Gonzalez S & Garnett A (2019), <i>Site appraisal plan</i> , The University of Queensland Surat Deep Aquifer Appraisal Project – Supplementary Detailed Report, The University of Queensland
Honari et al. 2019e	Honari V, Garnett A & Underschultz J (2019), <i>Risk register report</i> , The University of Queensland Surat Deep Aquifer Appraisal Project – Supplementary Detailed Report, The University of Queensland
Harfoush et al. 2019d	Harfoush A, Gonzalez S, Ribeiro A & Wolhuter A (2019), <i>Fluid substitution for seismic detection of plume</i> , The University of Queensland Surat Deep Aquifer Appraisal Project – Supplementary Detailed Report, The University of Queensland
Gamma Energy Technology 2019	Gamma Energy Technology (2019), <i>Hub development: Industrial-scale deployment via retrofitting sequencing and pipeline development</i> , Report for The University of Queensland Surat Deep Aquifer Appraisal Project – Supplementary Detailed Report, The University of Queensland
Garnett 2019a	Garnett A (2019), <i>Estimates of unit costs and discussion of the value of investment in appraisal</i> , The University of Queensland Surat Deep Aquifer Appraisal Project – Supplementary Detailed Report, The University of Queensland

Garnett 2019b	Garnett A (2019), <i>Experiences in adapting legacy oil and gas wells for CCS-related well testing</i> , The University of Queensland Surat Deep Aquifer Appraisal Project – Supplementary Detailed Report, The University of Queensland
Ampofo & Garnett 2019	Ampofo K & Garnett A (2019), <i>Reviews of previous work on costs in Australian CCS</i> , The University of Queensland Surat Deep Aquifer Appraisal Project – Supplementary Detailed Report, The University of Queensland
Garnett & Underschultz 2019	Garnett A & Underschultz J (2019), <i>Methodology for assessment of dynamic capacity</i> , The University of Queensland Surat Deep Aquifer Appraisal Project – Supplementary Detailed Report, The University of Queensland
Mahlbacher 2019	Mahlbacher A (2019), Hydrogeochemical investigation of the Precipice Sandstone aquifer in the Moonie Area, Southern Surat Basin, Australia: Assessing up-fault discharge potential, Masters of Science Thesis, The University of Queensland Surat Deep Aquifer Appraisal Project – Supplementary Detailed Report, The University of Queensland
Wye 2019	Wye D (2019), <i>The Lockyer Valley; Great Artesian Basin groundwater discharge to the east of the Great Dividing Range</i> , Masters of Mineral Resources Thesis, The University of Queensland Surat Deep Aquifer Appraisal Project – Supplementary Detailed Report, The University of Queensland
Robertson & Garnett 2018	<i>Robertson &amp; Garnett (2018), Discussion document - A regulatory review of greenhouse gas storage - governance of pressure impacts in the GAB, Queensland</i> , The University of Queensland Surat Deep Aquifer Appraisal Project – Supplementary Detailed Report, The University of Queensland

## 8. Glossary of terms, acronyms and abbreviations

Term	Definition
Abatement (carbon)	See definitions for Material Abatement and Feasible Abatement
Acentric factor	The acentric factor is a conceptual number introduced by Kenneth Pitzer in 1955, proven to be very useful in the description of matter. It has become a standard for the phase characterisation of single & pure components
Acritarchs	Acritarchs are defined as small, organic-walled microfossils of unknown biological affinity
Acoustic impedance	The ratio of the pressure over an imaginary surface in a sound wave to the rate of particle flow across the surface
AHP	Analytical hierarchy process
Allogenic	The term applied to the derived portion of a sediment, whether minerals or other constituents, which originated away from the area of sedimentation and is transported to it for final deposition
ANLEC R&D	Australian National Low Emissions Coal Research and Development
Anticline	A convex-upward formation of rock layers, which may form a trap for hydrocarbons
APCRC	Australian Petroleum Cooperative Research Centre
APLNG	Australia Pacific LNG (a joint venture between Origin, ConocoPhillips and Sinopec)
Aquifer	An underground layer of water-bearing permeable rock or unconsolidated materials (gravel, sand, silt or clay) from which groundwater can be extracted using a water well
Aquitards	An aquitard is a zone within the Earth that restricts the flow of groundwater from one aquifer to another
ASL	Above sea level
Autogenic	Internally generated, or autogenic, terrestrial and marine sediment-transport dynamics can produce depositional patterns similar to those associated with climatic, tectonic, or sea level changes
Bar	Unit of pressure
Barrel	42 US Gallons
Barrels of oil equivalent	Converting gas volumes to the oil equivalent is customarily done on the basis of the heating content or calorific value of the fuel. There are a number of methodologies in common use. Before aggregating, the gas volumes first must be converted to the same temperature and pressure. Common industry gas conversion factors usually range between 1.0 barrel of oil equivalent (boe) = 5.6 thousand standard cubic feet of gas (mscf) to 1.0 boe = 6.0 mscf
Baseload power	The baseload on a grid is the minimum level of demand on an electrical grid over a span of time, for example, one week. Synchronous power
Basin	A large, natural depression on the Earth's surface in which sediments, generally brought by water, accumulate
Bedding style	A bedding plane is a surface parallel to the surface deposition, which may or may not have a physical expression
Bellona	A Norwegian NGO that works across a range of issues, including energy
BHP	Bottom hole pressure
Biofuels	A fuel derived immediately from living matter
Biostratigraphy	Biostratigraphic correlation uses fossil assemblages constrained within rock strata to establish the relative ages of the rock layers. It is one of the most widely utilised methods for determining age-relationships of sediments in geological successions
Bioturbation	The disturbance of sedimentary deposits by living organisms
BI-scale	Bioturbation index

Term	Definition
Bitumen	A highly viscous form of crude oil resembling cold molasses (at room temperature). Bitumen must be heated or combined with lighter hydrocarbons for it to be produced. Contains sulfur, metals and other non-hydrocarbons in its natural form
BoD	Basis of design
Borehole	A hole in the earth made by a drilling rig
Bouguer gravity	In geodesy and geophysics, the Bouguer anomaly is a gravity anomaly, corrected for the height at which it is measured and the attraction of terrain
Bowen Basin	The foreland, Early Permian to Middle Triassic Bowen Basin of eastern Queensland occupies about 160,000 km <sup>2</sup> , the southern half of which is covered by the Surat Basin. It has a maximum sediment thickness of about 10,000 m concentrated in two north-trending depocenters, the Taroom Trough to the east and the Denison Trough to the west. Deposition in the basin commenced during an Early Permian extensional phase, with fluvial and lacustrine sediments and volcanics being deposited in a series of half-graben structures in the east, and a thick succession of coals and nonmarine clastics in the west
Braided channel complex	A stream consisting of interwoven channels constantly shifting through islands of alluvium and sandbanks
BREE	Bureau of Resources and Energy Economics
C1-C6	Hydrocarbons of varying chain lengths (where C1 is methane and C2-C6 are higher chain hydrocarbons such as ethane, propane, butane etc.)
CAPEX	Capital expenditure
Capillary pressure	In fluid statics, capillary pressure is the pressure between two immiscible fluids in a thin tube, resulting from the interactions of forces between the fluids and solid walls of the tube
Cap-rock	Impermeable layer of rock providing a seal to contain the reservoir fluids
Carbon abatement	The reduction of the amount of carbon dioxide that is produced when coal and oil are burned
Carbon capture and storage (CCS)	Process by which carbon dioxide emissions are captured and removed from the atmosphere and then stored, normally via injection into a secure underground geological formation
Carbon Capture and Storage Research Development and Demonstration (CCS RD&DA)	A fund set up by the Australian Government for research, development and demonstration activities in supporting Australian industry to innovate and adapt new technologies and processes, in particular for transport and storage of CO <sub>2</sub> . UQ-SDAAP is one of the projects funded under the scheme
Carbon dioxide equivalents (CO <sub>2</sub> e)	The quantity that describes, for a given mixture and amount of greenhouse gas, the amount of CO <sub>2</sub> that would have the same global warming potential (GWP) when measured over a specified timescale (generally 100 years)
Carbon sequestration	The fixation of atmospheric carbon dioxide in a carbon sink through biological or physical processes
Carbonic acid	Is a chemical compound with the chemical formula H <sub>2</sub> CO <sub>3</sub> (equivalently OC(OH) <sub>2</sub> ). It is also a name sometimes given to solutions of carbon dioxide in water (carbonated water), because such solutions contain small amounts of H <sub>2</sub> CO <sub>3</sub>
Carboniferous	A period named from the widespread occurrence of carbon in the form of coal in these beds. It extends from 345 to 280 m.y. and has a duration of 65 m.y
Casing	Thick walled steel pipe placed in wells to isolate formation fluids (such as fresh water) and to prevent borehole collapse
CCGTs	Combined cycle gas turbines (Condamine & Darling Downs plants in the study area)
CCS hubs	Central collection or storage distribution systems for CO <sub>2</sub>
CCTVs	Closed circuit televisions
CCUS	Carbon capture, utilisation and storage
CDR	Carbon dioxide removal
Cement bond integrity	Cement integrity logs are run to determine the quality of the cement bond to the production casing, and to evaluate cement fill-up between the casing and the reservoir rock. A poor cement bond may allow unwanted fluids to enter the well



Term	Definition
Cementation	The process of deposition of dissolved mineral components in the interstices of sediments
Cenozoic	The Cenozoic Era meaning “new life”, is the current and most recent of the three Phanerozoic geological eras, following the Mesozoic Era and extending from 66 million years ago to the present day
CH <sub>4</sub>	Methane
Clarence-Morton Basin	The Clarence Moreton Basin is a Mesozoic sedimentary basin on the easternmost part of the Australian continent. It is located in the far north east of the state of New South Wales around Lismore and Grafton and in the south east corner of Queensland
Clastic (rock)	Rock which has been formed from sediment of other rocks e.g. sandstone, shale, conglomerates, etc.
CMA	Cumulative Management Area (Office of Groundwater Impact Assessment, Queensland, terminology)
CMG GEM	GEM is CMG’s reservoir simulation software. It’s the equation-of-state (EoS) compositional and unconventional simulator that models the flow of three-phase, multi-component fluids
CO <sub>2</sub>	Carbon dioxide
COIs	Communities of interest (communities strategically chosen because of their exposure to energy projects)
Completion	Completion of a well. The process by which a well is brought to its final classification - basically a dry hole, producer, or injector. A dry hole is completed by plugging and abandonment. A well deemed to be producible of petroleum, or used as an injector, is completed by establishing a connection between the reservoir(s) and the surface so that fluids can be produced from, or injected into the reservoir. Various methods are utilised to establish this connection, but they commonly involve the installation of some combination of borehole equipment, casing and tubing, and surface injection or production facilities.
Condamine	Refers to the Condamine combined cycle gas turbines
Condensate	Mixture of hydrocarbons which are in a gaseous state under reservoir conditions and, when produced, become a liquid as the temperature and pressure is reduced
Conductor (casing)	Generally the first string of casing in a well
Container	For climate change mitigation to be accomplished through CCS, the large majority of CO <sub>2</sub> injected into the sub-surface must be securely contained indefinitely. To demonstrate containment requires the definition of a “container”. The leakage risk must be analysed within the context of this defined container. A container comprises the intended injection and storage reservoir and an overlying seal or seal complex that defines a vertical extent. The container also has to have defined, lateral boundaries. If CO <sub>2</sub> migrates outside the defined container (i.e. above the seal complex and/or beyond the lateral boundaries), it can be considered to have leaked
Containment	Containment, where geological features limit the migration of injected CO <sub>2</sub> (laterally or vertically) beyond its intended location
Conventional gas	Conventional gas is a natural gas occurring in a normal porous and permeable reservoir rock, either in the gaseous phase or dissolved in crude oil, and which technically can be produced by normal production practices
COP21 NDC commitments	Australia’s current Conference of Paris 21, nationally determined contributions
Core	A cylindrical sample taken from a formation for geological analysis
Coring	The process of cutting a vertical, cylindrical sample of the formations
Cretaceous	Rock formed in the last period of the Mesozoic era, between the Jurassic and the Tertiary periods
CSG	Coal seam gas. Natural gas contained in coal deposits, whether or not stored in gaseous phase
Cuttings	Small chips of rock retrieved from a well by the circulation of the mud, studied/logged by the well-site geologist
Darcy	Unit of measurement of rock permeability, the extent to which fluid will flow through it
Darling Downs	Refers to the Darling Downs combined cycle gas turbines
Decarbonisation	The reduction or removal of carbon dioxide from energy sources
Decollements	The plane of dislocation caused by an upper series of rocks folding and, in the process, sliding over a lower series of rocks, which may be unfolded or only slightly folded
DEM	Digital elevation model

Term	Definition
Density log	A wireline log parameter (measurement of density, a guide to porosity)
Depositional hiatuses	In geology a discontinuous succession of depositional layers would produce a hiatus or period of non-deposition between two orderly depositional units
Depth map	Relief map of sub-surface structure, contours relating to depths from surface datum level, (i.e. sea level)
Deterministic estimate	The method of estimation of reserves or resources is called deterministic if a single best estimate is made based on known geological, engineering, and economic data
Development well	A well drilled within the proved area of an oil or gas reservoir to the depth of a stratigraphic horizon known to be productive
Deviated (well)	Well diverted from the vertical
DFIT	Diagnostic fracture injection testing
DG	Decision gates for next stage investments
Dinoflagellate cysts	Dinocysts or dinoflagellate cysts are typically 15 to 100 µm in diameter and produced by around 15–20% of living dinoflagellates as a dormant, zygotic stage of their lifecycle, which can accumulate in the sediments as microfossils. Organic-walled dinocysts are often resistant and made out of dinosporin
Drawdown	The difference between the static and the flowing bottom hole pressures
Drilling fluid	Circulating fluid, removes cuttings from wellbore to surface, cools the bit and counteracts downhole formation pressure
DST	Drill stem test. Used to test the wells production potential with a temporary completion
Dynamic storage capacity	An estimate consistent with environmental and social context, for a given the geological environment (play) and a notional field development plan; the integral over time of the sustained (highest) injection rate supported by the analyses
EAs	Environmental approvals
EC	Electrical conductivity
Effective porosity	Effective porosity is most commonly considered to represent the porosity of a rock or sediment available to contribute to fluid flow through the rock or sediment, or often in terms of “flow to a borehole”
EIB	European Investment Bank
EIS	Environmental Impact Statement
Emissions	Emission of air pollutants, notably: Flue gas, gas exiting to the atmosphere via a flue. Exhaust gas, flue gas generated by fuel combustion. Emission of greenhouse gases, which absorb and emit
EMV analysis	Expected monetary value analysis
En-échelon	In structural geology, en-échelon veins or “en-échelon gash fractures” are structures within rock caused by noncoaxial shear. They appear as sets of short, parallel, planar, mineral-filled lenses within a body of a rock
Environmental assessment	A study that can be required to assess the potential direct, indirect and cumulative environmental impacts of a project
Environmental Protection and Biodiversity Conservation Act 1999	Australian Government’s central piece of environmental legislation
Environmental Protection Act 1994	The principal element of Queensland’s environmental legal system
EOR	Enhanced oil recovery. One or more of a variety of processes that seek to improve recovery of hydrocarbon from a reservoir after the primary production phase
EPCM	Engineering, procurement, construction and management
Eromanga Basin	The Eromanga Basin is a large Mesozoic sedimentary basin in central and northern Australia. It covers parts of Queensland, the Northern Territory, South Australia, and New South Wales, and is a major component of the Great Artesian Basin. The Eromanga Basin covers 1,000,000 km <sup>2</sup> and overlaps part of the Cooper Basin

Term	Definition
Eustatic sea level	Pertaining to absolute changes in sea level, i.e. to worldwide changes and not local changes produced by local movements of land or the sea floor
Evergreen Formation	Strata of the Surat Basin
EWR	Enhanced water recovery
EWT	Extended well test
Facies	The sum total of features such as sedimentary rock type, mineral content, sedimentary structures, bedding characteristics, fossil content, etc. which characterise a sediment as having been deposited in a given environment
Fault	A fracture in rock along which there has been an observable amount of displacement
FBHP	Flowing bottom hole pressure
FDP	Field development plan
Feasible Abatement	<p>UQ-SDAAP aimed to establish whether or not 'material' carbon Abatement was 'feasible' in the Surat Basin in southern Queensland via large-scale CCS.</p> <p>"Feasible Abatement" was defined to mean a combination of:-</p> <p>Lowest risk: Non-technical risk factors are known and demonstrably minimised and there is a clear work plan to address them before any deployment</p> <p>High technical confidence: High level of technical confidence that a high rate can be sustained for a long duration; and, that the CO<sub>2</sub> will be contained indefinitely</p> <p>A robust, conservative capture scenario with minimum disruption to generation (minimum price impacts)</p> <p>Pipeline routes possible with no obvious showstoppers</p> <p>Reasonable cost estimates: the unit costs of carbon abatement (\$/t) and LCOE (\$/Mwh) are in the range of published estimates for other CCS projects or literature</p>
FEED	Front end engineering design
FID	Final investment decision
Field	An area consisting of a single hydrocarbon reservoir or multiple geologically related reservoirs all grouped on or related to the same individual geological structure or stratigraphic condition
Flow test	An operation on a well designed to demonstrate the existence of moveable petroleum in a reservoir by establishing flow to the surface and/or to provide an indication of the potential productivity of that reservoir. Some flow tests, such as drill stem tests (DSTs), are performed in the open hole. A DST is used to obtain reservoir fluid samples, static bottomhole pressure measurements, indications of productivity and short-term flow and pressure build-up tests to estimate permeability and damage extent. Other flow tests, such as single-point tests and multi-point tests typically involve a measurement or estimate of initial or average reservoir pressure and a flow rate and flowing bottomhole pressure measurement. Multi-point tests are used to establish gas well deliverability and absolute open flow potential
Flue gas	Gas from industrial processes
Formation	A rock layer which has distinct characteristics (e.g. rock type, geologic age)
Formation damage	Reservoir damage due to plugging with mud, crumbling under pressure or high flow rate, etc.
Fossil	An organic trace buried by natural processes, and subsequently permanently preserved. The term 'organic trace' is here used to include skeletal material, impressions of organisms, excremental material, tracks, trails, and borings
Fossil fuel	A fuel source (such as oil, condensate, natural gas, natural gas liquids or coal) formed in the earth from plant or animal remains
Fracturing	Fracturing formation adjacent to well bore to improve well productivity (flow) by applying hydraulic pressure downhole
Free water level (FWL)	The free water surface is the highest elevation with the same oil and water pressure (zero capillary pressure)
Fugacity	In chemical thermodynamics, the fugacity of a real gas is an effective partial pressure which replaces the mechanical partial pressure in an accurate computation of the chemical equilibrium constant. It is equal to the pressure of an ideal gas which has the same temperature and molar Gibbs free energy as the real gas

Term	Definition
Galilee Basin	The Galilee Basin is a large inland geological basin in the western Queensland region of Australia. The Galilee Basin is part of a larger Carboniferous to Mid-Triassic basin system that contains the Cooper Basin, situated towards the south-west of the Galilee Basin, and the Bowen Basin to the east
Gamma ray	Log of the total natural radioactivity. Shales and clays are responsible for most natural radioactivity, so the gamma ray log is a good indicator of such rocks
Geobodies	Seismic bodies identified from different seismic attributes are analysed and calibrated with drilled wells to define their geological features
Geochronometric	A branch of stratigraphy aimed at the quantitative measurement of geologic time. It is considered a branch of geochronology
GEODISC	A program of APCRC that assessed and ranked sedimentary basins across Australia for their carbon storage potential relative to major point source emissions
Geomechanical	Geomechanics involves the geologic study of the behaviour of soil and rock
Geosequestration	Is the term used to describe the technology of capturing greenhouse gas emissions from power stations and pumping them into underground reservoirs. It is also referred to in some circles as carbon capture and storage (CCS)
Geothermal gradient	Increase of temperature with depth in the earth's crust
GHG	Greenhouse gas
GIS	Geographic Information Systems
Grain roundness	Rounding, roundness or angularity are terms used to describe the shape of the corners on a particle (or clast) of sediment. Such a particle may be a grain of sand, a pebble, cobble or boulder
Grain size	Grain size (or particle size) is the diameter of individual grains of sediment, or the lithified particles in clastic rocks. The term may also be applied to other granular materials. This is different from the crystallite size, which refers to the size of a single crystal inside a particle or grain
Grain sorting	Sorting describes the distribution of grain size of sediments, either in unconsolidated deposits or in sedimentary rocks
Great Artesian Basin (GAB)	The Great Artesian Basin, located in Australia, is the largest and deepest artesian basin in the world, stretching over 1,700,000 km <sup>2</sup> , with measured water temperatures ranging from 30–100 °C. The basin provides the only source of fresh water through much of inland Australia
Greenhouse gas	Atmospheric gases that are transparent to solar (short-wave) radiation but opaque to long-wave (infrared) radiation, thus preventing long-wave radiant energy from leaving Earth's atmosphere. The net effect of these gases is a trapping of absorbed radiation and a tendency to warm the planet's surface. The greenhouse gases most relevant to the oil and gas industry are carbon dioxide, methane and nitrous oxide
Greenhouse Gas Storage Act 2009	Queensland Government Act regulating storage of greenhouse gases
GRFS	Gaussian random function simulation
Gunnedah Basin	The Gunnedah Basin is in north-eastern New South Wales, between the Bowen Basin to the north and the Sydney Basin to the south. Marine and non-marine sequences from the Permian and Triassic are present in it, and it contains Permian coal deposits
GW	Gigawatts
GWDB	The Queensland Government's Groundwater Database
GWh	Gigawatt hours
HFB	Horizontal flow barrier
HI	Hydrogen index
Highstand systems tract	A systems tract bounded below by a downlap surface and above by a sequence boundary
HM	History matching

Term	Definition
Horner extrapolation	The Horner plot is a cross-plot of build-up (or drawdown) pressure (Pi) on the Y axis versus a dimensionless time coefficient (HTi), usually called Horner Time, on a logarithmic X axis
Hunter Bowen Orogeny	Late Permian and early Triassic resulted in deformation and basin inversion with uplift of nearly 4 km
Hutton Sandstone	The Hutton Sandstone is a geological formation of the Surat Basin in Queensland, Australia. The ferruginous sandstones and coal were deposited in a floodplain environment and dates back to the Bajocian Age
Hydraulic conductivity	Is a property of soils and rocks, that describes the ease with which a fluid can move through pore spaces or fractures
Hydraulic head	Hydraulic head or piezometric head is a specific measurement of liquid pressure above a vertical datum. It is usually measured as a liquid surface elevation, expressed in units of length, at the entrance of a piezometer
Hydrocarbons	An organic compound containing only carbon and hydrogen and often occurring in nature as petroleum, natural gas, coal and bitumen or in refined products such as gasoline and jet fuel
Hydrograph	A hydrograph is a graph showing the rate of flow (discharge) versus time past a specific point in a river, channel, or conduit carrying flow. The rate of flow is typically expressed in cubic meters or cubic feet per second (cms or cfs)
Hydrostatic	Pressure/head pressure exerted by a column of liquid at a given depth
Ichnology	Is the study of trace fossils, and is the work of ichnologists. Trace fossils may consist of impressions made on or in the substrate by an organism: for example, burrows, borings (bioerosion), urolites (erosion caused by evacuation of liquid wastes), footprints and feeding marks, and root cavities
IEA	International Energy Agency
Impermeable	Rock that will not allow hydrocarbons or groundwater to flow through it
Injection	The forcing or pumping of substances into a porous and permeable subsurface rock formation. Examples of injected substances can include either gases or liquids
Injectivity	Injectivity, where the storage reservoir has sufficient permeability and thickness to accept the injected CO <sub>2</sub> at an economic rate for an economic duration and preferably with minimum surface footprint (not too many injection wells) without exceeding critical pressure constraints where pressures in the formation are to be managed lower than (i) the temperature adjusted fracture pressure of the sealing formations at the injection well site; (ii) fault reactivation or fault valving pressures for any naturally occurring faults in the Play; and (iii) the CO <sub>2</sub> capillary entry pressure at the seal
Intermittent power	An intermittent energy source is any source of energy that is not continuously available for conversion into electricity and outside direct control because the used primary energy cannot be stored. Intermittent energy sources may be predictable but cannot be dispatched to meet the demand of an electric power system. Non-synchronous power
Intracratonic	Intracratonic sag sedimentary basins occur in the middle of stable continental or cratonic blocks. They are rarely fault bounded, although strike-slip faulting can occur within them
IPCC	Intergovernmental Panel on Climate Change
Isochores	A contour connecting points of equal true vertical thickness of strata, formations, reservoirs or other rock units
Jurassic	Rock formed in the second period of the Mesozoic era, between the Triassic and Cretaceous periods
Kogan Creek	A modern supercritical power plant located in the study area
Kriging	In statistics, originally in geostatistics, kriging or Gaussian process regression is a method of interpolation for which the interpolated values are modelled by a Gaussian process governed by prior covariances
LCOE	Levelised cost of electricity
Lease	A legal document executed between a mineral owner and a company or individual that conveys the right to explore for and develop hydrocarbons and/or other products for a specified period of time over a given area
Liquefied natural gas (LNG)	Natural gas that has been converted to a liquid by refrigerating it to 260°F. Liquefying natural gas reduces the fuel's volume by 600 times, enabling it to be shipped economically from distant producing areas to markets
Listric fault	A term applied to fracture planes which curve, either to near-horizontal ones which steepen, or to near-vertical ones which become less steep

Term	Definition
Lithology	A term usually applied to sediments, referring to their general characteristics
Lithostratigraphic unit	Lithostratigraphic units are bodies of rocks, bedded or unbedded, that are defined and characterised on the basis of their lithologic properties and their stratigraphic relations. Lithostratigraphic units are the basic units of geologic mapping
Logging (well)	Recording of information of subsurface formations. Logging includes records kept by the driller and records of mud and cutting analyses, core analyses, drill stem tests, and electric, acoustic and radioactivity logging
LOT	Leak-off test
Lowstand systems tract	A systems tract overlying a sequence boundary and overlain by a transgressive surface. Characterised by a progradational to aggradational parasequence set, this systems tract commonly includes a basin-floor fan, a slope fan and a lowstand wedge
LQC	Log quality control
M&V	Monitoring and verification
Machine learning	Machine learning is an application of artificial intelligence (AI) that provides systems the ability to automatically learn and improve from experience without being explicitly programmed. Machine learning focuses on the development of computer programs that can access data and use it learn for themselves
Magmatic arc	A magmatic/volcanic arc is a chain of volcanoes formed above a subducting plate, positioned in an arc shape as seen from above. Offshore volcanoes form islands, resulting in a volcanic island arc
Magnetics	Geophysical datasets used to depict regional structural grain or patterns using natural occurring rock magnetism
MAR	Managed Aquifer Recharge. Trials using fresh water from reverse osmosis plants. Using either the reinjection of water or CO <sub>2</sub> to raise water levels in the basin
Markov chain analysis	A Markov chain is a stochastic model describing a sequence of possible events in which the probability of each event depends only on the state attained in the previous event
MARPD	MAR Petrophysics Database
Material Abatement	<p>UQ-SDAAP aimed to establish whether or not 'material' carbon abatement was 'feasible' in the Surat Basin in southern Queensland via large-scale CCS</p> <p>"Material Abatement" was defined initially as <i>at least 5 Mtpa for at least 20 years</i>, roughly equivalent to the emissions of one of the large supercritical power stations</p> <p><i>Note: In the event, a working plateau rate of ~13 Mtpa was found technically robust. This was used as a reference case, representing the full retrofit of Millmerran and Kogan Creek and a partial retrofit at Tarong North. All reservoir models were run for longer than the lifetime of these plants indicating surplus dynamic capacity</i></p>
Maximum flooding surface (MFS)	In sequence stratigraphy, a maximum flooding surface is the surface that marks the transition from a transgression to a regression. Maximum flooding surfaces are abbreviated by MFS, synonyms for them include final transgressive surface, surface of maximum transgression and maximum transgressive surface
MCPD	Myall Creek Petrophysics Database
MEA	Monoethanolamine (MEA), an amine solvent used to remove CO <sub>2</sub> from flue gas (CO <sub>2</sub> scrubbing process). The process principle is based on the thermally reversible reaction between components in the liquid absorbent and CO <sub>2</sub> present in the flue gas
MEMs	Mechanical earth models
MFS	Maximum flooding surfaces
MICP	Mercury injection capillary pressure
Migration	Movement of hydrocarbons from source rock either into a reservoir or seeping to the earth's surface
Millmerran	A modern supercritical power plant located in the study area
Mimosa Syncline	The north-south axis along which the Surat Basin is aligned
MKTMK scenario	The highest rate scenario modelled has considered the partial sequential retrofitting of Millmerran, then Kogan Creek, then Tarong North, Millmerran and finally Kogan Creek
ML	Megalitres

Term	Definition
MMV	Measurement, monitoring and verification
Modflow	The U.S. Geological Survey modular finite-difference flow model, which is a computer code that solves the groundwater flow equation. The program is used by hydrogeologists to simulate the flow of groundwater through aquifers
Modflow-6 code	Modflow-6 is the most recent version of Modflow, one of the groundwater industry's standard codes that has been continually developed by the US Geological Survey since the late 1970s. It represents 3D fluid flow of a single water phase, with a wide variety of boundary condition options available.
Monocline	Is a step-like fold in rock strata consisting of a zone of steeper dip within an otherwise horizontal or gently-dipping sequence
Monte Carlo simulation	A type of stochastic mathematical simulation which randomly and repeatedly samples input distributions (e.g. reservoir properties) to generate a results distribution (e.g. recoverable petroleum volumes)
MTPA	Millions of tonnes pa
MWh	Megawatt hours
Natural gas	Natural gas is the portion of petroleum that exists either in the gaseous phase or is in solution in crude oil in natural underground reservoirs, and which is gaseous at atmospheric conditions of pressure and temperature. Natural gas may include amounts of non-hydrocarbons
NEM	National Electricity Market
NeuraLog™	Software used to digitise a significant number of legacy wireline logs
Neutron log	Normally synonymous with a neutron porosity log, however, the term is sometimes broadened to include an activation log. Guide to rock porosity
New England Fold Belt	The New England Fold Belt of eastern Australia comprises a number of variably deformed terrains, ranging in age from Early Palaeozoic to Late Triassic
NNM	Not normally manned
Normal fault	A fault with a major dip-slip component in which the hanging wall is on the downthrown side. See fault
Notional injection sites	Areas that may support large-scale injection and securely store by injecting into the deepest, lowermost aquifer of the Surat Basin. However, more site-specific data is required from these notional injection sites to increase technical confidence before development decisions can be made
NOx	Oxides of nitrogen, especially as atmospheric pollutants
nRMS	Normalised root mean square error
NTG	Net to gross
Offset well location	Potential drill location adjacent to an existing well. The offset distance may be governed by well spacing regulations. Proved volumes on the existing well are indicated by either conclusive formation test or production. For proved volumes to be assigned to an offset well location there must be conclusive, unambiguous technical data which supports the reasonable certainty of production of hydrocarbon volumes and sufficient legal acreage to economically justify the development without going below the shallower of the fluid contact or the lowest known hydrocarbon
OGIA	Office of Groundwater Impact Assessment, Department of Natural Resources, Mines and Energy, Queensland
Open-hole	An uncased section of well borehole
Operator	The entity responsible for managing operations in a field or undeveloped acreage position
OPEX	Operating expenditure
Organic	Substances derived from living organisms, such as oil in the natural state
Outcrop	The appearance of a rock formation at the surface
OzSEEBASE Map	Shows regional structural trends inferred from gravity maps
P&A	Plugged and abandoned
pa	per annum

Term	Definition
P50	P50 is defined as 50% of estimates exceed the P50 estimate (and by definition, 50% of estimates are less than the P50 estimate). It is a good middle estimate
Palaeozoic	The era ranging from 600-230 million years, a duration of 370 million years
Paleodepositional	Ancient depositional environment
Palynology	The study of fossil spores and pollen
Palynomorphs	Palynomorphs are broadly defined as organic-walled microfossils between 5 and 500 micrometres in size. Palynomorphs may be composed of organic material such as chitin, pseudochitin, sporopollenin and dinosporin
Paralic lakes	Of, relating to, or being interfingered marine and continental sediments
PCC	Post combustion capture refers to the separation of CO <sub>2</sub> from flue gas derived from the combustion of carbon-based fuel
Perforation	Holes shot through the casing in the pay zone (producing zone)
Permeability	The permeability of a rock is the measure of the resistance to the flow of fluid through the rock. High permeability means fluid passes through the rock easily
Permo-Triassic	Relating to the Permian to Triassic periods
Petrel	Software used for geological and reservoir engineering models
Petroleum	Petroleum is a naturally occurring mixture consisting predominantly of hydrocarbons in the gaseous, liquid or solid phase
Petrology/ Petrophysics	The study of rocks, their origin, chemical and physical properties and distribution
PHIE	Effective porosity
PHIT	Total porosity
Photoelectric factor	A wireline log parameter
PI	Well productivity index. PI defines the well deliverability, showing the flow rate of formation fluid that can be produced from the reservoir per unit pressure drawdown
Pilot project	A small-scale test or trial operation that is used to assess the suitability of a method for commercial application
Pipeline	A system of connected lengths of pipe, buried or surface laid for the transportation of fluids
Play	Recognised prospective trend of potential prospects, but which requires more data acquisition and/or evaluation to define specific leads or prospects
Plug/Plug and abandon	To seal a well with cement, e.g. before producing from a higher formation, side-tracking, or leaving the well permanently sealed and abandoned
Poro-perm	Porosity – permeability relationships
Porosity	The measure of a rock's ability to hold a fluid. Porosity is normally expressed as a percentage of the total rock which is taken up by pore space
PPA	Power purchase agreement
PPC	Post combustion capture
Precipice Sandstone	Strata of the Surat Basin. Considered to be the lowermost aquifer of the Great Artesian Basin
Present value	Also known as present discounted value, is a future amount of money that has been discounted to reflect its current value, as if it existed today
Produced water	Groundwater produced in connection with oil and natural gas exploration and development activities. Also known as formation water
Production casing	Innermost steel lining of a well cemented in place and perforated for production in the pay zone
psi	pounds per square inch; a unit of pressure



Term	Definition
PTA	Pressure transient analysis
Python	A programming language
QDEX	Queensland Digital Exploration Reports
QGC	Queensland Gas Company
QPED database	Queensland Petroleum Exploration Data
Regional Geological Model	<p>The UQ-SDAAP research created a Regional Geological Model of the Precipice Sandstone to Evergreen Formation strata in the Surat Basin. It integrates existing seismic data, well data, and their associated geological interpretations using Petrel 2016 software. The aim was to produce a 3D geological model that combines all the subsurface geological understanding to depict the spatial distribution of reservoirs and seals that is consistent with all available data. Subsurface data integration supported a conceptual geological model creation. In addition, using the play concept developed for the Precipice Sandstone and Evergreen Formation, subsurface fluid flow and its implications for CO<sub>2</sub> storage can then be assessed. Constructing large-scale models for the Surat Basin has limitations relating to areas of sparse data and this carries with it a relatively high degree of uncertainty. However, the uncertainty was mitigated by using our conceptual understanding of the geology to infill data gaps in a geologically consistent manner.</p> <p>The Regional Geological Model is used as the base case reference for the Regional Groundwater and Notional Injection Sector dynamic simulations</p>
Reserves	Estimated remaining quantities of oil and gas and related substances anticipated to be economically producible, as of a given date, by application of development projects to known accumulations. In addition, there must exist, or there must be a reasonable expectation that there will exist, the legal right to produce or a revenue interest in production, installed means of delivering oil and gas or related substances to market and all permits and financing required to implement the project
Reservoir	A subsurface rock formation containing one or more individual and separate natural accumulations of moveable petroleum that is confined by impermeable rock and is characterised by a single-pressure system
Reservoir pressure	The pressure at reservoir depth in a shut-in well
Resistivity log	A log of the resistivity of the formation made by an electrode device such as a laterolog, in this sense the term is used to distinguish the log from an induction measurement, which responds more directly to conductivity
Resources	Quantities of oil and gas estimated to exist in naturally occurring accumulations. A portion of the resources may be estimated to be recoverable, and another portion may be considered to be unrecoverable. Resources include both discovered and undiscovered accumulations
Reverse fault	A fault with a major dip-slip component in which the hanging wall is on the downthrown side
Rig (drilling)	The machine used to drill a wellbore
Risk	The probability of loss or failure. As “risk” is generally associated with the negative outcome, the term ‘chance’ is preferred for general usage to describe the probability of a discrete event occurring
ROI	Radius of investigation
Roma Shelf	Western margin of the Surat Basin
RTUPE	Real terms unit price earned (which would risk-cover the development, operating and appraisal costs)
SCADA	Supervisory control and data acquisition (SCADA) is a system of software and hardware elements that allows industrial organisations to control industrial processes locally or at remote locations. It is used to monitor, gather, and process real-time data
Schlumberger’s Techlog	Petrophysical analysis software
SDPD	Southern Depocenter Petrophysical Database
Seal	A relatively impermeable rock, commonly shale, anhydrite or salt, that forms a barrier or cap above and around reservoir rock such that fluids cannot migrate beyond the reservoir
Sedimentary rock	Rock composed of weathered materials transported by wind or water that have undergone lithification, e.g. sandstone, shale and limestone
Sedimentological	Relating to sedimentary rock forming processes. See Sedimentary rock

Term	Definition
Seismic survey	Exploration method in which strong, low-frequency sound waves are generated on the surface or in the water to find subsurface rock structures that may contain hydrocarbons
Seismogram	A seismogram is a graph output by a seismograph. It is a record of the ground motion at a measuring station as a function of time. Seismograms typically record motions in three cartesian axes (x, y, and z), with the z axis perpendicular to the Earth's surface and the x- and y- axes parallel to the surface
SEM image	Image produced from a scanning electron microscope
Sequence stratigraphic	Critical to confidence in injection and containment prediction is the lateral prediction of properties away from well control. Rather than rely on historic correlations, UQ-SDAAP has undertaken a fundamental revision of the lowermost Jurassic stratigraphy that comprise the storage play into a sequence stratigraphic framework. This has led to increased confidence in both injection and sealing prediction and performance
SGS	Sequential Gaussian Simulation
SIS	Sequential Indicator Simulation
Skid	Steel framework used to contain equipment or mount equipment for transport
Skin factor	Is a term introduced to account for any deviation from radial flow in the near well bore region and quantifies the pressure drop (positive skin) near the well bore due to formation damage induced during drilling operations, or flow improvement (negative skin) because of well stimulation such as acidisation
Solar PV	Solar photovoltaics
Sonic	A type of acoustic log that displays travel time of P-waves versus depth. Sonic logs are typically recorded by pulling a tool on a wireline up the wellbore. The tool emits a sound wave that travels from the source to the formation and back to the receiver
Source rock	Sedimentary rock with organic deposits that form into hydrocarbons
SOx	Oxides of sulfur, especially as atmospheric pollutants
Spacing	The distance between wells producing from the same reservoir. Spacing is often expressed in terms of acres (e.g. 8-acre spacing) and is often established by regulatory agencies
SPE	Society of Petroleum Engineers
SSSV	Subsurface safety valves
Static models	Static models can be defined as models that represent a phenomenon at a given point in time or that compare the phenomenon at different points in time
Stochastic	Adjective defining a process involving or containing a random variable or variables or involving chance or probability such as stochastic simulation
STOOIP	Stock-tank original oil in place, the volume of oil in a reservoir prior to production
Storage capacity	Storage capacity, where there is sufficient accessible pore space within the injection reservoir to accommodate the volume to be stored
Subsidence	Subsidence is the sudden sinking or gradual downward settling of the ground's surface with little or no horizontal motion. The definition of subsidence is not restricted by the rate, magnitude, or area involved in the downward movement. It may be caused by natural processes or by human activities
Supercritical power plant	A supercritical steam generator is a type of boiler that operates at supercritical pressure, frequently used in the production of electric power. In contrast to a subcritical boiler in which bubbles can form, a supercritical steam generator operates at pressures above the critical pressure – 3,200 psi or 22 MPa.
Surat Basin	The Surat Basin is a geological basin in eastern Australia. It is part of the Great Artesian Basin drainage basin of Australia. The Surat Basin extends across an area of 270,000 km <sup>2</sup> and the southern third of the basin occupies a large part of northern New South Wales, the remainder is in Queensland
Syncline	A downward, trough-shaped configuration of folded, stratified rocks. Compare with anticline
Tarong North	A modern supercritical power plant located in the study area
Taroom Trough	Bowen Basin major depocenter with up to 7 km of burial
TD	Total depth i.e. the drilled depth in a well at any one time

Term	Definition
TDR	Time-depth relationship
TDS	Total dissolved solids
Tectonics	The process of formation and evolution of the earth's solid surface crust
Tectono-stratigraphy	The degree to which local structures may have influence stratigraphy
Thermogenic hydrocarbon	The manufacture of thermogenic hydrocarbon gases usually occurs at sub-bottom depths exceeding 1,000 m. These hydrocarbon gases are produced under conditions of high temperature and great pressure from kerogens (which are derived from organic matter)
Tidal flats	Mudflats or mud flats, also known as tidal flats, are coastal wetlands that form when mud is deposited by tides or rivers. They are found in sheltered areas such as bays, bayous, lagoons, and estuaries
TOC	Total organic content
Toriacian to Bajocian	A period in the Early to Middle Jurassic
Total porosity	Total porosity is defined as the ratio of the entire pore space in a rock to its bulk volume. Effective porosity is the total porosity less the fraction of the pore space occupied by shale or clay. In very clean sands, total porosity is equal to effective porosity. See Porosity
Transgression	A marine transgression is a geologic event during which sea level rises relative to the land and the shoreline moves toward higher ground, resulting in flooding. Transgressions can be caused either by the land sinking or the ocean basins filling with water (or decreasing in capacity)
Transgressive surface	This is a marine-flooding surface that forms the first significant flooding surface in a sequence
Transgressive systems tract	The transgressive systems tract comprises the deposits accumulated from the onset of coastal transgression until the time of maximum transgression of the coast, just prior to renewed regression
Triassic	The period extends from 252 - 201 million years ago, a duration of -40 million years. It marks the beginning of the Mesozoic Era
TVD	True Vertical Depth; the vertical distance below surface datum reached by a deviated well
TVDSS	True vertical depth sub-sea
TWT	Two-way time
UCG	Underground coal gasification
Ultimate Seal	Acts as the final cap-rock which retains the CO <sub>2</sub>
Uncertainty	The range of possible outcomes in an estimate
Unconformity	An unconformity is a buried erosional or non-depositional surface separating two rock masses or strata of different ages, indicating that sediment deposition was not continuous
Unit play segment appraisal costs (UPSAC)	Unit costs for a specific plateau rate which probably uses the majority of the dynamic capacity appraised and is not limited by the project lifetime, again with the denominator as discounted injection rates. This could also be additive to UTC and assumes that, at some future point, additional sources of CO <sub>2</sub> are found to "use up" all of the storage resource
Unit project appraisal costs (UPAC)	Unit costs of appraisal for a specific project (which may not "use" the entire dynamic capacity appraised), limited by the project lifetime, with the denominator as discounted injection rates. This could be additive to UTC, but the capital spent has likely appraised more storage than the project has 'used'. It has benefited other future investors
Unit resource finding costs (URFC)	Unit costs of appraising a certain resource "volume", which is calculated as the integral of the maximum injection rate over time modelled with given pressure constraints and undiscounted rates over time. This is not additive to UTC
UPS	Uninterruptible power supply
UQ Centre for Coal Seam Gas Fault and Fractures project	Structural data and interpretations from the north were consolidated from the fault and fractures project
UQ-SDAAP	The University of Queensland Surat Deep Aquifer Appraisal Project. is part of the ongoing development of carbon capture and storage (CCS) to help reduce emissions from fossil fuel in Australia

Term	Definition
UTC	Unit technical cost
Variogram	A variogram is a description of the spatial continuity of the data. The experimental variogram is a discrete function calculated using a measure of variability between pairs of points at various distances. The exact measure used depends on the variogram type selected
Vegetation Management Act 1999	Queensland Government Act
Vent	Pipe/fitting on a vessel that can be opened to atmosphere
Vent stack	Open pipe and framework for discharging vapours into the atmosphere at a safe location without combustion
Viscosity	Property of fluids/slurries indicating their resistance to flow, defined as the ratio of shear stress to shear rate
VIT	Vertical interference test
Vitrinite reflectance	Thermal maturation indicators
VSMOW	Vienna Standard Mean Ocean Water (VSMOW) is a water standard defining the isotopic composition of fresh water
WACC	Weighted average cost of capital
Walloon Coal Measures (WCM)	The Walloon Coal Measures is an Aalenian to Oxfordian geologic formation in Queensland, Australia
Waste Reduction and Recycling Act 2011	Queensland Government Act
Water Act 2000	Queensland Government Act
Water drive	When the hydrocarbon reservoir in contact with underlying water table, the formation pressure will drive the water into the rock pores vacated by produced oil, thus maintaining reservoir pressure and aiding production
Water injection	The injection of water in order to maintain reservoir pressure and boost production
Water reinjection	Disposal of produced water into a disposal well as opposed to dumping to the environment (not for boosting the reservoir pressure)
Water saturation	Proportion of water in the pore spaces of a reservoir. See Porosity
Water table	The level in the earth below which rock pores are saturated with water
Well abandonment	The permanent plugging of a dry hole or of a well that no longer produces petroleum or is no longer capable of producing petroleum profitably. Several steps are involved in the abandonment of a well: permission for abandonment and procedural requirements are secured from official agencies; the casing is removed and salvaged if possible; and one or more cement plugs and/or mud are placed in the borehole to prevent migration of fluids between the different formations penetrated by the borehole
Well pad	A temporary drilling site, usually constructed of local materials such as gravel, shell or even wood
Well testing	Testing of an exploration or appraisal well to aid the estimation of reserves in communication with the well and well productivity. Testing in a production well also monitors the effects of cumulative production on the formation
Wellbore	The hole drilled by a drilling rig to explore for or develop oil and/or natural gas. Also referred to as a well or borehole
Wellhead	The “Wellhead” is descriptive of a location or function (including the ‘Christmas tree’ and hang offs) rather than a specific item of equipment Permanent equipment used to secure and seal the casings and production tubing and to provide a mounting for the Christmas tree. The Christmas tree is an assembly of valves, spools and fittings used to regulate the flow in all types of oil, gas and water wells (extraction and injection)
Wettability	Wettability is the tendency of one fluid to spread on, or adhere to, a solid surface in the presence of other immiscible fluids. Wettability refers to the interaction between fluid and solid phases. In a reservoir rock the liquid phase can be water or oil or gas, and the solid phase is the rock mineral assemblage
WHP	Wellhead pressure

Term	Definition
Wireline	Small-diameter metal line used in wireline operations; also called a slick line. A system in which a flexible cable and reel is used to lower a log or maintenance equipment into a well, rather than a rigid drill string, offering considerable savings of equipment, manpower and time
Wireline logs	See logging (wells)
WLF	Wireline log facies
WMIP	The Queensland Government's online Water Monitoring Information Portal
Zerogen Project	The ZeroGen Project was a Queensland Government initiative established to develop, construct and operate an Integrated Gasification Combined Cycle (IGCC) and carbon dioxide capture and storage (CCS) power plant and storage facility in Central Queensland, Australia
Zone	Interval between two depths in a well containing reservoir or other distinctive characteristics



THE UNIVERSITY  
OF QUEENSLAND  
AUSTRALIA

---

CREATE CHANGE